EUROPEAN
PHYSICAL
SOCIETY

INTERNATIONAL CONFERENCE ON HIGH-ENERGY PHYSICS

GENEVA, 27 JUNE – 4 JULY 1979

PROCEEDINGS

Volume 1

Sessions I to III

CERN, European Organization for Nuclear Research, Geneva 1979

EUROPEAN
PHYSICAL
SOCIETY

INTERNATIONAL CONFERENCE ON HIGH-ENERGY PHYSICS

GENEVA, 27 JUNE – 4 JULY 1979

PROCEEDINGS

Volume 1

Sessions I to III

CERN, European Organization for Nuclear Research, Geneva 1979

Copies of these Proceedings can be obtained from:

Scientific Information Service, CERN
CH-1211 Genève 23, Switzerland

Price (2 volumes) Sw.Fr. 30.-

CERN - Publications Group - RD/421 - 2000 - janvier 1980

FOREWORD

This year marks the 25th anniversary of CERN, the European Organization for Nuclear Research, which has played such a prominent role in European subnuclear physics. In order to celebrate this very significant event, the special gift offered by the European Physical Society was the decision to hold the EPS biennial High-Energy Physics Conference here in Geneva.

The Opening Ceremony of the Conference was honoured by the presence of prominent personalities who in their speeches expressed their support of the subnuclear physics research community -- a support which we value greatly.

* * *

A very large number of papers have been submitted to the Conference. They contain an impressive amount of very interesting results, which is the best proof of the importance of the role that subnuclear physics plays in modern research. We are at the turning point in our understanding of the laws of nature; and this turning point is based on three major breakthroughs in our experimental investigations. The *first* one is the study of lepton pairs produced in hadronic interactions. Started at CERN in 1964, this new way of looking at hadronic processes produced the celebrated J particle at BNL in 1974, and the Υ particle at Fermilab in 1977. The *second* breakthrough is in the study of $(e^{\pm}\mu^{\mp})$ pairs produced in (e^+e^-) collisions. Started in 1966 by CERN physicists working at Frascati, this original way of looking for leptons heavier than muons, produced in (e^+e^-) annihilation, led to the discovery in 1974 of the τ lepton at SPEAR. *Finally*, the study of muonless events in a heavy-liquid bubble chamber, started by CERN physicists, ended at CERN with the discovery of the "neutral weak currents" in 1973.

The discoveries of "charm", "bottom", "τ", and the "neutral weak currents" has produced a convincing picture of the existence of three families of quarks and leptons, and of the unification of electromagnetic and weak forces. For the first time quarks and leptons share the same quantum numbers: those of the symmetry groups $SU(2)_L \times U(1)_{L,R}$, which have the important property of being gauge groups. All this makes "classical" those fields of our physics which, at the International Conference on High-Energy Physics, held in London in 1974, just five years ago, were considered extremely interesting: for example, hadronic total and differential cross-sections with their rising behaviour and minima, Regge exchange processes, deep inelastic phenomena, and the like.

The structure of the Conference was as follows: five hours of Plenary Sessions and five hours of Parallel Discussion Sessions per day. This was the choice that the Scientific Advisory Committee considered as the best compromise in order to allow the greatest possible interaction between physicists working in the many branches of subnuclear physics: Parallel Discussion Sessions for specialized topics, and Plenary Sessions for everybody to follow the most important theoretical and experimental developments of subnuclear physics. It is a "format" which we would like to recommend to future conference organizers.

Neutrino physics and weak interactions; (e^+e^-) physics and deep inelastic phenomena; hadron spectroscopy; gauge theories and quark confinement -- all these are examples of some basic topics discussed at the Conference. One session was devoted to the new $(\bar{p}p)$ facility being built at CERN and another one to the future European accelerator possibilities.

I would like to express my gratitude and appreciation, and that of the Scientific Advisory Committee, to all those who have contributed to the success of the Conference.

* * *

Thanks are due in particular to the *Directors-General of CERN* for providing us with the invaluable support of various CERN services.

I am grateful to the *Members of the Scientific Advisory Committee*, to the *Chairmen, Rapporteurs and Speakers*, and to the *Scientific Secretaries*, for their excellent work and highly appreciated collaboration.

The considerable amount of material needed for these two volumes was collected by the *Proceedings Coordinator*, to whom I would like to extend my thanks. The efficient publication of the Proceedings was made possible by the combined expertise of *Members of the Text Processing* and *Visual Techniques Sections*, and by the careful work of the *Document Reproduction Section*, all of whom belong to the CERN *Publications Group*.

I would also like to thank the *Local Organizing Group*, and in particular the *CERN Conference Secretariat*, for taking good care of all the detailed arrangements.

The impressively large attendance at all the Conference sessions, right up to the last Lecture, and these Proceedings are the best proof that all the hard work of the physicists and staff was well worth while.

Antonino Zichichi
Conference Chairman

Geneva, 10 December, 1979

CONTENTS

Volume 1

SESSION CHAIRMEN

Aubert, J.-J.
Bellini, G.
Cheng, L.S.
Ekspong, G.
Ferrara, S.
Fiorini, E.
Fritzsch, H.
Fubini, S.
Gatto, R.
Jentschke, W.
Joos, H.
Martin, A.
Matthews, P.
Oades, G.C.
Perkins, D.H.
Prokoshkin, Yu.D.
Salmeron, R.A.
Schopper, H.
Sens, J.C.
Telegdi, V.L.
Ting, S.C.C.
Van de Walle, R.T.
Weisskopf, V.F.
Wetherell, A.M.
Zichichi, A.
Zumino, B.

SCIENTIFIC SECRETARIES

Aurenche, P.
Benvenuti, A.
Best, C.
Bigi, I.
Bonneaud, G.
Boratav, M.
Bosetti, P.
Bozzo, M.
Burns, A.
Calvetti, M.
Contin, A.
De Groot, J.
Del Papa, C.
Din, A.
Finjord, J.
Gavillet, P.
Geist, W.
Gennow, H.
Goggi, G.V.
Gregory, P.
Helgaker, P.
Hoffman, H.
Humpert, B.
Johansson, E.
Jones, D.R.T.
Kozanecki, W.
Lanceri, L.
Longo, E.
Loverre, P.
Martin, F.
Martin, J.P.
Maury, S.
Mouzourakis, P.
Nielsen, B.S.
Peroni, C.
Petronzio, R.
Plothow, H.
Poyer, C.
Reucroft, S.
Ross, R.T.
Scott, W.
Sorba, P.
Tovey, S.N.
Wahlen, H.
Weisz, S.
Zakrzewski, W.

CONFERENCE CHAIRMAN

Antonino Zichichi

SCIENTIFIC ADVISORY COMMITTEE

A. Białas, *Cracow, Poland*
I. Butterworth, *London, United Kingdom*
I.V. Chuvilo, *Moscow, USSR*
R.H. Dalitz, *Oxford, United Kingdom*
J. Fischer, *Prague, Czechoslovakia*
S. Fubini, *Geneva, Switzerland*
M. Gourdin, *Paris, France*
M. Guenin, *Geneva, Switzerland*
J. Hamilton, *Copenhagen, Denmark*
J. Laberrigue, *Paris, France*
G. Marx, *Budapest, Hungary*
G. Preparata, *Geneva, Switzerland*
Yu.D. Prokoshkin, *Protvino, USSR*
H. Wahl, *Geneva, Switzerland*
G. Wolf, *Hamburg, Fed. Rep. Germany*

LOCAL ORGANIZING GROUP

Chairman:	W.O. Lock
Organizing Secretary:	D.A. Caton
EPS Executive Secretary:	G. Thomas
Conference Secretariat:	I. Barnett
	M. Compoint
	I. Hansen
Proceedings Coordinator:	W.S. Newman
Coordinator for Scientific Secretaries:	H. Wahl
Social Programme:	C. Redman
Technical Services:	E. Bissa
Press & Visits:	R. Anthoine
Transport:	T. Kröwerath
Wagon-lits Tourisme:	P. Bouchardy

OPENING SESSION

A. Zichichi Introductory lecture

INTRODUCTORY LECTURE

A. Zichichi

CERN, Geneva, Switzerland

1. INTRODUCTION

Neutrino physics and weak interactions, (e^+e^-) phenomena, deep inelastic processes, hadron spectroscopy, quark theories and quark confinement: all these are hot topics in the field of subnuclear physics.

It is time to revive a long-discontinued practice; namely, the introductory lecture, which is intended to present a general review of the main themes and to correlate them in a unique picture. Let me try to do this.

2. THE DESERT AND THE PROTON DECAY

The main result to date in subnuclear physics is the existence of the three gauge symmetry groups: $SU(3)_{colour}$, $SU(2)_L$, and $U(1)_{L,R}$, which are believed to be at the origin of the superstrong and of the electroweak forces.

However, the main outcome of this great theoretical goal is the danger of a DESERT. We all expect the electroweak unification, $SU(2)_L \times U(1)_{L,R}$, to be at $\sim 10^2$ GeV. According to some theoretical speculations, the next unification -- between superstrong and electroweak forces -- should be not very far from the Planck mass (see Fig. 1), i.e. at $\sim 10^{15}$ GeV, the energy level appropriate to the celebrated SU(5) grand unification group; with nothing between 10^2 GeV and 10^{15} GeV (see Fig. 1).

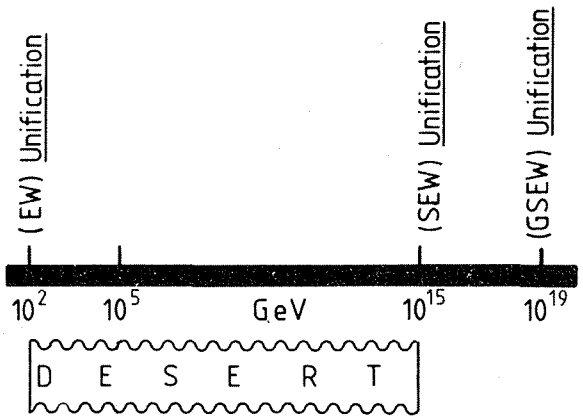

Fig. 1

Everybody agrees that there must exist a grand unifying gauge group "G", which contains

$$SU(3)_c \times SU(2)_L \times U(1)_{L,R} .$$

The great problem is to find how nature goes from the group "G" down to $SU(3)_c \times SU(2)_L \times U(1)_{L,R}$. If the descent is "direct", the desert is catastrophic: from 10^{15} GeV down to 10^2 GeV.

This theoretical energy range for the Desert should be compared with 10^4 GeV, the maximum energy we can hope to reach in the next two decades via a proton-antiproton collider or proton-proton intersecting storage rings (ISR): 5 TeV + 5 TeV.

If we believe in the theoretical desert, the only experiment left would be the study of proton decay. It is in fact a general feature of the grand unification, to predict that the "brick of the Universe" has to lose its stability. The reason is simple. Grand unified theories must put leptons and quarks in the same multiplet of the unifying group "G". The gauging of this group produces quark-lepton transformation: i.e. proton decay. The proton instability follows from the concept of grand unification. It is not the result peculiar to a particular grand unifying group chosen. The particular choice can produce different lifetimes. For example, if the grand unifying group is SU(5), τ_p is $\sim 10^{31}$ years. However, the various models investigated so far, produce lifetimes in the range 10^{28}-10^{34} years.

And now a few words about the decay channels. If quarks and leptons are put in the same multiplet (q,ℓ) (fermion number conserved), the predicted decays would be, with three leptons in the final state:

$$p \to \begin{cases} \to 3\nu + \pi^+ & (\sim 80\%) \\ \to 3\nu + \pi^+\pi^-\pi^+ & (\sim 8\%) \end{cases} .$$

If fermions and antifermions are put in the same multiplet $(q,\ell,\bar{q},\bar{\ell})$, the decay modes would be, with only one lepton:

$$p \to \begin{cases} \to e^+\pi^0, \omega^0, \rho^0, \eta^0 & (\sim 75\%) \\ \to \mu^+ K^0 & (\sim 10\%) \end{cases} .$$

The present best limit on the proton lifetime is $\tau_p \gtrsim 10^{30}$ years. The new experimental jump should be about 3 orders of magnitude: $\tau_p \gtrsim 10^{33}$ years. This implies the study of the stability of 10^4 tons of matter, with an expected counting rate of 5 events/year (for $\tau_p = 10^{33}$ years). The experiment should be planned with a minimum energy bias, in order to avoid the limitations of previous results, where the proton decay was investigated, assuming that its disappearance had to produce a large energy release.

3. THE LESSON FROM PAST DESERTS

As you know, Europe is planning to build a new machine, the greatest ever built. This is why it is important to recall our previous experience with predicted theoretical deserts and experimental findings.

• Let us start with the 30 GeV proton synchrotrons of CERN and BNL. The original theoretical motivations were: πp and pp scattering and phase-shift analyses, as well as tests of isospin and T invariances. What did we get with these machines?

- New particle states, which produced the celebrated SU(3) symmetry of Gell-Mann [not to be confused with $SU(3)_{colour}$].
- The first measurement of the $(\omega - \phi)$ mixing angle resolved the puzzle of the vector meson masses and provided the proof of the existence of such a symmetry.
- The measurement of e^+e^- and $\mu^+\mu^-$ production in hadronic interactions, started in 1964 at CERN, resulted in the discovery of the J particle at BNL in 1974.
- The first proof of the electromagnetic structure of the proton in the time-like region.
- The discoveries of: the existence of antinuclei ($\bar{d}$); two kinds of neutrinos ($\nu_e \neq \nu_\mu$); the fact that ν_μ is not equal to $\bar{\nu}_\mu$; CP and T violation; neutral currents.

All these findings had nothing to do with the original motivations.

• Some more examples: SLAC. The original physics aims were the study of the electromagnetic form factors of the nucleon, the electromagnetic transition form factors (N-N^*), and QED checks. Found: the very important phenomenon called deep inelastic effect, i.e. the proof that point-like structures exist inside the proton.

• Let us look at ADONE, the Italian 1-3 GeV e^+e^- machine; what were the motivations there? The list was extensive: QED and radiative correction checks; μe electromagnetic equivalence; electromagnetic form factors of pions, kaons, and protons; the study of the tails of vector mesons. It is probably interesting to recall that these vector mesons (ρ, ω, ϕ) were theoretically needed to understand the conserved hadronic currents associated with isospin, hypercharge, and baryon number. Notwithstanding all these motivations, a particularly relevant and totally unexpected fact was discovered: the ratio of hadronic to muonic cross-sections was shown to be much higher than the theoretically predicted value, based on the tails of the three known vector mesons. Finally there was the search for heavy leptons via the analysis of the μe final states but this search had no theoretical motivation.

• Now let us look at SPEAR and DORIS. SPEAR started with great enthusiasm because of ADONE's discovery of the high cross-section ratio mentioned above. However, they found three great new things: the J/ψ spectroscopy; the open charm states; and last but not least, the heavy lepton from the μe final-state analysis -- just what the Frascati people were looking for, but were prevented from finding because of insufficient energy.

• The ISR is a special case. It is a machine where the physics results could have been tremendous. Unfortunately, the general trend was to study small angle and small p_T physics. Then large p_T phenomena came. The observations of the J and, recently, of the T at the ISR show that the physics was there.

• Finally, the 400 GeV machines at Fermilab and CERN. These are too new to be of use in our historical survey. However, not very many people would have bet on the existence of the 9.5 GeV object discovered by Lederman at Fermilab.

What lessons can we learn from this experience?

Firstly, There should be no energy gap. The maximum energy of ADONE was 3 GeV. SPEAR started at 3 GeV but then jumped to higher energies and was for some time bound to miss the J/ψ. SPEAR's maximum lay at 8.5-9 GeV, whereas PETRA started above 10 GeV. Lederman's T was found at 9.5 GeV. *Secondly*, compared with the actual discoveries. the anticipated findings have the appearance of a desert of imagination. The conclusion we should draw from this is that however great and significant the physics motivations for the new (e^+e^-) machine appear to us now -- the Z^0, $W^\pm$; new hadronic thresholds and, hence, flavours; new heavy leptons; free quark states, leptonic or hadronic; QED checks -- the actual discoveries should make these motivations look as fruits of a desert of imagination.

4. QCD AND COLOUR EFFECTS

The world in which we live has no deserts. The extreme left-hand corner of the desert in Fig. 1 is very rich, as the following review will show.

When we started, the six fundamental interactions were as shown in Fig. 2: the strong interactions, namely the SU(3) invariant and the semistrong SU(3) breaking ones; the electromagnetic, weak, superweak and gravitational interactions. How they appear to us now is shown in Fig. 3. It is evident that we were on the wrong track, with regard to the celebrated SU(3) of Gell-Mann. Now we see that the superstrong coloured forces represent the basic fundamental interactions. The strong and the semistrong are a byproduct of the superstrong ones, these being originated by gauging $SU(3)_{colour}$. We were also wrong in thinking that electromagnetic, weak, and superweak interactions were just unrelated. At present it seems that, with six quarks and six leptons, the electroweak and the superweak interactions can all be merged together.

WHAT WE STARTED WITH ...

1) Strong : $SU(3)_f$ invariant
2) Semistrong: $SU(3)_f$ breaking
3) Electromagnetic
4) Weak
5) Superweak
6) Gravitational

Fig. 2

THE INTERACTIONS NOW

I. The Superstrong (coloured) $SU(3)_c$ { Strong, Semistrong

II. The Electroweak (6 quarks and 6 leptons) $SU(2)_L \times U(1)_{LR}$ { Electromagnetic, Weak, Superweak

III. The Gravitational

Unification of I and II with III needs Supersymmetry: (bosons ≷ fermions)

Fig. 3

Back to $SU(3)_{colour}$. What evidence is there for the existence of colour? The diagrams of Fig. 4 illustrate three types of measurement of colour effects. *Firstly*, if it were not for colour the π^0 lifetime should be nine times less (Fig. 4a). No new data on this topic are being presented at this Conference. *Secondly*, the ratio $R = \sigma(e^+e^- \to \text{hadrons})/\sigma(e^+e^- \to \to \mu^+\mu^-)$ should be three times larger than in the no-colour case (Fig. 4b). The *third* check for colour is provided by the so-called Drell-Yan mechanism (Fig. 4c), where an ocean (or valence) quark is annihilated with an ocean antiquark to produce a lepton pair. Here the probability for a quark to annihilate with an antiquark of the correct colour is ⅓ compared to the case of no colour. The existence of colour implies a factor of 27 when we go from π^0 decay to Drell-Yan pairs. At this Conference there will be new results from PETRA on R and from CERN on the Drell-Yan process.

Let us now see where we stand with QCD. This is shown in Fig. 5. At the very bottom, for $t = \infty$, $\alpha_s \to$ zero, there is asymptotic freedom, with quarks and coloured gluons obeying QCD. The first step, where quarks and gluons interact without becoming real particles, is relatively easy; this jump will be discussed in the theoretical sessions devoted to QCD. However, the most difficult jump is the second one, where quarks and gluons should produce the well-known particles and their associated phenomena, such as "quark jets" and "gluon jets". For $t \simeq (1 \text{ fermi})^{-1}$, i.e. for real hadrons, nobody knows what α_s becomes, and nobody

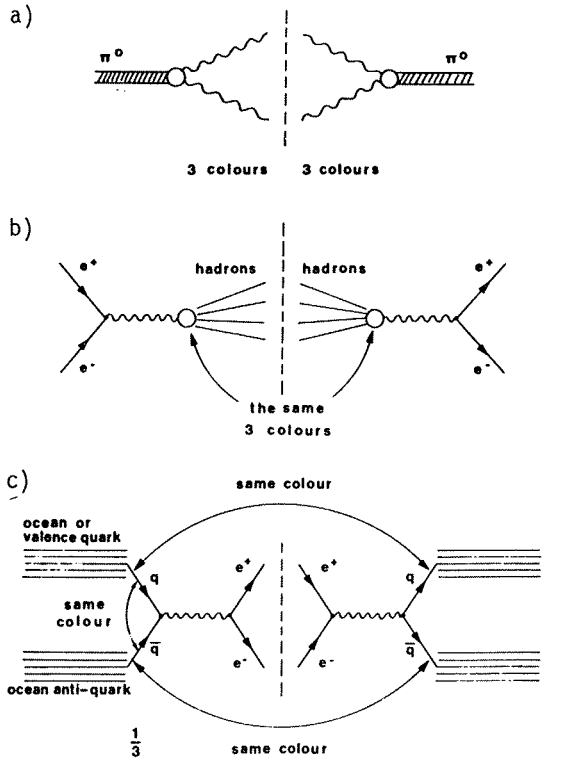

Fig. 4

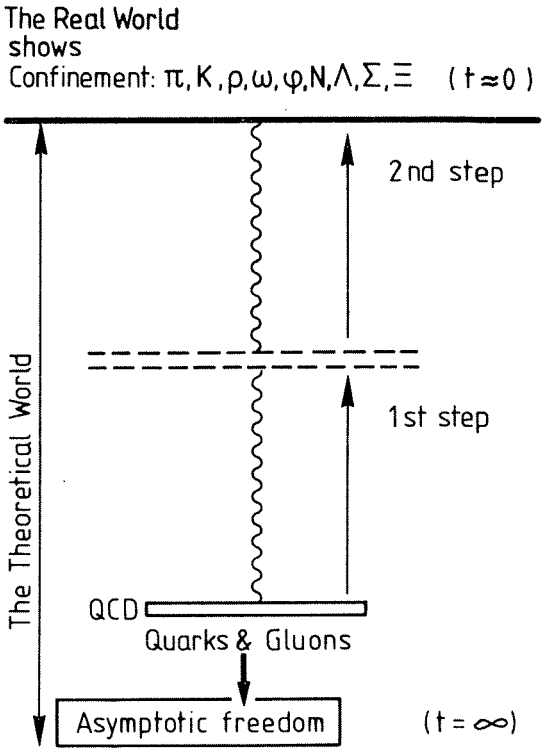

Fig. 5

has so far been able to prove confinement. If confinement were an exact result of a theory, there would be no point in looking for quarks. Sorry: it would be more exciting. But the present theoretical status on confinement is as follows: QCD at small distances produces asymptotic freedom, unlike QED; but QCD at large distances, like QED, does not produce confinement. Both results are perturbative, but they are the only ones available.

5. PRE-CHARM

Now let us consider the status of pre-charm physics. The baryons in the SU(6) multiplets given in Table 1 appear to be organized in such a way as to confirm our belief in the existence of (56, 0^+). There is also overwhelming evidence for the existence of (70, 1^-). Only a few states are missing. The question is whether the (70, 0^+) is really absent. The expected states are shown in Fig. 6, but only one candidate exists for this multiplet. Moreover, there is no evidence of the 20-plet for any L^P value. The absence of these states is a basic problem for the baryon multiplets. And it is related to the question of whether the baryon structure is of the "quark-diquark" type. All this will be discussed at the hadron sessions of the Conference.

The pre-Conference status of the mesonic multiplets is shown in Table 2. There are some problems with the (L = 1) multiplet of 108 states. These will be discussed in the hadron sessions, where new states with higher L-value will also be presented.

Table 1

Baryons in SU(6) multiplets

[SU(6), L^P]	$SU(3)_f$	J^P	Standard names of particle states
(56, 0^+)	8	$1/2^+$	N, Λ, Σ, Ξ
	10	$3/2^+$	N^*, Σ^*, Ξ^*, Ω^-
(70, 1^-)	1	$1/2^-$	Repeat singlet
	8	$1/2^-$	Repeat octet
	10	$1/2^-$	Repeat decuplet
	1	$3/2^-$	Repeat singlet
	8	$3/2^-$	Repeat octet
	10	$3/2^-$	Repeat decuplet
	8	$1/2^-$	Repeat octet
	8	$3/2^-$	Repeat octet
	8	$5/2^-$	Repeat octet

[Repeat means that the quantum numbers (isospin and strangeness) of the states are identical to the "octet" and "decuplet" already known for the 56-case.]

BARYON SUPERMULTIPLET

J	SU(3)	
½	1	(70, 0^+) only one state seems to be there
½	8	
½	10	
³/₂	8	

Fig. 6

Table 2

SU(6) mesonic multiplets

SU(6)	$SU(3)_f$	J^{PC}	Particle states	No. of states
$[(35 \oplus 1) \otimes 1]$; (L = 0)	8 ⊕ 1	0^{-+}	π, K, η, η′	36
	8 ⊕ 1	1^{--}	ρ, K^*, ω, φ	
$[(35 \oplus 1) \otimes 3]$; (L = 1)	8 ⊕ 1	1^{+-}	B, $Q_{1,2}$...?	108
	8 ⊕ 1	0^{++}	S, χ, S^*, ε	
	8 ⊕ 1	1^{++}	A_1, $Q_{1,2}$, D, E	
	8 ⊕ 1	2^{++}	A_2, K^{**}, f, f′	

At previous Conferences a lot of attention has been devoted to new multiquark hadronic states, baryonium and mesonium, made up of "peculiar" combinations of quarks and antiquarks. Earlier results supporting the existence of these types of quark-antiquark combinations will be confronted with new data -- some of which do not confirm these findings.

So much for pre-charm physics.

6. POST-CHARM

In post-charm physics the impressive fact is that so many states have been discovered in such a short period. Figure 7 shows the pre-Conference status of the "charmonium" and "bottomium" families. The χ(2830) and χ(3455) states will be questioned by new results, but everything else will remain as it is. A detailed analysis of the T decay from DORIS will be presented in the (e^+e^-) Session. These results deal with the problem of the T decay into three gluons.

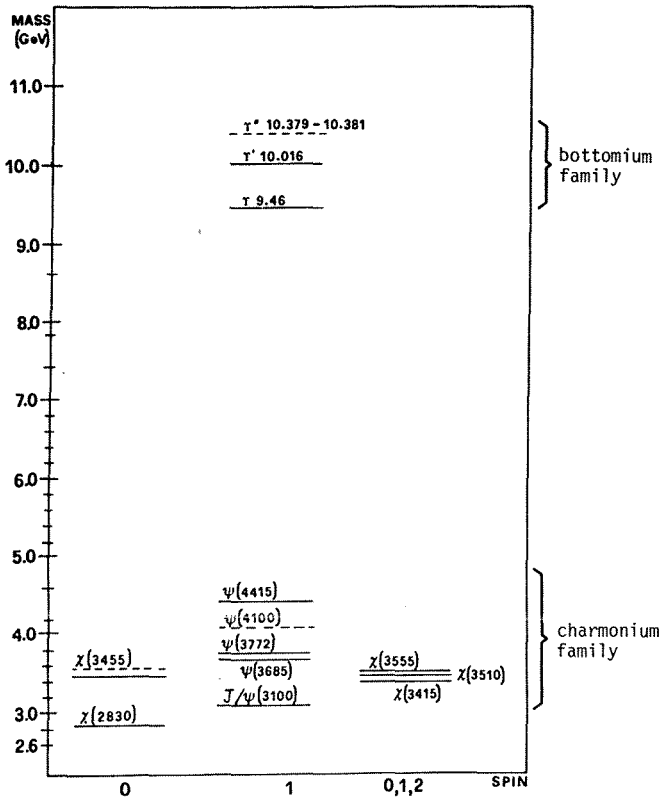

Fig. 7

If we now go into the "open-charm" states, Fig. 8 shows the status of the SU(4) flavour multiplet for the pseudoscalar mesons. The same SU(4) multiplet holds for the vector mesons; they have the same quark-antiquark content, the only difference being the spin state which here is a triplet. These two SU(4) multiplets are well established.

The status of open-charm baryons is quite different. Figure 9 shows the old baryon octet in the c = 0 plane, plus the new open-charm states. There are very many new states still to be discovered in the c = 1 and c = 2 planes. The only case reported so far is the Λ_1^+, and many new results will be presented at this Conference. In Fig. 10, the old, well-established baryonic decuplet in the c = 0 plane is reported with the new open-charm baryonic states, with c = +1, c = +2, c = +3, all to be discovered. An interesting result to be presented in the "charm" sessions is the measurement of the lifetime for open-charm states.

All the states mentioned so far can be obtained from five quarks, the sixth, the "top" quark, being predicted on the basis of the lepton-quark family structure (e, ν_e; u, d), (μ, ν_μ; c, s), (τ, ν_τ; t, b). Unfortunately up to the highest PETRA energies, there is no sign of t.

The status of the six quarks is shown in Table 3.

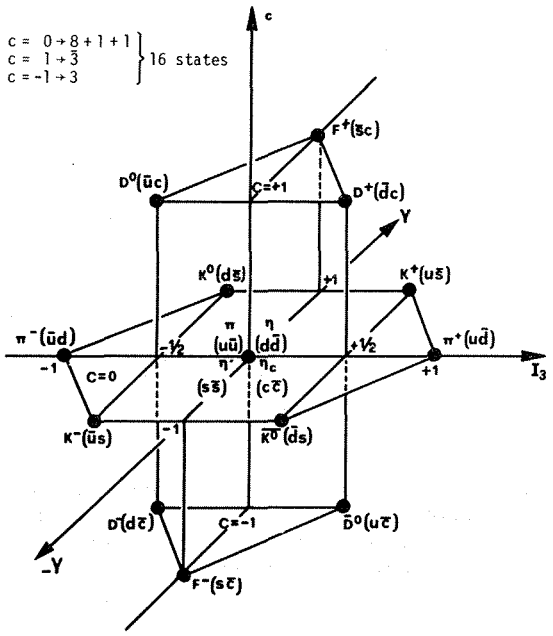

Fig. 8

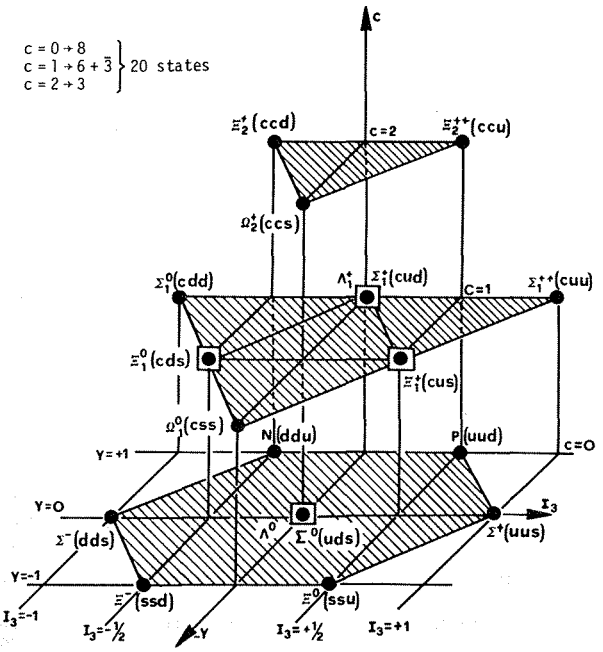

Fig. 9

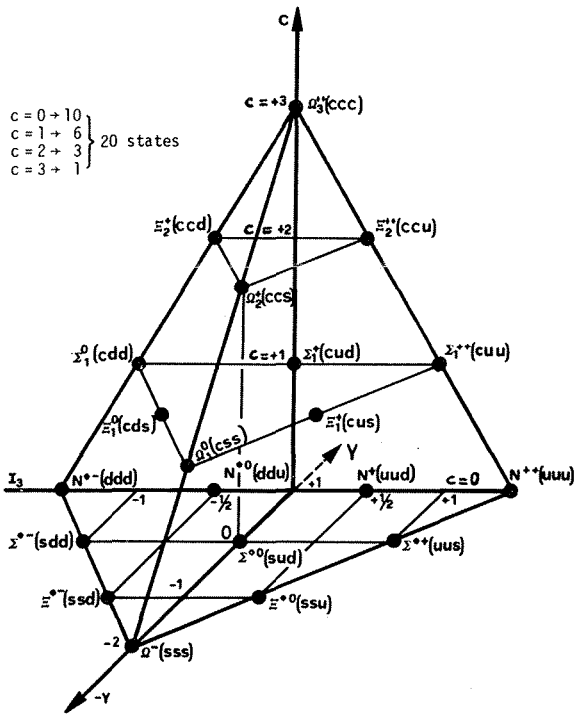

Fig. 10

Table 3

Six quarks

Quark	u	c	t	d	s	b
Mass	0.39	1.55	?	0.39	0.51	4.75
Q	+2/3			-1/3		

$m_u = m_d = \frac{1}{2}$ (ρ) mass; $m_s = \frac{1}{2}$ (φ) mass;

$m_c = \frac{1}{2}$ (J/ψ) mass; $m_b = \frac{1}{2}$ (Υ) mass.

7. THE ELECTROWEAK FORCES

Now we go to the celebrated electroweak interaction. Let me show you the basic ingredients of it. The reason why I do this, is because there is overwhelming evidence that Glashow, Salam and Weinberg (GSW) are indeed going to be right.

The basic coupling constant in $SU(2)_L \times U(1)_{L+R}$ is not "e", and the basic Lagrangian is made of two pieces, one which depends on the electroweak isospin $\vec{\tau}$ operator and the other which depends on the electroweak hypercharge Y:

$$\mathcal{L}_{\text{weak+em}} = g_\tau \left[\sum_i \bar{\psi}^i_L \frac{\vec{\tau}}{2} \psi^i_L \right] \vec{W} + g_Y \left[\sum_i \bar{\psi}_i \, Y \psi_i \right] W^Y \ , \qquad \text{(1a)}$$

where W^+, W^-, and W^3 are the intermediate vector Bose fields -- quanta of the electroweak isospin group SU(2) -- coupled to the electroweak isospin $\vec{\tau}$; and W^Y is the field coupled to the electroweak hypercharge Y and is a quantum of the electroweak group U(1). The complete symmetry is $SU(2)_L \times U(1)_{L+R}$. The index i runs over all leptons and quarks listed in Table 4.

The basic coupling constant is "g". The way in which this "electroweak" charge g is projected into the two electroweak axes $\vec{\tau}$ and Y is shown in Fig. 11. The thick lines indicate the observable coupling constants. Thus

$$\left.\begin{aligned} g_\tau &= g \cos\theta \\ g_Y &= g \sin\theta \end{aligned}\right\} \frac{g_Y}{g_\tau} = \tan\theta \ ,$$

where θ is the famous electroweak angle of the GSW theory. Notice the following equalities:

$$g^{\pm} = g_\tau \ , \quad g^Z = g \ ,$$

i.e. the "weak charged coupling" $g^{\pm}$ coincides with the "electroweak" isospin projection of g. Moreover, the "weak neutral coupling" g^Z coincides with the original electroweak charge g. This is why

$$g^{\pm}/g^Z = \cos\theta \ .$$

Table 4

The electroweak quantum numbers of the point-like particles

		T^3	Y	Q^{em}
LEPTONS	$\begin{pmatrix}\nu_e\\ e^-\end{pmatrix}_L \ \begin{pmatrix}\nu_\mu\\ \mu^-\end{pmatrix}_L \ \begin{pmatrix}\nu_\tau\\ \tau^-\end{pmatrix}_L$	$+\frac{1}{2}$ $-\frac{1}{2}$	-1 -1	0 -1
	$(e^-)_R \ (\mu^-)_R \ (\tau^-)_R$	0	-2	-1
	No neutrinos (R) because m_ν = all zero			
QUARKS × 3 COLOURS	$\begin{pmatrix}u\\ d_C\end{pmatrix}_L \ \begin{pmatrix}c\\ s_C\end{pmatrix}_L \ \begin{pmatrix}t\\ b_C\end{pmatrix}_L$	$+\frac{1}{2}$ $-\frac{1}{2}$	$+\frac{1}{3}$ $+\frac{1}{3}$	$+\frac{2}{3}$ $-\frac{1}{3}$
	$(d_C)_R \ (s_C)_R \ (b_C)_R$	0	$-\frac{2}{3}$	$-\frac{1}{3}$
	$(u)_R \ (c)_R \ (t)_R$	0	$\frac{4}{3}$	$+\frac{2}{3}$

$$Q^{em} = T^3 + \frac{Y}{2}$$

C = stands for Cabibbo mixed states

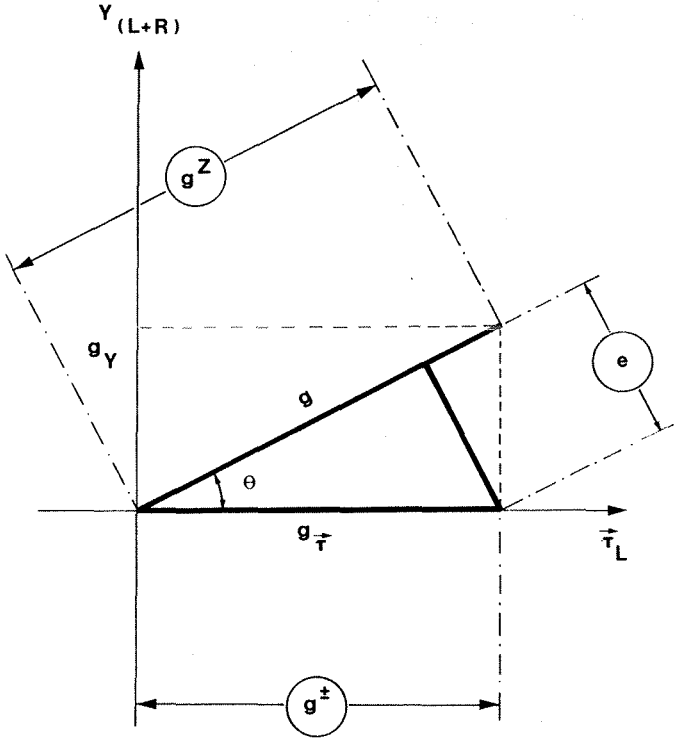

Fig. 11

As we will see later, if the simplest Higgs mechanism is at work, the damping factor between the "charged" and "neutral" intermediate boson masses is: $m_{W^{\pm}}/m_{Z^0} = \cos\theta$. This exactly compensates the above ratio of coupling constants, the key reason for the important result $\rho = 1$ (see page 18). Another interesting remark: the electric charge "e" is the result of the original "electroweak" charge g projected twice:

$$g \cdot \cos\theta \cdot \sin\theta = e \ .$$

It follows that

$$g_\tau = \frac{e}{\sin\theta} \ , \quad g_Y = \frac{e}{\cos\theta} \ .$$

The way in which the original field W_μ splits into the two axes, $\vec{\tau}$ and Y, is shown in Fig. 12a. Notice that in the $\vec{\tau}$ projections there are three fields: W^+_μ, W^-_μ, W^3_μ. These fields are coupled to left-handed currents only, while W^Y_μ is coupled to both left and right currents. The projections of W^3_μ and W^Y_μ to make up the electromagnetic field A_μ are shown in Fig. 12b. Finally, the projections making up the "neutral weak field" Z^0_μ are shown in Fig. 12c.

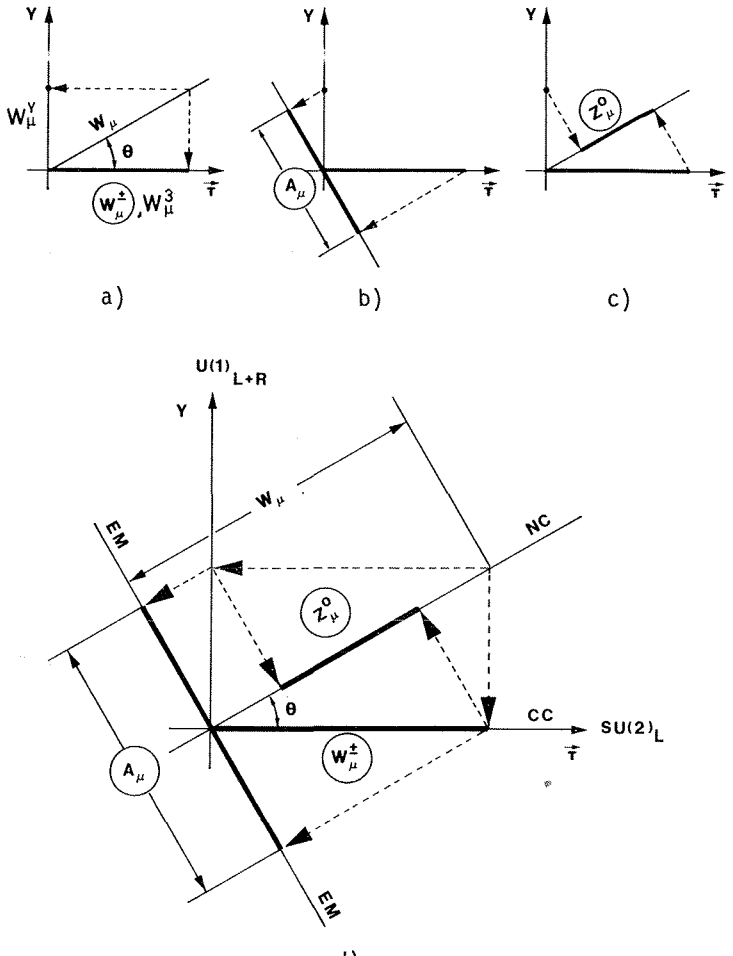

Fig. 12

The $SU(2)_L \times U(1)_{L+R}$ [or equivalently $SU(2)_{ew\ isospin} \times U(1)_{ew\ hypercharge}$] symmetric Lagrangian (1a) reproduces all results of the "charged" currents and electromagnetism. Obviously, the great new point of it is in the domain of the "neutral" currents; these currents should, more correctly, be called "electric charge not changing" currents. For brevity we will go on calling them "neutral currents" (NC). As we have seen above, there are two neutral intermediate vector bosonic fields, W^3 and W^Y, and two neutral currents, J^3_L and J^Y_{L+R}. So far, there are no masses in the theory. The physical particles corresponding to these are mixtures of W^3 and W^Y. This mixing has its origin (in the GSW theory) in spontaneous symmetry breaking, as a consequence of which W^3 and W^Y combine in such a way as to produce the other two neutral fields: one, A_μ, associated with massless quanta, the photon; the other, Z^0_μ, corresponding to massive quanta. In terms of the original electroweak isospin and hypercharge vector fields, the physical fields are:

$$A_\mu = W^Y_\mu \cos\theta + W^3_\mu \sin\theta$$

$$Z^0_\mu = -W^Y_\mu \sin\theta + W^3_\mu \cos\theta \ .$$

The summary of all this is shown in Fig. 12d. Notice that circled quantities indicate the fields whose quanta are observable. Thus $W^\pm_\mu$ correspond to the charged weak bosons; W^3_μ and W^Y_μ do not have observable quanta. Their mixing produces A_μ and Z_μ, whose quanta are the photon and the neutral weak boson, as we will see later. In Figs. 12a-d the thick lines indicate where the observable quantities come from.

Before the $SU(2)_L \times U(1)_{L+R}$ electroweak theory, our knowledge was all along the $\vec{\tau}$ axis, where we had the so-called charged currents (more correctly these currents should be called

"electric charge changing currents"). We knew that A_μ exist but we did not know of the existence of the neutral current NC axis, nor of the intimate connection between A_μ and Z^0_μ.

Note that $\vec{\tau}$ indicates the existence of the three components (τ^+, τ^-, τ^3). These are the generators of the group SU(2) while Y is the generator of the group U(1). The electroweak angle θ_{ew} (to be called θ for simplicity) determines the relative weight of these two basic gauge groups, whose merging generates the electromagnetic and the weak interactions.

We have learned that the e.m. field is not a fundamental field; it is made up of two other fields, W^3_μ and W^Y_μ. Their mixing generates A_μ and Z^0_μ; the quanta of these fields are the observable quantities. The A_μ is well known and is associated with a massless particle, the photon. The Z^0_μ is associated with a particle whose mass, as mentioned above, is expected to be near 85 GeV or so.

While only one of the two neutral fields is known, if we go from the fields to the currents we find out that both neutral currents are known. The electromagnetic neutral current is known since a long time, but not its structure in terms of J^3_L and J^Y_{L+R}, as shown in the formula

$$J^{em}_{L+R} = J^3_L + \tfrac{1}{2} J^Y_{L+R} \ .$$

The other neutral current is the so-called "weak neutral current", discovered in 1973 [1] and predicted much earlier by the $SU(2)_L \times U(1)_{L+R}$ theory, in spite of the experimental evidence against it[2].

It is in the field of the neutral weak currents that in these last years there has been a very intense experimental activity going on.

In order to understand how this "neutral weak current" is derived from the $SU(2)_L \times U(1)_{L+R}$ symmetric Lagrangian (1a), let us mention the basic steps. The first one is to write (1a) explicitly, omitting the spinors and other details for simplicity:

$$\mathcal{L}_{weak+em} = g_\tau (W^+_\mu J^-_\mu + W^-_\mu J^+_\mu + W^3_\mu J^3_\mu) + g_Y W^Y_\mu J^Y_\mu \ .$$

Once again we emphasize that the "neutral" part of this Lagrangian has two pieces:

$$\mathcal{L}^{\text{before mixing}}_{\text{neutral}} = g_\tau W^3_\mu J^3_\mu + g_Y W^Y_\mu J^Y_\mu \ . \qquad (1b)$$

After the mixing between W^3_μ and W^Y_μ, we have the other two fields A_μ and Z^0_μ coupled to the appropriate currents.

We know that electromagnetism exists, and that A_μ is coupled to the e.m. current J^{em}_μ with coupling "e": $e A_\mu J^{em}_\mu$.

By definition, the remaining "neutral" part is

$$g^Z Z_\mu J^{NC}_\mu \ ,$$

where g^Z is the "weak" neutral coupling constant and J^{NC}_μ is the weak neutral current. After the mixing has taken place the "neutral" Lagrangian is

$$\mathcal{L}^{\text{after mixing}}_{\text{neutral}} = e A_\mu J^{em}_\mu + g^Z Z_\mu J^{NC}_\mu \ . \qquad (1c)$$

Equating the two Lagrangians (1b) and (1c) we have:

$$g_\tau W^3_\mu J^3_\mu + g_Y W^Y_\mu J^Y_\mu = e A_\mu J^{em}_\mu + g^Z Z_\mu J^{NC}_\mu \ , \qquad (1d)$$

which gives "e" and g^Z in terms of the original coupling g and of the mixing angle θ:

$$e = g \cdot \sin\theta \cdot \cos\theta \ ; \quad g^Z = g \ ,$$

already illustrated in Fig. 11. The above equality (1d) gives J^{NC}_μ in terms of J^3_μ and J^{em}_μ. More precisely:

$$J^{NC}_{L,R} = J^3_L - \sin^2\theta \cdot J^{em}_{L+R} \ .$$

This formula tells us that in order to know the "neutral" weak coupling, all we need to know are the values of the electroweak isospin T^3_L, and of the electric charge of a given particle (leptons or quarks) as given by Table 4.

Notice that the electroweak isospin is only left; it contributes only to the "left" coupling constant. The electric charge is left and right; it therefore contributes to the "left" as well as to the "right" coupling constant. All this is shown below:

$$\begin{aligned} J^{NC}_{L,R} &= J^3_L - \sin^2\theta \cdot J^{em}_{L+R} \\ \longrightarrow g_L &= T^3_L - \sin^2\theta \cdot Q^{em}_L \\ \longrightarrow g_R &= \text{zero} - \sin^2\theta \cdot Q^{em}_R \end{aligned} \qquad (2)$$

For example, take the "up" quark. The electroweak isospin third component is $T^3_L(\text{up}) = +\frac{1}{2}$, while the electric charge is $+\frac{2}{3}$; the result is

$$g(u)_L = +\frac{1}{2} - \sin^2\theta \cdot \frac{2}{3} .$$

If $\sin^2\theta = \frac{1}{4}$, we have $g(u)_L = +\frac{1}{3}$.

The values of the weak neutral coupling constants for all known leptons and quarks are given in Table 5.

Table 5

Neutral weak coupling constants of leptons and quarks, as predicted by the $SU(2)_L \times U(1)_{L+R}$ standard theory.

Spinors	T^3_L	Q^{em}_L	Q^{em}_R	g_L	g_R	g_V	g_A
ν_e, ν_μ, ν_τ	$+\frac{1}{2}$	0	0	$\frac{1}{2}$	0	$\frac{1}{4}$	$-\frac{1}{4}$
e^-, μ^-, τ^-	$-\frac{1}{2}$	-1	-1	$\left(-\frac{1}{2} + \sin^2\theta\right)$	$\sin^2\theta$	$-\frac{1}{4} + \sin^2\theta$	$+\frac{1}{4}$
u, c, t	$+\frac{1}{2}$	$+\frac{2}{3}$	$+\frac{2}{3}$	$\left(\frac{1}{2} - \frac{2}{3}\sin^2\theta\right)$	$-\frac{2}{3}\sin^2\theta$	$\frac{1}{4} - \frac{2}{3}\sin^2\theta$	$-\frac{1}{4}$
d_C, s_C, b_C	$-\frac{1}{2}$	$-\frac{1}{3}$	$-\frac{1}{3}$	$\left(-\frac{1}{2} + \frac{1}{3}\sin^2\theta\right)$	$+\frac{1}{3}\sin^2\theta$	$-\frac{1}{4} + \frac{1}{3}\sin^2\theta$	$+\frac{1}{4}$
If $\sin^2\theta = 1/4$:							
Neutrinos (ν_e, ν_μ, ν_τ)				$+\frac{1}{2}$	0	$+\frac{1}{4}$	$-\frac{1}{4}$
Charged leptons (e^-, μ^-, τ^-)				$-\frac{1}{4}$	$+\frac{1}{4}$	0	$+\frac{1}{4}$
Up-like quarks (u, c, t)				$+\frac{1}{3}$	$-\frac{2}{12}$	$+\frac{1}{12}$	$-\frac{1}{4}$
Down-like quarks (d_C, s_C, b_C)				$-\frac{5}{12}$	$+\frac{1}{12}$	$-\frac{2}{12}$	$+\frac{1}{4}$

Notice that in $SU(2)_L \times U(1)_{L+R}$, $T^3_R = 0$ for all quarks and leptons. Therefore g_R, the "right" neutral weak coupling, can be $\neq 0$ only for particles with $Q^{em} \neq 0$. In other words, in the "standard" $SU(2)_L \times U(1)_{L+R}$ theory the "right" coupling is coming from the existence of "electrically" charged spinors. Otherwise the weak neutral coupling would be "left-handed" only.

Notice also that the "vector" (g_V) and "axial" (g_A) neutral weak couplings can be worked out in terms of the "chiral" neutral weak couplings (g_L, g_R) by

$$g_V = \frac{1}{2}(g_L + g_R) = \frac{1}{2}T^3_L - \sin^2\theta \cdot Q^{em} , \qquad g_A = \frac{1}{2}(g_R - g_L) = -\frac{1}{2}T^3_L .$$

All this explains how the weak neutral coupling constants of quarks and leptons, in terms of the "chiral" (g_L, g_R) or of the "vector" (g_V) and "axial" (g_A), are related. The results, shown in Table 5, are an example of the predictive power of the theory.

Let us review the experimental pre-Conference results. The neutral current experiments can be divided into four classes: I) lepton-hadron scattering; II) lepton-lepton scattering; III) lepton-hadron interference (free particle states); IV) lepton-hadron interference (bound particle states).

Class I: Lepton-hadron scattering

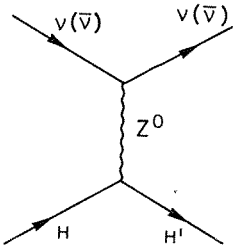

The typical diagram is shown here. In this class of experiments the leptons are electrically neutral, i.e. neutrinos (or antineutrinos). The target hadrons are "up" and "down" quarks. The "strange" quark is in the "ocean". More massive quark states are more damped by the ν-energy so far available. The final state can either be the same quark (elastic scattering) or any other hadronic state (inelastic processes), provided the known conservation laws are fulfilled. H stands for a hadronic state.

A series of 15 processes, using primary high-energy neutrino and antineutrino beams against either protons or neutrons, is the source of all experimental information to check how measurements compare with theoretical predictions. These processes are: inclusive neutrino and antineutrino on neutrons and protons; elastic neutrino and antineutrino scattering on protons; inclusive π production on neutrons and protons; exclusive π production on neutrons and protons.

The pre-Conference results[3,4] in terms of the basic weak neutral coupling constants $g(u)_L$, $g(u)_R$, $g(d)_L$, and $g(d)_R$, are given in Table 6, where the theoretical predictions of Table 5 are repeated for the sake of comparison.

Without the standard $SU(2)_L \times U(1)_{L+R}$ theory, many parameters would be needed to describe these 15 neutrino processes, and we would miss the link between electromagnetism and weak interactions.

Table 6

Comparison of the $SU(2)_L \times U(1)_{L+R}$ weak neutral coupling constant with experiments

GSW predictions	Taking $\sin^2\theta = 1/4$	Experimental
$g(u)_L = \frac{1}{2} - \frac{2}{3}\sin^2\theta$	+0.33	+0.35 ± 0.07
$g(d)_L$ [a] $= -\frac{1}{2} + \frac{1}{3}\sin^2\theta$	-0.42	-0.40 ± 0.07
$g(u)_R = -\frac{2}{3}\sin^2\theta$	-0.17	-0.19 ± 0.06
$g(d)_R$ [a] $= +\frac{1}{3}\sin^2\theta$	+0.08	0.00 ± 0.11

a) The Cabibbo angles are neglected here. The exact formula should read $g(d)_L = (\text{same}) \cdot \cos\theta_C$; $g(d)_R = (\text{same}) \cdot \cos\theta_C$. These effects are too small, compared with the experimental uncertainties.

Class II: Lepton-lepton scattering

The experiments performed so far have used as primary leptons ν_e and ν_μ. The target has always been "electrons". In these experiments the "target mass" is m_e, to be compared with the "target mass" of the previous class, m_N. In fact, for the same primary neutrino energy E_ν, the q^2 values for processes of classes I and II are in the ratio

$$\frac{q^2_I}{q^2_{II}} = \frac{E_\nu \cdot m_N}{E_\nu \cdot m_e} \simeq 2{,}000 \ .$$

The cross-sections in this second class of experiments are damped by about 3 orders of magnitude, with respect to the class I experiments. The order of magnitude of the cross-sections is

$$\sigma(\nu e \to \nu e) \sim 10^{-42} \text{ cm}^2 \ ,$$

where ν stands for ν_e and ν_μ. These are the smallest cross-sections measured on earth.

The diagram describing the elastic lepton-lepton processes $\nu_e e^- \to \nu_e e^-$, $\nu_\mu e^- \to \nu_\mu e^-$

is 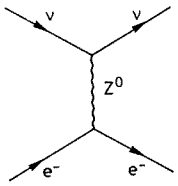

where ν can be either ν_μ or ν_e.

The experimental pre-Conference results are shown in Table 7.

Table 7

Comparison of the $SU(2)_L \times U(1)_{L+R}$ predictions for purely leptonic processes with experimental information

$\sigma(10^{-42}$ cm^2/GeV)	Theoretical predictions (with $\sin^2\theta = 0.27$)	Experimental value	Refs.
$\nu_e e^- \to \nu_e e^-$	5.2	(5.7 ± 1.2)	5
$\bar{\nu}_\mu e^- \to \bar{\nu}_\mu e^-$	1.6	(2.2 ± 1.0)	6
		$\left(1.0 \begin{smallmatrix}+2.1\\-0.9\end{smallmatrix}\right)$	7
$\nu_\mu e^- \to \nu_\mu e^-$	1.4	(1.1 ± 0.6)	6
		$\left(3.9 \begin{smallmatrix}+2.6\\-2.1\end{smallmatrix}\right)$	8
		(1.8 ± 0.8)	9

Class III: Lepton-hadron interference (free particle states)

Two experimental results are known since about a year. They come from the Taylor group at SLAC.

Using polarized electrons e_L and e_R, Taylor and co-workers[10] have established a non-zero value for the following ratio:

$$A = \frac{\sigma(e_L + D \to e_L + \text{any}) - \sigma(e_R + D \to e_R + \text{any})}{\sigma(e_L + D \to e_L + \text{any}) + \sigma(e_R + D \to e_R + \text{any})} ,$$

which is a "parity non-symmetric" quantity. This, according to $SU(2)_L \times U(1)_{L+R}$, arises from the interference between these two diagrams, where $\bullet \equiv \sqrt{\alpha}$ and $\Theta \equiv \sqrt{g_F} \equiv g^Z/m_{Z^0}$, and where T stands for target (i.e. protons or deuterons and their quark content). The parity properties of the "interference term" are as follows:

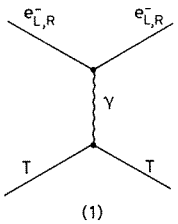

(1)

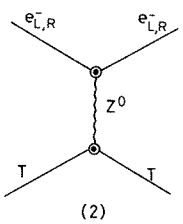

(2)

$$\begin{cases} J^V_e & \equiv \text{the vector current at the "electron" vertex} \equiv \bar{\psi}_e \gamma_\mu \psi_e \\ J^A_e & \equiv \text{the axial current at the "electron" vertex} \equiv \bar{\psi}_e \gamma_\mu \gamma_5 \psi_e \\ J^V_{\text{quark}} & \equiv \text{the vector current at the "quark" vertex} \equiv \bar{\psi}_q \gamma_\mu \psi_q \\ J^A_{\text{quark}} & \equiv \text{the axial current at the "quark" vertex} \equiv \psi_q \gamma_\mu \gamma_5 \psi_q \ . \end{cases}$$

Parity violation is due to two terms:

$$J_e^V \cdot J_{quark}^A \quad \text{and} \quad J_e^A \cdot J_{quark}^V \ .$$

Notice that the other terms

$$J_e^V \cdot J_{quark}^V \quad \text{and} \quad J_e^A \cdot J_{quark}^A$$

are also proportional to the product $(\alpha \cdot G_F)$ but conserve parity.

Notice also that the first diagram contributes purely vectorially, while the second diagram, with the Z^0, has both vector and axial currents at the "lepton" and "quark" vertices. The exact calculation predicts[11]

$$A = \frac{gG_F q^2}{20\sqrt{2}\,\pi\alpha}\left\{\underbrace{1 - \frac{20}{9}\sin^2\theta}_{\substack{\text{this term is generated by} \\ J_e^A \cdot J_{quark}^V}} + \underbrace{(1 - 4\sin^2\theta)\left[\frac{1 - (1 - y^2)}{1 + (1 - y^2)}\right]}_{\substack{\text{this term is generated by} \\ J_e^V \cdot J_{quark}^A}}\right\}, \qquad (3)$$

the experimental results being

$$A_D = (9.5 \pm 1.6) \times 10^{-5} \text{ in deuterium} ,$$

and

$$A_H = (9.7 \pm 2.7) \times 10^{-5} \text{ in hydrogen} ,$$

in excellent agreement with Eq. (3), for $\sin^2\theta = 0.20 \pm 0.03$.

We will see the newest data on the q^2- and the y-dependences, at the weak interactions sessions of the Conference.

This y-dependence is generated by the product $J_e^V \cdot J_{quark}^A$, and its detection is going to be as hard as $\sin^2\theta \to \frac{1}{4}$. For example, if $\sin^2\theta = \frac{1}{4}$, the asymmetry has no y-dependence, as can be deduced from the inspection of Table 5 without the need of any detailed calculation.

Class IV: Lepton-hadron interference (bound particle states)

Here we are in the field of atomic physics experiments. The "lepton" is charged (electrons in the atom), while the hadron is the nucleus. The basic diagrams are as shown here.

It is the interference between these two diagrams which produces the parity-violating effects. Notice that, in contrast to the class III experiments, the "electrons" as well as the target hadrons, or an assembly of quarks, are in bound states. Therefore atomic and nuclear physics structures come into play. Moreover, the q^2 values are very small, typical of atomic physics. And this is why the interference effects are much smaller than in the SLAC-type of experiments[10].

The pre-Conference results[12-21] are summarized in Table 8; two atoms have been investigated: bismuth and thallium.

The bismuth experiments. Bismuth is an atom with 83 electrons, of which 80 are in the core. Here a reliable theoretical calculation of the three-electron wave function at the site of the nucleus is needed.

In this class of experiments the trend has been towards a series of contradictory results. In 1977 the difficult laser experiment gave the first results reported in Table 8, in contradiction with the standard "electroweak" theoretical predictions. However, the three electron wave function calculations were later questioned by the same authors. The first evidence for the existence of a parity violation effect of the size expected in the standard theory was then reported by the Novosibirsk group[12,13], using the same spectral line investigated at Oxford (6476 Å) [14,15]. Later the Seattle group[16,18] reported new evidence which shows the existence of an asymmetry, even if the measured value is still far from the expected one. The most recent Novosibirsk data will be presented by L.M. Barkov at the Conference.

Table 8

The atomic physics experiments

Theoretical references	Theoretical predictions $\sin^2\theta = 0.27$	Experimental results	Refs. for experiments
	Atom used (bismuth) Z = 83		Oxford
20	1^{st} -25×10^{-8} } Line 6476 Å	$(2.7 \pm 4.7) \times 10^{-8}$	14
21	2^{nd} -12×10^{-8} }	$(-5 \pm 1) \times 10^{-8}$	15
			Seattle
20	1^{st} -18×10^{-8} } Line 8757 Å	$(0.7 \pm 3.2) \times 10^{-8}$	16
21	2^{nd} -9×10^{-8} }	$(-0.5 \pm 0.7) \times 10^{-8}$	17
		$(-2.4 \pm 0.9) \times 10^{-8}$	18
	Line 6476 Å	$\frac{\text{Experiment}}{\text{Theory}} = (1.10 \pm 0.30)$	Novosibirsk 12
		$(-19 \pm 5) \times 10^{-8}$	13
	Atom used (thallium) Z = 81		Berkeley
	2.6×10^{-3} Line 2927 Å	$(4.2 \pm 1.6) \times 10^{-3}$	19

Finally, a few words on the *thallium experiment*.

This is an element with only one external electron. Commins et al.[19] have selected a highly forbidden M1 transition, and the effect observed is due to the relative largeness of the quantity which is the imaginary part of the electric dipole moment divided by the (relatively) small M1 transition amplitude in the 2927 Å level of thallium.

The effect is called dichroism; it is, in fact, a measurement of the absorption cross-section for "left" and "right" helicity photons

$$(\sigma_R - \sigma_L)/(\sigma_R + \sigma_L) ,$$

just like the SLAC experiment[10] except that we are dealing with polarized photons rather than polarized electrons. In principle this experiment should be on better grounds when compared with the bismuth one. Here, in fact, we have a higher frequency of the spectroscopic line (2927 Å) and we are dealing with a one-electron system. Thus the core corrections should be much smaller than in the bismuth case.

The four classes discussed above can be characterized by the following parameters:

$$\varepsilon_i = \frac{\sigma(\text{wanted effect})}{\sigma(\text{other processes})} \qquad (i = 1, 2, 3, 4) ,$$

whose order of magnitude is given by the typical diagrams shown below (B = bound state).

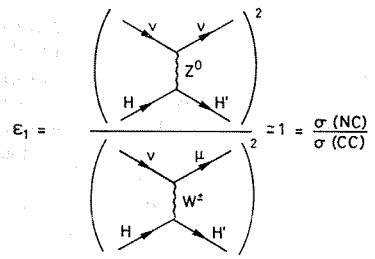

$\varepsilon_1 \simeq 1 = \frac{\sigma(\text{NC})}{\sigma(\text{CC})}$

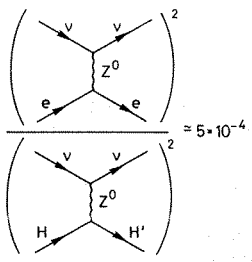

$\varepsilon_2 \simeq 5 \cdot 10^{-4}$

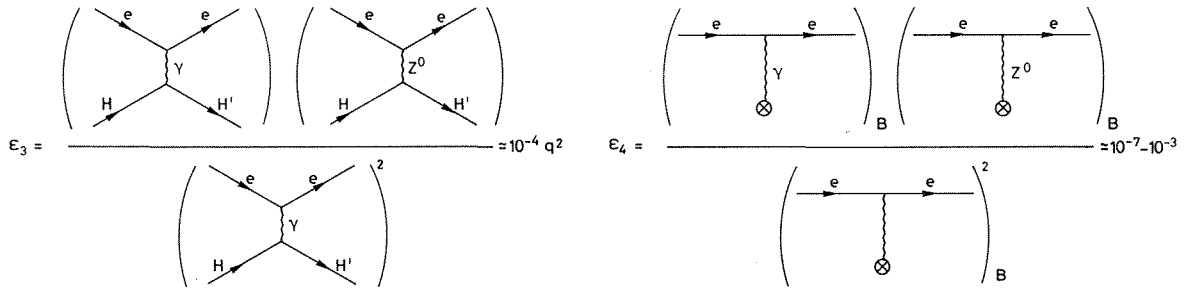

When comparing experimental results with theoretical predictions the value of ε_i should be taken into account, especially in order to understand the well-known history of the neutral current experiments. Thus we see that no problems have ever existed in the class I experiments, for which $\varepsilon_1 \simeq 1$. The class II experiments have produced some problems; here $\varepsilon_2 \simeq 5 \times 10^{-4}$. In class III we have a unique high-precision experiment. So, in spite of the small value of $\varepsilon_3 \simeq 10^{-4}$, no problem has existed. In the last class, we started with experiments characterized by $\varepsilon_4 \simeq 10^{-7}$ and many contradictory data have appeared in the literature. However, the Novosibirsk experiment and the recent thallium data (for which $\varepsilon_4 \simeq \simeq 10^{-3}$), have produced the first evidence for the existence of parity violation effects in accordance with the standard $SU(2)_L \times U(1)_{L+R}$ theoretical predictions. Table 9 summarizes the pre-Conference status of all neutral weak current experiments. At present there is not a single experiment that has proved to have results in contradiction to the standard theory of the electroweak interactions. We will see that the data to be presented at the Conference will confirm this trend.

Table 9

Neutral weak current experiments. Summary status.

Type of experiment	ε	Problems of inconsistency	At present [a]
Class I	1	No	OK
Class II	5×10^{-4}	Yes	OK
Class III	$10^{-4}\ q^2$	No	OK
Class IV	10^{-3}-10^{-7}	Yes	OK

a) Agreement with $SU(2)_L \times U(1)_{L+R}$

What have we learnt?

The knowledge of the following five quantities:

i) α, the fine structure constant,

ii) θ, the mixing angle between the two gauge groups $SU(2)_L$ and $U(1)_{L+R}$,

iii) the Clebsch-Gordan coefficients of the $SU(2)_L \times U(1)_{L+R}$ symmetry groups,

iv) the Fermi coupling constant, G_F, or one mass, $m_{W^\pm}$ or m_{Z^0},

v) the generalized Cabibbo angles,

is all that is needed to describe weak and electromagnetic processes, in the framework of a theory which is renormalizable. The old times when weak processes needed a cut-off are over.

Let me say a few words on the simple Spontaneous Symmetry Breaking (SSB).

Here comes an impressive experimental check, known since one year and to be reported with more precision at the Conference. In a weak interaction theory, with the Higgs mechanism unknown, there are two unknown parameters: the famous mixing angle θ; and the ratio ρ of neutral to charged currents, introduced in order to keep free the masses of the intermediate bosons:

$$\rho^2 = \frac{\text{rate of neutral currents}}{\text{rate of charged currents}} = \frac{g_{NC}^4}{g_{CC}^4} \cdot \frac{(1/m_{Z^0}^2)^2}{(1/m_{W^\pm}^2)^2} \ . \tag{4}$$

If SSB really takes place, as suggested by Salam-Weinberg[22], i.e. via the simplest Higgs mechanism, the masses of the charged and neutral intermediate bosons are related:

$$m_{W^\pm}/m_{Z^0} = \cos\theta \ . \tag{5}$$

In this case, as mentioned before, the damping of the neutral currents, with respect to the charged ones, is compensated exactly by the ratio of the coupling constants: $g_{CC}^2/g_{NC}^2 = \cos^2\theta$; in fact, $g_{CC} = g^\pm = g_{ew}\cdot\cos\theta$, and $g_{NC} = g_{ew}$, as we have already seen. Therefore

$$\rho^2 = \frac{m_{W^\pm}^4}{m_{Z^0}^4} \cdot \frac{1}{\cos^4\theta} = 1 \ . \tag{6}$$

The pre-Conference result[23] is

$$\rho = 0.98 \pm 0.05 \ .$$

Let me close by calling your attention to the following three features of the GSW theory:

i) the existence of the two quantum numbers, the electroweak isospin and the electroweak hypercharge, shared by quarks and leptons;

ii) the discovery of a new law which relates the weak neutral current to the electromagnetic current:
$$J^{NC}_{L,R} = J^3_L - \sin^2\theta \cdot J^{em}_{L+R} \ .$$

iii) the strength of neutral to charged current effects, i.e. $\rho = 1$, which implies that the simplest SSB is at work.

8. THE GENERALIZED CABIBBO MIXING

Here the great point of concern is to bring the PC- and T-violating interactions into the standard weak interaction scheme. This can be done if nature has, at least, six quarks to play with. These six quarks form three weak isospin doublets

$$\begin{pmatrix} u \\ d_C \end{pmatrix}, \quad \begin{pmatrix} c \\ s_C \end{pmatrix}, \quad \begin{pmatrix} t \\ b_C \end{pmatrix}. \tag{7}$$

Notice that "C" indicates a "Cabibbo" mixed state, as shown below. The transitions among the various states would be as given in Fig. 13.

Notice that there are no "charm-changing" neutral currents -- there will be new results presented at the Conference on this important topic -- in perfect analogy with the absence of the "strangeness-changing" neutral currents. In fact, the "horizontal" transitions in Fig. 13 are all "naturally forbidden", i.e. forbidden for any value of the mixing angles. This is indicated by ↔×↔ in Fig. 13.

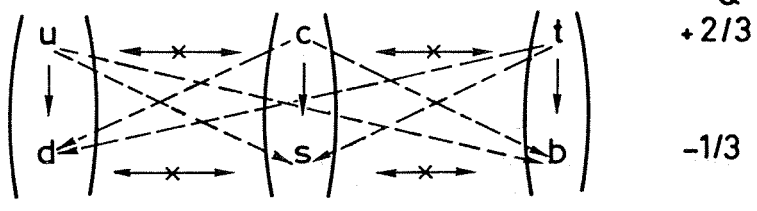

Allowed neutral currents:

$$\bar{u}u, \ \bar{c}c, \ \bar{t}t, \ \bar{d}d, \ \bar{s}s, \ \bar{b}b \ .$$

Generalized Cabibbo mixing opens the dashed channels. Without it, the dashed transitions would not exist. The only allowed transitions would be those inside a quark doublet, indicated by the full arrows.

Fig. 13

In this six-quark theory there are three Cabibbo angles: the original one and two more; plus a phase angle.

The generalized Cabibbo angles and the phase angle entering with the various weak transitions are shown in Fig. 14. Notice that there is no mixing in the lepton case if all neutrinos, ν_e, ν_μ, ν_τ, are massless.

Pre-Conference results already indicated that the process $\nu + d \to c + \mu^-$ is Cabibbo suppressed. Notice that "d" is a "valence" quark. New results will also be presented on the allowed one: $\nu + s \to c + \mu^-$, where "s" is of course an "ocean" quark. As shown in Fig. 14, $s \to c$ has only cos's $(C_1C_2C_3)$ whilst $d \to c$ has a sine: (S_1C_2).

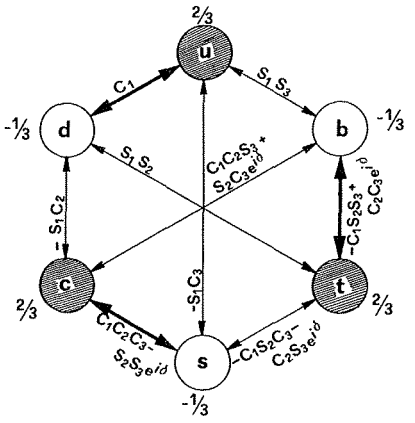

Six quarks mixing with CP violation
$S_i = \sin\theta_i$
$C_i = \cos\theta_i$

Fig. 14

9. SUPERSYMMETRY AND R ≠ 0 PARTICLES

All particles obey either Fermi or Bose statistics. Fermions and bosons exhaust all possible particle states. In his famous lecture at Erice in 1967, Coleman[24] discussed "All possible symmetries of the S-matrix". All but one. This one is the symmetry which tells you that if you have a boson you must have a fermion and vice versa. This supersymmetry can be traced back to the structure of space-time. Superspace tells us that we had forgotten the "fermionic" dimensions and have limited our concept of space to only the "bosonic" space-time dimensions.

The well-known "no go" theorems of SU(6) [i.e. $SU(3)_{flavour}$ combined with $SU(2)_{spin}$] are overcome; not because their proof was wrong, but simply because the nature of the space-time was too restrictive. It was only based on Lie algebra, i.e. no anticommutation relations were allowed in the basic algebra. The algebra related to superspace is a "graded" Lie algebra, i.e. anticommutation relations are allowed. One of the striking results of this new concept of superspace is the fact that a standard "space-time" translation is not the most elementary motion in superspace. In fact, the space-time displacement operator P_μ can be obtained as a result of the anticommutator of the spinoral operators[25] Q_α, Q_β:

$$\{Q_\alpha, Q_\beta\} = -2\gamma^\mu_{\alpha\beta}P_\mu \ .$$

The notion of superspace[26] provides us with the concept of a superelementary displacement, which can be thought of as the "square root" of the standard space-time displacement operator. This is reminiscent of the Dirac equation, which can be thought of as the "square root" of the Klein-Gordon equation. The concepts of mass and spin are on an equal footing in superspace. Its curvature is related to the "mass density"; its torsion to the "spin density".

Supersymmetric theories provide a theoretical motivation for the mutual occurrence of both FERMIONS and BOSONS through a symmetry principle which is related to the underlying geometrical structure of space and time.

A possible consequence of the supersymmetric approach to particle physics is shown in Table 10.

As we can easily deduce from this table, the existence of a photon would imply a massless spin $\frac{1}{2}$ particle, the photino. The gluon would be accompanied by a gluino. Quarks have as supersymmetric partners new "heavy leptons" -- not to be confused with the standard ones (R = 0). The existence of "gluinos" means that in hadron physics we should one day discover "mesons" behaving as "fermions" and "baryons" behaving as "bosons".

Table 10 [following Farrar and Fayet[27]]

The particle states are specified according to the quantum number R, which is zero for all known standard states. The values of R are indicated in parenthesis.

Multiplets	Vectors	Spinors	Scalars
$m = 0$ Gauge part.	Photon (0) Gluons (0)	Photino (1) Gluino (1)	
$m \neq 0$ Gauge part.	Intermediate bosons $W^{\pm}$, Z^0 (0)	Heavy leptons (1)	Higgs scalars (0)
Matter multiplets		Quarks (0)	Quarks (±1)
		e, ν_e (0)	Leptons (±1)
		μ, ν_μ (0)	Leptons (±1)
		τ, ν_τ (0)	Leptons (±1)
		.....	.....

10. PRESENT OUTLOOK

Excluding gravitational forces, all fundamental interactions of nature seem to share an impressive series of common features:

1) They are all described by the same basic diagram, where a pair of spinors (leptons and quarks) $(\bar{\psi}\psi)$ interact with another pair $(\bar{\psi}\psi)$, via the exchange of a spin-one particle (γ, $W^{\pm}$, Z^0, gluons).

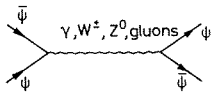

2) Each interaction is originated by a gauge symmetry group. These are:

$$\begin{array}{ccc} U(1) & SU(2) & SU(3)_C \\ \downarrow & \downarrow & \downarrow \\ g_Y & g_\tau & g_C \end{array}$$

where g_Y and g_τ are the electroweak "hypercharge" and "isospin" coupling constants whose mixing produces the electromagnetic and the weak couplings; and g_C is the "colour" coupling between coloured quarks and gluons. All (g_Y, g_τ, g_C) are dimensionless.

It is perfectly legitimate to think that a supergroup is at the origin of all the gauge symmetry groups; This needs to be a very large group. For example, SO(8) is too small, in fact: $SO(8) \not\supset SU(3)_C \times SU(2) \times U(1)$. However, as will be discussed at the Conference, the supersymmetric Lagrangian with SO(8) internal symmetry shows SU(8) properties.

It is interesting to remark that any group which contains $SU(3)_C$ and U(1) has the very interesting feature[28] that coloured states are associated with fractional charges, while colour singlet states have integral charges. If we identify the leptons with the colour-singlet basic fermions, and the quarks with the coloured basic fermions, this is exactly what seems to happen in nature.

Notice also that renormalizability requires strong interactions to be invariant under electroweak isospin $\vec{\tau}$ and hypercharge Y. As $SU(3)_C$ commutes with the gauge group of weak interactions and since the strong couplings occur through a gauge-invariant coupling of quarks and vector particles (the gluons), there are no parity-violation and no strangeness-violation effects to order α, as is found experimentally.

The Lagrangian of these basic unbroken interactions involves only massless gauge fields coupled minimally to conserved currents. These are basic features which guarantee the renormalizability of the theory. The masses of the real particles (intermediate bosons, leptons, and quarks) and the non-conservation of the currents are the result of spontaneous symmetry breaking. The basic point is that SSB does not spoil the renormalizability of the theory.

Conclusions: It seems that nature has constructed the world in such a way that we can always choose locally (i.e. at every space-time point) the angles of rotation: in one real dimension, U(1); in two complex dimensions, SU(2); in three complex dimensions, SU(3); and, if we add gravity, the reference system → {SO(3,1) + translations} {≡ Poincaré group}. This is shown synthetically in Table 11. The freedom to make these choices, without producing observable effects, generates the fundamental forces of nature and is at the origin of the vector nature of the gauge particles (photons, W's, Z^0, and gluons). Gravity is a special case. A point in space-time is already a vector quantity. To be free at every space-time point is another vector operation. This is why the graviton is a tensor.

To sum up the situation at the opening of this Conference: we are faced with what appears to be a grand synthesis. We must, however, remain open-minded, just in case ... .

Table 11: The Present Grand Synthesis

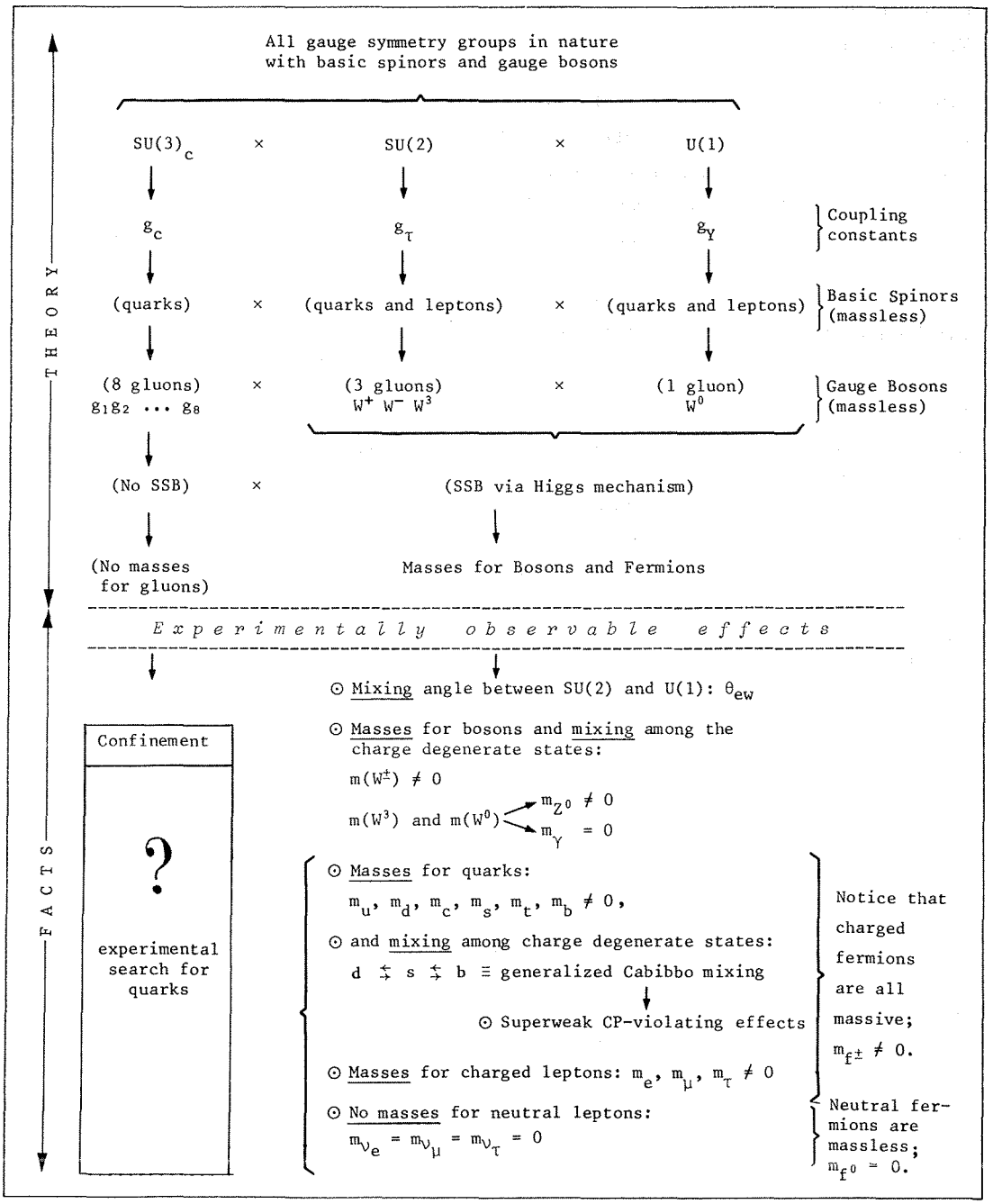

REFERENCES

1) F.J. Hasert et al., Phys. Lett. 46B, 138 (1973).

2) D.H. Perkins, Proc. Conf. on Weak Interactions, Argonne, 1965 (Argonne Nat. Lab. Report), Annex 1, p. 273.

3) L.M. Sehgal, Status of neutral currents in neutrino interactions, Aachen preprint PITHA-102 (1978).

4) M. Holder et al. (CDHS Collaboration), Phys. Lett. 71B, 222 (1977).

5) F. Reines, Phys. Rev. Lett. 37, 315 (1976).

6) M. Baldo Ceolin et al., Proc. "Neutrinos-78" Int. Conf. on Neutrino Physics, Purdue Univ., 1978 (Purdue Univ., West Lafayette, Ind., 1978), p. 387.

7) G. Blietschau et al., Nucl. Phys. B114, 189 (1976).

8) M. Haguenauer et al., Proc. 19th Int. Conf. on High-Energy Physics, Tokyo, 1978 (Phys. Soc. Japan, Tokyo, 1979), p. 360.

9) A.M. Cnops et al., Phys. Rev. Lett. 41, 357 (1978).

10) C.Y. Prescott et al., Phys. Lett. 77B, 347 (1978).

11) R.H. Cahn and F.J. Gilman, Phys. Rev. D 17, 1213 (1978).

12) L.M. Barkov and M.S. Zolotoryov, Zh. Eksper. Teor. Fiz. Pis'ma 27, 379 (1978).

13) L.M. Barkov, Proc. 19th Int. Conf. on High-Energy Physics, Tokyo, 1978 (Phys. Soc. Japan, Tokyo, 1979), p. 425.

14) P.E. Baird et al., Phys. Rev. Lett. 39, 798 (1977).

15) P.E. Baird et al., Reported at the Riga Conf. (USSR) 1978.
L.M. Barkov, Proc. 19th Int. Conf. on High-Energy Physics, Tokyo, 1978 (Phys. Soc. Japan, Tokyo, 1979), p. 425.

16) R.L. Lewis et al., Phys. Rev. Lett. 39, 795 (1977).

17) N. Fortson et al., Proc. "Neutrinos-78" Int. Conf. on Neutrino Physics, Purdue Univ., 1978 (Purdue Univ., West Lafayette, Ind., 1978), p. 417.

18) N. Fortson, private communication.

19) E. Commins et al., private communication.

20) E.M. Henley and L. Wilets, Phys. Rev. A 14, 1411 (1976). These authors are using a three-electron wave function with a "central field" for the nucleus.

21) P.G. Sanders, Proc. Conf. on Lepton and Photon Interactions, Hamburg, 1977 (DESY, Hamburg, 1977), p. 599. This author is using a three-electron wave function and a correction for the shielding of the 80 electrons in the core.

22) S. Weinberg, Phys. Rev. Lett. 19, 1264 (1967).
A. Salam *in* "Elementary Particle Theory", Nobel Symposium 8 (Almqvist and Wiksell, Stockholm, 1968), p. 367.

23) C. Baltay, Proc. 19th Int. Conf. on High-Energy Physics, Tokyo, 1978 (Phys. Soc. Japan, Tokyo, 1979), p. 882.

24) S. Coleman, All possible symmetries of the S-matrix, *in* "Hadrons and their Interactions", Proc. "Ettore Majorana" Int. School of Subnuclear Physics, Erice, 1967 (Academic Press, NY, 1968), p. 393.

25) J. Wess and B. Zumino, Nucl. Phys. B70, 39 (1974).
Yu.A. Gol'fand and E.P. Likhtman, JETP Letters 13, 323 (1971).

26) A. Salam and J. Strathdee, Nucl. Phys. B76, 477 (1974).
S. Ferrara, J. Wess and B. Zumino, Phys. Lett. 51B, 239 (1974).

27) P. Fayet, Phys. Lett. 70B, 461 (1977).
G. Farrar and P. Fayet, Phys. Lett. 76B, 575 (1978).

28) See, for example, M. Gell-Mann, P. Ramond and R. Slansky, Rev. Mod. Phys. 50, 721 (1978).

SESSION I

NEUTRINO PHYSICS AND WEAK INTERACTIONS

Chairmen: E. Fiorini
D.H. Perkins
V.L. Telegdi
A.M. Wetherell

Sci. Secretaries: G. Bonneaud
P. Bosetti
J. de Groot
W. Kozanecki
W. Scott
S.N. Tovey

Rapporteurs talks:

F. Dydak	Neutral currents
R. Turlay	Charged weak currents
B. Tallini	Hadronic final states in neutrino and antineutrino charged-current events
L.M. Sehgal	Neutrinos and nucleon structure

Invited papers:

L.M. Barkov	Atomic physics checks of parity violation
C.Y. Prescott	Further tests of parity violation in inelastic electron scattering
M.J. Rees	Neutrinos in astrophysics

Contributed papers:

M. Conversi	Lifetime of charmed hadrons produced in neutrino interactions
N. Schmitz	Fragmentation functions in neutrino hydrogen interactions
L. Pape	Measurement of the ratio of neutral to charged current cross sections of neutrino interactions in hydrogen
J. Ludwig	Flux normalized charged current neutrino cross sections up to neutrino energies of 260 GeV
M. Rollier	Results from Gargamelle neutrino experiment at CERN SPS
A. Rosanov	First results from the CERN-Hamburg-Amsterdam-Rome-Moscow neutrino experiment

NEUTRAL CURRENTS

F. Dydak
Institut für Hochenergiephysik der Universität, Heidelberg, Germany
and
CERN, Geneva, Switzerland

ABSTRACT

The present status of weak neutral currents is reviewed. Emphasis is put on the comparison of recent experimental results with earlier ones, and with predictions of gauge models of the SU(2) ⊗ U(1) type. The coupling constants governing the weak neutral current interaction are given, and their quantitative agreement with the Salam-Weinberg model is critically examined.

1. INTRODUCTION

The last year has been a period of consolidation for neutral current physics. Important new results and improvements of old results have been reported, but our picture of the neutral current interaction did not change compared to that of one year ago[1,2]. Hence the emphasis of this review is put on recent experimental results, and on a critical discussion of the precision of those experiments which yield the most stringent constraints on model parameters.

The processes which can occur via the weak neutral current interaction are depicted in the "Sakurai tetragon"[3] which is shown in Fig. 1. It is an analogue to the Puppi triangle for charged current interactions. The coupling constants governing the various neutral current interactions are based on the assumption that the neutral current interaction is effectively of the current-current form where the current is made up of a linear combination of vector and axial vector covariants, and the hadronic weak current comprises isoscalar and isovector pieces only. The effective Lagrangians of the neutral current interactions which have been explored experimentally are:

for the process $\nu + e \to \nu + e$:

$$L = -\frac{G}{\sqrt{2}}\left[\bar{\nu}\gamma_\lambda(1+\gamma_5)\nu\right]\left[\bar{e}\gamma^\lambda\left(g_V + g_A\gamma_5\right)e\right];$$

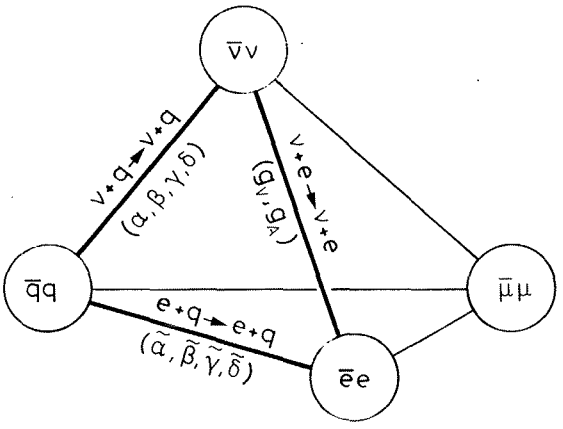

Fig. 1 The Sakurai tetragon of neutral-current interactions

for the process e + q → e + q (parity-violating parts only):

$$L = -\frac{G}{\sqrt{2}}\left\{\bar{e}\gamma_\lambda\gamma_5 e\left[\frac{\tilde{\alpha}}{2}\left(\bar{u}\gamma^\lambda u - \bar{d}\gamma^\lambda d\right) + \frac{\tilde{\gamma}}{2}\left(\bar{u}\gamma^\lambda u + \bar{d}\gamma^\lambda d\right)\right]\right.$$

$$\left. + \bar{e}\gamma_\lambda e\left[\frac{\tilde{\beta}}{2}\left(\bar{u}\gamma^\lambda\gamma_5 u - \bar{d}\gamma^\lambda\gamma_5 d\right) + \frac{\tilde{\delta}}{2}\left(\bar{u}\gamma^\lambda\gamma_5 u + \bar{d}\gamma^\lambda\gamma_5 d\right)\right]\right\};$$

and for the process ν + q → ν + q:

$$L = -\frac{G}{\sqrt{2}}\,\bar{\nu}\gamma_\lambda(1+\gamma_5)\nu\left[\frac{1}{2}\bar{u}\gamma^\lambda(\alpha+\beta\gamma_5)u - \frac{1}{2}\bar{d}\gamma^\lambda(\alpha+\beta\gamma_5)d\right.$$

$$\left. + \frac{1}{2}\bar{u}\gamma^\lambda(\gamma+\delta\gamma_5)u + \frac{1}{2}\bar{d}\gamma^\lambda(\gamma+\delta\gamma_5)d\right].$$

This definition of the coupling constants is due to Hung and Sakurai[4]. The relation between these coupling constants and the Lorentz covariants and the isospin components of the weak hadronic current is given in Table 1.

Table 1

The relation of the coupling constants (Hung and Sakurai notation) to the Lorentz covariants and the isospin components of the weak hadronic current

	Lorentz covariant	Isospin component
$\alpha(\tilde{\alpha})$	Vector	Isovector
$\beta(\tilde{\beta})$	Axial vector	Isovector
$\gamma(\tilde{\gamma})$	Vector	Isoscalar
$\delta(\tilde{\delta})$	Axial vector	Isoscalar

An alternative very useful notation has been made popular by Sehgal[5]. The "chiral coupling constants" are defined via the effective Lagrangian for the process ν + q → ν + q:

$$L = -\frac{G}{\sqrt{2}}\,\bar{\nu}\gamma_\lambda(1+\gamma_5)\nu\left\{\bar{u}\gamma^\lambda\left[u_L(1+\gamma_5) + u_R(1-\gamma_5)\right]u\right.$$

$$\left. + \bar{d}\gamma^\lambda\left[d_L(1+\gamma_5) + d_R(1-\gamma_5)\right]d\right\}$$

The meaning of the chiral coupling constants in terms of the chirality of the weak hadronic current and their relation to the coupling constants defined above is given in Table 2. The experimental challenge is to determine the various neutral current coupling constants as precisely as possible, and to compare them with theoretical predictions. As far as theory is concerned, there is only one model that has survived[2,5] a series of high-precision experiments: the model due to Salam[6] and Weinberg[7], based on the gauge group SU(2) ⊗ U(1), extended by the Glashow-Iliopoulos-Maiani (GIM)[8] scheme to include the weak interactions between the u-, d-, s-, and c-quarks. Hereafter it will be referred to simply as the "Salam-Weinberg" or "standard" model. It contains only one free parameter, the mixing angle θ_W between the third isospin component of the charged weak current and the electromagnetic

Table 2

Meaning of the chiral coupling constants

	Chirality	Quark
$u_L = \frac{1}{4}(\alpha+\beta+\gamma+\delta)$	Left-handed (V-A)	u
$d_L = \frac{1}{4}(-\alpha-\beta+\gamma+\delta)$	Left-handed (V-A)	d
$u_R = \frac{1}{4}(\alpha-\beta+\gamma-\delta)$	Right-handed (V+A)	u
$d_R = \frac{1}{4}(-\alpha+\beta+\gamma-\delta)$	Right-handed (V+A)	d

current which together constitute the weak neutral current in the standard model. The angle θ_W is referred to as the "electro-weak mixing angle", but is more commonly known as the "Weinberg angle".

The standard model has achieved such a degree of respectability that experimental results are usually quoted in terms of $\sin^2\theta_W$. This is a way of making a comparison with theory. However, it is more objective to determine the set of coupling constants experimentally and to compare them individually with theory. This is possible because of the high precision of today's neutral current experiments.

We note in passing that we have included only the contributions from u- and d-quarks in the effective Lagrangians. Today, high-precision experiments ought to apply small corrections for the s-quark content of the sea (assuming that the neutral current coupling of the s- and d-quark is the same, as predicted by the standard model). Future experiments, however, should provide experimental information on the neutral current coupling of s-, c, ... quarks.

So far we have considered only interactions between different corners of the Sakurai tetragon. There may exist also self-interactions within the same corner, e.g. ν-ν or q-q scatterings. These experiments are very hard. The best thing may be to look for parity-violating effects in nuclei due to the neutral current interaction between quarks[9].

2. NEUTRINO SCATTERING ON ELECTRONS

The particularly attractive feature of νe scattering is that there is no hadronic structure involved. Theoretical predictions are straightforward and unambiguous. A major drawback is the very small cross-section. All experiments performed so far have obtained very small data samples.

Four reactions are possible in neutral current νe scattering:

$$\nu_e + e^- \to \nu_e + e^-$$
$$\bar{\nu}_e + e^- \to \bar{\nu}_e + e^-$$
$$\nu_\mu + e^- \to \nu_\mu + e^-$$
$$\bar{\nu}_\mu + e^- \to \bar{\nu}_\mu + e^- \ .$$

Of these, ν_e and $\bar{\nu}_e$ can scatter via both neutral and charged currents, whereas ν_μ and $\bar{\nu}_\mu$ scatter only via the neutral current. The $\overset{(-)}{\nu}_\mu e$ scattering process is studied both in bubble chambers and counter experiments. Bubble chambers have the advantage of a good electron signature and low background, but suffer from small event numbers and scanning biases. Counter experiments are expected to accumulate several hundred events in the near future, because of their higher target mass. They have no problem with isolated γ background, as bubble chambers do. But other backgrounds are large, and the biases due to tight selection criteria have to be carefully examined.

2.1 The process $\nu_\mu + e^- \to \nu_\mu + e^-$

The experimental results[10-14] on the process $\nu_\mu + e^- \to \nu_\mu + e^-$ are summarized in Table 3. This process aroused a lot of interest in 1978 when a group working with Gargamelle reported[15] a cross-section, based on a subsample of their statistics, which was too large to be compatible with the standard model prediction with accepted values of $\sin^2\theta_W$. Shortly afterwards, Cnops et al.[13] reported a result based on an exposure to a neutrino flux bigger by a factor of 4. Their cross-section was in disagreement with the result of the Gargamelle group, but in agreement with the standard model with $\sin^2\theta_W = 0.2$.

Table 3

Summary of experiments on $\nu_\mu e$ scattering

Experiment	Sample of $\nu_\mu + N \to \mu^- + X$	$\nu_\mu e$ candidates	Background	σ/E [a]
GGM[10] CERN-PS		1	0.3 ± 0.1	< 3 (90% c.l.)
AP[11] Counter exp.		32	20.5 ± 2.0	1.1 ± 0.6
GGM[12] CERN-SPS	64,000	9	0.5 ± 0.2	$2.4^{+1.2}_{-0.9}$
CB[13] FNAL 15′	83,700	8	0.5 ± 0.5	1.8 ± 0.8
CHARM[14] Counter exp.	56,000	11	4.5 ± 1.4	2.6 ± 1.6
Average of the experiments				1.6 ± 0.4
Prediction of the standard model ($\sin^2\theta_W = 0.23$)				1.5

a) in units of 10^{-42} cm^2/GeV.

This discrepancy turned out to be largely due to a statistical fluctuation in the data sample of the Gargamelle group. The first result was based on 10 observed events in a sample of 24,000 charged current interactions. Later on, two events were removed because they were possibly due to bremsstrahlung from muons passing the chamber. This was accomplished by a cut in the fiducial volume around such muons, with a loss of a few percent in the fiducial volume. The increase in the statistics of charged current events from 24,000 to

64,000 resulted in only one more observed event, with a final sample of 9 events. This result is in good agreement with all other experiments as well as with the prediction of the standard model. The average of the slope of the cross-section from all experiments is

$$\sigma/E = (1.6 \pm 0.4) \times 10^{-42} \text{ cm}^2/\text{GeV} ,$$

yielding a Weinberg angle

$$\sin^2\theta_W = 0.22 \begin{matrix} + 0.08 \\ - 0.05 \end{matrix} .$$

A possible second solution at large values of $\sin^2\theta_W$ is excluded by experiments on the process $\bar{\nu}_\mu + e^- \to \bar{\nu}_\mu + e^-$ (see Section 2.2).

Very recently, the fine-grain calorimeter detector of the CERN-Hamburg-Amsterdam-Rome-Moscow (CHARM) Collaboration installed at the CERN-SPS, came up with a preliminary result on the cross-section of $\nu_\mu e$ scattering. As is evident from Table 3, this first result is in good agreement with other results. The authors hope soon to accumulate much more statistics and to increase the precision of their result substantially.

2.2 The process $\bar{\nu}_\mu + e^- \to \bar{\nu}_\mu + e^-$

The great interest in the process $\nu_\mu + e^- \to \nu_\mu + e^-$ initiated an intense search for the process $\bar{\nu}_\mu + e^- \to \bar{\nu}_\mu + e^-$. The results of these experiments[16-18] are summarized in Table 4, together with the results of two earlier experiments[10-11]. All three recent experiments performed in the high-energy domain reported only upper limits for σ/E. The

Table 4

Summary of experiments on $\bar{\nu}_\mu e$ scattering

Experiment	Sample of $\bar{\nu}_\mu + N \to \mu^+ + X$	$\bar{\nu}_\mu e$ candidates	Background	σ/E [a]
GGM[10] CERN-PS		3	0.4 ± 0.1	$1.0 \begin{matrix} + 2.1 \\ - 0.9 \end{matrix}$
AP[11] Counter exp.		17	7.4 ± 1.0	2.2 ± 1.0
GGM[16] CERN-SPS	7400	0	< 0.03	< 2.7 (90% c.l.)
FMMS[17] FNAL 15′	8400	0	0.2 ± 0.2	< 2.1 (90% c.l.)
BEBC TST[18] CERN-SPS	7500	1	0.5 ± 0.2	< 3.4 (90% c.l.)
Average of the experiments [b]				1.3 ± 0.6
Prediction of the standard model ($\sin^2\theta_W = 0.23$)				1.3

a) in units of 10^{-42} cm^2/GeV.

b) This average is obtained by adding the number of events observed in the experiments and dividing by the sum of the effective antineutrino fluxes.

results are in agreement with the earlier low-energy experiments[10-11], and with the prediction of the standard model with $\sin^2\theta_W = 0.23$. The average of the slope of the cross-section from all experiments is

$$\sigma/E = (1.3 \pm 0.6) \times 10^{-42} \text{ cm}^2/\text{GeV} ,$$

yielding a Weinberg angle

$$\sin^2\theta_W = 0.23 \begin{matrix} + 0.09 \\ - 0.23 \end{matrix} .$$

The cross-sections of all four possible νe scattering processes in the framework of the standard model have been calculated by 't Hooft[19] and are shown in Fig. 2. Since nature has chosen a value of $\sin^2\theta_W$ close to 0.25, a precise determination of $\sin^2\theta_W$ from the $\overset{(-)}{\nu}_\mu e$ cross-section is very hard because of its weak dependence on $\sin^2\theta_W$.

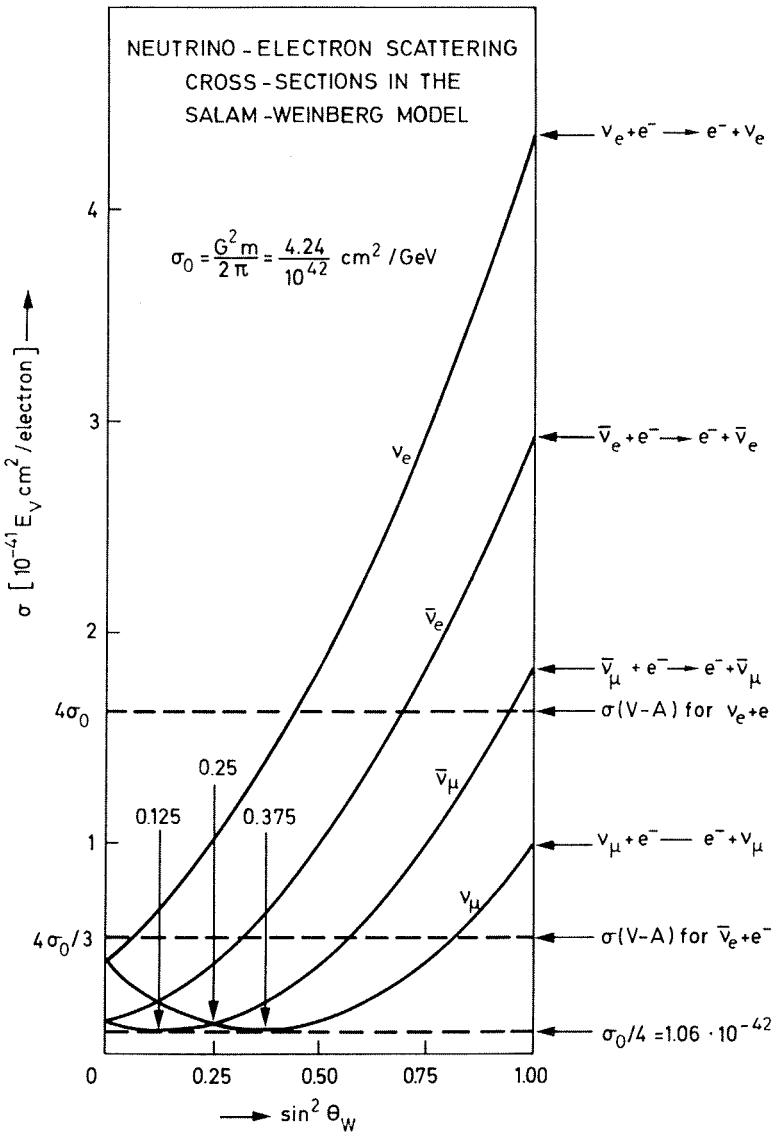

Fig. 2 Neutrino-electron scattering cross-sections in the Salam-Weinberg model

2.3 The coupling constants for neutrino-electron scattering

In terms of the coupling constants g_V and g_A defined above, the differential cross-section for νe scattering is given for high energies by

$$\frac{d\sigma}{dy} = \frac{G^2 m_e E_\nu}{2\pi} \left[(C_V + C_A)^2 + (C_V - C_A)^2 (1 - y)^2 \right] ,$$

where $y = E_e/E_\nu$ is the fraction of the neutrino energy transferred to the target electron. The relation of C_V and C_A to the coupling constants g_V and g_A is given in Table 5 for all four possible νe scattering processes. The total cross-section is obtained by integration over y between y = 0 and y = 1.

Table 5

Relation between C_V and C_A and the coupling constants g_V and g_A

Process	C_V	C_A
$\nu_e + e^- \to \nu_e + e^-$	$1 + g_V$	$1 + g_A$
$\bar{\nu}_e + e^- \to \bar{\nu}_e + e^-$	$1 + g_V$	$-1 - g_A$
$\nu_\mu + e^- \to \nu_\mu + e^-$	g_V	g_A
$\bar{\nu}_\mu + e^- \to \bar{\nu}_\mu + e^-$	g_V	$-g_A$

The cross-section defines an ellipse in the g_V, g_A plane. As can be seen in Fig. 3, the elliptic domains allowed by the measured $\nu_\mu e$ and $\bar{\nu}_\mu e$ cross-sections define four regions

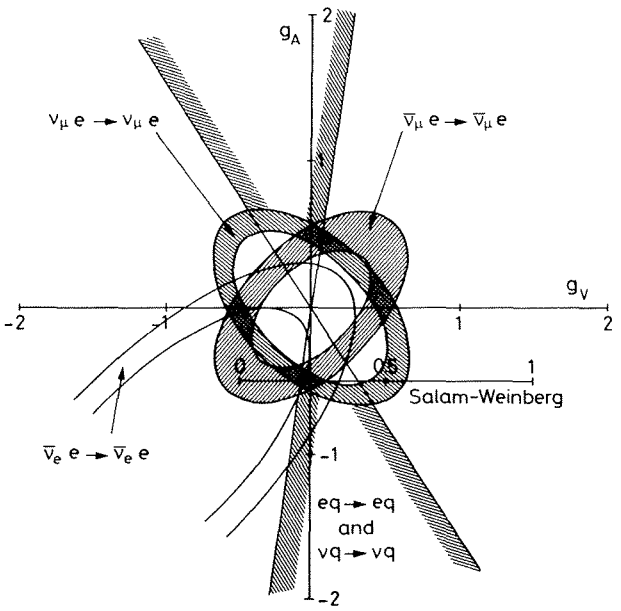

Fig. 3 Domains in the g_V, g_A plane allowed by νe scattering experiments

of overlap in part due to a sign ambiguity. The signs of the coupling constants g_V and g_A can be determined experimentally because of the interference between the charged and neutral current amplitudes in the $\nu_e e$ and $\bar{\nu}_e e$ scattering processes. The latter process has been observed by Reines et al.[20] at the Savannah River fission reactor. Although their measured cross-section is not significantly different from the V-A cross-section of the charged current channel process, in the framework of the standard model the mixing angle is constrained to $\sin^2\theta_W = 0.29 \pm 0.05$ thanks to the strong dependence of the cross-section on $\sin^2\theta_W$ (see Fig. 2). The elliptic domain allowed by the $\bar{\nu}_e e$ cross-section restricts the allowed domains of g_V, g_A to two. This remaining ambiguity cannot be resolved with νe scattering experiments alone. The two possible solutions correspond to a dominant vector or a dominant axial-vector current. A discrimination between the two solutions can be obtained with electron-quark and neutrino-quark scattering experiments, but not in a model-independent way (see Section 3.3).

The solution with axial vector dominance is in good agreement with the prediction of the standard model with $\sin^2\theta_W = 0.23$, as can be seen from Table 6.

In summary, all known results on νe scattering are consistent and in agreement with the predictions of the standard model. The precision of the experiments ought to be improved although there is little hope of getting a precise determination of $\sin^2\theta_W$ from $\nu_\mu e$ scattering experiments. Good precision on $\sin^2\theta_W$ is in principle expected from $\nu_e e$ scattering, which is the only channel not yet explored experimentally.

Table 6

Summary of the results on the coupling constants g_V, g_A

	Best fit value [a]	Standard model	$\sin^2\theta_W = 0.23$
g_V	0.06 ± 0.08	$-\frac{1}{2} + 2\sin^2\theta_W$	-0.040
g_A	-0.52 ± 0.06	$-\frac{1}{2}$	-0.500

a) Solution with axial vector dominance only.

3. ELECTRON SCATTERING ON QUARKS

Very recently, substantial progress has been made in the understanding of eq scattering via weak neutral current. This progress stems mainly from new results on parity-violating effects in the inelastic scattering of polarized electrons at SLAC, but also from new results on parity-violating effects in optical transitions of heavy atoms.

3.1 Polarized electron scattering on deuterium

The SLAC-Yale group reports on an extension of the previous measurement[21] of a parity-violating asymmetry in the inelastic scattering of longitudinally polarized electrons of about 20 GeV beam energy from unpolarized deuterium nuclei. The first measurement was done essentially for one value of the inelasticity y, namely $y \sim 0.2$. The new measurements[22] reported by Prescott to this conference give the asymmetry as a function of $y = (E_e - E'_e)/E_e$ covering the range $0.15 \leq y \leq 0.36$.

The new measurements open up new possibilities of testing the predictions of specific gauge models. The asymmetry for the inelastic scattering of right- or left-handed electrons on deuterium,

$$A = \frac{\sigma_R - \sigma_L}{\sigma_R + \sigma_L} ,$$

can be written as[23]

$$\frac{A}{Q^2} = a_1 + a_2 \frac{1 - (1-y)^2}{1 + (1-y)^2} ,$$

where Bjorken scaling and R = 0 are assumed (R is the ratio of the absorption cross-sections for longitudinal and transverse photons). The coefficients a_1 and a_2 depend in general on kinematic parameters; but with an isoscalar target such as deuterium they are expected to be constants, and can be expressed in terms of the relevant coupling constants $\tilde{\alpha}$, $\tilde{\beta}$, $\tilde{\gamma}$, and $\tilde{\delta}$, as follows[24]:

$$a_1 = (G/\sqrt{2}e^2)(9\tilde{\alpha} + 3\tilde{\gamma})/5 ,$$

$$a_2 = (G/\sqrt{2}e^2)(9\tilde{\beta} + 3\tilde{\delta})/5 .$$

An order of magnitude estimate for a_1 and a_2 is given by the constant $G/\sqrt{2}e^2 \sim 10^{-4}$ GeV^{-2}, which is the ratio of the weak to the electromagnetic amplitude giving rise to the observed interference effect.

The measurement of the y-dependence of the asymmetry permits a separate determination of the coefficients a_1 and a_2. The fit yielded[22]

$$a_1 = (-9.7 \pm 2.6) \times 10^{-5} \text{ GeV}^{-2}$$

and

$$a_2 = (4.9 \pm 8.1) \times 10^{-5} \text{ GeV}^{-2} ,$$

which gives in terms of the coupling constants the linear relations[24]

$$\tilde{\alpha} + \frac{\tilde{\gamma}}{3} = -0.60 \pm 0.16 ,$$

$$\tilde{\beta} + \frac{\tilde{\delta}}{3} = 0.31 \pm 0.51 .$$

Further experimental information is needed to determine the coupling constants individually.

Figure 4 shows the measured asymmetry as a function of y. The authors compare their results with the predictions of two gauge models, which differ in the assignment of the right-handed electron. In the standard model, right-handed quarks and leptons are placed in singlets. In the hybrid model, invented to explain the absence of parity violation in heavy atoms[25-26], the right-handed electron is placed in a doublet with a hypothesized neutral heavy lepton E^0, making the electronic current pure vector. As can be seen from Fig. 4, the data support the standard model predicting a small value of the slope a_2 with currently accepted values of $\sin^2\theta_W$, whereas the hybrid model predicting a large slope and an intercept $a_1 = 0$ appears to be ruled out.

The value of $\sin^2\theta_W$ as determined from a_1 and a_2 is $\sin^2\theta_W = 0.224 \pm 0.020$, where the error includes about equal contributions from statistical and systematic sources. The

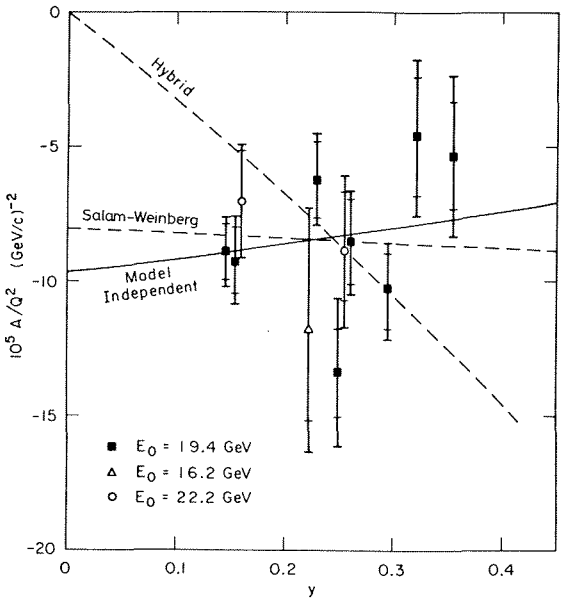

Fig. 4 Asymmetry of polarized electron scattering on deuterium as a function of the inelasticity $y = (E_e - E'_e)/E_e$. (Figure from Ref. 22.)

excellent agreement of this value of $\sin^2\theta_W$ with values determined in neutrino experiments is a great success for the standard model.

The interpretation of this experiment in terms of $\sin^2\theta_W$ depends on the validity of the quark-parton model, which is not likely to describe accurately the inelastic electron scattering at $Q^2 \sim 1$ GeV^2. To account for this theoretical uncertainty, the authors[22] allow an additional uncertainty of ±0.01 in the determination of $\sin^2\theta_W$, which is about comparable to the experimental error. Radiative corrections have been applied in the analysis. They do not produce an asymmetry but they change the effective values of y and Q^2.

The experimental error is not likely to be improved substantially. An extension of the measurements to large y appears impossible owing to an increasing pion contamination in the scattered electron yield, and the amount of running time is already such that it cannot be increased by a sizeable factor.

3.2 Parity-violating optical transitions in heavy atoms

The electronic current can also be studied in optical transitions between atomic levels. The existence of a parity-violating potential between the electron and the quarks in the atomic nucleus, due to weak neutral currents, implies that the atomic levels are not pure eigenstates of parity. They receive a small admixture of opposite parity which causes a mixture of electric and magnetic dipole transitions. Their interference causes a rotation of the polarization plane of a laser beam, or a different absorption of right- or left-circularly polarized laser light.

Parity violation in heavy atoms is primarily sensitive to the weak neutral charge[27] which is given in the notation of Hung and Sakurai[24] by

$$Q = -\tilde{\alpha}(Z - N) - 3\tilde{\gamma}(Z + N) \ ,$$

which depends only on the product of the axial electron current and the hadronic vector current.

The experimental situation on parity violation in atoms is not satisfactory. The experiments carried out at Seattle[25] and Oxford[26] measuring the rotation of the polarization plane of laser light going through bismuth vapour, showed essentially null results, with small statistical errors. A Novosibirsk team[28], however, reported evidence for a non-zero result in Bi, being consistent with the standard model prediction. Barkov[29] reported to this conference a new result of this team. The ratio of the experimental to the theoretical rotation (standard model with $\sin^2\theta_W = 0.25$) is 1.07 ± 0.14, which is clearly incompatible with parity conservation. Note that the Novosibirsk experiment is carried out on the same optical transition as the Oxford experiment, with conflicting results.

Recently, another experiment carried out at Berkeley[30] also reports parity violation observed in atomic thallium, although the effect has only a 2σ significance. The authors hope to improve the accuracy substantially in the near future.

The results of the four existing experiments are summarized in Table 7. The agreement is poor. All experiments are continuing to take data.

Table 7

Summary of experiments on parity violation in atoms

Experiment	Atom	Transition (nm)	R a)
Seattle[25]	Bi	876	0.0 to 0.2
Oxford[26]	Bi	648	0.0 to 0.1
Novosibirsk[29]	Bi	648	1.07 ± 0.14
Berkeley[30]	Tl	293	$2.3 \begin{smallmatrix}+3.1\\-1.4\end{smallmatrix}$

a) Ratio of the experimental result to the prediction of the standard model, with reasonable values of $\sin^2\theta_W$.

3.3 The coupling constants for electron-quark scattering

It is difficult to choose between the conflicting experimental results in order to determine the eq coupling constants. Tentatively, we go along with the positive results from the Novosibirsk and Berkeley groups and hope that the future development will justify this step (it cannot be justified at present on clear-cut experimental grounds).

Following Hung and Sakurai[24], we compare the weak neutral charges for the Bi and Tl nuclei

$$Q(\mathrm{Bi}) = 43\tilde{\alpha} - 627\tilde{\gamma}$$

and

$$Q(\mathrm{Tl}) = 42\tilde{\alpha} - 612\tilde{\gamma}$$

to the measured values[29-30]

$$Q(Bi) = -140 \pm 40$$

and

$$Q(Tl) = -280 \pm 140 \ .$$

It should be noted that the experimental error of the Novosibirsk experiment (see Table 7) allows a smaller error on Q(Bi), but the theoretical uncertainty of 15 to 20% in the atomic physics calculation of Bi [31] requires the quoted error for Q(Bi).

The SLAC polarized electron scattering experiment and the atomic physics experiments define nearly orthogonal linear relations between $\tilde{\alpha}$ and $\tilde{\gamma}$, as shown in Fig. 5. The domain in the $\tilde{\alpha}$, $\tilde{\gamma}$ plane which satisfies all experiments is given by

$$\tilde{\alpha} = -0.72 \pm 0.25$$

$$\tilde{\gamma} = \ 0.36 \pm 0.28 \ .$$

Both coupling constants agree with the prediction of the standard model for $\sin^2\theta_W = 0.23$.

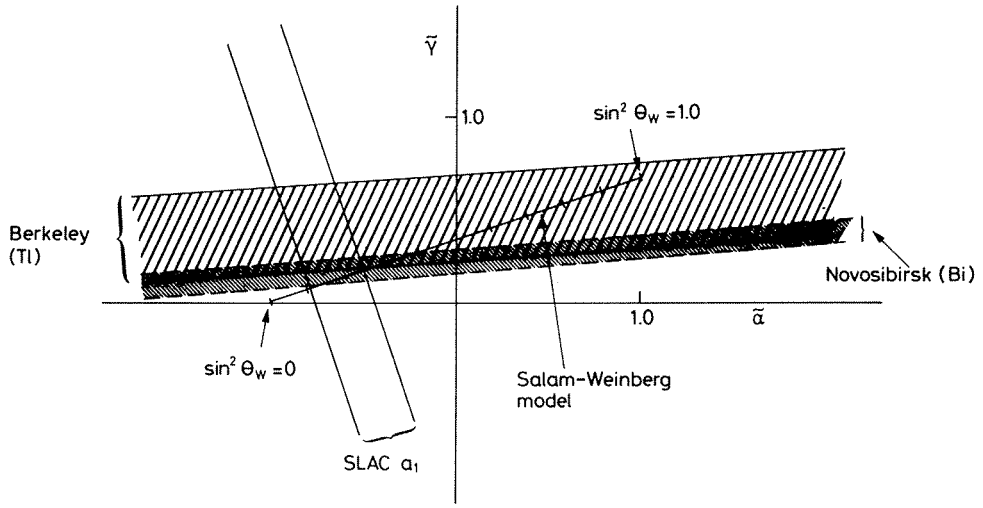

Fig. 5 Domains in the $\tilde{\alpha}$, $\tilde{\gamma}$ plane allowed by polarized electron scattering and atomic physics experiments (figure from Ref. 24)

A separation of the coupling constants $\tilde{\beta}$ and $\tilde{\delta}$ is not yet possible in a model-independent way.

In a single Z-boson model, only seven independent parameters denoting the coupling strengths of $u_{L,R}$, $d_{L,R}$, $e_{L,R}$, and ν_L are needed, compared to the 10 coupling parameters which appear in the Sakurai tetragon (Fig. 1). As pointed out by Hung and Sakurai[32], there must be three independent "factorization relations" among the 10 constants. They may be taken to be[24]

$$\frac{\tilde{\gamma}}{\tilde{\alpha}} = \frac{\gamma}{\alpha} \ , \quad \frac{\tilde{\delta}}{\tilde{\beta}} = \frac{\delta}{\beta} \ , \quad \frac{g_V}{g_A} = \frac{\alpha\tilde{\beta}}{\tilde{\alpha}\beta} \ .$$

A combination of these three relations gives

$$\frac{g_V}{g_A} = \frac{(\alpha + \gamma/3)(\tilde{\beta} + \tilde{\delta}/3)}{(\tilde{\alpha} + \tilde{\gamma}/3)(\beta + \delta/3)} \ ,$$

which can be tested in the g_V, g_A plane. Using the ratio a_2/a_1 as determined in the SLAC experiment[22], $a_2/a_1 = -0.50 \pm 0.74$, and using the results for α, β, γ, and δ given in Section 4, we can draw the allowed region in the g_V, g_A plane (see Fig. 3). As a consequence, the vector dominant solution for g_V, g_A appears to be ruled out, yielding the unique solution for g_V and g_A quoted in Table 6. Once more, this is the solution which is in good agreement with the standard model with $\sin^2\theta_W = 0.23$.

4. NEUTRINO SCATTERING ON QUARKS

4.1 The reaction $\bar{\nu}_e + d \to \bar{\nu}_e + p + n$

Recently, a 4σ signal of the weak disintegration of the deuteron via a neutral current, $\bar{\nu}_e + d \to \bar{\nu}_e + p + n$, has been reported by an Irvine group[33]. A well-shielded target of 268 kg D_2O was exposed to the high $\bar{\nu}_e$ flux originating from the Savannah River fission reactor. The reaction was identified via knock-on neutrons.

The process under consideration is, because of the low energy involved, essentially forbidden for vector-type (Fermi) interactions[34]. It proceeds only via the axial vector (Gamow-Teller) interaction and is therefore independent of the Weinberg angle, in the framework of the standard model. The reported cross-section is

$$(3.8 \pm 0.9) \times 10^{-45} \text{ cm}^2 ,$$

in agreement with the prediction of the standard model, 5.0×10^{-45} cm^2. The experiment is being continued to reduce the statistical error, which is claimed to dominate the uncertainties.

4.2 Inclusive neutral-current reactions on isoscalar targets

Inclusive neutral-current reactions on (nearly) isoscalar targets allow the most precise measurement of neutral current couplings. The measured quantities are the ratios of the inclusive neutral-to-charged-current cross-sections R_ν and $R_{\bar{\nu}}$. A study of the y-distribution ($y = E_{had}/E_\nu$) has given information on the space-time structure of hadronic neutral currents. A comparison of the results of different experiments can be found in Ref. 1. The hadronic neutral current on isoscalar targets is known to be dominated by V-A, with a small ($\sim$ 10%) admixture of V+A. Thus the current is neither pure in parity nor in chirality. It should be noted, however, that the V+A admixture has been seen so far only at a 4σ level by the CERN-Dortmund-Heidelberg-Saclay (CDHS) experiment[35]. It is an experimental challenge to improve the significance of the V+A contribution and to rule out a pure V-A structure of the hadronic current. The most sensitive place to look for this is the $\bar{\nu}$ y-distribution which at large y receives about equal contributions from V-A scattering from the antiquark content and from V+A scattering from the quark content of the nucleon. New results on the y-distribution from data obtained at CERN in a narrow-band beam exposure can be expected this autumn.

A new dimension in the study of the hadronic neutral current is opened up by the coming into operation of large devices capable of measuring the hadronic energy flow and thus determining the nucleon structure function via neutral currents.

The simplest and most precisely measurable quantities are R_ν and $R_{\bar{\nu}}$. The precision of $\sin^2\theta_W$, as determined in neutrino experiments, is essentially given by R_ν. It therefore seems appropriate to discuss in more detail the problems, both experimental and theoretical, of the measurement of R_ν and $R_{\bar{\nu}}$.

4.2.1 Experimental problems

The precision measurement of R_ν and $R_{\bar{\nu}}$ is a domain of counter experiments because large event numbers are important. The dominant sources of systematic errors are for R_ν the K_{e3} correction (ν_e from K_{e3} decays fake neutral-current events in a calorimeter detector) and the high-y charged-current background for neutral-current events. The latter correction is due to charged-current events where the muon is hidden in the hadronic shower. This is visualized in Fig. 6, where the maximum penetration length in Fe is plotted for the new CDHS data. Here a fine-grain calorimeter such as the CHARM detector offers an advantage since the minimum muon track length can be much reduced. At present, a limit of ±0.005 in the accuracy of R_ν, mostly due to uncertainties in the parent π/K ratio showing up in the K_{e3} correction, seems appropriate. This corresponds to a limit in accuracy for $\sin^2\theta_W$ of ±0.008.

The main source of uncertainty for $R_{\bar{\nu}}$ is the "wide-band" background arising from the decay of π's or K's before sign and momentum selection. This background is determined experimentally in separate "closed collimator" runs and statistically subtracted (see Fig. 6), which requires a precise knowledge of the relevant fluxes. The "new source" which has been discovered in the CERN beam dump experiments[36], and which is presumably due to a prompt neutrino flux from semileptonic charm decay, is automatically subtracted with this method.

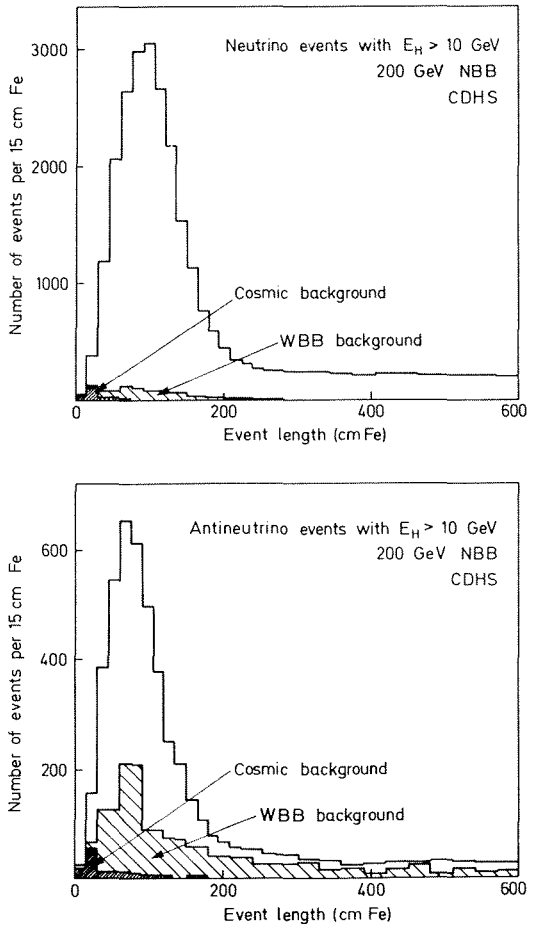

Fig. 6 Penetration length in Fe for ν and $\bar{\nu}$ events (CDHS data)

At present, a precision of ±0.015 for $R_{\bar{\nu}}$ seems within reach. This number is important as a check for the validity of the standard model, which predicts $R_{\bar{\nu}}$ once $\sin^2\theta_W$ is known from R_ν. However, $R_{\bar{\nu}}$ is not useful for a determination of $\sin^2\theta_W$ since $R_{\bar{\nu}}$ is very much independent of $\sin^2\theta_W$ around $\sin^2\theta_W = 0.23$.

4.2.2 Theoretical problems

The experimental information is of such a high precision that theoretical uncertainties in the analysis start to be of the same magnitude as the experimental errors. In this section we discuss the problems of radiative corrections, scaling violations, uncertainties in the sea, and elastic and quasi-elastic events. We restrict the discussion to y-distributions and to R_ν and $R_{\bar{\nu}}$, since structure functions (x-distributions) from neutral-current scattering are measured so far with low precision.

As long as the measurement of the hadronic energy is "electromagnetically" inclusive, as is the case in calorimeter targets (the final hadronic state comprises both hadrons and photons), only the radiative correction due to the lepton leg is to be considered in the "leading-log" approximation[37]. This correction is obviously different for neutral- and charged-current scattering and is expected to be in specific kinematical domains such as large y at the level of $\alpha/\pi \cdot \ln (Q^2/m_\mu^2) \sim$ several percent. This starts to be relevant for the experimental subtraction of the high-y charged-current background in the neutral-current sample (see Fig. 6) for the determination of R_ν and $R_{\bar{\nu}}$, and for a study of the space-time structure from the difference of the neutral- and charged-current y-distributions. Fortunately, the only relevant $\bar{\nu}$ y-distribution is less affected by radiative corrections at large y than is the ν y-distribution[37] (this holds for charged currents, whereas neutral currents need not be corrected).

Experimentalists have ignored the radiative correction problem up to now. Future precision experiments ought to worry about it.

In the analysis of hadronic neutral currents, the quark-parton model is employed. Gentle deviations from scaling, consistent with expectations from QCD, are established[38]. As a consequence of the slight changes in the amount of valence- and sea-quarks, and of the difference in the charged and neutral coupling to various quark flavours, scaling violation effects are to be considered for high-precision neutral-current work.

Fortunately, the effects of scaling violation are not very important at the present level of precision. Buras and Gaemers[39] and the Aachen-Bonn-CERN-London-Oxford-Saclay (ABCLOS) (BEBC) Collaboration[40] have shown, employing the Buras-Gaemers parametrization[39] of scaling violations with $\Lambda \sim 0.5$ GeV, that the effects at SPS and FNAL energies are small: R_ν changes by < 0.002 compared to a quark-parton model analysis, at $\sin^2\theta_W = 0.23$. Hence the determination of $\sin^2\theta_W$ is virtually unaffected by scaling violations.

On the contrary, $R_{\bar{\nu}}$ is more affected by scaling violations. They reduce $R_{\bar{\nu}}$ by typically 0.015, which is not negligible compared to the experimental error. This means that for future interpretations of $R_{\bar{\nu}}$ in terms of theoretical models, scaling violations ought to be taken into account.

The uncertainty in the amount of sea-quarks in the nucleon and in its flavour composition is in first approximation also irrelevant for the interpretation of R_ν (hence also for the

determination of $\sin^2\theta_W$). However, $R_{\bar{\nu}}$ changes by about ±0.01 if the relative amounts of all antiquarks and the strange antiquarks are changed within reasonable limits around the central values[38]:

$$\frac{\int x(\bar{u} + \bar{d} + 2\bar{s})dx}{\int x(u + d)dx} = 0.18$$

and

$$\frac{\int x2\bar{s}dx}{\int x(u + d)dx} = 0.03 .$$

In these estimates the coupling of the different quark flavours to the neutral current has been taken as predicted by the standard model, since there is no experimental information on the s-quark coupling.

We may conclude from this discussion that there is no point in substantially improving the measurement of $R_{\bar{\nu}}$ for a high-precision check of the standard model, without at the same time improving the precision of our knowledge of the nucleon structure.

Elastic and quasi-elastic events are not accounted for in the quark-parton model. They may confuse the comparison with the standard model at few GeV energies, but this should not matter very much at high energies. All neutral-current experiments require a minimum amount of hadronic energy. This cut removes essentially the elastic and quasi-elastic events from the sample, and the comparison with the standard model should be done with the same cut applied. This method, employing the quark-parton model with scaling violations, radiative corrections, and the correct quark structure of the nucleon, works well and yields a precise value for $\sin^2\theta_W$ derived from $R_\nu(E_{had} > E_{had}^{min})$. As an alternative, a model-independent method has been proposed by Paschos and Wolfenstein[41] long ago:

$$\frac{\sigma_\nu^{NC} - \sigma_{\bar{\nu}}^{NC}}{\sigma_\nu^{CC} - \sigma_{\bar{\nu}}^{CC}} = \frac{1}{2} - \sin^2\theta_W ,$$

where the total cross-sections may be replaced by a partial cross-section representing any kinematical domain. Hence experimental data need not be corrected for losses due to selection criteria. In practice, however, there are some problems to be overcome: since neutrino experiments use a continuous energy spectrum of incident particles, equal flux shapes for ν and $\bar{\nu}$ and the same energy-dependence of the cross-sections are necessary. This forbids the application at the threshold of a new quark flavour.

4.2.3 New experimental results

Preliminary new values of R_ν and $R_{\bar{\nu}}$ have recently been reported from the CERN-Dortmund-Heidelberg-Saclay (CDHS)[42] and CERN-Hamburg-Amsterdam-Rome-Moscow (CHARM)[43] Collaborations. The CHARM Collaboration uses a fine-grain calorimeter consisting of marble plates alternating with planes of drift-tubes and scintillators, which came into operation one year ago. The fiducial target mass of the CDHS detector is larger by a factor of 5, but the granularity of the CHARM detector and its construction allows some corrections to the neutral-current signal to be significantly reduced. The new results are consistent with the previous world average, as shown in Table 8.

Table 8

Experimental results on R_ν and $R_{\bar{\nu}}$

Experiment	R_ν a)	E_{had} cut	$R_{\bar{\nu}}$ a)	E_{had} cut
CDHS[42] prelim.	0.307 ± 0.008 (0.003)	10 GeV	0.373 ± 0.025 (0.014)	10 GeV
CHARM[43] prelim.	0.30 ± 0.02 (0.006)	∿ 8 GeV	0.39 ± 0.02 (0.014)	∿ 5 GeV
Previous average[1]	0.29 ± 0.01	None	0.35 ± 0.025	None

a) The statistical error is given in brackets.

Both new results are in good agreement with the standard model, as shown in Fig. 7. The CDHS result for $\sin^2\theta_W$, determined from the Paschos-Wolfenstein formula[41], is $\sin^2\theta_W$ = = 0.228 ± 0.018, which is in good agreement with the previous world average[1] $\sin^2\theta_W$ = = 0.23 ± 0.02.

In terms of the chiral coupling constants, R_ν and $R_{\bar{\nu}}$ can be used to extract[5] the combinations $u_L^2 + d_L^2$ and $u_R^2 + d_R^2$, respectively. This extraction from R_ν and $R_{\bar{\nu}}$ is independent of a possible violation of the Callan-Gross relation provided it is the same for neutral and charged currents.

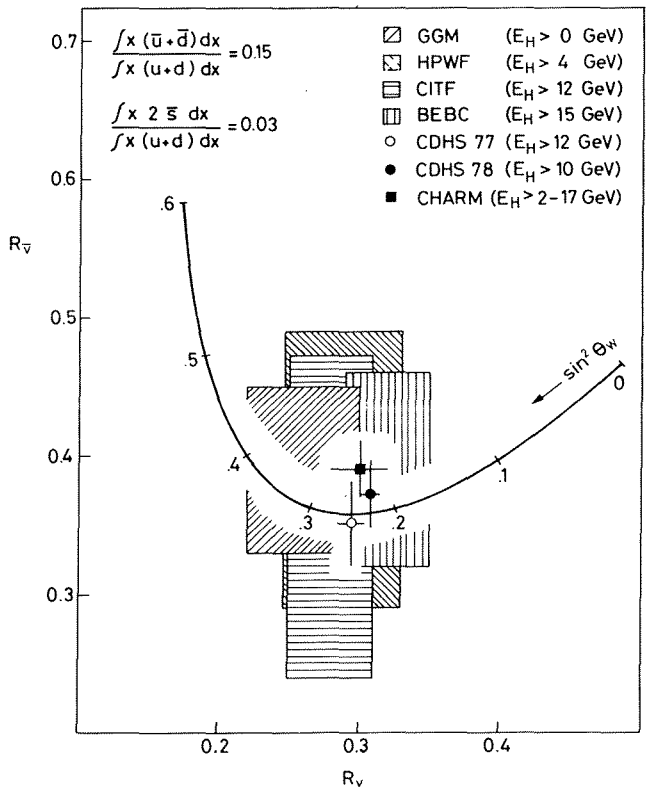

Fig. 7 Comparison of the results of various experiments on R_ν and $R_{\bar{\nu}}$ with the Salam-Weinberg model. The dimension of the rectangles indicate the error bars for R_ν and $R_{\bar{\nu}}$. The theoretical curve is drawn for the experimental conditions of the CDHS experiment. Corrections for scaling violation or radiative effects are not applied.

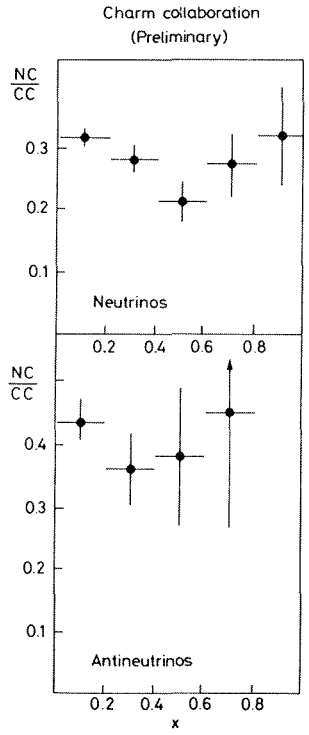

Fig. 8 Ratio of neutral-to-charged-current events as a function of x (figure from Ref. 43)

A first attempt to explore the structure function of the nucleon with neutral currents has been reported by the CHARM Collaboration[43]. Figure 8 shows their measured ratio of neutral-to-charged-current events as a function of the Bjorken variable x. For both neutral and charged currents, x has been determined from the hadronic energy flow. Although this result is preliminary and only a first step, it may be concluded that there is no large anomaly in the nucleon structure as determined by neutral currents. A qualitatively similar result, based on much smaller statistics, has recently been reported by a Columbia-Rutgers-Stevens group[44].

In the standard model, the hadronic neutral current conserves flavour by construction. A search for charm-changing reactions of the type

$$\bar{\nu} + N \to \bar{\nu} + C \quad \text{with} \quad C \to e^+ + \nu_e + \text{anything}$$

was carried out by a Fermilab-Michigan-Moscow-Serpukhov group[45]. The detector was the FNAL 15′ bubble chamber filled with a heavy neon mixture and exposed to a $\bar{\nu}$ wide-band beam. Only one candidate for a $\Delta C = 1$ neutral current was found, yielding an upper limit

$$\frac{\sigma(\text{charm-changing neutral current})}{\sigma(\text{all neutral currents})} < \frac{0.87 \times 10^{-3}}{0.38 \times 0.1} = 2.3\%$$

at the 90% confidence limit (where a semileptonic branching ratio of the charmed particle of 0.1 is assumed). This upper limit is similar in accuracy to a corresponding earlier limit for ν-induced charm-changing neutral currents[46].

4.3 Inclusive neutral-current reactions on protons

Owing to the different quark content of the proton compared to an isoscalar target, a measurement of R_ν^p and $R_{\bar\nu}^p$, the cross-section ratios of neutral-to-charged currents on a proton target, together with a measurement of R_ν and $R_{\bar\nu}$, allows a separate determination of u_L^2, d_L^2, u_R^2, and d_R^2. Previous attempts[47] to measure R_ν^p and $R_{\bar\nu}^p$ did not put stringent constraints on the coupling constants owing to lack of precision.

Neglecting the sea of $q\bar{q}$ pairs in the nucleon, the neutral-current coupling strength is given by $2u_L^2 + d_L^2$ for neutrinos, in contrast to $u_L^2 + d_L^2$ on an isoscalar target. The Aachen-Bonn-CERN-Munich-Oxford (ABCMO) (BEBC) Collaboration has just completed a measurement[48] of R_ν^p with BEBC filled with hydrogen exposed to a ν wide-band beam. Details of this measurement are found in the talk of L. Pape given at this conference.

The result is $R_\nu^p = 0.52 \pm 0.04$, where a cut $p_T^{had} > 1.9$ GeV/c is applied. This cut was found to provide a clean sample of neutral-current events. The interpretation of the result in terms of the coupling constants u_L^2 and d_L^2 is seen in Fig. 9. The intersect of the allowed domains for u_L^2 and d_L^2 yields

$$u_L^2 = 0.15 \pm 0.05$$

and

$$d_L^2 = 0.16 \pm 0.07 \ .$$

The result is consistent with the standard model, but requires a value of $\sin^2\theta_W = 0.18 \pm 0.03$ being somewhat lower than the currently accepted value.

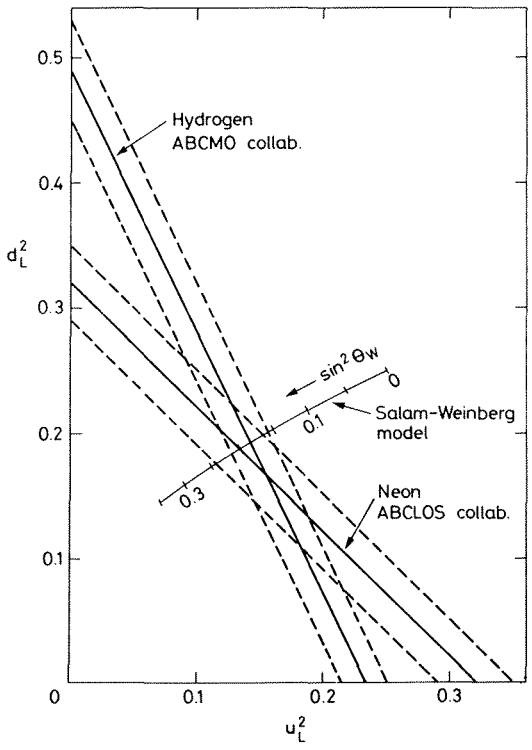

Fig. 9 Domains in the u_L^2, d_L^2 plane allowed by measurements of R_ν and R_ν^p (figure from Ref. 48)

4.4 Charge ratios of final-state hadrons

The analysis of charge ratios of final-state hadrons provides another way to disentangle u_L^2, d_L^2, u_R^2, and d_R^2. This method rests on the assumption that the composition of the hadronic system reflects in the "current fragmentation region" the flavour of the struck quark. As is visualized in Fig. 10 for neutrinos, the charged and neutral currents couple with different strengths to the quarks of an isoscalar target:

charged current: transforms $d \to u$ with coupling strength 1;

neutral current: couples with strength $u_L^2 + \frac{1}{3} u_R^2$ to u quarks and with $d_L^2 + \frac{1}{3} d_R^2$ to d quarks.

Further necessary ingredients are the fragmentation functions $D_q^{\pm}(z)$, which denote the probability for the quark q to give a positive or a negative hadron which carries a fraction z of the quark energy. Neglecting again for simplicity the sea of $q\bar{q}$ pairs in the nucleon, we get for the charge ratios of final-state hadrons in ν-induced reactions on isoscalar targets:

$$\frac{h^+}{h^-} = \frac{\left(u_L^2 + \frac{1}{3} u_R^2\right) D_u^+ + \left(d_L^2 + \frac{1}{3} d_R^2\right) D_d^+}{\left(u_L^2 + \frac{1}{3} u_R^2\right) D_u^- + \left(d_L^2 + \frac{1}{3} d_R^2\right) D_d^-} .$$

($L \leftrightarrow R$ for $\bar{\nu}$-induced reactions). The fragmentation functions can be determined from charged-current ν and $\bar{\nu}$ reactions. The positive and negative hadrons are predominantly pions, but kaons and protons are included in the data sample since in a bubble chamber the particles cannot be distinguished at momenta > 1 GeV/c.

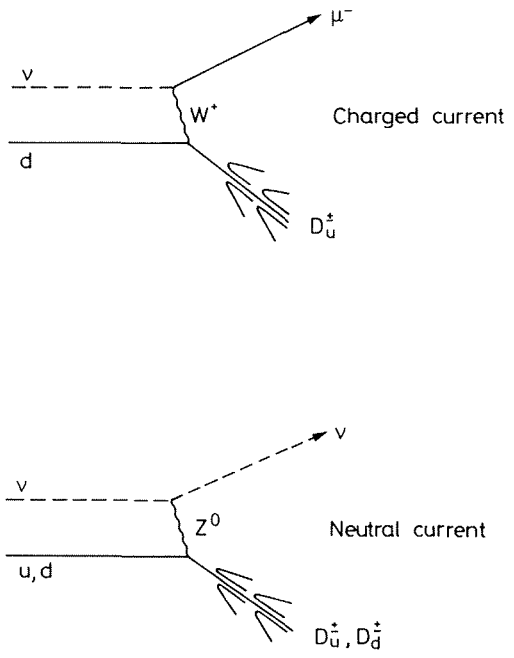

Fig. 10 Fragmentation of quarks struck by charged and neutral currents in ν and $\bar{\nu}$ reactions

The Aachen-Bonn-CERN-Demokritos-London-Oxford-Saclay (ABCDLOS) (BEBC) group[49] has reported a recent determination of h^+/h^- ratios at large z. They used BEBC filled with a heavy-neon mixture and exposed to ν and $\bar{\nu}$ narrow-band beams. From 300 ν and 140 $\bar{\nu}$ neutral-current events they deduce, together with the knowledge of $u_L^2 + d_L^2$ and $u_R^2 + d_R^2$ as determined in an earlier experiment[40],

$$u_L^2 = 0.11 \pm 0.05 \qquad d_L^2 = 0.21 \pm 0.05$$
$$u_R^2 = 0.01 \pm 0.03 \qquad d_R^2 = 0.03 \pm 0.03 \ .$$

The coupling constants are in agreement with the predictions of the standard model for $\sin^2\theta_W = 0.23$.

Sehgal[5] was the first to determine the squares of the individual coupling constants, employing π^+/π^- ratios measured in the fragmentation region of low-energy GGM data[50]. Since the validity of the quark fragmentation model may be questioned there, the confirmation of his earlier conclusions with high-energy data is gratifying. Still, one should not overestimate the systematic precision of the measurement of final-state charge ratios: the event selection is difficult, and corrections for various backgrounds are large.

The final-state charge ratios as determined in the ABCDLOS experiment are given in Table 9. The result for $\bar{\nu}$-induced hadrons agrees well with a recent measurement from the Fermilab-Michigan-Moscow-Serpukhov (FMMS) Collaboration[45] performed in the FNAL 15′ bubble chamber filled with a heavy-neon mixture and exposed to a $\bar{\nu}$ wide-band beam.

Table 9

Recent measurements of positive-to-negative final-state charge ratios

Experiment	$(h^+/h^-)_\nu$	$(h^+/h^-)_{\bar{\nu}}$
ABCDLOS[49]	1.07 ± 0.17 $(z > 0.3)$	1.54 ± 0.45 $(z > 0.3)$
FMMS[45]	-	1.60 ± 0.27 $(0.3 < z < 0.9)$

4.5 The coupling constants for neutrino-quark scattering

The concept of fitting the coupling constants of the most general Lagrangian to experimental data was pioneered by Hung and Sakurai, Sehgal, and Abbott and Barnett. This work resulted, in 1978, in the first complete set of neutral-current coupling constants[1,2,5], employing inclusive and semi-inclusive data from isoscalar targets, elastic scattering on protons, inclusive scattering on protons, and single-pion production.

Since then, many other authors have contributed to this field. Recently, Liede and Roos[51] and Langacker et al.[52] presented the results of global fits to all available neutral-current data. The fit gives a reasonable χ^2, which is rather surprising since the experimental errors quoted by the various experiments are presumably not Gaussian. All (but two) experimental results of the last two years are in good agreement with each other and with the standard model. Thus one single parameter, $\sin^2\theta_W$, is able to describe a host of experimental results. Properly adjusted small modifications of the standard model

(extension of the Higgs doublet, right-handed doublets of weak isospin, more than one Z) cannot be ruled out, but the standard model is at present sufficient.

Table 10 gives a summary of the best-fit values[24,52] for the neutral-current coupling constants. The fit did not yet include the very recent measurements on R_ν, $R_{\bar{\nu}}$, and R^p_ν.

The central value of $\sin^2\theta_W$ which best describes all data is the same as that of last year[1], but the error has decreased:

$$\sin^2\theta_W = 0.230 \pm 0.015 \ .$$

The central value is rounded in the last digit and represents a compromise between 0.229 ± 0.014 [51], 0.232 ± 0.009 [52] (this fit value includes the new results), and 0.228 ± 0.018 from the new CDHS measurement of R_ν (see Section 4.2). The quoted error on $\sin^2\theta_W$ contains an estimate of the systematic error from theoretical uncertainties as discussed in Section 4.2.

Table 10

Neutral-current coupling constants

Coupling constant	Best-fit value	Ref.	Salam-Weinberg model	For $\sin^2\theta_W = 0.23$
u_L	0.32 ± 0.03	52	$\frac{1}{2} - \frac{2}{3}\sin^2\theta_W$	0.347
d_L	-0.43 ± 0.03		$-\frac{1}{2} + \frac{1}{3}\sin^2\theta_W$	-0.423
u_R	-0.17 ± 0.02		$-\frac{2}{3}\sin^2\theta_W$	-0.153
d_R	-0.01 ± 0.05		$\frac{1}{3}\sin^2\theta_W$	0.077
α	0.58 ± 0.14	24	$1-2\sin^2\theta_W$	0.540
β	0.92 ± 0.14		1	1
γ	-0.28 ± 0.14		$-\frac{2}{3}\sin^2\theta_W$	-0.153
δ	0.06 ± 0.14		0	0
$\tilde{\alpha}$	-0.72 ± 0.25	24	$-1 + 2\sin^2\theta_W$	-0.540
$\tilde{\beta}$			$-1 + 4\sin^2\theta_W$	-0.080
$\tilde{\gamma}$	0.36 ± 0.28		$\frac{2}{3}\sin^2\theta_W$	0.153
$\tilde{\delta}$			0	0
g_V	0.06 ± 0.08		$-\frac{1}{2} + 2\sin^2\theta_W$	-0.040
g_A	-0.52 ± 0.06		$-\frac{1}{2}$	-0.500

In the standard model, the $W^{\pm}$ and Z^0 masses are related by $\rho = M_W^2/M_Z^2 \cos^2\theta_W = 1$. If we extend the standard model so as to include two Higgs doublets, ρ becomes a parameter to be determined by experiment. The simultaneous fit of ρ and $\sin^2\theta_W$ to all data yields[53]

$$\sin^2\theta_W = 0.235 \pm 0.030$$

and

$$\rho = 1.00 \pm 0.03 ,$$

where again theoretical uncertainties have been included in the quoted errors. Hence the extension of the Higgs sector does not seem to be necessary.

5. SUMMARY AND OUTLOOK

i) All (but two) more recent experimental results are consistent with each other.

ii) The Salam-Weinberg model gives a good description of all (but two) experimental results, with only one free parameter: $\sin^2\theta_W = 0.230 \pm 0.015$.

iii) Eight out of the ten phenomenological parameters governing νe, eq, and νq scattering are determined from data. All of them are consistent with the predictions of the Salam-Weinberg model with $\sin^2\theta_W = 0.23$.

iv) The experimental precision has reached such a level that theoretical uncertainties in the data analysis can no longer be ignored.

v) For the immediate future it is still worth while to improve the experimental accuracy. The experimental challenges are: a better determination of the V+A admixture on isoscalar targets; a better determination of the isoscalar-isovector interference (inclusive cross-section ratios on proton and neutron targets, charge ratios in final states); a study of the structure function for neutral currents; and a better determination of $\bar{\nu}_\mu e$ scattering.

vi) A new dimension of neutral current physics is opened up with the advent of high-energy colliding machines. The first step is the detection of the forward-backward asymmetry in $e^+e^- \to \mu^+\mu^-$ due to weak and electromagnetic interference. The big challenge is to find $W^{\pm}$ and Z^0 at the predicted masses, and to find the Higgs boson with its peculiar coupling properties.

Acknowledgement

I wish to thank Prof. K. Kleinknecht for a critical reading of the manuscript.

REFERENCES

1) C. Baltay, Proc. Int. Conf. on High-Energy Physics, Tokyo, 1978 (Physical Society of Japan, Tokyo, 1979), p. 882.

2) J.J. Sakurai, Proc. Topical Conf. on Neutrino Physics at Accelerators, Oxford, 1978 (Rutherford Laboratory, Chilton, Didcot, 1978), p. 338.

3) J.J. Sakurai, Proc. Int. Conf. on Neutrino Physics and Neutrino Astrophysics, Baksan Valley, USSR, 1977 (Nauka, Moscow, 1978), Vol. 2, p. 242.

4) P.Q. Hung and J.J. Sakurai, Phys. Lett. 63B, 295 (1976).

5) L.M. Sehgal, Proc. "Neutrino-78", Int. Conf. on Neutrino Physics, Purdue Univ., 1978 (Purdue University, West Lafayette, Indiana, 1978), p. 253.

6) A. Salam, Proc. 8th Nobel Symposium, Aspenäsgården, 1968 (Almqvist and Wiksell, Stockholm, 1968), p. 367.

7) S. Weinberg, Phys. Rev. Letters 19, 1264 (1967); Phys. Rev. D 5, 1412 (1972).

8) S.L. Glashow, J. Iliopoulos and L. Maiani, Phys. Rev. D 2, 1285 (1970).

9) E. Fiorini, Low-energy weak interactions, Review talk given at the "Neutrino-79", Int. Conf. on Neutrinos, Weak Interactions and Cosmology, Bergen, 1979.

10) J. Blietschau et al., Nucl. Phys. B114, 189 (1976); Phys. Lett. 73B, 232 (1978).

11) H. Faissner et al., Phys. Rev. Lett. 41, 213 (1978).

12) P. Alibran et al., High-energy elastic ν_μ scattering off electrons in Gargamelle, preprint CERN-EP/79-38 (1979).

13) A.M. Cnops et al., Phys. Rev. Lett. 41, 357 (1978).

14) A. Rosanov, talk given at this Conference (Abstract No. 235).

15) P. Alibran et al., Phys. Lett. 74B, 422 (1978).

16) D. Bertrand et al., An upper limit to the cross-section for the reaction $\bar{\nu}_\mu e^- \to \bar{\nu}_\mu e^-$ at SPS energies, preprint PITHA 79/07 (1979).

17) J.P. Berge et al., A search at high energies for antineutrino-electron elastic scattering, preprint Fermilab Pub 79/27-EXP (1979).

18) N. Armenise et al., Phys. Lett. 81B, 385 (1979).

19) G. 't Hooft, Phys. Lett. 37B, 195 (1971).

20) F. Reines, H.S. Gurr and H.W. Sobel, Phys. Rev. Lett. 37, 315 (1976).

21) C.Y. Prescott et al., Phys. Lett. 77B, 347 (1978).

22) C.Y. Prescott et al., Further measurements of parity non-conservation in inelastic electron scattering, preprint SLAC Pub 2319.
C.Y. Prescott, talk given at this Conference (Abstract No. 242).

23) J.D. Bjorken, Phys. Rev. D 18, 3239 (1978).

24) P.Q. Hung and J.J. Sakurai, Evidence for factorization and coupling constant determination in neutral-current processes, preprint UCLA/79/TEP/9.
J.J. Sakurai, talk given at "Neutrino-79", Int. Conf. on Neutrinos, Weak Interactions and Cosmology, Bergen, 1979.

25) L.L. Lewis et al., Phys. Rev. Lett. 39, 795 (1977).

26) P.E.G. Baird et al., Phys. Rev. Lett. 39, 798 (1977).

27) M.A. Bouchiat and C.C. Bouchiat, Phys. Lett. 48B, 111 (1974).
J. Bernabéu and C. Jarlskog, Nuovo Cimento 38A, 295 (1977).

28) L.M. Barkov and M.C. Zolotorev, JETP Lett. 26, 379 (1978); and Proc. "Neutrino-78", Int. Conf. on Neutrino Physics, Purdue Univ., 1978 (Purdue University, West Lafayette, Indiana, 1978), p. 423.

29) L.M. Barkov, talk given at this Conference.

30) R. Conti et al., Phys. Rev. Letters 42, 343 (1979).

31) V.N. Novikov, O.P. Sushkov and I.B. Khriplovich, Sov. Phys. JETP 44, 872 (1976).

32) P.Q. Hung and J.J. Sakurai, Phys. Letters 69B, 323 (1977).

33) H.W. Sobel, talk given at the "Neutrino-79", Int. Conf. on Neutrinos, Weak Interactions and Cosmology, Bergen, 1979.

34) A. Ali and C.A. Dominguez, Phys. Rev. D 12, 3673 (1975); and references cited therein.

35) M. Holder et al., Phys. Lett. 71B, 222 (1977); 72B, 254 (1977).

36) T. Hansl et al., Phys. Lett. 74B, 139 (1978).
P.C. Bosetti et al., Phys. Lett. 74B, 143 (1978).
P. Alibran et al., Phys. Lett. 74B, 134 (1978).

37) A. De Rújula, R. Petronzio and A. Savoy-Navarro, Nucl. Phys. B154, 394 (1979).

38) R. Turlay, Charged weak currents, Rapporteur's talk given at this Conference.

39) A.J. Buras and K.J.F. Gaemers, Nucl. Phys. B132, 249 (1978); Phys. Lett. 71B, 106 (1977).

40) P.C. Bosetti et al., Phys. Lett. 76B, 505 (1978).
H. Deden et al., Nucl. Phys. B149, 1 (1979).

41) E.A. Paschos and L. Wolfenstein, Phys. Rev. D 7, 91 (1973).

42) C. Geweniger, talk given at the "Neutrino-79", Int. Conf. on Neutrinos, Weak Interactions and Cosmology, Bergen, 1979.

43) A. Rosanov, talks given at this Conference (Abstracts No. 234 and 236).

44) H. French, talk given at the "Neutrino-79", Int. Conf. on Neutrinos, Weak Interactions and Cosmology, Bergen, 1979.

45) B.P. Roe, talk given at the "Neutrino-79", Int. Conf. on Neutrinos, Weak Interactions and Cosmology, Bergen, 1979.

46) M. Holder et al., Phys. Lett. 74B, 277 (1978).

47) F. Harris et al., Phys. Rev. Lett. 39, 437 (1977).
M. Derrick et al., Phys. Rev. D 18, 7 (1978).

48) L. Pape, talk given at this Conference (Abstract No. 93).

49) H. Deden, talk presented at the "Neutrino-79", Int. Conf. on Neutrinos, Weak Interactions and Cosmology, Bergen, 1979.

50) H. Kluttig, J.G. Morfin and W. Van Doninck, Phys. Lett. 71B, 446 (1977).

51) I. Liede and M. Roos, A neutral current evaluation of the standard model, contributed paper to the "Neutrino-79", Int. Conf. on Neutrinos, Weak Interactions and Cosmology, Bergen, 1979, and references cited therein.
M. Roos, talk presented at the "Neutrino-79", Int. Conf. on Neutrinos, Weak Interactions and Cosmology, Bergen, 1979.

52) P. Langacker, talk given at the "Neutrino-79", Int. Conf. on Neutrinos, Weak Interactions and Cosmology, Bergen, 1979.
H.H. Williams, private communication.

53) J.E. Kim, P. Langacker, M. Levine, H.H. Williams and D.P. Sidhu, to be published.

CHARGED WEAK CURRENTS

R. Turlay
CEN Saclay, Gif-sur-Yvette, France.

In this review of charged weak currents I shall concentrate on inclusive high energy neutrino physics. There are surely still things to learn from the low energy weak interaction but I will not discuss it here. Furthermore B. TALLINI will discuss the hadronic final state of neutrino interactions. Since the TOKYO conference a few experimental results have appeared on charged current interaction, I will present them and will also comment on important topics which have been published during the last past year.

The plan of this review is the following :

- General structure of charged current
- New results on total cross-section
- Callan-Gross relation
- Antiquark distribution
- Scaling violations and tests of QCD.

At the end I will give a very short summary on multilepton physics, because I think that it has some obvious connections with charged weak currents.

I. KINEMATICS

A charged current neutrino interaction can be represented by the following graph :

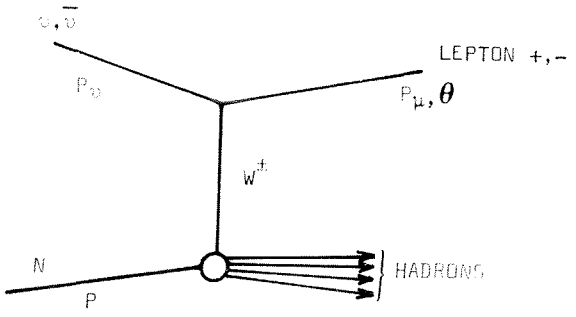

We can calculate the 3 invariants :

s total energy squared
$(p_\nu+p)^2 \simeq 2\ M\ E_\nu$

Q^2 fourth momentum transferred
$-(p_\nu-p_\mu)^2 = 4\ E_\mu E_\nu \sin^2 \frac{\theta}{2}$

$\nu = \frac{P}{M}(p_\nu-p_\mu) \simeq E_h$

and can define the two BJORKEN scaling variables :

$x = \frac{Q^2}{2M\nu}$ $\qquad$ $y = \frac{\nu}{E_\nu}$

An interesting kinematical aspect are the correlations which exist between the variables in the Q^2, ν plot. Figure 1 shows that one has two limitations in measuring the complete x distribution at fixed Q^2 which affect all neutrino experiments :

- for large Q^2 the low x region is missing because of the maximum available neutrino energy,
- for low Q^2 the large x region can be missing if one cannot detect events below a given

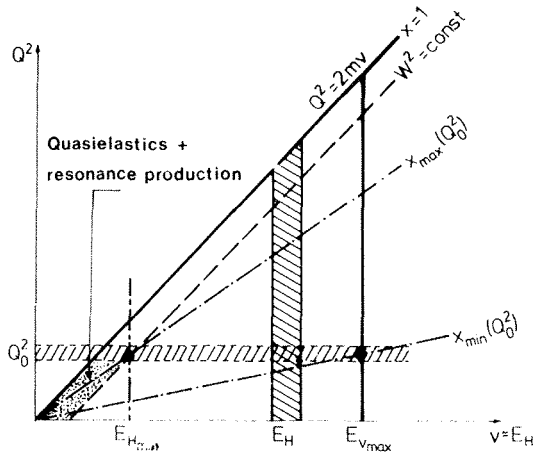

FIG. 1 - Q^2, υ plot and kinematical constraints.

value of E_h. This happens in counter experiments where the experimental resolution in hadron energy becomes poor at low energy.

On the other hand one sees on Figure 1 that the x distribution is complete for a fixed E_h value.

Because of these limitations some analyses on structure functions and particularly on moments of the structure functions have required experimental results from different experiments.

II. GENERAL STRUCTURE OF CHARGED WEAK CURRENT

The cross-section of neutrino nucleon interaction can be calculated assuming :

- the "current-current" form of the Lagrangian
- the V-A theory
- and the local interaction (no propagator effect).

One then obtains :

$$\left.\frac{d^2\sigma}{dQ^2 d\upsilon}\right|_{E_\upsilon} = \frac{G^2 M E_\mu}{2\pi E_\upsilon}\left[W_1^{\upsilon\bar{\upsilon}np}(Q^2,\upsilon)\, 2\sin^2\frac{\theta}{2} + W_2^{\upsilon\bar{\upsilon}np}(Q^2,\upsilon)\cos^2\frac{\theta}{2} \pm W_3^{\upsilon\bar{\upsilon}np}(Q^2,\upsilon)\frac{E_\upsilon + E_\mu}{M}\sin^2\frac{\theta}{2}\right] \qquad (1)$$

The 12 W_i's, structure functions of the nucleon necessary to study the υ, $\bar{\upsilon}$ interaction on neutron and proton, are functions of Q^2 and υ.

There are two new results on the general structure of charged current.

A - Inverse μ-decay GGM experiment [1].

The first observation of the reaction $\upsilon_\mu + e^- \rightarrow \mu^- + \upsilon_e$ has been made in the bubble chamber Gargamelle exposed to a wide band neutrino beam. A signal of 26 ± 6 candidates has been found. These events appear as isolated μ's and the main background is the reaction $\upsilon_\mu N \rightarrow \mu$ + hadrons, where hadrons escape detection.

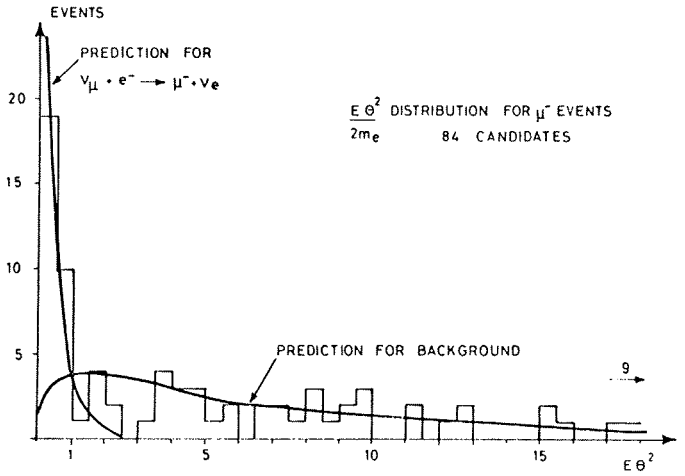

FIG. 2 - Signal of the reaction $\upsilon_\mu + e^- \rightarrow \mu^- + \upsilon_e$ from GGM experiment [1]

This reaction is predicted by V-A theory. The question was to know whether at high energy the form of the current is still the same as at low energy or if some new effects arise. The results of this experiment are in good agreement with the V-A theory (σ(inv. μ decay) / σ(V-A) = 0.9 ± 0.2) ruling out V+A coupling or right handed neutrinos.

B - Polarization of positive muons produced in high energy antineutrino interaction CHARM collaboration [2].

We already know that the y distributions of neutrino and antineutrino are consistent with V-A structure. However such distributions can also be obtained by mixtures of S, P, T currents (confusion theorem [3]). Since the V and A couplings preserve the helicity while S, P, and T couplings flip the helicity, a study of the polarization of the μ can resolve this ambiguity. In the CHARM experiment, antineutrinos interacted in the CDHS detector (which was used as target and muon spectrometer) and the produced muons stopped in the fine grained CHARM calorimeter which was then used as a polarimeter. The positron from μ^+ decay was detected in scintillator planes and the time dependence of the forward-backward decay asymmetry was observed (Figure 3).

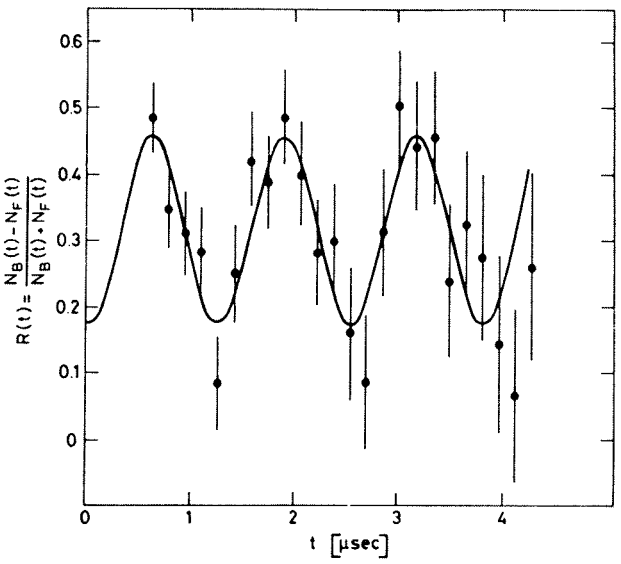

FIG. 3 - Time dependence of relative forward-backward position asymmetry. CHARM experiment [2].

The results yield a longitudinal polarization P = +(1.09 ± 0.22) consistent with a pure V,A form of the interaction and an upper limit for S, P, T couplings σ(S,P,T) / σ_{tot} < 18 % with 95 % confidence level.

III. FORMALISM AND QUARK PARTON MODEL

One has to simplify equation (1) to study the nucleon structure functions. First if one uses an isoscalar target one measures $W_i^{\upsilon N} = \frac{1}{2}(W_i^{\upsilon p} + W_i^{\upsilon n})$. This reduces the number of structure functions to 6. In the case of deviations from isoscalar target (i.e. Iron) where $N_n \neq N_p$ one applies a small correction (2 % for iron targets). The next step is to assume 3 hypotheses.

- Charge symmetry :

In the case of $\Delta S = 0$ transition, charge symmetry implies $W_i^{\upsilon n} = W_i^{\bar{\upsilon} p}$ and $W_i^{\upsilon p} = W_i^{\bar{\upsilon} n}$. Charge symmetry has been tested at a level of 5 % by different experiments CITF [4], BEBC [5], CDHS [6]. No new result is presented at this conference and charge symmetry is assumed to be valid.

- Callan Gross relation $2 \times F_1 = F_2$:

This relation will be discussed in the next chapter.

- BJORKEN scaling limit :

For Q^2, $\upsilon \to \infty$ at fixed $x = Q^2/2M\upsilon$, the structure functions are only functions of x :

$$MW_1\ (Q^2,\upsilon) \longrightarrow F_1(x)$$
$$\upsilon W_2\ (Q^2,\upsilon) \longrightarrow F_2(x)$$
$$\upsilon W_3\ (Q^2,\upsilon) \longrightarrow xF_3(x)$$

We then get cross-section as function of two structure functions :

$$\frac{d^2\sigma^{\upsilon\bar{\upsilon}}}{dx\,dy} = \frac{G^2 M E_\upsilon}{\pi}\left[F_2(x)\ (1-y+\frac{1}{2}y^2) \pm xF_3(x)\ (y-\frac{1}{2}y^2)\right]$$

In the frame of the quark parton model, using the quark and antiquark momentum distributions :

$$q(x) = u(x) + d(x) + s(x) + c(x)$$
$$\bar{q}(x) = \bar{u}(x) + \bar{d}(x) + \bar{s}(x) + \bar{c}(x)$$

we have :

$$\frac{d^2\sigma^{\bar{\upsilon}}}{dx\,dy} = \frac{G^2\ M\ E_\upsilon}{\pi}\left[q(x) + s(x) - c(x) + \left\{\bar{q}(x) - \bar{s}(x) + \bar{c}(x)\right\}\ (1-y)^2\right]$$
$$\frac{d^2\sigma^{\upsilon}}{dx\,dy} \quad \frac{G^2\ M\ E_\upsilon}{\pi}\left[\bar{q}(x) + \bar{s}(x) - \bar{c}(x) + \left\{q(x) - s(x) + c(x)\right\}\ (1-y)^2\right]$$

and :

$$F_2^{\upsilon} = F_2^{\bar{\upsilon}} = q + \bar{q}$$
$$\frac{1}{2}(x F_3^{\upsilon} + x F_3^{\bar{\upsilon}}) = x F_3 = q - \bar{q}$$

yielding the following properties :

- σ_{tot} is linear with E_ν
- Callan Gross relation holds (spin $\frac{1}{2}$ partons)
- $F_2^{ed} = \frac{5}{18}\left(1 - \frac{3}{5}\,\frac{s+\bar{s}}{q+\bar{q}}\right) F_2^{\nu N}$
- Gross-Llewellyn-Smith sum rule follows :

$$\int_0^1 F_3 \, dx = 3 \text{ (number of valence quarks)}$$

IV. TOTAL CROSS-SECTION

Table 1 gives the value of all measurements on total cross-section which are plotted on Figure 4. Four new measurements were presented during this year : two from GGM group [7,9] and one from BEBC WA-24 [10] at low energy and one preliminary result from the CFRR [8] group which has extended his measurements of total cross-section up to 260 GeV.

TABLE I : Slopes of neutrino and antineutrino cross-section in units of 10^{-38} cm^2 nucleon^{-1} GeV^{-1}

EXP	E_ν(GeV)	σ^ν / E_ν	$\sigma^{\bar{\nu}} / E_{\bar{\nu}}$	$\sigma(\bar{\nu}) / \sigma(\nu)$
GGM	2 - 10	0.74 ± 0.05	0.28 ± 0.02	0.38 ± 0.02
INEP / ITEP	10	0.72 ± 0.07	0.32 ± 0.03	0.44 ± 0.03
SKAT	3 - 30	0.73 ± 0.08		
BEBC	30 - 200	0.59 ± 0.04	0.29 ± 0.04	0.49 ± 0.07
CITFR	30 - 90 90 - 190	0.61 ± 0.02 0.62 ± 0.03	0.28 ± 0.01 0.34 ± 0.03	0.46 ± 0.02 0.55 ± 0.05
CDHS	30 - 200	0.62 ± 0.03	0.30 ± 0.015	0.48 ± 0.02
GGM [7]	3 and 9	0.69 ± 0.05 0.61 ± 0.06		
CFRR [8]	60 - 260	0.67 ± 0.04		
GGM [9]	10 - 90		0.30 ± 0.03	
BEBC [10]	28	0.73 ± 0.08	0.32 ± 0.06	0.44 ± 0.09

The point from BEBC WA-24 collaboration fills the gap in the neutrino cross-section left between the GGM measurements and the high energy results. However the significance of this new result is limited by the large statistical errors. The new results for antineutrinos are in good agreement with the earlier measurements.

The question of the possible variation with energy of the neutrino total cross-section in the range of 5 to 40 GeV is still unclear. Above 40 GeV the results are compatible with the linearity of total cross-section with energy. We would like to comment on this linearity.

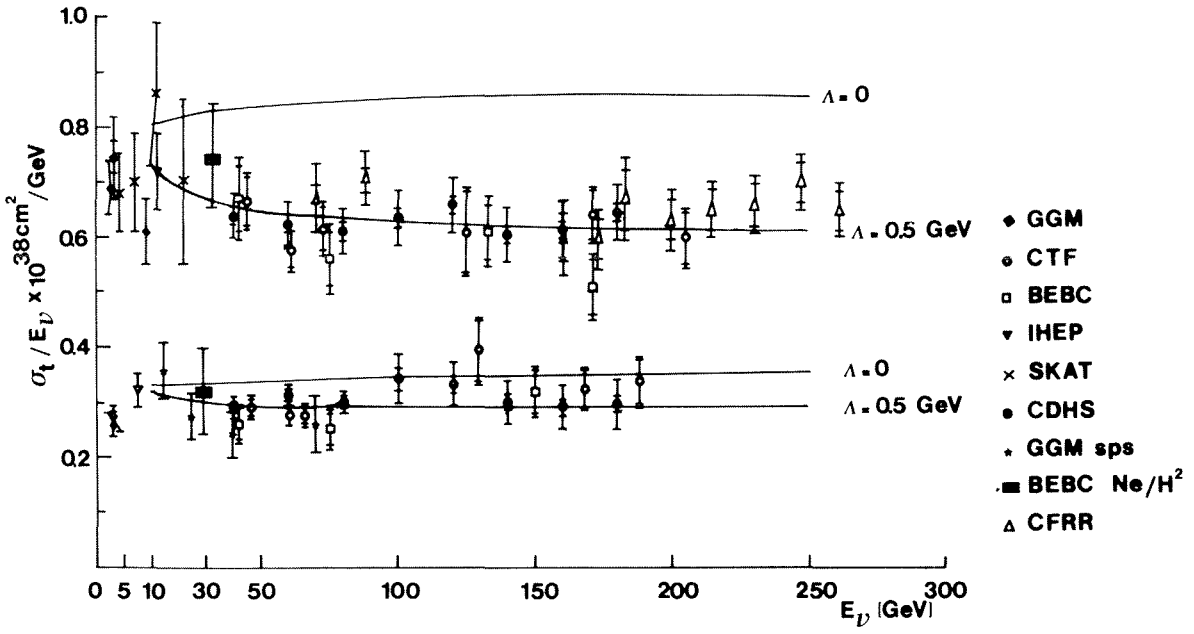

FIG. 4 - Slopes of total cross-sections.
The theoretical curves (QCD) have been calculated by GAEMERS [11].

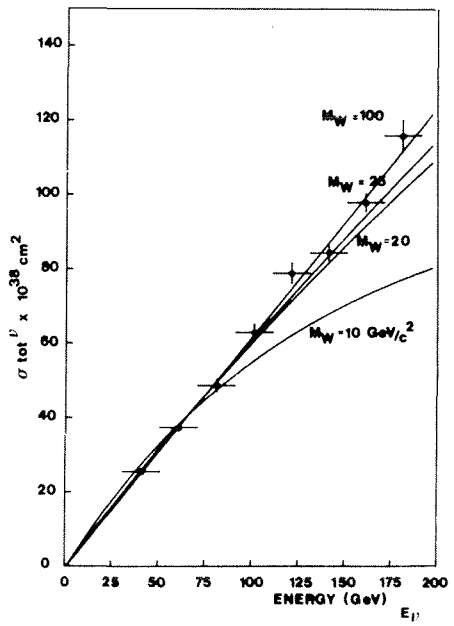

FIG. 5 - Propagator effect on linearity of total cross-section.

First, we would point out that Figure 4 is somewhat misleading in that groups are not consistent in reporting the errors of their measurements (i.e. in some cases the errors are only statistical, whereas for others they include systematic errors which can be of the same magnitude). Second, we want to ask what can be learned from a departure from linearity ?

- The first effect we expect is possibly due to propagator of the intermediate vector boson of mass M_W, $(1/1 + \frac{Q^2}{M_W^2})^2$.

Figure 5 shows the sensitivity to a M_W mass for the CDHS data. The lower limit on this mass is 19 GeV at 90 % confidence

level (this can be improved to 25 GeV with the present data from CDHS with a better knowledge of the $(\frac{K}{\pi})$ ratio for the narrow band beam). These limits are still far from the expected value of the M_W calculated with $\sin^2 \theta_W$.

- A second effect which can break the linearity of total cross-section are QCD scaling violations. In Figure 4 the curves are calculated by GAEMERS [11] for two different values of Λ. A value of Λ = 0.5 GeV fits very well the general slope of the neutrino cross-section and seems to explain the variation with energy. One should note that this is surely not the best way to determine Λ and that the QCD effect on the linearity is of the same order as the propagator term with M_W = 30 GeV : these two effects are mixed and thus complicate the problem.

Furthermore it is clear that to learn something from the non linearity of the total cross-section is difficult : measurements at a level of 1 % are a challenge that few experimentalists are ready to undertake.

V. CALLAN GROSS RELATION $2 \times F_1 = F_2$

The verification of this relation is important, since one can learn about the spin and the $P_\perp$ of the nucleon constituents. The ratio $2 \times F_1/F_2$ measures the ratio of magnetic to electric scattering off partons. It is equal to 1 for a parton of spin 1/2 and to 0 for a spin 0 parton. The equality $2 \times F_1 = F_2$ was also derived from current algebra in 1969 by CALLAN and GROSS [12] independently of the quark parton model. One can relate the Callan-Gross violation determined in the neutrino nucleon scattering to the ratio of longitudinal and transverse cross-section of virtual photons measured in electron or muon scattering on nucleon :

$$W_1 (\upsilon, q^2) = \frac{K}{4\pi^2 \alpha} \sigma_T (\upsilon, q^2)$$

$$W_2 (\upsilon, q^2) = \frac{K}{4\pi^2 \alpha} \left(\frac{q^2}{q^2+\upsilon^2}\right) \left[\sigma_T (q^2, \upsilon) + \sigma_L (q^2, \upsilon)\right]$$

$$R = \sigma_L / \sigma_T$$

In the quark parton model, R can be written $R = 4 (M_q^2 + P_\perp^2) / Q^2$ where M_q and $P_\perp$ are the mass and the transverse momentum of the valence quarks and R = 0 in the naïve quark parton model. If one defines $R_\upsilon = \frac{F_2 - 2 \times F_1}{F_2}$ then one has the relation :

$$R_\upsilon = R \left(1 + \frac{Q^2}{\nu^2}\right) - \frac{Q^2}{\upsilon^2}$$

If the $P_\perp$ of the quark is not zero, one expects a value of R different from zero. In both υ and e, μ scattering QCD predicts a variation of R with Q^2, thus providing an another test of this theory.

- How can we extract R ?

By analogy with the virtual photon, we can define cross-sections for right-handed, left-handed and scalar intermediate boson respectively :

$$F_R(x,Q^2) = 2 \times F_1(x,Q^2) - \times F_3(x,Q^2) \qquad 2\bar{q}$$

$$F_L(x,Q^2) = 2 \times F_1(x,Q^2) + \times F_3(x,Q^2) \qquad 2q$$

$$F_S(x,Q^2) = F_2(x,Q^2) - 2 \times F_1(x,Q^2) \qquad \underbrace{0}_{\text{Q.P.M.}}$$

The differential cross-sections become :

$$\frac{d\sigma^{\nu}}{dy} = \frac{G^2 M E_{\nu}}{\pi} \int \frac{F_L(x,Q^2)}{2} dx + \int \frac{F_R(x,Q^2)}{2} dx(1-y)^2 + \int F_S(x,Q^2)\, dx(1-y)$$

$$\frac{d\sigma^{\bar{\nu}}}{dy} = \frac{G^2 M E_{\nu}}{\pi} \int \frac{F_R(x,Q^2)}{2} dx + \int \frac{F_L(x,Q^2)}{2} dx(1-y)^2 + \int F_S(x,Q^2)\, dx(1-y)$$

A Callan Gross violation induces a (1-y) term in the neutrino and the antineutrino distributions, which can be measured directly. One can also add the two cross-sections $\frac{d\sigma^{\nu}}{dy} + \frac{d\sigma^{\bar{\nu}}}{dy}$ and look for y^2 terms,

$$\frac{d\sigma}{dy}(\nu+\bar{\nu}) \alpha \int F_2\, dx(1-y) + \int 2 \times F_1\, dx \frac{y^2}{2}$$

$$\alpha \int F_2\, dx(1+(1-y)^2) - \int F_2 - 2 \times F_1)\, dx\, y^2$$

These two approaches are equivalent.

- Choice of the variable and problems of systematic errors

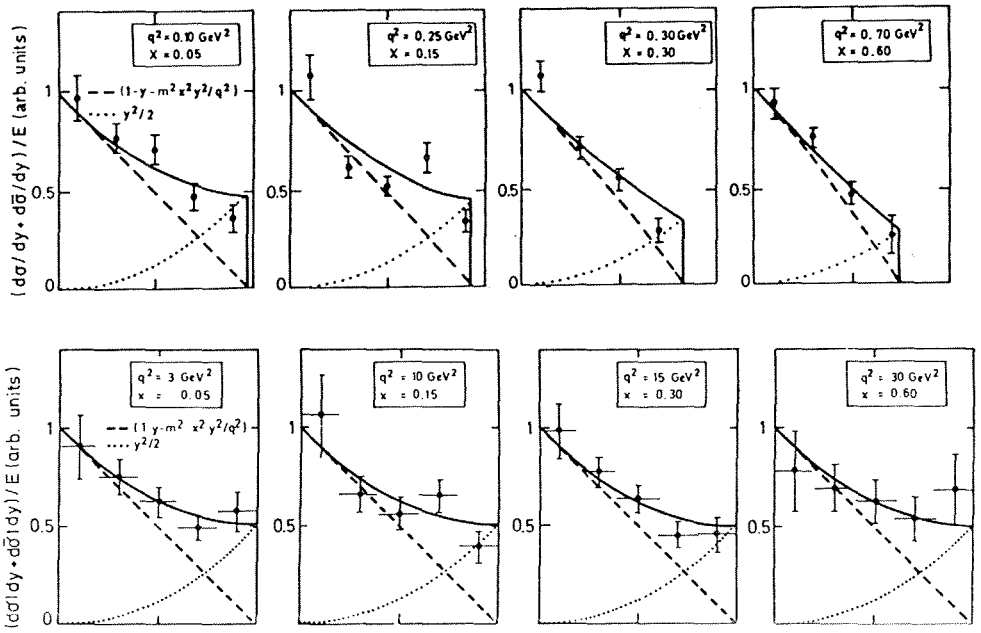

FIG. 6 - Fit on $\frac{d\sigma}{dy}(\nu+\bar{\nu})$ to determine R from BEBC [14].

Variations of R_υ with Q^2 and x can be compared with QCD predictions. However, we have emphazised at the beginning of this review the impossibility to obtain a complete x distribution for a given Q^2. Usually analyses of R_υ are made from a general fit on y distribution integrated over E_υ and then over Q^2. But since large y corresponds to large Q^2 and similarly small y to small Q^2, the result is affected by the a priori unknown Q^2 dependence of the structure functions. One could correct for this effect as measured in the structure function determinations, but as it has been pointed out [18], one uses in the determination of the structure functions the fact that $R_\upsilon = 0$, so this method of correction is not formaly correct and is circular. In the BEBC analysis [14], Q^2 bins have been used : however the binning is so large (due to statistics) that the previous criticism still applies. Their results are shown in Figure 6.

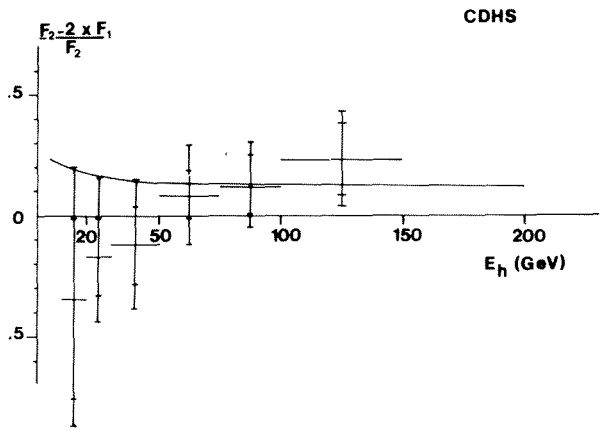

FIG. 7 - Results of the fit on $\frac{d\sigma}{dy}$ $(\upsilon+\bar{\upsilon})$ function of E_h to determine R_υ from CDHS data. The curve is the Altarelli Martinelli [22] calculation using CDHS fit to F_2.

An alternative binning in E_h has been used by the CDHS collaboration in a reanalysis of their data to overcome this problem. The results are presented in Figure 7.

The systematic errors for the CDHS data are large. This analysis is very sensitive to flux uncertainties (i.e. $\frac{K}{\pi}$ ratio) and on the other hand in E_h binning due to the correlation between y and E_h one does not see all the y distribution (at small E_h correspond small y and large E_h correspond large y) so the lever arm in the y distribution is reduced leading to a larger error to the fit.

- Experimental results

TABLE II : Experimental results on $R_\upsilon = (F_2 - 2xF_1)/F_2$

EXP	R	Q^2 (GeV/c)^2
GGM [13]	0.32 ± 0.15	$Q^2 < 1$
BEBC [14]	0.11 ± 0.14	$Q^2 > 1$
CDHS [6]	-0.03 ± 0.05	$\langle Q^2 \rangle \simeq 20$
HPWF [15]	0.18 ± 0.06 (± 0.04)*	$\langle Q^2 \rangle \simeq 20$
FMII [16]	-0.12 ± 0.16	$\langle Q^2 \rangle \simeq 5$
CDHS [17]	0.03 ± 0.05 (± 0.1)*	$\langle Q^2 \rangle \simeq 20$
	* with radiative correction	

A summary of neutrino data for R is presented in Table II. With the exception of the GGM result at small Q^2, the value of R_υ is compatible with zero. The average value of Q^2 in other experiments is generally large. Nevertheless the largest effect is expected from QCD at small Q^2, in qualitative agreement with these results. However, the tests of Callan-Gross are so far not very convincing.

- Comparison with $R_{e,\mu}$

The electron scattering data give a value of $R_e = 0.137 \pm 0.017$ from E.M.RIORDAN et al [19] in a Q^2 range $1 < Q^2 < 16$ $(GeV/c)^2$ and $0.1 < x < 0.8$. R.E. TAYLOR has reported in the TOKYO conference [20] an average value of $R_e = 0.21 \pm 0.10$. The results on μ scattering are known in a more restricted kinematical region (very low x) [21] : $R_\mu = 0.55 \pm 0.24$, $1 < Q^2 < 12$ $(GeV/c)^2$ and $0.009 < x < 0.1$. Very often one refers to this high value of R_μ but before any conclusion can be drawn, one would like to see a measurement of R in larger x and Q^2 region.

To summarize, it is not possible to seriously compare the value of R from different experiments and surely not to conclude that there is a discrepancy between the neutrino and the electron/muon experiments. The study of R_υ in neutrino physics is surely possible, but here one needs much more statistics and a better understanding of the systematic errors.

VI. Y AND X DISTRIBUTIONS INTEGRATED OVER THE ENERGY NEUTRINO RANGE

We have seen in the chapter concerning quark parton model formalism what neutrino and antineutrino differential cross-sections can tell us about nucleon constituants. Neglecting the charm sea quark contribution, assuming Callan-Gross relation is verified, correcting for non isoscalar target as well as for radiative processes, the two differential cross sections :

$$\frac{d^2\sigma}{dxdy}(\upsilon) \propto q(x) + s(x) + \left[\bar{q}(x) - \bar{s}(x)\right] (1 - y)^2$$

$$\frac{d^2\sigma}{dxdy}(\bar{\upsilon}) \propto \bar{q}(x) + \bar{s}(x) + \left[q(x) - s(x)\right] (1 - y)^2$$

can be used to obtain the total amount of quark and antiquark content and their x distributions. One may wonder why we have still considered these distributions integrated over the entire range of neutrino energies. It was simply the first logical step since in the quark parton model we assume scaling holds and we wanted to know precisely the quark and antiquark component. Their variation with q^2 is naturally the next step to consider.

A - Total antiquark, strange antiquark distributions.

From the above equations one can extract information on $\bar{q}$ and $\bar{s}$ in two ways :

i.) A fit of the neutrino y distribution determines $\bar{Q}-\bar{S}/\bar{Q}+Q$ and the antineutrino y distribution determines $\bar{Q}+\bar{S}/\bar{Q}+Q$, from which one can extract separately $\bar{Q}$ and $\bar{S}$.

ii.) Considering the antineutrino y distribution alone at large y, the term $\bar{Q}+\bar{S}$ is dominant and

$$\frac{d^2\sigma}{dxdy}(\bar{\upsilon})\Big/_{y\to 1} \longrightarrow \frac{G^2\, ME_\upsilon}{\pi}\left[\bar{q}(x) + \bar{s}(x)\right] .$$

One can thus correct by substracting the $(1-y)^2$ q(x) term of neutrino data at large y.

Information on the strange antiquark distribution can also obtained from dimuon production which is interpreted as charm production as described by the GIM mechanism.

The production cross-sections are given by :

$$\frac{d^2\sigma}{dxdy}(\upsilon+N\to\mu^-+\mu^++X) = \frac{G^2ME_\upsilon}{\pi}\left[(u(x)+d(x))\sin^2\theta_c + 2\,s(x)\cos^2\theta_c\right]$$

$$\frac{d^2\sigma}{dxdy}(\bar{\upsilon}+N\to\mu^++\mu^-+X) = \frac{G^2ME_\upsilon}{\pi}\left[2\,\bar{s}(x)\cos^2\theta_c + (\bar{u}(x)+\bar{d}(x))\sin^2\theta_c\right]$$

where θ_c is the Cabibbo angle.

If one neglects the $(\bar{u}+\bar{d})\sin^2\theta_c$ term and compares the dimuon production rates for neutrinos and antineutrinos one obtains :

$$\frac{2\bar{s}}{u+d} = tg^2\theta_c\,\frac{R_1}{R_2-R_1}$$

where $R_1 = \dfrac{\sigma\bar{\upsilon}}{\sigma\upsilon}$ and $R_2 = \dfrac{(2\mu/1\mu)_\upsilon}{(2\mu/1\mu)_{\bar{\upsilon}}}$

Another method to obtain the ratio $2\bar{s}/u+d$ is to fit the x distributions of both neutrino and antineutrino dimuon events ; assuming antineutrino events are only produced from strange quarks and that the neutrino events are the sum of u+d and s quark terms. In such a fit one uses the u+d distribution (the sum $u_\upsilon + d_\upsilon + \bar{d} + \bar{s}$) which is found from the charged current event analysis.

The experimental results obtained by these different methods are presented in tables III and IV.

TABLE III : Experimental results on total antiquark momentum $\bar{Q}$

EXP.	METHOD	$\bar{Q}$ / Q + $\bar{Q}$
GGM [23]	B parameter	0.05 ± 0.02
BEBC [14]	from F_2 and xF_3	0.11 ± 0.03
HPWF [24]	y distribution E_υ 40 GeV	0.08 ± 0.03
	y distribution E_υ 80 GeV	0.17 ± 0.03
CDHS [6]	y distribution υ and $\bar{\upsilon}$	0.15 ± 0.03
	y distribution $\bar{\upsilon}$ only (Q+S/Q+Q)	0.16 ± 0.01
FBHIIM [16]	y distribution $\bar{\upsilon}$	0.13 ± 0.02

TABLE IV : Experimental results on strange antiquark momentum

EXP.	METHOD	RESULTS
CDHS [6]	y distribution υ and $\bar{\upsilon}$	$\bar{s}/\bar{Q}+Q = 0.00 \pm 0.03$ *
CDHS [25]	dimuon production	$2s/Q+Q$ 0.035
HPWF [24]	dimuon production	$\bar{s}/U = 0.076 \pm 0.027$
PAC [26]	antineutrino-proton	$\bar{D}+\bar{S} = 0.036 \pm 0.013$
CDHS [27]	dimuon production rate υ and $\bar{\upsilon}$	$2\bar{s}/Q+\bar{Q} = 0.03 \pm 0.01$
	dimuon production fit on x distribution	$2\bar{s}/Q+\bar{Q} = 0.035 \pm 0.02$

* In this analysis one measure $\bar{s}-\bar{c}/Q+\bar{Q}$

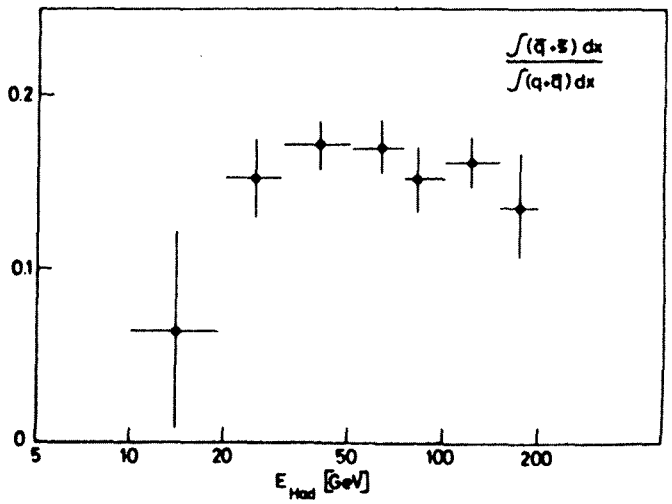

FIG. 8 - Antiquark fraction versus E_H.

All experiments agreed at high energy on an averaged value of $\bar{Q}/Q+\bar{Q} \simeq 0.16$. The variation with neutrino energy above 30 GeV is presently not very significant as can be seen in the figure 8 [6].

The smaller values of $\bar{Q}/Q+\bar{Q}$ at low energy which are found by GGM and HPWF groups are significant and the very low energy GGM point suggests a threshold effect due to charm production. A variation is predicted by QCD but its effect is difficult to observe in the variable E_υ. This q^2 variation of the sea will be discussed in the chapter concerning scaling violations.

Concerning the present experimental values of the strange sea 2s/u+d, they are definitely much smaller than what one would naïvely expect from a SU_3 symmetric model.

B - Structure functions averaged over neutrino energy.

From the sum and the difference of neutrino and antineutrino cross-sections one extracts respectively the total quark structure function $F_2(x) = q(x) + \bar{q}(x)$ and the valence quark structure $xF_3(x) = q(x) - \bar{q}(x)$. Experimental problems which arise in extracting the structure functions integrated over neutrino energy come mainly at small x due to the sea distribution correction term which can reach 20 % in the determination of $F_2(x)$ and the finite x resolution at $x = 0$ which limits the precision in determining the $xF_3(x)$ behaviour in this region. At large x the main problems come from a sensitivity to the smearing function and whether or not the fermi motion correction has been applied. This is why the cut-off for $x > 0.7$ has been applied in some analyses. In addition the absolute flux normalization and the relative neutrino and antineutrino flux uncertainty lead to an additional error of the order of 10 %.

Because no theory predicts the shape of these structure functions, experimental results have been fitted by rather simple analytical expressions using such theoretical prejudice as for instance that $xF_3(x) = 0$ for $x = 0$. One obtains the following results :

$$\text{VALENCE} \quad : \quad \sqrt{x}\,(1-x)^n$$

An exemple of valence quark distribution is given in figures 9 and 10.

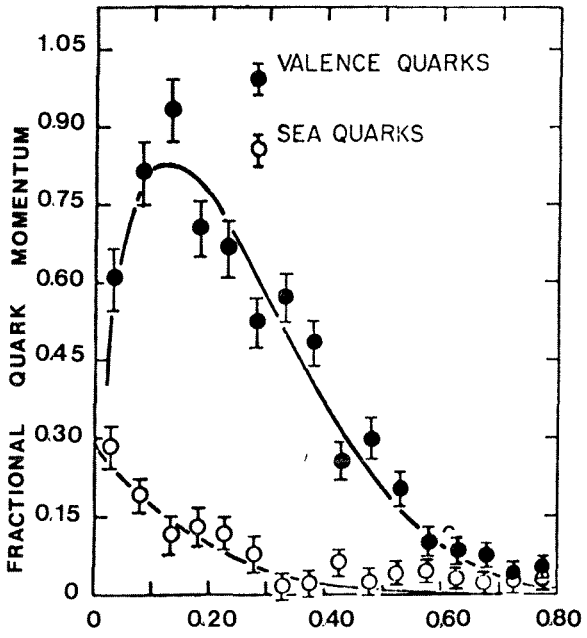

FIG. 9 - Valence and sea quark distribution from HPWF [15] for $20 < E_\upsilon < 220$ GeV.

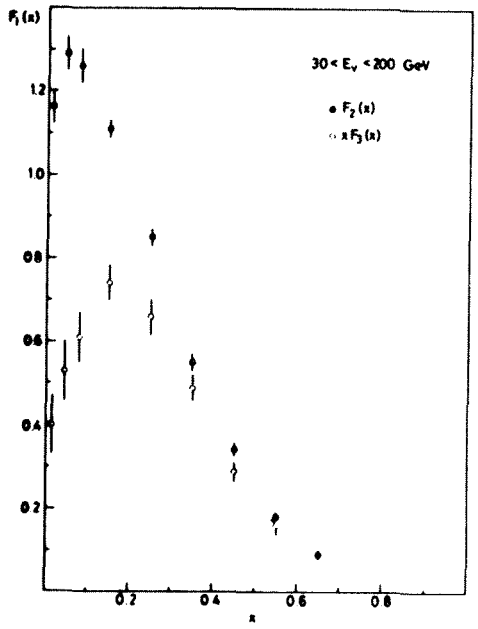

FIG. 10 - $F_2(x)$ and $sF_3(x)$ averaged over $30 < E_\upsilon < 200$ GeV from CDHS [6].

The value of n from the fit $\sqrt{x}(1-x)^n$ are the following :

HPWF [15]	3.7 ± 0.1 (±0.3)
CDHS [6]	3.5 ± 0.5
BEBC [14]	≃3. for x > 0.3

ANTIQUARK $(1 - X)^m$

The information on the antiquark structure function $\bar{q}(x) + \bar{s}(x)$ comes from the antineutrino cross-section at large y. An exemple is given in figure 11.

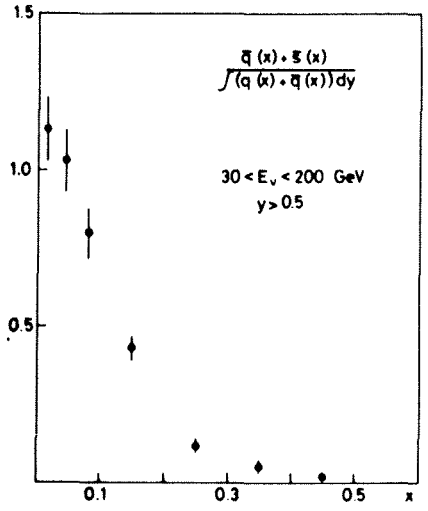

FIG. 11 - Antiquark structure function averaged over $30 < E_\upsilon < 200$ GeV [6].

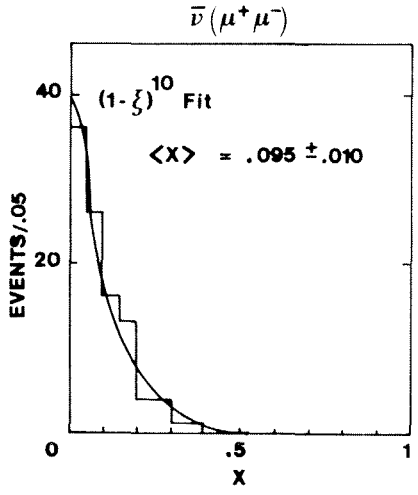

FIG. 12 - x distribution of dimuon events $\upsilon + N \rightarrow \mu^+ + \mu^- + X$ [27].

with $\xi = \dfrac{Q^2 - m_c^2}{2M\upsilon}$

One can also extract information on the x distribution of the strange sea, as already mentionned, from dimuon antineutrino production. Such a distribution is shown in figure 12 for 100 events $\bar{\nu} + N \rightarrow \mu^+ \mu^- + X$ obtained in a narrow band beam exposure [27].

The values of m from the fit of the form $(1-x)^m$ for the antiquark functions are listed below :

BEBC [14]	$4.9 \begin{smallmatrix} + 2.4 \\ - 1.7 \end{smallmatrix}$
HPWF [15]	4.6 ± 0.5 (± 0.6)
CDHS [6] : $(\bar{q}+\bar{s})$	6.5 ± 0.5
CDHS [27] ($\bar{s}$ only)	$10. \begin{smallmatrix} + 1.8 \\ - 1.4 \end{smallmatrix}$

The result for $\bar{s}(x)$ obtained from studies of antineutrino dimuon production is preliminary and it is too early to comment on the possible difference in m value of the fit between $\bar{q}+\bar{s}$ and the strange sea distribution alone. Clearly better values of the antiquark distribution are needed and the precision of the results should be improved. The scattered values of m presented above should converge very soon with new results from higher statistical experiments. One should also keep in mind that small variations are expected for these distributions as a function of q^2 (QCD) and that these fits are averaged over neutrino energy and should in the future be remplaced by more precise fits for different q^2 ranges.

VII. SCALING VIOLATION

It was from ed scattering results [19] that $F_2(q^2,\upsilon)$ was first shown not to follow the Bjorken scaling rule. In neutrino physics the energy dependence of total cross-section was compatible with linearity and variations with E_υ if the partial cross-sections for different variables was not seen. The mean-value $\langle Q^2/E \rangle = 2M\langle xy \rangle$ which should be constant in the scaling hypothesis is seen to be slowly decreasing in the interval from 2 GeV to 200 GeV, but still perfectly compatible experimentally with a constant value over the neutrino energy region between 40 and 200 GeV as is also seen for the integral of F_2 as a function of energy [28]. More convincing are the shapes of the structure function F_2 for different energies as shown in figure 13. Perhaps the cleanest test for scaling violations is to look at variations in F_2 and xF_3 as functions of q^2 and x. We had to wait for experiments with high statistics and well understood experimental systematics to conclude on the existence of scaling violations in neutrino physics.

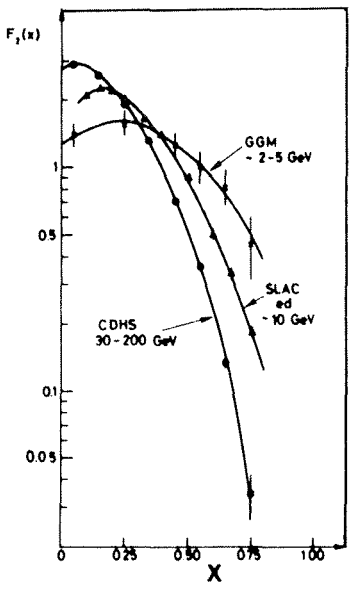

FIG. 13 - F_2 structure function for different energy of incident lepton.

Two experiments up to now have presented results in this way : ABCLOS-BEBC [14] collaboration and CDHS collaboration [6]. The results on F_2 and xF_3 are presented in figures 14(a,b) and 15(a,b).

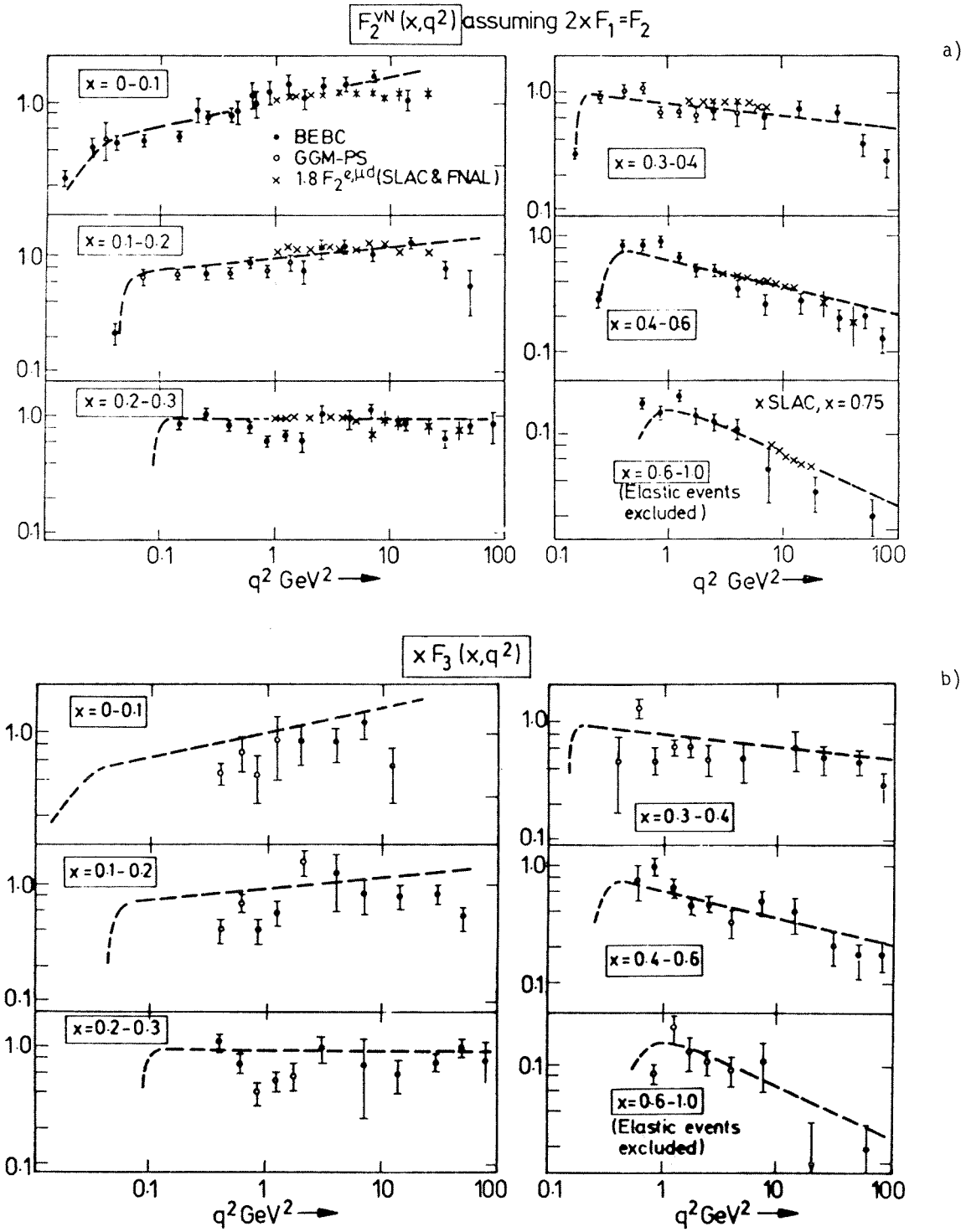

FIG. 14 - a) F_2 and b) xF_3 for various x ranges plotted versus q^2 from ABCLOS collaboration [14].

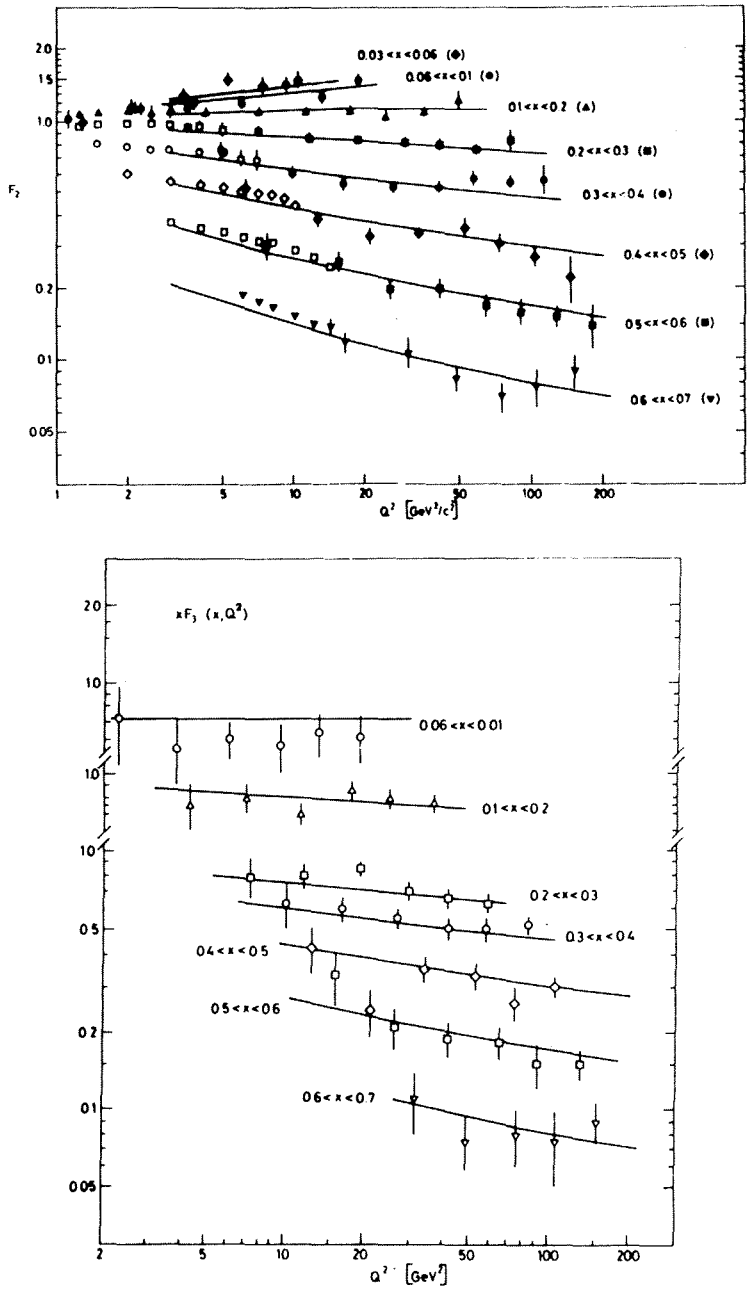

FIG. 15 - a) F_2 and b) xF_3 in different x bins as a function of $\ln q^2$ from CDHS collaboration [6].

- These figures show a positive slope of F_2 for small x, flat around x = 0.2 and negative for x >0.3. We would like to stress that in the BEBC data the variation of F_2 is more convincing when one includes the GGM points at small q^2. Their data obtained only in the same domaine of q^2 as CDHS would not allow any conclusion on scaling violation. The results of CDHS are precise enough to confirm the same tendency as ed scattering. The evidence for scaling violation on xF_3 is weaker. The statistical errors are much larger than for F_2. The lines of the fit are drawn on each figure, and we will point out in the next chapter, they help to indicate the scaling violation on xF_3.

- One sees on figure 15 the effect of kinematical constraints underligned in the first paragraph of this talk : for small x one has data at small q^2 and for large x at large q^2. This is why ed data were used tc complete the CDHS measurement and why both CDHS and BEBC have used respectively ed and GGM results to calculate the moments of these functions.

- The agreement of the neutrino data $F_2^{\upsilon N}$ compared with ed scattering results (corrected by the factor $F_2^{\upsilon N} = \frac{9}{5} F_2^{ed}$) is very good. The overlap region is very small in the case of CDHS experiment and perhaps it is better to state that the ed data at small q^2 are very well continued by υ-data at higher q^2.

VIII. QCD TESTS OF STRUCTURE FUNCTIONS

When the first scaling violations were found in ed scattering different models were proposed to fit the data [19]. When the neutrino data became available QCD theory was in full development and the neutrino data here are only compared to this theory. Starting from the Altarelli-Parisi equation [29] one can determine two sets of equation for the moments of the momentum distribution $Q(x,q^2)$ of the quarks. The moment or order N is defined as :

$$M(N,q^2) = \int X^{N-2} \; Q(x,q^2)dx$$

if $t = \ln q^2$ one has the two following sets of equations :

$$\frac{dM(N,t)}{dt} = \frac{\alpha_s(t)}{2\pi} \left[A_n \; M(N,t) + B_n \; G(N,t)\right]$$

$$\frac{dG(N,t)}{dt} = \frac{\alpha_s(t)}{2\pi} \left[C_n \; M(N,t) + D_n \; G(N,t)\right]$$

$$\alpha_s(Q^2) = \frac{12\,\pi}{(33-2f)\,\ln Q^2/\Lambda^2} \quad , \; f \text{ is the number of flavors}$$

The A_n, B_n, C_n, D_n, are calculated by the theory and are only functions of N and f.

- The ordinary moments or Cornwall-Norton moments are surely correct for large value of q^2. However in order to take care of target mass effects in a region of q^2 which is still small compared to the nucleon mass one generally uses the Natchmann moments [30] obtained using the variable $\xi = \frac{2x}{1+\sqrt{1+4\,\frac{M^2x^2}{q^2}}}$.

- The test of QCD Theory depends upon the variation of these moments with q^2 thus the way these moments are calculated experimentally is very important. We have seen that to improve their moment calculations, ie. to have the largest range of x for the structure functions, both neutrino experiments BEBC and CDHS have used complementary data from GGM and ed scattering, respectively. Even using these complementary data, the x range is not complete and one has to further rely upon extrapolations of these functions to x = 0 and x = 1.

The constraint $xF_3 = 0$ for $x = 0$ is very usefull in this way for extrapolation at small x and for large x the shape $\sqrt{x}(1-x)^n$ already discussed in the preceding chapter has been used. These constraints on xF_3 allow CDHS collaboration to calculate moments xF_3 only. Both F_2 and xF_3 moments have been calculated by the BEBC collaboration. The decision whether or not to include elastic events in the analysis is also very important for higher moment calculations (x near 1). All of these difficulties plus some additional systematic errors such as the relative normalization of the two experimental samples (GGM and BEBC) or (ed and CDHS) and the lack of Fermi motion corrections increase the total errors for the moments. Thus the comparison of these moments must be treated, rather carefully. As an example figure 16 shows comparison of BEBC and CDHS moments [31].

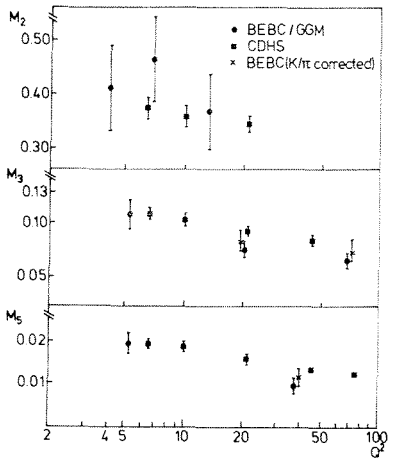

FIG. 16 - Moments of xF_3 measured by BEBC and CDHS experiment in overlapping Q^2 region [31].

The agreement between the experiments is good except for the higher moments. This discrepancy reflects a desagrement in the structure functions at high x and we know that the large x values are predominant in the high moment order calculation.

A - Moment analysis of xF_3 (non-singlet) structure function.

In the case of the non-singlet structure function xF_3, QCD predictions are simpler for the leading order. One can write the moments of xF_3 as :

$$M_3(N,q^2) = M_3(N,Q_0^2)\ e^{-d_N s}$$

with d_N = anomalous dimension $= \frac{4}{33-2f}\left[1 - \frac{2}{N(N+1)} + 4\sum_{J=2}^{N}\frac{1}{J}\right]$

$$s = \ln\left[\ln Q^2/\Lambda^2 \,/\, \ln Q_0^2/\Lambda^2\right]$$

Two tests come from QCD predictions.

i.) Test of vector character of gluons.

If we consider the logarithms of two moments i and j we can write :

$$\frac{\log M_i - \log M_i(0)}{\log M_j - \log M_j(0)} = \frac{d_i}{d_j}$$

a ratio which is independent of N and f and which is calculated by theory. It depends on the scalar or vector character of the gluon.

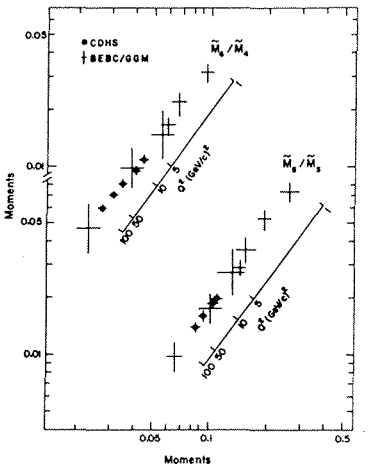

FIG. 17 - Nachtmann moments from CDHS and BEBC/GGM data in log-log plot.

Figure 17 shows the log-log plot of Nachtmann moments of BEBC and CDHS results. One sees that even though the results of CDHS are statistically much more precise, the lever arm used to determine the slope di/dj is longer for BEBC and thus the error on the results of the slope will be smaller in the BEBC analysis that in the CDHS one as shown in Table V.

TABLE V : di/dj from xF_3 moments.

di/dj	BEBC [14]	CDHS [33]		THEORY	
	NACHTMANN	CORNWALL NORTON	NACHTMANN	VECT. Gluon	SCAL. Gluon
d3/d5	1.50 ± 0.08	1.58 ± 0.12	1.34 ± 0.12	1.46	1.12
d4/d6	1.29 ± 0.06	1.34 ± 0.07	1.18 ± 0.09	1.29	1.06
d3/d6		1.76 ± 0.15	1.38 ± 0.15	1.62	1.21

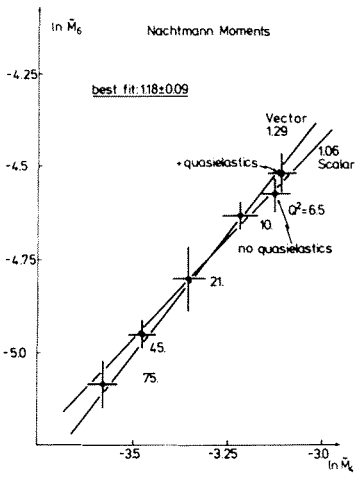

FIG. 18 - Nachtmann moment for different q^2 values. The effect of a quasielastic contribution is indicated [31].

- We see that the target mass effects are not small if we compare the columns of Cornwall-Norton moments versus Nachtmann moments in table V.

- If we consider only the Nachtmann moments the experimental results fall in between the vector and scalar gluon predictions for the CDHS results. The BEBC data are in very good agreement with the vector hypothesis.

- Inclusion of quasielastic events as shown in Figure 18, estimated by extrapolating the measured form factors [31], tends to increase the agreement between the CDHS data and the prediction of vector gluon. On the other hand, the

points at small q^2 which have obviously a large weight in the GGM/BEBC data may be somewhat doubtful in the lowest order QCD predictions.

In conclusion although data are presently consistent with the QCD predictions, there is not now enough precision to conclude on the vector or scalar character of the gluon. This impression is surely reinforced by the recent argument of Harari [32] on limits on the di/dj slope.

ii.) Variation of moments with q^2 : determination of Λ.

The second test of QCD prediction on xF_3 moment is simply understood if one considers the formula :

$$M_i^{-1/di} = \text{const } (\ln Q^2 - \ln \Lambda^2)$$

which gives non singlet moment behaviour in leading order in $\ln \frac{Q^2}{\Lambda^2}$

- The linear dependence in $\ln Q^2$ of this expression is well verified as shown in figure 19.

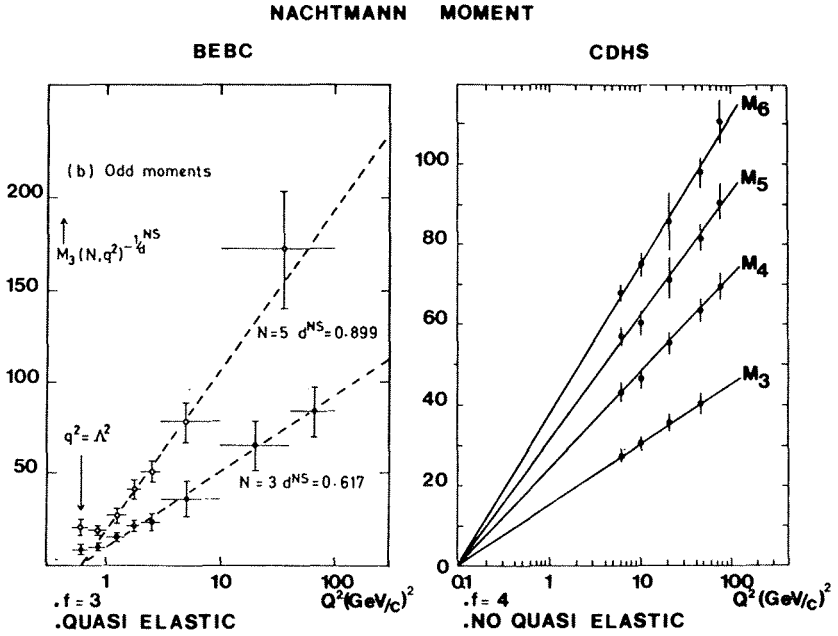

FIG. 19 - Nachtmann moment as function of Q^2 for BEBC and CDHS data.

- The intercept of these lines with zero must be obtained for $Q^2 = \Lambda^2$ and this is one way to measure Λ.

TABLE VI : leading order QCD

EXP		MOMENT	FLAVORS
BEBC [14]	0.74 ± 0.05	NACHTMANN	3
CDHS [33]	0.60 ± 0.15	CORNWALL-NORTON	4
	0.33 ± 0.15	NACHTMANN	4
BEBC [34]	0.72 ± 0.13	NACHTMANN	3

Table VI gives the value of Λ obtained in this way in leading order calculations.

- One sees a strong dependence of the value of Λ with the target mass corrections (0.6 compare to 0.33 in CDHS data).

- If one compares the result of BEBC and CDHS for Nachtmann moments the BEBC value is substantially higher. Can this discrepancy be due to a difference in the data ? As a first consideration the data should be compared only in the overlap q^2-region i.e. $q^2 > 6$ $(GeV/c)^2$. We have already seen (FIG. 16) that in the overlap q^2-region the xF_3 moment agreed. This agreement for xF_3 is even better with the new BEBC [34] analysis although their new value of Λ remains high (0.72 ± 0.13). One should stress again concerning the BEBC analysis that the low q^2 GGM data have a higher statistical significance. A trivial part of the discrepancy can be explained by differences in the way the analysis was done. Furthermore one should compare results where at least the same number of flavors have been used. The CDHS collaboration [33] has pointed out that their Λ would increase about 60 MeV for f = 3. Other corrections such as quasi elastic events if included, fermi motion, would raise the CDHS Λ value about 0.5 [35]. The discrepancy which is left (one standard deviation) could still be due to experimental differences but it is difficult to argue further because a large part of the data for q^2 range from 0.1 to 6 $(GeV/c)^2$ simply cannot be compared. In a different perspective, is the discrepancy due to the very different q^2 region studied by each experiment and more specificaly, can the formalism used in these analyses be the same for all q^2 value ? If one analyses data, as an example, including higher order α_s correction in the "minimum substraction" renormalization scheme [36] one finds :

BEBC [34] $\quad \Lambda = 0.43 \pm 0.12$

CDHS [17] $\quad \Lambda = 0.20 \pm 0.05$

where both values of Λ decrease.

To conclude and to be sure that we have really tested QCD in this way we need at least two experiments of the same statistical precision covering the same q^2 region and with the largest lever arm possible.

B - General fit of QCD on xF_3 and F_2

In this general analysis CDHS [37] has followed the parametrisation proposed by Buras and Gaemers [38].

i.) Valence distribution.

One assumes the following form

$$xF_3(x,q^2) = 3/B(n_1,n_2+1)\ x^{n_1(s)}\ (1-X)^{n_2(s)}$$

$$n_1(x) = n_{10} + n_{11} \cdot s \cdot 4/25$$

$$n_2(x) = n_{20} + n_{11} \cdot s \cdot 4/25$$

$B(n_1,n_2+1)$ is the Euler's beta function

where s was defined earlier in the chapter on QCD formalism.

For an average value of $Q^2 = 20\ (GeV/c)^2$ the results of the fit are the following :

$$n_1 = (0.51 \pm 0.02) - 0.83\ .\ s\ .\ 4/25$$

$$n_2 = (3.03 \pm 0.09) + 5.0\ .\ s\ .\ 4/25$$

$$\Lambda = 0.55 \pm 0.15\ \ (\pm 0.1 \text{ systematic}) \text{ GeV}.$$

One finds values of the constant parts of n_1 and n_2 pretty close to the coefficients of the parametrisation of the averaged x distribution $\sqrt{x}(1-x)^m$. The Q^2 dependence of s is very small as expected.

ii.) Commun fit to F_2 and xF_3

The sea distribution is parametrised as :

$$\bar{q}(x,q^2) = A(s)\ (1-x)^{P(s)} \qquad \text{and one writes}$$

$$F_2(x,q^2) = xF_3(x,q^2) + A(s)\ (1-x)^{P(s)}$$

Where one keeps the same parametrisation as above for xF_3 and the parameters A(s) and P(s) can be calculated from second and third moment of F_2. This involves the gluon distribution, essentially the third gluon moment $<G(x,q^2)>_3$ since the second gluon moment has been known from four-momentum conservation.

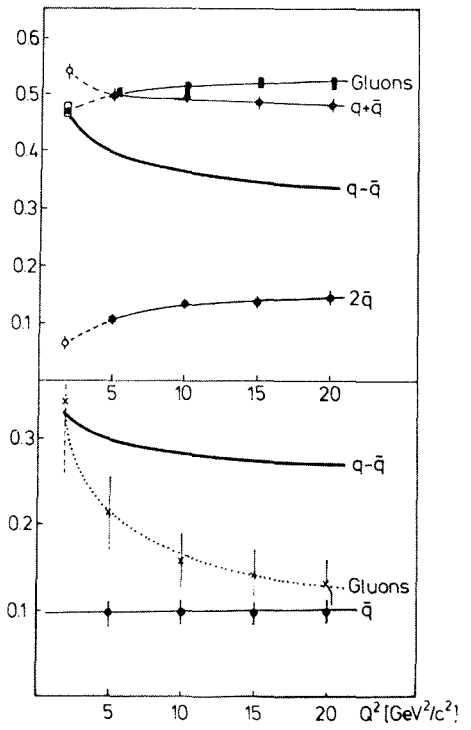

FIG. 20 - Total fractional momentum of all nucleon constituents and the average value of constituent momentum distributions [37].

For $Q_0^2 = 5\ (GeV/c)^2$ one obtains :

$$n_1 = (0.56 \pm 0.2) - 0.92\ .\ s\ .\ 4/25$$

$$n_2 = (2.71 \pm 0.11) + 5.08\ .\ s\ .\ 4/25$$

$$A(0) = 0.99 \pm 0.07 \qquad P(0) = 8.1 \pm 0.7$$

$$M_G\ (3,\ Q_0^2 = 5) = 0.105 \pm 0.02$$

$$\Lambda = 0.47 \pm 0.11\ (\pm 0.1 \text{ system}) \text{ GeV}.$$

The agreement between the result of these fits and the data is good as can be seen figure 15 where the lines are the results of these fits.

The result of the fit on the coefficient P(0) = 8.1 ± 0.7 is higher that the general fit on $\bar{q}(x) + \bar{s}(x)$ where we obtained (6.0 ± 0.5).

The value of $\Lambda = 0.5$ is perfectly compatible with the value of Λ obtained by the CDHS collaboration using the extrapolation method that we have lengthly discussed in the preceding chapter.

Figure 20 is a graphical presentation of these fits which shows the q^2 dependence of the data in the QCD formalism. One sees as predicted by QCD a decrease of the momentum carried by the valence quark and an increase of momentum carried by sea-quark with increasing q^2. The consequence is that $F_2(x)$ does not vary very much with q^2.

C - Gluon distribution

i.) From the general fits of F_2 and xF_3 from the CDHS analysis one obtains information on gluon moments. The value at $Q_0^2 = 5$ (GeV/c)^2 of the third moment $M_G(3, Q_0^2=5) = .105 \pm 0.02$ is obtained from the fit as a free parameter and figure 20 shows the q^2 dependence of the $<x>$ of gluon distribution. However the shrinkage which is seen is a consequence of the QCD moment equation and not a direct experimental measurement.

ii.) BEBC analysis of gluon distribution [14].

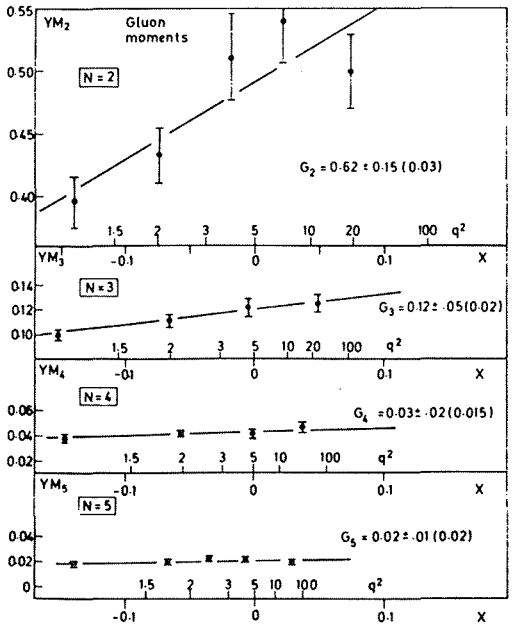

FIG. 21 - Plot of Y M_2 versus X from BEBC [14] analysis.

From the F_2 expression developped as sum of three terms related to the moments of quarks, antiquarks and gluons, one can calculate a linear relation between moment of F_2 and the gluon distribution :

$$Y\ M_2(N,q^2) = M_2(N,q_0^2) + X\ G(N,q_0^2)$$

where Y and X are expressions [14] which are calculated from QCD theory. As it is shown in figure 21 a plot of Y M_2 versus X yields a straight line with a slope equal to the gluon moment at $q^2 = q_0^2$. The result of such analysis is presented in table VII.

TABLE VII - Gluon moments $G(N,q_0^2)$ q_0^2=5 GeV^2

N	$G(N,q_0^2)$	q^2	xF_3
2	0.62 ± 0.15	1 - 20	0.45 ± 0.07
3	0.12 ± 0.05	1 - 100	0.12 ± 0.02
4	0.03 ± 0.02	1 - 100	0.045 ± 0.01
5	0.02 ± 0.01	1 - 100	0.027 ± 0.007

The conclusion of this analysis is that the momentum distribution of gluons is somewhat similar to that of the valence quark.

iii.) Direct extraction of the gluon distribution - BAULIEU AND KOUNAS METHOD

The gluon momentum distribution X G(x) may be obtained directly from the data of F_2, following a method developped by Baulieu and Kounas [39].

According to the Altarelli-Parisi equation :

$$I_2(x) = \int G(y,Q^2)\, P_{qG}\left(\frac{X}{Y}\right) \frac{dy}{y}$$

$$= \frac{1}{d_s(Q^2)} \times \frac{d}{d \ln Q^2} \left(\frac{F_2(x)}{x}\right) = \int_X^1 \frac{F_2(y)\; P_{qq}\left(\frac{X}{y}\right) \frac{dy}{y}}{I_1(x)}$$

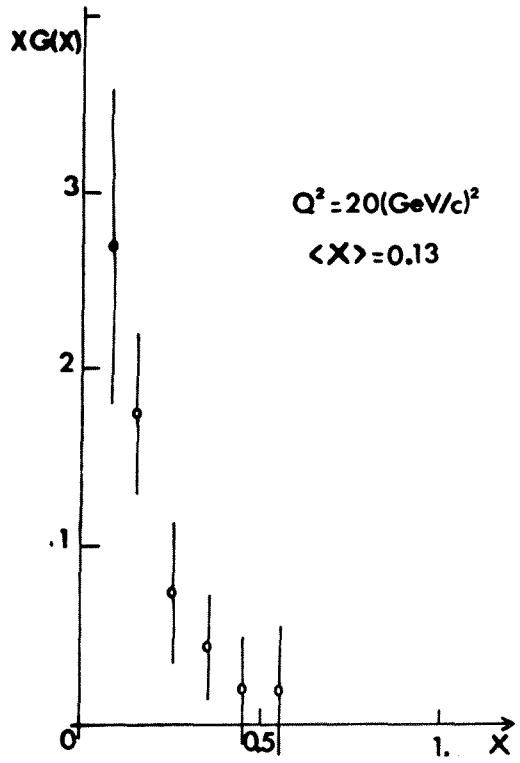

FIG. 22 - Gluon distribution determined by Baulieu-Kounas method with CDHS data.

The slope $\frac{d\, F_2(x)}{d \ln q^2}$ and the integral $I_1(x)$ can be computed at fixed q^2 from the data. No extrapolation to x=0 is needed and the value of $I_1(x)$ is much less sensitive to the extrapolation near (X=1) than it was in the moments evaluation. Integral $I_2(x)$ is then safety obtained.

Baulieu and Kounas have analytically computed the inverse $f_n(x)$ functions, such as :

$$X^n = \int f_n(y)\, P_{qG}\left(\frac{X}{y}\right) \frac{dy}{y}$$

In order to extract the gluon distribution X G(x) from $I_2(x)$ it is then necessary to fit I_2 by a simple polynomial expression

$$I_2(x) = \sum_n a_n\, x^n$$

The corresponding gluon distribution

$$X\, G(x) = \sum_n a_n\, X\, f_n(x)$$

is not sensitive to any particular choice of the polynomial parametrisation. Figure 22 shows the gluon distribution obtained with the CDHS data following this analysis at $Q^2 = 20\ (GeV/c)^2$. This distribution is well fitted by a distribution $(1-x)^5$.

This elegant method will be very interesting when high energy data will be available so that it can be used at different q^2.

These three independent analysis on gluon momentum distribution agree upon a value of $\langle x \rangle$ around 0.14 and show a distribution falling with x as $\sim (1-x)^5$.

IX. SUMMARY ON MULTILEPTON PHYSICS

What follows is a brief summary of multilepton physics. This topic was not covered elsewhere in this conference, neither by F. DYDAK (Neutral current) nor by B. TALLINI (Hadronic final states) except for exclusive production of charm. The lack of time limits the development of this topic.

A - Dimuon production : charm.

i.) Bubble chambers. Here we have followed a paper presented by G. MATTEUZZI [40] at BERGEN Conference. The sample of $\mu^-\mu^+$ events from the bubble chambers is now of the order of hundred (GGM) and the largest sample of μ^-e^+ events consists of 204 events (BNL-C). The results of these analyses have improved the already existing evidence that dilepton production is related to charm i.e. :

1. Large asymmetry between the momentum of the leading system and that of the "decay muon".
2. Number of V^0 per dilepton event now stabilised around 0.6.
3. The mass spectrum of the $K^0e^\pm$ system favors a $K\pi e\nu$ decay rather than a $Ke\nu$ one.
4. Missing energy such as $\langle Z_\nu \rangle = 0.24 \pm 0.09$.
5. Fragmentation function D(Z). If one parametrizes as $D(Z) = e^{-bZ}$ then $b = 1.25 \begin{smallmatrix} + 1.1 \\ - 0.75 \end{smallmatrix}$.
6. The rate is similar for neutrinos and for antineutrinos and is about 0.7 ± 0.3 % with respect to the charged currents.

ii.) Counter groups. The same general conclusion was already obtained earlier by counter experiments and there nothing new has been published since the TOKYO Conference. The new information which has been obtained by CDHS experiment concerning opposite sign dimuons involves the amplitude of production and the strange sea discussed earlier.

B - Trimuon production.

What was expected before the high statistic experiments was exotic decays of lepton cascades or heavy quarks as represented in the following graphs :

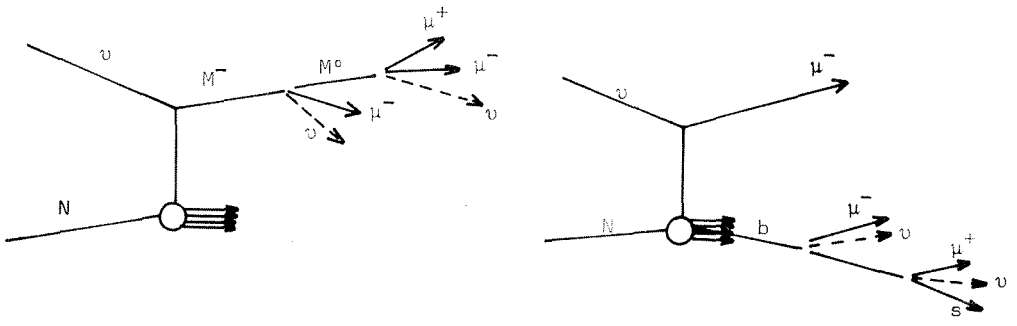

What we found CDHS [41] , HPWF [42] , was data consistent

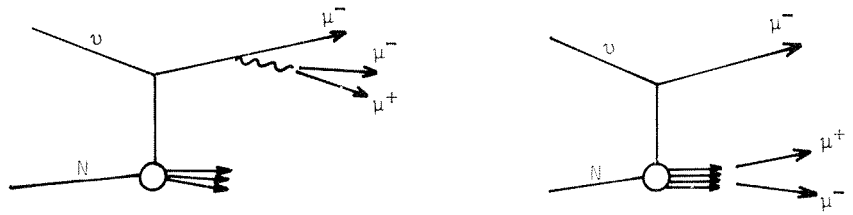

with charged current interaction with additional production of a muon pair by radiative and hadronic processes.

The measured 3μ/1μ rates are very compatible between the two different experiments for neutrino energies large enough to minimize the effect of the experimental cut on the second μ momentum.

			$E_\upsilon > 100$ GeV
υ	HPWF [24]	$(6.0 \pm 1.2)\ 10^{-5}$	$(1.2 \pm 0.5)\ 10^{-4}$
	CDHS [41]	$(3.0 \pm 0.4)\ 10^{-5}$	$(1.1 \pm 0.25)\ 10^{-4}$
$\overline{\upsilon}$	CDHS [43]	$(1.8 \pm 0.6)\ 10^{-5}$	$(0.9 \pm 0.5)\ 10^{-4}$

Furthermore antineutrino trimuon events are explained by the same processes used to describe neutrino trimuon production. No new sample of trimuon events has been presented since the TOKYO Conference. The limit on processes such as heavy lepton cascade (< 17% of trimuon sample at 90% C.L.) or new flavored quark cascade decay (< 10% of trimuon events at 90% C.L.) are still large and leave open a small but non-negligible possibility to discover new processes, but one needs at least a factor of 5 to 10 better statistics. The two trimuons "super events" found by HPWF [24] remain unexplained.

C - Like-sign dimuons.

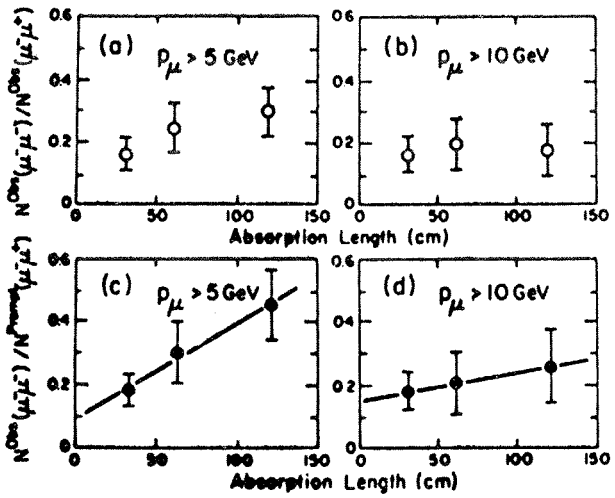

FIG. 23 - Ratio of the number of observed $\mu^-\mu^-$ events to $\mu^-\mu^+$ events in three targets of different absorption length [42] [24] .

Although we know that the "like-sign" dimuon sample is dominated by π-K decay processes it is still interesting to try to discover other processes in such a sample. It would be interesting in this light to have a large sample of μe events in which the probleme of π-K contamination is very much reduced. Like sign dimuon production can come from charm-anticharm production ($c\,\overline{c}$) or from the decay of a heavy quark. Two different methods to find such a prompt like-sign signal have been used up to now :

1. Using targets of different densities [42] one can try to find the prompt signal by extrapolation to infinite density, Fig.23.

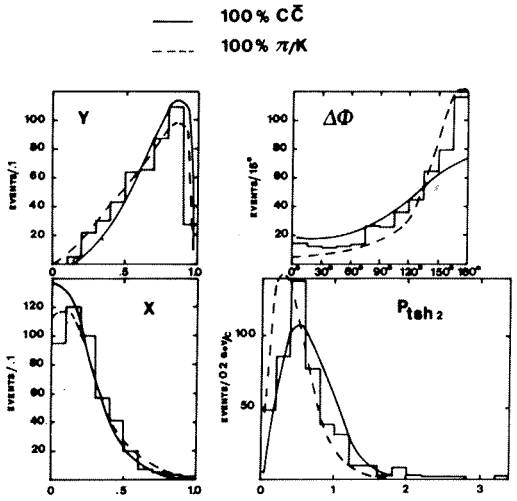

FIG. 24 - Distributions of $\mu^-\mu^-$ events in neutrino interactions.

This is perhaps the best way to detect a signal since it measures directly the π-K decay background, however statistics are quite low in this experiment (46 events).

2. Experiments which have larger statistics but only a single density target must rely upon a simulation of the π-K decay by Monte-Carlo. Then one can compare with the absolute rate or the distributions of measured quantities to find a signal, if the shape of the distributions for the different processes are sufficiently distinct. This method was used by the CDHS [27] collaboration, applied upon a sample of $\simeq$ 500 $\mu^-\mu^-$ and 60 $\mu^+\mu^+$. This demanded extremely great care in constructing the Monte-Carlo program. The difficulties are increased since it happens that the shape of distribution from π-K decay and c $\bar{c}$ production (as well as b decay) are quite similar as shown in figure 24.

Experimental results are presented in table VIII.

TABLE VIII : Prompt signal $\mu^-\mu^-$ ratio relative to $\mu^+\mu^-$

	$P_\mu > 5$ GeV	$P_\mu > 10$ GeV
HPWF [42]	(6.5 ± 5) %	(12 ± 5) %
CDHS [27]	(4.1 ± 2.2) % *	(2.0 ± 1.3) %

* This result is obtained for a P_μ of 6.5 GeV/c cut off.

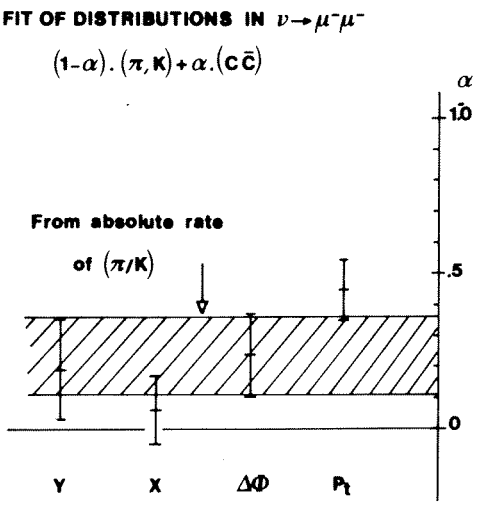

FIG. 25 - Fits of distribution of $\mu^-\mu^-$ events in neutrino interactions.

A fit to the shape of some variable distributions, X, Y, $\Delta\Phi$, $P_\perp$, by the CDHS collaboration assuming that the signal is due to c $\bar{c}$ production and π-K decays gives a comparable result for the prompt signal as shown in figure 25. Considering the similarities of the distributions for the two processes, one must take this last figure with caution.

On the other hand, if we attribute the signal to $\bar{b}$ production the limits obtained are not better than those obtained earlier from the trimuon event sample. It is certainly better to look for b production in the antineutrino process. Using the CDHS results one can calculate an upper limit on the transition coupling u→b (gG) giving g < 6 % [44].

We see here the intrinsic difficulty to disentangle b (or $\bar{b}$) production from c $\bar{c}$ production since the variable distributions of these two processes are quite comparable. It is mainly the $P_\perp$ of the second μ relative to the hadron shower direction which has been used to look for heavy particle production.

Because of the flavor changing nature of the charged weak current, neutrino physics has long had great hope to find new quarks. This capability has been already illustrated by the observation of charm in neutrino reactions where it is copiously produced. The experimental problem has become harder, but an increase in energy will certainly help to continue the hunting.

X. CONCLUSION

In two years of neutrino physics on the charged weak current enormous progress has been achieved. Starting from early questions on the Y distributions to test on elementary but vital laws of the weak interaction physics, we have arrived at a period of much more refined studies focusing upon nucleon structure , scaling violation, gluon distribution, and even new heavy quark searches. The picture is far from complete; after a very brilliant begining, the tests of QCD theory have to face the limitations of the present experimental data. Even the choice among different hypotheses in QCD calculations or the comparison between QCD and other theories need a new step of experimental data : higher statistics and more subtle analysis. Perhaps this means some tedious work rather than spectacular discoveries, however one can never exclude the possibility of a surprise. Neutrino studies are still essential for a growing understanding of weak interactions.

Acknowledgments :

I would like to thank Ph. BLOCH and F. EISELE for their great help when discussing several points. I would also like to thank B. PEYAUD, S. LOUCATOS, J. RANDER for their critical reading of the manuscript and Mrs G. BEUCHEY and S. ROUSSIEZ for the good work they did in doing all the typing and figures.

References.

1 N. ARMENISE et al - Phys. Letters 84B (1979) 137.

2 M. JONKER et al - Preprint CERN - presented at this conference - submitted to Physics Letter B.

3 M. GOURDIN - Proceedings of the International Neutrino Conference, Aachen 1976,p.234.

4 CALTECH : B.C. BARISH et al - Phys. Rev. Letters 39 (1977) 741.

5 BEBC : P.C. BOSETTI et al - Phys. Letters 70B (1977) 273.

6 CDHS : J.G.H. de GROOT - Z. Physik C, Particles and fields 1,143-162 (1979).

7 S. CIAMPOLILLO et al - Phys. Letters 84B (1979) 281.

8 J. LUDWIG - International Conference on Neutrino, BERGEN 1979.

9 GGM Collaboration : H. WEERTS - International Conference on Neutrino, BERGEN 1979.

10 BEBC - WA24 Collaboration : D.C. COLLEY et al - Rencontre de Moriond, Mars 1979.

11 GAEMERS - private communication to the CDHS Group.

12 CALLAN-GROSS - Phys. Rev. Letters 22 (1969) 156.

13 P. MUSSET et J.P. VIALLE - Neutrino physics with GGM - Physics Report 39C (1978).

14 P.C. BOSETTI et al - Nucl. Phys. B142 (1978) 1.

15 A. BENVENUTI et al - Phys. Rev. Letters 42 (1979) 1317.
B.M. HEAGY : International Conference on Neutrino, BERGEN 1979.

16 D. SINCLAIR - presented to the International Conference on Neutrino, BERGEN 1979.

17 CDHS Collaboration - A. SAVOY-NAVARRO - Int. Conf. on Neutrino, BERGEN 1979.
- J. WOTSCHAK - This conference.

18 This question was raised by F. SCIULLY.

19 E.M. RIORDAN et al - SLAC-PUB - 1634.

20 R.E. TAYLOR - 19th International Conference on High Energy Physics, TOKYO 1978.

21 B.A. GORDON et al - Phys. Rev. Letters 41 (1978) 615.

22 G. ALTARELLI et al - Nuclear Physics B143 (1978) 521.

23 T. EICHTEN et al - Phys. Letters 46B (1973) 275.

24 A.K. MANN - Recent results on Neutrino reactions - Proceeding of the 19th International Conference on High Energy Physics, TOKYO 1978.

25 M. HOLDER et al - Phys. Letters 69B, 3 (1977) 377.

26 V.E. BARNES - Perdue, Argonne, Carnegie Collaboration - International Conference on Neutrino, BERGEN 1979.

27 H.G. WILLUTZKI - CDHS Collaboration - International Conference on Neutrino, BERGEN 1979.

28 K. TITTEL - Neutrino reactions I. - Proceeding of the 19th International Conference on High Energy Physics, TOKYO 1978.

29 G. ALTARELLI and G. PARISI - Nuclear Physics B126 (1977) 298.
G. ALTARELLI - Cours d'été de l'Ecole de Gif-sur-Yvette (1978).

30 O. NACHTMANN - Nuclear Physics B78 (1974) 455.

31 F. EISELE - Compte-rendus de la 14e Rencontre de Moriond - Les Arcs (France) 1979.

32 H. HARARI - SLAC-PUB - 2254. January 1979.

33 J.G.H. de GROOT et al - Phys. Letters 82B (1979) 292.

34 G. MORFIN - ABCDLOS Collaboration - International Conference on Neutrino, BERGEN 1979.

35 F. EISELE - private communication.

36 W.A. BARDEEN et al - Phys. Rev. D18 (1978) 3998.

37 J.G.H. de GROOT et al - Phys. Letters 82B (1979) 456.

38 A.J. BURAS and K.J.F. GAEMERS - Nucl. Phys. B132 (1978) 249.

39 L. BAULIEU and C. KOUNNAS - Preprint LPTENS 78/27 (1978).

40 C. MATTEUZZI - Multilepton production in bubble chambers - International Conference on Neutrino, BERGEN 1979.

41 T. HANSL et al - Nuclear Physics B142 (1978) 381.

42 A. BENVENUTI et al - Phys. Rev. Letters 41 (1978)725.

43 J.G.H. de GROOT et al - Trimuon events observed in high energy antineutrino interactions accepted by Phys. Letters to be published.

44 J. SMITH and G.H. ALBRIGHT - Like sign dimuon production by neutrinos and antineutrinos - preprint T.H. 2666 - CERN.

* * *

DISCUSSION

Chairman: V.L. Telegdi
Sci. Secretaries: J. de Groot and W. Scott

A. Bodek: For the same value of Q^2 how well do the absolute values of the CDHS and BEBC agree with each other?

R. Turlay: There is a discrepancy in the value of F_2 for the large x bin. So the moments which have been published have a systematic 20% disagreement. But when you take these moments at the power of -1/dW you have to be careful to use the same number of flavours if you want to compare the results.

K. Winter: When you are plotting the logarithm of one moment against the log of another you are introducing large correlations which give a trend which is not too different from the QCD prediction. Have these correlations been taken into account when the slope fit has been performed? If not, I think the agreement is to some degree fortuitous because the errors of the slopes are expected to be much larger.

R. Turlay: It is true that there are strong correlations between these different moments. For example, the correlation ellipses have the larger axis parallel to the line we want to fit. These correlations have been taken into account.

J. Ludwig: Why can BEBC go to higher Q^2 values (by a factor 2) than CDHS in the log-log plot of moments?

R. Turlay: BEBC cannot have higher Q^2 values than CDHS: the beam energy is the same for the two experiments and the number of events in BEBC experiments is smaller than in CDHS. But in the log-log plot the Q^2 scale disappears and the points reflect the magnitude of the scaling violation. For the same Q^2 range the two points from BEBC and CDHS are not at equal values of $\log M_i / \log M_j$.

HADRONIC FINAL STATES IN NEUTRINO AND ANTINEUTRINO CHARGED-CURRENT EVENTS

B. Tallini
DPhPE, CEN Saclay, France

ABSTRACT

The results of the analyses concerning the hadronic systems produced in $\nu/\bar{\nu}$ nucleon interactions are reviewed. Particular attention is devoted to the questions of factorization, scaling deviations of fragmentation functions, and the behaviour of $\langle p_T^2 \rangle$ of individual hadrons as a function of Q^2. Tests of QCD ideas concerning these effects are discussed. Also the present status of the production of charmed states in $\nu/\bar{\nu}$ interactions in bubble chambers is summarized.

In this report I will discuss the following topics:

1. Fragmentation functions.
2. Inclusive single-hadron average transverse momentum $\langle p_T \rangle$ distributions.
3. Charmed states.

The papers reviewed here are from this Conference and from the Bergen "Neutrino 79" Conference.

1. FRAGMENTATION FUNCTIONS

1.1 Single-moment analysis

The single particle inclusive cross-section for the process $\nu N = \mu h^{\pm} X$ can be written as

$$\frac{d^2\sigma^h(Q^2)}{dxdz} = \frac{G^2 mE}{\pi} F(x,Q^2) \cdot D_q^h(z) \ , \qquad (1)$$

where

$x = Q^2/2M\nu$
$\nu = E_\nu - E_\mu$
$z = E_h/\nu$ (E_h = energy of the hadron h)
$W^2 = M^2 + Q^2[(1/x) - 1]$ = square of the total invariant mass of the hadronic system (h + X).

$F(x,Q^2)$ is the structure function of the nucleon and represents the quark momentum distribution, whereas $D_q^h(z)$ is the fragmentation function and represents the probability that the quark q gives a hadron h with a fraction z of the total hadron energy ν. In the naïve parton model the D_q^h fragmentation functions are expected to factorize and to scale, i.e. the $D_q^h(Z)$ are independent of x and Q^2.

At this Conference the Aachen-Bonn-CERN-Munich-Oxford (ABCMO) Collaboration has presented an analysis of fragmentation functions for νH_2 cc events in a wide-band beam (WBB) in BEBC[1]. This analysis is appearing in these same Proceedings and I have no space to repeat it here except for the main results, which are the following:

- Factorization does not hold, i.e. the D_u^h's are functions of z and x.
- There is evidence for scaling deviations in the fragmentation functions, i.e. the D_u^h's are functions of Q^2.

- The variation with Q^2 of the fragmentation functions is such that the single z moments of the non-singlet (NS) combination $(D_u^{h^+}-D_u^{h^-})$ defined as

$$D_M^{NS}(Q^2) = \int_0^1 z^{M-1}\left(D_u^{h^+}-D_u^{h^-}\right) dz \qquad (2)$$

follow the predictions of perturbative QCD, that is

$$D_M^{NS}(Q^2) = \frac{C_n^{NS}}{\left[\ln(Q^2/\lambda_2)\right]^{d_{NS}}} , \qquad (3)$$

where the d_{NS} are parameters (function of M) predicted by the theory. Using these $D_M^{NS}(Q^2)$ moments the ratios of d_{NS}'s have been determined experimentally and agree satisfactorily with the theory (spin-1 gluons).

Concerning this analysis the following comments are appropriate:

i) In order to obtain the NS combination $(D_u^{h^+}-D_u^{h^-})$ from the νp events, it was imposed that

$$xF_1 = F_2 = xF_3 , \qquad (4)$$

which is equivalent to neglecting the sea contribution. This is a strong assumption, especially for small x-values where the sea contribution is supposedly important. In order to release the condition (4) it will be necessary, in future analyses, to fit the $y = \nu/E_\nu$ distributions.

ii) Factorization was assumed in the (single) moment analysis.

1.2 Double-moment analysis

In a situation of non-factorization it is most natural (and more rigorous) to use double moments in x and z of the fragmentation functions. This analysis has been performed by Scott[2] on the same νH_2 BEBC data and was presented at the Bergen Neutrino 79 Conference. Theoretically the double moments, first discussed by Ellis et al.[3], are defined as follows:

$$D(M,N,Q^2) = \frac{\iint x^{N-2}\, z^{M-1}\, F(x,Q^2)\, D_u^h(x,z,Q^2)\, dxdz}{\int x^{N-2}\, F(x,Q^2)\, dx} . \qquad (5)$$

To determine the $D(M,N,Q^2)$ experimentally, single-particle inclusive cross-sections are used, $d^2\sigma^h(x,z,Q^2)/dxdz$ and $d\sigma(x,Q^2)/dx$ corrected for the neutrino flux $\phi(E_\nu)$:

$$D(M,N,Q^2) = \frac{\iint x^{N-2}\, z^{M-1}\, \frac{\pi}{G^2 M E_\nu}\, \frac{d^2\sigma^h}{dxdz}\, (x,z,Q^2)\, dxdz}{\int x^{N-2}\, \frac{\pi}{G^2 M E_\nu}\, \frac{d\sigma}{dx}\, (x,Q^2)\, dx} . \qquad (6)$$

In evaluating Eq. (6), x was replaced by the Nachtmann variable

$$\xi = 2x\Big/\left(1+\sqrt{1+\frac{4m^2x^2}{Q^2}}\right)$$

which is supposed to take into account effects due to target fragments[4]: The Z of a given track was calculated in the Breit frame:

$$Z_{BF} = \frac{E + p_L}{\sqrt{Q^2}} , \tag{7}$$

where E and p_L are the track energy and longitudinal momentum in the Breit frame. Finally, in order to select the current fragments, tentatively only tracks with $p_L > 0$ were used in the integrals.

The double moments of the NS combination,

$$D^{NS}(M,N,Q^2) = D^{h^+}(M,N,Q^2) - D^{h^-}(M,N,Q^2) , \tag{8}$$

are shown in Fig. 1 for different values of M and N. If factorization was valid, the $D^{NS}(M,N,Q^2)$ dependence on Q^2 should only be a function of M and not of N, which is clearly not the case. Thus the M and N dependence of the D^{NS} seen in Fig. 1 proves that x, z factorization does not hold. Further, the evolution of the $D^{NS}(M,N,Q^2)$ with Q^2 is in good agreement with QCD, as shown in Fig. 2, which represents the log $D^{NS}(M,N,Q^2)$ versus log $D^{NS}(M,N,Q^2)$ [5] for various pairs of values (M,M') and for different N's. The experimental points are predicted to lie on straight lines, the slope of which are the ratios of the $d_{NS}(M)/d_{NS}(M')$ independent of N. Both of these predictions seem to be well verified experimentally; with the exception, perhaps, of the N = 1 case, which suffers most from assumption (4) above.

It is important to note that the double-moment analysis permits us to study and test the original Q^2 dependence of the $D^{NS}(M,N,Q^2)$ by unfolding any possible Q^2 dependence which might be introduced by the assumption of factorization.

In QCD, factorization is expected to hold in leading order in the coupling constant α_s, and deviations from factorization are presumably due to next to leading order corrections. Such calculations have been carried out by Sakai[6], and the comparison with the data is shown in Fig. 3. It appears that the agreement is not too good, especially for small M and N; this implies that either the α_s corrections are not sufficient to account for all non-factorization effects observed, or that the assumptions made in the determination of the experimental moments -- as in Eq. (4) above -- are too strong. It should also be pointed out that this comparison is still preliminary, and more work is in progress.

2. TRANSVERSE MOMENTUM OF SINGLE HADRONS

I now turn to the discussion of the properties of the transverse momentum p_T of single hadrons produced in $\nu/\bar{\nu}$ interactions. Here the p_T is defined with respect to the vector resultant of the measured hadronic system. The measurement of p_T can best be done in a heavy-liquid bubble chamber where the single hadrons are well measured and where most of the hadron shower is reconstructed. However, in order to reduce the possible systematic bias in the determination of this hadron shower direction introduced by undetected neutrals, also the variable $p_{T,out}$ is used, which is the component of p_T on the perpendicular to the ν-μ plane. If we

assume azimuthal isotropy, $\langle p_{T,out} \rangle$ is related to $\langle p_T \rangle$ by the relation $\langle p_T \rangle = \sqrt{2} \cdot \langle p_{T,out} \rangle$. Note that $p_{T,out}$ is well determined since it is defined by means of well-measured quantities only: the ν and μ directions and the single hadron vector.

In the narrow-band beam (NBB) ν experiment in BEBC filled with a Ne/H_2 mixture, an increase of $\langle p_T^2 \rangle$ with Q^2 or W^2 was observed[7] mainly for $z > 0.2$, a cut devised to eliminate most of the target fragments. No significant effect was observed in the NBB $\bar{\nu}$ events nor in the WBB ν experiments[8]; this apparent discrepancy could be explained by the softer energy spectra of the $\bar{\nu}$ NBB or of the ν WBB which limits the Q^2 and W^2 ranges of the events.

An increase of $\langle p_T^2 \rangle$ with Q^2 is expected in QCD as due to gluon radiation from quarks. Quantitatively, perturbative QCD predicts[9] that $\langle p_T^2 \rangle \approx Q^2/\ln (Q^2/\Lambda^2)$, which is in reasonably good agreement with the ν NBB data[7,10]. New $\bar{\nu}$ data have been presented by the FNAL-IHEP-ITEP-Michigan (FIIM) Collaboration[11] obtained with the 15' bubble chamber filled with Ne/H_2 at FNAL. In this experiment half of the data was taken in a standard WBB, while the other half was obtained in a sign-selected "bare target" $\bar{\nu}$ beam which, with its harder $\bar{\nu}$ energy spectrum, allows the Q^2 range explored to be extended up to $Q^2 \sim 150$ $(GeV/c)^2$. A total of 7000 charged-current $\bar{\nu}$ events were analysed, and Figs. 4 show, for these events, the $\langle p_{T,out}^2 \rangle$ as a function of Q^2 and W^2 for positive and negative hadrons. Using the cut $z > 0.2$, an increase of $\langle p_{T,out} \rangle$ with Q^2 and W^2 is observed, in good quantitative agreement with QCD predictions[9b]. As is apparent in Fig. 4, this effect is only observed for negative hadrons h^-, which could imply that the h^-'s carry the information of the original p_T of the fragmenting quark better than do the h^+'s.

Also in the same experiment[12], the inclusive study of the V^0 sample consisting of 900 K^0's and 400 Λ's shows an increase of $\langle p_{T,out} \rangle$ with Q^2, W^2, and $1/x$ for the K^0's in the current fragmentation region ($z > 0.2$) but not for the Λ's (mostly associated with target fragments), as can be seen in Figs. 5 to 7. For the K^0 mesons the behaviour of p_T^2 follows closely the predictions of QCD, as indicated in the same figure.

I wish to remark, however, that part of the increase of p_T^2 of the K^0's, as $x \to 0$, could be also explained by charm production and decay which, in $\bar{\nu}$ interactions, would also correlate large p_T's -- due to the large mass of the charmed states -- with the small x region of the sea, as we will see in Section 3. For this purpose a comparison with the properties of the V^0's produced in neutrino experiments will be most useful.

As interesting result from the same collaboration is the determination of the Λ polarization. Figure 8 shows this polarization as a function of Q^2 and x. There is some indication of a non-zero Λ polarization perpendicular to the production plane and associated with the small x region:

$$\langle p_N \rangle = 0.34 \pm 0.18 \ . \qquad (8)$$

The Aachen-Bonn-CERN-Demokritos-IC London-Oxford-Saclay (ABCDLOS) Collaboration[13], using the SPS narrow-band $\nu/\bar{\nu}$ beam in BEBC filled with Ne/H_2, with improved ν statistics (by a factor of ~ 2), confirm the linear increase of $\langle p_T^2 \rangle$ with Q^2 (Fig. 9a) and with W^2 (Fig. 9b) originally observed in the same experimental conditions.

Altarelli[9] and Odorico et al.[10] have shown that the predicted variation of $\langle p_T^2 \rangle$ versus Q^2,

$$\langle p_T^2 \rangle \approx Q^2/\ln(Q^2/\Lambda^2) \ , \qquad (9)$$

has an important x dependence which -- according to QCD -- can be absorbed into a change of variable $Q^2 \to W^2$, i.e. the function

$$\langle p_T^2 \rangle = f(W^2) \text{ is independent of } x \ . \qquad (10)$$

The new BEBC NBB ν data, shown in Fig. 10, are in good agreement with this prediction (10). This makes the W^2 a more convenient variable to use phenomenologically. The same BEBC NBB data are being analysed in terms of non-singlet moments of the "transverse" variable $z_T = 2p_T/W$; these moments, defined as

$$D_T^M = \int z_T^{M-1} \left(D_u^{h^+} - D_u^{h^-} \right) dz_T \ , \qquad (11)$$

are expected[14] to show in QCD a characteristic logarithmic dependence with Q^2. Figure 11 represents some of these moments versus Q^2 and versus W^2. Experimentally the factorization properties of Eq. (10) seem to be verified, in a more general way, also for the higher moments of z_T as shown in Fig. 12. This moment analysis is still in progress.

3. CHARMED STATES

Two important developments have been achieved on this subject this year:

a) The lifetime of charmed particles has been measured by the direct observation of their decay, both in emulsions and in bubble chamber neutrino experiments, with the result $\tau_c \simeq (1\text{-}5) \times 10^{-13}$ s, in good agreement with the theoretical predictions. This topic has been reviewed at this Conference by M. Conversi, and I refer the reader to his report.

b) More direct evidence for the existence of charmed states -- especially charmed baryons -- has been accumulated in inclusive or exclusive analyses of ν, $\bar{\nu}$ charged-current interactions. In the inclusive studies, important progress in the charm search has been made by both the ABCMO Collaboration working with BEBC[15] and by the BNL-Columbia Collaboration in the 15' FNAL bubble chamber[16]. This has been achieved by assuming that some of the D^0 or Λ_c resonances produced are the decay products of higher-mass charmed resonances (lying $\sim$ 150 MeV above) in the processes

$$D^{*+}(2005) \to D^0(1860) + \pi^+ \qquad (12a)$$

or

$$\Sigma_c^{++}(2420) \to \Lambda_c^+(2260) + \pi^+ \qquad (12b)$$

which are predicted[17] to be the most favoured decay modes of the D^{*+} and Σ_c^{++}. Experimentally this is done by looking at the correlation between the effective mass M_1 of the D^0 or Λ_c system S_1 in a given decay mode and the mass difference Δm between this mass M_1 and the effective mass of the system obtained by adding an extra π^+ to S_1: $\Delta m = M(S_1 + \pi^+) - M_1$. The success of this method is due to the fact that i) the Q values involved in the decay processes (12) are small ($\sim$ 150 MeV), and ii) the determination of Δm is very precise (a few MeV) since the errors on all tracks are eliminated in the difference except for the extra π^+. The results are displayed in Figs. 13 and 14, which give the distributions of Δm for the processes (12a) and (12b), respectively, for various decay modes of the D^0 and of the Λ_c^+; peaks are observed at $\Delta m = 145$ MeV for the D^0 and at $\Delta m \sim 166$ MeV for the Λ_c^+ cases. For the charmed baryon case,

selecting combinations with Δm in the range 166 ± 6 MeV the BNL-Columbia Collaboration obtained the mass distributions shown in Fig. 15, where sharp peaks at the Λ_c mass are observed with widths compatible with zero, for the various decay modes. This additional clear evidence in favour of the Λ_c^+ and Σ_c^{++} comes at the appropriate time to clarify the somewhat confused situation of the charmed baryons of last year[18].

The total number of events observed in the four decay modes of the Λ_c, i.e. $\Lambda\pi^+$, $\bar{K}^0 p$, $K^{*-}p\pi^+$, $Y^{*+}\pi^+\pi^-$, is 20, with an estimated background of 6 from which a production rate in ν-Ne-cc interactions for the $\Sigma_c^{++} \to \Lambda_c^+\pi^+$ of $\sigma \cdot B(\Sigma_c^{++} \to \Lambda_c^+\pi^+)/\sigma_{tot} = (6 \pm 2) \times 10^{-4}$ is obtained, after correction for the K^0 and Λ^0 neutral decay modes and for detection efficiency. Figure 16 shows for the Σ_c^{++} candidates the decay angular distribution which is compatible with isotropy as expected for spin $\frac{1}{2}$. As for the $D^{*+}(2009)$ state, its production rate in νp-cc interactions has been estimated by the ABCMO Collaboration to be

$$\frac{\sigma(\nu p \to \mu^- D^{*+} + X)}{\sigma(\nu p \to \mu^- + X)_{W>2.9GeV}} = (4.1 \pm 2.4)\% ,$$

where the following branching ratios have been assumed: $D^{*+} \to D^0\pi^+ = 60 \pm 15\%$, $D^0 \to K^-\pi^+ = 1.8 \pm 0.5\%$, and $D^0 \to K^-\pi^+\pi^+\pi^- = 3.5 \pm 0.9\%$.

More indirect evidence for charm production in antineutrino interactions comes from the Argonne-Carnegie Mellon-Purdue Collaboration[19] in an inclusive study of V^0 events produced in $\bar{\nu}p$ cc reactions. As the authors point out, in $\bar{\nu}$ interactions the V^0's, which are the decay products of charm states, are expected to be mostly at large y and small x ($\bar{\nu}\bar{s} \to \mu + \bar{c}$). Figures 17a and 17b show the ratios $f_s(x,y)$ of the x and y distributions, respectively, between events with V^0 and all events. The data is compared with the predictions obtained using Feynman and Field quark distributions:

		V^0 probability
$\bar{\nu}u \to \mu^+ d$ $\bar{\nu}\bar{d} \to \mu^+ \bar{u}$	$(1-y)^2 xu(x) \cos^2\theta_c$ $x\bar{d}(x) \cos^2\theta_c$	-0.005 + 0.35 in W (V^0 associated production)
$\bar{\nu}u \to \mu^+ s$	$(1-y)^2 xu(x) \sin^2\theta_c$	0.25
$\bar{\nu}\bar{s} \to \mu^+ \bar{c}$	$x\bar{s}(x) \cos^2\theta_c$	0.50

As can be seen in Fig. 17, the data are in very good agreement with the charm model prediction.

Finally, concerning the exclusive production of charmed states, Table 1 summarizes the present status of the 3-C fits detected so far. In all cases the masses of all outgoing secondaries have been identified, and therefore the signature for a charmed state is the fact that for these events $\Delta S = -\Delta Q$.

Acknowledgements

I would like to thank Prof. D.H. Perkins and Dr. W.G. Scott for enlightening discussions and comments.

Table 1

Charm hadron production exclusive fits ($\Delta S = -\Delta Q$)

Baryons $\Sigma_c^{++}(2427)$, $\Lambda_c^+(2260)$		
BNL 7' [a] νH_2, νD_2	$\nu p \to \mu^- \Sigma_c^{++}(2426 \pm 12$ MeV) $\hookrightarrow \pi^+ \Lambda_c^+(2260)$ $\hookrightarrow \Lambda^0 \pi^+ \pi^+ \pi^-$	$M_{\Sigma_c^{++}} - M_{\Lambda_c^+} = 166 \pm 15$ MeV
BNL 7' [a] νH_2, νD_2	$\nu n \to \mu^- \Lambda_c^+(2254 \pm 12)$ $\hookrightarrow p\pi^+ K^{*-}(913 \pm 8)$ $\hookrightarrow K^0 \pi^-$ ($\therefore S = -1$)	
FNAL 15' [b] ν, Ne/H_2	$\nu p \to \mu^- \Sigma_c^{++}(2439)$ (candidate: Ne target) $\hookrightarrow \pi^- \pi^+ \Lambda_c^+(2776)$ $\hookrightarrow \pi^+ Y^*(1385)$ $\hookrightarrow \Lambda^0 \pi^+$	$M_{\Sigma_c^{++}} - M_{\Lambda_c^+} = 163 \pm 5$
Emulsion/BEBC [c]	$\nu p \to \mu^- \Lambda_c^+(2295 \pm 15)$ $\hookrightarrow p\bar{K}^{*0}(866 \pm 10)$ $\hookrightarrow K^- \pi^+$	$\tau_{\Lambda_c} = (7.3 \pm 0.1)\ 10^{-13}$ s 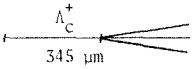
Mesons $D^{*+}(2009)$, $D^0(1863)$		
BEBC [d] νH_2	$\nu p \to \mu^- p D^{*+}(2009 \pm 1$ MeV) $\hookrightarrow \pi^+ D^0(1863 \pm 1)$ $\hookrightarrow K^- \pi^+$	$M_{D^{*+}} - M_{D^0} = 145.2 \pm 0.5$ MeV
BEBC [d] νH_2	$\nu p \to \mu^- p \pi^+ \pi^- D^{*+}(2013 \pm 4)$ $\hookrightarrow \pi^+ D^0(1865 \pm 4)$ $\hookrightarrow K^- \pi^- \pi^+ \pi^+$	$M_{D^{*+}} - M_{D^0} = 145.2 \pm 0.6$ MeV
BEBC [d] νH_2	$\nu p \to \mu^- \Delta^{++}(1201 \pm 2) D^0(1866 \pm 9)$ $\hookrightarrow K^- \pi^- \pi^+ \pi^+$	(K^- not identified)

a) E.G. Cazzoli et al., Phys. Rev. Lett. 34, 1125 (1975).
A.M. Cnops et al., Phys. Rev. Lett. 42, 197 (1979).

b) C. Baltay et al., BNL-Columbia Collaboration, Confirmation of the existence of the Σ_c^{++} and Λ_c^+ charmed baryons, Paper A1-103 presented by H.G. Kirk at the "Neutrino-79" Internat. Conf. on Neutrinos, Weak Interactions and Cosmology, Bergen, 1979.

c) Ankara-Brussels-CERN-UC Dublin-UC London-Open University-Pisa-Roma-Torino Collaboration, Lifetime of charmed hadrons produced in neutrino interactions, Paper reviewed by Prof. M. Conversi at this Conference.

d) Aachen-Bonn-CERN-Munich-Oxford Collaboration, Production of charmed mesons in neutrino interactions in hydrogen, Paper presented by D. Lanske at this Conference.

REFERENCES

1) Aachen-Bonn-CERN-Munich-Oxford (ABCMO) Collaboration, Fragmentation functions in neutrino-hydrogen interactions, Paper presented by N. Schmitz at this Conference.

2) W.G. Scott (ABCMO Collaboration), Experimental study of inelastic single-hadron production by neutrinos, Paper presented at the "Neutrino-79" Internat. Conf. on Neutrinos, Weak Interactions and Cosmology, Bergen, 1979.

3) J. Ellis, M.K. Gaillard and W.J. Zakrzewski, CERN TH-2595 (1978).

4) O. Nachtmann, Nucl. Phys. B63, 237 (1973); B78, 455 (1974).

5) Aachen-Bonn-CERN-IC London-Oxford-Saclay Collaboration, P. Bosetti et al., Nucl. Phys. B142, 1 (1978).

6) N. Sakai, CERN TH-2641 (1979).

7) Aachen-Bonn-CERN-IC London-Oxford-Saclay Collaboration, P. Bosetti et al., Nucl. Phys. B149, 13 (1979).

8) V. Stenger, Proc. Topical Conf. on Neutrino Physics, Oxford, 1978 (Science Research Council, Rutherford Lab., Didcot, 1978), p. 99.

9) a) G. Altarelli, Proc. Topical Conf. on Neutrino Physics, Oxford, 1978 (Science Research Council, Rutherford Lab., Didcot, 1978), p. 119;
b) A. Mendez, ibid., p. 135.

10) P. Mazzanti, R. Odorico and V. Roberto, Phys. Lett. 81B, 219 (1979).

11) V. Assomov et al., FNAL-IHEP-ITEP-Michigan Collaboration, Average transverse momentum behaviour of hadrons in antineutrino-nucleon charged-current interactions, Paper E18 submitted to the "Neutrino-79" Internat. Conf. on Neutrinos, Weak Interactions and Cosmology, Bergen, 1979.

12) V. Assomov et al., FNAL-IHEP-ITEP-Michigan Collaboration, Properties of K^0 and Λ inclusive production in charged current antineutrino-nucleon interactions, Paper E20 submitted to the "Neutrino-79" Internat. Conf. on Neutrinos, Weak Interactions and Cosmology, Bergen, 1979.

13) Preliminary data from the Aachen-Bonn-CERN-Demokritos-IC London-Oxford-Saclay Collaboration: ν-CC events from the NBB in BEBC filled with a 74% Ne/H_2 mixture, to be published.

14) J. Ellis, private communication.

15) Aachen-Bonn-CERN-Munich-Oxford Collaboration, Production of charmed mesons in neutrino interactions in hydrogen, Paper presented by D. Lanske at this Conference.

16) C. Baltay et al., BNL-Columbia Collaboration, Confirmation of the existence of the Σ_c^{++} and Λ_c^+ charmed baryons, Paper A1-103 presented by H.G. Kirk at the "Neutrino-79" Internat. Conf. on Neutrinos, Weak Interactions and Cosmology, Bergen, 1979.

17) A. De Rújula, H. Georgi and S.L. Glashow, Phys. Rev. D12, 147 (1975).

18) S. Wojcicki, SLAC-PUB-2232 (1978);
B. Tallini, CEA/DPhPE-Saclay 78-10 (1978).

19) S.J. Barish et al., Carnegie Mellon-Argonne-Purdue Collaboration, Strange particle production in $\bar{\nu}p$ interactions, Paper A3-2 presented at the "Neutrino-79" Internat. Conf. on Neutrinos, Weak Interactions and Cosmology, Bergen, 1979.

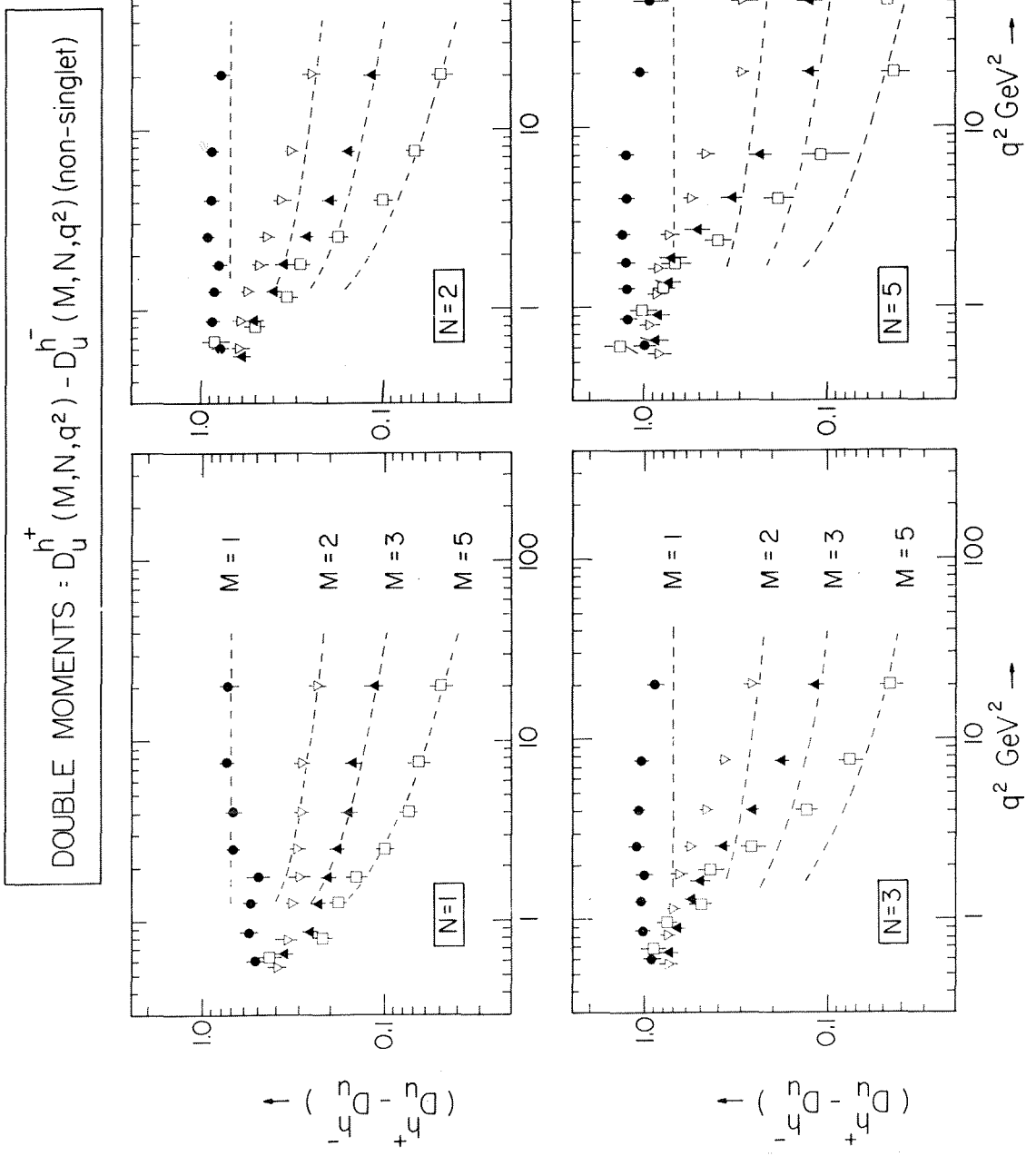

Fig. 1 Double moments of the non-singlet fragmentation functions versus Q^2 for different N's and M's. The broken lines are QCD predictions [Eq. (3) with Λ^2 = 0.5 GeV^2] normalized to the N = 1 data and repeated in the three other sets of M moments for N = 2, 3, and 5.

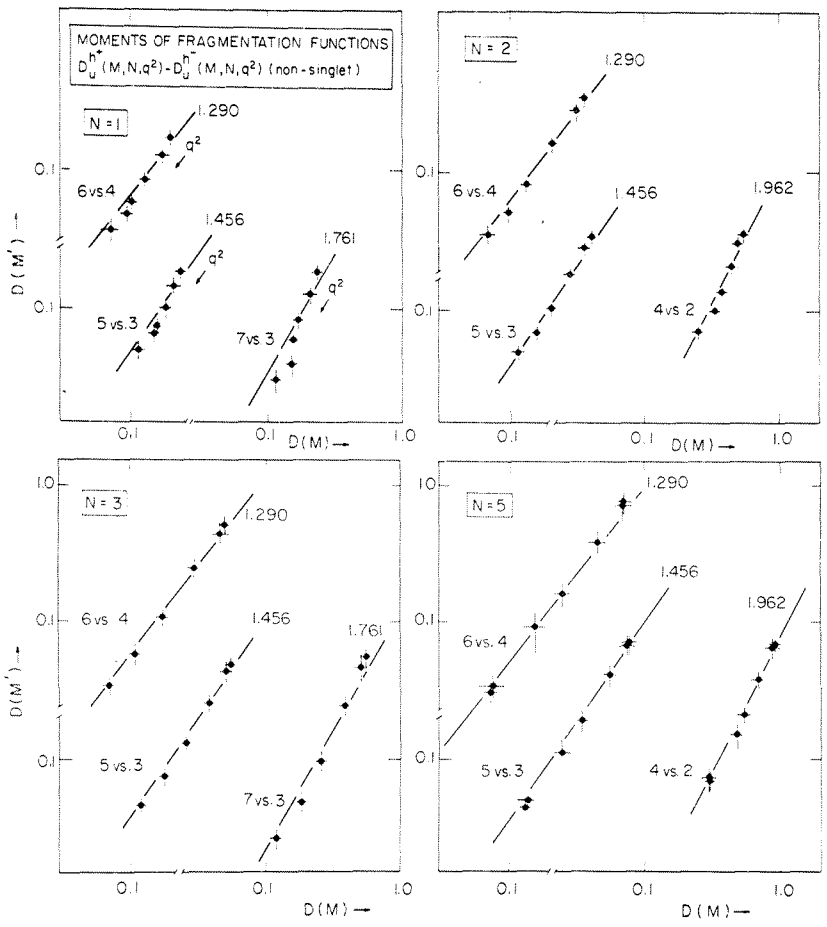

Fig. 2 Plots of log $D^{NS}(M,N,Q^2)$ versus log $D^{NS}(M',N',Q^2)$ for different pairs of values (M,M') and for different N's.

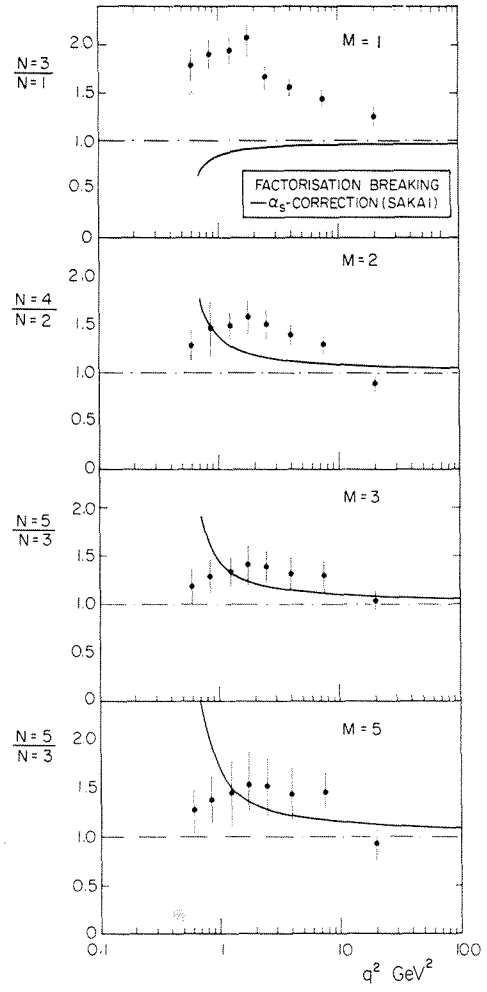

Fig. 3 Ratio of normalized double moments for selected values of M, N, N' compared with the predictions of Sakai (Ref. 6).

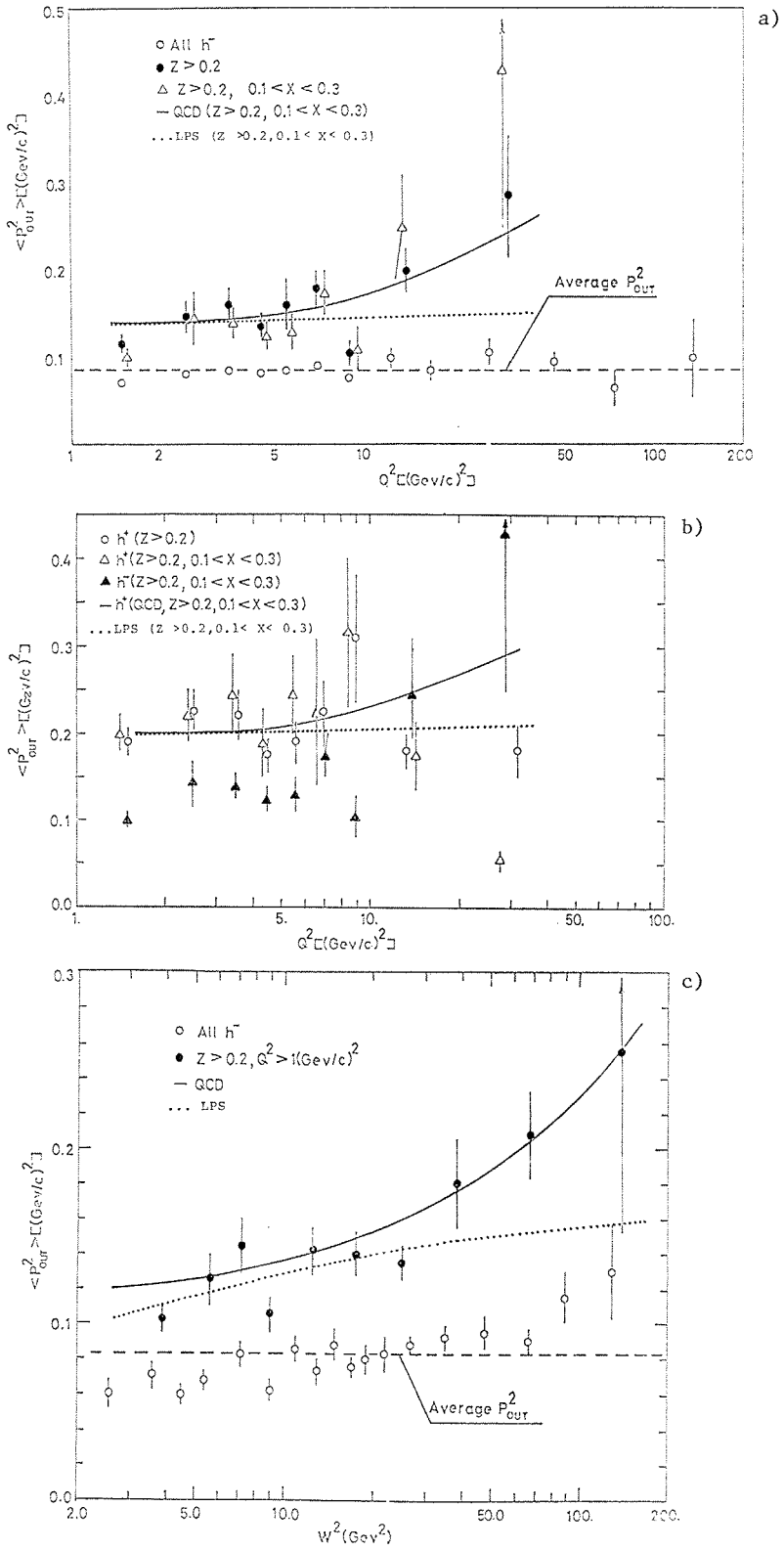

Fig. 4 $p^2_{T,out}$ of charged tracks in $\bar{\nu}$-cc events: a) for negative hadrons versus Q^2; b) for positive hadrons versus Q^2; c) for negative hadrons versus W^2.

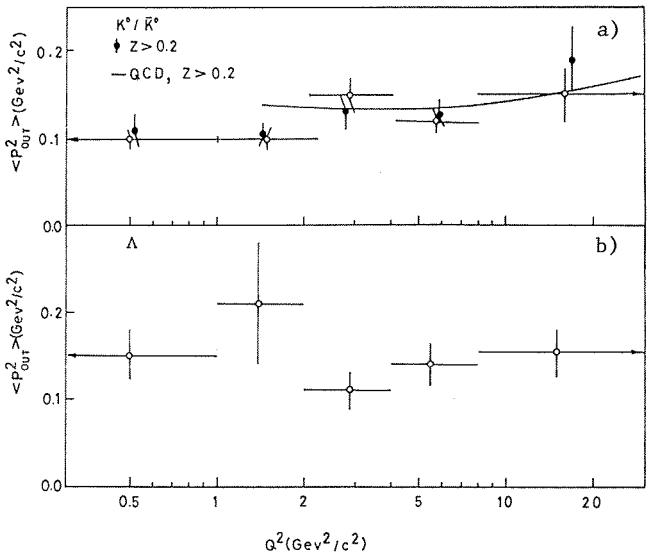

Fig. 5 $\langle p^2_{T,out}\rangle$ for V^0 tracks versus Q^2 in $\bar{\nu}$-cc events: a) for K^0's; b) for Λ^0's.

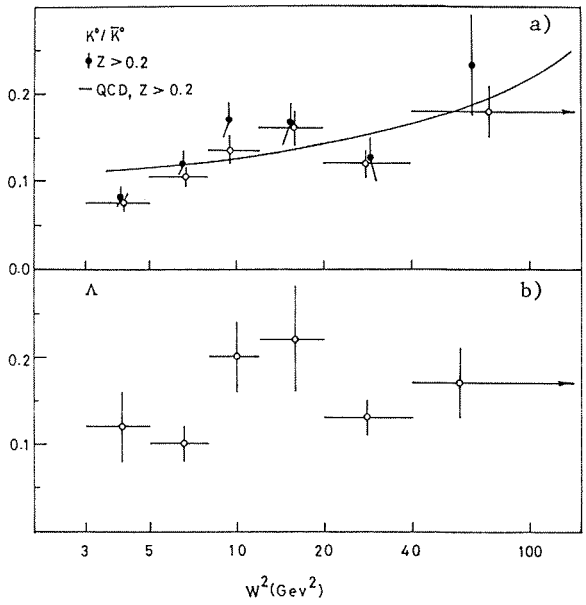

Fig. 6 $\langle p^2_{T,out}\rangle$ for V^0 tracks versus W^2 in $\bar{\nu}$-cc events: a) for K^0's; b) for Λ^0's.

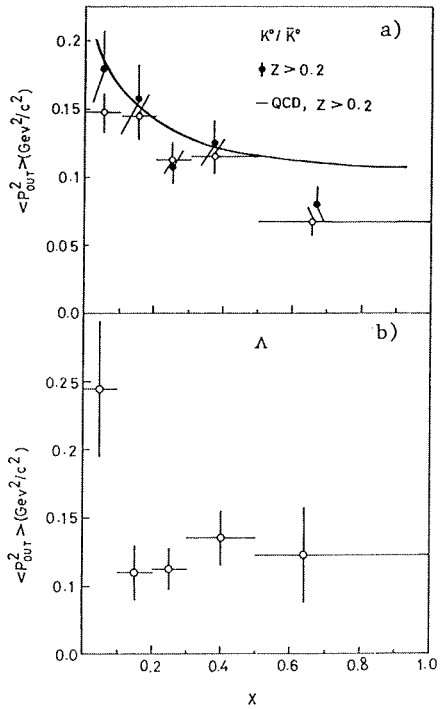

Fig. 7 $\langle p^2_{T,out}\rangle$ for V^0 tracks versus x in $\bar{\nu}$-cc events: a) for K^0's; b) for Λ^0's.

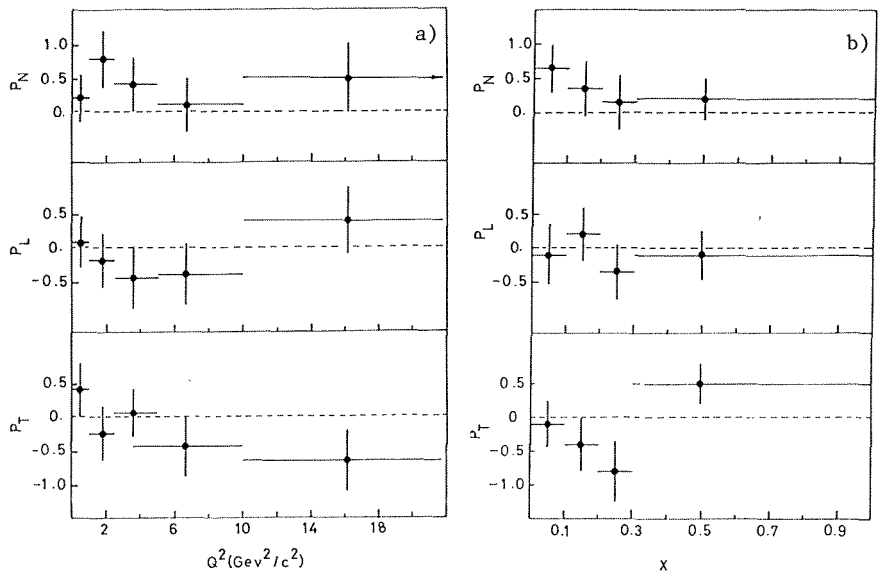

Fig. 8 Λ^0 polarization in $\bar{\nu}$-cc interactions: a) as a function of Q^2; b) as a function of x. p_N = component along the direction $\vec{e}_z = (\vec{e}_\Lambda \times \vec{e}_{\bar{\nu}})/|\vec{e}_\Lambda \times \vec{e}_{\bar{\nu}}|$; p_L = component along $\vec{e}_x = \vec{e}_\Lambda$; p_T = component along $\vec{e}_y = \vec{e}_z \times \vec{e}_x$.

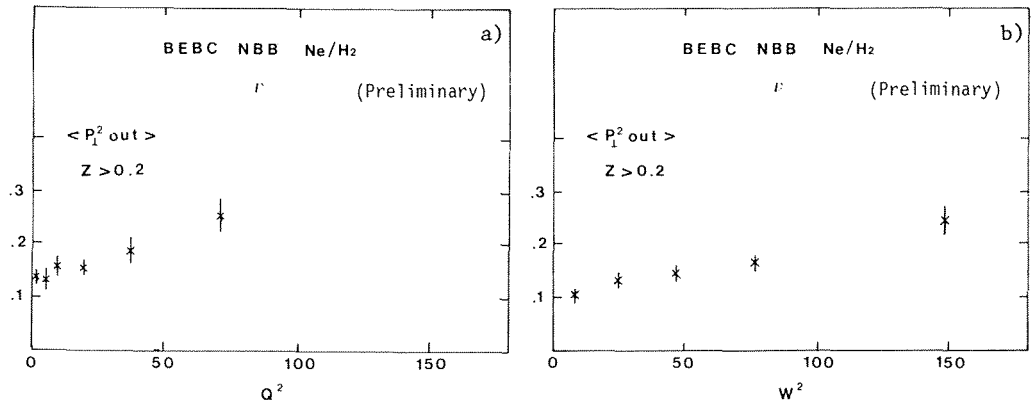

Fig. 9 $\langle p^2_{T,out} \rangle$ of charged tracks with z > 0.2 in ν-cc events: a) versus Q^2; b) versus W^2. PRELIMINARY DATA.

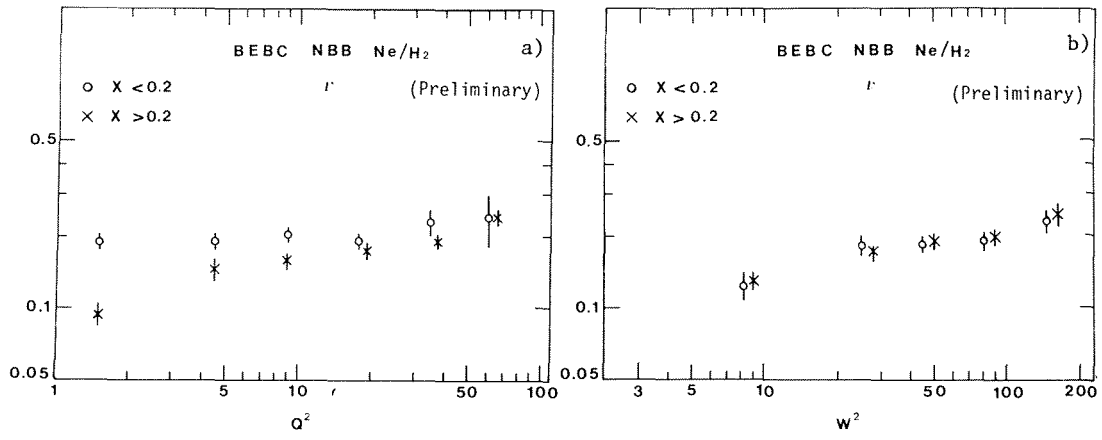

Fig. 10 $\langle p^2_T \rangle$ for charged tracks with z > 0.2 for ν-cc events for two cuts in $x_{Bjorken}$. a) versus Q^2; b) versus W^2. PRELIMINARY DATA.

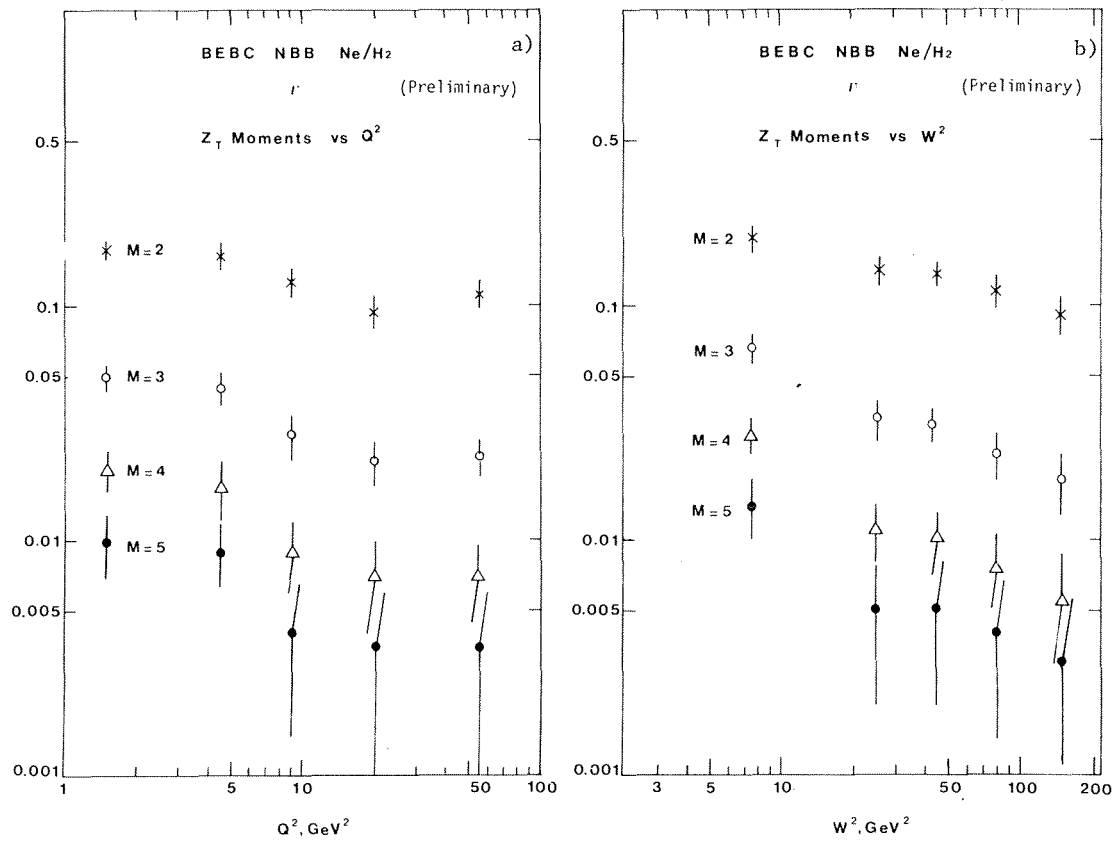

Fig. 11 Moments D_T^M of the variable z_T [Eq. (11)] for different M-values; a) versus Q^2; b) versus W^2. PRELIMINARY DATA.

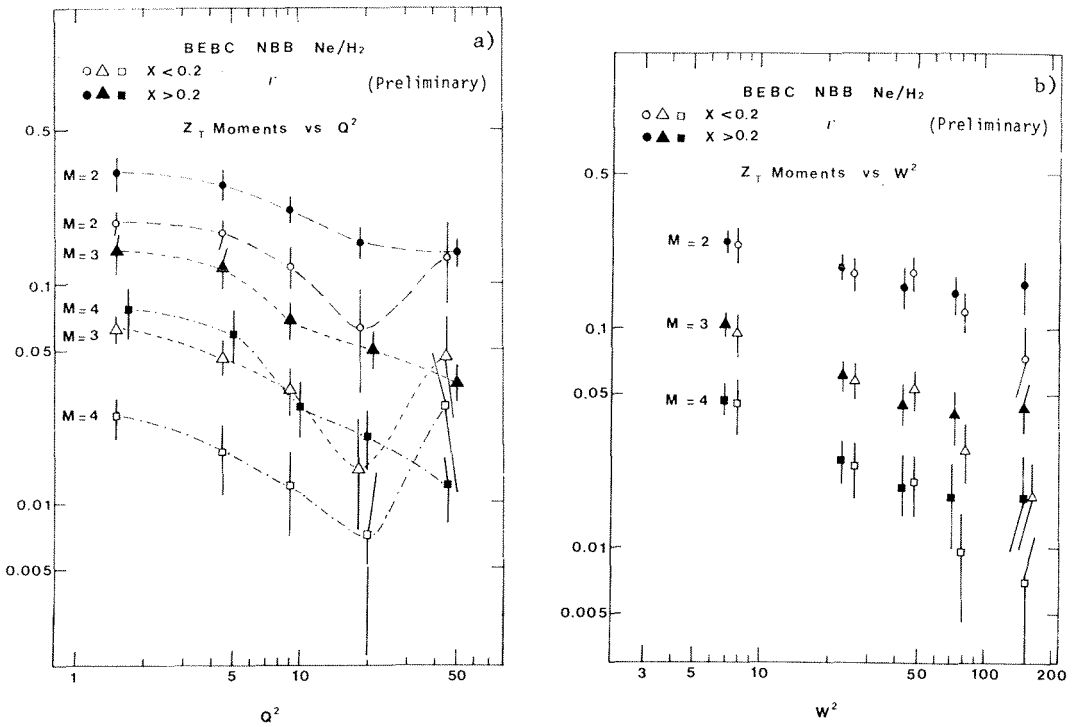

Fig. 12 Moments D_T^M of z_T for different values of M and for two different cuts in $x_{Bjorken}$. a) versus Q^2; b) versus W^2. PRELIMINARY DATA.

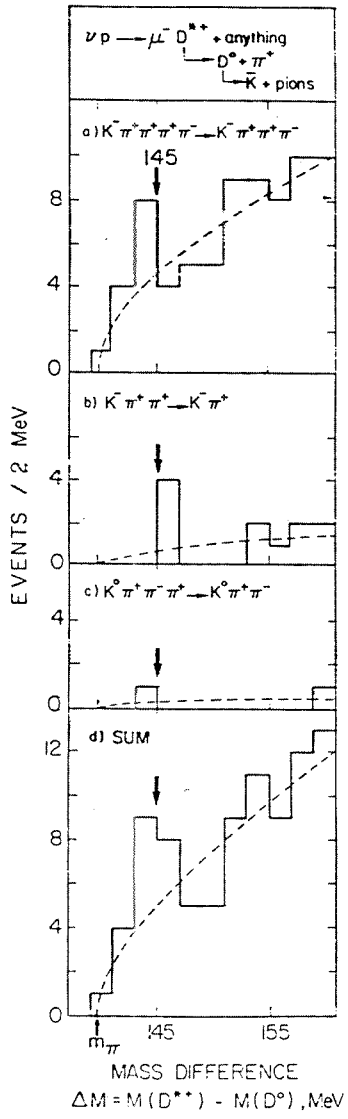

Fig. 13 Distribution in the mass difference $\Delta m = M(D^{*+}) - M(D^0)$, as explained in the text, for three decay modes of the D^0; a) $D^0 \to K^-\pi^+\pi^+\pi^-$; b) $D^0 \to K^-\pi^+$; c) $D^0 \to K^0\pi^+\pi^-$; d) sum of (a) to (c). The D^0 mass range taken is, in the three cases, 1840 to 1890 MeV.

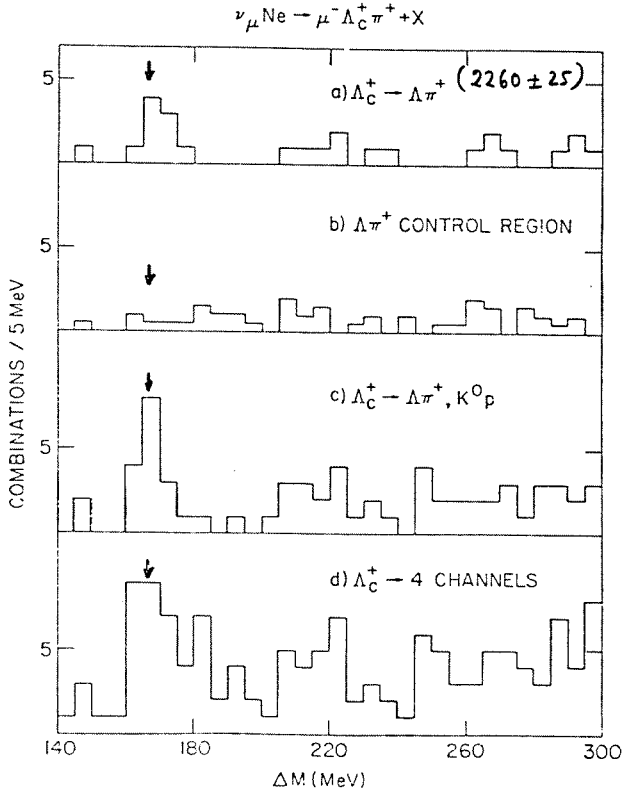

Fig. 14 Distribution in the mass difference $\Delta m = M(\Sigma_c^{++}) - M(\Lambda_c^+)$ for a) $\Lambda_c^+ \to \Lambda\pi^+$ decays; b) average of the control regions above and below the Λ_c^+ mass: $M(\Lambda\pi^+) = 2210 \pm 25$ MeV and $M(\Lambda\pi^+) = 2310 \pm 25$ MeV, respectively; c) $\Lambda_c^+ \to \Lambda\pi^+$ and $\Lambda_c^+ \to \bar{K}^0 p$ decays; d) Λ_c^+ decays into $\Lambda\pi^+$, $\bar{K}^0 p$, $Y^{*+}(1385)\pi^+\pi^-$, and $K^{*-}p\pi^+$. The Λ_c^+ mass range taken in (a), (c), and (d) is 2260 ± 25 MeV.

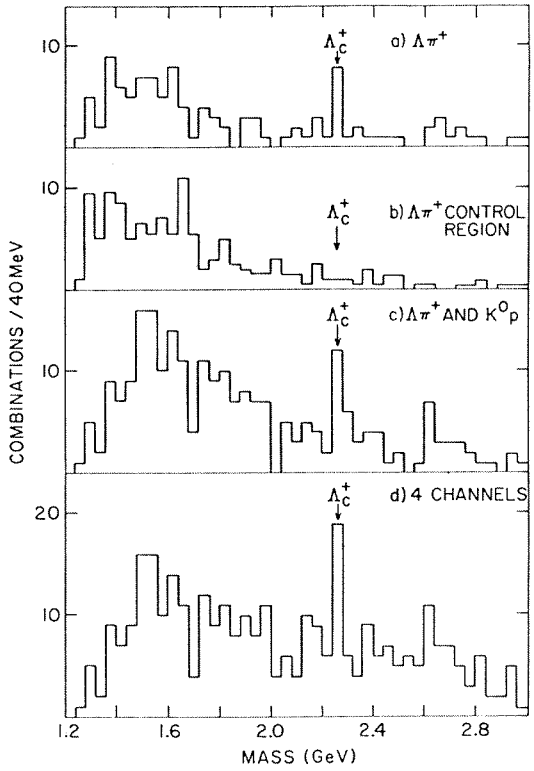

Fig. 15 a) $\Lambda\pi^+$ mass distribution for $\Delta m =$ $= 166 \pm 6$ MeV; b) $\Lambda\pi^+$ mass distribution for the average of the control regions defined by $\Delta m =$ $= 154 \pm 6$ MeV and 178 ± 6 MeV; c) combined $\Lambda\pi^+$ and $\bar{K}^0 p$ mass distribution for $\Delta m = 166 \pm 6$ MeV; and d) $\Lambda\pi^+$, $\bar{K}^0 p$, $Y^{*+}\pi^+\pi^-$, and $K^{*-}p\pi^+$ mass distribution for $\Delta m = 166 \pm 6$ MeV.

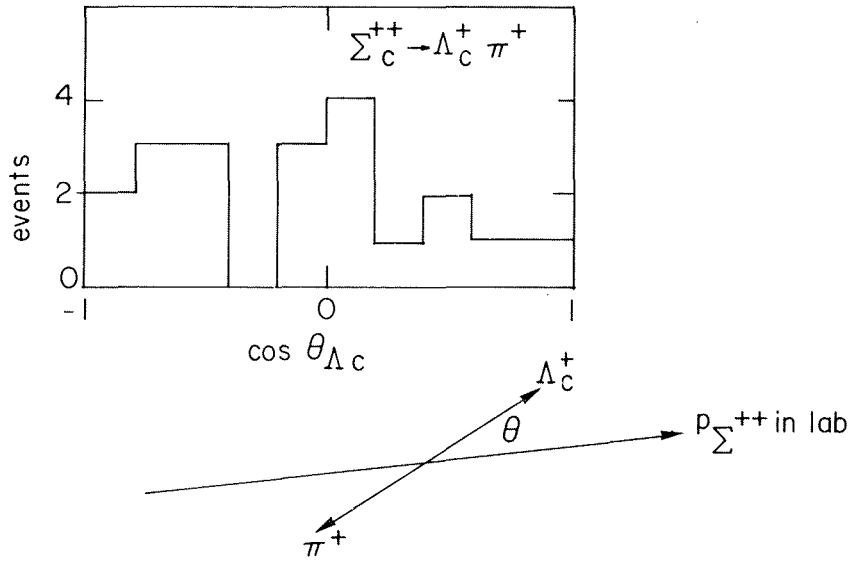

Fig. 16 Decay angular distribution for the Σ_e^{++} candidates.

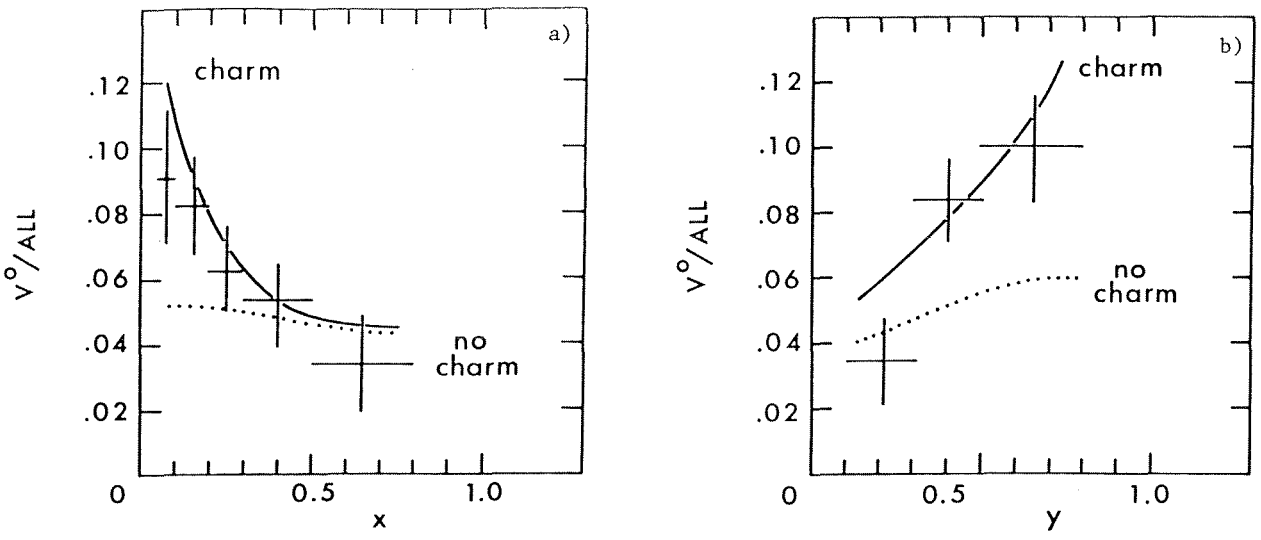

Fig. 17 $\bar{\nu}$ charged current events: a) ratio of x distributions between events with V^0's and all events: $\int_{0.1}^{0.8} f_S(x,y)\,dy$; and b) ratio of y distributions between events with V^0's and all events: $\int_{0.05}^{1} f_S(x,y)\,dx$. In (a) and (b) the dotted curves assume no charm, while the solid curves include charm.

DISCUSSION

Chairman: V.L. Telegdi

Sci. Secretaries: J. de Groot and W. Scott

G. Preparata (comment): The peculiar W^2-dependence of the fragmentation functions in deep-inelastic neutrino-nucleon interactions, that Prof. Schmitz and you have shown, seems to be in contradiction with the notion of "asymptotic freedom". In fact in order for the "fragmenting quark" to know about W, the hadron total mass, it must be able to talk to the "spectator quarks". But this is what asymptotic freedom forbids; because otherwise the fragmenting quark would not be free at all. Any calculation which produces dependences on variables close to W^2 cannot be a consequence of asymptotic freedom, but rather of physically unjustified use of leading logs in QCD perturbation theory.

B. Tallini (comment): Concerning the $\langle p_T^2 \rangle$ versus W^2 or Q^2 behaviour, which I have discussed, it appears that W^2 is a much more convenient variable to use phenomenologically than Q^2. Indeed it has been shown by G. Altarelli (Oxford Conference, 1978) and by R. Odorico et al. [Phys. Lett. 81B (1979) 219] that according to QCD the change of variable from Q^2 to W^2 absorbs most of the x_{Bj} dependence of $\langle p_T^2 \rangle$, as the ν-neon data seem to support.

G. Altarelli (comment): At the moment what is seen in the data is a violation of factorization and scaling at small values of Q^2 or W^2. I think that these effects are normal deviations from the parton model to be expected for small values of the energies involved. In fact they tend to disappear quite rapidly, and a cut at $W^2 > 4$ is sufficient to reduce them substantially.

NEUTRINOS AND NUCLEON STRUCTURE

L.M. Sehgal

III. Physikalisches Institut, Technische Hochschule, Aachen, Germany.

ABSTRACT

The study of neutrino interactions in matter is yielding a wealth of information on the form factors and structure functions of the nucleon. These data allow tests of models of nucleon structure and of dynamical theories of quarks and gluons. We attempt a critical appraisal of recent facts and their impact on our theoretical understanding.

One of the primary aims of neutrino physics has been to use the charged current interaction of neutrinos as a probe of nucleon structure and, in particular, to study how the response of the nucleon to an axial vector current differs from that to a vector current. Such studies began with attempts to determine the weak form factors of the nucleon with a view to testing our ideas about chiral symmetry and vector meson dominance. Today, the focus has moved to the investigation of the scaling phenomenon at high energies and its confrontation with a very elegant and provocative theory, the theory of quantum chromodynamics. While these latter developments are currently at the centre of interest, it is clear that a comprehensive understanding of nucleon structure requires a careful correlation of many features revealed by a variety of measurements at low as well as high energies. For this reason I have attempted to review the subject in broad terms, including areas that are presently receiving only peripheral attention. The talk is divided into four parts.

1. The Nucleon at Rest
2. The Excited Nucleon
3. The Nucleon at Infinite Momentum
4. The Hadronic Vacuum.

1. THE NUCLEON AT REST

1.1 Elastic Scattering

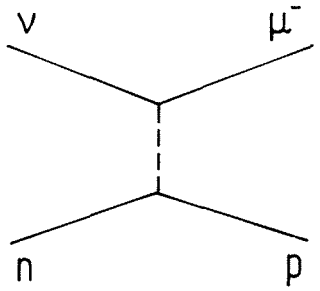

Our understanding of the static properties of the nucleon requires a careful study of the primeval neutrino process: elastic neutrino scattering on a nucleon. The principal object of interest is the axial vector form factor $F_A(Q^2)$. The customary procedure has been to assume a dipole behaviour

$$F_A(Q^2) = (1 + Q^2/M_A^2)^{-2} \qquad (1)$$

by analogy with the vector form factor F_V, and to fit simultaneously the energy dependence of the cross section $\sigma(E_\nu)$ and the differential distribution $d\sigma/dQ^2$. A number of experiments proceeding along this line have determined M_A = 0.9 - 1.0 GeV.[1)]

The above procedure must be considered somewhat disappointing. One must remember that the dipole structure determined in electron scattering remains to this day a mystery, and our objective should be to resolve mysteries, and not to elevate mysteries to superstitions. There is no basis for a dipole other than the fact that it is an approximate empirical representation of the vector form factor. And so the whole thrust of the axial vector measurement should be to look for subtle differences in the shape of F_V and F_A that may provide clues to an understanding of these form factors.

There is, in principle, a straightforward way of measuring $F_A(Q^2)$, and that is to compare $d\sigma/dQ^2$ for ν and $\bar{\nu}$ at the same value of energy. The difference

$$\frac{d\sigma^{\nu}}{dQ^2} - \frac{d\sigma^{\bar{\nu}}}{dQ^2} \propto F_V(Q^2)\, F_A(Q^2) \qquad (2)$$

isolates the VA interference term, and so knowing $F_V(Q^2)$ one can determine $F_A(Q^2)$. There is, to my knowledge, only one record of such an attempt, and that was by the Gargamelle-Freon experiment at the PS.[2] The result obtained is shown in Fig. 1, along with dipole curves for $M_A = 1.0 \pm 0.1$ GeV. One has the impression from this Figure that a dipole is <u>not</u> a particularly good representation of the data. There is, if anything, a hint of an excess in the low Q^2 region.

That being the situation, it is perhaps time to revive our basic thinking about the meaning of form factors in order to consider possible alternatives to a dipole. Let us revert to the idea of a form factor as being a fourier transform of a spatial distribution of charge. A realistic description ought to take account of two important facts of life: first, that a nucleon is a bound state of quarks that are the basic carriers of charge, and second, that for low Q^2 phenomena, a virtual photon appears to couple predominantly to

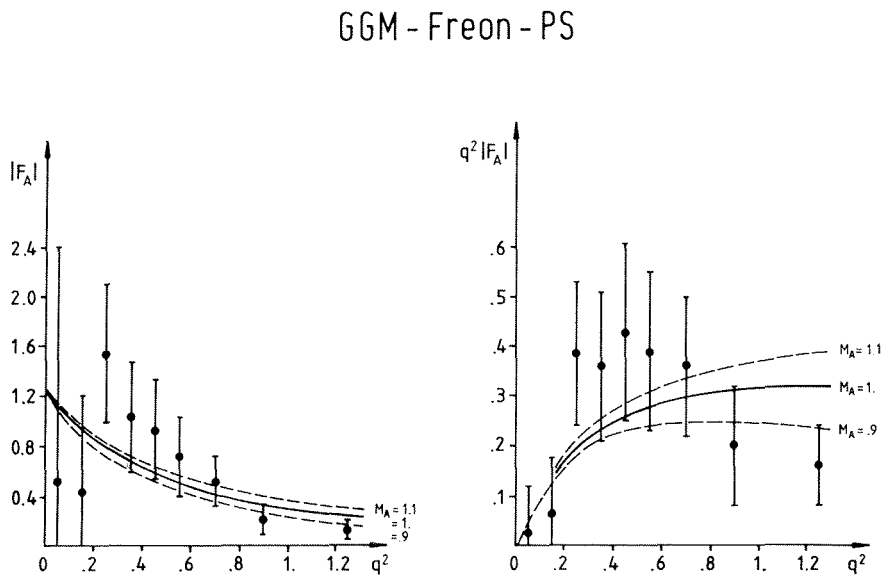

Fig. 1 Axial vector form factor deduced by Gargamelle experiment (Ref. 2) from comparison of ν and $\bar{\nu}$ elastic scattering.

the lowest vector meson state (vector dominance). A geometrical picture that accommodates both facts is to view the nucleon as a distribution of quarks with a radial extent $\langle R^2 \rangle_{QM}$ determined by the bound-state wave-function, and to ascribe to each quark a vector meson cloud whose extent $\langle R^2 \rangle_{VD}$ is determined by the Compton wave-length of the vector meson.[3] In such a picture, the mean square radius of the nucleon as measured in elastic scattering will be approximately

$$\langle R^2 \rangle \simeq \langle R^2 \rangle_{QM} + \langle R^2 \rangle_{VD} \tag{3}$$

Accordingly, the form factor $F(Q^2)$ will be a product of two factors

$$F(Q^2) = F_{QM}(Q^2)\, F_{VD}(Q^2) \tag{4}$$

where the first involves a mass scale characteristic of quark confinement (e.g. the average $k_\perp$ of quarks in the nucleon) and the second the mass scale of vector mesons, being essentially the vector meson pole

$$F_{VD}(Q^2) = (1 + Q^2/M_V^2)^{-1} \tag{5}$$

There is, of course, no unique prescription for the factor F_{QM}. For the purpose at hand, one could simply choose it empirically so as to reproduce the observed behaviour of the vector form factor. The following function has been advocated in some discussions based on the quark model:[4]

$$F_{QM} = \exp\left[-\tfrac{1}{6} Q^2R^2/(1 + Q^2/4M^2) \right] \tag{6}$$

This is a Gaussian, with a Lorentz-contraction factor in the exponent, originally suggested by Licht and Pagnamenta.[5] With such a choice, the vector form factor of the nucleon is

$$F_V(Q^2) = (1 + Q^2/m_\rho^2)^{-1} \exp\left[-\tfrac{1}{6} Q^2R^2/(1 + Q^2/4M^2) \right] \tag{7}$$

In Fig. 2 we have plotted this function for $R^2 = 6\ \mathrm{GeV}^{-2}$ along with the standard dipole.[6] The two functions coincide within the thickness of the curve.[7]

Suppose we use the above model as a basis for our intuition about the axial vector form factor. The obvious procedure would be to replace the ρ-pole by the A_1-pole, leaving the factor F_{QM} intact[8] (we take the A_1 mass to be $\sqrt{2}\, m_\rho$). Thus

$$F_A(Q^2) = (1 + Q^2/m_{A1}^2)^{-1} \exp\left[-\tfrac{1}{6} Q^2R^2/(1 + Q^2/4M^2) \right]. \tag{8}$$

Fig. 3 compares this form with the traditional dipole parametrization (with a dipole parameter $M_A = 0.96$ GeV). One now sees a delicate difference: the QM-VD form is larger by about 10% in the interesting domain $Q^2 \lesssim 1$. This difference will obviously show up in the distribution $d\sigma/dQ^2$. As seen from Fig. 4, the above form factor (as compared to the dipole) produces an excess of $\sim$ 10% in the neighbourhood of $Q^2 = 0.5\ \mathrm{GeV}^2$.

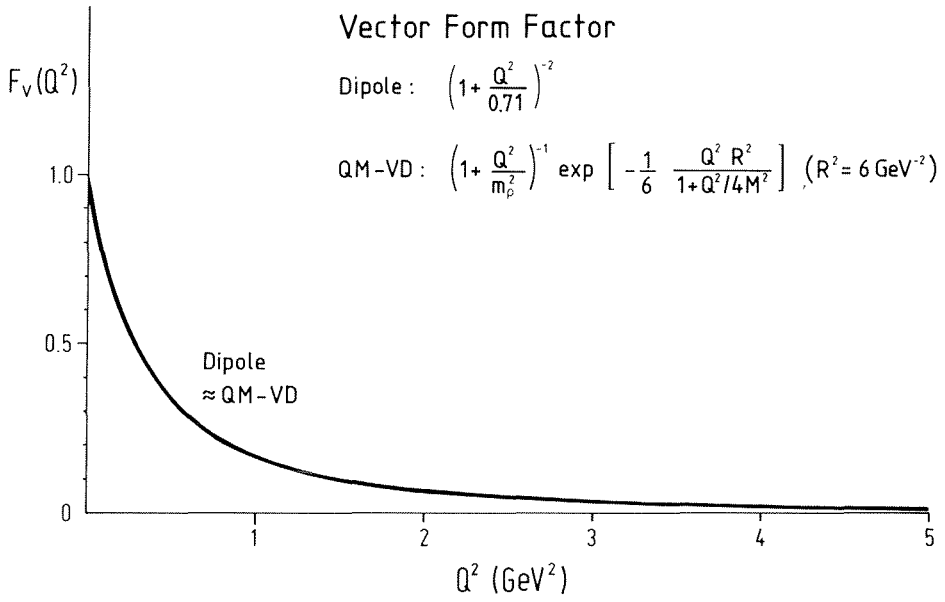

Fig. 2 Comparison of two parametrisations of vector form factor. For $R^2 = 5.8\ \mathrm{GeV}^{-2}$ the functions coincide to 3% for $Q^2 < 2\ \mathrm{GeV}^2$ and to 7% for $Q^2 < 10\ \mathrm{GeV}^2$.

Do the data show evidence of such an effect? We present in Fig. 5 the result of the Argonne experiment[9] along with their best dipole fit. As noted by the authors, there is an excess of events in the form of a shoulder in the region $Q^2 = .3 - .4\ \mathrm{GeV}^2$. Qualitatively, this is what we have anticipated above. While it is too early to claim that a departure from the dipole form for F_A has been established or that the explanation invented above is correct, there is certainly grounds for a serious re-examination of all data on the

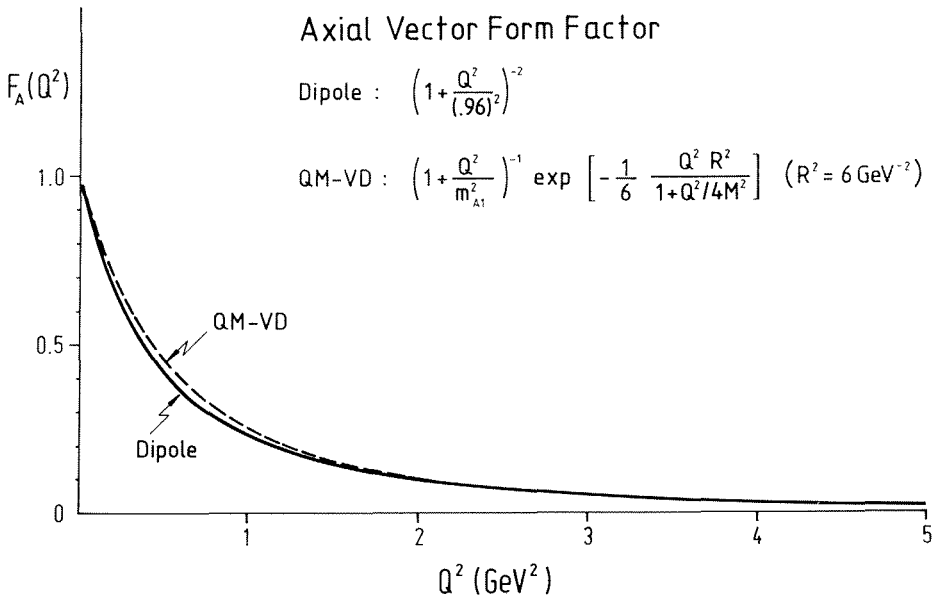

Fig. 3 Comparison of two parametrisations of axial vector form factor.

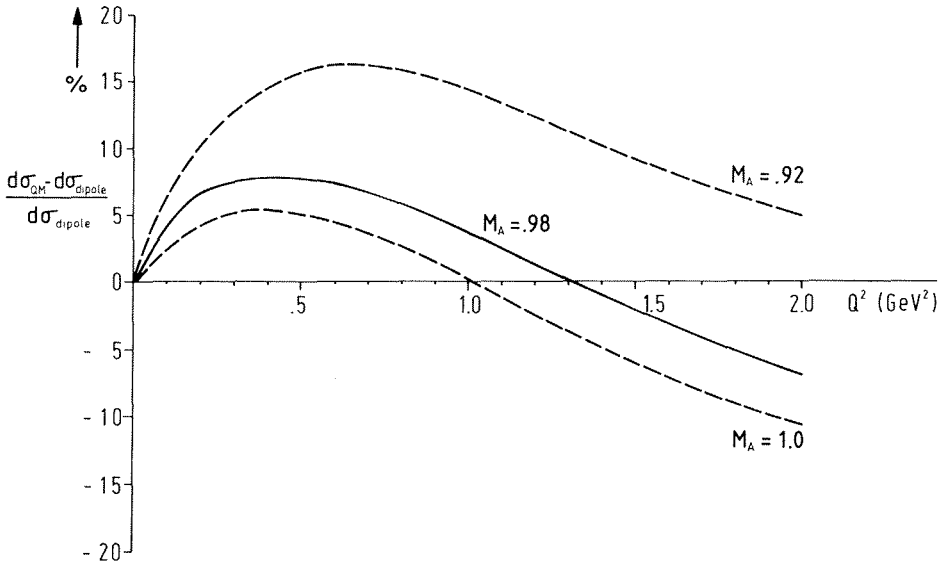

Fig. 4 Comparison of differential cross section of $\nu n \to \mu^- p$ resulting from two different choices of axial form factor.

elastic process.[10] The issue is fundamental.

One should note here that one symptom of the inadequacy of the dipole form for F_A would be that the value of M_A deduced from fits to $\sigma(E_\nu)$ will not always agree with that deduced from $d\sigma/dQ^2$, and may vary with neutrino energy, or in going from ν to $\bar{\nu}$. It should be noted also that the behaviour of $F_A(Q^2)$ affects predictions for the distribution of the neutral current process $\nu p \to \nu p$, particularly since in the Weinberg-Salam model for

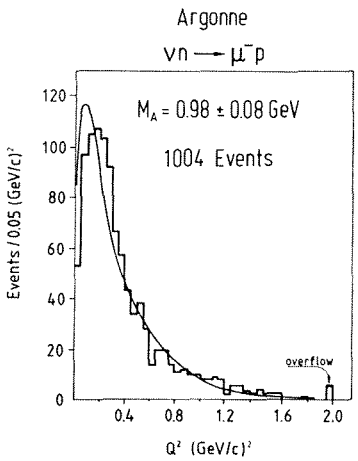

Fig. 5 Differential cross section observed in the Argonne experiment (Ref. 9) together with best dipole fit.

$\sin^2\theta \simeq 1/4$, the dominant contribution to the process is axial vector.[11]

1.2 Charmed Baryon Excitation

Another fundamental reaction where the form factor plays a role is the transformation of the nucleon into the lowest charmed baryons, in particular the C_o^+ and C_1^{++}. The standard calculation[12] of this process assumes the matrix elements at $Q^2 = 0$ to be given by SU(4) symmetry and the form factors to have the dipole behaviour

$$F_{V,A} = (1 + Q^2/M_{D^*}^2)^{-2} \quad , \quad M_{D^*} = 2 \text{ GeV} \tag{9}$$

The resulting cross section saturates at energies above 5 - 10 GeV to the values

$$\begin{aligned} \sigma(C_o^+) &= 2.0 \times 10^{-39} \text{ cm}^2 \\ \sigma(C_1^{++}) &= 0.6 \times 10^{-39} \text{ cm}^2 \end{aligned} \tag{10}$$

Our discussion above, however, leads us to contemplate an alternative choice of form factor, namely

$$F_{V,A} = (1 + Q^2/M_{D^*}^2)^{-1} \tilde{F}_{QM} \tag{11}$$

where the factor $\tilde{F}_{QM}$ is the analogue of the quark model factor F_{QM}. Because of the uncertainty in incorporating SU(4) symmetry breaking, it is not clear precisely how $\tilde{F}_{QM}$ should be related to F_{QM}. For some simple assumptions[12a] one finds that the resulting cross section is a factor 3 lower than the dipole estimate. In an explicit quark model constructed by the Orsay group[13], the factor $\tilde{F}_{QM}$ is calculated as an overlap integral between charmed and uncharmed baryon wave-functions. In such an approach, there is a substantial renormalization of $\tilde{F}_{QM}$ as a result of SU(4) symmetry-breaking[14] ($\tilde{F}_{QM}$ $(Q^2 = 0) \simeq 0.5$) and the overall suppression in the cross-section is a factor 6. These considerations lead us to conclude that the cross section for charmed baryon excitation with the alternative form factor (11) is a factor 3 - 6 lower than the standard estimate given in Eq. (10).

The data on quasi-elastic charm production are still fragmentary, but it is worth noting that the Columbia-Brookhaven[15] experiment has found only one possible example of $\nu p \to \mu^- C_1^{++}$ in 10^5 charged current events. With reasonable allowance for branching ratios and acceptances, there appears to be a hint of a suppression compared with the standard expectation. Improved data on these channels will be awaited with great interest, not only for the intrinsic interest in studying charmed baryons but also as a test of our ideas about elastic and quasi-elastic form factors.

2. THE EXCITED NUCLEON

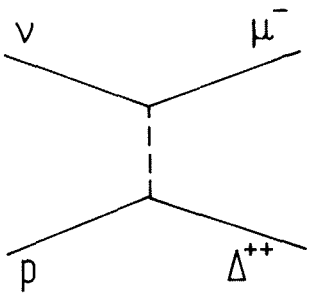

We turn now to the transition of the nucleon to its first excited level, the Δ resonance. In neutrino physics, one has the unique situation that by impinging with neutrinos on protons one can create a πN state which has two units of charge, and which is therefore purely I = 3/2. Thus it is possible to study the Δ resonance in an environment that is completely free of any interfering I = 1/2 background. As evidence of the clarity with which the Δ shows up in $\nu p \to \mu^- \Delta^{++}$, Fig. 6 shows the mass plot obtained by BEBC[16]: in the Δ region the data are almost perfectly reproduced by a Breit-Wigner resonance.

Our interest is to test our ideas about the form factors of this process. The vector matrix element $\langle \Delta^{++}|V|p\rangle$ is determined using electroproduction data and CVC, so that the main unknown is the axial vector part $\langle \Delta^{++}|A|P\rangle$. For practical purposes this is characterised by three form factors C_3^A, C_4^A, C_5^A (the nomenclature is standard[17]). Of these, the normalization of C_5^A at $Q^2 = 0$ may be fixed by appealing to PCAC and one finds $C_5^A(0) \simeq 1.2$. The remaining two factors C_3^A and C_4^A are model dependent; it turns out that in the simplest descriptions of this process (e.g. the quark model, the static model or the Adler model) they are predicted to be small or zero. The Q^2 dependence is basically that of the elastic process $F_A(Q^2)$ with some modulation that varies from model to model. In the case of C_5^A, the Q^2-dependence is $\left[m_\pi^2/(m_\pi^2 + Q^2) \right] F_A(Q^2)$.

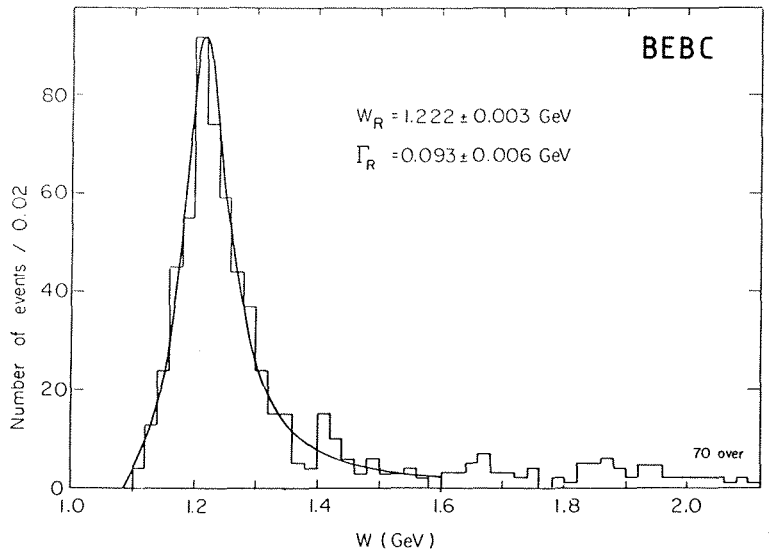

Fig. 6 Invariant mass distribution of $\nu p \to \mu^- p\pi^+$ measured in BEBC (Ref. 16).

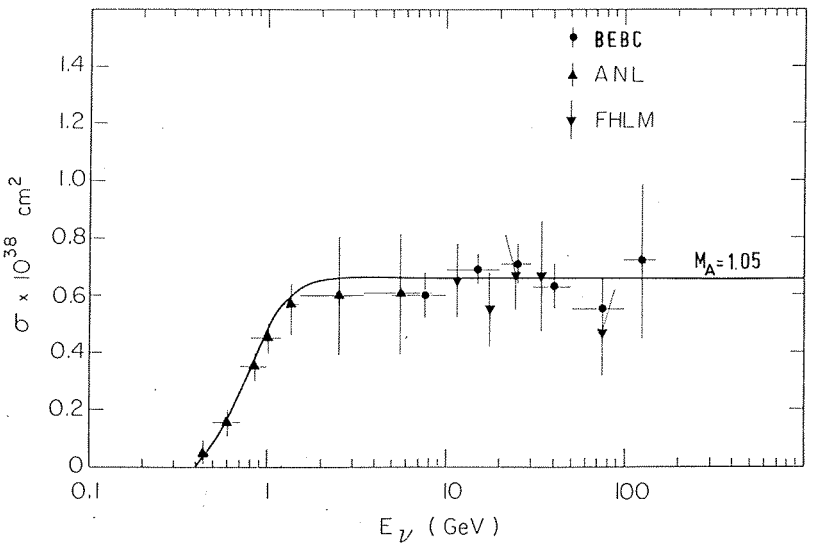

Fig. 7 Energy-dependence of cross section for $\nu p \to \mu^- p \pi^+$ compared with Adler model. Data from Refs. 9, 16, 19.

Fig. 7 shows how the total cross section calculated with the above assumptions compares with data obtained from three experiments:[16,18,19] the energy dependence is well-reproduced with a dipole parameter $M_A \simeq 1.0$ GeV. An attempt has been made to test directly the prediction that the form factors C_3^A and C_4^A have small static values. The result obtained by ANL[18] is shown in Fig. 8: the allowed domain encloses the origin.

A study of the Q^2-dependence does reveal some problems[19]. For instance, fits to the Adler model tend to give a rather large value for M_A. This may reflect a failure of the dipole form factor, or may be a limitation of the model itself. The density matrix elements are in broad agreement with expectations (there is a discrepancy between the BEBC[16] and 15'[19] experiments in the measured value of ρ_{33}). Finally, the angular distribution of the pion in the Δ region shows some asymmetries around $\cos\theta = 0$ and around $\phi = \pi$ (Fig. 9) which are enhanced when Q^2 is large (> 1 GeV^2)[16,19]. These asymmetries are indicative of an interfering non-resonant background under the Δ. One of the interesting challenges for models is to reproduce the sign and magnitude of this asymmetry.

Because of the fact that the reaction $\nu p \to \mu^- p \pi^+$ isolates I = 3/2 states, it is an excellent laboratory for studying the higher partial waves in this isospin channel. The data, in fact, show evidence for the excitation of resonances in the 1.7 and 1.9 GeV regions, the estimated cross sections being[16]

$$\begin{aligned} \sigma(1.7) &= 0.1 \times 10^{-38} \text{ cm}^2 \\ \sigma(1.9) &= 0.1 \times 10^{-38} \text{ cm}^2 \ . \end{aligned} \tag{12}$$

These are in good agreement with the predictions of the quark model.[20]

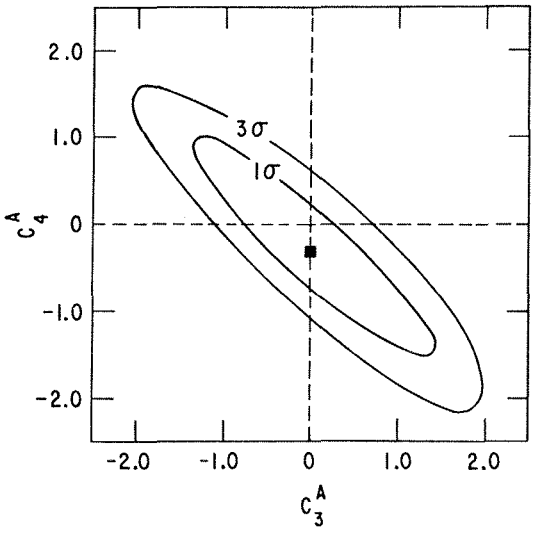

Fig. 8 Constraint on static values of form factors C_3^A and C_4^A derived from Argonne experiment (Ref. 9). Black dot denotes Adler model.

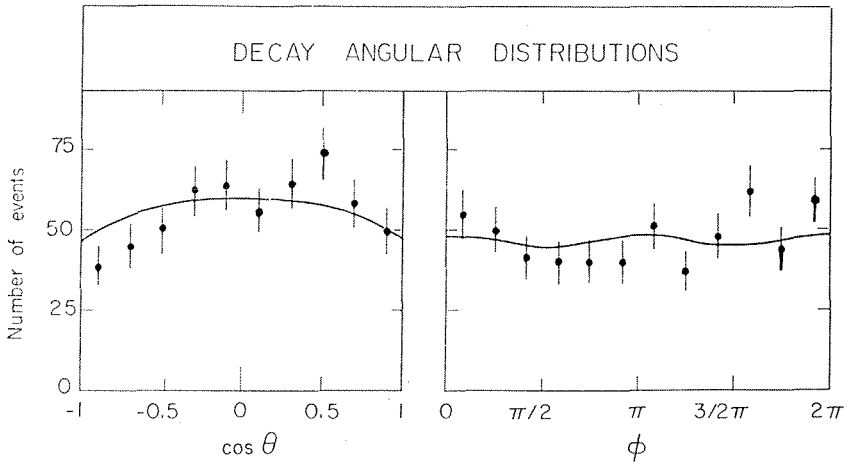

Fig. 9 Angular distribution of pion in $\nu p \to \mu^- \Delta^{++}$, $\Delta^{++} \to p\pi^+$, as measured in BEBC (Ref. 16). Curve is prediction of Adler model.

3. THE NUCLEON AT INFINITE MOMENTUM

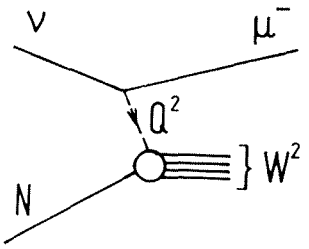

We proceed to the investigation of nucleon structure at high energies: the process of deep inelastic scattering $\nu N \to \mu^- X$. The inclusive cross section for this process is described quite generally by three structure functions which depend on Q^2 and W^2. These may be chosen in a variety of ways: in addition to the standard representation (F_1, F_2, F_3), one can define structure functions according to the helicity of the incoming current $(\sigma_L, \sigma_R, \sigma_S)$ or according to a decomposition in vector, axial vector and interference terms $(\sigma_V, \sigma_A, \sigma_I)$.[21]

Now as one goes up in Q^2 and W^2, three important phenomena are supposed to take place:

(i) approximate scaling in Q^2/W^2

(ii) approximate chiral symmetry, i.e. $\sigma_V = \sigma_A$

(iii) approximate vanishing of the zero-helicity structure function, i.e. $\sigma_S = 0$.

Let us recall briefly the evidence for these phenomena. The evidence for Bjorken scaling (which is what the first statement is) is well-known; one knows that it is a good first approximation to the behaviour of the inclusive cross section at high energies. The evidence for chiral symmetry is contained in the comparison of the electromagnetic and the weak structure functions (usually expressed by the relation $F_2^{\nu N} = \frac{18}{5} F_2^{eN}$); the validity of this result may be judged from Fig. (10), and one may conclude that $\sigma_V = \sigma_A$ to about 10%.[22] Finally the result $\sigma_S = 0$ translates into the Callan-Gross relation $F_2 = 2x F_1$.

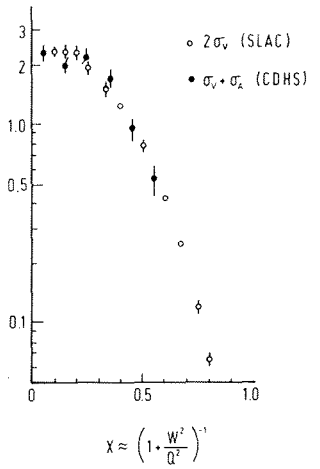

Fig. 10 Test of chiral symmetry in inclusive scattering at high energies.

The evidence for this has been reviewed by Turlay[23], and in its integral form, the relation appears to hold at the 10% level.

It is instructive to contrast the above behaviour at high W^2 and Q^2 with that observed for low values of these invariants. One knows, for instance, that in the neighbourhood of a resonance, scaling in Q^2/W^2 cannot be valid, the behaviour of the cross section being

$$\sigma \sim f_{BW}\,(W^2)\; g(Q^2) \tag{13}$$

where f_{BW} is a Breit-Wigner function. Again, the elastic and Δ channels discussed so far manifestly violate chiral symmetry. The V and A cross sections for these processes are displayed in Fig. 11, and they differ, both because of the fact that the V and A couplings are renormalized in different ways and because the associated form factors are different. Note, in particular that for any inelastic channel such as $\nu N \to \mu^- \Delta$, the vector cross section is forced to vanish in the forward direction ($Q^2 = 0$) because of current conservation, but no such constraint applies to the axial vector cross section. Finally, what is the status of the scalar structure function σ_S at low Q^2 and W^2? The behaviour of σ_S/σ_T for the elastic and Δ channels is shown in Fig. 12a. This ratio can be quite large at low Q^2, but dies with increasing Q^2 at a rate that is typically $[m_\pi^2/(m_\pi^2 + Q^2)]^2$. In the limit $Q^2 = 0$, the scalar structure function σ_S for any final state mass $W > M$ can, in fact, be predicted on the basis of PCAC.[24] The result is

$$\lim_{Q^2 \to 0} \sigma_S = \frac{1}{\pi}\,(\sqrt{2}\,F_\pi)^2\,\sigma_{\pi N}\,(W^2) \tag{14}$$

and is exhibited in Fig. 12b. For large W^2, σ_S has a numerical value close to $1/\pi$. We see, therefore, that for $Q^2 \lesssim m_\pi^2$, σ_S is not negligible and can actually be calculated.

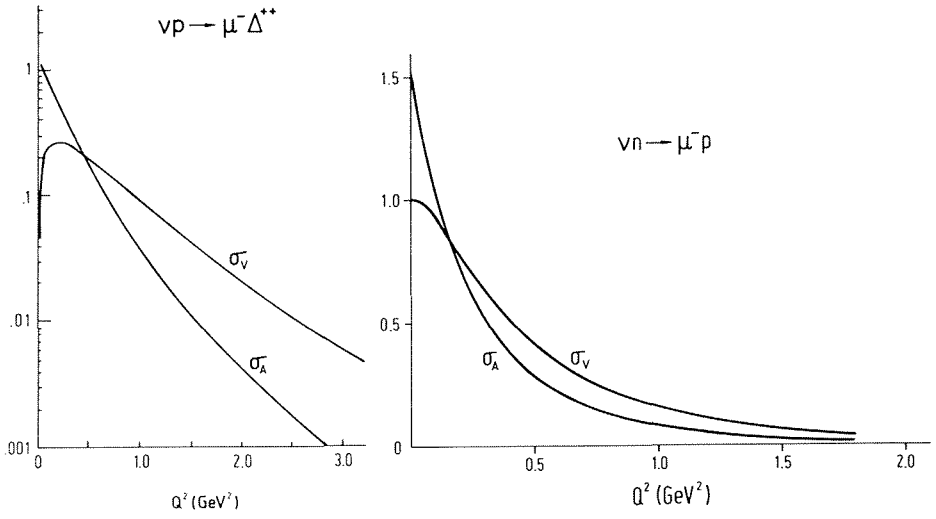

Fig. 11 V and A contributions to elastic and Δ channels. (Examples of chiral symmetry breaking at low energies.)

How does one interpret the simple behaviour at high energies? We are familiar with the parton model explanation: for Q^2 large compared to $\langle k_\perp^2 \rangle \sim (0.3\ \text{GeV})^2$, neutrino scattering is assumed to occur off quarks that are essentially free, so that the cross section may be computed in the impulse approximation. The scaling behaviour is supposed to be a consequence of the point-like character of quarks, chiral symmetry arises because the quarks have negligible masses, and the scalar structure function vanishes because quarks have spin $\frac{1}{2}$. The structure functions are interpreted as linear combinations of quark and antiquark densities in a proton at infinite momentum.

Fig. 13 shows the momentum profile of the proton as revealed by deep inelastic scattering. This profile is necessarily somewhat diffuse, because scaling is not exact, but it is a profile nevertheless and the figure shows the structure as seen at $Q^2 = 5\ \text{GeV}^2$. Neutrinos have the unique advantage of being able to tell quarks from antiquarks, and the left half of Fig. 13 is derived from a comparison of ν and $\bar{\nu}$ scattering on isoscalar targets.[22] On the other hand, electrons are uniquely equipped to distinguish u quarks from d quarks, and electron data when combined with neutrino measurements, yield the right half of the figure.[25] In the conventional sense of the term, Fig. 13 represents the most detailed knowledge that we possess about the "structure" of the proton.

There is a wealth of information contained in the above profile: one has not yet absorbed the many nuances to the shapes of the quark and antiquark distributions. Most important, the profile reveals an intricate pattern of symmetry-breaking, exemplified by $u \neq 2d$. There is even a weak indication from electron scattering (based on the apparent failure of the Gottfried sum rule) that $\bar{u} \neq \bar{d}$.[26] Neutrino measurements in hydrogen could make a contribution here, by filling in our knowledge of u/d and $\bar{u}/\bar{d}$ in domains of x

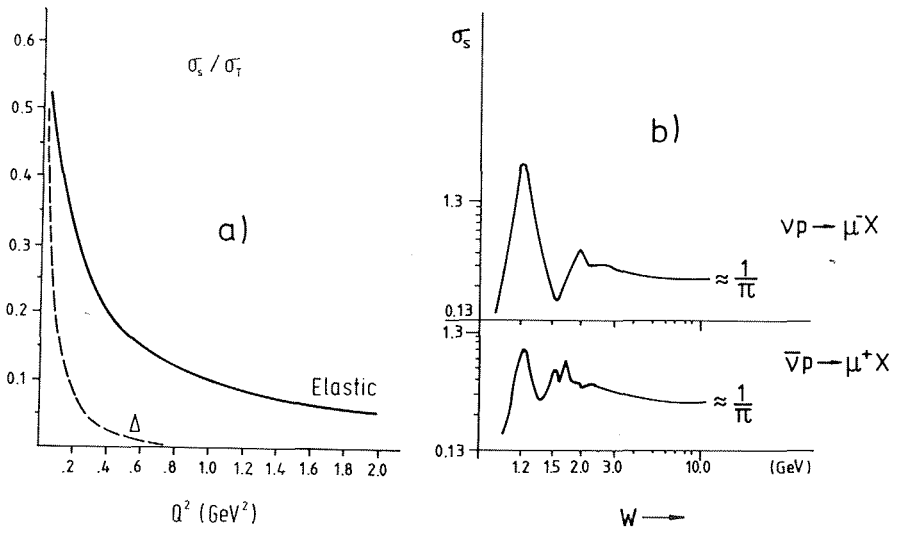

Fig. 12 (a) σ_S/σ_T for elastic and Δ channels. b) PCAC prediction for σ_S at $Q^2 = 0$.

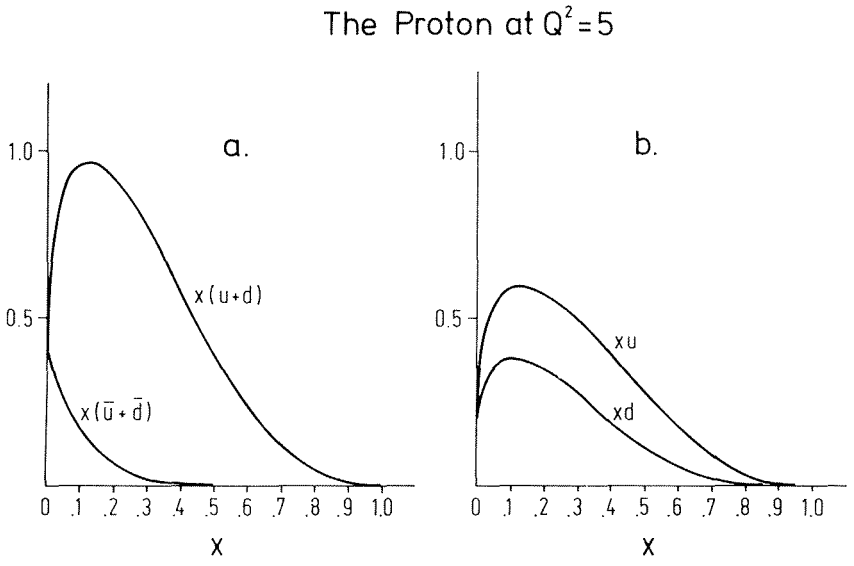

Fig. 13 Momentum profile of proton at Q^2 = 5 GeV^2 (a) based on ν data (Ref. 22) and (b) based on u/d ratio extracted from electron data (Ref. 25).

where electron scattering has weaknesses. Finally, there is the interesting theoretical challenge to relate the symmetry-breaking pattern observed in the parton densities to manifestations of symmetry-breaking in the static properties of the nucleon. In particular, one ought to be able to correlate the non-vanishing charge radius of the neutron with the fact that u(x) and d(x) differ in shape.[27] One can probably argue also that the Σ^o is heavier than the Λ^o as a consequence of the fact that u(x) is a broader distribution than d(x).[28]

The above discussion summarises what one has learnt from high energy scattering in the scaling approximation.

4. THE HADRONIC VACUUM

We come now to the last part of this survey, and that refers to the recent development of a theory of quarks and gluons interacting via colour (QCD). The interesting feature of this theory in its present form is that it has almost nothing to say about the structure of the nucleon in the sense that we have discussed it so far. It is not a theory of the form factors, transition matrix elements or the parton wave function of the proton. There is, however, one domain in which the theory makes contact with observation, and that is in the deviations from scaling behaviour at high energies. And in this domain, the theory makes predictions which are exquisitely precise and universal.

The consequences of the theory derive from two fundamental features. (a) The primitive vertices of the theory (Fig. 14) which determine the probabilities for the transitions

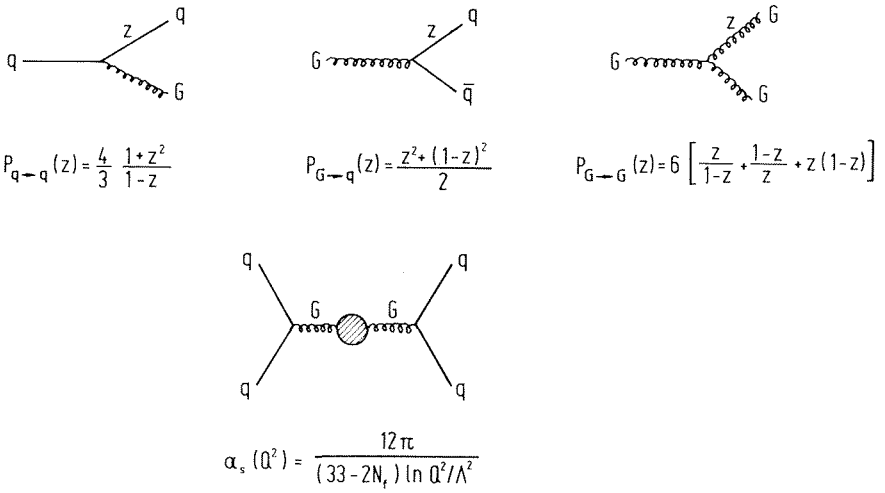

Fig. 14 Primitive vertices and vacuum polarization in QCD.

$q \to qG$, $G \to q\bar{q}$ and $G \to GG$ (the splitting functions). (b) The effective coupling constant of the theory resulting from the effect of vacuum polarization, which is calculable in the leading-logarithm approximation, and has the behaviour

$$\alpha_S(Q^2) = \frac{12\pi}{(33 - 2N_f)\ln Q^2/\Lambda^2} \tag{15}$$

exhibiting the remarkable property of asymptotic freedom. It is this property (the asymptotic vanishing of α_S for $Q^2 >> \Lambda^2$) that rationalises the success of the parton model based on the assumption of nearly free quarks. Furthermore, the precise manner in which $\alpha_S(Q^2)$ decreases with Q^2 implies a precise pattern of scaling violations in the structure functions. It should be stressed that this pattern is a universal pattern that does not depend on the properties of the target, but rather on the polarization properties of the hadronic vacuum as given in Eq. (15). Thus, in studying the nonscaling behaviour of structure functions, one is testing the idea that the hadronic vacuum is the vacuum of quarks and gluons interacting via QCD.

The predictions of QCD, to lowest order in α can be written as evolution equations for the parton densities $q \equiv u + d$ and $\bar{q} \equiv \bar{u} + \bar{d}$. These in turn are related to the structure functions of an isoscalar target by

$$\begin{aligned} xF_3 &= q_{NS} \equiv q - \bar{q} \\ F_2 &= q_S \equiv q + \bar{q} \end{aligned} \tag{16}$$

For instance, the non-singlet density q_{NS} is predicted to evolve as

$$\frac{\partial q_{NS}(x,t)}{\partial t} = \frac{\alpha_S}{2\pi} \int q_{NS}(y,t)\, \tilde{P}_{q\to q}(z)\, \delta(x - yz)\, dydz$$

$$\tilde{P}_{q\to q} = P_{q\to q}(z) - \delta(1 - z) \int P_{q\to q}(z')\, dz'$$

$$t = \ln Q^2/\Lambda^2 \qquad (17)$$

which implies that the moments of xF_3 have a Q^2-dependence given by

$$M_3(N,Q^2) = M_3(N,Q_0^2) \left[\frac{\ln Q^2/\Lambda^2}{\ln Q_0^2/\Lambda^2} \right]^{-d_N}$$

$$d_N = \frac{A_N}{2\pi b} \; ; \; A_N = \int dz\, z^N \tilde{P}_{q\to q}(z) \; ; \; b = \frac{12\pi}{33 - 2N_f} \qquad (18)$$

In particular

$$\left[M_3(N,Q^2) \right]^{-1/d_N} = \text{const} \left[\ln Q^2 - \ln \Lambda^2 \right] \qquad (19)$$

This linear dependence of the left-hand side on $\ln Q^2$ has been tested in the BEBC and CDHS experiments[30,31], and is compatible with the data for $Q^2 \gtrsim 1$ GeV^2 (Fig. 15). The value of Λ determined from the intercept is

$$\Lambda = \begin{matrix} 0.74 \pm 0.05 \text{ GeV (BEBC}^{30}\text{)} \\ 0.33 \pm 0.15 \text{ GeV (CDHS}^{31}\text{)} \end{matrix} \qquad (20)$$

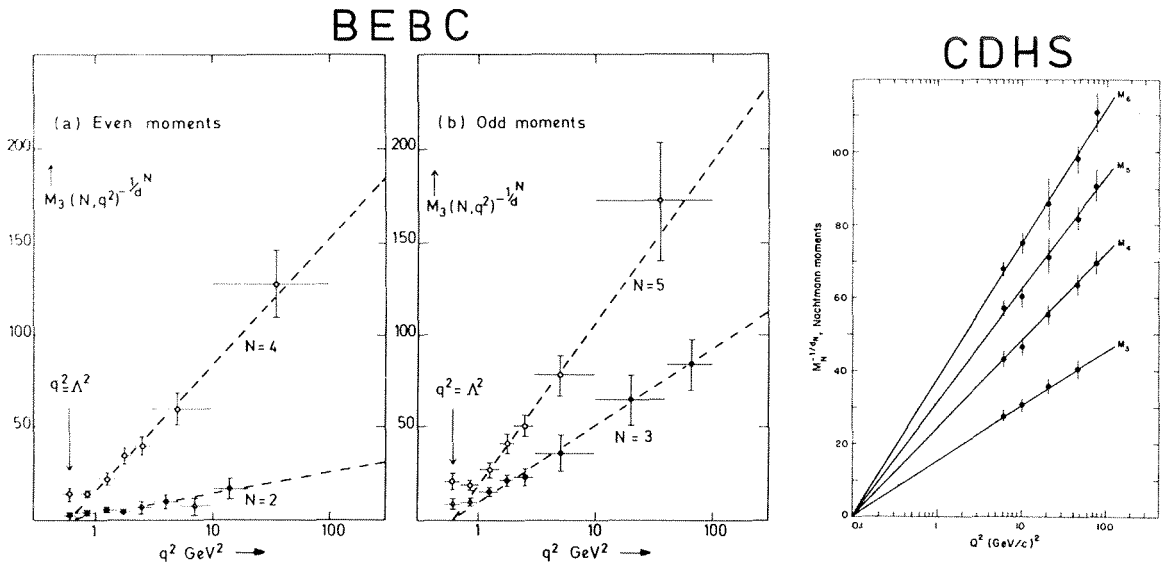

Fig. 15 Test of QCD based on moments of xF_3.

The disparity between these two estimates is, in part, a reflection of the fact that the two experiments have different acceptance in Q^2 and a different treatment of the elastic and quasi-elastic channels. That such differences arise at all is an indication that preasymptotic effects may not be negligible.

To test the theory more incisively, one must also examine the evolution of the singlet quark density q_s, which is the structure function F_2.[32] A convenient procedure is based on the observation of Buras and Gaemers[25] that for a steeply falling antiquark distribution (as indicated by data), the evolution equations have an approximate solution which can be parametrised as

$$\begin{aligned} q-\bar{q} &= [3/B\ (\eta_1, \eta_2 + 1)]x^{\eta_1(s)}\ (1 - x)^{\eta_2(s)} \\ \bar{q} &= A(s)\ (1 - x)^{P(s)} \end{aligned} \qquad (21)$$

where η_1 and η_2 are linear functions of $s = \ln \left[(\ln Q^2/\Lambda^2)/(\ln Q_0^2/\Lambda^2) \right]$, and A(s) and P(s) are constrained so as to agree with the first two moments of F_2 at a given s value. An analysis of the CDHS data[22,33] shows that such a fit is indeed possible, and yields $\Lambda = 0.47 \pm 0.11$ GeV.

Fig. 16 shows how the various components of the proton evolve with Q^2 when the data are analysed according to the constraints of QCD. Fig. 16a shows how the momentum of the proton is partitioned and Fig. 16b how the average width (or "hardness") of the different x-distributions changes with Q^2. It is interesting to note that whereas the momentum fraction carried by the gluon is roughly constant at about 50%, the gluon distribution is in fact rapidly evolving between Q^2 = 2 and 20 GeV^2, as witness the change in <x>.

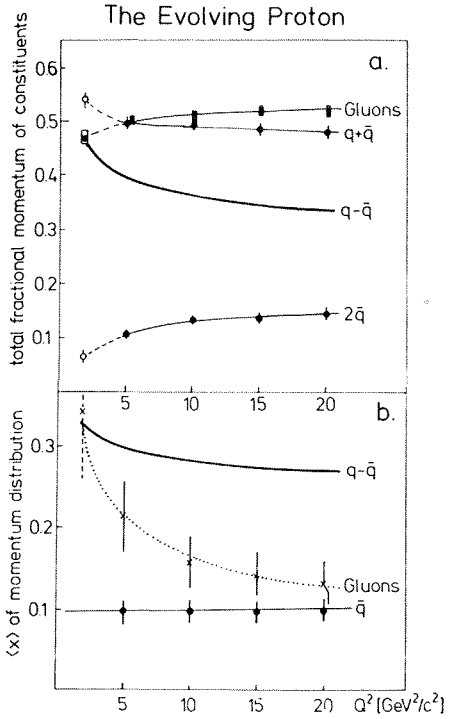

Fig. 16 Evolution of quarks, antiquarks and gluons in the proton based on QCD-interpretation of data. (a) Momentum fractions (b) Average width of distributions (Ref. 33).

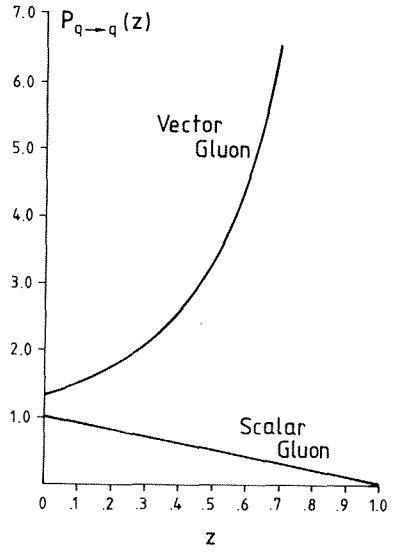

Fig. 17 Splitting function $P_{q\to q}(z)$ for scalar and vector gluon theories.

Thus, from the standpoint of QCD, the gluon is not simply a piece of ballast attached to the proton that accounts for half of the proton's momentum; it is in fact playing a dynamical role, and is a living and vital component of this system.[34)]

In conclusion, one must caution that quantitative tests of QCD can be complicated by subasymptotic effects of the type $1/Q^2$ and $1/\ln Q^2$.[35)] Also, the uniqueness of QCD is extremely difficult to establish, because observables such as structure functions are related to the primary quantities of the theory, e.g. the splitting functions, only through cascade-type equations; and we know from cosmic ray experience that by looking at the end-product of a cascade, it is very difficult to establish the nature of its origin. Perhaps one way to analyse the data to test the theory more objectively is to state what constraints the data place on the shape of the splitting function (contrast, for instance the behaviour of $P_{q\to q}$ in vector and scalar gluon theories shown in Fig. 17). And finally, one must not forget the outstanding theoretical challenge: to go from a theory of the hadronic vacuum to a theory of real hadrons.

Acknowledgements:

I wish to thank Uli Samm for his help in the numerical exploration of the form factors discussed in Sec. 1. For helpful discussions on theoretical matters, I thank P. Zerwas, D. Rein and S. Ono. I am indebted to many experimental colleagues for information and encouragement, and should like to thank particularly H. Faissner, J. Morfin, P. Fritze, H. Deden and D. Lanske.

REFERENCES

1) For a summary, see F. Sciulli, Proc. Oxford Conf., Ed. A. Michette and P. Renton (Rutherford Lab 1978) p. 405.

2) M. Rollier (Gargamelle Collab.), Proc. Paris Colloquium "La Physique du Neutrino a Haute Energie", CNRS (Paris) 1975, p. 349.

3) For examples of such a viewpoint, see S. Ishida et al., Prog. Theor. Phys. 36, 1243 (1966); K. Fujimara et al., Prog. Theor. Phys. 43, 73 (1970); A. Le Yaouanc et al., Nucl. Phys. B37, 522 (1971).

4) See e.g. A. Le Yaouanc, Ref. 3.

5) A. Licht and A. Pagnamenta, Phys. Rev. D2, 1150 (1970).

6) In the harmonic oscillator quark model, the spacing between adjacent levels is $(M_q R^2)^{-1}$, where M_q is the quark mass. Assuming $M_q = M_N/3$, the choice $R^2 = 6\ \text{GeV}^{-2}$ gives a spacing of about 0.5 GeV, a not unreasonable result.

7) It should be noted that the dipole is not a perfect representation of the electromagnetic form factor. See P.N. Kirk et al., Phys. Rev. D8, 63 (1973); S. Stein et al., Phys. Rev. D12, 1884 (1975).

8) This is suggested by the fact that the electric and magnetic radii of the proton appear to be nearly the same. (Recall that in the non-relativistic limit, the axial vector operator is proportional to the magnetic moment operator.)

9) M. Derrick et al., ANL-HEP-CP-78-31; Proc. Oxford Conf. p. 58; S. Barish et al., Phys. Rev. D16, 3103 (1977)

10) A similar effect may well be present in the BNL data. See remarks on p. 67, Proc. Oxford Conf. (Ref. 1).

11) It may be relevant to note here that the distribution $d\sigma/dQ^2$ for the reactions $\overset{(-)}{\nu}p \to \overset{(-)}{\nu}p$ measured by the HP-BNL experiment was not easily reproduced at low Q^2 using conventional form factors. See data in L. Sulak et al., Proc. Purdue Conf., Ed. E. Fowler (Purdue University, 1978) p. 355.

12) R.E. Shrock and B.W. Lee, Phys. Rev. D13, 2539 (1976); G. Köpp et al., Nucl. Phys. B123, 61 (1977).

12a) Assumptions we have tried are (i) $\tilde{F}_{QM} = F_{QM}$; (ii) replace R^2 by the mean value of charmed and uncharmed baryon parameters, estimated from the quark model ($R^2 \to 0.8\ R^2$); (iii) replace $(1 + Q^2/4M^2)^{-1}$ by the Lorentz factor $(1 - \beta^2)$ appropriate to the transition N → C viewed in an equal-velocity frame.

13) A. Amer et al., Phys. Lett. 81B, 48 (1979); M. Gavela, Ph.D. thesis, Orsay (1979)

14) One consequence of this renormalization effect is to reduce the absolute decay width of $\Gamma(C_o^+ \to \Lambda^o e\nu)$ (and similarly of $D \to Ke\nu$). It may be possible to check this with the help of measurements of charmed particle lifetimes.

15) C. Baltay et al. (Columbia-Brookhaven), BNL preprint OG482 (1979).

16) J. Blietschau et al. (ABCMO collaboration), paper presented at the Bergen Neutrino Conference, CERN/EP/B. Conforto/ap, July 1979.

17) P. Schreiner and F. von Hippel, Nucl. Phys. B58, 333 (1973).

18) S.J. Barish et al., ANL-HEP-PR-78-30 (1978).

19) J. Bell et al., Phys. Rev. Lett. 41, 1008 (1978).

20) P. Andreadis et al., Ann. Phys. 88, 242 (1974); F. Ravndal, Nuovo Cimento 18A, 385 (1973); T. Abdullah and F. Close, Phys. Rev. D5, 2332 (1972).

21) For a discussion of the kinematics, see for instance C. Llewellyn Smith, Phys. Rep. 3C, 263 (1972).

22) J.G.H. de Groot et al. (CDHS collaboration), Zeitschrift f. Physik C1, 143 (1979).

23) R. Turlay, these Proceedings.

24) See e.g. F. Ravndal, Ref. 20.

25) A. Buras and K. Gaemers, Nucl. Phys. B132, 249 (1978).

26) R. Field and R.P. Feynman, Phys. Rev. D15, 2590 (1976); D. Ross and C. Sachrajda, Nucl. Phys. B149, 497 (1979).

27) For tentative attempts in this direction, see R.D. Carlitz et al., Phys. Lett. 68B, 443 (1977) and references therein; L.M. Sehgal, Phys. Lett. 53B, 106 (1974)

28) See, for instance, J. Gunion et al., Nucl. Phys. B123, 445 (1977); A. Le Yaouanc et al., LPTHE 76/27 (1976).

29) Useful reviews are J. Ellis, Lectures at SLAC Summer Institute, SLAC-PUB-2177 (1978); R. Field, Lectures at La Jolla Summer Workshop, CALT-68-696 (1978).

30) P.C. Bosetti et al., (ABCLOS Collaboration), Nucl. Phys. B142, 1 (1978); D. Perkins, Oxford preprint 2/79 (1979); J. Morfin, paper presented at the Bergen Neutrino Conference (1979).

31) J.G.H. de Groot et al. (CDHS Collaboration), Phys. Lett. 82B, 292 (1979).

32) E. Reya, DESY preprint 79/02 (1979).

33) J.G.H. de Groot et al. (CDHS Collaboration), Phys. Lett. 82B, 456 (1979).

34) On the other hand, as noted correctly by D. Perkins in the discussion, this conclusion concerning gluons is necessarily dependent on the assumption of QCD being the correct theory. The data per se do not enjoin us to believe in such an interpretation.

35) W. Bardeen and A. Buras, Fermilab-Pub-79/31-THY (1979); E.G. Floratos et al., CERN preprint TH.2566 (1978); D.W. Duke and R.G. Roberts, Rutherford preprint RL-79-025 T.238 (1979).

DISCUSSION

Chairman: D.H. Perkins

Sci. Secretaries: G. Bonneaud and S.N. Tovey

A. Bodek: There is accurate electron scattering data from SLAC on $F(q^2)$ [up to $|q^2| > 20$ $(GeV/c)^2$]. These data show 2-10% deviations from the dipole form. Do these deviations agree with those predicted by your proposed (vector-dominance)-(quark-model) formula for $F(q^2)$?

L.M. Sehgal: I have not really attempted such a fit because, for the purpose of the problem that I was trying to investigate, the really essential part of $|q^2|$ is the region below 1 GeV^2. Essentially the cross-section disappears beyond that. But I think there are papers in the literature which have invented form factors which draw their intuition from the quark model, and they claim that these fit the electron scattering data as well as or better than the dipole form factor.

D.H. Perkins: You showed experimental points of gluon moments (from CDHS) as a function of Q^2, and also curves showing the predictions of QCD, and implied that the observed Q^2 evolution of gluons is strong support for QCD. I just wanted to remark that the evolution (in Q^2) of the moments of the quarks and the gluons, in QCD, is described by two coupled equations, which are not independent. To determine the gluon moments from the moments of $F_2(Q^2,x)$, using the first equation, and then show that these fulfil the second development equation, is just a consistency check, not an independent test of QCD.

L.M. Sehgal: I agree. It is a consistency check. I cannot answer that right away. It is an interesting point.

S. Fubini: I am asking a question about the formula for nucleon form factor which takes into account both the ρ pole and quark structure. Since the ρ is made out of $q\bar{q}$, do the authors see any risk of double counting?

L.M. Sehgal: I think I would for the moment not attach any fundamental significance to this parametrization. Clearly the theoretical behaviour of form factors has been an outstanding problem for many years and I think as long as one is trying an ansatz or an assumption one might as well use something which is transparent, even if it turns out to be wrong, and this particular parametrization has the outstanding virtue of transparency.

O. Pène: You noted that there may be a relation between the symmetry breaking in the charge square radius of the neutron and in the structure function of the proton. But there seems to be a difficulty in relating the signs of these two effects: the negative charge square radius implies that the down quarks are further away in configuration space in the neutron, which, by charge symmetry and uncertainty principle would imply dominance of down quark in proton structure function for $x \to 1$. This is contradicted by experiment.

L.M. Sehgal: I think the point I am making is, not that we know what the relation between those two things is, but rather that we know definitely that if the u- and the d-quark distributions in the proton were identical, this charge radius would vanish. The fact that in the infinite momentum frame one actually sees these two distributions as being distinct, ought in some way to be related to the fact that in a proton at rest, the u- and d-quarks are differently distributed. Now I am not suggesting that we know what that connection is, but a connection like that must exist and that is a theoretical challenge.

S.J. Brodsky: The electromagnetic and weak nucleon form factors at large Q^2 can be evaluated in QCD. The correct power law is $1/Q^4$ with logarithmic modifications from $\alpha_s(Q^2)$ and the anomalous dimensions of the nucleon wave functions at short distances. The forms you have used for the nucleon form factors are in conflict with these QCD predictions, and, I believe, the high Q^2 SLAC data for $G_n^p(Q^2)$.

L.M. Sehgal: This is not a form that is expected to be asymptotically correct. It is a form that describes the data in the low Q^2 region. Certainly the analytic properties of the form factors were not a consideration in choosing this.

J.G. Taylor: Which is the most important feature in the suggested vector dominance/quark model, the vector dominance term or the quark bound state wave function? Is there much sensitivity of the suppression brought about by this revised form factor to the quark masses?

L.M. Sehgal: The vector dominance part is more important. I think I should acknowledge here that ideas of this type, that the form factor may be a product of a quark type form factor and a vector meson pole, have been around in the literature and I believe I mentioned the Orsay group as one of the proponents of this idea. The form I have used is not identical to what they have, because when one tries to modify a non-relativistic expression for relativistic effects, there is always a certain measure of arbitrariness and ambiguity, and they have some additional factor there.

J.G. Taylor: The results then, that you obtain, in particular in the damping by a factor of 5, are not very sensitive to the quark masses that are assumed.

L.M. Sehgal: No, they are not. At least the way I have estimated the SU(4) symmetry breaking corrections, there is no large renormalization. On the other hand, there can be several opinions on that. I think in the paper by the Orsay group there is a substantial renormalization of that matrix element which accounts partly for a decrease in the cross-section.

D.J. Broadhurst: Yesterday Turlay showed that Duke and Roberts' second order calculation agrees better with the BEBC data than with the CDHS data. Do you have any reason to prefer one data set to the other in a comparison with QCD? In particular, could the different treatment of quasi-elastic events be significant?

L.M. Sehgal: I think that is a very complicated question. It seems clear that if one is trying to test a theory which is valid at very short distances, it is best to go to the highest momentum transfers available. It is also safest to exclude the elastic and quasi-elastic channels, because, as we saw, these manifestly violate chiral symmetry which is one of the underpinnings of the theory. Theoretical papers suggest that second order corrections (in α) are large at the currently available Q^2 and the effect then could be, to give values of Λ arising from lowest order fits which have nothing to do with the true Λ value. I have not really looked at this very critically. The second order fits do not appear to be much better than the lowest order. They just give Λ values about a factor two smaller.

G. Preparata: It should be clearly recognized that your parametrization of the form factor with a vector meson factor and a factor depending on the wave function of the nucleon implies a breakdown of usual dispersion relations for form factors. A thing I find most interesting.

L.M. Sehgal: All I can say is this choice was not dictated by any considerations of analyticity.

P.J. O'Donnell: In addition to alternative parametrizations of form factors there is the problem of choice of form factor. In the electromagnetic case one can choose the Sachs or Dirac form factors. How does this affect your analysis?

L.M. Sehgal: It seems to me that at least as far as the axial-vector form factor is concerned, there is no ambiguity, there is only one. I do not know what the situation is in electron scattering, how crucial it is to separate the electric and the magnetic form factors, to see this dipole behaviour and this scaling of electric and magnetic form factors. I do not know.

M. Bace: During the discussion there was a statement that the situation about the QCD parameter Λ is confused. In fact there is no confusion. Experiments give different values, so obviously, it will take more work to achieve agreement. Theoretically there is a small subtlety (explained in a note in Phys. Letters by myself) but no confusion.

L.M. Sehgal: I think there is a well-known paper of Bace .... (he is Bace!) ... so you know about it!

ATOMIC PHYSICS CHECKS OF PARITY VIOLATION

L.M.Barkov and M.S.Zolotorev
Institute of Nuclear Physics, Novosibirsk, USSR

ABSTRACT

The results of the new run of measurements of the parity violation in atomic bismuth on $^4S_{3/2} - {}^2D_{5/2}$ MI - transition at $\lambda = 648$ nm are presented. The value $R = Im(EI/MI)$ measured on $F = 6 - F' = 7$ and $F = 6 - F' = 6$ hyperfine structure components is found to be $(-20.6 \pm 3.2)\cdot 10^{-8}$. The average value for all our measurements $\langle R \rangle = (-20.2 \pm 2.7)\cdot 10^{-8}$ is in agreement with the theoretical prediction obtained in the framework of the standard gauge model with $\sin^2\theta = 0.25$.

In the previous works[1,2] we reported the observation of the parity nonconservation in atomic transitions caused by the weak interaction of electrons with nucleons. In those experiments the rotation of the polarization plane of light at $\lambda = 648$ nm in bismuth vapor was observed. The results of our experiments were consistent with the theoretical predictions[3], based on the standard gauge model[4,5], and were in contradiction with null results of the experiments in Seattle[6,7] and Oxford[8].

As it was noted for the first time by Zel'dovich[9], the parity violation in the interaction of the electrons and nucleons should induce natural optical activity of the matter. The possibility to find the optical activity in atoms in real experiments was shown in the works[10-12], in which it was proposed to search for the optical activity in MI - transitions of some heavy atoms.

In this paper the results of the new run of measurements of the optical activity in bismuth vapor at the $F = 6 - F' = 7$ and $F = 6 - F' = 6$ hyperfine structure components of the MI - transition $^4S_{3/2} - {}^2D_{5/2}$ at $\lambda = 648$ nm are presented.

The scheme of the experiment is shown in Fig. 1. A Spectra-Physics 375 dye laser with an additional element, which permitted to have a single-frequency light beam and to modulate this frequency by 416.3 MHz steps was used. The frequency modulated light passed through the prism polarizer, the bismuth-vapor cell and the prism analyzer, after which two space separated beams with orthogonal polarization were detected by photomultipliers. The bismuth cell was situated inside double magnetic shield so that the spurious magnetic field along the cell axis was smaller than $2\cdot 10^{-5}$Gs. Inside the magnetic shields seven sections of the coil were placed. The Faraday rotation from each section of the coil permitted to find out the atomic bismuth vapor pressure distribution along the cell axis. The helium buffer gas stabilized the bismuth vapor pressure and ensured the safety of the analyzer and polarizer prisms, which were used as the entrance and exit windows of the cell. The design of the support

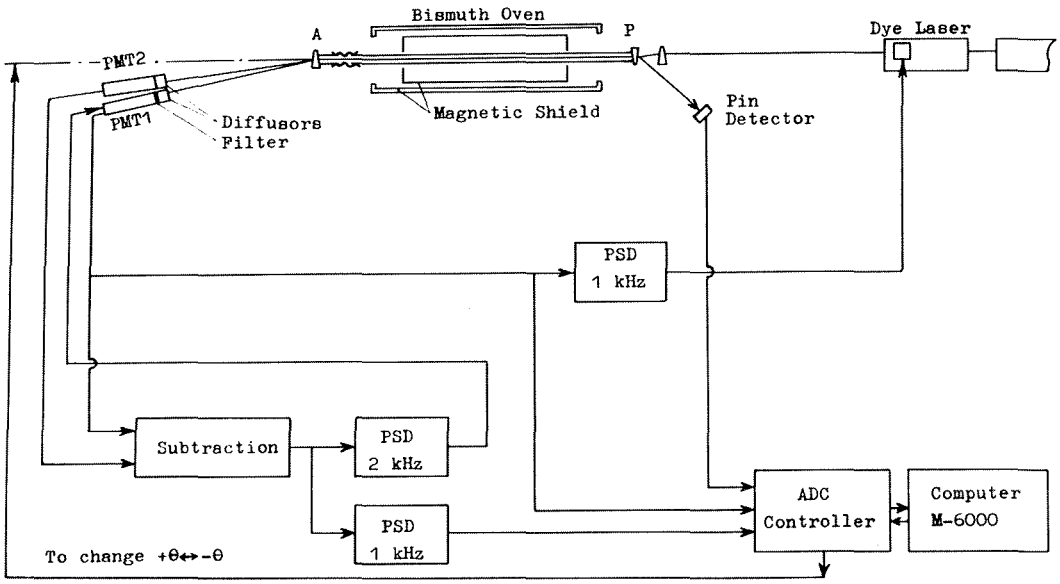

Fig. 1 The scheme of the experiment. P-prism polarizer, A-prism-analyzer, PMTI and PMT2-photomultipliers, PSD-phase-sensitive detectors, ADC-analog-digital converter.

of the analyzer and the photomultipliers allowed to rotate them about initial direction of the light beam without change of the deflected beam position relative to the multipliers. In front of the photomultipliers the cavities covered inside with white paint were placed, which ensured diffused scattering of the light before hitting the photocathodes.

The signals from the photomultipliers PMTI and PMT2 are

$$V_1 \sim I \cos^2(\theta + \Psi_{PNC}) \simeq I ,$$

$$V_2 \sim I \sin^2(\theta + \Psi_{PNC}) \simeq I\theta^2(1 + 2\Psi_{PNC}/\theta) ,$$

where I is the intensity of the light passed through the bismuth vapor, $\theta = \pm 4 \cdot 10^{-3}$ rad is the angle between the axes of the analyzer and polarizer, Ψ_{PNC} is the angle of rotation of the polarization plane due to the parity nonconserving interaction between the electrons and nucleons. As the angle is proportional to the real part of the refraction index and its wavelength dependence has dispersion curve shape (see Fig. 2a), during wavelength modulation near the absorption line centre Ψ_{PNC} must contain the first harmonic of the scanning frequency, which in the experiment was 1 kHz. To minimize the false 1 kHz signal, two feedback circuits were used (see Fig. 1), one of which provided the symmetry of scanning position so that the signal of the first harmonic from PMTI was more than 10^3 times suppressed. Another 2 kHz feedback circuit regulated the high voltage supply of PMT1 to provide good quality substraction of the signals from photomultipliers so that the subtracted signal had the second harmonic amplitude 10^3 times smaller than that from PMT2. Preliminary the signals from PMT2 were levelled with the help of a grey filter installed before

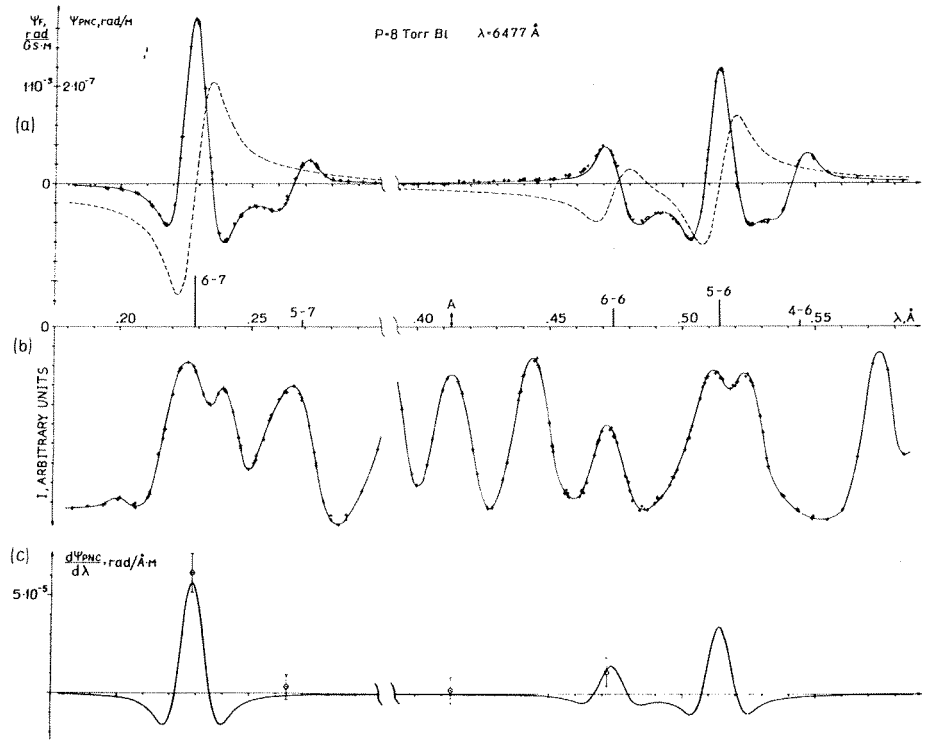

Fig. 2 a) Dashed line - the theoretical prediction for PNC optical rotation of bismuth vapor, solid line - the calculated Faraday rotation;
b) observed absorption spectrum;
c) the calculated curve and the results of the measurements.

the photocathode of PM1 and by the choice of the high voltage supply of the photomultipliers. In these conditions the subtracted signal $\Delta = V_2 - V_1 \sim I\theta\Psi_{PNC}$ must contain the first harmonic of the scanning frequency only through Ψ_{PNC}. It does exist if the parity is not conserved in the electron-nucleon interactions. The difference of the phase detected signals in Δ, found for $+\theta$ and $-\theta$ positions of the analyzer, served as the measure of the parity violation.

In this experiments were done on four absorption lines shown as 1,2, 3 and A in Fig. 2. The measurements on the quadrupole transition $F = 5 - F' = 7$ and on the molecular absorption line A permitted to control the spurious magnetic field and symmetric errors. During the experiment the measurements were performed alternatively on the working and control lines. Each measurement continued 30 minutes. During that time the sign of θ changed 20 times. On the 1,2 and A lines 26 measurements were done, and only 13 on the line 3. At the end of each measurement the magnetic field was switched on and $d\Psi_F/d\lambda$ was measured (Ψ_F is the Faraday rotation angle), which was used subsequently for normalization of measured value of $d\Psi_{PNC}/d\lambda$. The information about intensity of the light beam before and after the bismuth oven, about the shape of the absorption line and the value of the first harmonic of the subtracted signal was accumulated and processed with the help of the computer M-6000.

In Fig. 2a the results of the Faraday rotation measurements and the theoretical curve, calculated for null collisional broadening and the value of radial integral $\langle r^2 \rangle = 9\, a_0^2$, where a_0 is a Bohr radius of hydrogen atom, are shown. Also shown in the figure is the dependence of Ψ_{PNC} on λ . The theoretical curves were found on the basis of works[3,13] where the amplitude of MI-transition was taken[14] to be equal to $-0,55\,M$ Bohr with $\pm 2\%$ estimated error instead of the usually used value $-\ 0,584\,M$ Bohr. More precise value of R, calculated by the Novosibirsk group of theorists, was found to be $R_{theor} = -18,8 \cdot 10^{-8}$ for $\sin^2\theta = 0.25$. The Faraday rotation measurements were carried out in separate experiment in which a Faraday cell was placed additionally between the polarizer and the bismuth cell, and 2 Gs magnetic field was applied along the bismuth vapor cell axis. In these measurements the wavelength was scanned at 0.01 Hz frequency and at the same time the polarization plane of the laser light was modulated at 1 kHz with the help of the Faraday cell. The optical length of the atomic bismuth vapor, which was found from comparison of measured and calculated Faraday rotation, within several percent accuracy coincides with that found from measurements of the atomic bismuth vapor density distribution along the cell axis, known total pressure in the bismuth vapor cell and the partial atomic bismuth pressure taken from[15].

The value of $d\Psi_{PNC}/d\lambda$ measured on the lines 1,2,3 and A and the calculated curve $d\Psi_{PNC}/d\lambda$ are presented in Fig. 2c. The results obtained on the lines 1 and 3 correspond to the value

$$R_{exp} = (-20.6 \pm 3.2) \cdot 10^{-8},$$

and the measurements on the control lines 2 and A show zero effect. Together with the previous results of the work[2] we get average value for all our measurements

$$\langle R_{exp} \rangle = (-20.2 \pm 2.7) \cdot 10^{-8}$$

and in comparison with the theoretical prediction

$$\langle R_{exp} \rangle / R_{theor} = 1.07 \pm 0.14$$

The latest unpublished results from Oxford[16] and Seattle[17] show parity violation effect in atomic bismuth. However, the results of their new experiments have too poor reproducibility to make definite conclusions about its value. The method of measurements of small angle rotation of the plane of polarization used in our experiments possesses a series of advantages. The main of them consists in the large number of measurements on different control lines. Before each run of measurements durable work on the control lines for search, artificial enlargement and then suppression of false effects had been done. Durable work on the control lines, as we are sure, allowed us to expose possible systematic errors and to get rid of them.

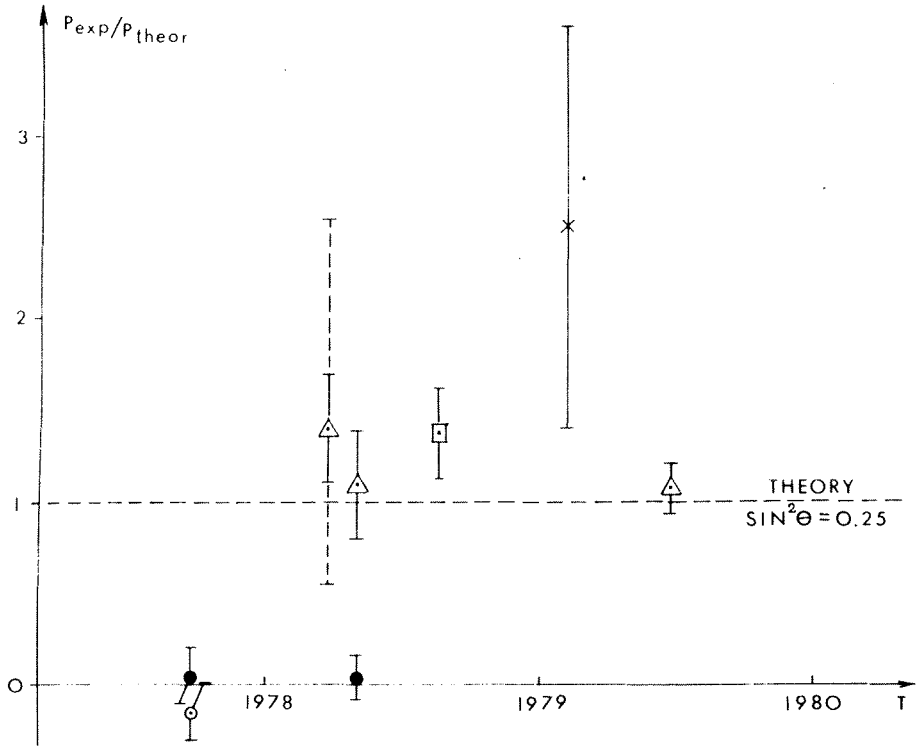

Fig. 3 Chronological sequence of the results of measurements of PNC interaction of electrons and nucleons. P - parity nonconservation parameter, P_{theor} - predicted value in Weinberg-Salam model with $\sin^2\theta = 0.25$. ● - Seattle[6,7], ⊙ - Oxford[8], ▲ - Novosibirsk[1,2], ⊡ - Stanford[21], × - Berkeley[18].

The result of Berkeley experiment[18] for a measurement of the circular dichroism in the forbidden M1-transition at $\lambda = 293$ nm in thallium also shows the parity violation in atoms, however with large statistical uncertainty

Recently some people declared doubt the reliability of atomic calculations for such heavy atoms like bismuth[19]. From our point of view the most reliable predictions for PNC effects in heavy atoms were made by the Novosibirsk group of theorists, who succeeded in noncontradictory way to calculate a great number of known experimental atomic characteristics, using for this the theoretical scheme with a few number of phenomenological parameters. The calculations, performed recently by this group[14], gave the value of the effect differing only by 6% from that found in 1976[3]. All this gives us confidence that the accuracy of their calculations, estimated by the authors as 15-20%, is true.

As is known[20], in the atomic experiments and in the experiment at Stanford[21], where the deep inelastic scattering of polarized electrons by deutrons and protons was investigated, two independent linear axial and vector constants of the weak interaction can be measured. Thus, the results of our and Stanford experiments indicate the validity of the Weinberg-Salam model.

REFERENCES

1) L.M.Barkov and M.S.Zolotorev, Pis'ma Zh. Exp. Teor. Fiz. 27, 379 (1978). /JETP Lett. 27, 357 (1978)/.

2) L.M.Barkov and M.S.Zolotorev, Proc. of the Conf. Neutrino-78; Pis'ma Zh.Exp. Teor. Fiz. 28, 544 (1978).

3) V.N.Novikov, O.P.Sushkov and I.B.Khriplovich, Zh. Exp.Teor. Fiz. 71, 1665 (1976). /Sov. Phys. JETP 44, 872 (1976)/.

4) S.Weinberg, Phys. Rev. Lett. 19, 1264 (1967).

5) A.Salam, Elementary Particle Physics (ed. by N.Svartholm, 1968) p. 367.

6) L.L.Lewis et al., Phys. Rev. Lett. 39, 795 (1977).

7) E.N.Fortson, Proc. of the Conf. Neutrino - 78.

8) P.E.Baird et al., Phys. Rev. Lett. 39, 798 (1977).

9) Ya.B.Zel'dovich, Zh. Exp. Teor. Fiz. 36, 964 (1959). /Sov. Phys. JETP 9, 682 (1959).

10) I.B.Khriplovich, Pis'ma Zh. Exp. Teor. Fiz. 20, 686 (1974). /JETP Lett. 20, 315 (1974).

11) P.G.H.Sandars, in Atomic Physics, Vol. 4 (ed. by G.Zh.Putlitz) (Plenum, New York, 1975), p. 71.

12) D.C.Soreide and E.N.Fortson, Bull. Am. Phys. Soc. 20, 491 (1975).

13) V.N.Novikov, O.P.Sushkov and I.B.Khriplovich, Opt. Spectr. 43, 621 (1977); 45, 413 (1978).

14) O.P.Sushkov, V.V.Flambaum and I.B.Khriplovich, Report at the Conf. on the Theory of Atoms and Molecules, Vilnius (1979).

15) R.Hultgen et al., Selected Values of the Thermodynamic Properties of the Elements, American Society for Metals (1973).

16) P.E.G.Baird, Talk at the 4 Intern. Conf. on Atomic Physics, Riga, p. 653 (1978); P.E.G.Baird, private communication (1979).

17) E.N.Fortson, private communication (1979).

18) R.Conti et al., Phys. Rev. Lett. 42, 343 (1979).

19) S.Weinberg, Proc. of the 19 Intern.Conf. on High Energy Physics, Tokyo, p. 907 (1978).

20) See, for example, G.Altarelli, Proc. of the 19 Intern. Conf.on High Energy Physics, Tokyo, p. 411 (1978).

21) C.Y.Prescott et al., Phys. Lett. 77B, 347 (1978).

DISCUSSION

Chairman: D.H. Perkins

Sci. Secretaries: G. Bonneaud and S.N. Tovey

E. Fiorini: Due to the importance of this result, I would like to know if somebody in the audience can comment on its disagreement with the result obtained by the Oxford Group on the same line?

L.M. Barkov: Oxford work on one line, the head line of the hyperfine structure, and find a null result. At the Riga Conference, they announced their new result. But, it was not reproducible and varied between the theoretical prediction and zero. In our experiment we had non-reproducible results about 2½ years ago. Now, we switch on the apparatus, change what we want, then begin to work with the control lines where one sees zero effect, and then find the non-zero results on the working lines. On the head line we have 26 measurements, of half an hour each, in which the effect was about the same. With this working line, only one result was near zero. I think that, in the experiments at Oxford and Seattle, they achieved small statistical errors while they still had systematic spurious effects.

G. Barbiellini: How large are the corrections due to the Coulomb potential of the electrons with bismuth atoms?

L.M. Barkov: The corrections for these effects made in the calculations were about 10 to 15%. This is not very dangerous in the Novosibirsk calculations, as the corrections can be well checked by comparison with many well measured experimental quantities: fine structure, lifetimes of states, their positions, polarizability of the atoms and so on. And they are based on the whole range of heavy atoms, not only bismuth. During the last 3 years, the change in the theoretical predictions due to the atomic calculations was only 6%.

FURTHER TESTS OF PARITY VIOLATION IN INELASTIC ELECTRON SCATTERING

C.Y. Prescott

Stanford Linear Accelerator Center, Stanford, California, USA

ABSTRACT

Further measurements of parity violating asymmetries in inelastic scattering of polarized electrons from deuterium have been made for a range of y values from 0.15 to 0.36. Only a small y-dependence is observed in the asymmetries. Using the quark-parton model our results are in good agreement with the Weinberg-Salam predictions. We obtain a value of the parameter $\sin^2\theta_W = 0.224 \pm 0.020$.

The evidence for parity non-conservation in electron scattering was reported last year.[1] Today I wish to report on further measurements of the parity violating asymmetries we have made in the process

$$e(\text{polarized}) + D(\text{unpolarized}) \rightarrow e' + X \quad . \tag{1}$$

These further measurements refine and extend our earlier results over a wider kinematic range and provide more stringent tests of gauge theory models. The parity violating asymmetry we measure is defined as

$$A = (\sigma_R - \sigma_L)/(\sigma_R + \sigma_L) \tag{2}$$

where $\sigma_{R(L)}$ is the cross-section $d^2\sigma/d\Omega dE'$ for right-handed (left-handed) electrons scattering from deuterium.

If we make the usual quark-parton model assumptions that the electrons scatter off spin ½ constituents of the nucleons, the asymmetry has the general form

$$A/Q^2 = a_1 + a_2 \frac{(1 - (1 - y)^2)}{(1 + (1 - y)^2)} \tag{3}$$

where Q^2 is the invariant four-momentum transfer-squared, and $y = (E_o - E')/E_o$ is the fractional energy transferred from the electron to the hadrons.[2] For an isoscalar target such as deuterium, the coefficients a_1 and a_2 are expected to be constants. Gauge theory models predict values for a_1 and a_2, and in the Weinberg-Salam version of the SU(2) x U(1) gauge theory, equation (3) becomes[3,4,5]

$$A/Q^2 = \frac{G_F}{2\sqrt{2}\pi\alpha} \cdot \frac{9}{10} \left[(1 - \frac{20}{9} \sin^2\theta_W) + (1 - 4 \sin^2\theta_W) \frac{1 - (1 - y)^2}{1 + (1 - y)^2} \right] \quad . \tag{4}$$

Under these more restrictive assumptions, measurements of the reaction (1) can be used to determine a value for the mixing parameter $\sin^2\theta_W$. I will show fits to our data for the Weinberg-Salam model, equation 4, for the more general form, equation 3, and for a second SU(2) x U(1) model which assigns the right-handed electron to a doublet with an hypothesized heavy neutral lepton. I will conclude my remarks with a brief discussion of the sources of errors in our results, and connections our results have to parity violation in the atomic physics experiments.

The asymmetry A arises from weak-electromagnetic interference and was expected to be less than 10^{-4} in our kinematic range. The experimental objective, therefore, was to control statistical and systematic errors at the 10^{-5} level. The smallness of this error made the measurements technically difficult. Figure 1 shows the experiment in a highly schematic form.

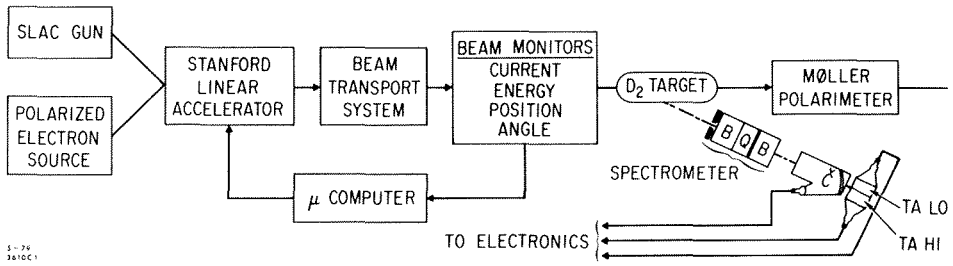

Fig. 1

We had available for our use either ordinary unpolarized electrons from the SLAC gun, or polarized electrons from the newly developed GaAs photoemission source. The polarized electron source was developed over the past 4 years as a high intensity injector for SLAC, based on a proposal in 1974 by Garwin (SLAC), Pierce and Siegmann (Zurich) that circularly polarized laser light could photoemit longitudinally polarized electrons from gallium arsenide crystal surfaces. Such a device was developed at SLAC and installed as an injector for the accelerator in late 1977. It now routinely provides full SLAC beam intensities at a polarization around 40%. Polarization is fixed for the short 1.5 μsec long beam pulses at SLAC, but can be reversed between beam pulses by reversing the circular polarization of the laser light. Most importantly, influences these reversals have on beam parameters such as current, position, or phase space are virtually non-existent, and cross-section comparisons between + and - helicity can be meaningfully made. We chose to randomize the pattern of + and - pulses to remove any biases due to systematic drifts in apparatus or periodic effects in the accelerator. The accelerator operated at 120 pulses per second for this work, at energies from 16.2 GeV to 22.2 GeV. No problems with depolarization of longitudinal spin were seen (or expected). A beam transport system defined the energy of the beam ($\Delta E/E$ = 1.5% FW) and delivered it to the target. The beam transport system is instrumented with beam toroids that measure the charge delivered in each pulse to the target, and with resonant microwave position monitors to monitor position and angle of each beam pulse at the target. A microwave cavity placed in the beam transport system where energy is dispersed horizontally permitted measurement of beam energy within the 1.5% acceptance. Signals derived from these cavities were monitored by a microcomputer and correction signals were generated to null out drifts seen in beam energy, position and angle. The phase of two of the accelerating klystrons was varied forward or backward from 90^{o} to add or subtract beam energy, and currents in beam magnets were adjusted to correct position and angle. This procedure significantly improved stability in these beam parameters.

Signals from these monitors were read for each beam pulse and stored along with other data for analysis. This information was later used in the analysis of our systematic errors. The beam passed first through a 30 cm long liquid D_2 target (0.04 radiation lengths) and then through a polarimeter which monitors beam polarization. By scattering longitudinally

polarized beam electrons off polarized target electrons (Møller scattering) the beam polarization could be measured. Polarized target electrons are obtained by magnetizing an iron foil. This process, calculated to good accuracy in QED, provides an important normalization for the measurements. The experimental asymmetries are related to the parity violation asymmetry, Eq. (2) by

$$A_{exp} = P_e A \ . \tag{5}$$

The Møller polarimeter was used frequently during the course of the data (several times per day), and obtained an average polarization, $P_e = 37 \pm 2\%$. We also monitored the polarization at the source by the traditional low energy technique of Mott scattering from gold foils. For the latter technique the value obtained was $P_e = 39 \pm 4\%$. We use the more accurate high energy value.

Cross-sections for electrons scattered at 4^o were measured in a spectrometer. The spectrometer defined acceptances in angles and momentum which varied from 11 to 16.5 GeV/c. Electrons passing through the acceptances are counted by two counters. The first was a 3 meter long gas Cerenkov counter, and the second a lead glass shower counter divided into high and low momentum halves. These counters operated independently through separate electronic channels (never in coincidence), and served as a cross check on each other. Because of the high counts needed to achieve $\Delta A < 10^{-5}$, cross-sections were measured by counting fluxes of scattered electrons. For each beam pulse, the photomultiplier anode currents were integrated and digitized for each counter. These signals, taken as a measure of the flux of electrons, were normalized in the computer to the charge delivered to the target. For each beam pulse we obtained in each counter a cross-section in arbitrary units. Although the spectrometer was calibrated, precise normalization is not important because such factors cancel for asymmetries defined in equation 2. By averaging over sufficiently large numbers of beam pulses, the statistical errors could be reduced to the 10^{-5} level. But at this level, the question of non-statistical sources of error becomes a primary concern.

One critical source of error could arise if reversals of polarization between + and - helicity caused changes in beam parameters. Extensive monitoring of all important parameters (current, energy, position and angle) ruled out systematic errors of this nature at the 10^{-5} level. To rule out other sources of systematic errors, we appeal to the several null measurements included in our measurements. An example is found in the next figure, which also shows the best evidence we have for parity violation in this process.

Owing to the anomalous magnetic moment of the electron, and to the $24\frac{1}{2}^o$ bend in the transport system, the electron spin will precess ahead of the momentum by an amount

$$\begin{aligned} \theta_{prec} &= \gamma \frac{g-2}{2} \theta_{bend} \\ &= \frac{E_o \pi}{3.237(GeV)} \quad \text{radians.} \end{aligned} \tag{6}$$

The majority of our data were taken at 19.4 GeV ($\theta_{prec} = 6\pi$) where positive helicity at the source resulted in positive helicity at the target. But at 16.2 GeV and 22.2 GeV this was not so. The experimental asymmetries measured by our computer relative to the source polarization should be modulated by the g-2 precession according to

$$A_{exp}/Q^2 = P_e A/Q^2 \cos\left(\frac{E_o \pi}{3.237}\right) . \qquad (7)$$

Figure 2 shows the asymmetries measured separately in two counters for four energies, and a fit of the form given by equation 7. The point at 17.8 GeV corresponds to spin transverse to the scattering plane, where asymmetries are expected to vanish. This point limits the contribution due to unobserved systematic effects, and rules out asymmetries arising from transverse spin components which would be maximum for this point. No systematic errors we know of can mimic the g-2 modulation of our results, and we take the results of Figure 2 to be clear evidence of parity violation in electron scattering.

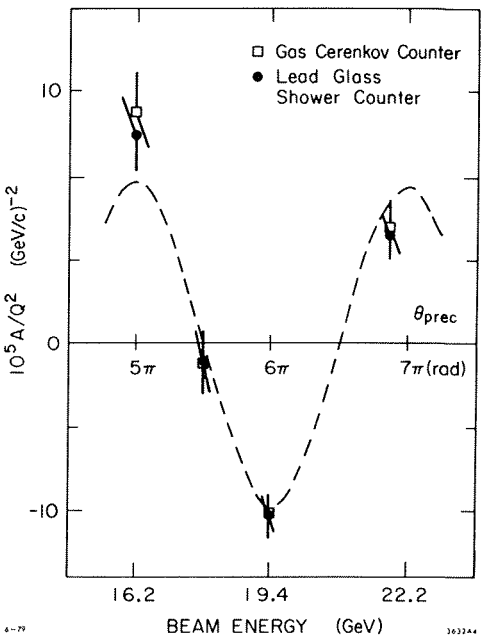

Fig. 2

Figure 3 shows the latest results taken mostly at $E_o = 19.4$ GeV for secondary energies E' = 11 to 14.5 GeV. Earlier data taken at $E_o = 16.2$, 19.4, and 22.2 GeV are also included. We plot asymmetries normalized to Q^2 for the different mean y values of each setting. For these points, the separate high and low momentum halves of the lead glass counter are used, resulting in two points per kinematic setting. For the lowest energy, 16.2 GeV, one half has been deleted because it contained strong elastic peak and resonance production contributions. This results in 11 data points. Each point is shown with double error bars. The inner errors are the statistical part only. The outer errors are the systematic and statistical errors combined. An additional ± 5% uncertainty in overall scale, due to the error on P_e, is not shown.

We fit these data to three models. The first is the Weinberg-Salam model combined with the simple quark-parton model for the nucleon, equation (4). The fit depends on a single parameter, $\sin^2\theta_W$. The best value is

$$\sin^2\theta_W = 0.224 \pm 0.020 \qquad (8)$$

and the chi-squared value for the fit is 1.04 per degree of freedom.

A second SU(2) x U(1) model, which assumes the right-handed electron has a heavy neutral partner, $(e^{E_o}-)_R$, is shown. In this "hybrid" model the asymmetry must go to 0 at y = 0 due to the vanishing of the electron axial-vector coupling. The data rule this case out. A third fit to the data is shown for the "Model Independent" form of equation 3. "Model Independent" refers to the absence of gauge theory assumptions, although quark-parton model ideas are still used. This fit is a two parameter form, nearly a straight line. I will return to

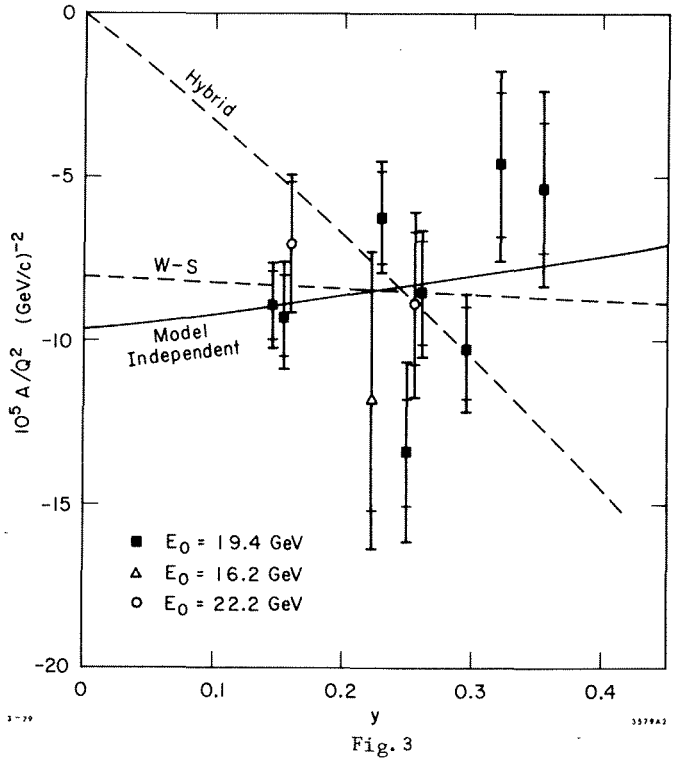

Fig. 3

this fit in a moment. But first let me say a few words about errors.

Within the context of the Weinberg-Salam model and the simple quark-parton model, the parity violating asymmetry, equation (2), is expressed in terms of a single parameter, $\sin^2\theta_W$. We determine the best value and its errors by fitting the experimental data to the form, equation (4). The error consists of a statistical part (0.012) and a systematic part (0.008) added linearly. The systematic error comes from several sources; beam monitoring and background subtractions contribute point-to-point systematic errors and uncertainty in P_e contributes the largest part, an overall scale uncertainty in A. Beyond these experimental errors, there exist uncertainties in the "theory" due to the quark-parton model assumptions. If we add a 10% $q\bar{q}$ sea contribution, the best value for $\sin^2\theta_W$ is a nearly-identical 0.226. Quark-antiquark sea terms have insignificant effects on A. However, what about effects outside the framework of the simple parton model? Several authors have addressed this specific question, and we use their parametrizations for estimating effects on $\sin^2\theta_W$ values.[2,6,7] Equation (4), from the simple-quark parton model, is a special case of equation (2). Modified forms replace equation (4); the a_1 part is modified ± a few percent by coherent scattering effects. The form of the y-dependence is modified by finite non-zero $R = \sigma_L/\sigma_T$ values, and a_2 picks up factors from non-scaling effects at low - Q^2 that probably exist, based on neutrino bubble chamber data. For the modified forms of equation (4), and for the range of variations suggested, best fits are obtained for $\sin^2\theta_W$ that vary from 0.210 to 0.230. The limits on $\sin^2\theta_W$ are not precisely defined, but we find an error due to parton model uncertainties of ± 0.010. We have not included this in the experimental error of ± 0.020, but conclude that the error on the "theory" may be as large as experimental errors.

I would like to conclude with a few brief remarks about the connections this work has to parity violation in atomic physics. We have taken note of the remarkable success of the Weinberg-Salam model of weak and electromagnetic interactions, but in the spirit of objective experimental investigation let's ignore for now all gauge theory ideas and look at the model independent approach. This approach has been emphasized by a number of authors,[8] particularly with regard to neutrino neutral current interactions, but can be extended to parity violating effects in electron-hadron interactions. Parity violation phenomenology has its basis in the neutral current piece of the interaction between electron and quarks, where the form of the interaction is regarded as an unknown. The leptonic neutral current interaction has both a vector part and an axial-vector part. Likewise, the hadronic part couples to neutral currents through vector and axial-vector couplings. The parity-violation part of the interaction arise from the cross-products; that is, from the leptonic vector-hadronic axial-vector product and the leptonic axial-vector-hadronic vector product. Vector-vector and axial vector-axial vector terms in the neutral current interaction exist but do not contribute to parity violation. Likewise, S, P, or T terms, if they exist in neutral currents, do not contribute. The most general parity violation effective Lagrangian can be written as

$$\mathscr{L}_{eff} = -\frac{G}{\sqrt{2}} \sum_{\text{quarks}} \varepsilon_{VA}(e,q)\ \bar{e}\gamma_\mu e\ \ \bar{q}\gamma_5\gamma_\mu q + \varepsilon_{AV}(e,q)\ \bar{e}\gamma_5\gamma_\mu e\ \ \bar{q}\gamma_\mu q \qquad (9)$$

where the ε coefficients (Bjorken's notation[2]) are undetermined, but can be related to measureable parameters in different processes. In the simple quark-parton model the heavier quarks (s, c, ...) are neglected, while the light quarks (u, d) are summed over. In terms of these phenomenological couplings, the asymmetry in e D scattering becomes[2]

$$A/Q^2 = -\frac{3G}{10\pi\alpha\sqrt{2}} \left\{ \left[2\varepsilon_{AV}(e,u) - \varepsilon_{AV}(e,d)\right] + \left[2\varepsilon_{VA}(e,u) - \varepsilon_{VA}(e,d)\right] \frac{1-(1-y)^2}{1+(1-y)^2} \right\} \qquad (10)$$

which is the basis of equation (3). The model independent fit of figure 3 gives

$$a_1 = -\frac{3G}{10\pi\alpha\sqrt{2}} \left[2\varepsilon_{AV}(e,u) - \varepsilon_{AV}(e,d)\right] = (-9.7 \pm 2.6) \times 10^{-5}$$

and $$a_2 = -\frac{3G}{10\pi\alpha\sqrt{2}} \left[2\varepsilon_{VA}(e,u) - \varepsilon_{VA}(e,d)\right] = (4.9 \pm 8.1) \times 10^{-5} \qquad (11)$$

which is insufficient information to determine the fundamental parity violating coupling parameters between electron and quarks.

To make the separations, we must turn to other processes which can provide different combinations of the ε's. Inelastic scattering from protons in principle provides new information, but the difference from e D scattering is so small ($\lesssim$ 10%) that in practice this case would provide no new information. Elastic scattering at high Q^2 is prohibitively difficult but at medium energies, elastic scattering off protons, deuterons, and higher Z nuclei, is possible, and experiments being planned may ultimately provide us new information. At present we are limited to atomic physics parity violation measurements from bismuth and thallium,[9-12] where the results are sensitive to the nearly orthogonal combination

$$\varepsilon_{AV}(e,u) + 1.15\ \varepsilon_{AV}(e,d) \quad . \qquad (12)$$

For high Z nuclei, the hadronic axial-vector terms do not contribute measurable effects but in atomic hydrogen they do, and we may have to wait for atomic hydrogen parity violation results to obtain experimental separation of the hadronic axial-vector terms.

Figures 4a and 4b summarize the present experimental situation. The SLAC e D results can be separated into hadronic vector parts, which contribute to the intercept parameter a_1, and hadronic axial-vector parts which contribute to a_2. In figure 4a, the two axes correspond to $\epsilon_{AV}(e,u)$ and $\epsilon_{AV}(e,d)$, and the SLAC e D results map out a stripe in this two-parameter space. The atomic physics parity violation results map out stripes that are nearly orthogonal to the SLAC results. I show four experimental results, three from bismuth and one from thallium. Two of the bismuth experiments, Oxford and Seattle groups, have reported absence of parity violating effects at the level predicted by the Weinberg-Salam model, and two experiments, Novosibirsk (bismuth) and Berkeley (thallium) have reported evidence for parity violation at the level consistent with the Weinberg-Salam model. The discrepancies between the groups is at present not resolved. I also wish to point out that in the model independent framework, our results from e D parity violation can be regarded as consistent with any of the results from atomic physics. The Weinberg-Salam model predicts values for these phenomenological couplings, and they are shown in figures 4a and 4b. In figure 4b, we see the stripe mapped out by the slope parameter a_2 from our e D results. At present this is the only experiment sensitive to these hadronic axial-vector parameters.

In conclusion, we have measured parity violating asymmetries in inelastic e D scattering at SLAC for a range of y values from 0.16 to 0.36. In the framework of the Weinberg-Salam model and using the simple quark parton model for the nucleon, we find good agreement with our data for a value of $\sin^2\theta_W$ that is consistent with the world average for that parameter in neutrino interactions.[13] The experimental errors approach the errors we obtain from uncertainties in the quark-parton model. From the model independent point of view, the experimental determination of the parity violating neutral current couplings is still unresolved, and much difficult experimental work is still needed to measure these parameters.

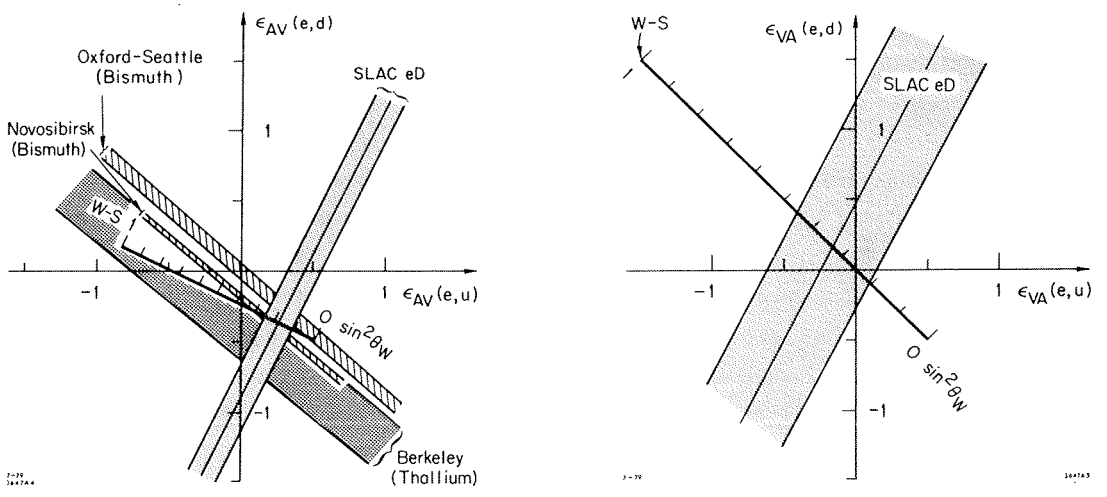

Fig. 4

REFERENCES

1) C.Y. Prescott, et al., Phys. Lett. 77B, 347 (1978).

2) J.D. Bjorken, SLAC-PUB-2146 (1978).

3) S.M. Berman, R.J. Primack, Phys. Rev. D9, 2171 (1974).

4) W.S. Wilson, Phys. Rev. D10, 218 (1974).

5) R.N. Cahn and F.J. Gilman, Phys. Rev. D17, 1313 (1978). A comprehensive list of references is found in this publication.

6) L. Wolfenstein, COOO-3066-111 (1978).

7) H. Fritzsch, CERN report 2607-CERN (1978).

8) L.M. Sehgal, Phys. Lett. 71B, 99 (1977); P.Q. Hung and J.J. Sakurai, Phys. Lett. 72B, 208 (1977); L.F. Abbott and R.M. Barnett, Phys. Rev. Lett. 40, 1303 (1978); J.J. Sakurai, UCLA/78/TEP/18, published in Proceedings of the Topical Conference on "Neutrino Physics at Accelerators", Oxford, July 1978; J.D. Bjorken, ref. 2; J.J. Sakurai, UCLA/78/TEP/27, published in AIP Proceedings on the III International Symposium on High Energy Physics with Polarized Beams and Polarized Targets, Argonne National Laboratory, Oct. 1978.

9) L.L. Lewis, et al., Phys. Rev. Lett. 39, 795 (1977). E.N. Fortson, Proceedings of the International Conference on Electronic and Atomic Collisions, Kyoto (1979).

10) P.E.G. Baird, et al., Phys. Rev. Lett. 39, 798 (1977).

11) L.B. Barkov and M.S. Zolotorev, JETP 27, 357 (1978).

12) R. Conti, et al., Phys. Rev. Lett. 42, 343 (1979).

13) C. Baltay, Proceedings of the 19th International Conference on High Energy Physics, Tokyo, Japan, Aug. 1978.

* * *

DISCUSSION

Chairman: D.H. Perkins

Sci. Secretaries: G. Bonneaud and S.N. Tovey

G. Barbiellini: At large y you have a substantial contribution of π. Did you check if this cross-section of π is spin-independent?

C.Y. Prescott: Yes we did. The systematic errors include measurements of the asymmetry for these pions. We had a device behind the lead-glass shower counter, a wall of lead which filtered out electrons and another counter which measured the pion yields and monitored the asymmetry of the pions. We measured the fraction of the pions which contribute so we can make corrections. We made corrections for these backgrounds and included uncertainties in the systematic errors. The asymmetries at the highest y I might mention; the number was $\sim (2 \pm 2) \times 10^{-5}$ for the asymmetry and it contributed 25% of the counting. That was the worst case.

V.A. Khose: Can you say a few words about proton data?

C.Y. Prescott: We have not taken very much proton data. We have reported in the publication last summer the one point we measured; it was consistent with the deuterium data. There is no new proton data.

M. Konuma (comment): According to your last figure, your result appears to be consistent both with the Novosibirsk result and with the Oxford and the Seattle results on the parity violation of the atomic Bi. If we, however, assume the factorization of the leptonic and the quark contributions in the model independent analysis, we can conclude that your result is compatible with the Novosibirsk data but not with the other two experimental results.

NEUTRINOS IN ASTROPHYSICS

Martin J. Rees
Institute of Astronomy, Madingley Rd, Cambridge, England.

ABSTRACT

The amount of ^{4}He synthesised in the "big bang" is sensitive to the early particle content and to the expansion rate. If there was indeed a "big bang", surprisingly strong conclusions can be drawn about the number of species of neutrinos, and about the possibility that such particles have non-zero rest mass. The dynamics of supernovae are sensitive to the details of neutrino physics; such explosions would yield 10^{52}-10^{53} ergs of $\sim$10 Mev neutrinos, in a burst lasting a few milliseconds. Galactic nuclei, cosmic ray sources and other high energy cosmic phenomena could yield a low background of $\gtrsim$10 Gev neutrinos.

1. INTRODUCTION

In this paper, I shall focus on those astrophysical contexts where the observed phenomena may be rather sensitivity dependent on neutrino physics - and where, as a corollary, astronomical observations can complement experimental data on weak interaction physics. The present written version is intended solely as a brief summary: references are given to recent papers where more extensive discussions may be found.

2. COSMOLOGICAL EVIDENCE

Helium is much more abundant, and much more uniformly distributed, than the heavier elements. The latter could all be the products of stellar nucleosynthesis. The helium, on the other hand, is commonly attributed to the hot dense early phase of the big bang: indeed, the most compelling reason for taking seriously the earlier phases (t = 1-100 sec) of a big bang is that the simplest assumptions (i.e. homogeneity, isotropy, no "new physics", Einstein's general relativity, etc.) yield a He abundance in gratifying accordance with observations[1]. The crucial process that determines the amount of He is the neutron/proton "freeze-out" which occurs when the reactions $p + e^- \rightarrow n + \nu$, $p + \bar{\nu} \rightarrow n + e^+$ become slower than the expansion timescale. In a standard radiation-dominated Friedmann model, the reaction rate goes as T^5 (since the particle density goes as T^3 and the cross sections as T^2) and the expansion rate $\propto (G\rho)^{\frac{1}{2}} \propto T^2$. The respective timescales are equal at kT $\simeq$ 1 Mev. The neutron/proton ratio is then approximately $e^{-1.5}$, most of these neutrons being subsequently incorporated into D, and then into ^{4}He, before they have time to decay freely.

The expansion rate of a Friedmann cosmological model depends on $\rho^{\frac{1}{2}}$. During the relevant early phases of a hot big bang cosmology (in which photons outnumber baryons by 10^8-10^9) the main contribution to ρ comes not from the baryons, but from the photons and other species of particle that are in thermal equilibrium. At kT $\simeq$ 1 Mev these include electron-positron

pairs, ν_e, $\bar{\nu}_e$, ν_μ, $\bar{\nu}_\mu$, and any other low-mass leptons that may exist. The "known" species of particles raise the energy density to $\frac{9}{2}aT^4$, where a is the Stefan-Boltzmann constant. Any extra species would raise this coefficient $\frac{9}{2}$ by an amount $\frac{7}{16}$ times its statistical weight, thereby increasing the total density, at a given T, by a factor $(1 + \frac{7}{72}\Delta g_\nu)^{\frac{1}{2}}$, Δg_ν denoting the sum of the statistical weights (2 or 4) of each new particle species[2,3].

Schwartzman[2] pointed out in 1969 that the observed fractional abundance of ^{4}He can place interesting constraints on the number of lepton species. If the universe were expanding somewhat faster than in the standard model, neutron/proton freeze-out would occur at a higher temperature, resulting in more neutrons, and a (possibly) unacceptable amount of primordial He. Recent calculations by Yang et al.[3] show the following: if the primordial helium abundance by mass (denoted by Y) is < 0.25, then the "speed-up factor" cannot exceed 1.09; if Y < 0.29, then the speed-up factor is $\lesssim$ 1.40. Most astronomers would be somewhat unhappy with a "primordial" Y exceeding 25%, and 29% seems the maximum consistent with the observations (bearing in mind that some further ^{4}He is produced by the same processes that must be invoked to account for the heavy elements). These limits clearly place stringent constraints on Δg_ν.

Note that this line of argument depends on the idea of an isotropic Friedmann-type "big bang". If much of the helium, or much of the background radiation, were generated out at processes at later epochs (cf. Rees[4]) the conclusion would be strengthened, unless one were prepared to jettison the idea of a "smooth" and homogeneous early universe. Even though there might be alternative mechanisms for producing a 25% cosmic helium in a pregalactic era, there is no feasible way of destroying He. Thus the upper limit of 25% to primordial helium abundance is a firm constraint on the nature of the big bang and the physical constituents of the "primordial fireball".

If there were an excess of ν over $\bar{\nu}$ (or vice versa), then not only is the expansion rate increased, but the neutron/proton equilibrium ratio is shifted, thereby modifying nucleosynthesis[1,5,6]. Consideration of the other light elements that may be relics of the big bang (D, ^{3}He, ^{7}Li) sets further constraints on the baryon density and on neutrino degeneracy[5,6], but are less relevant to other lepton species.

The above arguments would apply to neutrinos of non-zero rest mass, provided that this mass were $\lesssim$ 1 Mev, so that they could be assumed to be present with their thermal density, and behaving like relativistic particles at the epoch of nucleosynthesis. The density of very heavy leptons ($\gtrsim$ 2 Gev) would be greatly reduced because $e^{-mc^2/kT}$ becomes very small while T is still high enough for them to be coupled to other species. This line of argument therefore cannot directly constrain the number of lepton species with mass $\gtrsim$ 3 Gev.

Cosmological considerations of a different kind do, however, set strong limits on the masses of any leptons stable enough to survive to the present day. Such particles (provided their masses were $\lesssim$ 2 Gev) would be about as numerous as the thermal photons in the microwave background - in other words they would outnumber baryons by a factor 10^8-10^9. Dynamical arguments, applied to the deceleration of the whole universe, or the equilibrium of individual clusters or galaxies, can exclude masses between 50 ev and $\sim$2 Gev. Any neutrinos with masses above 2 Gev would be much less abundant than photons (comparable in abundance, perhaps, to the baryons). Such particles could in principle provide "missing mass" in the universe. The possibility of detecting γ-rays arising from annihilation of these particles (and a variety of other constraints on unstable leptons) are reviewed by Gunn et al.[7].

3. SUPERNOVAE

It is in the supernova explosion that terminates the life of (at least some) massive stars that neutrinos play their most crucial astrophysical role. When a stellar core collapses to nuclear densities, the bulk of the resultant neutron star's $\sim 10^{53}$ ergs of binding energy is radiated as a sudden surge of neutrinos. The dynamics of the ejection of supernova envelopes are sensitive to the neutrino opacities within stellar matter. According to Colgate and White's 1966 analysis[8], neutrino diffusion was of prime importance: the neutrinos liberated in the core were able to diffuse outward and deposit their energy and momentum in the less tightly bound outer layers. More recent work[9-13] has suggested that neutrino mean-free paths are short enough to make the behaviour resemble a hydrodynamic bounce, leading to an outward-propagating neutrino shock. Current detailed work on supernova theory takes account of neutrino degeneracy, coherent scattering, neutrino "thermalisation", etc.: the quantitative details of the models may eventually allow sensitive observational tests of weak interaction theory; but at present the astrophysical uncertainties (the nature of the pre-collapse star, the role of rotation and magnetic fields, etc.) are larger still.

Supernovae within our Galaxy occur once every 10-30 years; the neutrino pulse from such an event would be detected by existing detectors. The energy output in 10-50 Mev neutrinos may be $\sim 10^{53}$ ergs; but 10^{52} is a fairly firm lower limit, since this is the flux released by neutronisation of the core material. To detect an event rate exceeding $\sim$ 1 per year, however, one must be able to detect supernovae as far away as the Virgo Cluster of galaxies. To construct a neutrino detector capable of this sensitivity ($\sim 10^9$ tons) seems an even more daunting task than the detection of gravitational waves from the same phenomena.

4. HIGH ENERGY ($\gtrsim$ 10 Gev) NEUTRINOS

The variety of cosmic processes (involving cosmic ray sources, pulsars, galactic nuclei, etc) giving rise to high energy neutrinos ($\gtrsim$ 10 Gev) have been reviewed elsewhere[14]. This is the energy range detectable by a large-

scale instrument such as the proposed DUMAND array. As Schramm[15] has pointed out, a large-scale neutrino detector would be useful also for searching for evidence of proton decay - indeed, attempts to set limits exceeding 10^{31} yrs to the proton lifetime would be bedevilled by the neutrino background from high energy astrophysical processes, and from cosmic ray interactions in the atmosphere.

* * *

REFERENCES

1) R.V. Wagoner, W.A. Fowler and F. Hoyle, Astrophys. J. 148, 3 (1967).

2) V.F. Schwartzman, J.E.T.P. Letters 9, 184 (1969).

3) J. Yang, D.N. Schramm, G. Steigman and R.T. Rood, Astrophys. J. 227, 697 (1979).

4) M.J. Rees, Nature 275, 35 (1978).

5) R.V. Wagoner, Astrophys.J. 179, 343 (1973).

6) H. Reeves in Proceedings of conference on Origin and Early Evolution of Galaxies (W.H. McCrea and M.J. Rees eds). Phil.Trans.Roy.Soc. (in press).

7) J.E. Gunn, B.W. Lee, I. Lerche, D.N. Schramm and G. Steigman, Astrophys. J. 223, 1015 (1978).

8) S.A. Colgate and R.H. White, Astrophys. J. 143, 626 (1966).

9) S.W. Bruenn, W.D. Arnett and D.N. Schramm, Astrophys. J. 213, 213 (1977).

10) W.D. Arnett, Ann.N.Y. Acad. Sci. (in press).

11) D. Kazanas, Astrophys. J. (submitted).

12) D.Z. Freeman, D.N. Schramm and D. Tubbs, Ann. Rev. Nuc. Sci. 27, 37 (1977).

13) H. Bethe, G. Brown, J. Applegate and J. Lattimer, NORDITA preprint (1979).

14) D.N. Schramm, Ann. N. Y. Acad. Sci. (in press).

15) F.W. Stecker, Astrophys. J. 228, 919 (1979).

* * *

DISCUSSION

Chairman: D.H. Perkins

Sci. Secretaries: G. Bonneaud and S.N. Tovey

J.G. Taylor: Are there any recent developments in the search for solar neutrinos?

M. Rees: The latest published results will show that the estimated count rate is about a factor of 2 below the lowest plausible estimates based on stellar models for the sun. There are two uncertainties which are being explored. One concerns the opacities in the solar interior, the other concerns the possibility that one might redo some of the basic experiments on which the cross-sections are based. More important for settling this question will be the proposed Gallivan neutrino experiment, which will be sensitive to neutrinos produced in the basic proton-proton reaction and not the rare chain which produces the high-energy neutrinos to which Davis' experiment is sensitive.

LIFETIME OF CHARMED HADRONS PRODUCED IN NEUTRINO INTERACTIONS

M. Conversi

Istituto di Fisica dell'Università di Roma, Italy

ABSTRACT

Examples of the decay of charmed hadrons produced by high-energy neutrinos in an emulsion hybrid experiment (WA17, CERN) and in a bubble chamber exposure (E546, Fermilab) have been directly observed.

The decay paths of the five charmed candidates found in experiment WA17 (three positively charged and two neutral range from about 50 to 900 μm, giving charmed hadron proper decay times well consistent with the meanlife expected from current theoretical models ($\sim 5 \cdot 10^{-13}$ s). One of the events represents the production of a Λ_c^+ baryon which decays after $(7.3 \pm 0.1) \cdot 10^{-13}$ s to a $pK^-\pi^+$ final state. The identification of the final state is made possible by the combined information from the emulsion and the associated bubble chamber photo (BEBC).

In experiment E546 two neutral and one charged short decays have been detected in the FNAL 15' bubble chamber, in addition to one of undetermined charge. Two of them are interpretable as $D^0 \to e^+K^-\nu_e$ and $D^+ \to e^+K^-\pi^+\nu_e$ decays, yielding decay times consistent with those of the five events found in experiment WA17.

The status of another emulsion hybrid experiment at Fermilab (E553) is also briefly reported.

1. INTRODUCTION

Until recently rather conflicting results have been reported from experiments based on different techniques[1], concerning the lifetime τ_c of charmed particles. Thus, some three years after these new states of hadronic matter were found[2] as predicted by the "GIM mechanism"[3], no conclusive answer could be given to the fundamental question of whether or not the decay rate of charmed hadrons is governed basically by the Fermi weak coupling constant as expected.

The theoretical prediction is that charmed particles all have lifetimes of the same order of magnitude, essentially determined by the rate of the charmed quark β-decay ($c \to s + e^+ + \nu_e$) which is given by the same formula as for μ decay.*) Including first-order gluon effects and a correction for the finite mass of the s-quark the value $\tau_c = 5 \cdot 10^{-13}$ s has recently been reported[4] assuming a mass $m_c = 1.75$ GeV/c^2 for the c-quark as suggested from an analysis of D meson decays.

There is, of course, still a large uncertainty in the estimated value of τ_c, mostly due to the uncertainty in the value of m_c.

My task is to review briefly - in the 20 minutes allocated for my talk - the experimental situation concerning the decay of charmed hadrons produced in neutrino interactions. The review will be based on three contributed papers selected by the Conference Scientific Advisory Committee:

---

*) Then $\tau_c = B_{sl}\,(m_\mu/m_c)^5\tau_\mu$, where B_{sl} = semileptonic inclusive branching ratio; m_μ = muon mass; m_c = mass of the c-quark; τ_μ = muon lifetime.

1) "Estimate of the lifetime of charmed hadrons produced in neutrino interactions" (Abs 26 rev.), by the Ankara-Brussels-CERN-Dublin UC-London UC-Open University-Pisa-Rome-Turin Collaboration - CERN exp. WA17.

2) "Bubble-chamber detection of short-lived particles produced by high energy neutrinos" (Abs 229), by the Berkeley-Fermilab-Hawaii-Seattle-Wisconsin Collaboration - FNAL exp. E-546.

3) "Study of neutrino interactions producing short-lived particles" (Abs 111), by the Cornell-Lund-Pittsburg-Sydney-York University Collaboration - FNAL exp. E-553.

Before presenting these new results I wish to recall that the first likely example of the decay of a charmed hadron produced in neutrino interactions was found in an experiment carried out at Fermilab in 1976[5] using a hybrid technique introduced in 1965.[6]

2. CERN EXPERIMENT WA17

2.1 Apparatus

This experiment uses a combination of emulsion, bubble chamber and counter techniques[7] in an experimental set-up schematically illustrated in Fig. 1.

Large stacks of 600 μm thick pellicles of nuclear emulsion are located in front of the beam entrance window of the Big European Bubble Chamber, BEBC, which is filled with liquid hydrogen and operates in a 35 KG magnetic field.

Tracks of secondary particles from ν-interactions occurring in the emulsion are observed and measured in BEBC to predict the position of the interaction vertices.

A large MWP chamber (D) covering BEBC window allows one to correlate the BEBC and emulsion reference frames. This correlation is achieved by locating in chamber D and in BEBC 2000 passing-through muons. The position of chamber D, and consequently of the emulsion stacks in BEBC frame, could thus be located with an accuracy of 3 mm in the beam direction (x) and 0.3 mm in the transverse directions (y and z).

A veto-coincidence counter system (VCS) coupled to chamber D, provides a time correlation with the "external muon identifier" (EMI) of BEBC. It also provides further information useful in the analysis of the recorded events.

2.2 Exposure

During two runs, 10 and 20 litres respectively of emulsion were exposed to the CERN SPS wide-band neutrino beam, with neutrino energy peaking at ∿ 25 GeV.

A total of 10^{18} protons of energy 350 GeV hit the neutrino target and 206.000 BEBC photos were recorded.

2.3 Event search procedure

BEBC photos are scanned to select event configurations with at least three tracks apparently converging to a point inside the emulsion, at least one of which has to have a momentum larger than 3.5 GeV/c. Selected events are then measured and processed, and their possible vertices in emulsion are predicted with errors by a "vertex program". The errors are typically 9 mm in the x direction and ∿ 1 mm in y and z. "Found ν-events" are

those exhibiting a good matching between tracks seen in emulsion and BEBC*) and no incoming minimum ionization track. For the found ν-events all minimum ionization tracks are followed for 5 mm, to search for "charged decays". The search for "neutral decays" (V^0) is made by scanning in a forward cone of $\pm 30^o$ aperture, 2 mm long.

2.4 Detection losses

The selection criteria just outlined reduce drastically (by a factor $\sim$ 30) the number of BEBC photos to retain for measurement but they introduce a large loss of "good" ν-events: 35-40% for ordinary charged current (c.c.) ν-events, as well as for c.c. events with production of charmed particles.**)

Even larger losses occur at the emulsion level, due to "white starts" (at least 10%), over-all scanning inefficiency including edge effects ($\sim$ 20%), limited "search volume" ($\sim$ 15%), nuclear interactions of hadrons from the ν-vertex ($\simeq$ 10%) and poor quality of emulsion in part of the stacks. Additional losses are expected for the "charmed ν-events" due to the difficulty of observing neutral decays and 1-prong charged decays.

As a consequence, the estimated $\sim$ 700 c.c. ν-interactions which occurred in the emulsion during the exposures should lead to 400-450 good vertex predictions, 160-170 "found c.c. ν-events" and, among the latter, 6 to 7 expected "charmed events".

2.5 Results

To date $\sim$ 90% of the BEBC photos have been fully analysed and about 3/4 of the corresponding vertex predictions have been searched for leading to 150 "found c.c. ν-events", in each of which the μ^- is unambiguously identified by the VCS-EMI system and its momentum determined by BEBC. Among these are the 5 charmed candidates listed in the table.

Event	Short-lived particle				
	Charge	Decay path	Final state	Nature	Decay time[a]
1	+	96 μm	$\begin{cases}\Delta S = \Delta C \\ \geq 4 \text{ body}\end{cases}$	?	$0.5\text{-}1.2 \times 10^{-13}$ s
2	+	354 μm	$pK^-\pi^+$	Λ_c^+ baryon	$7.3\pm0.1 \times 10^{-13}$ s
3	+	906 μm	≥ 4 body	?	$1.6\text{-}5.3 \times 10^{-13}$ s
4	0	54 μm	≥ 3 body	meson	$0.2\text{-}4.2 \times 10^{-13}$ s
5	0	115 μm	≥ 3 body	?	$0.4\text{-}2.5 \times 10^{-13}$ s

a) The two values reported for all events except No. 2 correspond to those obtained from the kinematical two-fold ambiguity mentioned in the text.

*) The requirement is that the differences between azimuth and dip angles of tracks measured in emulsion and those extrapolated from BEBC be smaller than 3^o.

**) These losses are estimated on the basis of data kindly made available for WA17 by a parallel experiment with BEBC (WA21) and, for the "charmed events", by the FNAL 15' bubble chamber exposure of C. Baltay et al. in which 182 $e^+\mu^-$ charm decays were detected.

Three of them - already reported recently elsewhere[8] - have the same general features of the first charm candidate produced in a ν-interaction[5]: the track of a charged particle of minimum ionization, emitted from the ν-interaction occurring at a point A of the emulsion, splits at a point B into three tracks also of minimum ionization. There is no sign of either nuclear excitation or recoil at point B, so that the events are best interpreted in terms of the decay at B of unstable particles produced at A. Indeed the probability that the three new events[8] and the old one[5] are due to nuclear interactions of high energy hadrons presenting the observed decay topology is estimated[8a] to be less than 10^{-7}. The decay paths AB are in the range from $\sim$ 100 to $\sim$ 900 μm, as reported in the table. The matching between tracks observed in emulsion and in BEBC fulfills the requirements mentioned above for virtually all associated tracks of the three new events. Furthermore the charges of the three secondary particles, and therefore that of the primary parents, are determined in the new events by the curvature of the corresponding tracks observed in BEBC. Parents of positive charge are thus found in all cases, as expected from the dominant quark transformation for charmed hadron production in ν_μ interactions ($\nu_\mu + d \to \mu^- + c$).

For two of these three positively charged charmed candidates the over-all information derivable from the apparatus is not sufficient to identify the final state, nor the mass of the decaying particle. There are several decay modes of known charmed hadrons which are kinematically compatible with them, and for each assumed decay mode there is a twofold ambiguity for the momentum, and therefore for the decay time of the parent charmed hadron, as briefly discussed in reference 8a. The third event is instead identified as the decay at B (Fig. 2) of a charmed baryon Λ_c^+ produced at A by a high energy neutrino. The arguments for such an identification can be briefly summarized as follows:

a) The transverse momentum imbalance, as derived from the momenta of the secondary particles measured in BEBC and the angles measured in emulsion, is compatible with zero (46 $\pm$ 28 MeV/c). Hence the event is interpretable as a 3-body decay;

b) One of the two positive secondary particles is identified as a proton by the kinematical analysis of the interaction it undergoes in BEBC (a p-p elastic scattering). Hence the primary particle is a baryon.

c) The negative particle is identified as a K^- meson by combining curvature measurements in BEBC with ionization measurements in emulsion, assuming that the third (positive) secondary particle, which crossed the same emulsion pellicles traversed by the negative particle, is a π^+ meson. Hence the event is most probably due to the production at A of a charmed baryon, Λ_c^+, which undergoes the decay process $\Lambda_c^+ \to pK^-\pi^+$ after travelling a path AB = 354 $\pm$ 3 μm.

The mass*) M_c, momentum p_c, and proper decay time t_c, of the primary baryon can be derived from the momenta measured in BEBC and the decay path AB measured in emulsion. The results are: $M_c = (2.29 \pm 0.015)$ GeV/c^2; $p_c = (3.74 \pm 0.02)$ GeV/c; $t_c = (7.3 \pm 0.1) \cdot 10^{-13}$ s. The invariant mass of the $K^-\pi^+$ system in this event is 0.866 GeV/c^2 suggesting a decay scheme $\Lambda_c^+ \to p\overline{K^*} \to p\pi^+K^-$.

*) The mass value given below does not take into account possible systematic errors. It is somewhat larger, but not inconsistent, with that reported for the few examples[2a)9)] of the Λ_c^+ baryon produced in bubble chamber.

In addition to the three charged charmed candidates mentioned above and reported in more detail elsewhere[8], two neutral candidates have been found. One of them, (event no. 5) found in the course of the search for c.c. ν-interactions, can be interpreted as the production at a point A of the emulsion of a neutral short-lived particle which, after travelling a path AB = 115 ± 3 μm, decays at B into two charged secondaries ("V^0"). The line AB makes an angle of 6^0 with the V^0 plane, indicating that if the event is indeed due to a neutral decay, at least one neutral particle has to be present among the decay products. Unfortunately, since no fully satisfactory correlation with a BEBC picture has been established as yet, the analysis of this event relies, for the moment, only on what is seen in emulsion. The opening angle of the V^0 is 20^0. The two charged secondaries, followed up to the edge of the stack, have $p\beta$ values of 1.15 ± 0.25 and 1.75 ± 0.45 GeV/c, as derived from multiple scattering measurements. The V^0 particle cannot be due to a $\Lambda^0 \to p\pi^-$ decay since the π^- momentum should then be smaller than 0.32 GeV/c. Even though it is consistent with a $K^0_s \to \pi^+\pi^-$ decay, the probability of a random coincidence of a K^0_s decay with a neutral induced interaction is negligible. In fact no other example of V^0 decay was found in the scan under high magnification of 500 mm^3 of emulsion.

The other neutral charmed candidate (Fig. 3) has similar features, with a decay path AB = 54 ± 3 μm and an opening angle of the V^0 of 23^0. Although there is good correlation with the BEBC photo used to predict its vertex, the analysis of this event has to be based again only on what is observed in the emulsion, since neither of the two tracks from the V^0 decay reaches BEBC sensitive volume.*) Multiple scattering measurements made on the $\sim$ 3 cm available track lengths yield $p\beta$ values of $\sim$ 0.9 ± 0.2 and $\sim$ 0.2 ± 0.02 for the two charged secondary particles, V_1 and V_2 respectively.

The magnetic field is strong enough over the stack region to allow significant curvature measurements, by which it is concluded that V_1 is a negative particle and V_2 a positive one. Furthermore, accurate ionization measurements on both tracks, and differential $p\beta$ measurements on the V_2 track which traverses $\sim$ 1 radiation length, lead to mass assignments which make V_1 compatible with being only an e^-, a μ^- or a K^- meson, and V_2 with either a μ^+ or a π^+ meson.

The line of flight of the V^0, derived from the vector momenta of particles V_1 and V_2, of which angles of emission and $p\beta$ values are known, is 12 ± 2 μm off the primary vertex A. Hence at least a neutral particle has to be present among the decay products of the V^0 in order to balance the momenta. A few Cabibbo-favoured decay modes of the D^0-meson are found to be compatible with the event ($D^0 \to \pi^+\pi^-K^0$, $\pi^+K^-\pi^0$, $\mu^+K^-\nu_\mu$...). For each decay mode there is, however, a kinematical ambiguity which leads to two values of the momentum, and therefore of the decay time of the parent particle. These decay times are within the interval 0.3-4 x 10^{-13} s.

*) This is because one of the two secondary tracks (V_2, see below) has a low momentum ($\sim$ 200 MeV/c) and the other (V_1) is emitted with $\sim$ 900 MeV/c momentum at a large angle with respect to the direction of the ν-beam.

3. FNAL EXPERIMENT E-546

This is a pure bubble chamber experiment in which short-lived decays of dilepton events have been detected in neutrino interactions of the highest energies. The results are based on an exposure of the Fermilab 15' bubble chamber (3.4×10^{18} p on target, 326,000 photos) to the quadruple triplet neutrino beam for which the average ν-event energy is as large as $\sim$ 90 GeV.

Careful examination of a sample of 89 high-energy ν-induced dilepton events, out of $\sim$ 12,000 charged current events, has led to the observation of the production and semi-leptonic decay of 4 charmed candidates, of which one is positively charged, two are neutral and one is of undetermined electric charge. The decay paths are reported to be between about 6 and 9 mm, measured with a 15%-20% error.

The charged candidate is consistent with the hypothesis $D^+ \to e^+ K^- \pi^+ \nu_e$ (not with $\Lambda_c^+ \to pK^- e^+ \nu_e$); the two neutral candidates are consistent with $D^0 \to e^+ K^- \nu_e$. One of them, shown in Fig. 4, is not consistent with a K^0 decay. The charge of the remaining candidate is uncertain because the e^+ emerges from a tight jet. The event is reported to be again consistent with a D decay (not with a K^0 decay).

The estimated total background (largest contribution comes from asymmetric γ conversion with a low energy, undetectable e^-, and the random overlay of a negative hadron) is less than 0.14 neutral and less than 0.11 charged events.

Using the charged event and one of the two neutrals,*) an estimate of the decay times is obtained from a likelihood method based on the remaining 85 dilepton events for which no decay vertex is seen. The decay times for these two events are $(2.5 \,^{+\,3.5}_{-\,1.5}) \cdot 10^{-13}$ s for the D^+ and $(3.5 \,^{+\,3.5}_{-\,1.5}) \cdot 10^{-13}$ s for the D^0.

4. FNAL EXPERIMENT E553

This again uses a hybrid emulsion technique. The track sensitive target consists of 14 litres of Kodak NTB3 emulsion, exposed as horizontal pellicles, 600 μm thick, stacked in two separate slabs, each 2 cm along the beam direction. Spark chambers with aluminized glass electrodes, placed immediately downstream of each stack, allow one to find the vertices of the ν-events by extrapolation from measured positions of the spark-evaporated holes in the electrodes. Further downstream there is first a magnetic spectrometer and then a track-sensitive "plastic flash calorimeter"[10], which detects and separates in general electromagnetic and hadronic showers, and identifies passing-through muons. Two examples of dimuon events detected in this calorimeter are shown in Fig. 5.

The apparatus just outlined was exposed to the Fermilab broad band horn ν-beam early this year and more than 200 ν-events are expected to have occurred in the emulsion. To date several ν-events have been located in the emulsion, but no example of a charmed hadron candidate has been found. The analysis is in progress.

---

*) The other neutral event occurred in a region of liquid turbulence.

5. CONCLUSIONS

With the inclusion of the first candidate observed in a previous experiment[5] there is now a sample of 8 charmed hadron candidates produced in neutrino interactions which decay with lifetimes all well consistent with expectations based on current theoretical ideas. The sample includes a charmed baryon[8b] (a Λ_c^+) for which decay mode, mass and lifetime have all been determined. Thus the last of the most important open questions about charm particle physics seems to be settled.

REFERENCES

1) a) K. Niu: Proc. XIX Intern. Conf. on High Energy Physics (ICHEP), Tokyo 1978, p. 371, also for references to previous emulsion works; M.M. Chernyavski et al.: Lebedev Phys. Institute, preprint no. 149 (1978); N. Ushida et al.: Lett. Nuovo Cimento 23, 577 (1978).

b) D.S. Baranov et al.: Phys. Lett. 70B, 269 (1977); Proc. Topical Conf. on Neutrino Physics, Oxford 1978, p. 167; A. Blondel: ibid p. 217.

c) G. Diabrini-Palazzi: Proc. ICHEP, Tokyo 1978, p. 297.

2) a) E.G. Cazzoli et al.: Phys. Rev. Lett. 34, 1125 (1975);

b) G. Goldhaber et al.: Phys. Rev. Lett. 37, 225 (1976).

3) S.L. Glashow, J. Iliopoulos and L. Maiani: Phys. Rev. D2, 1285 (1970).

4) N. Cabibbo, G. Corbo and K. Maiani: Nuclear Physics (in press).

5) E.H.S. Burhop et al.: Phys. Lett. 65B, 299 (1976);
A.L. Read et al.: Phys. Rev. D19, 1287 (1979).

6) E.H.S. Burhop et al.: Nuovo Cimento 39, 1037 (1965).

7) M. Conversi: CERN NP Int. Rep. 75-17 (28 Nov. 1975).

8) a) A. Angelini et al.: Phys. Lett. 80B, 428 (1979).

b) A. Angelini et al.: Phys. Lett. 84B, 150 (1979).

9) B.Knapp et al.: Phys. Rev. Lett. 37, 882 (1976);
A.M. Cnops et al.: Phys. Rev. Lett. 42, 197 (1979).

10) L. Federici et al.: Nucl. Instr. and Meth. 151 (1978) 103, also for previous references.
F.E. Taylor et al.: Proc. IEEE Nuclear Science Symp., San Francisco (19-21 October 1977).

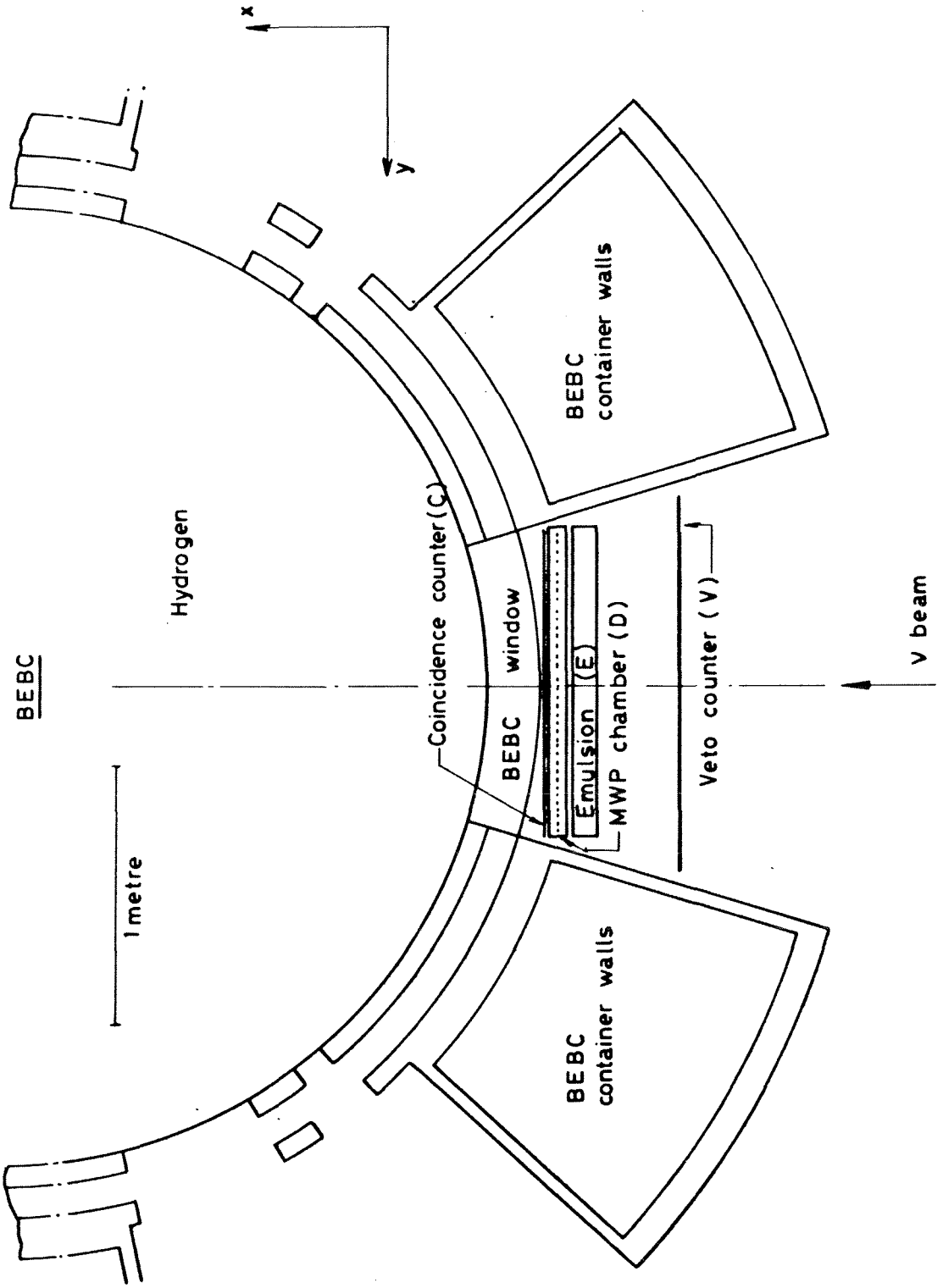

Fig. 1 The experimental set-up of CERN SPS experiment WA17

a) Event No. 2 as seen in the emulsion

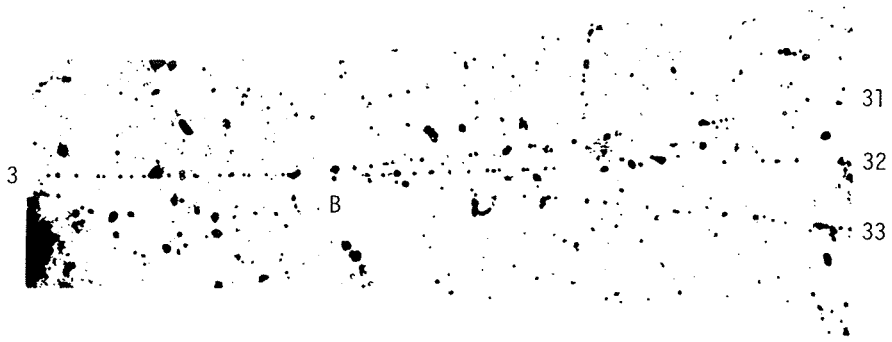

b) The decay of the identified Λ_c^+ baryon at point B, as seen under high magnification

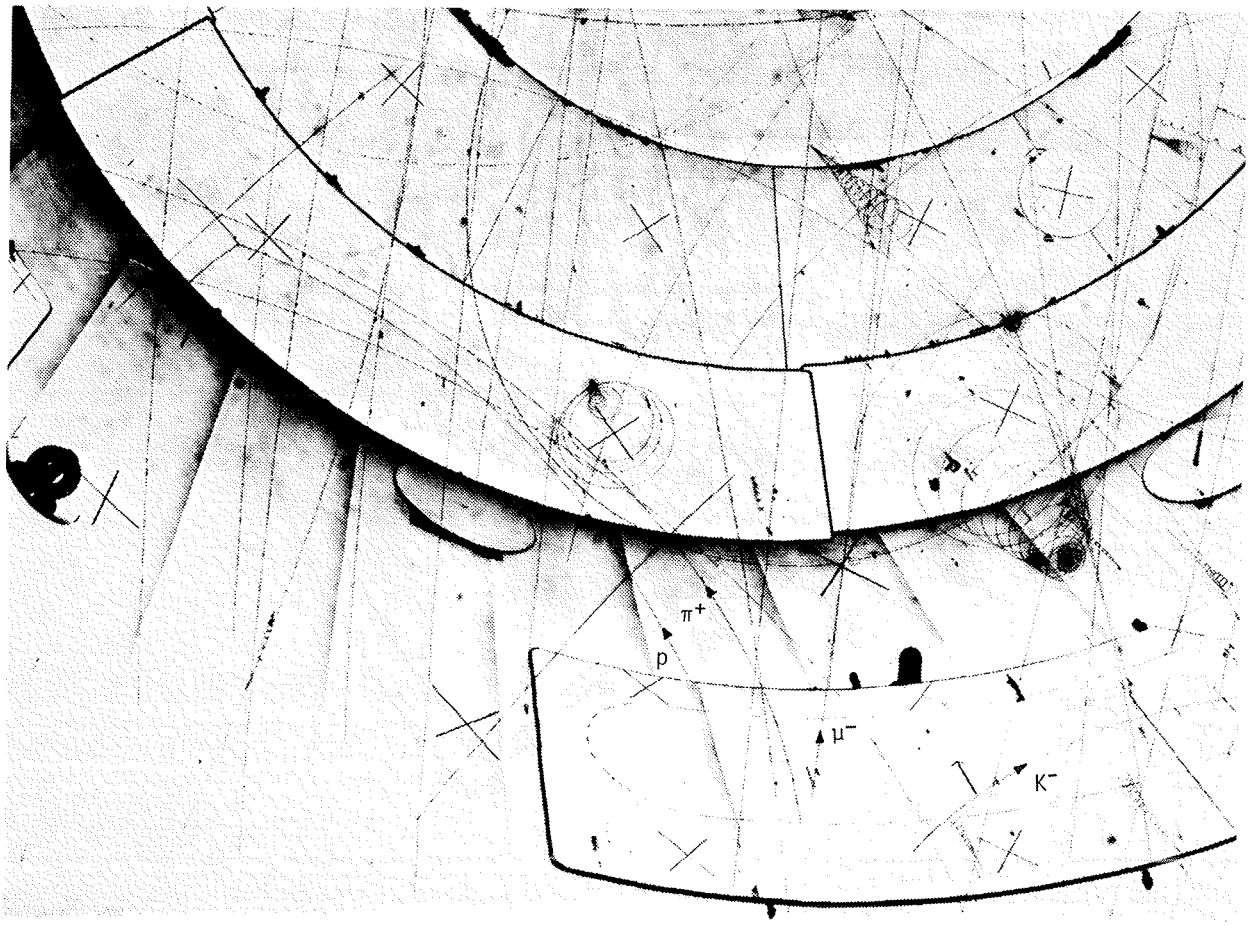

c) Event No. 2 as seen in BEBC

Fig. 2

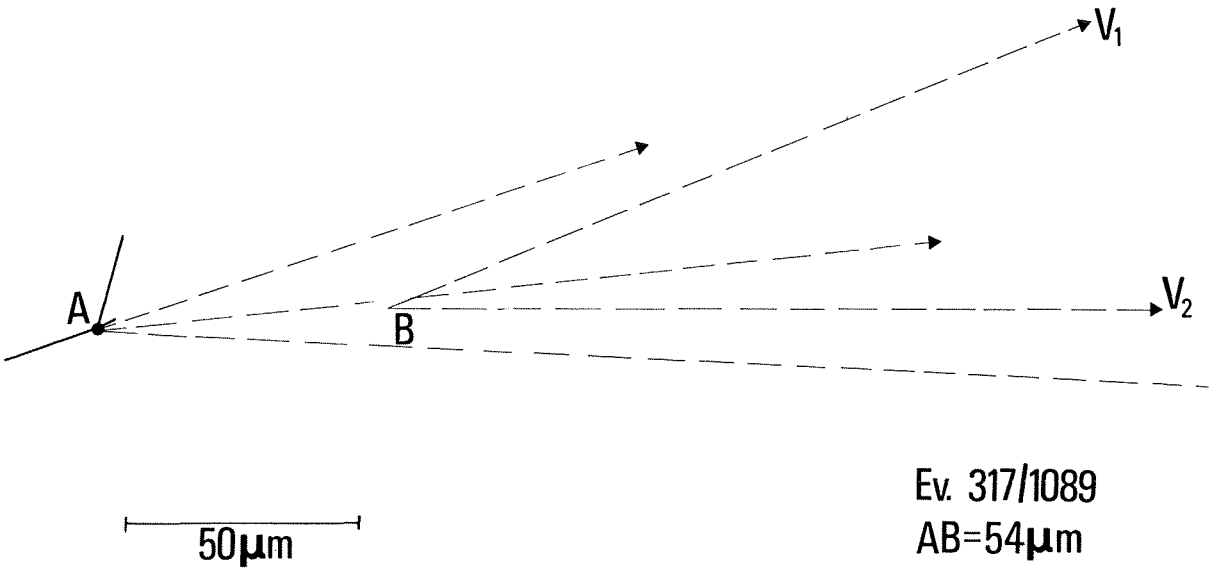

Fig. 3 Sketch of a probable example of ν-induced production and decay of a neutral charmed particle in emulsion (event No. 4). One of the tracks emerging from point A is well correlated with that of a negative muon seen in BEBC and identified by the EMI of BEBC.

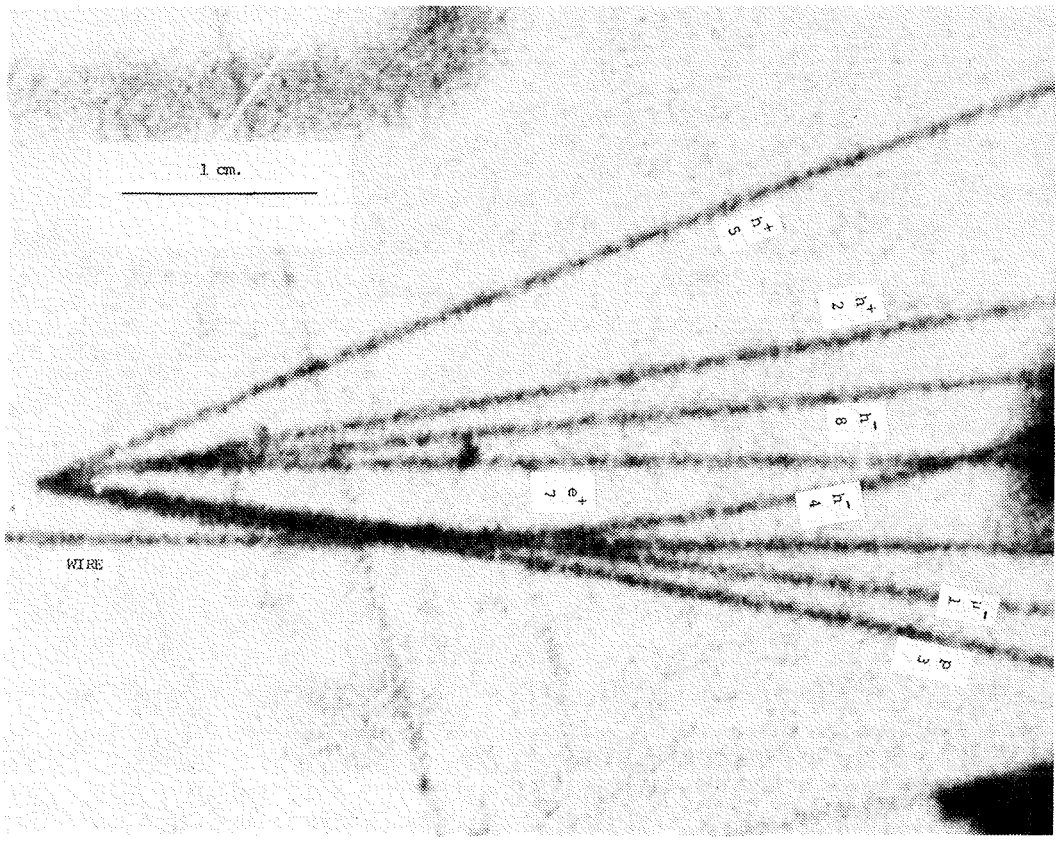

Fig. 4 Probable example of ν-induced production and decay of a neutral charmed particle in the 15' Fermilab bubble chamber (FNAL experiment E246)

Fig. 5 Two examples of dimuon events recorded in the large plastic flash chamber calorimeter of FNAL experiment 553. The two electromagnetic showers which can be seen on the left of the top photo possibly originate from a π^0 meson decay.

FRAGMENTATION FUNCTIONS IN NEUTRINO HYDROGEN INTERACTIONS

Aachen-Bonn-CERN-München (MPI)-Oxford Collaboration

J. Blietschau, J. Grässler, W. Krenz, D. Lanske, R. Schulte and H.H Seyfert
III. Physikalisches Institut der Technischen Hochschule, Aachen, Germany.

K. Böckmann, C. Geich-Gimbel, H. Heilmann, T. Kokott, B. Nellen and R. Pech
Physikalisches Institut der Universität Bonn, Bonn, Germany.

L. Bacci, P. Bosetti[1], D.C. Cundy, A. Grant, P.O. Hulth, D.R.O. Morrison, R. Orava[2], L. Pape, Ch. Peyrou, H. Saarikko[3], W.G. Scott, E. Simopoulou[4], A. Vayaki[4] and H. Wachsmuth
CERN, European Organisation for Nuclear Research, Geneva, Switzerland.

M. Aderholz, N. Schmitz, R. Settles, K.L. Wernhard and W. Wittek
Max-Planck-Institut für Physik und Astrophysik, München, Germany.

R. Giles, P. Grossmann, R. McGow, G. Myatt, D.H. Perkins, D. Radojicic, P. Renton and B. Saitta
Department of Nuclear Physics, Oxford, U.K.

presented by N. Schmitz

ABSTRACT

The fragmentation of the u-quark is studied in the reaction $\nu_\mu p \to \mu^- h^\pm$ + anything. It is found that the single particle inclusive cross section does not factorize. Scaling deviations are observed in the fragmentation functions and are found to be in agreement with the leading order QCD prediction.

In this paper we report on a study of the distribution in fractional energy (z distributions) of secondary hadrons in charged current neutrino interactions in BEBC filled with hydrogen and exposed to a wideband horn-focussed neutrino beam from the CERN SPS. The data sample consists of 5,600 charged current events with muons of $p_\mu > 3$ GeV/c identified in a two-plane External Muon Identifier. The average neutrino energy of the events is 40 GeV.

For each secondary hadron $h^\pm$ in the semi-inclusive reaction

$$\nu_\mu p \to \mu^- h^\pm X \qquad (1)$$

we define the energy fraction z carried by the hadron as $z = E_h/E_H$, where E_h is the laboratory energy of the hadron and E_H that of all secondary hadrons including the correction for unobserved neutral particles. The z distribution for positive or negative hadrons $h^\pm$ is given by the single particle inclusive cross section divided by the total inclusive cross section:

---

1) CERN fellow from III. Physikalisches Institut der Technischen Hochschule, Aachen

2) Now at Fermilab

3) CERN visitor from University of Helsinki

4) Now at Demokritos, Athens

$$D^{\pm}(z,q^2) = \frac{d\sigma^{h^{\pm}}_{incl}(x,q^2,z)}{dx\, dq^2\, dz} \Big/ \frac{d\sigma(x,q^2)}{dx\, dq^2} \qquad (2)$$

The m-th moment of this distribution is defined as

$$D^{\pm}(m,q^2) = \int_0^1 z^{m-1}\, D^{\pm}(z,q^2)\, dz. \qquad (3)$$

Fig. 1a shows $D^{\pm}(z,q^2)$ for low and high q^2 for those hadrons which travel forward in the overall hadronic center-of-mass system ($x_F > 0$). The latter selection (which is applied throughout this paper) is made in order to reduce contributions from target fragments so that according to the naive quark-parton model for reaction (1) $D^{\pm}(z,q^2)$ may be interpreted as the fragmentation function of the u-quark (contributions from sea quarks are neglected in this analysis). All values of W, the effective mass of the hadronic system, are included in Fig. 1a. For both positive and negative hadrons a significant q^2 dependence of $D^{\pm}(z,q^2)$ is observed, the distributions becoming narrower with increasing q^2.

In the naive quark-parton model the single particle inclusive cross section factorizes, which means that $D^{\pm}(z,q^2)$ as defined in (2) is independent of $x = q^2/(2M\nu)$. To test this hypothesis we have plotted in Fig. 1b $D^{+}(m = 3,q^2)$ versus x as an example for three different intervals of q^2. One observes indeed that at high q^2 the fragmentation moment is independent of x; however at smaller q^2 $D^{+}(3,q^2)$ increases significantly with x implying non-factorization in this q^2 region.

It is suggestive to test whether the observed scaling violation is consistent with the prediction of leading order QCD. The prediction for the q^2 evolution of non-singlet fragmentation moments is[1)]

$$D^{NS}(m,q^2) = c_m \cdot \ln\left(\frac{q^2}{\Lambda^2}\right)^{-d_m^{NS}} \qquad (4)$$

where c_m are unknown constants, d_m^{NS} are the anomalous dimensions and Λ is the scale parameter of the theory. Experimentally a non-singlet combination is obtained by taking the difference of $D^{+}(m,q^2)$ and $D^{-}(m,q^2)$. This follows from charge conjugation invariance and with the assumption that the z distributions in (2) are the fragmentation functions of a u-quark:

$$D_u^{NS}(m,q^2) = D_u^{+}(m,q^2) - D_{\bar{u}}^{+}(m,q^2) = D_u^{+}(m,q^2) - D_u^{-}(m,q^2) \qquad (5)$$

This formula is valid irrespective of the nature of the hadron ($\pi^{\pm}$,$K^{\pm}$,$p/\bar{p}$). Fig. 2 shows $D_u^{NS}(m,q^2)$ for m = 2 to 7 and for all W together with the result (solid lines) of a global fit (i.e. for all m simultaneously) of equation (4) to the data in the region $q^2 > 1$ GeV^2. The data are well reproduced by the QCD formula yielding a value for Λ of $\Lambda = (0.54 \pm 0.08)$ GeV.

It should be pointed out, that the observed q^2 dependence in Fig. 2 is associated with the region of small W values; for W > 4 GeV no q^2 dependence is found.

According to (4) two non-singlet moments of order m_1 and m_2 when plotted against each other on a log-log scale are expected to fall on a straight line with slope $d^{NS}_{m_2}/d^{NS}_{m_1}$. Fig. 3 shows plots of (D^+-D^-) and (for comparison) (D^++D^-) for $m_2 = 6$, $m_1 = 4$ and $m_2 = 7$, $m_1 = 3$. In all cases the plots can be fitted by straight lines with experimental slopes as indicated. The slopes of the non-singlet moments (D^+-D^-) are in good agreement with the QCD prediction; the combinations (D^++D^-) on the other hand give substantially bigger slopes.

In conclusion, both Figs. 2 and 3 show surprising agreement of the measured non-singlet moments with the QCD prediction. This agreement may however be coincidental since the q^2 dependence is observed only if small values of W are included.

. . .

REFERENCES

1) J.F. Owens, Phys. Lett. 76B, 85 (1978); T. Uematsu, Phys. Lett. 79B, 97 (1978).

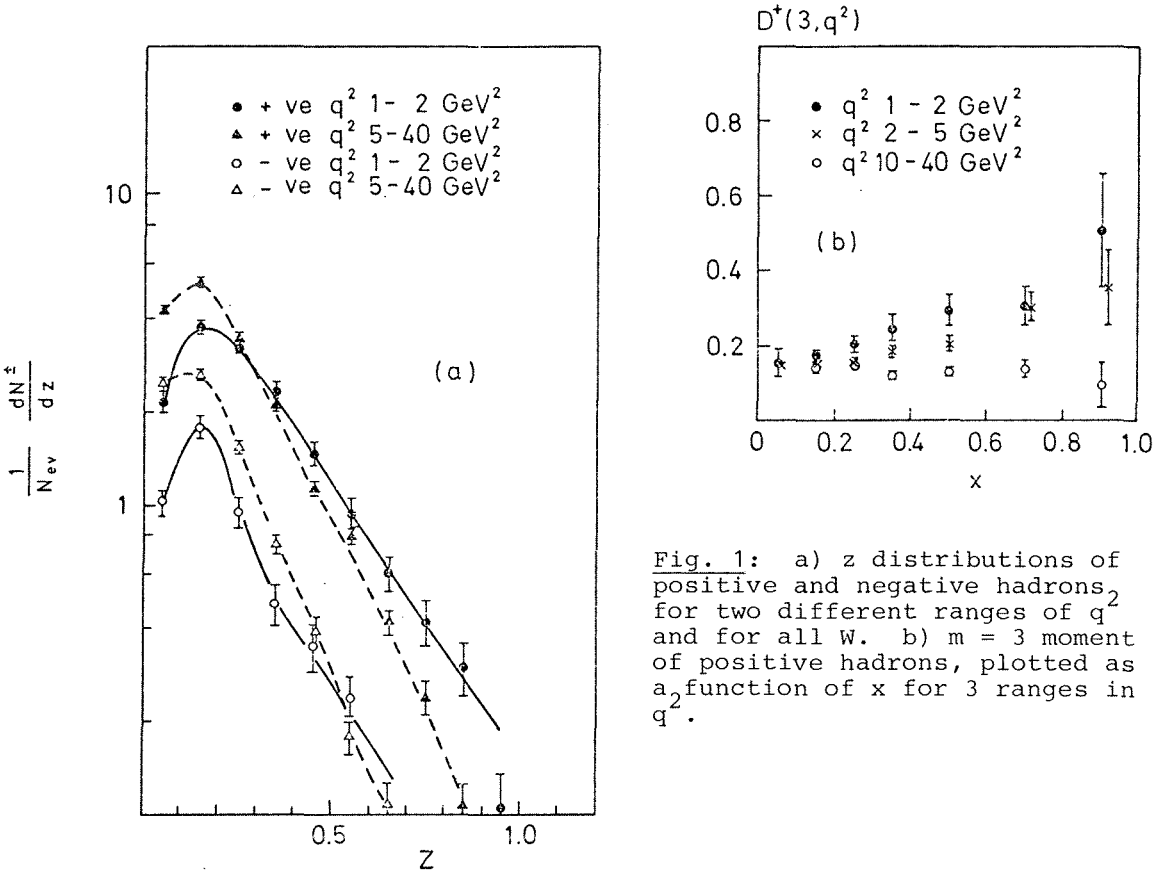

Fig. 1: a) z distributions of positive and negative hadrons for two different ranges of q^2 and for all W. b) m = 3 moment of positive hadrons, plotted as a function of x for 3 ranges in q^2.

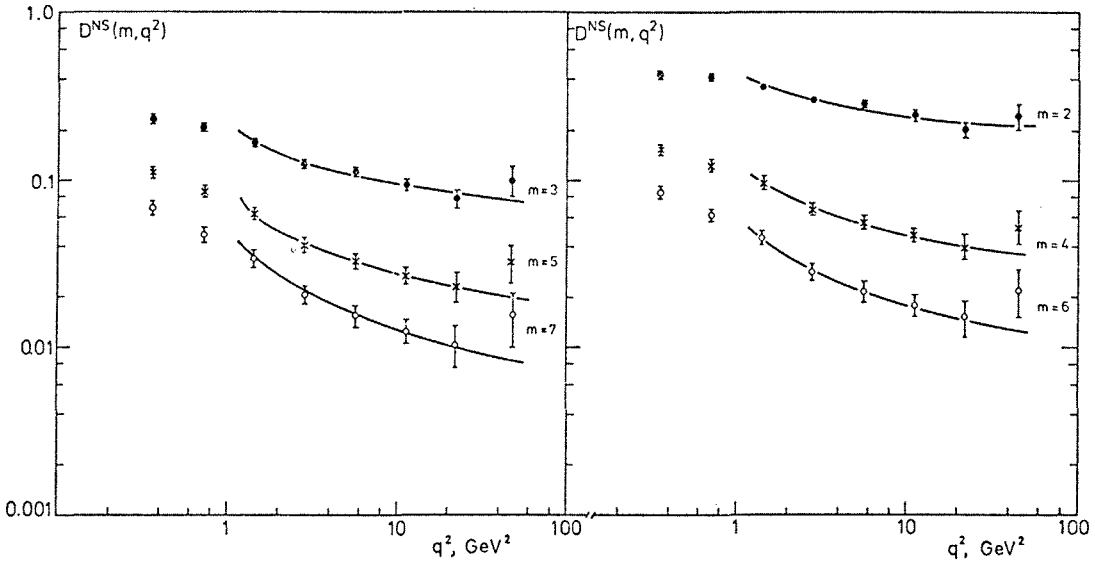

Fig. 2: Moments of the non-singlet combination $D^{NS}(m,q^2) = D^+(m,q^2) - D^-(m,q^2)$ plotted against q^2 for all W. The curves show the results of a fit to the logarithmic dependence predicted by leading order QCD.

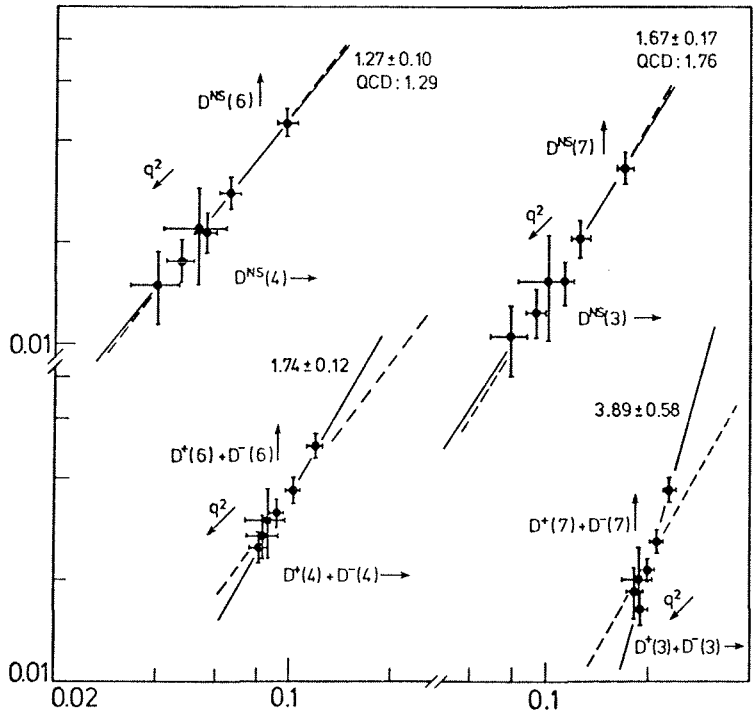

Fig. 3: Logarithmic plots of $m_= 6$ versus m = 4 and m = 7 versus m = 3 moments for $q^2 > 1$ GeV^2 and for the hadron combinations (D^+-D^-) and (D^++D^-). The full lines show the fitted slopes while the broken lines show those predicted for D^{NS} by leading order QCD.

MEASUREMENT OF THE RATIO OF NEUTRAL TO CHARGED CURRENT CROSS SECTIONS OF NEUTRINO INTERACTIONS IN HYDROGEN

Aachen-Bonn-CERN-Munich-Oxford Collaboration

presented by

L. Pape
CERN, European Organization for Nuclear Research, Geneva, Switzerland

1. INTRODUCTION

We present a measurement of the ratio R_p of Neutral Current (NC) to harged urrent (CC) cross sections from neutrino interactions or protons. Similar measurements exist for the interactions of ν and $\bar{\nu}$ on isoscalar targets [1,2], from which the magnitude of the left- and right-handed couplings of the neutral current to quarks have been determined [3]. But, because of of the isospin symmetry of the target, the contributions of the up and down quarks to the couplings cannot be separated. Used together with the measurement of NC/CC on protons, the magnitude of the couplings to u and d quarks can be determined separately. However, the only published measurement of neutrinos on protons $R_p = 0.48 \pm 0.17$ [4] does not reach the precision required to put significant constraints on the couplings. In the present experiment, we determine R_p to a precision which is better than 10%.

2. EXPERIMENTAL CONDITIONS

The experiment was carried out in the CERN SPS wideband neutrino beam, obtained from 350 GeV protons. A total of about 285 000 pictures were taken in the bubble chamber BEBC filled with hydrogen. The pictures were double-scanned for events with ≥ 3 charged tracks. The chamber was equipped with a two-plane External Muon Identifier (EMI) [5]. The subsample used for this analysis consists of 2750 events with an EMI identified muon with $p_\mu > 3$ GeV/c (CC events) and 3900 events where no muon is detected (NC candidates), both with measured hadronic energy $E_H \geq 5$ GeV and in a fiducial volume of 18 m^3 corresponding to ~ 1 t of H_2.

3. SELECTION OF NEUTRAL CURRENT EVENTS

The sample of events without a detected muon contains, in addition to the real neutral current events, a considerable number of background events. The main sources contributing to this background are: (a) CC events where the muon is not identified because of the limited EMI geometrical acceptance; from a Monte-Carlo simulation it is estimated that the geometrical acceptance is 98% for $p_\mu > 10$ GeV/c, but that it decreases rapidly for smaller p_μ and is essentially zero below 3 GeV/c. The corresponding contamination in the NC candidates is approximately 70% of the true number of NC events. (b) Interactions in the liquid produced by incoming neutral hadrons (K^0's and neutrons) originating from neutrino interactions in the material in front of the chamber. A Monte-Carlo program was used to simulate the production of the neutral hadrons in the material surrounding the bubble chamber, to follow their cascade and to determine the number of neutral hadron interactions in the bubble chamber. The contamination from neutral hadron interactions was found to be approximately 40% of the true number of NC events.

The uncertainties in these corrections are large, and do not allow to reach the accuracy mentioned above. An efficient way of reducing this background is to select events with large transverse momentum p_T^H of the hadronic system with respect to the neutrino beam direction. This is illustrated by the examples given in fig. 1, and can qualitatively be understood as follows: as the neutrals are in general not detected in this experiment, p_T^H corresponds, in the case of true CC or NC events (fig. 1(a)), to $\sim 2/3$ of the true hadronic p_T (or the p_T of the muon). When the muon is not identified and hence counted with the hadrons, p_T^H measures the unbalance in p_T, which is $\sim 1/3$ of the true hadronic p_T. Fig. 1(b) shows that the p_T^H of misclassified CC events is indeed about half of the p_T^H of the identified events. Finally, the total hadronic p_T is shared by several hadrons, which have each a small p_T component with respect to the direction of the hadronic system. It is therefore expected that the p_T of any individual hadron, with respect to the neutrino direction, is on the average small compared to the total hadronic p_T. This is supported by the p_T distribution of V^0's, given in fig. 1(c). In conclusion, the events coming from the main sources of background in the NC candicates are concentrated in the region of small p_T^H.

4. NEUTRAL CURRENT TO CHARGED CURRENT RATIO

The raw ratio R_p for events with p_T^H, greater than a given value p_T^{MIN} is shown as a function of p_T^{MIN} in fig. 2. The fast drop of the ratio as p_T^{MIN} increases reflects the presence of contaminations in the NC sample, together with the loss of CC events due to inefficiencies in muon identification. In addition to the two dominant corrections discussed above, corrections have been applied for:

- The "electronic" inefficiency of the EMI and accidental association of hadrons to hits on the EMI due to background.
- Background due to $\bar{\nu}_\mu$, $\bar{\nu}_e$ and ν_e events.
- One-prong events, which are not recorded at the scanning.
- The value of the hadronic p_T^H is determined from the measured particles only, hence the contribution due to neutral hadrons is in general missing. A calibration of the measured p_T^H was obtained from CC events by comparing p_T^H to the p_T^μ of the muon. It was found that the measured p_T^H corresponds on average to 0.8 of p_T, with a spread of 0.3. The calibration of p_T^H in NC events could be different if the p_T carried by neutral hadrons were different in NC and CC events. From a Monte-Carlo calculation differences in the π^0 and neutron production are estimated to lead to a systematic loss of $\sim$ 4% of the NC events.

The NC to CC ratio R_p, after all corrections have been applied, is shown in fig. 2 as a function of p_T^{MIN}. The value of p_T^{MIN} which makes the systematic errors due to uncertainties in the correction procedure about equal to the statistical errors corresponds to 1.5 GeV/c (measured transverse momentum). It can be clearly seen that the corrections are drastically reduced by the cut in p_T. The best estimate of R_p is therefore

$$R_p = 0.52 \pm 0.04 \text{ for } p_T^H > 1.5 \ (1.9) \text{ GeV/c} , \qquad (1)$$

where the statistical and the systematic errors each contribute ± 0.03. The cut $p_T^H > 1.5$ GeV/c measured p_T corresponds to a cut on the true $p_T^H > 1.9$ GeV/c. As seen from fig. 2, the value of R_p is not very sensitive to the exact value of p_T used.

5. STRUCTURE OF THE NEUTRAL CURRENT

The analysis of the inclusive scattering of ν and $\bar{\nu}$ on isoscalar targets has given an accurate measurement of the left and right-handed couplings of neutral currents. The chiral couplings, as used in the analysis of Sehgal [3], are u_L, u_R, d_L, d_R, where u and d refer to the up and down quarks and L and R refer to left- and right-handed couplings respectively. The ABCLOS Collaboration [2] used the ratios of total cross sections to determine the combinations $(u_L^2 + d_L^2)$ and $(u_R^2 + d_R^2)$ and their best estimate is

$$u_L^2 + d_L^2 = 0.32 \pm 0.03 , \ u_R^2 + d_R^2 = 0.04 \pm 0.03 . \qquad (2)$$

The coupling constants u_L^2 and d_L^2 can be determined individually by combining the above result with the NC to CC cross section ratio on protons.

In the quark parton model the differential cross sections for ν-proton inclusive scattering are

$$\frac{d^2\sigma}{dxdy}(CC) = \frac{2G^2ME}{\pi} x\left[(d_V + d_S + s_S) + (u_S + c_S)(1 - y)^2\right]$$

$$\frac{d^2\sigma}{dxdy}(NC) = \frac{2G^2ME}{\pi} x\left\{u_V\left[u_L^2 + u_R(1 - y)^2\right] + d_V\left[d_L^2 + d_R(1 - y)^2\right]\right. \quad (3)$$
$$\left. + \left[(u_S + c_S)(u_L^2 + u_R^2) + (d_S + s_S)(d_L^2 + d_R^2)\right]\left[1 + (1 - y)^2\right]\right\}$$

where u_V, u_S, d_V and d_S are the quark density distributions for u and d valence or sea quarks, s_S (c_S) are the density distribution of strange (charmed) quarks, these quark densities being functions of x and Q^2 [6]. In the above expression, it has been assumed that the sea quark and anti-quark density distributions are identical and that the couplings are the same for quarks with the same charge.

Integrating the differential cross sections over x and y gives for the ratio R_p of NC to CC total cross sections

$$R_p = f_1\, u_L^2 + f_2\, d_L^2 + f_3\, u_R^2 + f_4\, d_R^2, \quad (4)$$

where the f_i are ratios of integrals over the known quark density distributions.

For the evaluation of the integrals f_i, we have used the Q^2 dependent parametrization of the quark density distributions proposed by Buras and Gaemers [7], with a non SU(3) symmetric contribution of strange quarks in order to reproduce the dimuon production in ν and $\bar{\nu}$ interactions [8]. The quark density distributions were used as input in a Monte-Carlo program which takes into account the energy distribution of the neutrino wideband beam and the effect of the cut on p_T^H. The values obtained for the integrals f_i with a cut $p_T^H > 1.5$ GeV/c and $E_H > 5$ GeV are:

$$f_1 = 2.1 \qquad f_2 = 1.0 \qquad f_3 = 0.70 \qquad f_4 = 0.36\ . \quad (5)$$

These values are not sensitive to the detailed shape of the beam, the neutrino energy entering only via the Q^2 dependence of the quark density functions. This dependence is known to be small and it is partially absorbed as the f_i are ratios of quark densities.

Using the above value of $u_R^2 + d_R^2$ and the values for f_3 and f_4, the right-handed contribution R_p^{RH} to the NC/CC ratio R_p is bound to lie inside the limits $R_p^{RH} = 0.03 \pm 0.02$ and $R_p^{RH} = 0.02 \pm 0.01$ corresponding to $d_R = 0$ and $u_R = 0$ respectively. As this difference is small compared to the errors of the experiment, we have assumed that $R_p^{RH} = 0.025 \pm 0.02$. Taking the value of $u_L^2 + d_L^2$ from eq. (2) and the estimate of eq. (1) for R_p, we get

$$u_L^2 = 0.15 \pm 0.05$$

$$d_L^2 = 0.16 \pm 0.07.$$

Fig. 3 displays the constraints on u_L^2 and d_L^2 coming from the measurement on isoscalar targets and from this experiment. It also shows that the results agree with the standard SU(2) × U(1) model [9]. The value of $\sin^2\theta_W$ determined from the R_p value obtained in this experiment is

$$\sin^2\theta_W = 0.18 \pm 0.03$$

in good agreement with other determinations.

* * * *

REFERENCES

[1] J. Blietschau et al., Nucl. Phys. B118 (1977) 218;
P. Wanderer et al., Phys. Rev. D17 (1978) 1679;
F. Merrit et al., Phys. Rev. D17 (1978) 2199;
M. Holder et al., Phys. Lett. 71B (1977) 222, Phys. Lett. 72B (1977) 254.

[2] P.C. Bosetti et al., Phys. Lett. 76B (1978) 505.

[3] L.M. Sehgal, Phys. Lett. 71B (1977) 99 and Aachen preprint PITHA 102 (1978) whose notation we followed here.

[4] F. Harris et al., Phys. Rev. Lett. 39 (1977) 437.

[5] R. Beuselinck et al., Nucl. Inst. and Meth. 154 (1978) 445.

[6] P.C. Bosetti et al., Nucl. Phys. B142 (1978) 1.

[7] A.J. Buras and K.J.F. Gaemers, Nucl. Phys. B132 (1978) 249 and Phys. Lett. 71B (1977) 106.

[8] M. Holder et al., Phys. Lett. 72B (1977) 254.

[9] S. Weinberg, Phys. Lett. 19 (1967) 1264;
A. Salam, Proceedings of the 8th Nobel Symposium, ed. N. Svartholm, Stockholm (1978);
S.G. Glashow, J. Iliopoulos and L. Maiani, Phys. Rev. D2 (1970) 1285.

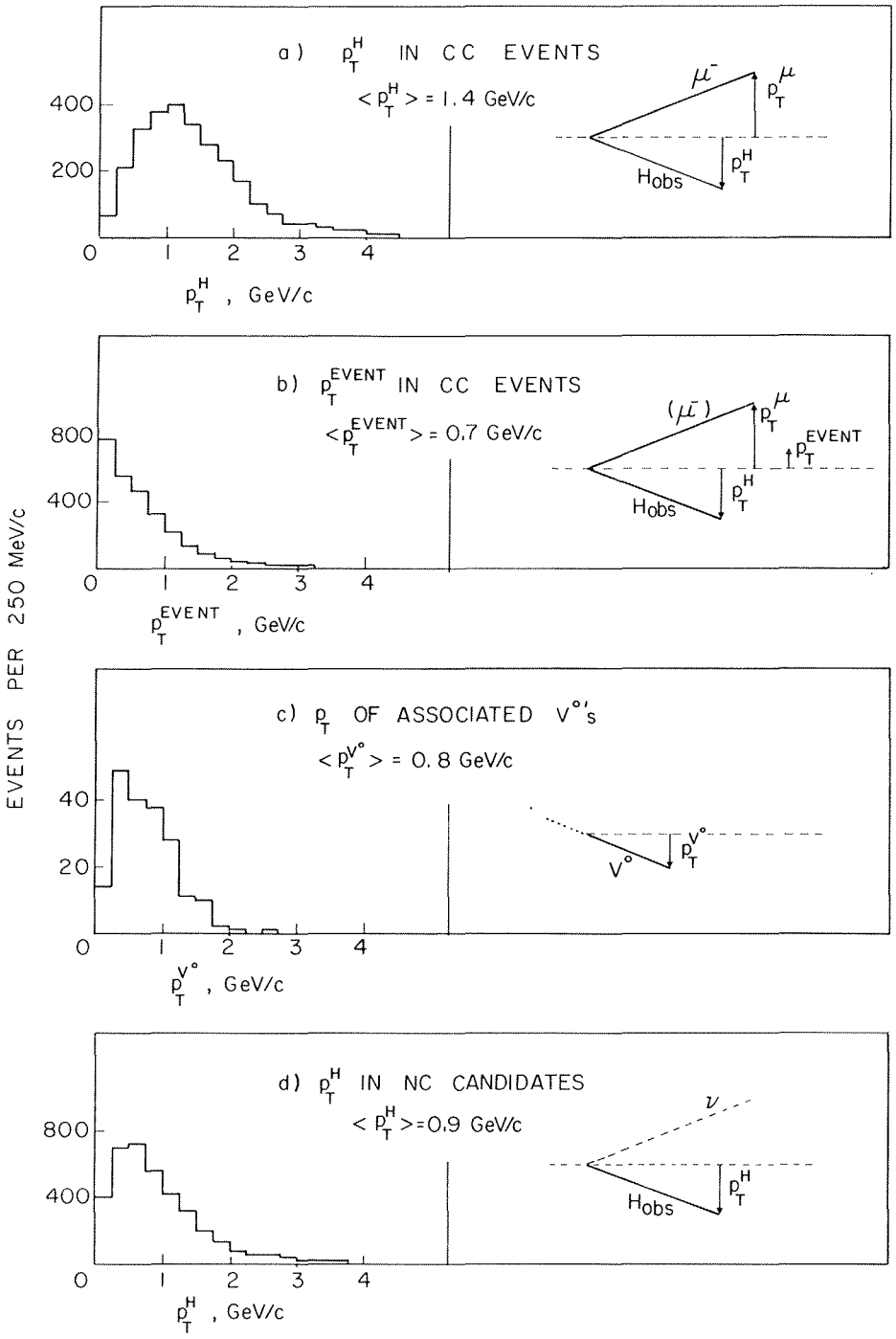

Fig. 1

Event distributions as functions of the transverse momentum p_T with respect to the ν-direction:

(a) the p_T of the detected hadronic system p_T^H in CC events;

(b) the p_T of all tracks, including the muons, in CC events;

(c) the p_T of neutral hadrons, obtained from V^0's associated to neutrino interactions;

(d) the p_T of the detected hadrons p_T^H in NC candidates, including background.

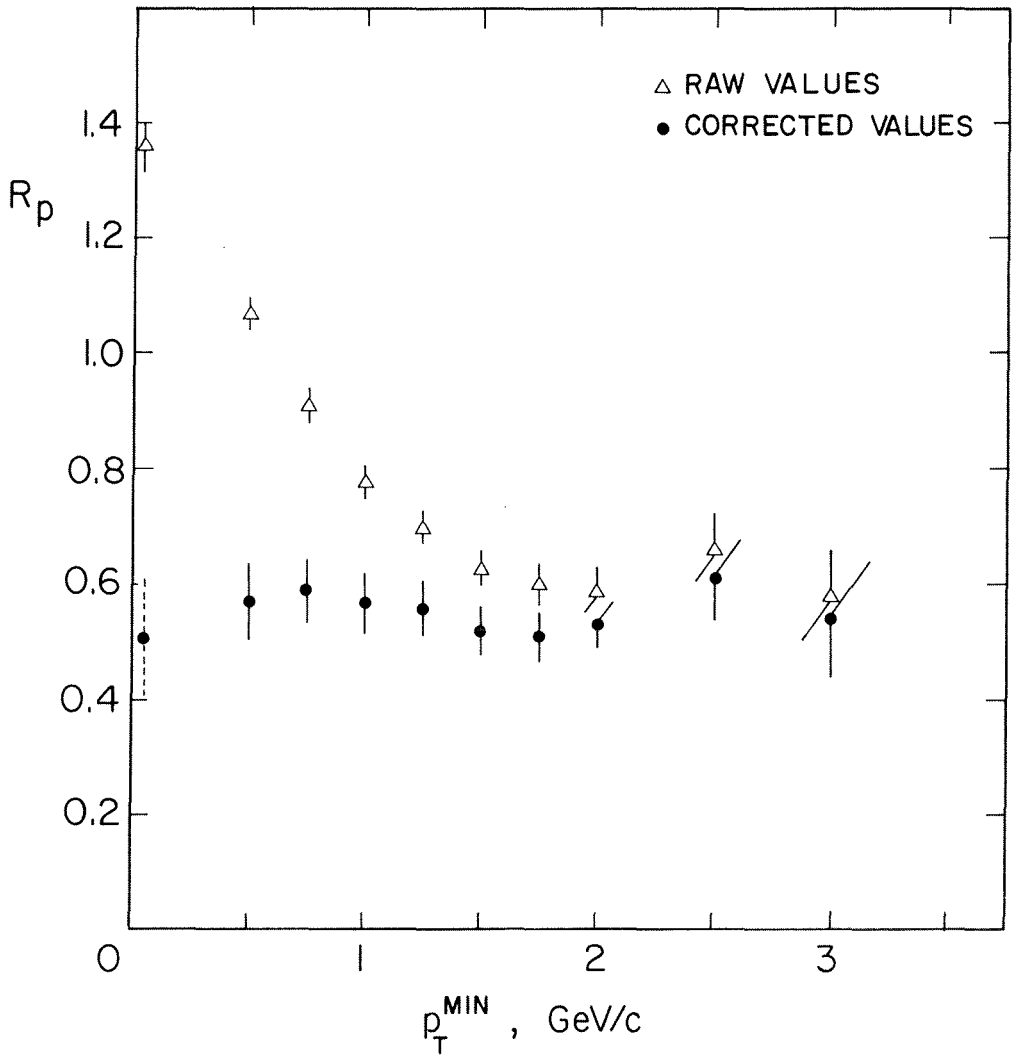

Fig. 2

Ratio R_p of NC to CC events with p_T^H above a given p_T^{MIN} and plotted as a function of p_T^{MIN}. Only events with $E_H \geq 5$ GeV are included. The values of R_p are displayed before corrections (Δ) and after all corrections have been applied (dots).

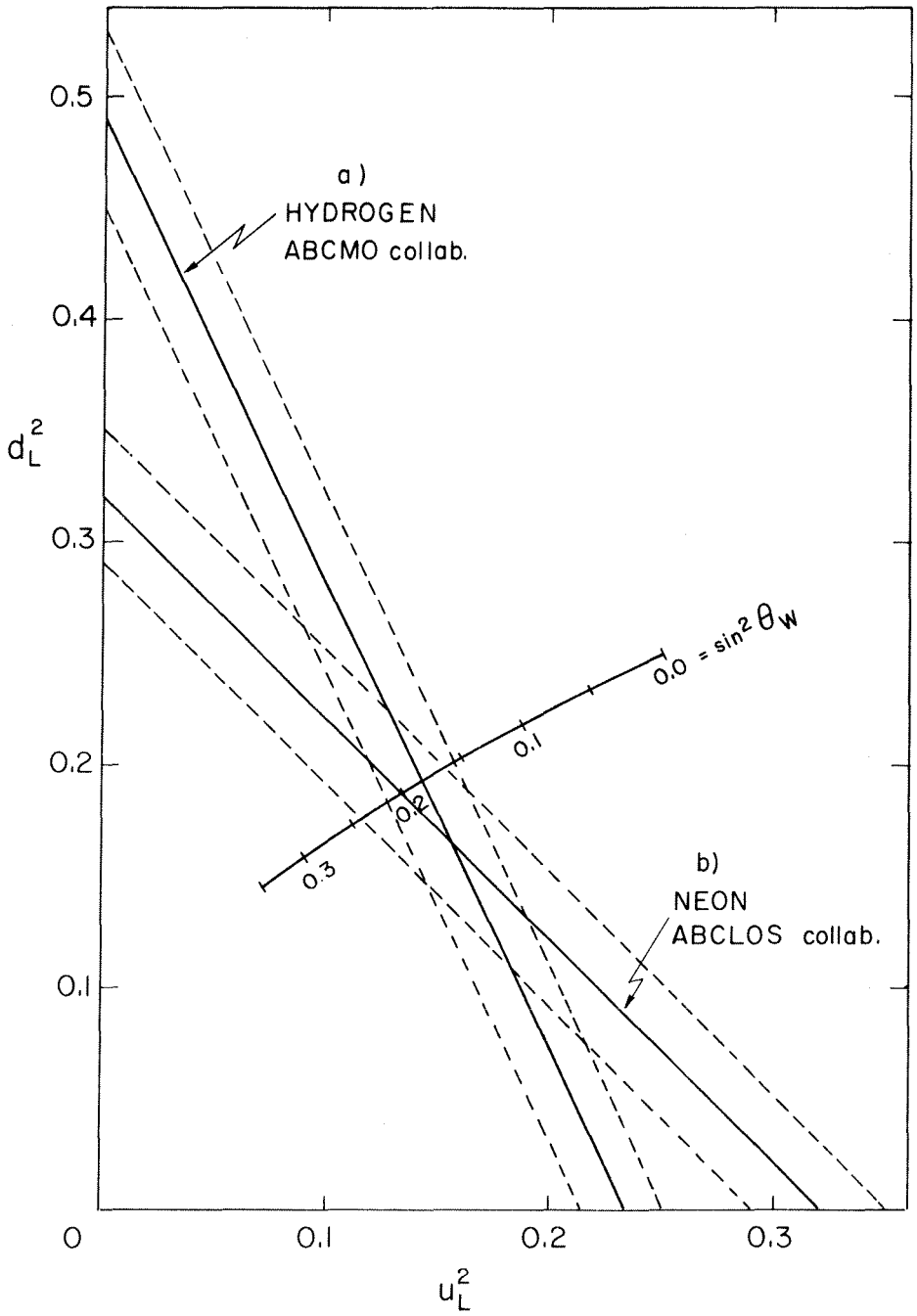

Fig. 3

The relations between the coupling constants u_L^2 and d_L^2 obtained from isoscalar data (line a) [2] and from νp interactions in this experiment (line b). The errors indicated by dotted lines correspond to 1 standard deviation. Also shown is the prediction of the standard SU(2) × U(1) model as a function of the single parameter $\sin^2\theta_W$ (curve c).

FLUX NORMALIZED CHARGED CURRENT NEUTRINO CROSS SECTIONS UP TO NEUTRINO ENERGIES OF 260 GeV*

B. Barish, R. Blair, J. Lee, P. Linsay, J. Ludwig, R. Messner, F. Sciulli and M. Shaevitz
California Institute of Technology, Pasadena, California 91125, USA.

F. Bartlett, D. Edwards, H. Edwards, E. Fisk, G. Krafczyk, Y. Fukushima, Q. Kerns, T. Kondo, D. Nease, S. Segler and D. Theriot
Fermi National Accelerator Lab, Batavia, Illinois 60510, USA.

A. Bodek and W. Marsh
University of Rochester, Rochester, New York 14627, USA.

O. Fackler and K. Jenkins
Rockefeller University, New York, New York 10021, USA.

ABSTRACT

Preliminary measurements of flux normalized charged current neutrino cross sections are presented. From a sample of 6000 neutrino events with energies between 50 and 260 GeV we find that

$$\sigma_\nu/E_\nu = (0.67 \pm 0.04) \times 10^{-38}\ \mathrm{cm}^2/\mathrm{GeV}$$

independent of neutrino energy.

INTRODUCTION

The simplest model which describes deep inelastic neutrino scattering well is the quark-parton model. It predicts that the cross section should rise linearly with the incident neutrino energy. The simple scaling may be modified at low energies by the quark mass and transverse momentum corrections. The effects of gluon Bremsstrahlung, as calculated from QCD, lead to logarithmic deviations from scaling. At high energies there are propagator effects due to the mass of the W boson. Thus a measurement of the total neutrino cross section from the lowest to the highest possible energy provides us with important information on our current understanding of the nucleon and its interactions.

We present here the first measurement of the charged current neutrino total cross section up to an energy of 260 GeV.

BEAM AND APPARATUS

The measurements that are described here were made with a new narrow band neutrino beam and a new neutrino detector at Fermilab.

The new narrow band beam is designed to minimize wide band background and has a narrow momentum bite and small angular divergence in order to produce a neutrino energy spectrum as close as possible to the ideal flat distribution of two body π and K decay. The characteristics of this new beam are listed in Table I. The present data were taken with the secondary beam energy set to 200 and 300 GeV respectively.

The secondary particles (π/K) decayed in a 340m long evacuated pipe which began just downstream of the last beam magnet. They were monitored at the expansion port located about 100m downstream of this last magnet. The total particle intensity was measured by an ion chamber. The particle ratios π/K/p were measured by an integrating differential Cerenkov counter.

* Work supported in part by the U.S. Department of Energy under Contract No. DE-AC-03-79ER0068 for the San Francisco Operations Office.

Table I

Beam Parameters

Incident Proton Energy	400 GeV/c
Target Material	BeO
Incident Spot Size	2 x 0.5mm^2
Targeting Angles	
Horizontal:	11.96mr
Vertical:	1.125mr
Momentum Bite	±9%
Angular Divergence	
Horizontal:	±0.15mr
Vertical:	±0.18mr
Secondary Energy	100 - 300 GeV

Particle ratios are listed in Table II for different mean pion momentum.

Table II

Polarity	Pπ [GeV/c]	K/π	P/π
+	198 ± 18	0.15 ± 0.009	3.94 ± 0.08
+	289 ± 26	0.25 ± 0.012	36.8 ± 0.7

The new separated function neutrino detector located downstream of a 910m muon shield is shown in Figure 1. The upstream portion is a 680 ton instrumented iron target followed by a 420 ton muon spectrometer. The entire detector has been moved into a hadron beam for calibration.

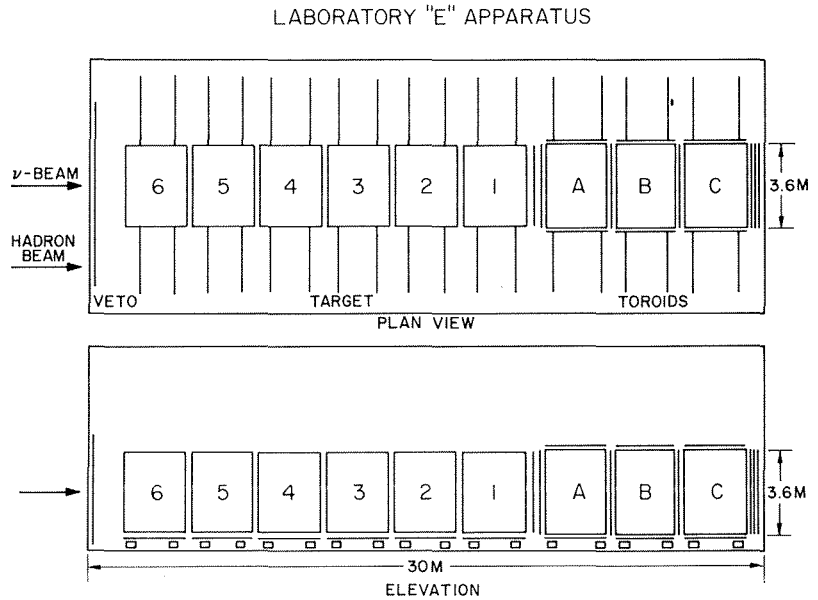

Fig. 1 Counter ν-experiment of the CFRR-Group at Fermilab

The iron target is instrumented with liquid scintillation counters for calorimetry and with spark chambers to track muons. The muon spectrometer is a magnetized iron toroid instrumented with acrylic scintillation counters to measure hadron energy and with spark chambers to track muons. A complete description is given in Table III. The calorimetric response was empirically determined from measurements made in a hadron beam.

Table III

Lab E Neutrino Detector

Target/Calorimeter	
Dimensions	3m x 3m x 20m
Weight	680 tons: Fe
Counters	10cm spacing
Hadron Energy Resolution	$\Delta E/E = 0.93/\sqrt{E[GeV]}$
Spark Chambers	20cm spacing
Angular Resolution	$\Delta\theta_\mu[mrad] = 0.30 + \frac{68}{p_\mu[GeV/c]}$
Muon Spectrometer/Calorimeter	
Dimensions	3.4m dia. x 10m
Weight	420 tons
Counters	20cm spacing
Hadron Energy Resolution	$\Delta E/E = 1.85/\sqrt{E[GeV]}$
Spark Chambers	80cm spacing
Muon Momentum Resolution	$\Delta p/p = 10\%$

ANALYSIS

The results presented here are based on 6000 charged neutrino interactions found in a cylindrical fiducial volume 1.27m in radius and 13.2m long. For each event the hadron energy was corrected for the measured attenuation in the scintillation counters and the muon energy was corrected for the energy loss in iron. In addition, a model independent azimuthal geometric efficiency was calculated for each event.

A correction was also made to account for the unsampled region of acceptance at very large x and y. This loss is less than 10% for low ν energies and decreases to about 2% for high energies.

The calculation of the neutrino cross section is quite straightforward with a dichromatic beam. The events in any given radial bin on the target may be divided into high energy neutrinos from K decay and low energy neutrinos from π decay due to the nature of the beam. The neutrino flux into each radial bin from each type of decay is readily calculated from the measured composition and properties of the beam and two body kinematics. As an example, Figure 2 shows the measured high energy neutrino distribution in the radial bin from 0 to 50cm compared with the predictions of a Monte Carlo which simulates the beam. The measured energies are based on calibrations done in the hadron beam. The means of these distributions differ by less than 1%.

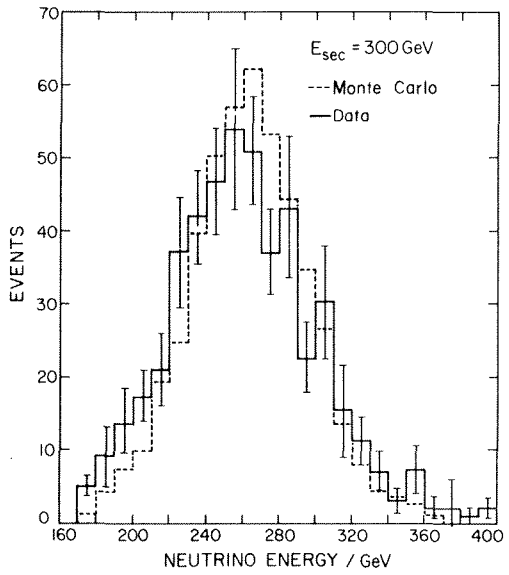

Fig. 2 Comparison of ν-energy distribution obtained from data and Monte Carlo

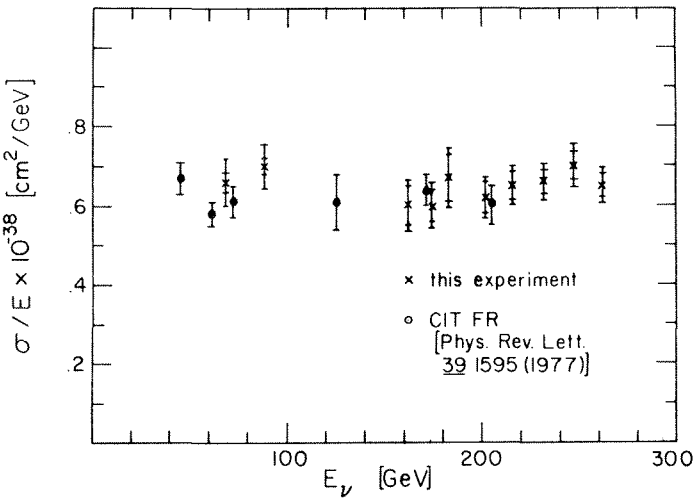

Fig. 3 Total cross section divided by the ν-energy for charged current events plotted against neutrino energy

The cross section divided by the energy is shown in Figure 3. These results have been corrected for a minimum muon energy of 2.4 GeV and empirically determined wide band background. The overall result is

$$\frac{\sigma}{E} = (0.67 \pm 0.04) \times 10^{-38} \text{ cm}^2/\text{GeV}.$$

A previous result is also shown for comparison. There is no indication in the total cross-section data at the present level of experimental precision for any deviation from exact scaling up to neutrino energies of 260 GeV.

RESULTS FROM GARGAMELLE NEUTRINO EXPERIMENT AT CERN SPS

WA14 Collaboration - Bari,CERN,Ecole Polytechnique, Milan, Orsay

Presented by M. Rollier

Istituto di Fisica dell'Università and INFN Milan, Italy

ABSTRACT

Three results are presented: a) from the study of 117 neutrino induced dimuons events a production rate of $\sigma(\mu^+\mu^-)/\sigma(\mu^-)=(0.72 \pm 0.14)\cdot 10^{-2}$ has been measured. The $\mu^+\mu^-$ channel is found to be dominated by D-meson production and decay. b) the inverse muon decay reaction is observed for the first time with a clear signal of 26 ± 6 events in good agreement with predictions from standard V-A theory. c) results with the complete statistics are presented for the pure leptonic neutral current reaction ($\nu_\mu e^- \to \nu_\mu e^-$). The measured cross section is now in agreement with other experiments and with the predictions from the standard SU(2)×U(1) model.

1. INTRODUCTION

Results will be presented on these three topics:

i) study of dimuons production from neutrinos ($\nu_\mu N \to \mu^+\mu^- X$)

ii) observation of the inverse muon decay ($\nu_\mu e^- \to \mu^-\nu_e$)

iii) measurement of the production cross section for the purely leptonic reaction: ($\nu_\mu e^- \to \nu_\mu e^-$)

2. EXPERIMENTAL APPARATUS

The heavy liquid bubble chamber Gargamelle (∿4 m^3 fiducial volume), filled with a propane freon mixture (90% C_3H_8 and 10% CF_3Br in moles, 61 cm radiation length and 0.51 g/cm^3 density) has been exposed to the CERN-SPS wide band neutrino beam using a total of $2.3\cdot 10^{18}$ protons on the target. The chamber was operated with a set of counters[1] all around the chamber (Fig.1) which allows the muon identification and also the scanning of selected topologies. Upstream the first plane of MWPC (veto counter) eliminate the incoming particles, downstream the "picket fence" selects the exact time of each interaction in the chamber. The EMI (two MWPC planes separated by 160 cm of iron) identifies the outgoing muons.

Our experiment using this hybrid technique offers the advantages of an efficient selection of rare events, and at the same time, the possibility to study all the details of the interactions.

3. DIMUONS

From the counter data candidates for the reaction:

$$\nu_\mu + N \to \mu\mu X \qquad (1)$$

have been selected requiring:

- no particle in the veto
- at least one particle in the "picket fence"
- two possible muons coming from GGM and crossing the two EMI planes in the same time slot defined in the picket fence.

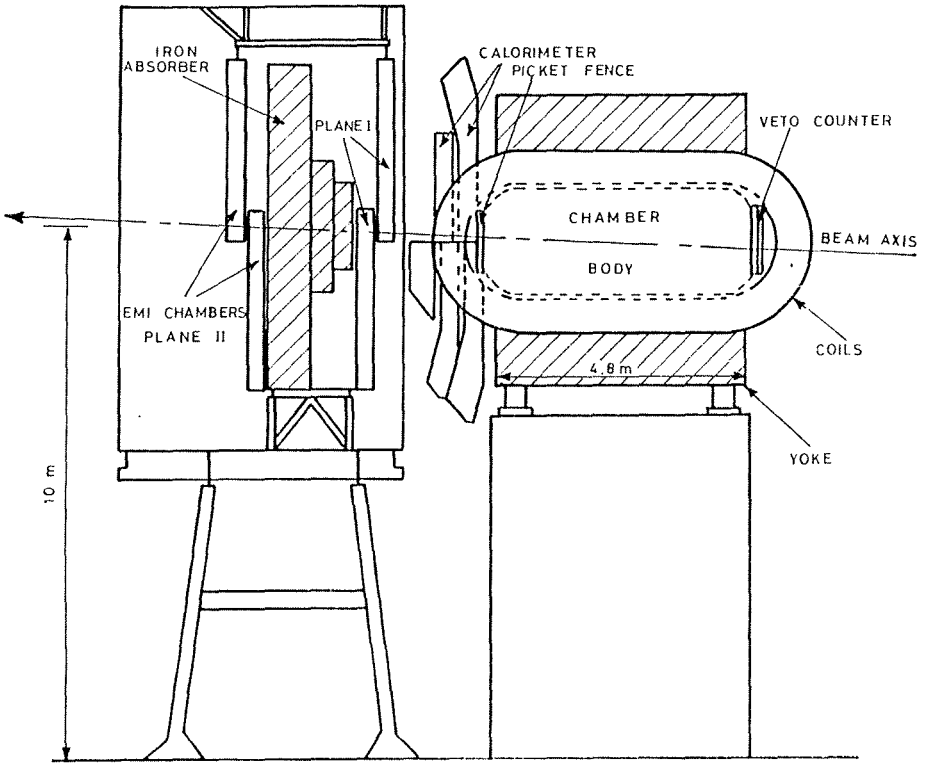

Fig.1 Experimental apparatus with counters around GGM.

All events selected by these criteria have been carefully analyzed and the possible candidates measured. All muon tracks are described in terms of a χ^2 of association with the nearest hit in each EMI plane.

Events were retained as dimuons candidates when at least two tracks had a χ^2 less than 40. Results are presented in Table I for 420.000 pictures corresponding to 39.000 CC events obtained with $2.3 \cdot 10^{18}$ protons on the target.

	$\mu^- \mu^+$	$\mu^- \mu^-$
events $\chi^2 < 40$	117	41
after cut at $\chi^2 < 10$	94	25
Background		
π decay in flight	24.2 ± 2	14.5 ± 1
K decay in flight	3.9 ± 1	2.5 ± 1
Punch through + random association	4 ± 2	3 ± 2
Total background	32.1 ± 3	20 ± 2.5
SIGNAL	62 ± 10	5 ± 6

TABLE 1: Summary of background calculations

The background comes from the following sources:

- B1 - decay in flight of π's and K's.
- B2 - punch through of an hadron which can reach with its shower the second EMI plane.
- B3 - association of random hits in the EMI.

A cut at $\chi^2=10$ eliminate most of the background B2 and B3 and background B1 can be computed by Montecarlo.

We conclude from Table I that no significant signal of $\mu^-\mu^-$ is observed, but a signal of $\mu^+\mu^-$ is clearly present.

Dimuons events ($\mu^+\mu^-$) are currently interpreted as being due to the production of charmed particles and their semileptonic decay:

If this hypothesis is correct we expect: high V^0 production and missing energy due to the undetected neutrino.

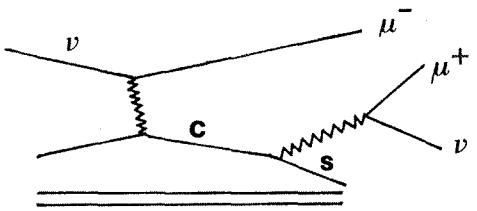

In the 94 $\mu^+\mu^-$ events there are 9 K^0s and 3Λ^0. If we take into account our detection efficiencies (0.25 ± 0.02 for K^0s and 0.48 ± 0.03 for Λ^0) and we correct for background the rates are:

$$0.53^{+0.25}_{-0.20}\ K^0 \text{ per dimuon event} \qquad 0.03^{+0.06}_{-0.04}\ \Lambda^0 \text{ per dimuon event}$$

showing no evidence for Λ^0 production.

As all $K^0\mu^+$ masses are compatible with the decay of the highest known charmed meson D, we conclude that our sample is probably dominated by D production. At our energies the production of charmed barions is desfavoured by our acceptance which requires high energy μ^+.

The missing energy due to undetected neutrals can be estimated [2] from the transverse momentum balance, and the best and almost unbiased measure of the fraction of the total hadronic energy actually measured is given by:

$$f = \frac{P_\perp(h)}{P_\perp(\mu^-)}$$

where $P_\perp(h)$ is the transverse momentum of hadrons projected on the $\nu\mu$ plane and $P_\perp(\mu^-)$ the transverse momentum of the negative muon.

In Fig.2 this function f is shown for our $\mu^+\mu^-$ sample (signal) and for the $\mu^-\mu^-$ sample (background). Clearly the signal has a lower mean value of f. If we interpret this to be due to the missing energy of the undetected neutrino, we can estimate the mean fraction $\langle Z_\nu \rangle$ of hadronic energy carried by the neutrino:

$$\langle Z_\nu \rangle = 0.25 \pm 0.09$$

Assuming the $\mu^+\mu^-$ sample to be due to D production and subsequent leptonic decay, we can compare the experimental inclusive properties of our events with the predictions of a standard quark parton model [3]. Assuming from e^+e^- data [4] the branching ratios for the

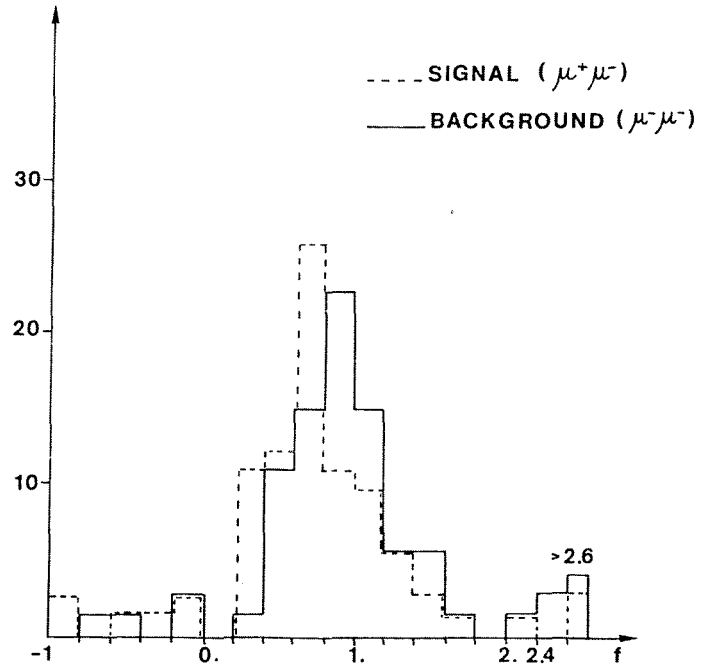

Fig.2 Fraction of hadronic energy actually measured for signal events ($\mu^+\mu^-$) and background events ($\mu^-\mu^-$)

decay modes $D \to K\mu\nu$ and $D \to K\pi\mu\nu$ to be 0.4 and 0.6 respectively, we see that the most sensitive parameter in the model is the "parton fermentation function" $D(Z_D)$ where Z_D is the fraction of the hadronic energy carried by the D meson.

With a Z_D dependence of the type e^{+bZ_D} we can fit the b parameter from same experimental distributions (Z_μ, y, E_{vis}). In Fig. 3 the expected distributions for Z_{μ^+} for different values of the b parameter is compared with experimental data. The best estimate for b is $b=1.25^{+1.1}_{-0.75}$ and as shown in Fig.4 negative b values, as found for usual hadrons, seems to be excluded by our data.

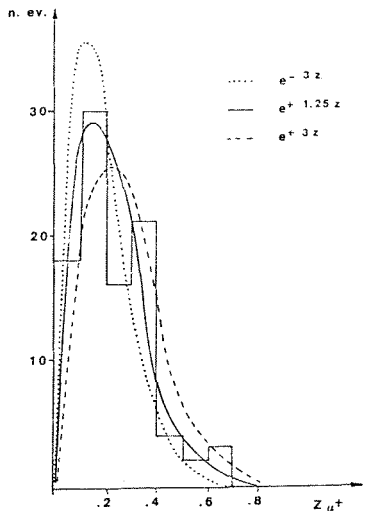

Fig.3 Distribution of $Z_{\mu^+} = P_{\mu^+}/E_H$.

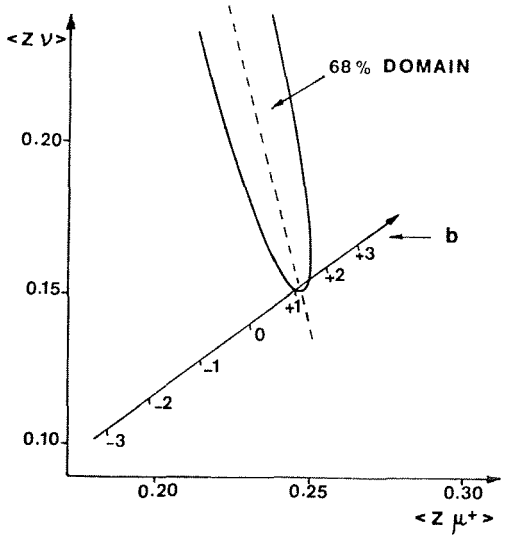

Fig.4 Comparison of this experiment with predictions of the D production model for different b values.

In order to compute the $\mu^+\mu^-$ production rate as a function of neutrino energy, the data were corrected for the geometrical and kinematical acceptance of the EMI.

The efficiency ranges from 14% at low neutrino energies to 55% for high energy with a mean value of 28 ± 4%.

In Fig.5 the rate $\sigma(\mu^+\mu^-)/\sigma(\mu^-)$ is shown for different energies and compared with the results of other experiments for dilepton production. The GGM mean value $(7.2 \pm 1.4)\cdot 10^{-3}$ is in good agreement.

In our sample no clear vertex for the D decay has been seen. It is only possible to give a limit on the D mean life defining for all events the maximum lengths after which clearly none of the considered D decay have occured.

With assumptions on the branching ratio of the D to take into account when the decay is clearly visible in the bubble chamber, and assumptions on the mean D momentum, it is possible, by a likelihood method, to give an upper limit at 90% confidence level for the D mean life:

$$\tau_D < 0.8 \cdot 10^{-12} \text{ sec}$$

in agreement with the experimental results presented at this Conference [5].

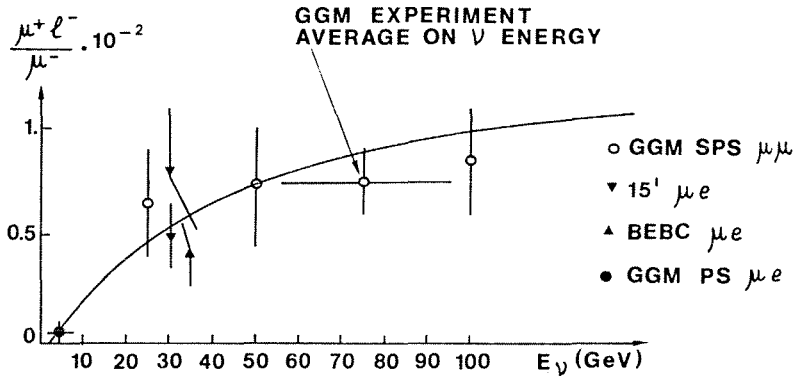

Fig.5. Rate of dilepton production as a function of the neutrino energy.

4. INVERSE MUON DECAY

The inverse muon decay reaction predicted by the V-A theory [6]:

$$\nu_\mu e^- \rightarrow \mu^- \nu_e \qquad (2)$$

has never been observed due to the high threshold (≃10.9 GeV) and to the low cross section [7]:

$$\sigma_{V\text{-}A} = 1.55 \frac{(E_\nu - 10.9)^2}{E_\nu} \cdot 10^{-41} \text{ cm}^2$$

From the kinematics we expect high energy muons ($E_\mu > 10.9$) emitted in a very small angle with the neutrino beam ($\vartheta_{\mu\nu} < 5$ mrad). The $q^2 = \tilde{p}_\mu - \tilde{p}_\nu$ region allowed by the reaction ranges

up to about $\sim$0.1 GeV^2 (for E_ν=100 GeV) in a wide region far from the point $q^2 = -m_\mu^2$ of the muon decay.

Events candidates for reaction (2) were selected using the data from the counters around the bubble chamber requiring only one muon track of high energy with a small $\vartheta_{\mu\nu}$ angle.

This procedure reduces by a big factor the number of pictures to be scanned and increase the detection efficiency for finding "isolated muons" which was found to be 94 ± 3%.

84 isolated μ^- with $E_\mu > 10$ GeV and $\vartheta_{\mu\nu} < 100$ mrad were selected.

The background mainly comes from two sources:

i) the quasi elastic reaction on nucleons $\nu\mu + N \rightarrow \mu^- +$ unseen proton.

ii) the reaction on nuclei, by excitation of the giant dipole resonance $\nu_\mu + {}^{12}C \rightarrow \mu^- + {}^{12}N$

Both background processes have different kinematical properties than the signal. First in the background reaction the muon carries almost all the neutrino energy, whereas for reaction (2) the muon takes about half neutrino energy. In Fig.6 the muon energy is plotted and compared with what expected for signal and background.

Secondly in the reaction (2) the angle $\vartheta_{\mu\nu}$ is severely limited and satisfy the constraint $\rho = E_\mu \vartheta_{\mu\nu}/2m_e < 1$. On the contrary for the background reactions, very low values of q^2, and consequently of $\vartheta_{\mu\nu}$, are suppressed and we expect a broader distribution of the ρ variable. The experimental distribution (Fig.7) show a very clear peak at low values as expected from the inverse muon decay reaction.

By a likelihood method based on both variable E_μ and $\vartheta_{\mu\nu}$ the signal was estimated to be, after scanning efficiency correction, 26 ± 6 events. We conclude that for the first time a clear signal of reaction (2) is observed.

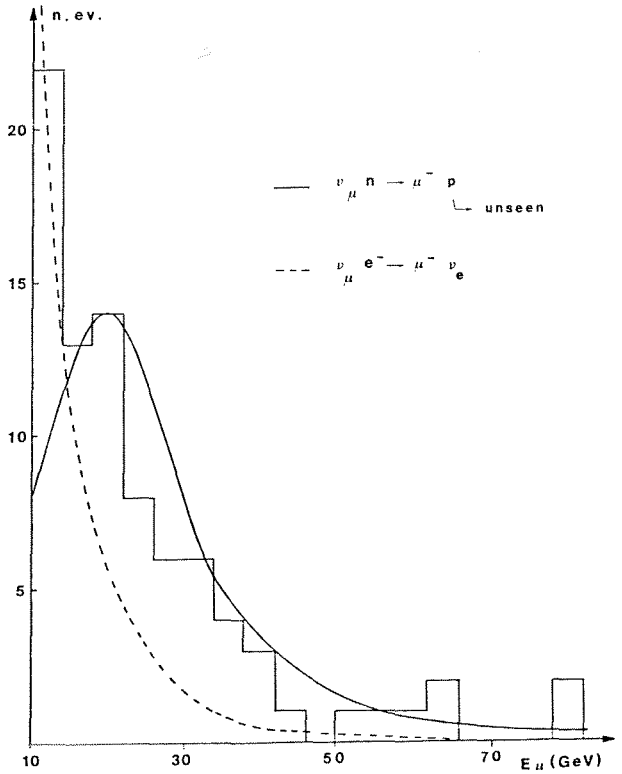

Fig.6 Muon energy distribution.

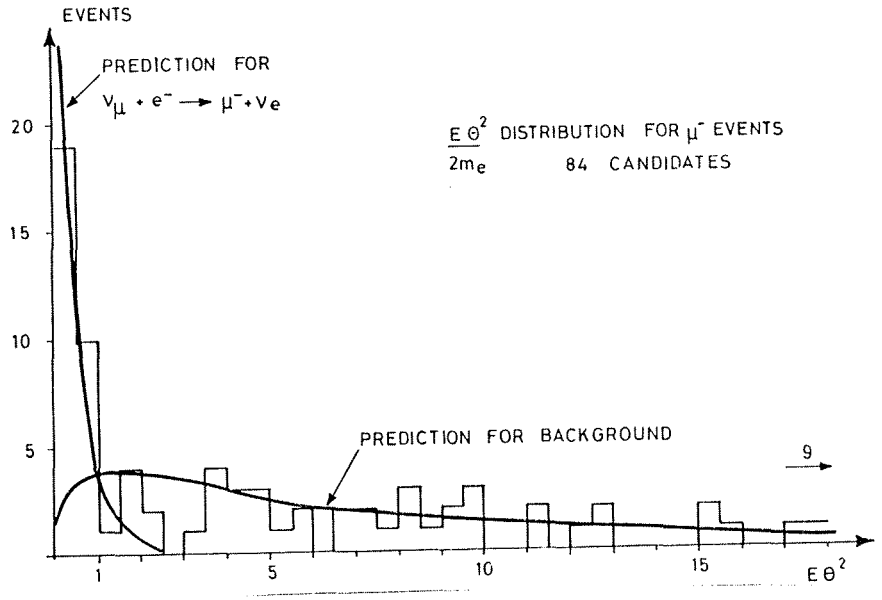

Fig.7 $\rho = E_\mu \vartheta_\mu / 2m_e$ distribution.

With the ν flux information if we compared the expected cross section from V-A theory (29 events predicted) with the experiment. We find a good agreement:

$$\frac{\sigma^{exp}}{\sigma^{V-A}} = 0.9 \pm 0.2$$

In a more general way, assuming only V and A contributions, we can write the expected number of events only as a function of two parameters $\lambda = 2g_A g_V / (|g_A|^2 + |g_V|^2)$ (axial and vector contributions) and $p = N_R - N_L / (N_R + N_L)$ (contribution from right and left handed neutrino):

$$N = \frac{29}{32} \{(1+p)(1-\lambda)\cdot 3 + 8(1-p)(1+\lambda)\}$$

The result of this experiment, illustrated in Fig.8, is in agreement with V-A theory ($\lambda=1$) with only left handed neutrinos ($p= -1$) and rules out exotic possibilities like V+A coupling or right handed neutrinos.

5. NEUTRAL CURRENT REACTION $\nu_\mu e^- \rightarrow \nu_\mu e^-$

One year ago [8] our collaboration published a preliminary result (based on 1/3 of the statistics) on the total cross-section for the purely leptonic reaction: $\nu_\mu e^- \rightarrow \nu_\mu e^-$ which was unexpectedly high.

We present here the final result based on the total statistics of the experiment. The total neutrino flux was increased by a factor 2.6 and the results come from the analysis of 410.000 pictures corresponding to $2.2 \cdot 10^{18}$ protons on the target and 64.000 CC events.

I will not go into the details of the analysis which is similar to the previous one.

Only one new selection criterion was added in order to eliminated the possible background coming from the bremsstrahlung of muons tracks crossing the chamber.

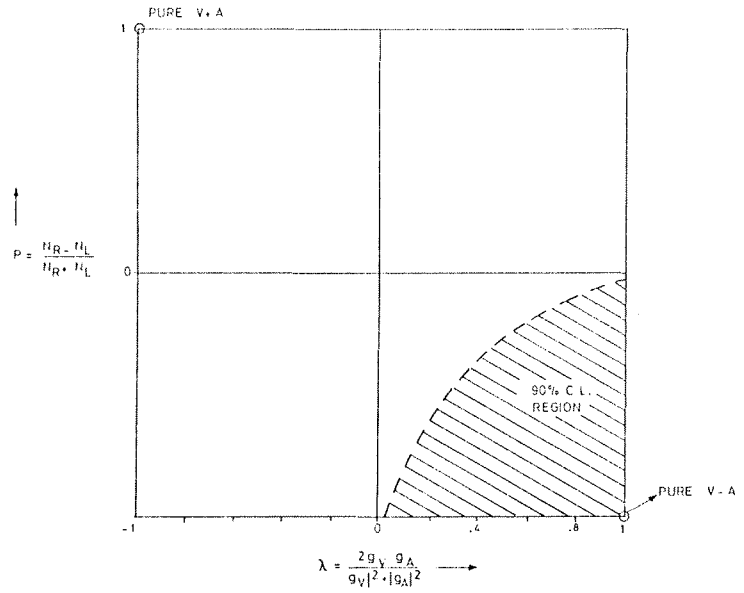

Fig.8 Allowed domain at 90% CL from GGM experiment in the p,λ plane.

For that we required the isolated electrons or gammas to be at a distance from all muon tracks larger than 2 cm and with an angle with the muon track of more than 20 mrad. With this new criterion two of the previously selected electrons were rejected and the final sample is now 9 events in the cuts $E_e>2$ GeV and $\vartheta_e<3^0$

From background calculation we expect only 0.5 ± 0.2 events mainly coming from the quasi-elastic reaction $\nu_e n \to e^-(p)$ and from asymmetric isolated γ rays.

After corrections for losses and for background the experimental total cross section is now:

$$\sigma = 2.4^{+1.2}_{-0.9} \cdot 10^{-42} \cdot E_\nu \quad cm^2/electron$$

which is in agreement with other experiments [9] as shown in Table II.

TABLE II

Experiment	n. events	background	cross sections ($\times E_\nu \cdot 10^{-42}$)
GGM PS	≤ 1	0.3 ± 0.1	≤ 3
AACHEN-PADOVA	32	21	1.1 ± 0.6
COLUMBIA-BNL	11	0.7 ± 0.7	1.8 ± 0.8
GGM SPS	9	0.5 ± 0.2	$2.4^{+1.2}_{-0.9}$

If we consider the predicted cross section:

$$\frac{d\sigma}{dE_e} = \frac{G^2 m_e}{2\pi} \{(g_V+g_A)^2+(g_V-g_A)^2(1-\frac{E_e}{E_\nu})^2\}$$

our result defines an allowed domain at 90% confidence level in the g_A,g_V plane (Fig.9).

In Fig.9 also the prediction from SU(2)×U(1) model in which g_A=- 1/2 and g_V= 1/2+2sinϑ_W is shown. The two allowed values for $\sin^2\vartheta_W$ are:

$$\sin^2\vartheta_W=0.12^{+0.11}_{-0.07} \qquad \sin^2\vartheta_W=0.6 \pm 0.10$$

The first value is in good agreement with the $\sin^2\vartheta_W$ values obtained in other reactions [10].

If we compare the present result with the one published in 1978 we find:

$$\sigma^{1979} = \sigma^{1978}/3.1$$

Let us remark that only a factor 1.2 is due to the new selection criteria, but the big factor 2.6 is apparently only due to a very large statistical fluctuation which has a probability of $3.1\cdot10^{-3}$

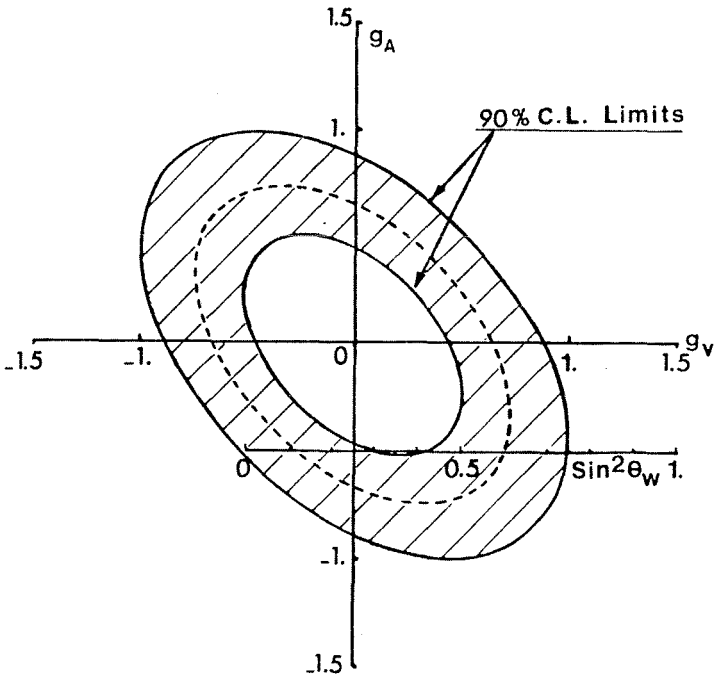

Fig.9 Allowed domain at 90% level from the GGM experiment in the g_V,g_A plane.

REFERENCES

1) C. Brand et al., CERN/EF 77-3

2) A. Blondel, Ph.D Thesis Orsay (1978)

3) R.M. Barnett, Phys. Rev. Lett. 36, 1163 (1976)

4) J. Kirkby SLAC Pub. 2231 (1978)

5) M. Conversi, Communication to this Conference

6) R.P. Feynman and M. Gell-Mann, Phys. Rev. 109, 193 (1958)

7) C. Jarlskog, Lettere al Nuovo Cimento 1,4,377 (1970)

8) P. Alibran et al., Phys. Lett. 74B, 422 (1978)

9) J. Blietschau et al., Phys. Lett. 73B, 232 (1978)
H. Faissner et al., Phys. Rev. Lett. 41, 213 (1978)
C. Baltay et al., Phys. Rev. Lett. 41, 357 (1978)

10) S. Weinberg, Tokyo Conference 1978
C. Baltay, Tokyo Conference 1978
C.Y. Prescott, Phys. Lett. 77B, 347 (1978)

FIRST RESULTS FROM THE CERN-HAMBURG-AMSTERDAM-ROME-MOSCOW NEUTRINO EXPERIMENT

M. Jonker, J. Panman and F. Udo

NIKHEF, Amsterdam, The Netherlands

J.V. Allaby, U. Amaldi, G. Barbiellini[a], A. Baroncelli, G. Cocconi, W. Flegel, P.D. Gall[b], W. Kozanecki, E. Longo, K.H. Mess, M. Metcalf, J. Meyer, R.S. Orr, F. Schneider, A.M. Wetherell and K. Winter

CERN, Geneva, Switzerland

F.W. Büsser, H. Grote, P. Heine, B. Kröger, F. Niebergall, K.H. Ranitzsch and P. Stähelin

II. Institut für Experimentalphysik der Universität[*], Hamburg, Germany

P. Gorbunov, E. Grigoriev, V. Kaftanov, V. Khovansky and A. Rosanov

ITEP, Moscow, USSR

R. Biancastelli[c], B. Borgia[c], C. Bosio[d], A. Capone[c], F. Ferroni[c], P. Monacelli[c], F. de Notaristefani[c], P. Pistilli[c], C. Santoni[d] and V. Valente[e]

INFN, Rome, Italy

(Presented by A. Rosanov)

ABSTRACT

Preliminary results of the neutrino counter experiment carried out by the CHARM collaboration are presented. They cover the following topics:

Study of the strength and the structure of the neutral current in inclusive reactions on an isoscalar target.

Neutrino scattering on electrons.

Measurement of the polarization of positive muons produced in high-energy antineutrino interactions[**].

We present preliminary results of three neutrino experiments which make use of the novel features of the new neutrino detector of the CHARM (CERN-Hamburg-Amsterdam-Rome-Moscow) Collaboration. The experiments were performed in the neutrino beams of the 400 GeV Super Proton Synchrotron (SPS) accelerator at CERN.

1. THE APPARATUS

The CHARM neutrino detector[1] (see Fig. 1) consists of a fine-grained marble calorimeter which allows the measurement of the energy and the direction of the hadron or electromagnetic showers, and of a magnetized iron spectrometer which allows the measurement of the momentum of muons. The target calorimeter contains 78 submodules. Each of these submodules consists of:

---

a) On leave of absence from Laboratori Nazionali INFN, Frascati, Rome, Italy.

b) On leave of absence from II. Institut für Experimentalphysik, Universität Hamburg, Germany.

c) Istituto di Fisica dell'Università di Roma and INFN, Sez. di Roma, Italy.

d) INFN Sez. Sanità and Istituto Superiore Sanità, Rome, Italy.

e) Laboratori Nazionali INFN, Frascati, Rome, Italy.

*) Supported by the Bundesministerium für Forschung und Technologie, Bonn, Germany.

**) In collaboration with CDHS: J.G.H. de Groot, F.L. Navarria and A. Savoy-Navarro.

i) a marble plate, 8 cm thick and of 300 × 300 cm^2 cross-sectional area, surrounded by a magnetized iron frame;

ii) a plane of 128 proportional drift tubes, each having dimensions of 3 × 3 cm^2 in cross-section and 400 cm in length;

iii) a plane of 20 plastic scintillators, each 3 cm thick and 15 × 300 cm^2 in cross-sectional area, oriented at 90° with respect to the proportional drift tubes.

The total weight of the target calorimeter is 175 tons. The marble calorimeter is followed by the muon spectrometer, made of four toroidal magnetized iron modules.

2. INCLUSIVE NEUTRAL CURRENTS

Inclusive neutral-current (NC) reactions were studied in the 200 GeV narrow-band neutrino beam[2]. The data sample obtained in the autumn of 1978 yielded 9200 neutrino and 2700 antineutrino events in a fiducial volume with a mass of 61 tons.

The special features of this experiment are:

i) the low hadron energy cut: 0.5 GeV trigger threshold and 2 GeV off-line cut, and good energy resolution: $\Delta E_h/E_h = [1 + 43/(E/GeV)^{\frac{1}{2}}]\%$;

ii) low muon momentum cut of $\sim$ 1.5 GeV/c;

iii) automatic pattern recognition of muons;

iv) measurement of the hadron shower direction.

The dichromatic narrow-band beam provides a relation between the radial position of the event vertex and the energy of a neutrino from pion or kaon decay. The Lorentz structure of the neutral currents can be studied using the inelasticity ($y = E_H - M/E_\nu$) distributions.

To resolve the pion-kaon neutrino energy ambiguity, a statistical method has been developed which makes essential use of neutrino flux information. After a few iterations, this method is independent of the initial assumptions on y distributions. It has been tested by comparing the y distribution of charged current (CC) events, which was determined using the measured muon momentum, with the statistical one obtained using hadron energy only. The detailed description of the method employed can be found in Ref. 2.

Preliminary y distributions obtained for neutrino and antineutrino data are shown in Figs. 2 and 3. In this analysis the CC events were treated in the same way as NC events. No corrections are applied to these distributions. The data show the dominance of (V-A) coupling. The dots represent the Monte Carlo predictions with the weak mixing angle $\sin^2\theta_W = 0.25$. The Monte Carlo predictions are in satisfactory agreement with the data. Another way to test the structure of the neutral currents is to determine the ratio of NC to CC cross-sections. These ratios are shown as a function of y in Fig. 4. The Monte Carlo predictions of the quark-parton model with $\sin^2\theta_W = 0.25$ follow the data reasonably well. The ratios integrated over all y are:

$$R = 0.30 \pm 0.006 \pm 0.02$$

$$\bar{R} = 0.39 \pm 0.014 \pm 0.02 \ ,$$

where the first error is statistical and the second is an estimate of systematic uncertainties. Figure 5 shows a comparison of this result with other experiments[3-7], and the

prediction of the quark-parton model[8] and its modification by QCD effects[9]. Our data are in good agreement both with other experiments and with theoretical predictions.

The knowledge of the neutrino energy-radius correlation and the measurement of the hadron shower direction allow us to determine the scaling variable $x = Q^2/2M\nu$ and to study the structure functions of the nucleon with the neutral current. Preliminary results on the ratio of NC to CC cross-sections as a function of x are obtained in a way similar to that used for the y distributions, but with a cut of $E_h > 20$ GeV (Fig. 6). They indicate the similarity of structure functions obtained with neutral and charged currents, as expected in the quark-parton model.

3. NEUTRINO SCATTERING ON ELECTRONS

Measurements of neutrino electron scattering, $\nu_\mu + e^- \rightarrow \nu_\mu + e^-$, give information on the coupling constants of the weak leptonic neutral current. The extremely low cross-section [$\sim 10^{-4}$ of the neutrino nucleon cross-section[10]] requires a detector comprising special features, which combines some of the advantages of bubble chambers in the event selection and of a massive calorimeter to obtain good event rates.

There are two main experimental problems that have to be solved in this experiment. The first one is the separation of hadronic showers from electromagnetic ones, which is achieved in the fine-grained CHARM calorimeter owing to the difference in their transversal profile.

Figure 7 shows the distribution of the width of electron and pion showers obtained in calibration runs. It can be seen that electron (solid lines) and pion (dotted lines) showers can be well separated using both scintillator counters and proportional tubes.

The narrow angular distribution of electrons recoiling in the reaction $\nu_\mu e \rightarrow \nu_\mu e$ [$\theta_e \sim (2m_e/E_\nu)^{\frac{1}{2}}$] allows this reaction to be separated from various backgrounds which have a wider angular distribution. Thus, the second experimental problem is to achieve good angular resolution for electron showers. Results of calibration measurements, performed in an electron beam at 6, 15, and 20 GeV, are well approximated by the expression

$$\Delta\theta_{proj} = \frac{1}{\left(\ln \frac{E}{\varepsilon} + 0.4\right)} \left[3 \times 10^{-3} + \frac{4 \times 10^{-2}}{E}\right]^{\frac{1}{2}} \text{ mrad},$$

where the electron energy E is measured in GeV and $\varepsilon = 0.05$ GeV. This corresponds to an angular resolution of $\Delta\theta = 11$ mrad at 20 GeV. As can be seen from this equation, the angular resolution is a function of the electron energy. If the measured angle is expressed in units of the angular resolution, the distribution of events as a function of $(\theta/\Delta\theta)^2$ becomes energy independent.

The experiment was performed during the summer of 1978 in the 350 GeV neutrino wide-band beam with a partly equipped apparatus[11]. A data sample of 73,000 neutrino interactions with shower energy in the range $5 \leq E_{sh} \leq 50$ GeV was collected in a fiducial target of 22 tons. Several cuts were applied to the data, rejecting events with single tracks longer than 180 g/cm^2, large shower angles ($\theta^2/\Delta\theta^2 > 10$), proportional tube multiplicity at the vertex > 2, or with energy deposition in the first scintillator plane after the vertex > 8 minimum-ionizing particles. Events with a transverse width of the shower in scintillators

and proportional tubes, as expected for electrons, were retained. Twenty-one events satisfied these criteria. Contributions from the following background processes must be subtracted from the data:

a) hadronic CC events with very low energy muons and a large electromagnetic component;

b) semileptonic neutral currents with a large electromagnetic component e.g. $\nu_\mu + N \to \nu_\mu + \pi^0 + N$;

c) quasi-elastic CC events induced by the $\overset{(-)}{\nu}_e$ component of the neutrino beam.

Backgrounds (a), (b), and (c) are expected to have wider angular distributions than $\nu_\mu e$ scattering. Figure 8a shows the distribution of 21 candidates as a function of $\theta^2/\Delta\theta^2$. The dashed line shows the flat angular distribution of backgrounds (a) and (b) normalized to the observed number of events for $\theta^2/\Delta\theta^2 > 3$. The shaded area represents the angular distribution of events due to the background (c), which was obtained by multiplying the observed number of events of the reaction $\nu_\mu + N \to \mu^- +$ (invisible hadrons) by the computed ratio[12] of electron and muon neutrino fluxes $(\nu_e + \bar{\nu}_e)/\nu_\mu = 1.9\%$. We observe a peak containing 11 events with $\theta^2/\Delta\theta^2 < 2.25$ with a background of 4.5 ± 1.4 events. The energy distribution of the 11 candidates is shown in Fig. 8b, together with the expected spectrum for $\sin^2\theta_W = 0.23$. The over-all efficiency for selecting $\nu_\mu e$ events by the criteria given above is $\varepsilon = (58 \pm 17)\%$. Normalizing the excess of 6.5 ± 2.6 events to the total number of NC and CC neutrino events using a cross-section of $\sigma/E_\nu = 0.85 \times 10^{-38}$ (cm^2/GeV) and assuming a linear energy dependence of the $\nu_\mu e$ cross-section with energy, we find

$$\frac{\sigma(\nu_\mu e)}{E} = \left(2.5 \begin{matrix} + 1.4 \text{ statistical error} \\ - 0.8 \text{ systematical error} \end{matrix}\right) \times 10^{-42} \text{ (cm}^2\text{/GeV)} .$$

This result is consistent with earlier experiments[10] and with the Weinberg-Salam model.

3. POLARIZATION OF POSITIVE MUONS PRODUCED IN ANTINEUTRINO INTERACTIONS

This experiment was performed using the massive CDHS (CERN-Dortmund-Heidelberg-Saclay) neutrino detector[13] as a target for $\bar{\nu}_\mu$ interactions and the fine-grained CHARM detector as a muon polarimeter. Positive muons produced in $\bar{\nu}_\mu$ interactions are focused in the toroidal field of the CDHS detector, and $\sim$ 5% of them stop in the CHARM polarimeter (see Fig. 9). The longitudinal polarization of positive muons can be determined by the forward-backward asymmetry of positrons emitted in μ decay at rest. A magnetic field of 0.0058 T perpendicular to the beam direction is produced inside the polarimeter, causing the spin of the stopped μ to precess with a period of 1.3 μs. Conventional V and A currents preserve the lepton helicity, whereas possible S, P, T interactions flip the helicity and produce muons with negative helicity. The helicity of muons emitted in pion and kaon decays has been measured[14,15], but no corresponding measurements exist at higher centre-of-mass energies, confirming directly the V and A nature of the current.

The data sample was obtained in spring 1978 in an antineutrino wide-band beam exposure[16]. It consists of 13,000 muons produced in the target and stopping in the polarimeter; 3400 decay positrons were detected. The observed time dependence of the backward-forward asymmetry,

$$R(t) = \frac{N_B(t) - N_F(t)}{N_B(t) + N_F(t)} = R_0 \cos(\omega t + \phi) + R_1 ,$$

is shown in Fig. 10. The method of spin precession is insensitive to systematic forward-backward asymmetries of the apparatus. The data are well fitted by the oscillating curve, and the values of the polarimeter analysing power and positron detection efficiency are in good agreement with Monte Carlo predictions. The results are

i) the measured phase of the oscillations $\phi = -3.1 \pm 0.2$ (rad) is in perfect agreement with $-\pi$ predicted for muons of positive helicity;

ii) the absolute value of the polarization is $P = 1.09 \pm 0.22$. Within the experimental errors the helicity is +1, consistent with a pure V, A structure of the interaction. One can put an upper limit $\sigma_{S,P,T}/\sigma_{tot} < 18\%$ at the 95% confidence level on the S, P, T helicity-flipping contribution to the charged-current interaction at an average four-momentum transfer of $\langle Q^2 \rangle = 3.2$ GeV^2.

The authors wish to thank all the members of the CDHS Collaboration for their help in performing the μ^+ polarization experiment.

* * *

REFERENCES

1) M. Jonker et al., CHARM Collaboration, A detector for neutral-current interactions of high-energy neutrinos, to be published in Nucl. Instrum. Methods.

2) CHARM Collaboration (presented by K.H. Mess), Analysis of neutral current events in the CERN 200 GeV narrow band beam, Neutrino 79 Int. Conf., Bergen, 1979 (to be published).

3) J. Blietschau et al., GGM Collaboration, Nucl. Phys. B118, 218 (1977).

4) P. Wanderer et al., HPWF Collaboration, Phys. Rev. D 17, 1679 (1978).

5) F. Merrit et al., CITF Collaboration, Phys. Rev. D 17, 2199 (1978).

6) M. Holder et al., CDHS Collaboration, Phys. Lett. 71B, 222 (1977) and 72B, 254 (1977).

7) P.C. Bosetti et al., BEBC-ABCLOS Collaboration, Phys. Lett. 76B, 505 (1978). H. Deden et al., BEBC-ABCLOS Collaboration, Nucl. Phys. B149, 1 (1979).

8) CDHS Collaboration (presented by C. Geweniger), New measurement of R and $\bar{R}$, this conference.

9) J.E. Kim et al. (presented by P. Langacker), A new analysis of neutral current data, this conference.

10a) F.J. Hasert et al., Phys. Lett. 46B, 121 (1973). J. Blietschau et al., Nucl. Phys. B114, 189 (1976).

b) J. Blietschau et al., Nucl. Phys. B114, 189 (1976).

c) H. Faissner et al., Phys. Rev. Lett. 41, 213 (1978).

d) P. Alibran et al., Phys. Lett. 74B, 422 (1978).
N. Armenise et al., Phys. Lett. B (to be published).

e) A.M. Cnops et al., Phys. Rev. Lett. 41, 357 (1978).

11) CHARM Collaboration (presented by E. Longo), Measurement of the cross-section of neutrino scattering on electrons with a digitized calorimeter, Neutrino 79 Int. Conf., Bergen, 1979 (to be published).

12) H. Wachsmuth, private communication.

13) M. Holder et al., Nucl. Instrum. Methods 148, 235 (1978).

14) G. Backenstoss et al., Phys. Rev. Lett. 6, 415 (1961).

15) C.A. Coombes et al., Phys. Rev. 108, 1348 (1957).

16) M. Jonker et al., Polarization of positive muons produced in high-energy antineutrino interactions, Phys. Lett. 86B, 229 (1979).

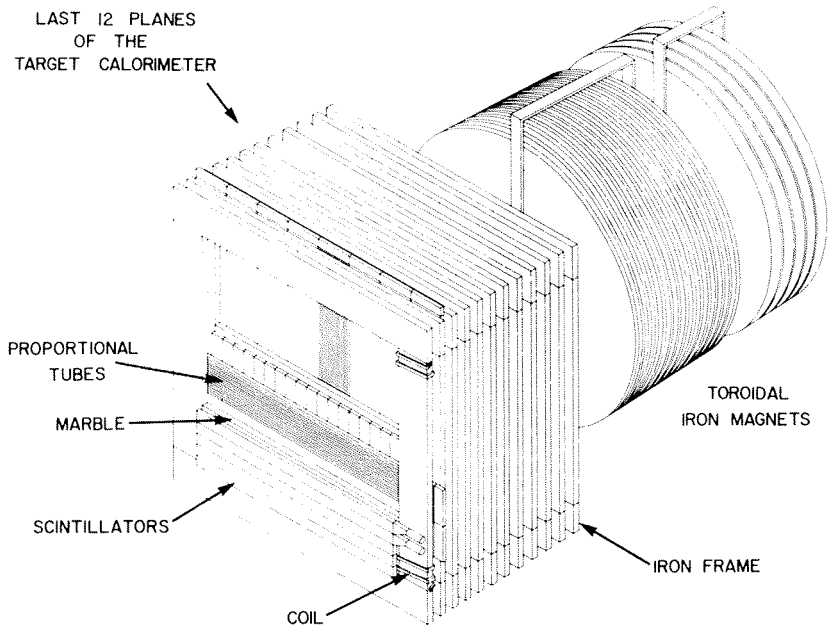

Fig. 1 Perspective view of part of the CHARM detector

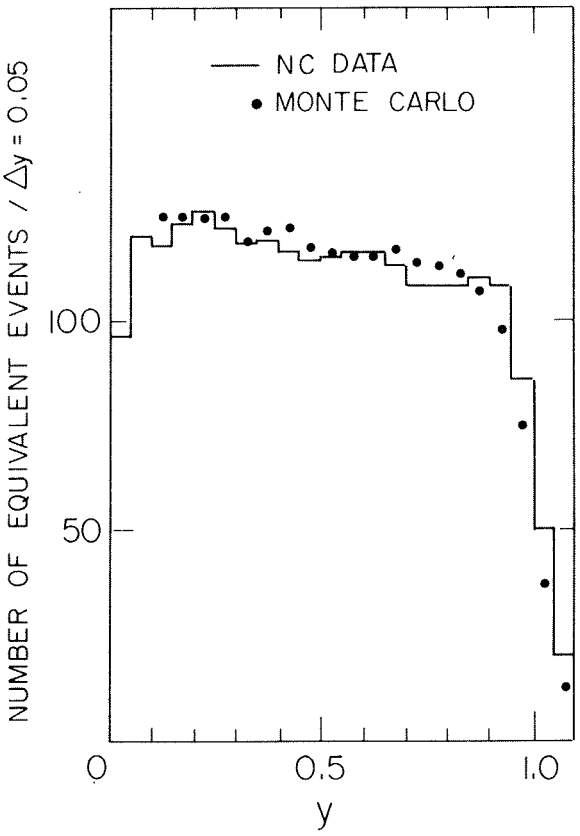

Fig. 2 Preliminary y distribution for NC events induced by neutrinos. Dots represent the Monte Carlo predictions with $\sin^2 \theta_W = 0.25$.

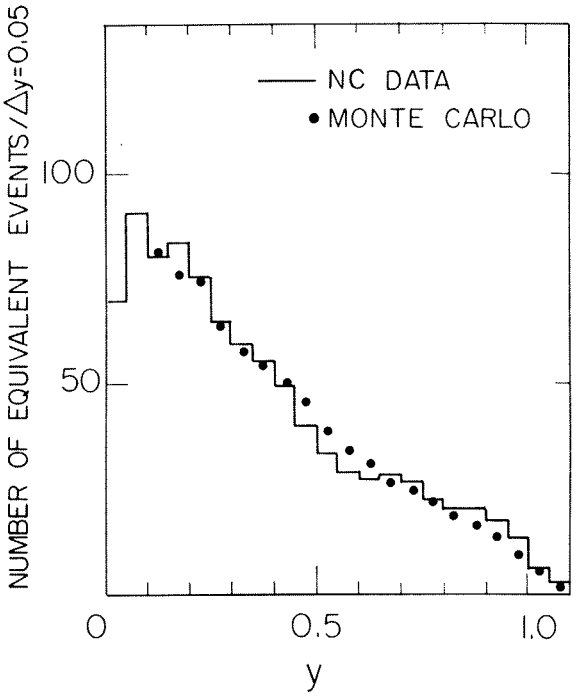

Fig. 3 Preliminary y distribution for NC events induced by antineutrinos

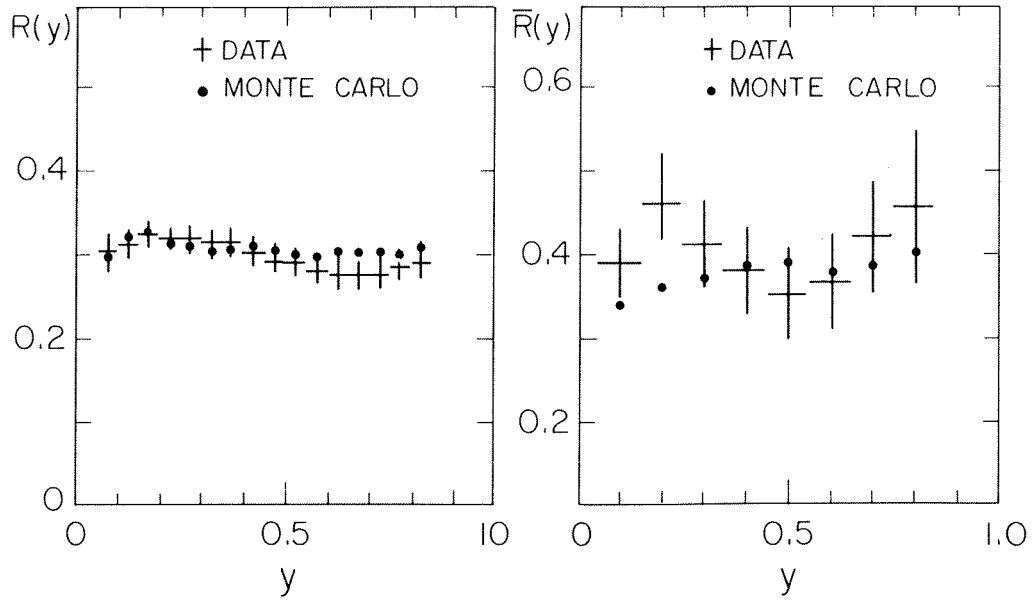

Fig. 4 Preliminary results on the ratio of neutral to charged current cross-sections as a function of $y = \nu/E_\nu$.

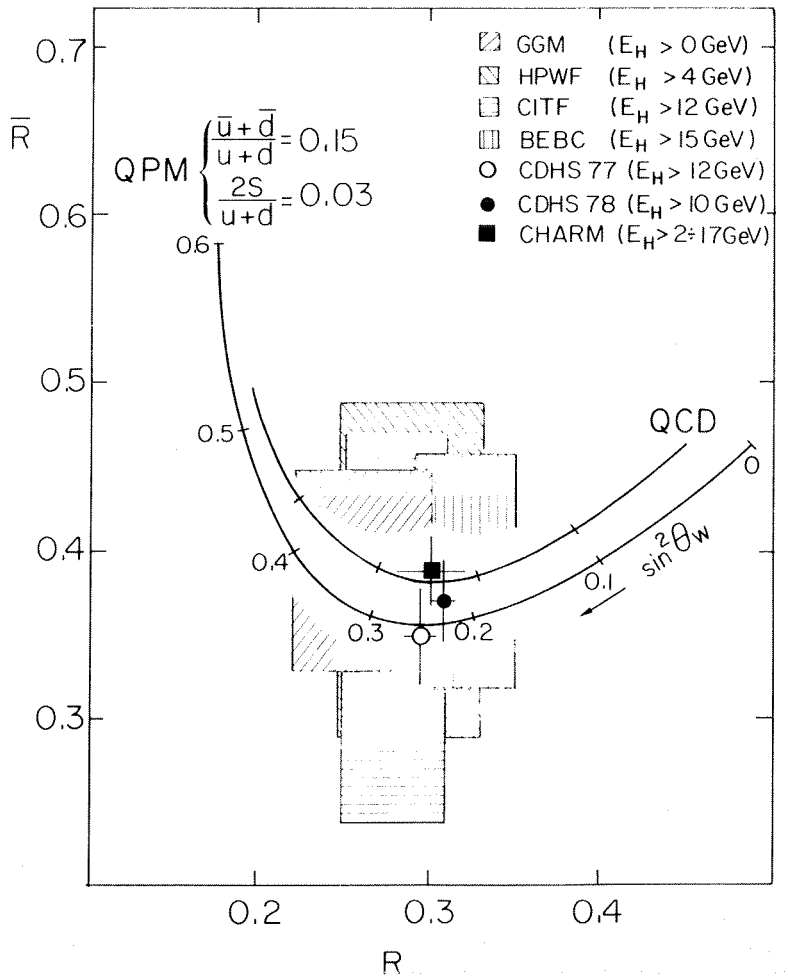

Fig. 5 The comparison of the integrated ratios R and $\bar{R}$ with other experiments. The lower curve is a quark-parton model prediction[8], the upper curve includes QCD corrections[9].

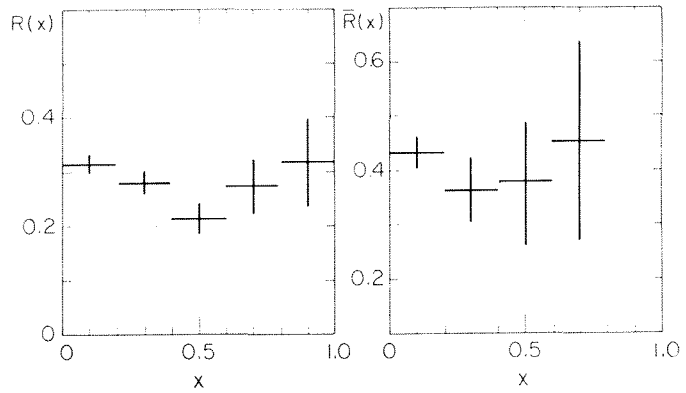

Fig. 6 Preliminary results on the x dependence of the NC/CC ratio for neutrinos and antineutrinos.

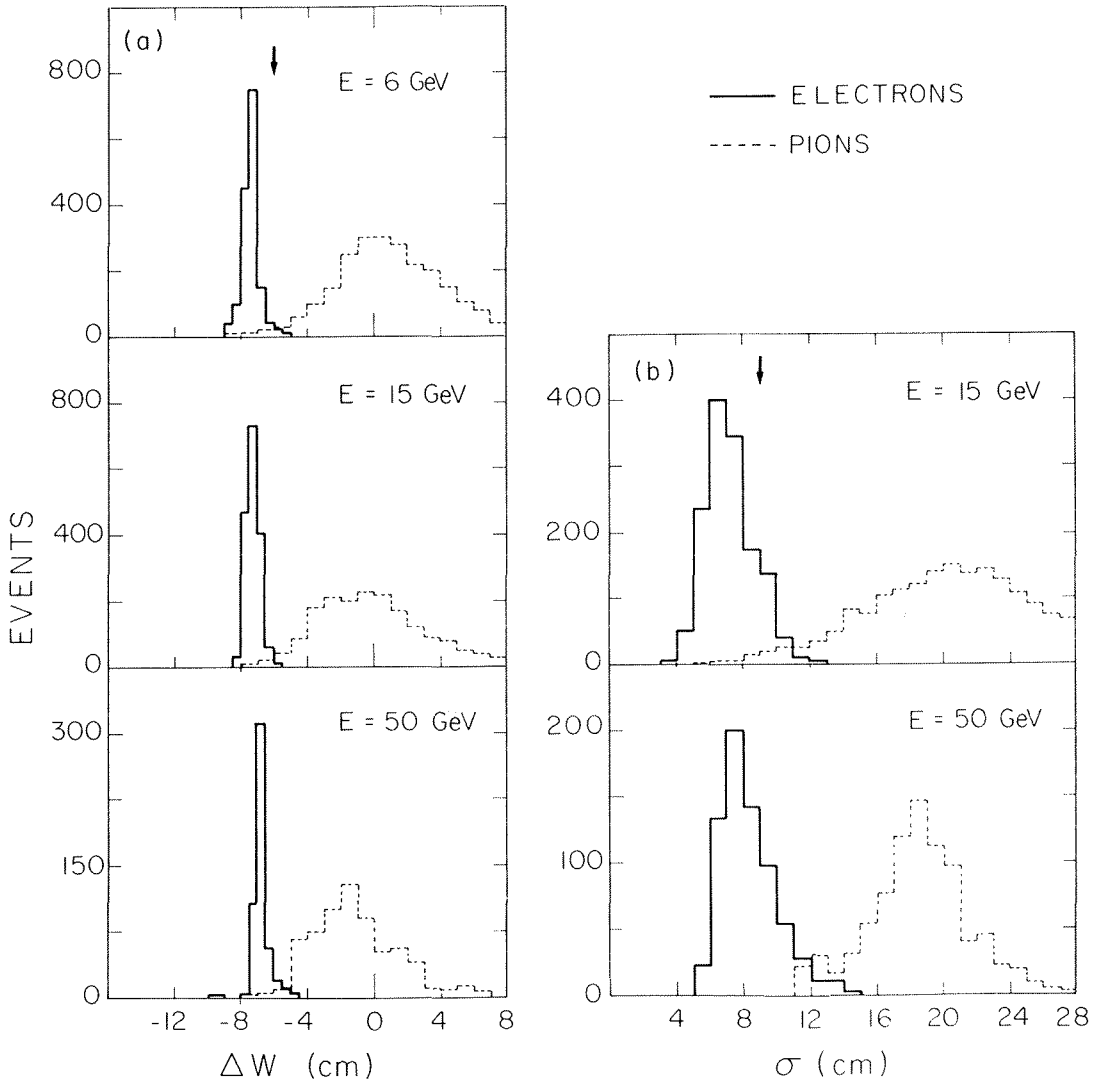

Fig. 7 a) Distributions for incident electrons and hadrons of 6, 15, and 50 GeV of the difference ΔW between the observed width of showers and that expected for a hadron shower, as measured by the scintillators. The arrow indicates the cut at $\Delta W = -6$ cm.

b) Distributions of the normalized r.m.s. width of the energy deposited in the proportional tubes by electrons and pions at 15 and 20 GeV. The arrow indicates the cut at $\sigma = 9$ cm.

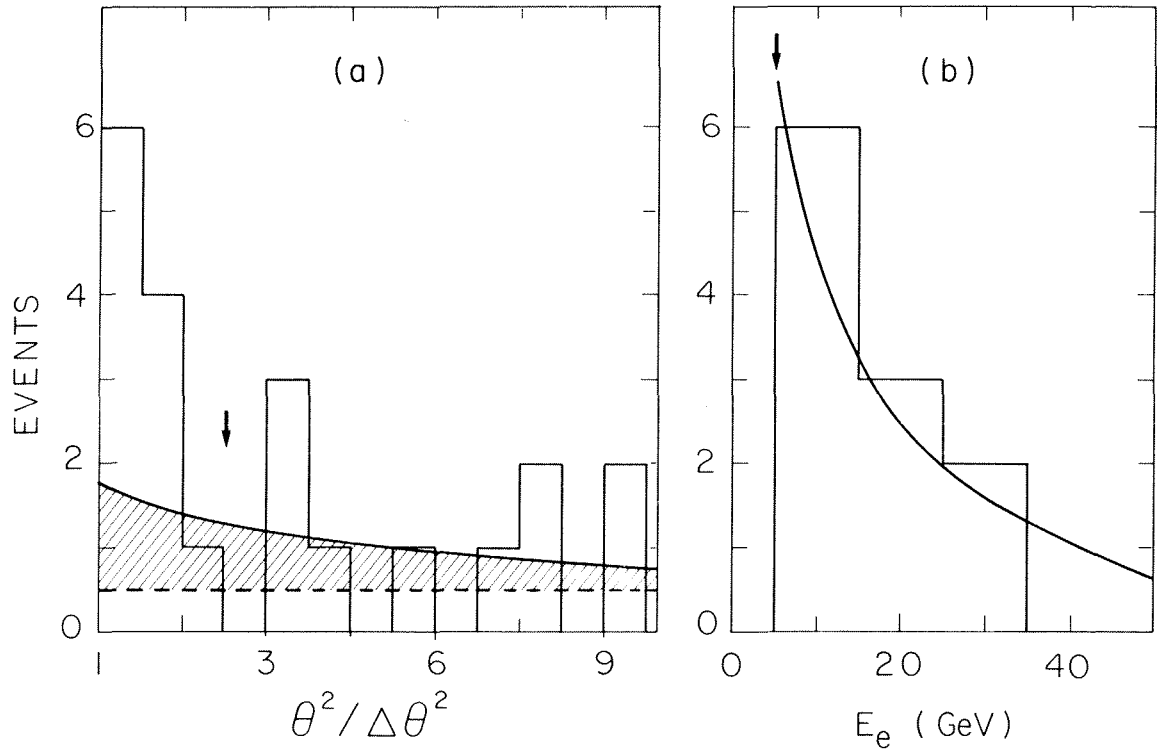

Fig. 8 a) Distribution of $\nu_\mu e^- \to \nu_\mu e^-$ candidates as a function of $\theta^2/\Delta\theta^2$. The dashed line represents the background due to semileptonic NC events initiated by ν_μ's. The shaded area is the computed contribution of elastic and quasi-elastic events induced by the $(\bar{\nu})_e$ contamination of the beam.

b) Energy distribution of the events with $\theta^2/\Delta\theta^2 \leq 2.25$. The line is the expected distribution for $\sin^2 \theta_W = 0.23$.

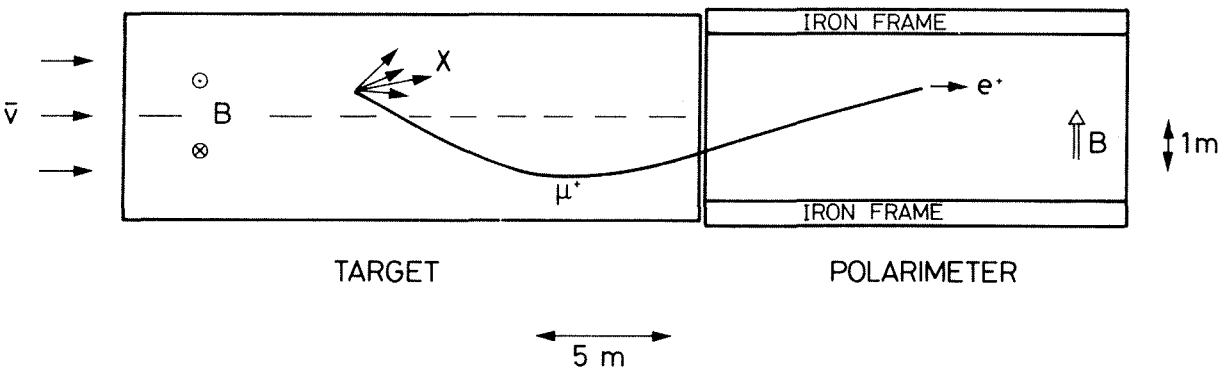

Fig. 9 Layout of the μ^+ polarization experiment

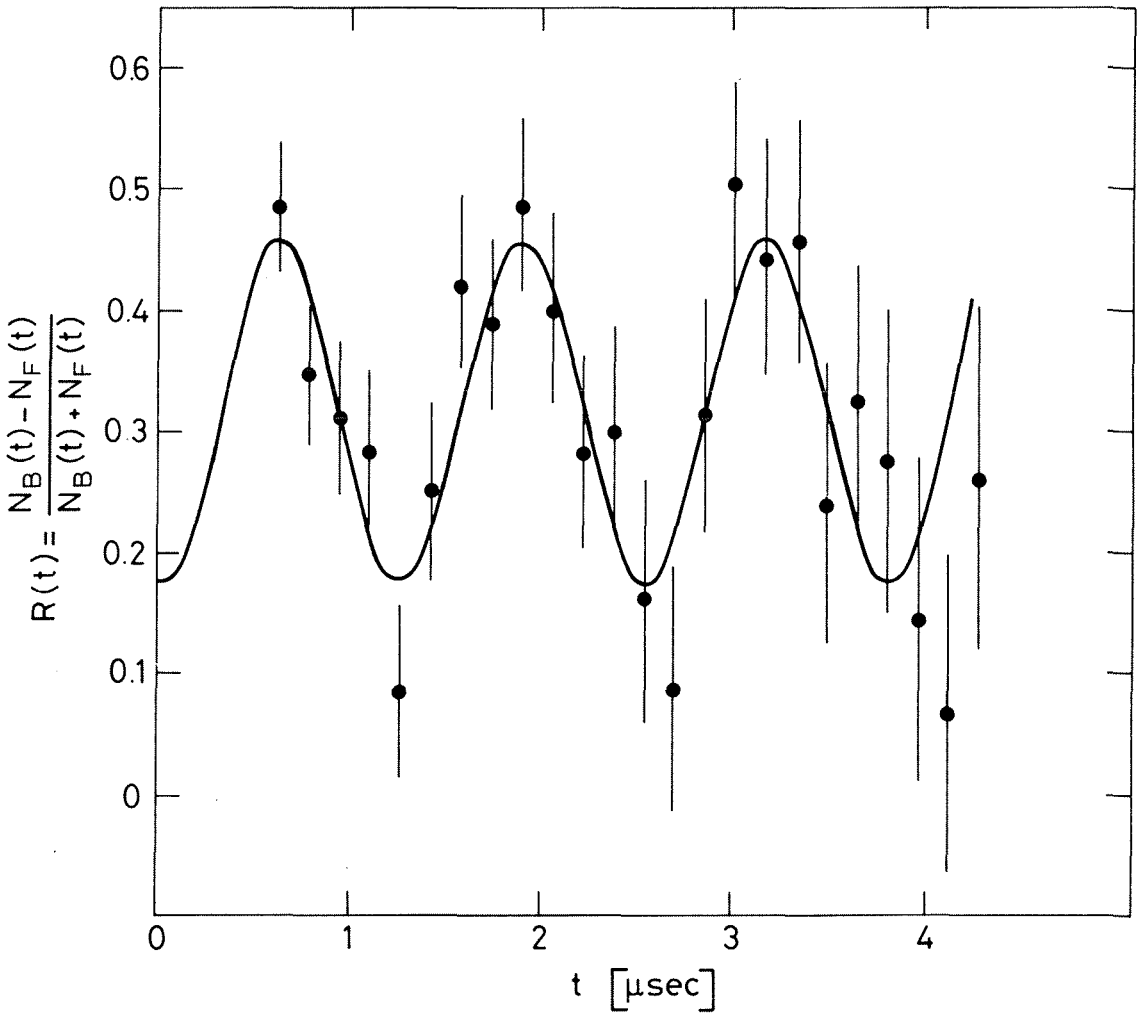

Fig. 10 Observed time dependence of relative backward-forward positron asymmetry. The sinusoidal function is the best fit to the experimental points for a phase $\phi = -3.1 \pm 0.2$ and a polarization $P = +(1.09 \pm 0.22)$, in agreement with helicity +1.

SESSION II

e^+e^- PHYSICS

Chairmen: L.S. Cheng
W. Jentschke
A. Martin
H. Schopper
V. Sidorov
S.C.C. Ting

Sci. Secretaries: C. Best
M. Calvetti
A. Contin
C. del Papa
H. Gennow
G.V. Goggi
C. Peroni
R.T. Ross

Rapporteurs talks:

M. Davier	e^+e^- physics: heavy quark spectroscopy
G. Wolf	High energy trends in e^+e^- physics
J.D. Bjorken	Electron-positron annihilation: some remarks on the theory

Invited papers:

G. Flügge	Heavy leptons
P. Söding	Jet analysis
J. Augustin	e^+e^- physics below J/ψ resonance
C.M. Kiesling	Results on charmonium from the Crystal Ball
G. Gidal	Results from the Mark II detector at SPEAR

Contributed papers:

J.G. Branson	Tests of quantum electrodynamics at PETRA
J.G. Branson	A measurement of $e^+e^- \to$ hadrons at $\sqrt{s}$ = 27.4 GeV
R. Cashmore	The hadronic final state in e^+e^- annihilation at c.m. energies of 13, 17, and 27.4 GeV
S. Brandt	Experimental search for Υ decay into 3 gluons
V. Blobel	Results from PLUTO at PETRA
R. Baldini-Celio	Results from ADONE
J. Weiss	Some first results from the Mark II at SPEAR
J.C. Bizot	A study of e^+e^- annihilation into hadrons in the 1600-2200 MeV energy range with the magnetic detector DM1 at DCI

e^+e^- PHYSICS : HEAVY QUARK SPECTROSCOPY

M. DAVIER
Laboratoire de l'Accélérateur Linéaire
Université de Paris-Sud, Orsay, France.

ABSTRACT

We review the situation of charmonium and charmed meson spectroscopy in e^+e^- annihilations in the light of the new experimental results presented at this conference. New information on bottomonium decays is also discussed.

1. INTRODUCTION

Since the ψ and ψ' discoveries at SPEAR in November 1974 [1], experiments using e^+e^- annihilations have provided a wealth of information on the spectroscopy of heavy narrow bound states. The subsequent discovery of D mesons [2] with the expected properties established the "existence" of the charmed quark (c) and allowed a comprehensive description of the new phenomena in e^+e^- around 3-5 GeV in the centre of mass energy. Last year the confirmation of the T and T' states [3] in e^+e^- collisions at DORIS [4] gave a strong support of their assignment to bound states of new heavy quarks (b).

We are going to review progress in this field over the last year, particularly through important contributions made to this conference from the DORIS and SPEAR colliding rings.

2. CHARMONIUM

Figure 1 represents the experimental situation on charmonium states prior to this conference. New results have been obtained at SPEAR on the P states and the pseudoscalar states which affect strongly the picture in figure 1.

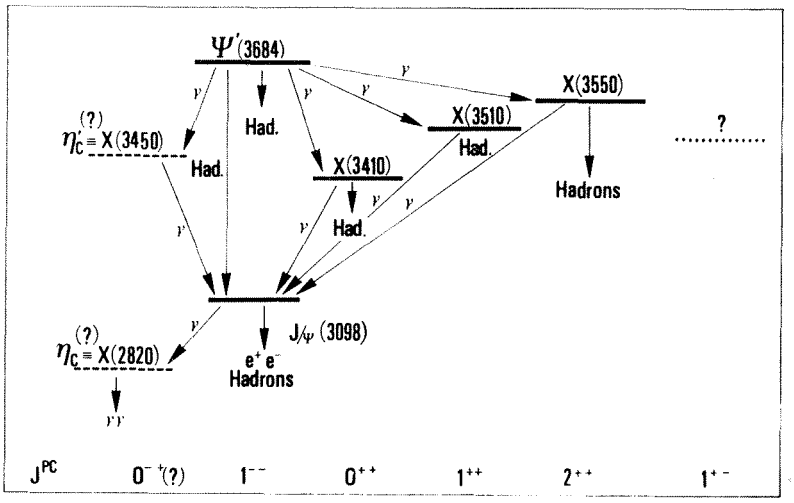

Figure 1 : Experimental knowledge of the narrow charmonium states in 1978.

2.1 P states

The C = +1 P states of charmonium are expected to lie between J/ψ and ψ' and can therefore be seen through radiative decays as shown in figure 2. The C =-1 P state cannot be produced easily in e^+e^- annihilations and has not been detected as yet.

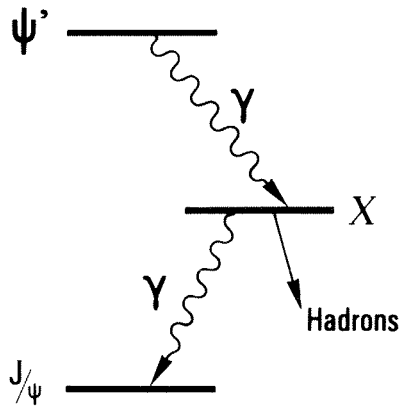

Figure 2 : Radiative decays of ψ' into C = +1 P states

Three techniques have been used so far to identify and study these particles :

i) Inclusive γ energy spectrum from ψ' : $\psi' \to \gamma X$

Since the decay $X \to \gamma\ J/\psi$ also takes place, two peaks are expected for a given X state : a monochromatic line and a Doppler-broadened peak.

ii) Cascade decays : $\psi' \to \gamma X \hookrightarrow \gamma\ J/\psi \hookrightarrow \ell^+\ell^-$

Here, one or two photons are detected together with the constrained lepton pair from the J/ψ decay.

iii) Hadronic decays of X : $\psi' \to \gamma X \hookrightarrow$ hadrons

If the soft photon is unseen, only constrained systems can be studied.

2.1.1 Previous situation

The expected 3 states $^3P_{0,1,2}$ have been seen : X(3410), X(3510) and X(3550). Using technique (i) the MP^{2}S^{3}P^5) and DESY-Heidelberg[6] experiments are in agreement and give a branching ratio (BR) for all 3 states $BR(\psi' \to \gamma X) \sim 7$ %. Method (ii) has been used by 5 experiments[5-9] which are in reasonable agreement although their experimental techniques for photon detection are widely different. The main virtue of method (iii) has been to assign quantum numbers to the X states[8] : if 0^{++} is well established for X(3410), there is no unique assignment for X(3510) and X(3550) although 1^{++} and 2^{++} are favoured. Confirmation of these assignments can also come from situation (ii) looking at angular correlations between photons and $\ell^+\ell^-$ pair.

This ideal picture (for charmonium) has been spoiled by the observation of 2 additional "states" : X(3590) seen in the cascade decays[6] and X(3450) also seen in the cascade decays but not in hadronic modes[8]. Both states are not well established, their existence relying on very small statistics. It has been suggested that X(3450) could be the pseudoscalar partner of ψ' ; this will be discussed in the next section.

The situation on P states before this conference is best summarized by the cascade-decay plot of the two possible X mass compiled from previous experiments[10]

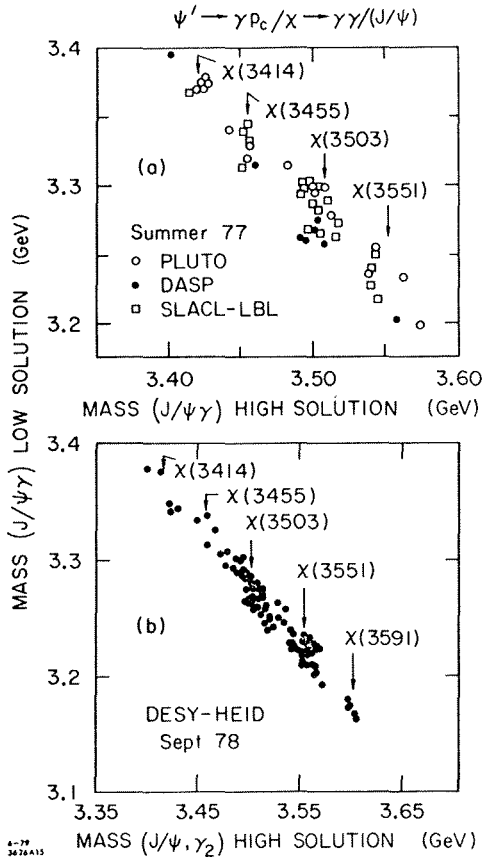

Figure 3 : Plot of the 2 solutions for the γ J/ψ invariant mass in the ψ' cascade decays from experiments before this conference.

2.1.2. New experimental data

SLAC-LBL (Mark II)[11]

Clean results have been presented on the cascade decays where both photons are detected in the liquid argon calorimeter of the Mark II detector together with the leptonic decays of ψ. The final state is therefore very well constrained and the background from $\psi' \to \eta^\circ\psi$ is subtracted out (see fig. 4).

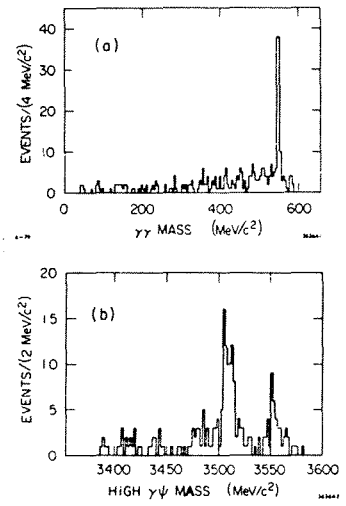

Figure 4 : New SLAC-LBL data[11] on ψ' cascade decays

In general, there is good agreement with previous data although X(3450) is not confirmed :

$$BR(\psi' \to \gamma X(3450))\ BR(X(3450) \to \gamma\psi) < 1.2\ 10^{-3} \qquad (90\ \%\ C.L.)$$

as compared to $(8 \pm 4)10^{-3}$ in the Mark I experiment. Nothing can be said for or against the existence of X(3590) since the low energy γ escapes detection for this high mass.

Crystal Ball[10,12]

This is a powerful neutral detector with large solid angle and good photon energy resolution : so far $\Delta E_\gamma/E_\gamma \sim 8$ % has been achieved at E_γ = 100 MeV and the resolution should still be increased with better calibration.

The γ inclusive spectrum at ψ' is shown in figure 5 : again good agreement with "old" experiments with better and cleaner data. There is no evidence for X(3450) but no limit is given so far since a detailed study of the detector is necessary.

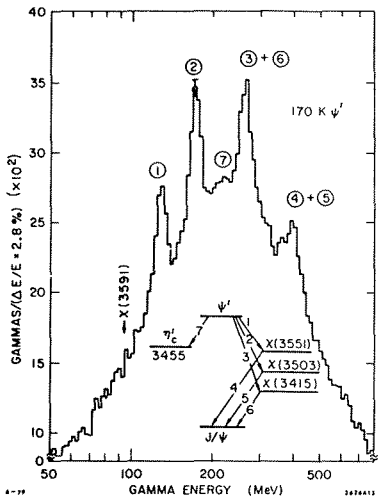

Figure 5 : Inclusive γ energy spectrum at ψ'[12] with expected transitions

Figure 6 displays the results from the cascade decays showing the strong signals of X(3510) and X(3550); as already known X(3410) shows up only weakly because of the small branching ratio for $X(3410) \to \gamma\psi$. Also some events are seen around 3450 and 3590 MeV but with a very small rate.

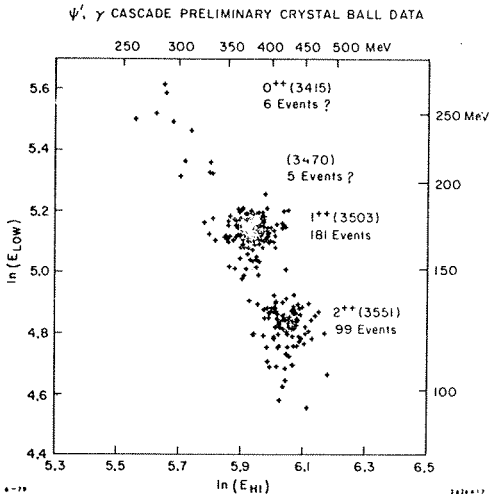

Figure 6 : Two-dimensional γ energy spectrum from ψ' cascade decays[12]

2.1.3. Conclusions

The simple picture of the 3 P states is confirmed by the new experiments which are in general cleaner and more constrained than previous ones. The consistency of all the experiments is demonstrated in figure 7.

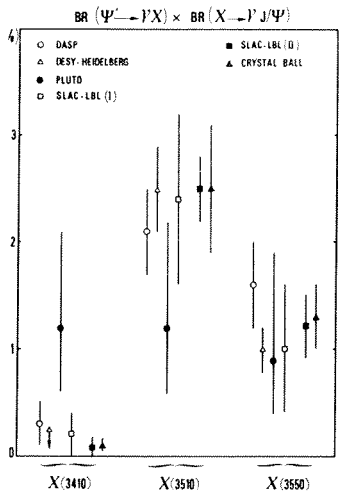

Figure 7 : Compilation of branching ratios $BR(\psi' \to \gamma X) \times BR(X \to \gamma\psi)$ for the 3 states.

No strong conclusions can be reached regarding new states at 3450 and 3590 MeV : however their rate is definitely much smaller than observed previously. The measured rate has become so small that one should seriously consider the possibility of a purely electromagnetic decay of ψ' into $\gamma\gamma\psi$ without X states. A preliminary calculation[13] gave a branching ratio : $BR_{QED}(\psi' \to \gamma\gamma\psi) \lesssim 3\ 10^{-3}$, quite consistent with the small background level around the most prominent X peaks.

Better results should be available soon since Mark II and Crystal Ball have only analyzed about 1/4 of their data sample.

2.2. Pseudoscalars

One expects the $^1S_0$ states to lie just below the corresponding $^3S_1$ states with a possible M1 radiative transition between them (fig. 8).

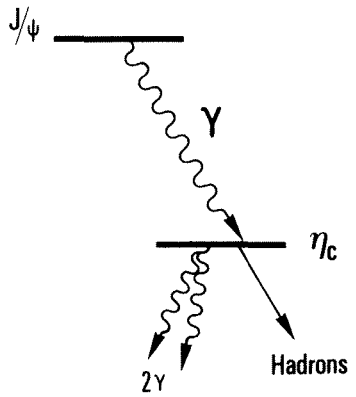

Figure 8 : Radiative transition between $^3S_1$ and $^1S_0$ levels of charmonium

$$J/\psi \to \gamma\eta_c$$
$$\psi' \to \gamma\eta_c'$$

η_c and η_c' are then expected to decay into hadrons with a characteristic 2γ decay mode.

2.2.1. Situation before conference

There was a strong indication for a state decaying in 2γ in the decay of $J/\psi \to 3\gamma$ seen by the DASP experiment[14] at DORIS with the following properties :

$$M_X = 2820 \pm 14 \text{ MeV}$$
$$\Gamma_X(\text{exp}) = 40 \pm 14 \text{ MeV} \quad \text{consistent with experimental resolution}$$
$$BR(J/\psi \to \gamma X) \times BR(X \to \gamma\gamma) = (1.4 \pm 0.4)\ 10^{-4}$$

Although the $^3S_1$ - $^1S_0$ mass-splitting might look too large, it was proposed at that time that X(2820) be associated with the sought η_c ; this assignment prompted many theoretical investigations trying to explain the large splitting.

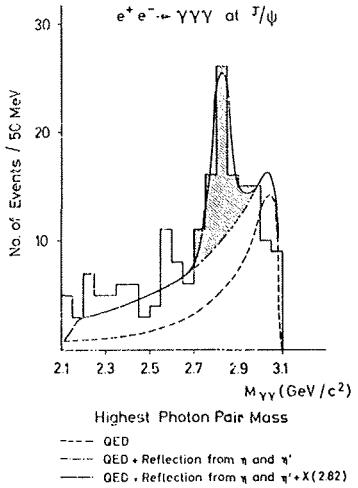

Figure 9 : High $\gamma\gamma$ mass solution in the decay $J/\psi \to 3\gamma$ observed by DASP[14] showing evidence for X(2820)

Only an upper limit could be given by the DESY-Heidelberg experiment : $BR(J/\psi \to \gamma X) \times BR(X \to \gamma\gamma) < 2.8\ 10^{-4}$ but, most disturbing, was the non-observation of any hadronic mode by the SLAC-LBL collaboration.

As previously mentioned it was also suggested that X(3450) could be identified with η_c', this proposal being no less problematic than the previous one.

2.2.2. Crystal Ball results[12]

Again this experiment makes a powerful contribution to the field.

Inclusive γ spectrum at ψ

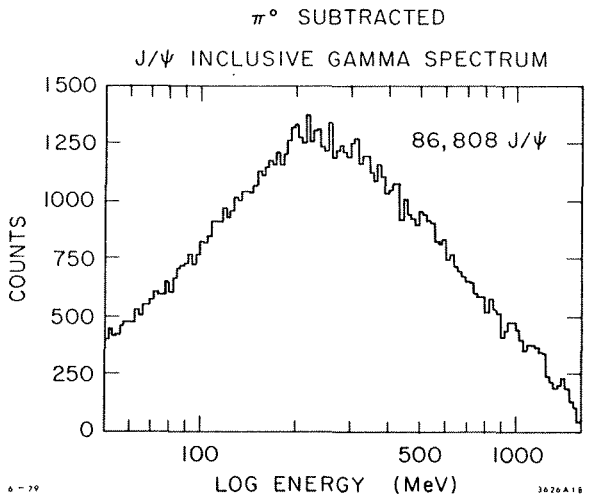

Figure 10 : Inclusive γ spectrum at ψ from Crystal Ball experiment[10]

Figure 10 shows the γ energy spectrum on about 10 % of their data. In contrast to the ψ' spectrum there is no indication for a signal anywhere above 50 MeV. In particular :

$$BR(\psi \to \gamma\ X(2820)) < 5\ 10^{-3} \quad (90\ \%\ C.L.)$$

This result, taken together with the DASP combined branching ratio, implies - if the X(2820) state seen by DASP is real - :

$$BR(X(2820)) > 2\ \%$$

3γ decay of ψ

For this mode the full sample of nearly one million ψ decays has been analyzed. The full information can be derived from the Dalitz plot in figure 11(a). The two bands corresponding to η and η' production are clearly visible and are projected in figure 11(b) : both correspond to the expected mass resolution. As already clear in the Dalitz plot, the high mass projection shown in figure 11(c) does not indicate any enhancement around 2820 MeV in clear contradiction to the DASP result. In fact they quote an upper limit for X(2820) production

$$BR(\psi \to \gamma X) \times BR(X \to \gamma\gamma) < 3\ 10^{-5} \quad (90\ \%\ C.L.)$$

$$(DASP\ (14 \pm 4)\ 10^{-5})$$

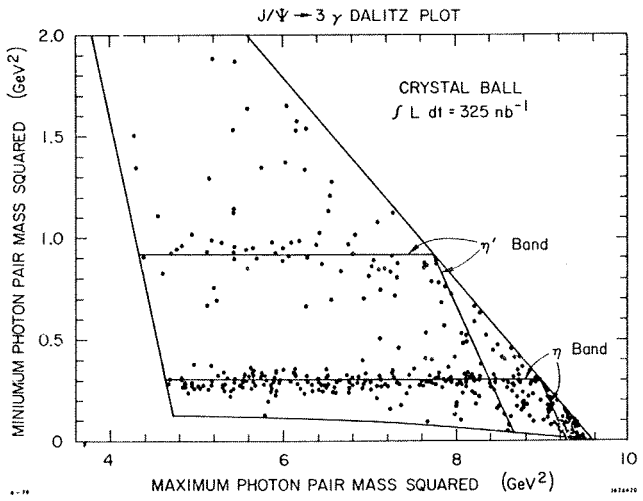

Figure 11(a) : Dalitz plot for $\psi \to 3\gamma$ obtained in the Crystal Ball experiment[12])

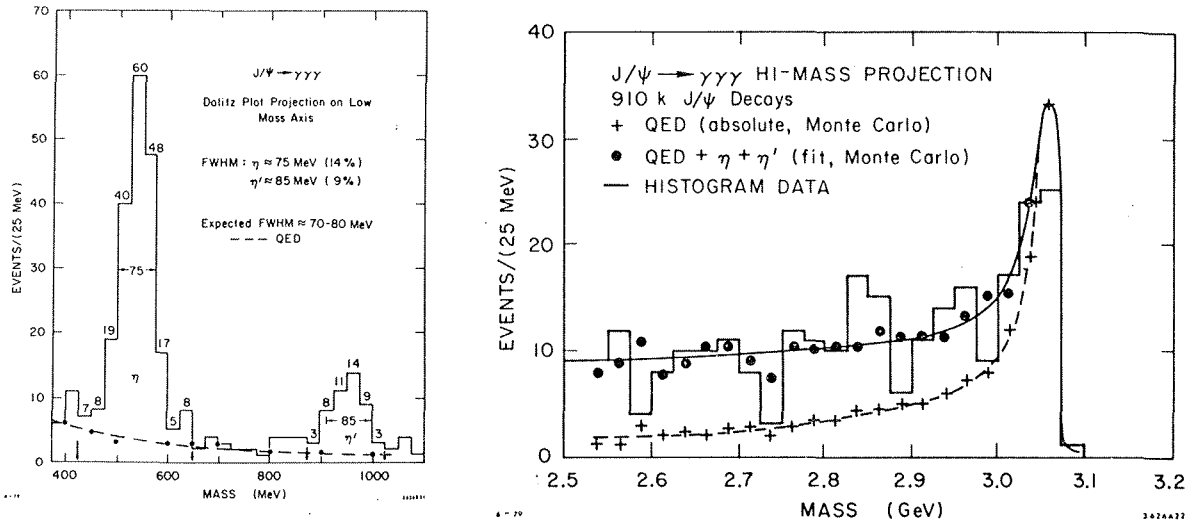

Figure 11(b) (c) : Low and high γγ mass projections

A major discrepancy between the two experiments lies in the relative ratio of η' and X(2820) production : DASP has a weak η' signal in the main band of the Dalitz plot. To further compare we list in table 1 the respective branching ratios for η and η' as seen by the different experiments.

Table 1

Branching ratios for $J/\psi \to \gamma\eta$ and $\gamma\eta'$

Experiment	$10^3 \times BR(J/\psi \to \gamma\eta)$	$10^3 \times BR(J/\psi \to \gamma\eta')$
Crystal Ball[12]	1.15 ± .17 *	6.3 ± 1.6 *
DASP[14]	.82 ± .10 *	2.2 ± 1.1 *
DESY-Heidelberg[6]	1.3 ± .4 *	2.4 ± .7 **
SLAC-LBL (Mark I)[15]		3.8 ± 1.3 **
SLAC-LBL (Mark II)[15]		3.4 ± .7 **

* γγ decay mode

** $\pi^+\pi^-\gamma$ decay mode

It should be noted that some uncertainty still exists on the γγ branching ratio of η'[16]. At that point it seems to us that the Crystal Ball experiment is cleaner and more convincing although no clear-cut argument can be made against the DASP finding.

2.2.3. Implications of X(2820) and X(3450) as η_c and η_c' candidates

Most charmonium experts were unhappy about last year's situation[17]. We review the main points of disagreement with the simple charmonium picture :

i) $J/\psi - \eta_c$ mass splitting

Assuming that the only spin-spin force is generated by one-gluon exchange, we expected :

$$M(J/\psi) - M(\eta_c) = \frac{\alpha_s}{2\alpha^2}\left(\frac{M_\psi}{m_c}\right)^2 \Gamma(\psi \to e^+e^-)$$

$$= 36 \text{ MeV (instead of 280 MeV observed)}$$

if $\alpha_s = .19$ and $m_c = 1.5$ MeV

ii) Radiative rate of $J/\psi \to \gamma\eta_c$

Using the Crystal Ball limit on inclusive production :

$$BR(J/\psi \to \gamma\eta_c) < 5\ 10^{-3}$$

we deduce :

$$\Gamma(J/\psi \to \gamma\eta_c) < 350 \text{ eV}$$

in contradiction with charmonium estimates of M1 transition by 2 orders of magnitude :

$$\Gamma(J/\psi \to \gamma\eta_c) = \frac{16}{27}\alpha\frac{k^3}{m_c^2}\left|\langle\psi|\eta_c\rangle\right|^2 = 32 \text{ keV}$$

iii) 2γ branching ratio of η_c

A branching ratio $BR(\eta_c \to \gamma\gamma) > 2$ % disagrees with the theory by a factor 15 since :

$$BR_{th}(\eta_c \to \gamma\gamma) = \frac{\Gamma(\eta_c \to \gamma\gamma)}{\Gamma(\eta_c \to gg)} = \frac{8}{9}\left(\frac{\alpha}{\alpha_s}\right)^2$$

$$= .13 \text{ \%}$$

Here one should be more cautious since corrections to 1st order QCD are expected to be rather large[18] as we shall discuss later.

Similar discrepancies occur[17] if one assigns the previously proposed X(3450) to be the η_c'. Since new experiments do not confirm either state this will bring some relief to afflicted theorists but we now have to address the question of finding the true η_c and η_c' particles.

2.2.4. Future searches

i) $J/\psi \to \gamma\eta_c$

The transition rate depends on the mass splitting as seen in figure 12(a). The expected η_c has a branching ratio of about 10^{-3} which could just possibly be reached by the Crystal Ball experiment. Right now they can exclude an η_c with a mass splitting larger than 75 MeV but their increased statistics and resolution should bring their sensitivity down to about 35 MeV[12].

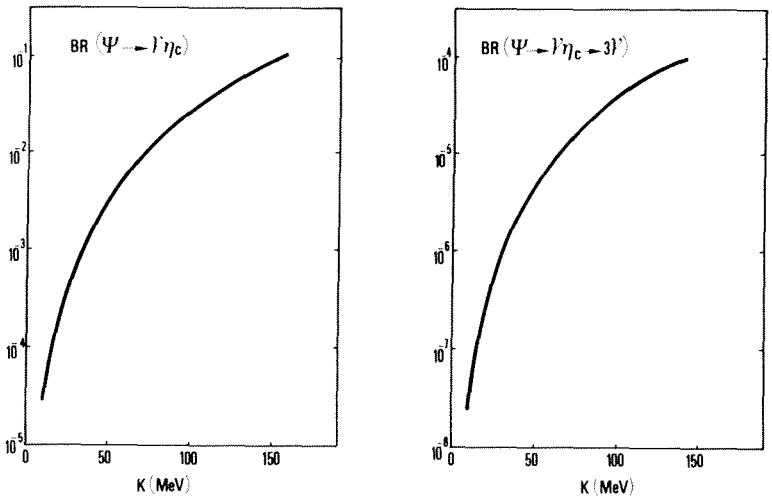

Figure 12 : Estimates for branching ratios in charmonium model[17]
as a function of mass splitting
(a) $BR(J/\psi \to \gamma\eta_c)$
(b) $BR(J/\psi \to \gamma\eta_c) \times BR(\eta_c \to \gamma\gamma)$

The 3γ mode appears extremely hard to detect if the splitting is small as indicated by figure 12(b), with the additional disadvantage of the QED background.

In general things are worse for η_c' with an expected smaller splitting from ψ'.

ii) $\psi' \to \gamma\eta_c$

This decay rate is difficult to evaluate theoretically because of the strong suppression of the ψ' and η_c wave function overlap. Since its value depends on small corrections to the model estimates range from 1 to 10 keV[19] or possibly even smaller. The lower limit of 4 keV from the MP^2S^3D experiment has been improved by the Crystal Ball

$$BR(\psi' \to \gamma\eta_c) < 0.9 \text{ keV}$$
$$(\text{for } M_{\eta_c} \sim M_\psi)$$

This value should be decreased in the near future.

iii) η_c production in two-photon collisions

This process, shown in figure 13, has a measurable cross section :

$$\sigma(ee \to ee\eta_c) \simeq \frac{64\alpha^2}{M_{\eta_c}^3} \Gamma(\eta_c \to \gamma\gamma) \ln^2\frac{E}{2m} \ln\frac{2E}{M_{\eta_c}}$$

$$\simeq 60 \text{ pb} \quad \text{at} \quad \sqrt{s} = 2E = 30 \text{ GeV}$$

using the expected partial width $\Gamma(\eta_c \to \gamma\gamma) = 8$ keV. Such a measurement should be possible

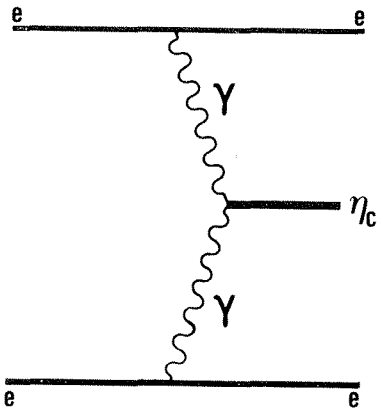

Figure 13 : Diagram for η_c production in 2γ collisions

- given enough luminosity - and separation from background could make use of sphericity : hadron production by 2γ should be predominantly at low p_T around the beam whereas η_c production should lead to essentially isotropic events.

2.3. Strong coupling constant α_s in charmonium

2.3.1. Mass spectrum

The mass spectrum of $c\bar{c}$ states can be reproduced with a phenomenological potential between the two quarks. We know that such a potential deviates considerably from the simple Coulomb potential generated by gluon exchange. In all phenomenological treatments one adds to it a confining part taken generally as a linear term in r :

$$V(r) = -\frac{4}{3}\frac{\alpha_s}{r} + a\,r$$

Since the Coulomb part do not play a strong role in charmonium, we do not expect α_s to be well determined from the particle spectrum alone. Fits are obtained with a range :

$$\alpha_s \sim 0.2 - 0.4$$

2.3.2. Hadronic width of quarkonia

In the heavy quarkonium model direct hadron decays of 1^{--} states are mediated by three gluons as depicted in figure 14.

This yields :

$$\frac{\Gamma(Q\bar{Q} \to 3g)}{\Gamma(Q\bar{Q} \to \ell^+\ell^-)} = \frac{10(\pi^2 - 9)}{81\,\pi\,e_Q^2}\frac{\alpha_s^3}{\alpha^2}$$

giving the following values for the known narrow states :

$$\begin{array}{ll} J/\psi & \alpha_s = .19 \pm .02 \\ \psi' & \alpha_s \lesssim .26 \pm .02 \text{ (cascade decays removed)} \\ \Upsilon & \alpha_s = .19\,\sqrt[3]{\Gamma_\Upsilon(\text{keV})/50} = .19\,^{+\,.05}_{-\,.03} \end{array}$$

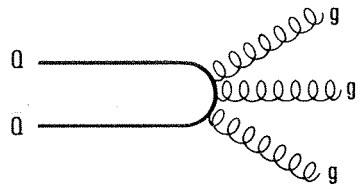

Figure 14 : Hadronic decay of 1^{--} $Q\bar{Q}$ state into 3 gluons (lowest order QCD)

2.3.3. Scaling violation in deep inelastic lepton scattering

Scaling violations in deep inelastic eN, μN and νN scattering are now manifest and can be interpreted in the framework of QCD[20]. We have learned that such an interpretation was quantitatively difficult, but in general analyses point to a larger value of the coupling α_s

$$\alpha_s(J/\psi) \sim 0.4 - 0.7$$

2.3.4. Radiative decays of quarkonia

Photon emission from 1^{--} $Q\bar{Q}$ states is expected through the QCD diagram in figure 15.

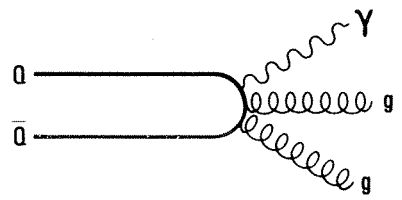

Figure 15 : Radiative decay of 1^{--} $Q\bar{Q}$ state giving two gluons (lowest order QCD)

Therefore such a process yields an independent measurement of α_s through the ratio :

$$\frac{\Gamma(Q\bar{Q} \to \gamma 2g)}{\Gamma(Q\bar{Q} \to 3g)} = \frac{72\ e_Q^2}{10}\ \frac{\alpha}{\alpha_s}$$

For the J/ψ state such a relation gives :

$$\frac{\Gamma(J/\psi \to \gamma \text{ hadrons})}{\Gamma(J/\psi \to \text{hadrons})} = \frac{.023}{\alpha_s} \sim 0.1$$

The observation of the total radiative decay of J/ψ is therefore a good test of QCD since usually radiative decays are more typically $\lesssim 10^{-2}$ of hadronic decays.

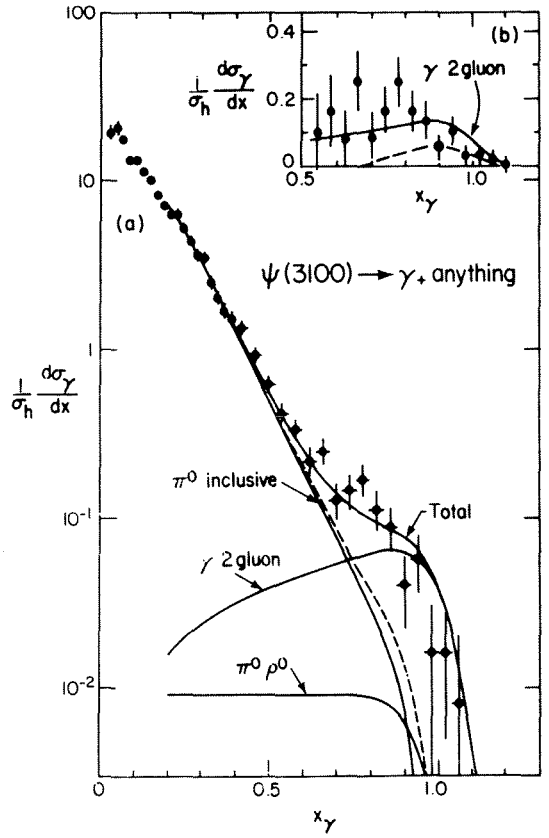

Figure 16 : Photon spectrum at ψ observed by the Mark I-LGW[21] at SPEAR. The excess of events at large x is attributed to direct photons.

New data have been obtained by the Mark I detector at SPEAR supplemented by a lead-glass array detector[21]. They have observed the inclusive γ distribution from ψ decays : this spectrum is dominated by photons from π° decay except for the large x part where they see an excess of events which they attribute to the direct radiative transition (fig. 16). This is some uncertainty in the determination of the π° background at large x since the measured π° spectrum is not statistically precise enough and the authors rely on the average of $\pi^\pm$ which agrees with the π° data within uncertainties.

They obtain :

$$BR(J/\psi \to \gamma \text{ hadrons}) = (4.9 \pm 0.7)\ 10^{-2}$$

corresponding to :

$$\alpha_s = .35 \pm .12$$

We must however be cautious about the QCD interpretation of this result because most of the calculated γ2g spectrum corresponds to a hadronic mass less than 2 GeV where resonances certainly play an important role. Adding up known rates, $\psi \to \gamma\pi^\circ$, $\gamma\eta$, $\gamma\eta'$ and γf, yields at most a branching ratio of 0.7 to 1 %. Where is the observed rate coming from ?

2.3.5. A word of caution

As pointed out by Barbieri et al.[18] higher order QCD corrections to transition rates in charmonium may be uncomfortably large. For example they have computed the second order correction to this ratio :

$$r = \frac{\Gamma(\eta_c \to 2g)}{\Gamma(\eta_c \to 2\gamma)} = r_1(1 + 22.1 \frac{\alpha_s}{\pi})$$

where r_1 is the first order calculation.

This remark brings a cloud of pessimism over applications of QCD to charmonium states. One should not therefore be too much worried about the dispersion in α_s values obtained from different methods and be happy enough if a qualitative description of transition rates is achieved.

3. CHARMED PARTICLES

3.1. D mesons

3.1.1. Semileptonic decays

All experiments[22-24] are in agreement giving a branching ratio :

$$BR(D \to e^+X) = (8.3 \pm 1.1)\ \%$$

averaged over D° and D^+ decays. Such a value disagrees with the naive argument using quark counting and colour giving a value of 20 % (3 coloured quarks for each lepton), but the difference seems well accounted for by QCD corrections[25].

The hadronic final state connected to the upper vertex in figure 17 has been studied mostly looking at $K^{\mp}e^{\pm}$ mass distributions.

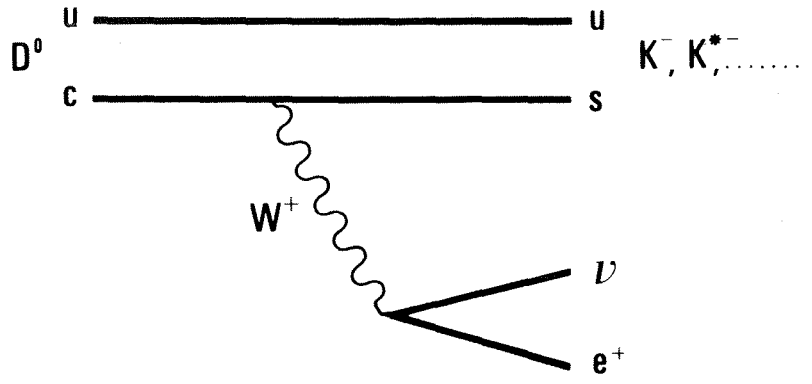

Figure 17 : Semi-leptonic decay of D° into strange particles and lepton pair.

Experiments at different energies disagree on the amount of K versus K^* production as can be seen in figure 18 from the Mark I-LGW experiment[21]

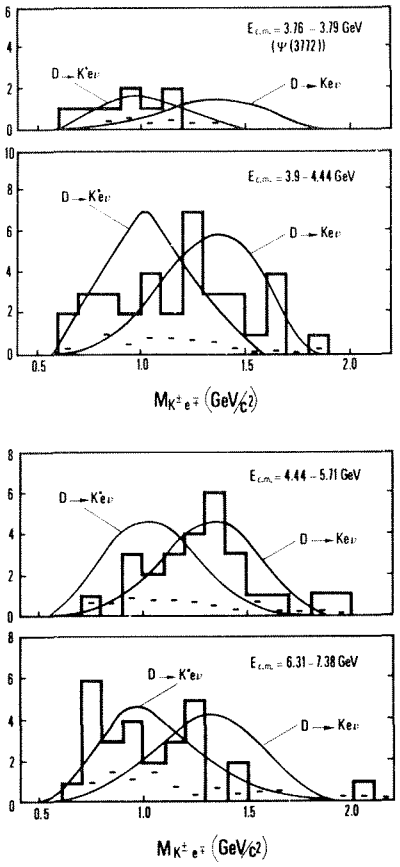

Figure 18 : $K^{\mp}e^{\pm}$ invariant mass distributions for different centre of mass energies[21]. The dashed line is the background from hadrons misidentified as electrons.

The cleanest test is at energy of $\psi''(3770)$ since $D\bar{D}$ are produced there. A higher energies there might be contributions from F production but the largest uncertainty comes from the ratio of D^+ to D° production which give different contributions to the observed spectra. Indeed :

$$D^\circ \to K^- \ , \ K^{*-} \hookrightarrow K^-$$

$$D^+ \to K^{*\circ} \hookrightarrow K^- \quad \text{only}$$

D° and D^+ production has been crudely measured[21] but one can say that the spectra shown in figure 18 are not understood in detail. From the ψ'' data alone one may nevertheless conclude that K^* is dominant over K in semi-leptonic decays.

3.1.2. Cabibbo suppressed transitions

This can truly be classified into the second generation of charm experiments in e^+e^-

annihilations. Roughly one expects :

$$\frac{\Gamma(D^\circ \to K^-K^+)}{\Gamma(D^\circ \to K^-\pi^+)} \sim \frac{\Gamma(D^\circ \to \pi^-\pi^+)}{\Gamma(D^\circ \to K^-\pi^+)} \sim \tan^2\theta_c \sim 0.05$$

where θ_c is the Cabibbo angle.

A nice measurement of these decay modes has just been completed by the SLAC-LBL collaboration using the Mark II detector[15]. From about 50 000 ψ'' decays into $D\bar{D}$ (an ideal tagged source of monochromatic D mesons) with K/π separation using time-of-flight, they have obtained the spectra in figure 19 where the $\pi^+\pi^-$ and K^+K^- modes are well apparent together with the spurious peaks from misidentified $K^-\pi^+$ modes appearing at the expected places.

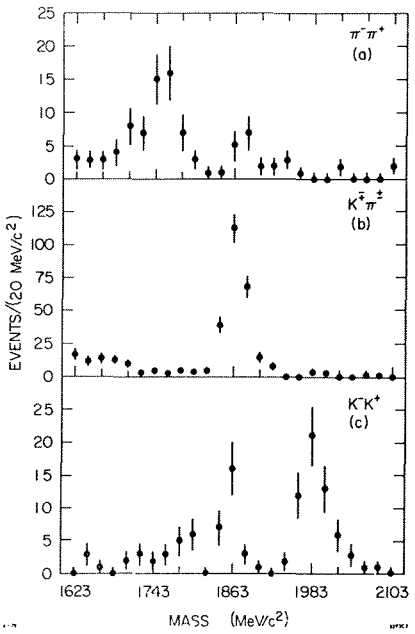

Figure 19 : K^-K^+, $K^-\pi^+$ and $\pi^-\pi^+$ invariant mass distributions[15] at $\psi''(3770)$ showing the Cabibbo-suppressed modes of $D^\circ(1863)$.

The following ratios are obtained :

$$\frac{\Gamma(D^\circ \to \pi^-\pi^+)}{\Gamma(D^\circ \to K^-\pi^+)} = .033 \pm .014$$

$$\frac{\Gamma(D^\circ \to K^-K^+)}{\Gamma(D^\circ \to K^-\pi^+)} = .113 \pm .030$$

$$\frac{\Gamma(D^\circ \to \pi^-\pi^+)}{\Gamma(D^\circ \to K^-K^+)} = .29 \ {}^{+\ .17}_{-\ .12}$$

Roughly these values are in agreement with the expected level for a Cabibbo-suppressed

transition. Can we go any further to understand them more quantitatively ?

The charged hadronic weak current can be described in the 6-quark model by the expression :

$$J_\mu \sim (\bar{u}\ \bar{c}\ \bar{t})\ \gamma_\mu(1 - \gamma_5)\ U\begin{pmatrix} d \\ s \\ b \end{pmatrix}$$

where U is a 3 × 3 unitary matrix which depends on 3 Cabibbo-like missing angles θ_1, θ_2, θ_3 and phase δ related to CP violation[26]. Explicitly we have :

$$U = \begin{pmatrix} c_1 & -s_1c_3 & -s_1s_3 \\ s_1c_2 & c_1c_2c_3 - s_2s_3e^{i\delta} & c_1c_2s_3 + s_2c_3e^{i\delta} \\ s_1s_2 & c_1s_2c_3 + c_2s_3e^{i\delta} & c_1s_2s_3 - c_2c_3e^{i\delta} \end{pmatrix}$$

where $c_i = \cos\theta_i$ and $s_i = \sin\theta_i$, i = 1, 2, 3.

One can proceed to compute the amplitude for each measured transition, a procedure summarized in Table 2.

Table 2

Transition amplitudes for Cabibbo-suppressed D decays

Process	Amplitude	Phase-space correction
D° ($\bar{u}c$) → K^- ($\bar{u}s$) + π^+ ($u\bar{d}$)	$c_1(c_1c_2c_3 - s_2s_3e^{i\delta})$	1.0
D° ($\bar{u}c$) → K^- ($\bar{u}s$) + K^+ ($u\bar{s}$)	$s_1c_3(c_1c_2c_3 - s_2s_3e^{i\delta})$	.92
D° ($\bar{u}c$) → π^- ($\bar{u}d$) + π^+ ($u\bar{d}$)	$s_1c_1c_2$	1.07

We therefore expect : $$\frac{\Gamma(D^\circ \to K^-K^+)}{\Gamma(D^\circ \to K^-\pi^+)} = .92\ \tan^2\theta_1\ \cos^2\theta_3$$

which should range from .39 to .051 using θ_1 and θ_3 values derived from semi-leptonic decays of n, Λ , K[27,28]. However it is well-known that SU(3) breaking plays a significant role in these two-body processes : for example we have a similar situation in the leptonic decays of π and K.

$$\frac{\Gamma(K \to \mu\nu)}{\Gamma(\pi \to \mu\nu)} \times \text{phase space} = \left(\frac{f_K}{f_\pi}\right)^2 = .075$$

which is again larger than the theoretical estimate and in agreement with the K^-K^+ measured rate.

As far as the $\pi^+\pi^-$ decay rate is concerned it is harder to make a casual comparison since it depends on all angles and δ. Estimates of the relative ratio based on calculations made in Ref. 28 range between .02 and .14 in agreement with experiment. Provided SU(3) breaking can be handled the $\pi^+\pi^-$ mode contains useful information on the weak mixing matrix and can be used to narrow the possible range for the less well-known angles. This is important since these angles control the weak decays of b and t quarks.

As a final remark it is possible that SU(3) breaking could be less important if inclusive D decays could be measured along the same lines :

$$D^\circ \to K\bar{K} + \text{pions}$$
$$D^\circ \to \bar{K} + \text{pions}$$
$$D^\circ \to \text{pions}$$

This is of course much harder experimentally.

3.2. Other charm states

3.2.1. F mesons

No new information has been contributed since the original DASP finding[29] on

$$e^+e^- \to F\bar{F}^* \quad (\to \gamma\bar{F}) \qquad \text{with} \quad F^\pm \to \eta\pi^\pm \quad (\to \gamma\gamma)$$

Both Mark II and Crystal Ball experiments have data which is being analysed.

3.2.2. Charmed baryons

The evidence for charmed baryons in e^+e^- reactions is only indirect : no mass peak has been deemed significant enough to be shown officially. On the other hand new data have been presented by the Mark II collaboration[11] on the inclusive $\bar{p}$, Λ and $\bar{\Lambda}$ production between 4.5 and 6 GeV. They are shown in figure 20 : a smooth rise occurs in both p and Λ production between 4.5 and 5 GeV with a levelling-off above. This is consistent with charmed baryon threshold with a Λ_c^+ mass around 2260 MeV.

The step is more important for $\bar{p}$ than for Λ, $\bar{\Lambda}$:

$$2\Delta R_{\bar{p}} \simeq .35$$
$$\Delta R_{\Lambda,\bar{\Lambda}} \simeq .06$$

Also we know[30] that $2\Delta R_{\bar{\Sigma}^{\pm}} = .24 \pm .10$.

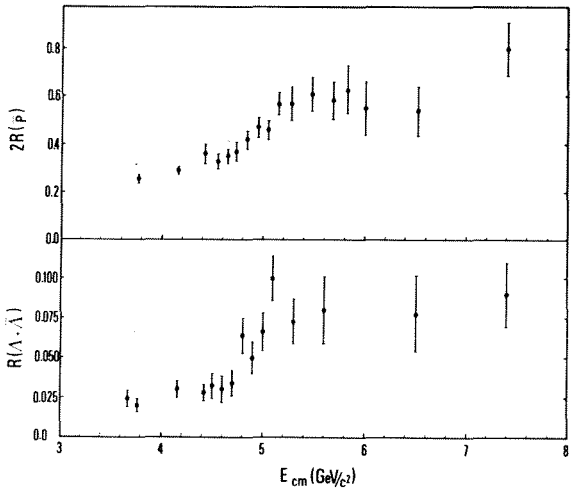

Figure 20 : Inclusive $\bar{p}$ and Λ, $\bar{\Lambda}$ production[11]

From these results we learn that charmed baryon decays yield $\bar{K}N$.... and Σ.... final states rather than Λ.... final states. This is maybe not too surprising according to the naive quark-model picture in figure 21 :

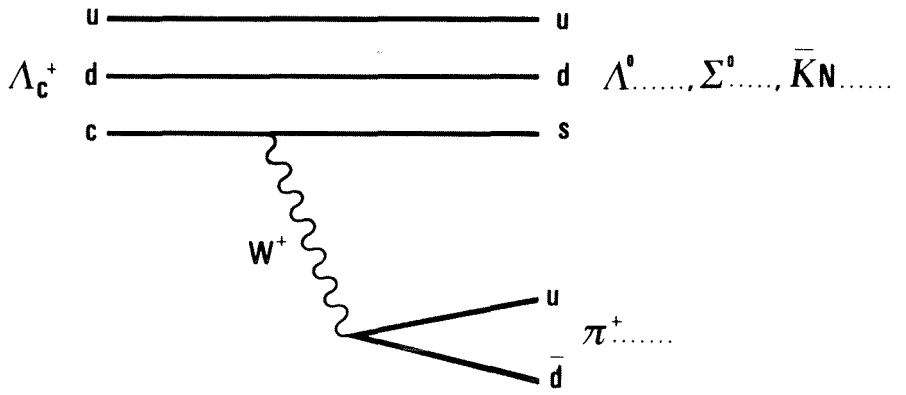

Figure 21 : Quark diagram for Λ_c^+ decay

The known Y^* spectroscopy below 2 GeV tells us that $\bar{K}N$ states are more coupled than $\Sigma\pi$, itself larger than $\Lambda\pi$ (except for one state, Y(1385)). Also Σ decays are probably counted in the p, $\bar{p}$ inclusive rate since their detection is hardly feasible experimentally.

3.3. Charmed quark fragmentation

3.3.1 Inclusive D production

D meson production has been studied in an inclusive way between 3.7 and 5.8 GeV by a SLAC-LBL collaboration[31] observing the $D^\circ \to K^-\pi^+$ and $D^+ \to K^-\pi^+\pi^+$ decay modes. The D^+

production is systematically lower than D°, but the results have been averaged to give the total D inclusive cross section :

$$\sigma_D = \frac{1}{2}\left[\sigma_{D^+} + \sigma_{D^-} + \sigma_{D^\circ} + \sigma_{\bar{D}^\circ}\right]$$

which is best expressed as :

$$R_D = \frac{\sigma_D}{\sigma_{\mu\mu}}$$

The observed value for R_D is 1.5 with an uncertainty of about 0.5 above charm threshold and resonances. This is consistent with the total charm step in R although some room ($\sim$ .5) could be allowed for F production. This is best displayed in figure 22 showing the various contributions to R : $R_{old}(u\,d\,s)$, $R_{\tau^+\tau^-}$ and $R_{B\bar{B}}$ inferred from $R_{p,\bar{p}}$ and $R_{\Lambda,\bar{\Lambda}}$ and R_D represented as data points. There is good agreement with the top curve drawn through R data.

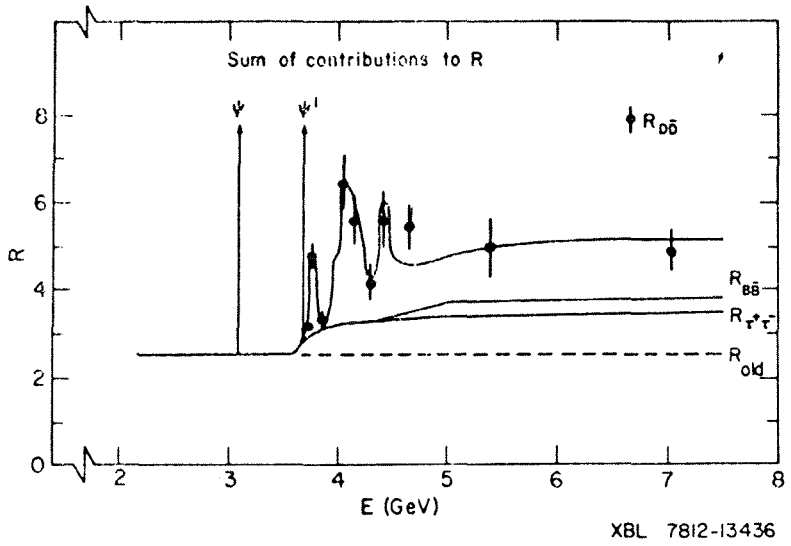

Figure 22 : Various contributions to R including D inclusive production[21] (see text for explanations).

This is additional evidence of our understanding of the charm phenomenology in e^+e^-.

3.3.2. Fragmentation of c quark into D mesons

The energy distribution of produced D mesons has been measured around 7 GeV centre of mass energy[32]. Since the primary process is thought to be the creation of a $c\bar{c}$ pair, this measurement offers the possibility to study how c quarks fragment into hadrons. One usually expects D mesons to appear as leading particles due to the heavy mass of the c quark. Unfortunately the energy may be somewhat too low since only a small range is accessible. Defining the energy fraction

$$z = \frac{2E_D}{\sqrt{s}}$$

we have here $0.54 < z < 1$. Data are shown in figure 23 for the scaling cross section $s\frac{d\sigma}{dz}$.

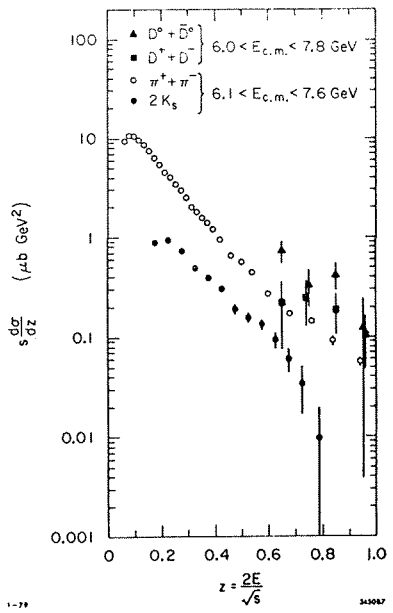

Figure 23 : Inclusive spectra for D° and D^+ production[32] compared to π and K°_S spectra[33]

Although statistics is not very large, one may say that D^+ and especially D° productions are not as flat in z as expected, the latter one being as steep as π production. There is certainly a need for more statistics[34] and also higher energies, since there seems to be some disagreement with di-lepton analyses in ν reactions which appear to call for a flat z distribution. The e^+e^- data is a much direct approach and should be improved in the future.

4. BOTTOMONIUM

4.1. Υ and Υ' parameters

No new information has come out this year on Υ and Υ' spectroscopy from e^+e^- machines which were not operating at these energies. In table 3 we recall the properties of these states established by experiments last year at DORIS[4]. When these studies resume, possibly this coming fall, the most pressing measurement will remain the leptonic branching ratio of Υ and Υ' which are needed in order to extract the total width of these particles. This is important for their understanding in the framework of QCD applied to heavy quarkonia.

Table 3

Mean values for Υ and Υ' parameters[35]

State	Mass (GeV)	Γ_{ee} (keV)	$B_{\mu\mu}$ (%)	Γ_{tot} (keV)
Υ	9.46 ± 0.01	1.2 ± 0.2	2.6 ± 1.4	> 25 95 % C.L.
Υ'	10.02 ± 0.02	.33 ± .10	?	?

4.2. Final state in Υ decays

Heavy $Q\bar{Q}$ quarkonia are predicted to decay into 3 gluons according to QCD (fig. 14). Given enough energy one expects the final state in their decays to be different from the hadronic background in e^+e^- which is dominated by $q\bar{q}$ production. At J/ψ there no evidence for a significant change in the hadronic final state, in particular there is no multiplicity change going through the resonance. Owing to the larger Υ mass there is a chance to test the 3 gluon mechanism predicted by QCD.

Good data from the PLUTO group[36,37] on some 1250 Υ direct decays have been presented and are discussed below.

4.2.1. Multiplicity

An increase in charged multiplicity is seen at the Υ from (4.9 ± 0.1) at 9.4 GeV to (5.9 ± 0.1) for the direct Υ decays. This is in qualitative agreement with the fact that more quanta are active in the decay.

4.2.2. Sphericity

Although hadronic production at 9.4 GeV is strongly jet-like - as seen through the average sphericity - there is a marked increase of sphericity at the Υ, corresponding to a much more isotropic configuration. This behaviour, striking in figure 24, is well reproduced by a Monte-Carlo model of 3-gluon production with gluons fragmenting like quarks[36].

The sphericity distribution of direct Υ decays is also in very good agreement with 3-gluon model disagreeing with a simple phase-space simulation (fig. 25). Agreement with 3-gluon model is also seen in the angular distribution of the sphericity main axis with respect to the e^+e^- beam line.

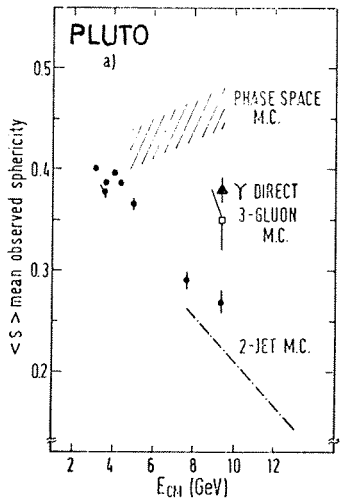

Figure 24 : Mean observed sphericity <S> as a function of centre of mass energy[36]

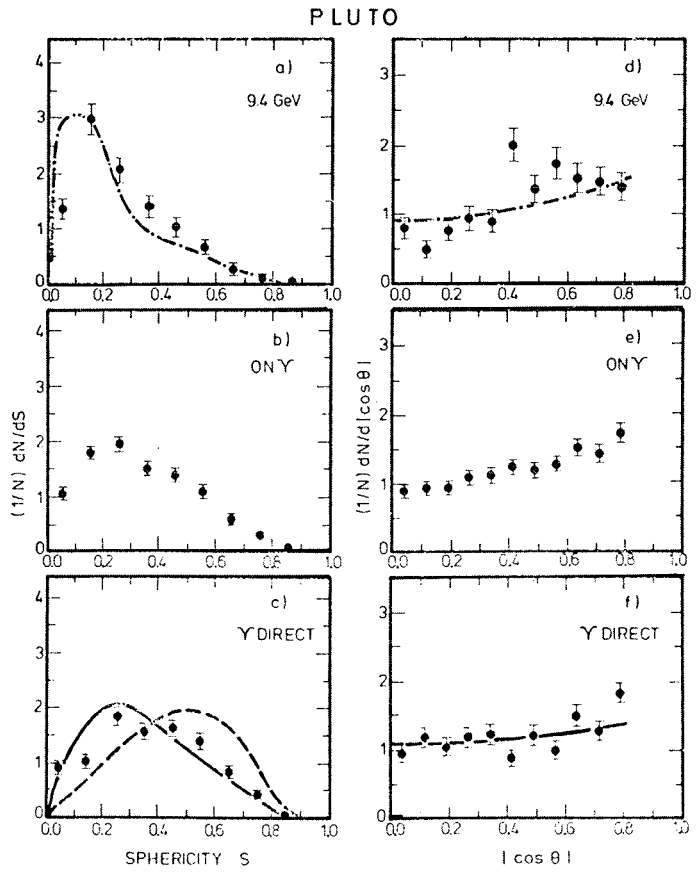

Figure 25 : Sphericity and angular distributions around Υ resonance[36]. The dashed-dotted line in (a) and (d) represents the 2-jet model while the dashed and solid lines in (c) and (f) correspond respectively to phase space and 3-gluon models.

More elaborate quantities (for example triplicity) have been constructed to exhibit more clearly the "planar" 3-gluon topology[37]. In all these investigations we may summarize in saying that the 3-gluon model is a much better representation of the data than simple phase space. It is not clear however what modification of the phase space model (resonances ?) it would take to improve its comparison with the data. So at present QCD is well supported by Υ decays, but it certainly does not prove it either. The next step would be to see clear evidence for gluon jets.

4.2.3. Search for gluon jets

The PLUTO group has made an extensive search for gluon jets with a negative conclusion. A method using energy flow diagrams with superimposed events[38] has proved to be tricky in generating fake 3-jet structure[37]. On the other hand, to see jets on an event-to-event basis is very difficult at the Υ because its mass is still not high enough.

To be more quantitative about the last statement we must look at the way the 3 gluons share the available energy. Figure 26 shows the distribution, broken down into the most energetic (F), less energetic (S) and intermediate (I) gluons[39]

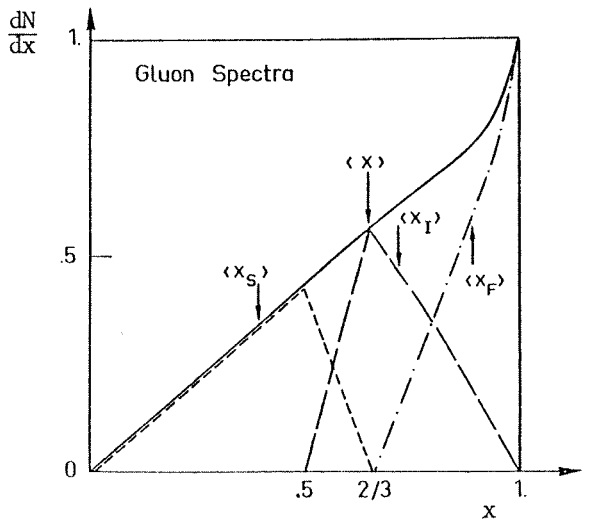

Figure 26 : Gluon energy spectrum in Υ decays (see text for explanations).

This allows one to quote average values for the 3-gluon energy sharing and charged multiplicity assuming gluons fragment like quarks :

$$\langle x_F \rangle = .89 \qquad \langle n_{ch} \rangle = 2.45$$
$$\langle x_I \rangle = .72 \qquad \langle n_{ch} \rangle = 2.35$$
$$\langle x_S \rangle = .39 \qquad \langle n_{ch} \rangle = 1.60$$

giving a total charged multiplicity of 6.4 not too different from the experimental value of 5.9 ± 0.1.

A typical configuration is drawn in figure 27 where the cones indicate a 50 % containment of energy for the respective jets assuming they behave like quark jets.

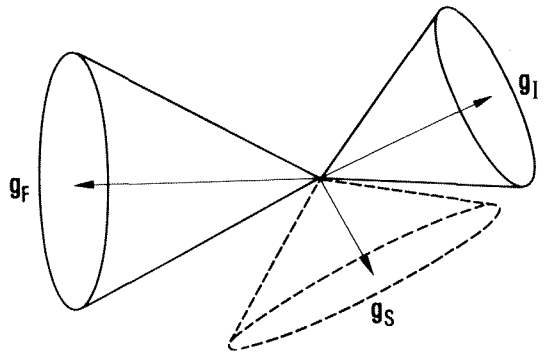

Figure 27 : Typical configuration for Υ decay with 50 % of energy of each jet contained in each corresponding cone.

If the 2 softer jets are likely to merge into one another, there is a good chance to study the fast jet[39] and learn about gluon fragmentation in a less global way than before. It could be possible to see if gluon jets are indeed similar to quark jets or if they are softer with larger multiplicities as one would naively expect.

4.3. Gluon jets in heavier quarkonia

The decay dynamics of heavy $Q\bar{Q}$ states is determined by the relative amount of electromagnetic ($\ell^+\ell^-$, $q\bar{q}$), 3g and γ2g decays. Provided they can be separated, 3g decays should be more transparent at higher mass.

Expressing partial widths in unit of the leptonic width Γ_{ee} for each state we can make the following estimates in table 4 :

Table 4

Partial widths of $Q\bar{Q}$ states relative to Γ_{ee}

$Q\bar{Q}$	e_Q	α_S	$\Sigma\ell^+\ell^-$	$\Sigma q\bar{q}$	3g	γ2g	$\frac{3g}{\text{hadrons}}$	$\frac{\gamma 2g}{\text{hadrons}}$	$\frac{\gamma 2g}{\text{hadrons}}$
$J/\psi(c\bar{c})$	2/3	.19	2	2.5	10	1.2	.73	.088	.12
$\Upsilon(b\bar{b})$	1/3	.15	3	4.0	20	0.8	.81	.032	.04
$T(t\bar{t})$	2/3	.12	3	4.3	2.5	0.5	.34	.068	.20

One notes the dominant $q\bar{q}$ decay mode of toponium states which can be separated out by a sphericity cut. Large-sphericity events will show 3 jets since $\langle E_S \rangle \gtrsim 6$ GeV and radiative events will represent a larger fraction. The latter decays are particularly well suited for looking for gluon jets : in the system recoiling against the radiated photon, it should be easy to find out the back-to-back gluon jets using sphericity. A similar argument can be applied to P states of the $t\bar{t}$ system accessible from radiative decays of T'.

5. CONCLUSIONS

The main points of this review are the following :

1. e^+e^- annihilations have provided us with a wealth of detailed information on $c\bar{c}$ states : J/ψ, ψ', ψ'' and P states (X).
2. An outstanding problem is the finding of the pseudo-scalar states η_c and η_c' since previously proposed candidates seem to have been ruled out.
3. Understanding of transition rates in charmonium is at a qualitative level.
4. Data on D decays are reaching rare modes at a time when hadron and neutrino reactions start to unveil D mesons through main decay modes. Cabibbo suppressed decays are in qualitative agreement with expectations.
5. Although charmed baryons seem to be produced at a sizeable level, no invariant mass plot has been allowed to leave Stanford as yet.
6. Direct observation of D production is a clean way to study c quark fragmentation. More statistics and higher energy are needed.
7. Υ decay dynamics has given us a first glimpse into gluon physics : the 3-gluon decay mechanism is well supported by data but gluon jets will have to wait for toponium.

ACKNOWLEDGEMENTS

I am indebted to A. Barbaro-Galtieri, A. Billoire, E. Bloom, S. Brandt, G. Flügge, M.K. Gaillard, G. Gidal, C. Kiesling, L. Maiani, B. Richter, J. Weiss and G. Wolf for their help in the preparation of this talk.

* * *

REFERENCES

1) J.E. Augustin et al., Phys. Rev. Lett. 33, 1406 (1974).
G.S. Abrams et al., Phys. Rev. Lett. 33, 1453 (1974).

2) G. Goldhaber et al., Phys. Rev. Lett. 37, 255 (1976).
I. Peruzzi et al., Phys. Rev. Lett. 37, 569 (1976).

3) S.W. Herb et al., Phys. Rev. Lett. 39, 252 (1977).
W.R. Innes et al., Phys. Rev. Lett. 39, 1240 (1977).

4) C. Berger et al., Phys. Lett. 76B, 243 (1978).
C.W. Darden et al., Phys. Lett. 76B, 246 (1978).
J.K. Bienlein et al., Phys. Lett. 78B, 360 (1978).
C.W. Darden et al., Phys. Lett. 78B, 364 (1978).

5) C.J. Biddick et al., Phys. Rev. Lett. 38, 1324 (1977).

6) W. Bartel et al., Phys. Lett. 79B, 492 (1978).
W. Bartel, Proceedings of the Rencontre de Moriond (1977).

7) W. Braunschweig et al., Phys. Lett. 57B, 407 (1975).
G. Grindhammer, Proceeding of the Rencontre de Moriond (1978).

8) W. Tannenbaum et al., Phys. Rev. D17, 1731 (1978).
J.S. Whitaker et al., Phys. Rev. Lett. 37, 1596 (1976).

9) V. Blobel, Proceedings of the Rencontre de Moriond (1977).

10) E.D. Bloom, Proceedings of the Rencontre de Moriond (1979).

11) J.M. Weiss et al., this Conference.

12) C. Kiesling et al., this Conference.
13) E. Pelaquier and F.M. Renard, Nuovo Cimento 32A, 421 (1976).
14) W. Braunschweig et al., Phys. Lett. 67B, 243 (1977).
15) G. Gidal et al., this Conference.
16) Particle Data Group, Phys. Lett. 75B, 1 (1978).
17) See for example, A. Billoire, Proceedings of the Rencontre de Moriond (1979).
18) R. Barbieri et al., CERN preprint TH.2622 (1979)
19) J.S. Kang and J. Sucher, Phys. Rev. D18, 2698 (1978).
20) R. Turlay, rapporteur talk at this Conference.
21) A. Barbaro-Galtieri, Proceedings of the Rencontre de Moriond (1979).
22) J.M. Feller et al., Phys. Rev. Lett. 40, 274 and 1677 (1978).
23) R. Brandelik et al., Phys. Lett. 70B, 387 (1978).
B. Wiik and G. Wolf, DESY 78/23 (1978).
24) W. Bacino et al., Phys. Rev. Lett. 40, 671 (1978)
J. Kirkby, Proceedings of the 1978 SLAC Summer Institute, SLAC-PUB-2231.
25) J. Ellis, M.K. Gaillard and D. Nanopoulos, Nucl. Phys. B100, 313 (1975).
N. Cabibbo and L. Maiani, Phys. Rev. Lett. 73B, 418 (1978).
D. Fakirov and B. Stech, Nucl. Phys. B133, 315 (1978).
26) M. Kobayashi and K. Maskawa, Progr. of Theoret. Phys. 49, 652 (1973).
27) H. Harari, Proceedings of the 1977 SLAC Summer Institute, SLAC-204.
V. Barger, W. Long and S. Pakvasa, Phys. Rev. Lett. 42, 1585 (1979).
28) R. Schrock, S. Treiman and L.L. Wang, Phys. Rev. Lett. 42, 1589 (1979).
29) R. Brandelik et al., Phys. Lett. 70B, 132 (1977).
30) T. Ferguson et al., SLAC-PUB-2081 (1979).
31) M. Piccolo et al., SLAC-PUB-2323 (1979).
32) P. Rapidis et al., SLAC-PUB-2184 (1979).
33) V. Luth et al., Phys. Rev. Lett. 70B, 120 (1977).
G. Hanson, Proceedings of the Rencontre de Moriond (1978).
34) More data have been taken recently by Mark II at SPEAR : G. Gidal, private communication.
35) G. Flügge, invited talk at the XIX International Conference on High Energy Physics, Tokyo (1978).
36) C. Berger et al., Phys. Lett. 82B, 449 (1979).
37) S. Brandt et al., this Conference.
38) A. De Rujula et al., Nucl. Phys. B138, 387 (1978).
39) A. Morel, Saclay preprint, DPhT 79-70 (1979)

* * *

DISCUSSION

Chairman: L.S. Cheng

Sci. Secretaries: G.V. Goggi and C. Peroni

M. Derrick: Is there any evidence that the leptonic branching ratios of the neutral and charged D mesons are different?

M. Davier: Right now they are consistent and in the average values that I have quoted they are combined. There is no evidence for a difference at the level of, say, 2%.

I. Butterworth: There was a claim to see η_c at Serpukhov in a large γ detector. Is there anything new on that experiment?

M. Davier: I have no new experimental information. A two-photon peak was seen, although statistically not compelling, just an indication of a 2γ mode.

HIGH ENERGY TRENDS IN e^+e^- PHYSICS

Günter Wolf
Deutsches Elektronen-Synchrotron DESY, Hamburg, Germany

1. INTRODUCTION

With the advent of PETRA the Q^2 range over which e^+e^- annihilations can be studied has been extended by an order of magnitude:

	SPEAR/DORIS I	DORIS II	PETRA
Q^2_{max}	~60 GeV^2	100 GeV^2	1000 GeV^2

Although still preliminary and limited in statistics the data convey already a clear and exciting picture of what is happening at these high energies in certain areas.

As it turns out many things become simpler at high energies. For instance the occurence of jets is no longer the result of a complex analysis but can be seen with the naked eye. Fig. 1 shows a jet event as seen by MARK J. The hadronic showers are contained in two narrow cones.

Another example is the production of the heavy lepton τ. It took around 2 years of data taking at energies between 4 and 5 GeV in order to establish the existence of the τ. At PEP and PETRA energies the existence of the τ would have been firmly demonstrated within a month of running. This may be seen from Fig. 2 which displays a typical τ event of the kind

$$e^+e^- \to \tau^- \;\; \tau^+$$
$$\quad\;\; |_{\to \nu + 3\ \text{charged}} \quad |_{\to \mu^+ \nu\bar{\nu}}$$

observed at 13 GeV. The probability for hadronic events of this topology with which τ events could be confused is very small.

Other features of e^+e^- analyses become more difficult at high energies and require care. One of them is the separation of annihilation from two photon events. While at low energies two photon contributions are mostly of the order of a few percent at PETRA energies the relative proportion of the two processes is reversed. However, e.g. by summing the total visible hadron energy a separation of the two processes can be achieved to an accuracy of a few percent. This is illustrated in Fig. 3 showing the sum of the observed charged and neutral energy as measured by PLUTO at 27.4 GeV.

2. STATUS OF PETRA

The new DESY e^+e^- colliding ring PETRA (= Positron Electron Tandem Ring Anlage) was gradually brought into operation in the second half of last year. Fig. 4 shows a layout of

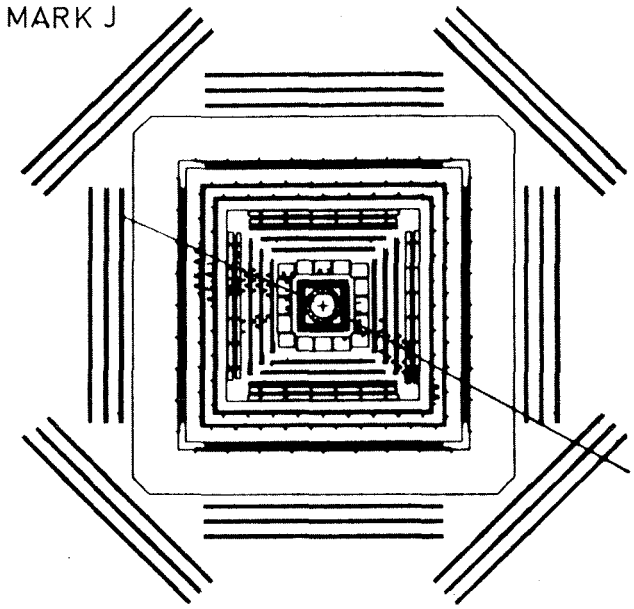

Fig.1 Hadron event observed in the MARK J detector at 27.4 GeV.

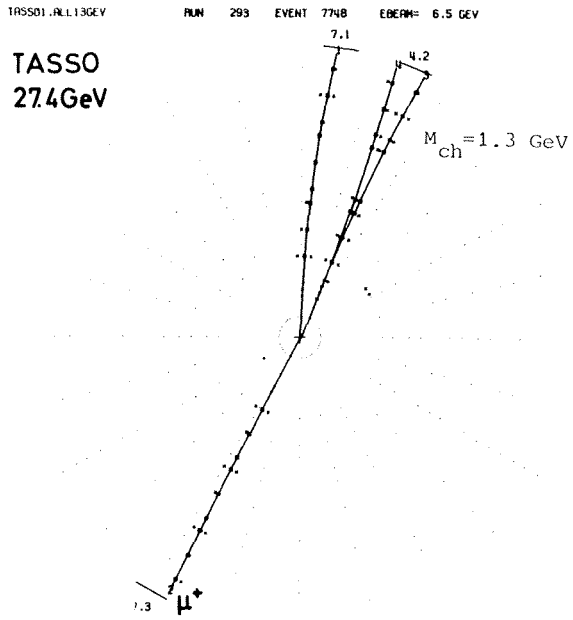

Fig.2 Candidate for τ pair production, $e^+e^- \to \tau^+ \tau^-$ as observed by TASSO at 13 GeV.

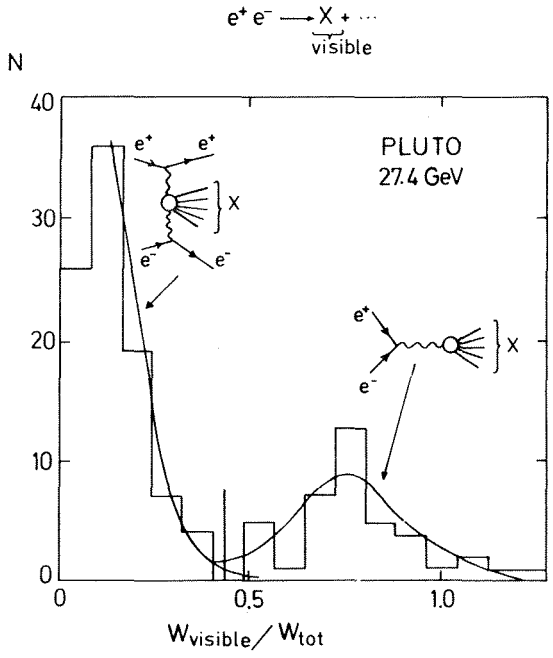

Fig.3 Distribution of the total visible energy as observed by PLUTO at 27.4 GeV. The curves indicate the shape of the contributions expected from two photon exchange and one photon annihilation.

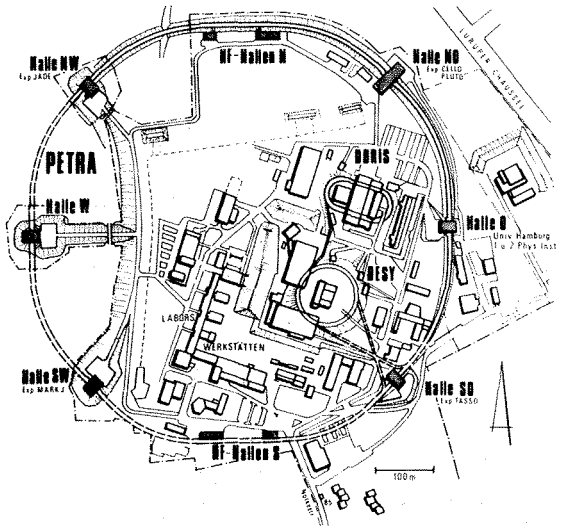

Fig.4 Layout of PETRA

the accelerator complex with the synchrotron (DESY) serving as injector and the storage ring DORIS as accumulator for positrons. Some of the PETRA parameters are listed in Table I. There are four short and four long straight sections. Two of the long straight sections are used for the accelerating RF structures. The other six straight sections are available for experiments.

At present five experiments have been installed or are being setup in the four short sections:

North-East: PLUTO, CELLO
North-West: JADE
South-West: MARK J
South-East: TASSO

The number of RF cavities and therefore the maximum energy attainable has been/is being increased in steps. Until February of this year four RF cavities were used providing a maximum total energy of $W = 2E_{beam} = 22$ GeV. With this configuration MARK J, PLUTO and TASSO have taken data at W = 13 and 17 GeV. Since March 32 cavities are installed increasing the maximum energy to 32 GeV. The three experiments mentioned above, together with JADE which has moved into the ring just recently, have carried out measurements at 27.4 GeV. By the end of this year a total of 64 cavities will be available allowing PETRA to reach energies as high as W = 38 GeV.

The maximum luminosity obtained at 27.4 GeV was $3 \cdot 10^{30}$ $cm^{-2} sec^{-1}$ with two positron and two electron bunches and 8 mA current per beam.

Table I
PETRA parameters

maximum beam energy	19 GeV
circumference	2.3 km
magnetic bending radius	192 m
number of interaction regions	6
length of interaction region	15 m
RF frequency	500 MHz
number of klystrons	8
power per klystron	0.5 MW
max. number of cavities	64

3. ENERGY DEPENDENCE OF R

The total cross section σ_{tot} for

$$e^+e^- \rightarrow \text{hadrons}$$

is given in terms of the cross section for μ pair production ($\sigma(e^+e^- \rightarrow \mu^+\mu^-) \simeq \frac{4\pi\alpha^2}{3s} = \frac{87.7 \text{ nb}}{s \text{ (GeV}^2)}$. $s = W^2$ = square of total c.m. energy):

$$R = \sigma_{tot} / \sigma_{\mu\mu}$$

Fig. 5 shows a compilation of measurements from near threshold up to an energy of W = 3 GeV.[1-5]

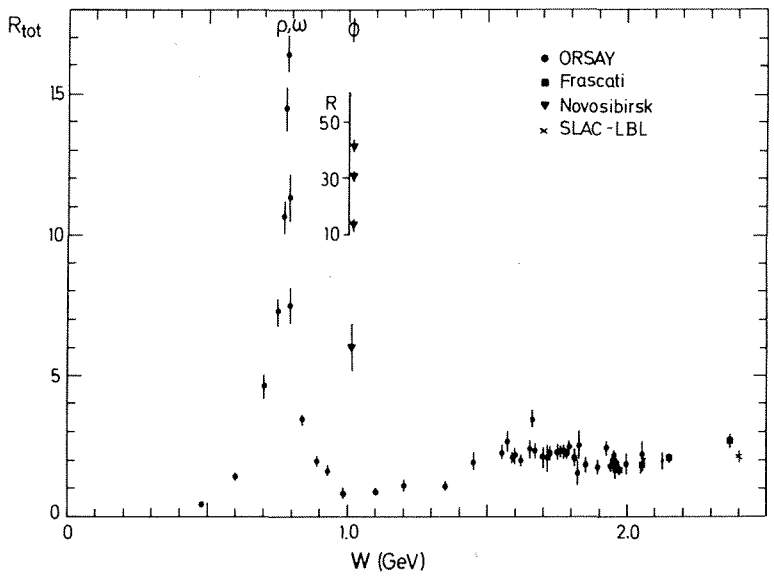

Fig.5 Measurements of R from Refs. 1-4.

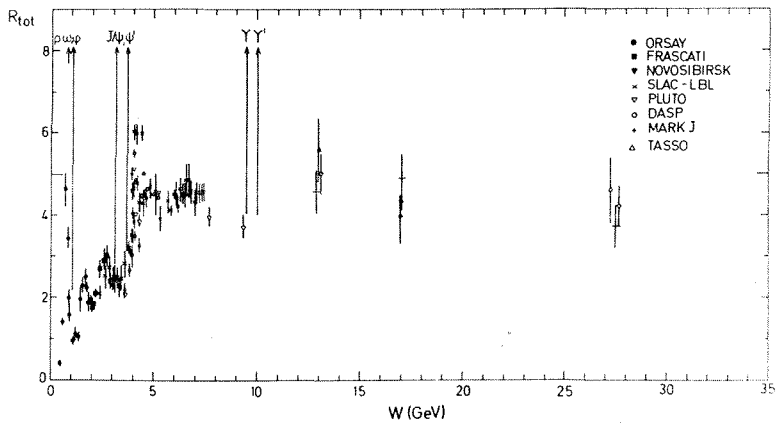

Fig.6 Measurements of R from Refs. 1 - 4, 6 - 10.

The error bars shown in this and the subsequent figure are only statistical. The systematic uncertainties are at the level of 10 - 20 %. The new data from ADONE[2] and DCI[3] presented at the Tokyo conference have clarified the behaviour of R in the region between 1 and 2 GeV. Below 1 GeV is the regime of the ground state vector mesons ρ, ω and ϕ. Above 1 GeV R shows a rather smooth behaviour despite the fact that individual channels (e.g. 4π, 5π) are dominated by the excitation of higher mass vector mesons such as the $\rho(1500)$, the $\omega(1700)$ and possibly others[2,3]. We see that R is near 1 between 1.1 and 1.4 GeV and then rising to a level of about 2 above 1.5 GeV. The rise is probably related to the onset of K production; above 1.6 GeV final states with kaons contribute approximately one unit in R[5].

The high energy region[4,6-10] together with the low energy data is shown in Fig. 6. The highest energy data points at 13, 17 and 27.4 GeV were measured by the MARK J[8], PLUTO[9] and TASSO[10] experiments at PETRA. A description of these new setups and the analysis procedures can be found in the reports of Drs. Branson[8], Blobel[9] and Cashmore[10] to this conference. The R values measured in these experiments are listed in Table 2:

Table 2

Measured R values at high energies

	13 GeV	17 GeV	27.4 GeV
MARK J	4.6 ± 0.5 ± 0.7	4.9 ± 0.5 ± 0.7	3.7 ± 0.5 ± 0.7
PLUTO	5.0 ± 0.5 ± 1.0	4.3 ± 0.5 ± 0.8	4.2 ± 0.5 ± 0.8
TASSO	5.6 ± 0.7 ± 1.1	4.0 ± 0.7 ± 0.8	4.6 ± 0.8 ± 0.9

The errors give the statistical and the systematic uncertainties.
The outstanding features of R as observed above 3 GeV are the spikes from the excitation of $J/\psi,\psi',\ldots$ and of Υ,Υ' ,... plus the fact that in between the two particle families and above Υ,Υ' R is almost constant.

Note that the final value for R measured by PLUTO just below the Υ at 9.4 GeV is 3.7 ± 0.3 ± 0.5. The high energy data points are consistent with R being constant or slightly falling between 13 and 27.4 GeV. A rise of R e.g. by two units from 17 to 27.4 GeV appears to be improbable.

The simple quark model is in striking agreement with the general behaviour of R. In the quark model hadron production proceeds via the formation of a quark antiquark pair (see Fig. 7). Assuming that the produced quarks turn into hadrons with unit probability R measures the sum of the square of the quark charges:

$$R(s) = \sum \frac{\sigma_{q\bar{q}}}{\sigma_{\mu\mu}} = 3 \sum e_q^2 \qquad (1)$$

$$q = u,d,s,c,\ldots$$

$$M_q > W/2$$

The factor of 3 accounts for the colour degree of freedom. R is predicted to be a step function with a rise above each new quark threshold. The comparison with the data is shown in Figs. 8 and 9. Up to 3 GeV only u,d and s contribute and therefore R = 2 in good accord with the data between 1.5 and 3 GeV. Above charm threshold (near 4 GeV) R should rise to a level of 3.3. The data are larger mainly because of resonance effetcs; above 4.5 GeV the measured R values seem to descend slowly towards the quark model value. Beyond the Υ,Υ'...

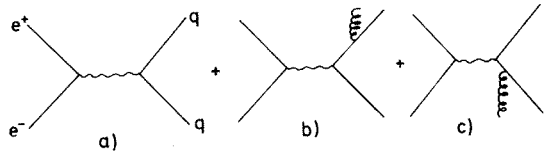

Fig.7 Diagram for quark pair production (a) plus gluon corrections (b), (c)

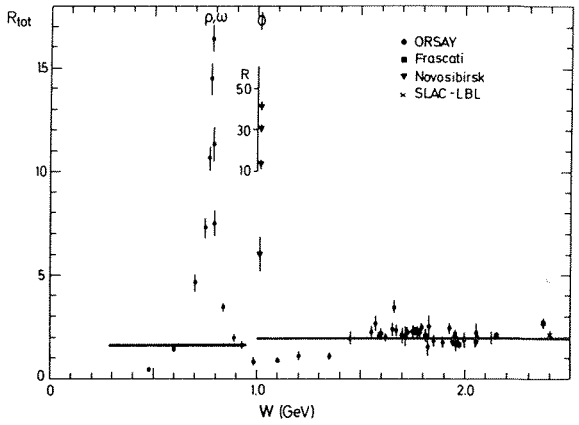

Fig.8 Measurements of R and the prediction of the quark model (solid lines)

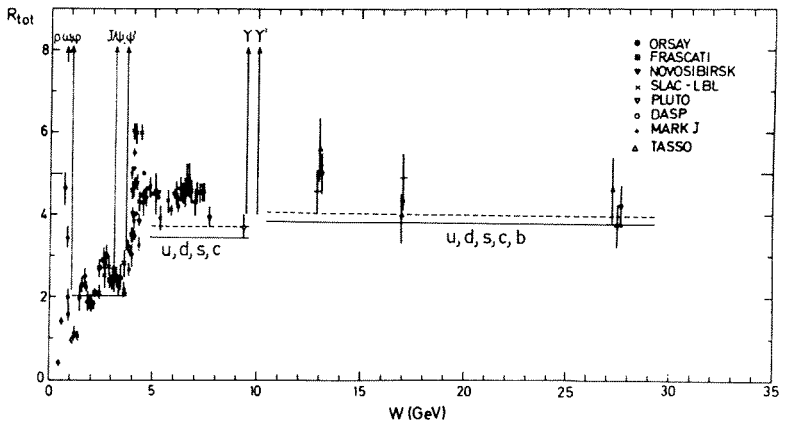

Fig.9 Measurements of R. The solid lines show the prediction from the quark model. The dashed lines show the quark model predictions corrected for gluon emission.

family the data are again higher than the theoretical value of 3.7 but tend to approch this value as the energy increases. A possible sixth quark contribution will be discussed later.

In QCD gluon emission (diagrams b and c in Fig. 7) modifies the result of the quark model; R_0:

$$R = R_0 \left(1 + \frac{\alpha_s(s)}{\pi}\right) \qquad (2)$$

Here, α_s measures the strength of the gluon quark coupling

$$\alpha_s = \frac{12\pi}{(33-2\ N_f)\ \ln s/\Lambda^2}$$

with N_f being the number of quark flavours (e.g. $N_f = 4$ for u,d,s,c) and Λ a constant which from neutrino experiments is found to be ~500 MeV. The QCD correction increases the predicted R values by approximately 10 % (see dashed lines in Fig. 9). This is well within the accuracy of the experimental data points.

4. GROSS FEATURES OF THE FINAL STATES

a) Multiplicity

In Fig. 10 the average charge multiplicity $\langle n_{ch} \rangle$ is plotted as a function of s[2,9-11]. Although the data are preliminary since most of them have not yet been published and corrections for acceptance, for photons converting in the beampipe, etc. may not always have been made in the same way, they suggest, that the multiplicity above ~10 GeV is rising (logarithmically) faster than at lower energies.

The dashed curve in Fig. 10 gives the energy dependence of $\langle n_{ch} \rangle$ for pp collisions[12]. The pp multiplicity is lower by 0.5 to 1 units but has almost the same behaviour with energy.

A good fit to the e^+e^- data is obtained with the function (see solid curve)

$$\langle n_{ch} \rangle = 2 + 0.2\ \ln s + 0.18\ (\ln s)^2$$

The decomposition of $\langle n_{ch} \rangle$ into charged pion, kaons and nucleons is shown in Fig. 11 for the 3.6 to 5.2 GeV region[11]: the majority of the charged hadrons are pions (~83 %); kaons account for ~15 %, protons and antiprotons for ~2 %. As the energy increases and the phase space effect due to the larger kaon mass is reduced one expects the fraction of kaons to rise. Whether this is so remains to be seen.

b) Inclusive particle spectra

The differential cross section for producing a particle h with momentum and energy P,E and angle Θ relative to the beam axis (see Fig. 12) can be expressed in terms of two structure functions $\overline{W}_1$ and $\overline{W}_2$ which are closely related to W_1 and W_2 measured in inelastic lepton hadron scattering:

$$\frac{d^2\sigma}{dx d\Omega} = \frac{\alpha^2}{s}\ \beta x\ \{m\overline{W}_1 + \frac{1}{4}\ \beta^2\ x\ \nu\overline{W}_2\ \sin^2\Theta\} \qquad (4)$$

where m is the mass of h, $\beta = P/E$, $x = E/E_{beam} = 2E/\sqrt{s}$ and ν is the energy of the virtual photon as seen in the h rest system, $\nu = E/m\sqrt{s}$.

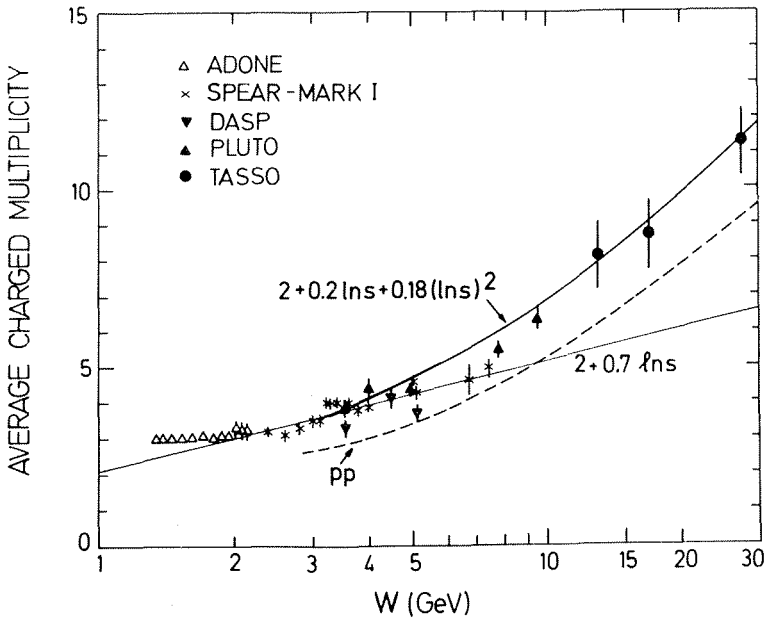

Fig.10 Average charge multiplicity (Refs. 2, 9-11). The dashed line shows the result for pp collisions (Ref. 12).

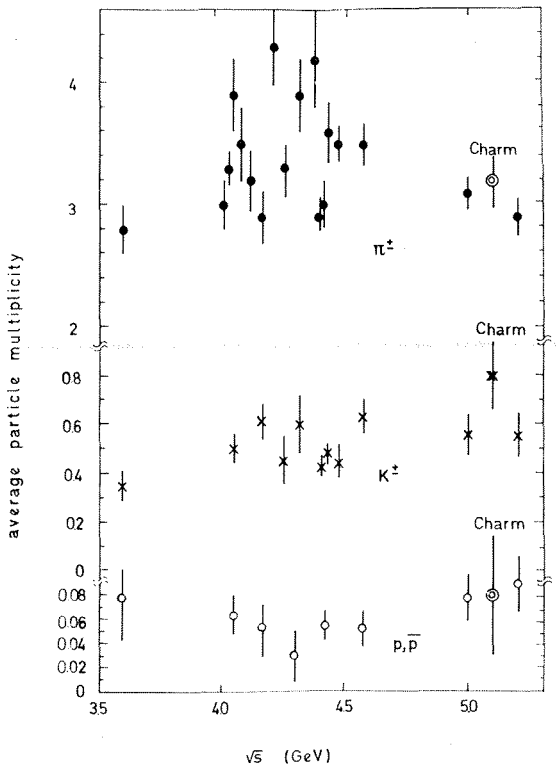

Fig. 11 Average multiplicity of $\pi^{\pm}$, $K^{\pm}$ and $p,\bar{p}$ per event. The points labelled "charm" give the multiplcities for charmed events alone. (Ref. 11)

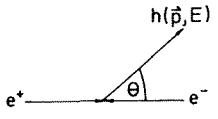

Fig. 12 Diagram for inclusive particle production

After integrating over the angles one has

$$\frac{d\sigma}{dx} = \frac{4\pi\alpha^2}{s} \beta x \{ m\bar{W}_1 + \frac{1}{6}\beta^2 x \nu\bar{W}_2 \} \quad (5)$$

Since the first term is dominating

$$\frac{d\sigma}{dx} \simeq \frac{4\pi\alpha^2}{s} \beta x m\bar{W}_1 \quad (6)$$

The structure functions $\bar{W}_1$ and $\bar{W}_2$ in general are functions of two variables e.g. s and the scaling variable x which corresponds to the scaling variable $x = 1/\omega$ used in inelastic lepton nucleon scattering. If scale invariance holds $\bar{W}_1$ and $\nu\bar{W}_2$ are functions of x alone and the so called scaling cross section $s/\beta\, d\sigma/dx$ is almost the same for all values of s (see eqs. 5, 6).

Scaling behaviour is e.g. expected from the hypothesis of quark fragmentation: at energies large enough that particle masses can be neglected, the number of hadrons h produced by a quark q with fractional energy x, $D_q^h(x)$, is independent of s. This leads to

$$\frac{d\sigma}{dx}(e^+e^- \to q\bar{q} \to h) = \sigma_{q\bar{q}} \cdot 2D_q^h(x) = \frac{8\pi\alpha^2}{s} e_q^2 D_q^h(x) \quad (7)$$

Fig. 13 shows the scaling cross section as measured between 3.6 and 5.2 GeV for $\pi^{\pm}$, $K^{\pm}$ and $2\cdot\bar{p}$. Most remarkable is the similarity between the three types of particles. Within a factor of two their cross sections fall on a common curve. Scaling is tested in Fig. 14 where pion data are compared at 3.6 and 5.0 GeV. For $x > 0.3$ scaling is satisfied to within 30 %. Between 3.6 and 5.0 GeV the charmed threshold is crossed leading to a rise of the total cross section by almost a factor of two. From Fig. 14 we see that the additional cross section produces only low x pions.

Fig. 15 compares the scaling cross sections for pions and kaons with inclusive ρ^0 production measured by PLUTO[13] and D production measured by SLAC-LBL[14]. A striking similarity in shape as well as in size is observed for π, K, ρ^0 while D production is a factor of 5 to 10 larger.

At higher energies inclusive cross sections have been measured for the sum of all charged particles. Since the mass of the particle is not known, the scaling variable $x = E/E_{beam}$ is replaced by $x_p = P/E_{beam}$ and the quantity $sd\sigma/dx_p$ is measured instead of $s/\beta\, d\sigma/dx$. (In the following x is used for x_p).

Fig. 16 displays the data from TASSO measured at energies of 13, 17 and 27.4 GeV together with measurements from SLAC-LBL[15] at 3 GeV and DASP[11] at 5 GeV. At $x > 0.2$ the scaling cross sections are found to be the same between 5 and 27.4 GeV within errors (~20-30 %). The rise of the charged multiplicity we saw in Fig. 10 is related to the dramatic increase of the particle yield a low x; for instance at $x = 0.06$ the increase is an order of magnitude going from 5 to 27.4 GeV. The 13 GeV data are somewhat special in that for $x > 0.2$ they are above the values measured for 17 GeV. Since 13 GeV is still close to the $b\bar{b}$ threshold this may indicate copious $B\bar{B}$ production (and decay).

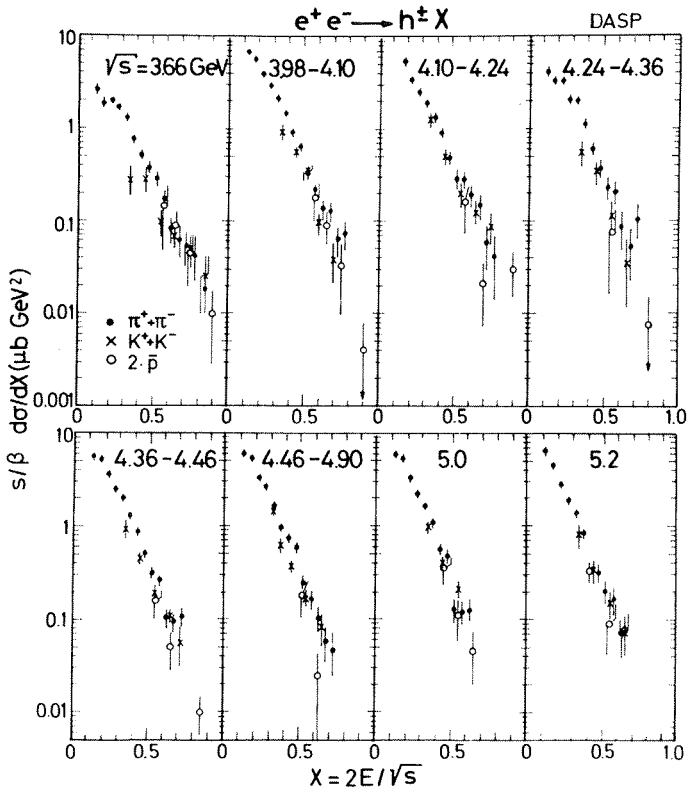

Fig. 13 The scaling cross section $s/\beta\ d\sigma/dx$ ($x = 2E/\sqrt{s}$) as a function of x for the sum of $\pi^+\pi^-$, K^+ and K^- and twice the $\bar{p}$ production for different intervals of the total energy.

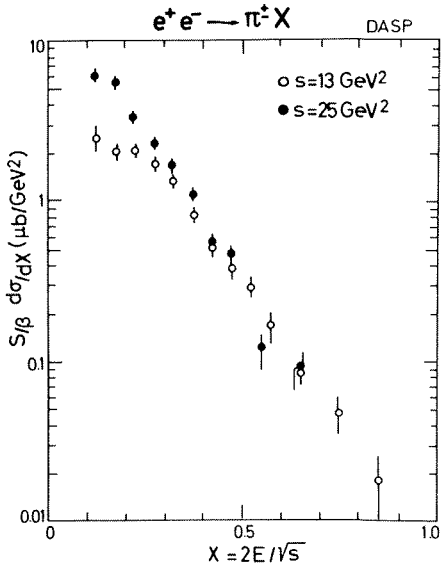

Fig.14 Comparison of the scaling cross sections $(s/\beta)\ d\sigma/dx$ for $\pi^\pm$ at s = 13 and 27 GeV^2 (Ref. 11).

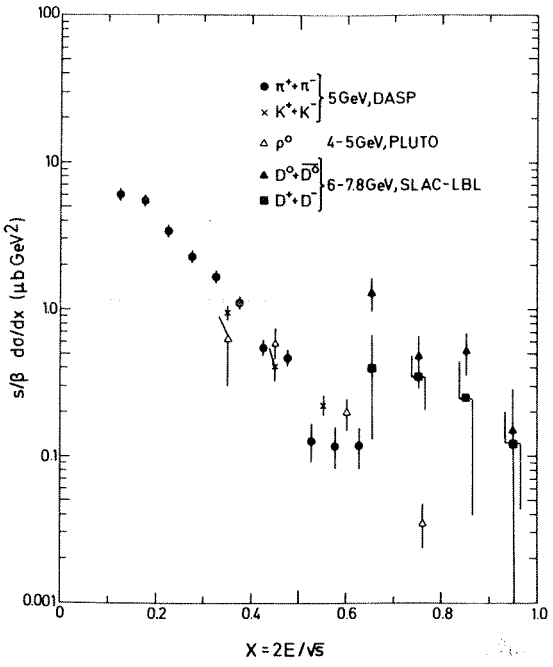

Fig.15 The scaling cross section $s/\beta\ d\sigma/dx$ ($x = 2E/\sqrt{s}$) for $\pi^\pm$, $K^\pm$ (Ref. 11) ρ^0 (Ref. 13), $D^0, \bar{D}^0$ and $D^\pm$ production (Ref. 14).

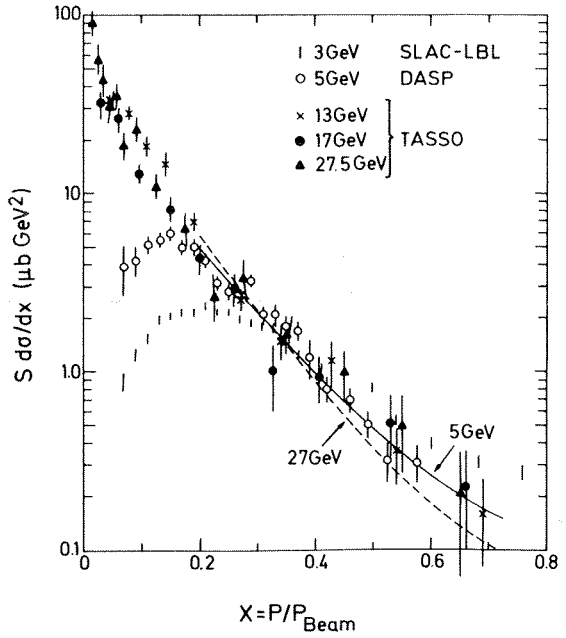

Fig.16 The scaling cross section $s\ d\sigma/dx$ ($x = p/p_{beam}$) for inclusive charged particle production as measured at 3 GeV by SLAC-LBL[15] at 5 GeV by DASP[11] and at 13, 17 and 27.4 GeV by TASSO[10]. The curves show the QCD scale breaking effect predicted for going from 5 to 27.4 GeV[16].

Gluon emission will lead to scale breaking effects: the primary momentum is now shared by quark and gluon resulting in a depletion of particles at high x and an excess of particles at low x values. The curves in Fig. 16 indicate the size of the expected scale breaking[16]. It amounts to a 30 % effect at x = 0.6 comparing 5 and 27.4 GeV cross sections. The precision of the data does not allow to test the predicted change.

5. JET FORMATION

As mentioned before the quark model views annihilation into hadrons as a two step process: first, a pair of quarks is produced which then fragment into hadrons (see Fig. 17). If the hadron momenta transverse to the quark direction of flight are limited and the number of produced hadrons grows only logarithmically with energy the emitted hadrons will be more and more collimated around the primary quark directions as the total energy increases and one will observe jets. Let $\langle n \rangle = a + b \cdot \ln s$ be the average particle multiplicity, $\langle p_T \rangle$ and $\langle p_{\parallel} \rangle \approx \langle p \rangle \approx \frac{\sqrt{s}}{\langle n \rangle}$ the average transverse and longitudinal hadron momenta then the mean half angle of the jet cone is given by

$$\langle \lambda \rangle = \frac{\langle p_T \rangle}{\langle p_{\parallel} \rangle} \approx \frac{\langle p_T \rangle \cdot \langle n \rangle}{\sqrt{s}} = \frac{\langle p_T \rangle \, (a + b \cdot \ln s)}{\sqrt{s}} \sim \frac{1}{\sqrt{s}} \qquad (8)$$

The jet cone opening angle decreases roughly proportional to $s^{-1/2}$ as the energy increases.

The occurrence of jets in e^+e^- annihilation was first demonstrated in the pioneering work of SLAC-LBL[17]. This work was followed by measurements of PLUTO at energies up to 10 GeV and including neutrals in the jet analysis[18]. The experiments done at PETRA and reported at this conference have extended the jet studies up to 27.4 GeV[8-10,19]. Jet structure is commonly tested in terms of sphericity S and thrust T:

$$S = \frac{3}{2} \frac{\sum p_{\perp i}^2}{\sum p_i^2} \qquad 0 \leq S \leq 1 \qquad (9)$$

and

$$T = \frac{\sum |p_{\parallel i}|}{\sum p_i} \qquad \frac{1}{2} \leq T \leq 1 \qquad (10)$$

where $p_{\parallel i}$, $p_{\perp i}$ are the longitudinal and transverse particle momenta relative to the jet axis which is shosen such that $\sum p_{\perp i}^2$ ($\sum |p_{\parallel i}|$) is minimal (maximal) for sphericity (thrust). Extreme jettiness yields S = 0 and T = 1.

Comparing eq(8) with (9) we see that sphericity has a simple meaning: S measures the square of the jet cone opening angle:

$$S \approx \frac{3}{2} \langle \lambda^2 \rangle \; ; \qquad (11)$$

likewise

$$T \approx \sqrt{1 - \langle \lambda \rangle^2} \qquad (12)$$

In general not all final state particles are detected; e.g. neutrals are usually not registered. As a consequence the reconstruction of the true jet axis is only approximate. The effects of acceptance, detection efficiency and measuring accuracy have to be studied by an elaborate Monte Carlo analysis in order to separate physics effects from systematic biases.

a) Tests for quark jets

Fig. 18 displays the observed mean sphericity as a function of energy measured by SLAC-LBL. This measurement gave the first evidence for jet formation. The sphericity is approximately constant up to 4 GeV and then decreases with increasing energy. The solid and dashed curves show the Monte Carlo results for jet and phase-space like produced events. The theoretical curves have been corrected for acceptance and detection efficiencies. In the jet calculation an average $\langle p_T \rangle$ of 0.315 GeV/c was assumed. At low energies ($\lesssim$4 GeV) where $\langle p_{//} \rangle$ is of the same order as $\langle p_T \rangle$ both models predict the same average sphericity. Above 4 GeV phase space predicts sphericity to rise contrary to the data while the jet model describes the data well.

Fig. 19 shows a compilation of average sphericity values $\langle S \rangle$ from PLUTO and TASSO. One finds $\langle S \rangle$ to decrease from 0.4 at the J/ψ to ~0.15 at 27.4 GeV. The trend to ever stronger collimation persists up to the highest energy explored in agreement with the simple quark model. The jet cone opening angle deduced from $\langle S \rangle$ is ~31^o at 4 GeV dropping to 18^o at 27.4 GeV. A straight line fit to the data in Fig. 19 yields

$$\langle S \rangle = 0.8\ s^{-1/4}$$

The shrinkage of the jet cone is slower than expected from the naive arguments given above, $\langle S \rangle \sim s^{-1}$.

A jet analysis in terms of thrust leads to the same conclusions (Fig. 20). The curve shows the prediction of De Rujula et al. [20].

In Fig. 21 T distributions are shown at low and high energies. The trend towards more and more jetlike events is clearly visible.

The analyses described sofar included only charged particles. PLUTO has investigated also neutral particle (photons) distributions[18]. Define $dE/d\lambda$ to be the energy emitted at an angle λ with respect to the jet axis. Fig. 22 shows at 9.4 GeV the neutral and charged energy flow $dE^0/d\lambda$ (data points) and $dE^C/d\lambda$ (histograms) with respect to the thrust axis which had been determined from charged particles alone. The neutral energy is seen to be concentrated near the jet axis in much the same way as charged particles.

The jet axis distribution around the beam direction provides another test of the quark model. Since quarks have spin 1/2 the polar angular distribution is of the form (neglecting mass effects)

$$d\sigma/d\cos\Theta \sim 1 + \cos^2\Theta \qquad (13)$$

For comparison, spin 0 quarks would lead to

$$d\sigma/d\cos\Theta \sim \sin^2\Theta$$

The experimental data have been found to be consistent with a $1 + \cos^2\Theta$ distribution. The cleanest test has been made by SLAC-LBL studying jet production with beams polarized transverse to the storage ring plane[17]. In this case the angular distribution is of the form

$$d\sigma/d\Omega \sim 1 + \alpha\cos^2\Theta + \alpha P_+P_- \sin^2\Theta \cos 2\Phi \qquad (14)$$

where the azimuthal angle Φ of the jet axis is measured with respect to the storage ring plane, $P_+(P_-)$ is the degree of polarization and $\alpha = 1$ for $q\bar{q}$ production. Fig.23 shows the Φ distribution measured with $P_+P_- = 0.5$. A fit to the Φ distribution yielded $\alpha = 0.97 \pm 0.1$ in agreement with the quark model.

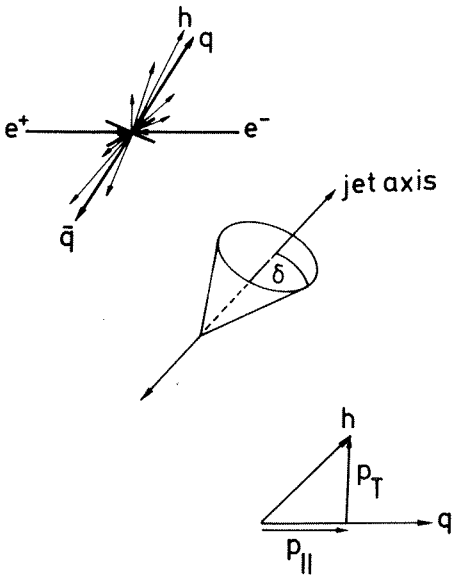

Fig.17 Jet formation

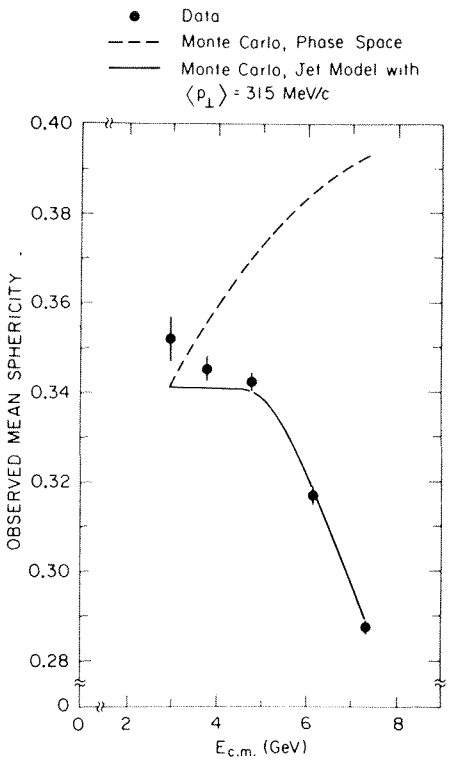

Fig.18 Observed mean sphericity versus total energy. The solid curve is the result of a jet model calculation with $\langle p_T \rangle$ = 0.315 GeV/c. The dashed curve is the invariant phase space prediction (Ref. 17).

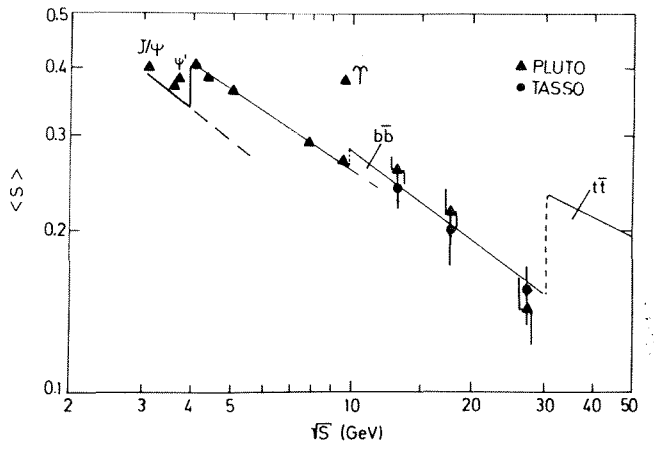

Fig. 19 The average sphericity as a function of the total energy as observed by PLUTO (Ref. 9, 18) and TASSO (Ref. 10). The curves indicate the expected contributions from u, d, s, c, b and t quark pairs.

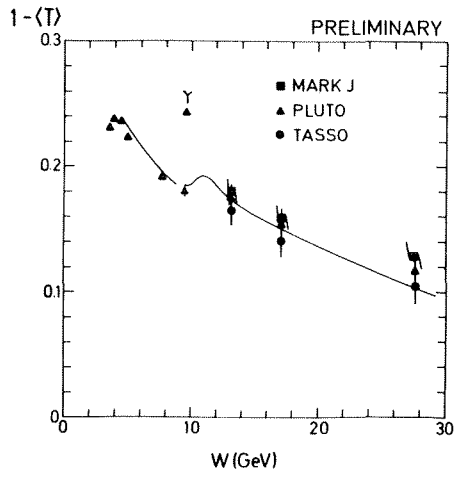

Fig.20 Energy dependence of 1 - <T> as measured by MARK J[8], PLUTO[9,18] and TASSO[10]. The curve shows the theoretical prediction[20].

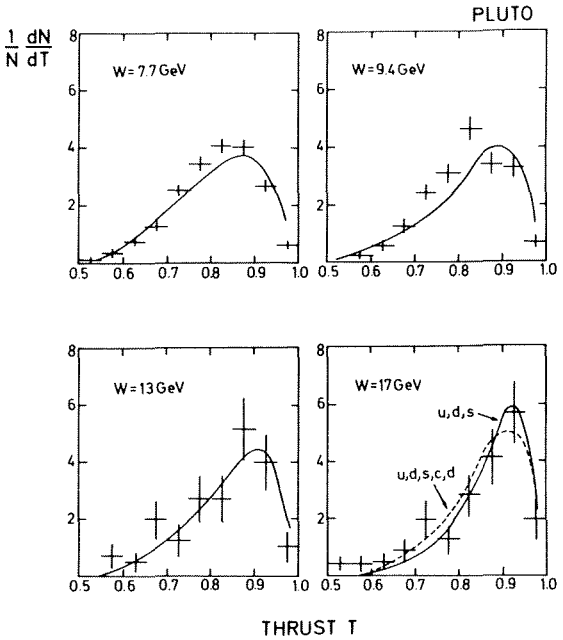

Fig.21 Thrust distributions for different total energies from Ref. 9. The solid and dashed curves show the quark model predictions using Field and Feynman fragmentation functions[21].

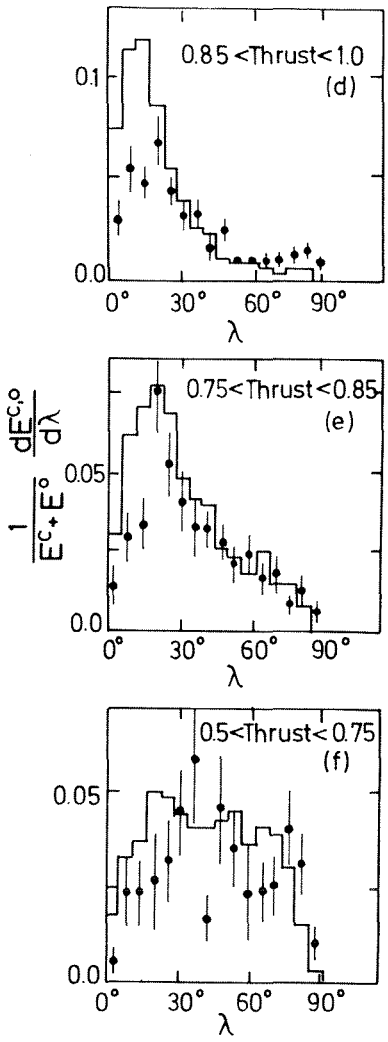

Fig.22 The angular distributions $1/(E^C + E^O)\cdot dE^O/d\lambda$ of neutral energy (data points) and charged energy $1/(E^C + E^O)\, dE^C/d\lambda$ (histograms) with respect to the thrust axis at 9.4 GeV for different T intervals. PLUTO (Ref.18).

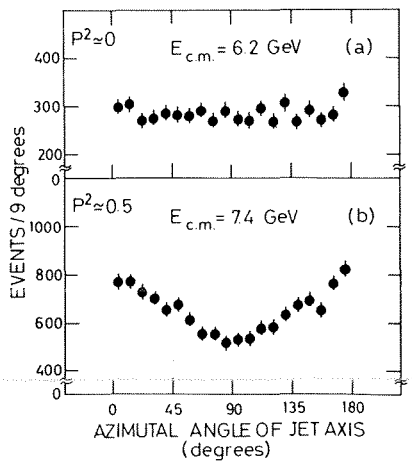

Fig.23 Azimuthal distribution of the reconstructed jet axis; zero degree is in the ring plane = plane of polarization.
(a) for a total energy of 6.2 GeV where the beam polarization is zero;
(b) for a total energy of 7.4 GeV where the product of the e^+ and e^- beam polarization is $p^2 = 0.5$. SLAC-LBL (Ref.17).

b) Structures in the energy dependence of sphericity

The energy dependence of <S> shown in Fig. 19 exhibits interesting structures. It is large at the J/ψ, ψ' and Υ with values close to those predicted by pure phase space (<S> $\approx$ 0.4 - 0.5) and it shows a rise at 4 GeV above the charm threshold. This rise can be understood as follows. Close to threshold the charm quarks are slow and the final state particles are emitted phase space like. Defining $\langle S_{ps} \rangle$ and $\langle S_{2jet} \rangle$ as the average sphericities for phase space and u,d,s produced events respectively, and R_c, $R_{u,d,s}$ the contributions from $c\bar{c}$ and $u\bar{u}$, $d\bar{d}$, $s\bar{s}$ production, the average sphericity just above charm threshold can be computed:

$$\langle S \rangle = \frac{\langle S_{ps} \rangle R_c + \langle S_{2jet} \rangle R_{u,d,s}}{R_c + R_{u,d,s}} \qquad (15)$$

One finds e.g.that at 4.5 GeV <S> increases due to the charm contribution by 0.06 from 0.32 to 0.38 in agreement with the data.

As the energy increases the velocity β of the charm quarks grows and the $c\bar{c}$ final states start to become jet like too. One may guess that for $\beta \approx 0.7$ the increase of <S> due to the $c\bar{c}$ contribution is only half of its value near the threshold. This "half width" point for the $c\bar{c}$ contribution is reached around 5 GeV.

Applying the same receipe to the $b\bar{b}$ contribution <S> is found to increase by $\approx$0.02 at 10 GeV. The increase is small due to the (expected) small $b\bar{b}$ contribution ($R_{b\bar{b}} = 0.3 - 0.6$). The half width point is near 13 GeV.

c) Particle emission with respect to the jet axis

The production of hadrons with respect to the jet axis has been extensively studied. If the quark model is correct these analyses permit in a very clean manner a study of quark fragmentation, clean since e.g. smearing effects due to quark fermi motion in the target are absent. The data have been analysed in terms of the longitudinal and transverse momenta, $p_{\parallel}$ and p_T, the rapidity $y = 1/2 \ln \left[(E + p_{\parallel})/(E - p_{\parallel})\right]$ and the fractional longitudinal momentum $x_{\parallel} = p_{\parallel}/E_{beam}$. Fig. 24 shows rapidity distributions for charged particles for energies between 4.8 and 27.4 GeV. To compute y the particles were assumed to be pions. The normalization is such that $1/\sigma \, d\sigma/dy$ gives the normalized yield per jet. The width of the y distributions increases and some sort of plateau is developing as the energy increases. The height of the plateau is not constant but is rising too. The fragmentation region is approximately two units wide which is equal to what is observed in hadron scattering. The fragmentation region is scaling. That can be seen when the data are plotted with respect to $y_{max} - y$ ($y_{max} \approx \frac{1}{2} \ln \frac{s}{m^2}$) as shown in Fig. 25.

Provided that only one kind of quark pair is produced and that the quarks fragment into pions only, theory predicts a plateau width Δy that grows logarithmically with energy,

$$\Delta y \approx y_{max} - 2 \approx \frac{1}{2} \ln s/m^2 - 2$$

a constant plateau height and scaling in the fragmentation region. The experimentally observed rise of the height of the plateau is related to the more rapid growth of the average particle multiplicity above 10 GeV (see Fig. 10).

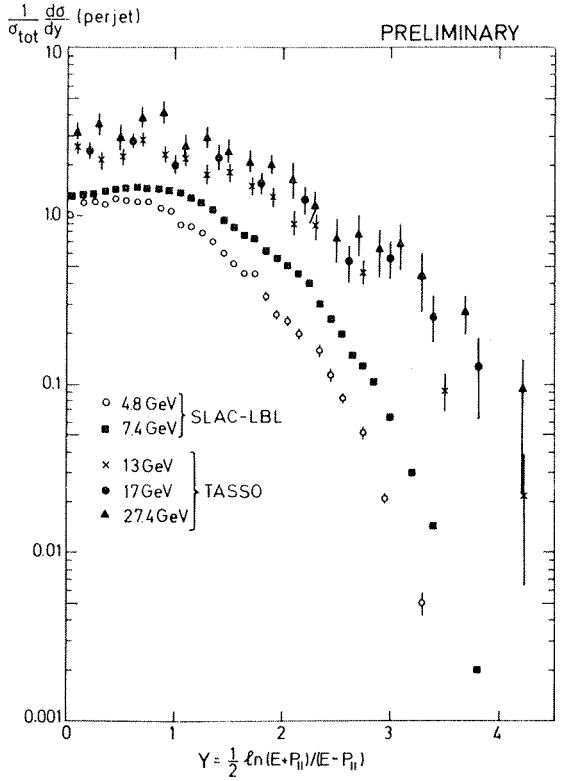

Fig.24 Rapidity distribution for charged particles assuming m = m_{π}: Yield per jet, normalized to the total cross section. Measurements by SLAC-LBL (4.8 and 7.4 GeV, Ref.17) and TASSO (13, 17 and 27.4 GeV, Ref.10).

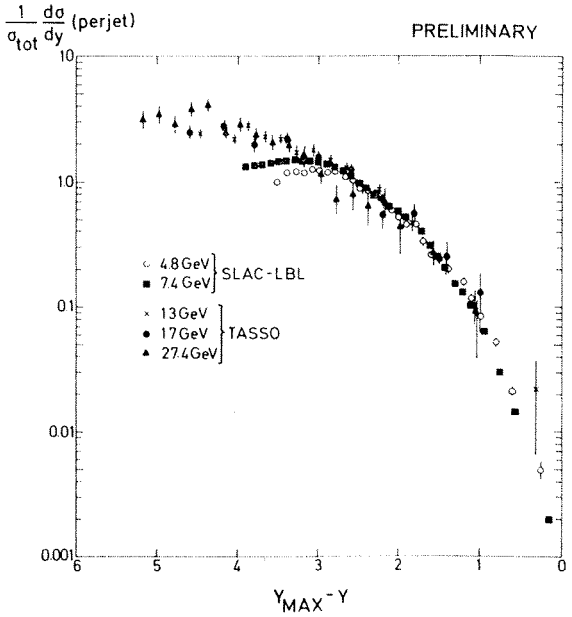

Fig.25 Rapidity distributions for charged particles as a function of y_{max} - y assuming m = m_{π}: Yield per jet normalized to the total cross section. Measurements by SLAC-LBL (4.8 and 7.4 GeV, Ref.17) and TASSO (13, 17 and 27.4 GeV, Ref.10).

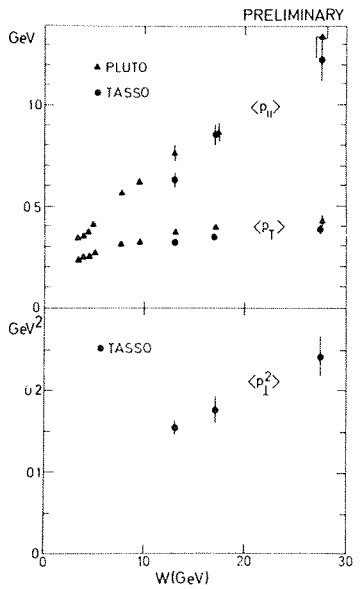

Fig.26 The energy dependence of $\langle p_{\parallel} \rangle$, $\langle p_T \rangle$ and $\langle p_T^2 \rangle$ relative to the thrust axis for charged particles (from Refs. 9, 10).

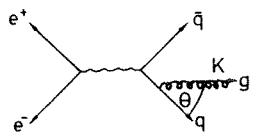

Fig.27 Schematic diagram for gluon emission.

Fig. 26 shows the energy dependence of the average $p_{\parallel}$ and p_T values. The average longitudinal momentum grows almost linearly in accordance with our expectation. The transverse momentum shows a rapid rise below 5 GeV which must be due to the increase in phase space. The data between 6 and 13 GeV are consistent with a constant $\langle p_T \rangle$. The measurements at the highest energy, 27.4 GeV, show that $\langle p_T \rangle$ is rising between 17 and 27.4 GeV:

Table 3
Average p_T and p_T^2 values (preliminary)

W (GeV)	$\langle p_T \rangle$ in GeV/c		$\langle p_T^2 \rangle$ in GeV^2/c^2
	PLUTO	TASSO	TASSO
13	0.37±0.01	0.329±0.009	0.145±0.010
17		0.363±0.013	0.175±0.014
27.4	0.43±0.02	0.422±0.020	0.276±0.029

As has been discussed by Professor Söding measuring errors can lead to a widening of the $\langle p_T \rangle$distribution. However, the increase in $\langle p_T \rangle$ and in particular in $\langle p_T^2 \rangle$, observed by TASSO cannot be accounted for by instrumental biases or by the larger phase space which allows quarks to fragment more frequently into heavier particles (kaons).

The widening of the p_T distribution is an important prediction of QCD which we will discuss briefly.

6. JET BROADENING BY QCD EFFECTS

Hard gluon emission illustrated by the diagrams b and c of Fig. 7 leads to a broadening of the p_T distribution and of the jet cone as shown by Ellis, Gaillard and Ross [22]. Qualitatively, the broadening of $\langle p_T \rangle$ can easily be understood. Similar to the emission of photons from an electron the gluon distribution radiated off a quark is approximately given by[23]

$$\frac{d\sigma(qqg)}{dk\,d\cos\Theta} = \frac{\alpha_s}{K(1-\cos\Theta)^2}\,\sigma_{qq} \qquad (16)$$

or

$$\frac{d\sigma(qqg)}{dk\,d\Theta} \approx \frac{\alpha_s}{K\sin\Theta}\,\sigma_{qq}$$

where K and Θ are the gluon energy and emission angle relative to the quark direction of flight (see Fig. 27). The average transverse momentum of the (hard) gluon jet is

$$\langle K_T \rangle \approx \frac{\alpha_s \cdot \sigma_{qq} \iint \frac{K\sin\Theta}{K\sin\Theta}\, dK\,d\Theta}{\sigma_{qq}\,(1+\frac{\alpha_s}{\pi})} \qquad (17)$$

$$\approx \alpha_s \cdot E_{beam} \qquad \text{(up to log terms)}$$

The remarkable result is that contrary to many other predictions of QCD which lead to logarithmic deviations from the pure quark model, and are therefore difficult to test experimentally, the transverse momentum is predicted to rise linearly with energy. A direct consequence is that the jet cone will not shrink indefinitly but will have an almost constant opening angle, $\delta = \langle p_T \rangle / \langle p_{\parallel} \rangle$ since both, longitudinal and transverse momenta, will grow linearly with energy above a certain minimum energy.

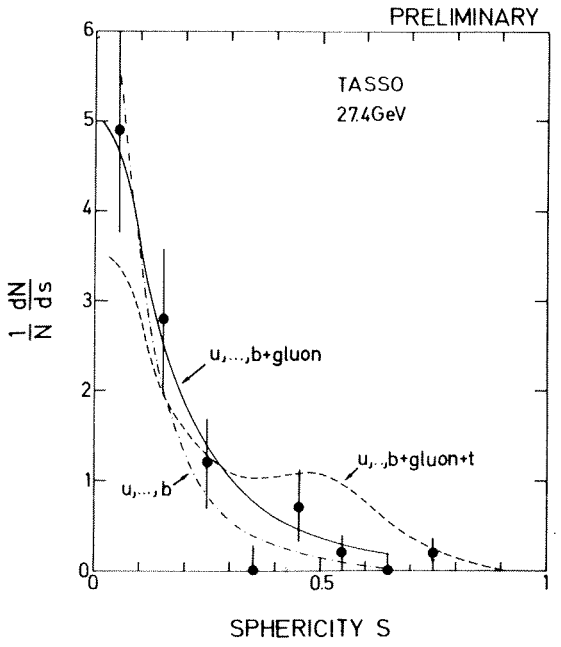

Fig.28 The sphericity distribution at 27.4 GeV as measured by TASSO (Ref.10). The curves show predictions[24] of the quark model with u, d,...b quarks (dashed-dotted) plus gluon corrections (solid) plus a t quark contribution (dashed).

Fig. 28 shows the measured sphericity distribution at 27.4 GeV together with the predictions from the pure quark model (including u,d,s,c,b quarks) and the QCD corrections to it[24]. The statistical accuracy is insufficient to prefer one over the other.

The QCD broadening of jets has been extensively studied [20,22,24-27], devising many tests to establish this phenomenon. The distinction between the QCD broadening and e.g. a mere rise of the average p_T for quark fragmentation is possible. The hard gluon emission leads to three jet events or, if you like one fat and one small jet while the latter would produce two fat jets. As shown by Professor Söding in his talk the available data are consistent with QCD. More statistics at high PETRA energies will make the QCD effects clearly discernible from other possible sources.

7. SEARCH FOR THE t QUARK

The observed symmetry between leptons and quarks suggests besides u, d, s, c, b the existence of a sixth quark, t. The charge of the t quark is predicted to be +2/3 if one groups the quarks in weak isospin doublets, viz

$$\begin{pmatrix} u \\ d \end{pmatrix}, \begin{pmatrix} c \\ s \end{pmatrix}, \begin{pmatrix} b \\ t \end{pmatrix}$$

The theoretical predictions for the t mass populate mass values between 10 and 40 GeV[28]. Forgetting about theory one can look at the ψ, J/ψ, Υ mass spacing,

$$m_{J/\psi}/m_{\phi} \simeq m_{\Upsilon}/m_{J/\psi}$$

which suggests the $t\bar{t}$ vector ground state to be found at

$$m_{V_t} = m_{\Upsilon}^2/m_{J/\psi} \approx 28 \text{ GeV}$$

which is in the reach of PETRA. The peak height of the total cross section at the position of V_t depends on the leptonic decay width Γ_{ee} and on the energy spread of the storage ring beams. The Breit-Wigner without energy spread reads

$$\sigma(e^+e^- \to V_t) = \frac{3\pi}{s} \frac{\Gamma_{ee}\,\Gamma}{(M_o - W)^2 + \Gamma^2/4} \tag{18}$$

The energy spread of the beams, ΔE, reduces the peak cross section - very roughly - to

$$\sigma_{peak} \simeq \frac{3\pi}{s} \cdot \frac{\Gamma_{ee}}{\Delta W} \tag{19}$$

where $\Delta W = \sqrt{2} \cdot \Delta E$. For PETRA

$$\Delta E/E = 6.5 \cdot 10^{-5}\, E, \qquad E \text{ in GeV} \tag{20}$$

For a mass of 28 GeV (E = 14 GeV) the energy spread is ΔE = 13 MeV. The leptonic width Γ_{ee} depends on the shape of the $t\bar{t}$ potential. Various models studied[29] suggest that Γ_{ee} is approximately the same as for the J/ψ, Γ_{ee} = 5 keV. This yields

$$\sigma_{peak}(28\ \text{GeV}) \simeq 1.3\ \text{nb}$$

or

$$R_{peak}(28\ \text{GeV}) \simeq 11.$$

The signal to noise ratio is 11:4 or ~3. This may be compared with the J/ψ seen at SPEAR or DORIS where the signal to noise ratio is roughly 100.

The $c\bar{c}$ system has two bound $^3S_1$ vector states, J/ψ and ψ'; the $b\bar{b}$ system probably has three while the $t\bar{t}$ is expected[29] to have 6 or 7 bound states $1^3S_1, \ldots, 6^3S_1$ as sketched in Fig. 29. One may guess that the $t\bar{t}$ continuum is likely to begin two or three pion masses above the $T\bar{T}$ threshold (where T denotes a $t\bar{q}$ meson), i.e. $W_{continuum} \approx M(6^3S_1) + 2 \div 3\ m_\pi \simeq M(V_t) + 2$ GeV.

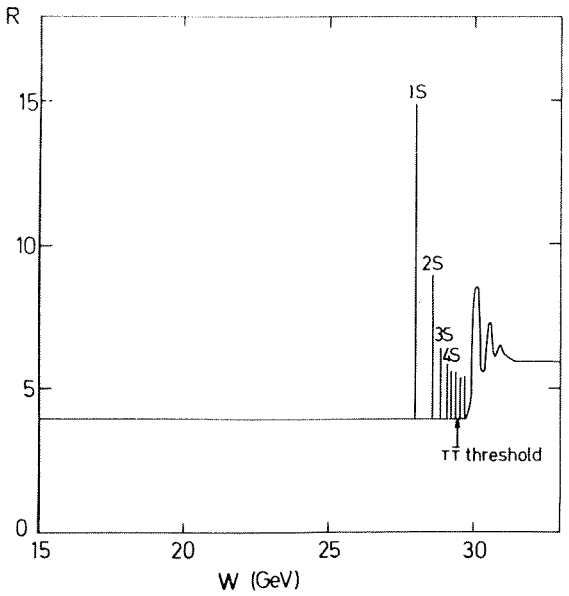

Fig.29 The energy dependence of R expected near the $t\bar{t}$ threshold.

While it will require a large effort to localize the vectorstates it should be straight forward to detect the $t\bar{t}$ continuum contribution provided the available energy is sufficient. The asymptotic $t\bar{t}$ contribution should be $R_t = 3 \cdot (\frac{2}{3})^2 = \frac{4}{3}$. Near threshold it is likely to be larger. Comparing with the charm contribution near 4 - 4.5 GeV, one may expect $R_t = 2$ or $R \simeq 6$ above $t\bar{t}$ threshold. The R values measured by MARK J, PLUTO and TASSO up to 27.4 GeV (see Fig. 6) do not show this expected rise in R from 4 to 6. They are consistent with no rise between 13 and 27.4 GeV. However, the systematic uncertainties quoted are of the order of 10 - 20%.

A quantity more sensitive to the $t\bar{t}$ contribution is the sphericity. Events from $t\bar{t}$ decay can be expected to have high multiplicity and a phase space like configuration near threshold. According to the Kobayashi-Maskawa[30] generalized Cabibbo matrix the favored decay sequence for t quarks is $t \to b \to c \to s$. As a consequence $T\bar{T}$ hadronic decays have no less than 14 (or more) quarks in the final state (see Fig. 30). The same line of argument used to explain the step in <S> above the charm threshold predicts a large increase of S by ~ 0.08 from roughly 0.15 below threshold to 0.23 above threshold (see curve in Fig.19). A similar effect would be seen in thrust. The data at 27.4 GeV are consistent with what one expects for u,d,s,c,b contributions alone (see Fig. 19).

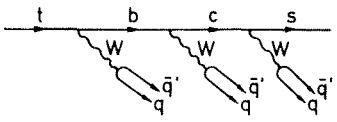

Fig.30 (Hadronic) decay scheme for t quarks.

Finally, one can investigate the sphericity and thrust distributions at 27.4 GeV. Above the $t\bar{t}$ threshold e.g. the T distribution should be a superposition of a rapidly falling distribution from the first 5 quarks including QCD broadening plus a broad gaussian like distribution centered around $T \simeq 0.7$ describing $t\bar{t}$ events. In Fig. 31 the

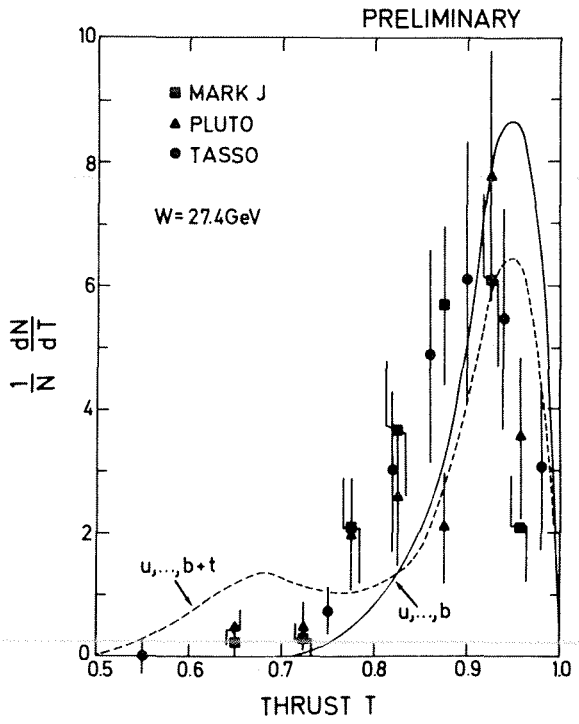

Fig.31 Thrust distribution at 27.4 GeV (Refs. 8-10). The curves show the predictions of the quark model for u, d,...b and for a t.

thrust distribution as measured by MARK J, PLUTO and TASSO at 27.4 GeV are compiled. The data agree well with the distribution expected from u,...,b quarks; there is no evidence for a $t\bar{t}$ contribution. Table 4 summarized the observed and expected number of low thrust events.

Table 4
Observed number of events with thrust T < 0.75 at 27.4 GeV and expected number of events above the $t\bar{t}$ threshold

	$N_{observed}$	$N_{expected}$
MARK J	1	15
PLUTO	3	11
TASSO	2	9

The absence of a $t\bar{t}$ signal can mean either one of two things : the $t\bar{t}$ threshold is above 27.4 GeV or it is below 27.4 GeV but the $t\bar{t}$ contribution is small because 27.4 is in a valley between two $t\bar{t}$ resonances.+

8. TWO PHOTON PROCESSES

So far we have been discussion hadron production through annihilation of electron and positron. As first pointed out by Low[31] there is another class of ee processes where the (virtual) photon clouds of the two beams interact with each other and produce hadrons by $\gamma\gamma$ scattering (see Fig. 32). The cross section is of the fourth order in α but logarithmically rising with energy $\sigma(ee \to eeX) \sim \alpha^4 \ell n^2 \frac{E}{m_e}$; the logarithms result from integrating the photon spectra. Because of its energy dependence the two photon cross section overtakes the annihilation cross section ($\sigma \sim \alpha^2/E^2$) at some point and two photon scattering becomes the dominant source of hadrons at high energies.

Owing to the bremsstrahlung type energy spectrum of the two photons the total c.m. energy M of the hadron system produced by $\gamma\gamma$ scattering is rapidly falling with M, viz.[32]:

$$\frac{d\sigma(ee \to eeM)}{dM^2} \approx \frac{\alpha^2}{\pi^2}\left(\ell n \frac{4E^2}{m_e^2}\right)\left(\ell n \frac{4E^2}{M^2}\right)\frac{\sigma(\gamma\gamma \to M)}{M^2} \qquad (21)$$

This permits to separate the two types of processes experimentally even at high energies (see Fig. 3).

The PLUTO group[9] has made a first attempt to measure the cross section for $\gamma\gamma$ scattering into hadrons. One of the scattered electrons has been detected (tagged) in a forward hodoscope while the hadrons produced have been observed in the central detector. The event selection required

1. energy of the tagged electron more than 3 GeV,

+ Note added in proof : Data taken at 27.72 GeV did not show any evidence for $t\bar{t}$ events either which renders the valley hypothesis unlikely.

2. three or more tracks in the central detector, two of which have to have a transverse momentum relative to the beam pipe of more than 0.3 GeV/c.

The scattering angle of the tagged electron had to lie between 23 and 70 mrad which lead to average Q^2 values of one of the virtual photons of 0.09, 0.11 and 0.3 GeV^2 at total energies of 13, 17 and 27.4 GeV, respectively. In evaluating $\sigma_{\gamma\gamma}$ the Weizsäcker-Williams approximation was applied. This can lead to deviations from the exact result as large as factors of 1.5-2 as shown recently by Kessler and coworkers[33].

Fig. 33 shows $\sigma_{\gamma\gamma}$ as a function of the visible hadron energy. The 13 and 17 GeV data for which $\langle Q^2 \rangle \approx 0.1$ GeV^2 the $\gamma\gamma$ cross section can be described by $\sigma_{\gamma\gamma} \simeq (0.3 + 0.9/M_{vis})$ μb, M_{vis} in GeV. The 27.4 GeV data with $\langle Q^2 \rangle = 0.4$ GeV^2 are consistently lower above $M_{vis} = 2$ GeV. Simple vector dominance, replacing the two photons by vector mesons, predicts for $M \gtrsim 2$ GeV

$$\sigma_{\gamma\gamma}^{VDM} \approx \frac{2}{3} \sigma_{\pi N} \left(\frac{\sigma_{\gamma p}}{\sigma_{\pi N}}\right)^2 \approx 0.4 \ \mu b$$

in qualitative agreement with the data. The factor of 2/3 accounts for the fact that the nucleon is made of three quarks and vector mesons of two. To the VDM result the excitation of resonances specific to the $\gamma\gamma$ channel[34] and possibly quark box diagrams[35] have to be added.

The fact that the $\gamma\gamma$ cross sections deduced from the 27.4 GeV data are lower is expected since at least one of the virtual photons is further off the mass shell. The results on virtual photon nucleon scattering suggest for <u>one</u> photon being off the mass shell

$$\sigma_{\gamma\gamma}(Q^2) \approx \frac{1}{1 + Q^2/0.6 \ GeV^2} \sigma_{\gamma\gamma}(0)$$

in rough accord with Fig. 33.

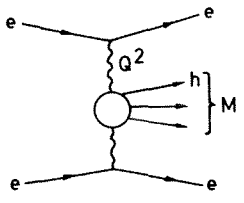

Fig.32 Diagram for $\gamma\gamma$ scattering.

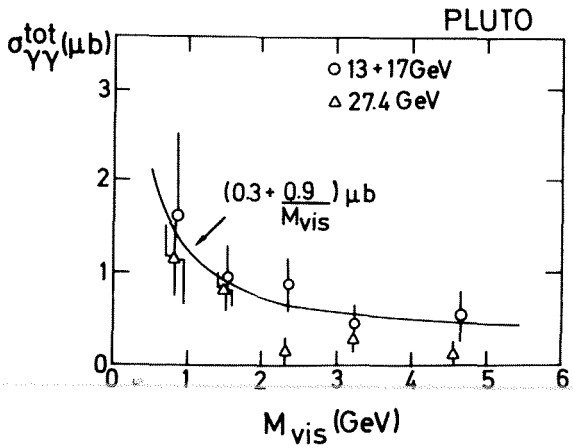

Fig.33 The $\gamma\gamma$ cross section as measured by PLUTO at $\langle Q^2 \rangle = 0.1$ GeV^2 (13 and 17 GeV data) and 0.4 GeV^2 (27.4 GeV data). (Ref. 9).

CONCLUSIONS

1. Hadron production at high energies is dominantly jet-like. The jet cone is shrinking $\sim W^{-1/2}$ as the energy increases.

2. The shape and magnitude of the total cross section, the observed scaling behaviour of the inclusive cross sections, the occurance of jets and their gross features are in astonishing agreement with the quark hypothesis.

3. First evidence for corrections to this hypothesis have been presented to this conference. The momentum distribution of hadrons transverse to the jet axis is broadening at very high energies. The data indicate that only one of the two jets is broadening and that the broadening occurs in a plane. This makes it unlikely that the broadening can be understood as a general widening of the (nonperturbative) P_T distribution with energy. The details of the effects are consistent with QCD where one of the quarks radiates off a hard gluon.

   Deep inelastic lepton nucleon scattering and e^+e^- annihilation complement each other in this respect. The scale breaking observed in the first one is caused by forward emission ($\theta = 0$) of the gluon, the latter by the transverse momentum component X_T ($\theta \neq 0$) carried away by the gluon (see Fig. 34).

4. In the energy range up to 27.4 GeV no evidence has been found for the existence of a sixth quark.

5. A first attempt has been made to measure the total $\gamma\gamma$ - cross section. This marks the beginning of a new field : hadron production by the scattering of photons on photons.

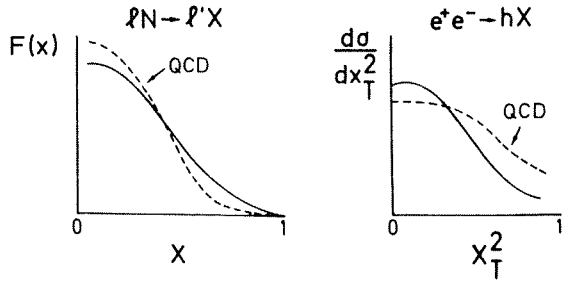

Fig.34 Illustration of QCD effects in lepton nucleon scattering and e^+e^- annihilations.

Acknowledgements

I am grateful to my colleagues for numerous discussions, in particular to J. Ellis, Y. Eisenberg, T. Meyer, E. Reya, P. Söding, B.H. Wiik and S.L. Wu.

REFERENCES

1) A. Quenzer, thesis, Orsay report LAL 1294 (1977);
A. Cordier et al., Phys. Lett. 81B (1979) 389;
A.V. Sidorov, rapporteur talk, 1976 Tbilisi Conference, N46

2) G.P. Murtas, 1978 Tokyo Conference, B2;
R. Baldini, invited speaker at this conference

3) J. Perez-y-Jorba, 1978 Tokyo Conference

4) R.F. Schwitters, rapporteur talk, 1976 Tbilisi Conference, B34

5) Bizot, invited speaker at this conference
J. Augustin, rapporteur talk to this conference

6) PLUTO collaboration, J. Burmester et al., Phys. Lett. 66B (1977) 395

7) DASP collaboration, R. Brandelik et al., Phys. Lett. 76B (1978) 361

8) MARK J collaboration, D. Barber et al., Phys. Rev. Lett. 42 (1979) 1113

9) PLUTO collaboration, Ch. Berger et al., Phys. Lett. 81B (1979) 410
and V. Blobel, invited speaker at this conference

10) TASSO collaboration, R. Brandelik et al., Phys. Lett. 83B (1979) 261

11) DASP collaboration, R.Brandelik et al., Nucl. Phys. B148 (1979) 189

12) E. Albini, P. Capiluppi, G. Giacomelli and A.M. Rossi, Nuovo Cimento 32A (1976) 1o1

13) PLUTO collaboration, G. Knies, rapporteur talk, 1977 Hamburg Conference, p.93

14) P.A. Rapidis et al., SLAC-PUB 2184 (1979)

15) R.F. Schwitters, rapporteur talk, 1975 Stanford Conference, p.5

16) R. Baier, J. Engels and B. Peterson, University of Bielefeld report BI-TP 79/1o (1979)
adn B. Peterson, private communication;
W.R. Frazer and J.F. Gunion, University of California report UCD-78-5 (1978)
and J.F. Gunion, private communication

17) R.F. Schwitters, rapporteur talk, 1975 Stanford Conference, p.5;
R.F. Schwitters et al., Phys. Rev. Lett. 35 (1975) 1320;
G.G. Hanson et al., Phys. Rev. Lett. 35 (1975) 1609;
G.G. Hanson, results presented at the 13th Rencontre de Moriond (1978), Vol. II,
ed. by J. Tran Thank Van

18) PLUTO collaboration, Ch. Berger et al., Phys. Lett. B78 (1978) 176

19) P. Söding, rapporteur talk at this conference

20) A. de Rujula, J. Ellis, E.G. Florates and M.K. Gaillard, Nucl. Phys. B138 (1978) 387;

21) R.D.Field and R.P. Feynman, Nucl. Phys. B136 (1978)1;
The production and fragementation of c and b quarks has been incorporated by T. Meyer.

22) J. Ellis, M.K. Gaillard and G. Ross, Nucl. Phys. B111 (1976) 253

23) see e.g. H. Fritzsch, Schladming Lectures 1978, Acta Physica Austriaca Suppl. XIX, p.249

24) P. Hoyer, P. Osland, H.G. Sander, T.F. Walsh, and P.M. Zerwas, DESY report DESY 79/21 (1979);
and H.G. Sander, private communication.

25) G. Sterman and S. Weinberg, Phys. Rev. Lett. 39 (1977) 1436

26) T. De Grand, Y.J. Ng and S.H. Tye, Phys. Rev. D16 (1977) 3251
G. Kramer and G. Schierholz, DESY report, DESY 78/62 (1978);
G. Kramer, G. Schierholz and J. Willrodt, Phys. Lett. 79B (1978) 249

27) G. Fahri, Phys. Rev. Lett. 39 (1977) 1587;
S. Brandt et al., Phys. Lett. 12 (1964) 57;
G.C. Fox and S. Wolfram, Nucl. Phys. B149 (1979) 413;
S.Y. Pi, R.L. Jaffe and F. Low, Phys. Rev. Lett. 41 (1978) 142

28) see e.g. C.J. Aubrecht II and D.M. Scott, COO-1545-247;
G. Preparata, CERN TH 2599 (1978);
M.A. Combrugghe , Phys. Lett. 80 B (1979) 365;
H. Georgi and D.V. Nanopulos, HUTH-78/A039 (1978);
H. Harari, H. Haut and J. Weyers, Phys. Lett. 78B (1978) 459;
S. Pakvasa and H. Sugawara, Phys. Lett. 82B (1979) 1o5;
J.D. Bjorken SLAC-PUB 2195 (1978)
T.F. Walsh, DESY Report DESY 78/68 (1978)

29) C. Quigg and J.C. Rosner, Phys. Lett. 72B (1978) 462;
G. Bhanot and S. Rudaz, Phys. Lett. 78B (1978) 119;
H. Krasemann and S. Ono, DESY-Report DESY 79/09 (1979)

30) M. Kobayashi and K. Maskawa, Pro. Theor. Phys. 49 (1973) 652

31) F.E. Low, Phys. Rev. 120 (1960) 582;
F. Calogero and C. Zemach,Phys. Rev. 120 (1960) 1860;
A. Jaccarini, N. Arteaga-Romero, J. Parisi and P. Kessler,
Compt. Rend. 269 B (1969) 153, 1129; Nuovo Cimento 4 (1970) 933;
S. Brodsky, T.Kinoshita and Terazawa, Phys. Rev. Lett. 25 (1970) 972;
H. Terazawa, Rev. Mod. Phys. 45 (1973) 615

32) S. Brodsky, SLAC-PUB 2240 (1978)

33) C. Carimalo, P. Kessler and J. Parisi, Collège de France report L.P.C. 79-06 (1979)

34) see e.g. B. Schrempp-Otto, F. Schrempp, and T.F. Walsh, Phys. Lett. 36B (1971) 463;
G. Schierholz and K. Sundermeyer, DESY Report 71/49 (1971)

35) M. Greco and Y. Srivastava, University of Rome preprint (1978)

ELECTRON-POSITRON ANNIHILATION: SOME REMARKS ON THE THEORY*

James D. Bjorken
Stanford Linear Accelerator Center, Stanford University, Stanford, California 94305, USA.

ABSTRACT

We review some topics in e^+e^- annihilation, including high-quality QCD tests, jet production, production of old and new leptons and quarks, gluonium, Higgs-bosons, and unconfined quarks.

It is difficult for me to try to review the status of e^+e^- theory; I feel very much an amateur at this point. Since the early days, the field has matured and flourished a great deal. More than a half dozen very large experimental groups are well prepared to exploit the expected physics forthcoming from PETRA and soon from PEP. These groups are served by a large number of theoretical gurus, e.g., one expert on sphericity, another on spherocity, another for thrust, and so on. So the phenomenology expected from QCD and the Kobayashi-Maskawa six-quark version of electroweak $SU(2) \otimes U(1)$ has been rather thoroughly worked out, and it is now a matter of waiting for the returns to come in. We have had abundant evidence at this meeting that thus far there is no trouble for the theory. It is a far cry from the early ADONE days, when existence of a large multihadron cross section was considered something of a surprise, or the days of the CEA and SPEAR startups. Then the most popular hypothesis had R less than $s^{-1} \log s$, while $R = 2/3$ was considered a large estimate[1]. This time around, everything is working remarkably well — almost too well. It is tangible evidence of the great progress that has been made in the last decade.

This talk will not try to be a detailed or balanced review of the phenomenology, and will consist only of remarks on a few aspects I feel may be important, along with others that are perhaps a bit neglected. The topics are listed below:

(1) Gold-plated tests of QCD.
(2) Comments on jet properties.
(3) Leptons, old and new.
(4) New quarks.
(5) Higgs.
(6) Gluonium.
(7) Unconfined quarks.

1. GOLD-PLATED TESTS OF QCD

Many QCD calculations are actually judicious mixtures of the parton-model and QCD perturbation theory. Others stretch the limits of applicability of the short distance, perturbative quark-gluon aspect of the theory. But there are a few tests which appear to be especially clean, and therefore deserve special attention. The best candidate is the colliding beam total cross section, or R. The theoretical value is

$$R = \left(\sum_i Q_i^2\right)\left[1 + \frac{\alpha_s}{\pi} + (1.98 - .12N_f)\left(\frac{\alpha_s}{\pi}\right)^2 + \ldots\right] \qquad (1)$$

* Work supported by the Department of Energy under contract number DE-AC03-76SF00515.

The second order term has only been recently calculated[2]. The result above is expressed in a modified minimal-subtraction renormalization scheme, one which allows a definition of α_s comparable to the one used in analyses of deep inelastic lepton-nucleon scattering.

It is probably better to evaluate the real part of the vacuum polarization at spacelike Q^2; this has been recently carried out by Sanda[3]. It should come as no surprise that the agreement with QCD is satisfactory. Nevertheless the systematic errors in the experiments are still large ($\Delta R \gtrsim 0.5$) and it is important to refine, if possible, the measurements to sharpen the comparison as much as possible. For example, it is not ruled out that there is a $J = 0$ pointlike integer-charged boson ($R = 0.25$) being produced along with the quarks.

Another test which appears quite clean is the production of energy (gluon jets) at large angles to the quark-jet direction[4]. A gluon with finite fraction ε of the total energy and large angle (greater than some fixed angle δ) relative to the quark jet is emitted at very short distances $\sim s^{-\frac{1}{2}}$, and therefore calculable in perturbation theory[5]. This short-distance process should lead to a distinct 3-jet final state. Hence measurement of the cross section and distribution in the Dalitz plot of these "gold-plated" 3-jet events should lead to an especially clean test of QCD perturbation theory and an independent determination of α_s.

Another candidate for a clean test is annihilation of onium into three gluons. However recent calculations[6] show very large radiative corrections for these processes, $\sim(10\text{-}20)\ \alpha_s/\pi$. Thus doubt is shed on quantative tests based on hadronic width. However, the data[7] on 3-jet final states in T decay remain of course a nice piece of general evidence in support of QCD.

We may also mention in this connection recent work of Peskin[8], who constructs a strict multipole expansion for gluon systems coupled to massive onia, based on operator product expansions. However in this case, it can only be applied to extremely heavy onia (which are essentially Coulombic), with level spacing large compared to the confinement scale Λ (Peskin optimistically estimates $m_Q \gtrsim 25$ GeV, but this number could well be considerably higher). This again suggests that QCD tests involving onia may not be all that gold-plated.

2. JET PROPERTIES

It takes a distance scale ~10-20 f for a PETRA/PEP jet to evolve from its parent parton into a group of distinct, approximately collinear hadrons. After the original $q\bar{q}$ pair have separated by no more than 1 fermi, one must expect that non-perturbative confinement effects are operative, in order that each jet screens the fractional charge and color it possesses at birth[9]. It is not clear to what extent (if any) such effects influence, say, the inclusive distribution of leading hadrons. Nevertheless, one must exercise extra caution in interpreting inclusive hadron distributions (parton fragmentation) in terms of perturbative QCD.

The question of the time-evolution and screening of QCD jets has recently attracted theoretical attention. The tree-structure of quark and gluon emissions present in the leading-logarithm approximation to QCD suggests a time-evolution for jet formation similar to the Weiszacker-Williams approximation in QED. The QED evolution does occur on a long time scale[10] (proportional to $\sqrt{s}$) so that one may suspect perturbative QCD to be deficient in being able to account for the evolution of color confinement[11]. However, the situation appears to be not that bad[12]. Owing to the high multiplicity of low-rapidity gluons emitted at short times — times short enough ($t \ll 1f$) for the perturbative calculations to

be trusted — there is enough filling of the central rapidity-region to allow soft confining effects to easily proceed at early times[13]. Indeed it has been found by Amati and Veneziano[14] that the distribution in rapidity of virtual quarks produced at early proper time (i.e., very near the light cone) allow — in the $1/N_c$ approximation — the quarks to be grouped into color-singlet combinations of relatively low mass. This phenomenon, which is dubbed "preconfinement," sets the stage for the action of only soft confining forces in producing the observed hadrons out of the groups of virtual quarks and gluons.

However, these calculations are strictly valid only in the very asymptotic limit of high multiplicity of virtual gluons ($n_g \sim \exp \sqrt{Q^2/\mu^2}$) and thus very high Q^2. It would also be nice to see a more explicit space-time description of how the jets evolve. Another interesting question concerns what role would be played by pre-confining processes in a world without light quarks u,d,s. On the one hand, at sufficiently high energies $\sqrt{s}$, the time-evolution of the perturbative QCD jet should be insensitive to quark masses m_Q for times $t < m_Q^{-1}$. On the other hand, one intuitively suspects that in a world with only heavy quarks, confinement is implemented at all energies via strings connecting the heavy quarks, and not by pair-creation of $Q\bar{Q}$. Is this intuition wrong?

While jet structure has its theoretical uncertainties, it does mean we might learn more about non-perturbative aspects of QCD by studying it. The approximate scaling behavior of the leading hadrons is compatible with parton model ideas, suggesting that use of perturbative methods may be applicable. This phenomenology has had some success and is discussed here[15] by M. K. Gaillard. An important experimental question concerns charge correlations of the leading hadrons. The observed hadron distributions in neutrino-nucleon interactions are in good agreement with the general notions of parton fragmentation[16]. While much of the observed correlations of leading hadrons with parent-quark charge in charged-current ν and $\bar{\nu}$ processes may be attributed to phase-space and overall charge-conservation effects[17], this criticism cannot be made for the neutral-current processes, where a distinct difference in the π^+/π^- ratio for leading mesons has been seen in νN vs. $\bar{\nu}$N processes. [In fact, it may now be time to use neutral currents as a tool in studying QCD and parton-model dynamics, accepting the applicability of the Weinberg-Salam effective Lagrangian for the basic coupling.] In colliding-beam reactions, one must therefore expect a negative charge correlation of the leading hadron in the quark jet with that of the antiquark jet, reflecting the negative charge correlation of their parents. A search for such an effect was made in SPEAR data, with results somewhere between inconclusive and negative[18]. It seems hard to find an excuse for this effect not being present at the higher energies now available.

Another question of considerable interest concerns the inclusive production of D and D^*. One naturally expects that their momentum distributions should be flatter than the pion distribution because of the heavy quark inside, which is difficult to decelerate. Existing SPEAR data[19] is too close to threshold to give a good inclusive distribution. The situation in the neutrino data is consistent with a flat D spectrum; however, the arguments are rather indirect[20].

3. LEPTONS, OLD AND NEW

The e^+e^- physics of μ and e centers about the QED tests. Of course we now expect QED to break down. The photon is supposed to die at a distance scale of ~100 GeV, presumably to be replaced by the U(1) generator of electroweak SU(2) $\otimes$ U(1) at shorter distances.

The most salient tests are well known and well studied, namely $\delta R_{\mu^+\mu^-}$ and the front-back asymmetry in $e^+e^- \to \mu^+\mu^-$.

The τ lepton is by now almost an "old" lepton. But it should not be taken for granted; we saw already[21] that PEP/PETRA should be especially clean sources of τ's. What is interesting?

(i) Lifetime: Georgi and Glashow have recently played with assigning τ to a higher grand-unified SU(5) representation[22], leading to a reassignment of τ to an electroweak triplet $(\nu_\tau\, \tau^-\, L^{--})_L$. This leads to a τ lifetime a factor two shorter than the standard value. On the other hand, were ν_τ mixed with a massive neutral lepton, the lifetime could be longer.

(ii) Branching ratios: Kane, motivated by the apparently large branching ratio of $D \to K\bar{K}$ observed at SPEAR, has suggested[23] that charged Higgs-exchange contributes to this weak decay as well as the usual $W^\pm$ exchange. His scheme then implies that this Higgs should contribute to τ-decay. This leads to branching ratios for $\tau \to K\nu$ and $\tau \to \pi\nu$ at variance with the standard (gold-plated) predictions coming from W-exchange. The effect is a factor $\sim$1.4 for $K\nu$ and $\sim$1.1 for $\pi\nu$.

(iii) Rare decays: We know so little about intergeneration relations that one should watch for other unanticipated rare decays such as $\tau \to eee$, μee, $\mu\gamma$, $e\gamma$, $\mu\pi$, μK, $e\pi$, eK, ...

Given the cloning of fermions into three generations, we cannot rule out the possibility of a fourth charged sequential lepton λ. If the trend $m_\mu/m_e > m_\tau/m_\mu > m_\lambda/m_\tau$ is correct[24], there is a good chance that λ production would be within the PETRA/PEP energy range. The final states and branching fractions would be (for $E_{CMS} \sim 30$ GeV)

$$\begin{aligned} e^+e^- \to \lambda^+\lambda^- &\to q\,q\,q\,q\,\nu\,\nu \sim 45\% \\ &\to q\,q\,\ell\,\nu\,\nu\,\nu \sim 45\% \\ &\to \ell\,\ell\,\nu\,\nu\,\nu\,\nu \sim 10\% \end{aligned} \qquad (2)$$

Signatures are high sphericity, relatively low visible energy, and considerable numbers of energetic associated charged leptons which are not correlated with the quark jets. It seems unlikely that such a particle has been already produced at PETRA unless the threshold is rather near 27.4 GeV.

Neutral leptons, while less conventional, should not be forgotten. They naturally appear, for example[25], in the grand-unified theory based on the exceptional group E6. [This model can be arranged[26] so as to give just as satisfactory a value for $\sin^2\theta_W$ as SU(5).] There was a time when a neutral lepton N^o, paired with the right-handed electron in a weak doublet, helped in understanding the null result of the Seattle and Oxford atomic parity violation experiments. Such an N^o could be produced in $e^+e^- \to N_0\nu_e$ via W-exchange, or in $\tau^- \to \nu_\tau \bar{N}_0 e^-$. A search[27] at SLAC for the latter mode set a limit $M_{N^o} > 1.2$ GeV. However, the SLAC polarized electron-scattering experiments[28] have disallowed this assignment. The remaining way to produce an N_0 in e^+e^- annihilation is pair production via an intermediate Z^o (or Higgs). The R for such a process[29] is $\lesssim 10^{-2}$ at $E_{CMS} \sim 30$ GeV. Provided N_0 communicates with μ or τ, a good signature is two leptons (+ other charged particles as well) in the final state. If N_0 is of low mass, the $\pi^\pm\mu^\mp$ channel is an especially nice signature. If N_0 is of high mass, the high sphericity (plus two leptons), or more than two charged leptons are good signatures.

4. NEW QUARKS

The signatures for new-quark production have been much discussed[30] and will not be reviewed here again in detail. They include increases in sphericity, $\bar{n}_{ch}$, inclusive lepton yields, and various multilepton configurations as one crosses the production threshold. As one has seen[31], the detection is relatively easy for tops, and difficult for bottoms.

While one may discover such quarks without too much grief, it is harder to do something with them once one has them. For example, the decay

$$t \to qqq \tag{3}$$

with $m_t \sim 15$-20 GeV will yield a better 3-jet final state than $T \to qqq$. But with two t-quarks per event, it will be hard to disentangle all those jets.

For the bottom-quark the situation is similar. There is expected to be a flavor cascade

$$b \underset{W}{\to} c \underset{W}{\to} s \underset{W}{\to} u \tag{4}$$

and inclusive properties as well as multilepton, multikaon events will provide a fair amount of information. But it will be rather indirect. To find direct exclusive decay channels of B will probably be harder than for D. Leading candidates are $B \to D\pi\pi$ or $D^*\pi\pi$. An interesting idea[32] is to use the decay channel $b \to c(\bar{c}s)$ which is not too badly repressed by phase-space effects. One has modes $B \to D\bar{D}\bar{K}$ or $B \to \psi\bar{K}$. Observable branching ratios, however, are not better than 10^{-3}, so that one needs $> 10^4$ bottom-mesons just to enter the game[33].

The orthodoxy gives a reasonably definite picture of bottom-quark properties, but these properties could change radically were the orthodoxy to be abandoned. If bottom is an electroweak singlet, one does not understand at all the decay-mechanism, and the lifetime could be anything. Even within the doublet assignment, crazy things might happen. For example, Derman[34] uses permutation symmetry to relate fermion generations to each other, and ends up, because of multiplicative conservation laws, with b decaying only semileptonically, e.g., $b \to q\mu e$. It will not take long to settle that issue.

5. HIGGS

The final, least understood, and least established piece of the orthodoxy is the Higgs sector. The minimal scheme has one neutral Higgs-boson of mass somewhere between ~10 GeV and ~10^3 GeV. There has been increased enthusiasm[35),36] of late for supposing that the only mechanism which gives the Higgs-boson its mass is essentially the virtual emission and absorption of $W^{\pm}$ and Z. With the present value of $\sin^2\theta_W \cong 0.23$, this puts the Higgs-mass at $\cong$ 10 GeV, approximately degenerate with the T system. This mass range for the Higgs is rather advantageous from the point of view of early detection[35]. If toponium does turn up at a mass ~30 GeV, the branching ratio for $(t\bar{t}) \to h^o + \gamma$ is $\sim 5 \times 10^{-3}$. In addition, the decays of T states (especially T' and T'') into $h^o + \gamma$ is enhanced by mixing of the h^o with the 0^{++} P-wave bottomonium states. Branching ratios are $\sim 10^{-4}$, and with some luck could even be bigger. The situation is summarized in Fig. 1.

The Higgs sector might suffer proliferation, just like the fermion-sector does. If so, there should exist charged Higgs particles, which should be pair-produced by e^+e^-, with an $R = 0.25$. However, not much guidance can be given on masses, coupling constants, or decay modes[37].

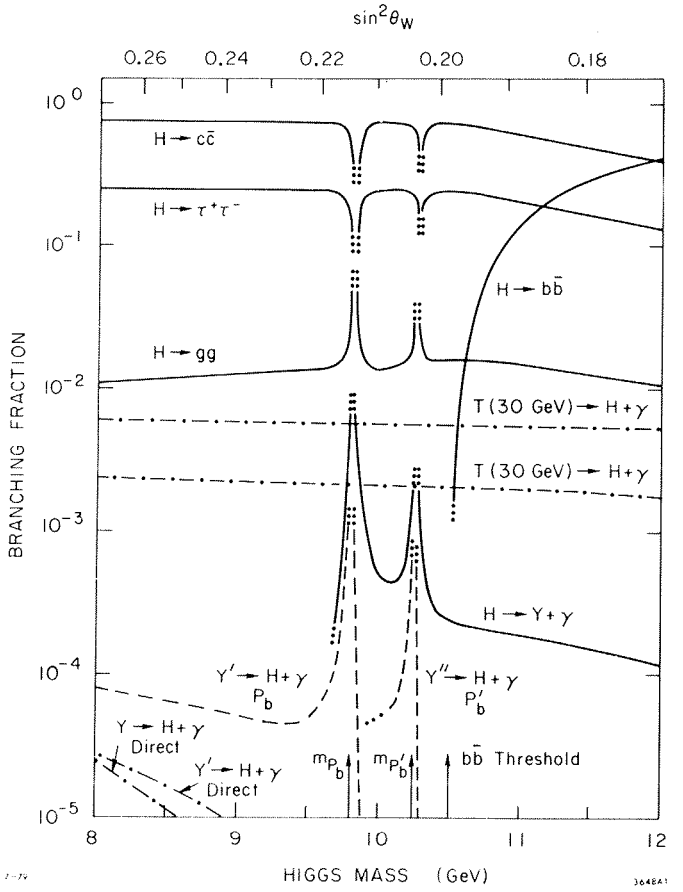

Fig. 1. Properties of a standard model Higgs-boson of mass ~10 GeV (the "scalon"). Taken from Ref. 35).

6. GLUONIUM

We now turn to a less-discussed feature[38] of the orthodoxy — that of gluonium. Gluonia are the physical quanta of pure QCD (i.e., QCD without the quarks): quarkless, colorless, flavorless mesons with mass probably in the range of 1 to 2 GeV. We emphasize that QCD implies that they should exist. Why? Let us start with pure QCD and consider the well known process

$$\nu + \bar{\nu} \rightarrow g + g \tag{5}$$

This is neutrino-antineutrino annihilation into two gluons via a virtual graviton. At short distances asymptotic freedom tells us that the cross section can be calculated perturbatively. Let

$$R_\nu = \frac{\sigma(s)}{\sigma(s)_{point}} \tag{6}$$

be defined as usual, and consider the behavior as s decreases. As s approaches the confinement scale, perturbation theory breaks down, and we expect some wiggles in the true R_ν along with possible discrete resonances, as shown in Fig. 2. There are two choices for the mass scale M: either it is small (1-2 GeV) or it is large. If it is large, gluonia could be heavy, but then perturbation theory breaks down at an unexpectedly high mass scale. Such

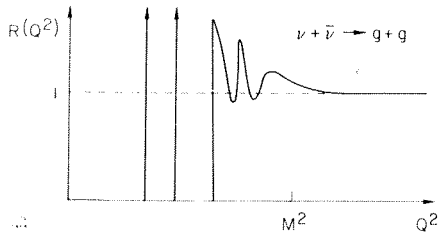

Fig. 2. Hypothetical cross section for the process $\nu + \bar{\nu} \to$ hadrons (gluonia) in pure quarkless QCD, normalized to the point cross section.

a conclusion would undermine the applicability of perturbative QCD at a moderate mass scale. On the other hand, if the mass scale is small, then the gluonia have small masses and there is no problem with convergence of perturbation theory.

However, this is still pure, quarkless QCD, not the real world. What happens when the quarks are introduced? Again, there are two possibilities: either the gluonia mix strongly with the ordinary $q\bar{q}$ meson states, or else the mixing is small. Consider the first possibility. The gluonia (some of which were stable) become very broad and difficult to see as resonances. But this threatens to introduce large violations of the OZI rule, with possibly large violations of the ideal nonet mixing in the 1^{--} ($m_\rho \approx m_\omega$) and 2^{++} ($m_{A2} \approx m_f$) nonets, along with broadening of ψ and ψ' widths.

Despite these problems, a group at ITEP in Moscow have recently advocated this viewpoint[39]. Their basic starting point is the set of QCD sum rules used not only to successfully describe the charm sector, but even to determine the parameters of ρ^0 and ω resonances[40]. Emboldened by this success, they analyze two-point functions such as $\langle 0|F^2(x)\ F^2(0)|0\rangle$ and $\langle 0|F\tilde{F}(x)\ F\tilde{F}(0)|0\rangle$ in the same way as the electromagnetic vacuum polarization, and conclude that the sum rules which they construct should (or could) be saturated by the 0^{++} ε meson (the broad $\pi\pi$ "resonance" at ~700 MeV) for F^2, and the η' for $F\tilde{F}$. They estimate the radiative decays $\psi \to \eta\gamma$ and $\psi \to \eta'\gamma$ with this picture[41], finding satisfactory agreement with experiment. Nevertheless the calculations do not look too clean (for example, instanton effects enter in a poorly controlled way). The success of the straightforward quark-model estimate[42] of $\Gamma(\eta' \to \gamma\gamma)$ is no longer understood. And one wonders whether a systematic study of OZI forbidden processes (e.g., $\psi' \to \psi\pi\pi$) would allow compatibility with this scheme[43].

I think it fair to say that most QCD theorists favor the second alternative, that gluonia mix very little with ordinary $q\bar{q}$ mesons and are narrow. This is a feature of the topological expansion or 1/N expansion[44]. [An eloquent exposition and summary of this line of argument has been recently given by Witten[45].] What then are the properties? Theory is hard put to give a sharp answer to this question (it is a challenge for nonperturbative, pure QCD to give us a spectrum — even qualitative — in terms of α_s). As a first terribly simple-minded attempt, we may try a naive gluonium model[38], at least as naive as the naive parton model, naive Drell and Yan, or naive SU(6) quark spectroscopy. Just take two or three massive "constituent gluons" and bind them together into an S-wave bound state with spin-independent central potential. One gets a plethora of candidate states (cf., Table I), not all of which need be low-lying — or even exist — in the real world. Some typical decay channels are also listed in the table. Nothing very distinguished emerges. One must have (approximate) SU(3) — singlet states, suggesting that channels with η, η', ϕ, K's may be advantageous. Robson[38] suggests a 1^{-+} gluonium decay into $\eta + \eta'$ might be a good possibility.

Where should gluonia be produced? No doubt in hadron collisions (are "clusters" gluonia?), but they may be hard to dig out of the background. $\pi\pi$ and KK phase-shift analyses

might be promising places to look for narrow 0^{++} and/or 2^{++} states. Resonant e^+e^- annihilation is of course good for any 1^{--} gluonium state. However, one has to go rather far down the list of candidates in Table I to find one, and the leptonic width would be hard to estimate and quite likely rather small.

TABLE I

	Type	J^{PC}	Typical Decays
1.	E_iE_j	0^{++}, 2^{++}	$\pi\pi$,KK,$\eta\eta$,$\eta'\eta'$,$\rho\rho$,$\omega\omega$,K^*K^*,$\phi\phi$
2.	E_iB_j	0^{-+}, 1^{-+}, 2^{-+}	$\pi\delta$,Kκ,ηS^*,$\eta'\varepsilon$,ρB,K^*Q;$\pi A1$,KQ,...
3.	B_iB_j	0^{++}, 2^{++}	Same as (1)
4.	$E_iE_jE_k$	0^{-+}, 1^{--}, 3^{--}	$\pi\delta$,Kκ,$\eta'\varepsilon$,$\pi\rho$,KK^*,$\eta\omega$,$\eta'\phi$,ωf,$\phi f'$,...
5.	$E_iE_jB_k$	0^{++}, 1^{++}, 2^{++}	Same as (1); $\pi\delta$,Kκ,ηS^*,...
		1^{+-}, 2^{+-}, 3^{+-}	$\pi\rho$,KK^*,$\eta\omega$,$\eta'\phi$,πB,KQ,ηD,...
6.	$E_iB_jB_k$	0^{-+}, 1^{-+}, 2^{-+}	Same as (2)
		1^{--}, 2^{--}, 3^{--}	πB,KQ,$\rho A2$,K^*K^{**},ωf,$\phi f'$,...
7.	$B_iB_jB_k$	0^{++}, 1^{+-}, 3^{+-}	Same as (1); πB,KQ,$\rho A1$,$\rho A2$,...

The best chance for finding gluonia probably lies in radiative ψ decays[46]: $\psi \to \gamma +$ gluonium. In QCD the branching ratio is estimated to be ~10% although the aforementioned large radiative corrections makes this at best a semiquantitative guess. The γ-ray spectrum from the lowest order perturbative calculation is shown in Fig. 3(a); it is essentially 3-body phase-space. Radiative corrections[6] will change it to something like Fig. 3(b), while replacing the low-mass gg parton final-states with a more realistic resonance spectrum (assuming duality) will provide something like Fig. 3(c).

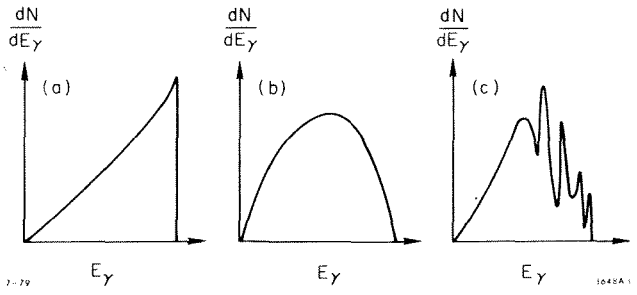

Fig. 3. (a) Lowest-order γ spectrum as calculated for $\psi \to \gamma gg$.
(b) The γ-spectrum (schematic) only after radiative corrections.
(c) The conjectured real spectrum after inclusion of gluonium resonances (with use of duality).

The known decays $\psi \to \gamma\eta$, $\gamma\eta'$, γf give a total width of $\lesssim 1\%$. The Mark I lead-glass wall collaboration at SPEAR has reported[47] a single-γ continuum contribution (with mass recoiling against the γ of $\lesssim$ 1.7-1.8 GeV) consistent with a total radiative branching ratio of ~5%. If this result holds up, the gluonia may in fact be already observed.

A large fraction of the final gg state is expected[48] to be 0^{++} and 2^{++}. Krammer[49] has estimated the $\pi\pi$ angular correlation in the decay $\psi \to \gamma gg \to \gamma f \to \gamma\pi\pi$ expected from QCD. The correlation observed experimentally agrees nicely with expectations. However, only a quite weak $q\bar{q} \leftrightarrow gg$ coupling is needed, so that this does not imply that the f is a gluonium state. It is also curious that $\psi \to \gamma f'$ has not been seen.

7. UNCONFINED QUARKS

Unconfined quarks may seem a radical departure from orthodox QCD, but it may not be so at all. De Rujula, Giles and Jaffe[50] have studied a slightly multilated version of QCD which appears to produce unconfined quarks of large mass and large size. The procedure is as follows:

(1) Give gluons a small "Lagrangian" mass μ_g (we will be considering $\mu_g \sim$ 5-20 MeV, of order the bare-quark "Lagrangian" masses).

(2) Do this by the Higgs-mechanism. [Otherwise nonrenormalizable effects probably occur at an unacceptably low mass scale.] The Higgs representation(s) must be 8 (or 10, 27,...), not 3 (or 6, 15,...) in order to avoid low-mass colorless fermions of fractional charge built from quarks bound to the Higgs-bosons[51].

(3) Unbroken QCD (omitting temporarily the light quarks) probably implies a quite stable string connecting a widely separated pair of very heavy quarks Q. If the distance exceeds the gluon Compton wavelength μ_g^{-1} it is plausible (but not self-evident and far from proven) that this string breaks, owing to the replacement of a power-law potential with a Yukawa-like potential. A single quark Q with a piece of broken string then has a mass $M \sim m_Q + T\mu_g^{-1}$, where T is the energy per unit length of the string (string-tension), ~1 GeV/f. If this picture can be maintained, it implies that both size and mass of unconfined quark are $\sim\mu_g^{-1}$, i.e., tend to infinity as the breaking tends to zero.

(4) Adding in the light quarks u,d,s may profoundly change the situation. Vacuum structure is probably modified, and in unbroken QCD the string breaks by Heisenberg-Euler pair creation[52]. This probably means that the color field surrounding the unconfined quark contains a large component of virtual pairs of light quarks. It may even be that a degenerate sea of q's and $\bar{q}$'s form in order to suppress further pair creation. However this is at best wild speculation.

In addition to the large size, large mass, and complicated internal structure, such an unconfined quark would accrete nucleons in its passage through matter. The mass of the resultant system versus baryon number A is estimated by De Rujula, Giles and Jaffe[50] to look like Fig. 4(a). McLerran and I, motivated by a desperate effort to understand the Centauro cosmic-ray event, have tried going one step further[53]. We considered a situation (Fig. 4(b)) where the primeval quark with $|A| < 1$ can spontaneously decay into a lighter system of large A with emission of ~A antibaryons. This might happen were the region of color field surrounding the quark source stabilized from pair-creation by the presence of a degenerate sea of either light quarks or light antiquarks, but not both (thereby avoiding the cost of the extra kinetic energy). Again, this is wild speculation.

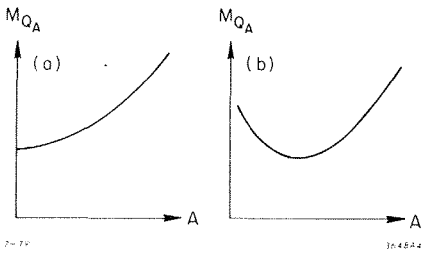

Fig. 4. (a) Mass of an unconfined quark + baryonic matter system as function of A according to De Rujula, Giles and Jaffe (Ref. 50). (b) Extreme variant used by McLerran and me (Ref. 53) as model of Centauro event.

If large, heavy quarks do exist, how might they be produced? In e^+e^- annihilation, probably a necessary condition is that a newly formed $q\bar{q}$ pair separate by a distance μ_g^{-1} without any quark pair breaking the string. Since the probability per unit time of Heisenberg-Euler pair creation is some constant, say

$$\frac{d\Gamma}{dz} \sim 20 \text{ MeV/f} \quad , \tag{7}$$

then the survival probability $P_{Q\bar{Q}}$ will be

$$P_{Q\bar{Q}} \sim \exp - \left(\frac{M_Q}{m}\right)^2 \tag{8}$$

with the scale factor m^{-2} proportional to $d\Gamma/dz$ in Eq. (7). With the above guess for the decay rate of the string, one gets $m \sim 3$ GeV. This would lead, for $M_Q \sim 10$ GeV, to a yield $R_{Q\bar{Q}}$ of unconfined quarks in e^+e^- annihilations of

$$R_{Q\bar{Q}} \sim 10^{-4} \tag{9}$$

But this is clearly very uncertain; the exponent is not reliable to better than a factor ~3-10.

What is the mass of the unconfined quark? Recently Steigman and Wagoner[54] have reconsidered the problem of quark production in the big bang. They estimate the quark/baryon fraction by regarding, at the time when quark matter makes the phase transition to nuclear matter (temperature T ~ 100-200 MeV), those quarks of energy $E > m_Q$ as the remanent physical quarks. This results in a quark mass estimate of ~15-30 GeV, provided the quark abundance is to be $\sim 10^{-18}$-10^{-20} per nucleon, as indicated by the Stanford experiments[55]. It may not make sense to identify in that epoch those energetic quark-partons with the heavy, large unconfined quarks we discussed. If one only allows non-equilibrium quark production by hadron-hadron collisions after the phase transition, the mass estimate goes down[56] to ~10 GeV. In either case the mass range is of experimental interest.

What messages are there in all this crazy speculation? For theorists there is a challenge: one clearly need not believe a word of what we have said. But if anyone really claims to understand confinement in QCD, he should also be able to understand what happens were QCD to be slightly broken in the way we described.

And what is the message for experimentalists? It is simply that, were they to observe an e^+e^- event with two highly charged heavy tracks, accompanied by fireballs composed of several baryons and antibaryons, they should let us all know about it. After all, it may turn out to be another test of QCD.

8. SUMMARY

The present experimental situation exhibits a remarkably good agreement with theoretical expectations. There exists opportunities of making truly incisive tests of QCD by study of R and of gold-plated 3-jet events. Somewhat less incisive, but still an important issue for QCD, is the search for gluonium in radiative ψ decays and elsewhere. And while it is somewhat premature to draw any firm conclusion from the new data, it already appears that

if truly new and surprising phenomena exist in the energy range 13-27 GeV, they do so at best at a rather low level. One should of course pursue the search for possible kinds of low-level hidden phenomena, such as charged Higgs-bosons, or the standard neutral Higgs in onium-decays, or neutral lepton production, or even unconfined quarks. And we may still have major surprises as the energies increase from the 28 GeV at present to ~40 GeV in the near future.

* * *

REFERENCES

1) J. Bjorken, Proc. of the 6th Internat. Symp. on Electron and Photon Interactions at High Energies, ed. by H. Rollnik and W. Pfeil, North-Holland (Amsterdam), 1974; also J. Ellis, Proc. of the 17th Internat. Conf. on High Energy Physics, London, 1974.

2) M. Dine and J. Sapirstein, SLAC preprint SLAC-PUB-2332; K. Chetyrkin, A. Kataev and F. Tkachov, Moscow INR preprint P-0126.

3) A. Sanda, Rockefeller preprint COO-2232B-178, also Phys. Rev. Lett. 42, 1658 (1979). See also G. Moorhouse, R. Pennington and G. Ross, Nucl. Phys. B124, 285 (1977).

4) P. Hoyer, P. Osland, H. Sander, T. Walsh and P. Zerwas, DESY preprint DESY 79/21 and references therein.

5) This infrared freedom of jet properties has been especially emphasized by G. Sterman and S. Weinberg, Phys. Rev. Lett. 39, 1436 (1977).

6) R. Barbiera, E. d'Emilio, G. Curchi and E. Remiddi, CERN preprint CERN-TH-2262, January 1979.

7) See the talk of P. Söding, these proceedings.

8) M. Peskin, Harvard preprint HUTP-79/A008, March 1979; G. Bhanot and M. Peskin, Harvard preprint HUTP-79/A015, March 1979.

9) I have in mind the inside-outside cascade picture of particle production; cf., J. Kogut and L. Susskind, Phys. Rev. D10, 732 (1974); also J. Bjorken, in Lecture Notes in Physics 56, "Current-Induced Reactions," ed. by J. Korner, G. Kramer and D. Schildknecht, Springer-Verlag (N.Y.), 1975.

10) A nice exposition is given by E. Feinberg, Zh. Exp. Teor. Fiz. 50, 202 (1966) [English translation, JETP 23, 132 (1966)].

11) C. Chiu and J. Szwed, Max Planck Institute preprint MPI/PAE/PTh 15/79 (May 1979).

12) L. Caneschi and A. Schwimmer, Weizmann Institute preprint WIS-79/24 Ph.

13) K. Konishi, A. Ukawa and G. Veneziano, Phys. Lett. 78B, 243 (1978) and Rutherford Laboratory preprint RL-79-026.

14) D. Amati and G. Veneziano, Phys. Lett. 83B, 87 (1979).

15) M.-K. Gaillard, these proceedings.

16) For reviews, see R. Field, Proc. of the 19th Internat. Conf. on High Energy Physics, Tokyo, Japan, 1978 (CALT 68-696); L. Sehgal, Proc. of the 19th Internat. Symp. on Lepton and Photon Interactions at High Energies, Hamburg, Germany, August 1977.

17) For example, cf., J. Vander Velde, Michigan preprint UMBC-78-9; J. Bell et al., Phys. Rev. D19, 1 (1979).

18) G. Hanson, Proc. of the 13th Rencontre de Moriond, Les Arcs, France, March 1978; also SLAC preprint, SLAC-PUB-2118, May 1978.

19) M. Piccolo, I. Peruzzi and P. Rapidis et al., SLAC-PUB-2323, May 1979; P. Rapidis et al., SLAC-PUB-2184, August 1978.

20) R. Odorico and V. Roberto, Nucl. Phys. B136, 333 (1978).

21) G. Wolf, these proceedings.

22) H. Georgi and S. Glashow, Harvard preprint HUTP 79/A027.

23) G. Kane, SLAC preprint SLAC-PUB-2326, May 1979.

24) For example, see J. Bjorken, SLAC-PUB-2195 (unpublished); A. Barut, Phys. Rev. Lett. 42, 1251 (1979); T. Walsh, DESY preprint DESY 78/58.

25) F. Gursey, P. Ramond and P. Sikivie, Phys. Lett. 60B, 177 (1976).

26) Y. Achiman and B. Stech, Phys. Lett. 77B, 389 (1979).

27) D. Meyer and H. Nguyen et al., Phys. Lett. 70B, 469 (1977).

28) C. Prescott et al., Phys. Lett. 77B, 347 (1978) and SLAC-PUB-2319, May 1979; also C. Prescott, these proceedings.

29) A. Ali, Phys. Rev. D10, 2801 (1974); C. Ragiadakis, Strasbourg preprint CRN/HE 77-15 (1977).

30) J. Ellis, M.-K. Gaillard, D. Nanopoulos and S. Rudaz, Nucl. Phys. B131, 285 (1977); A. Ali, J. Korner, G. Krammer and J. Willrodt, DESY preprints DESY 78/47, 78/51, and 78/67.

31) G. Wolf, these proceedings.

32) H. Fritzsch, CERN preprint CERN-TH-2648, March 1979.

33) A positive signal in π^- production at 150 GeV is reported by the Goliath collaboration; cf., D. Treille, these proceedings.

34) E. Derman, Phys. Rev. D19, 317 (1979) and references therein.

35) J. Ellis, M.-K. Gaillard, D. Nanopoulos and C. Sachrajda, Phys. Lett. 83B, 339 (1979).

36) I. Bars and M. Serardoglu, Yale preprint COO-3075-188; S. Weinberg, Phys. Lett. 82B, 387 (1979).

37) H. Haber, G. Kane and M. Sterling, Michigan preprint UM HE-78-45, December 1978.

38) D. Robson, Nucl. Phys. B130, 328 (1977), provides a nice survey of the subject and references to other work; see also P. Roy and T. Walsh, Phys. Lett. 78B, 62 (1978). We follow here the arguments of H. Fritzsch and P. Minkowski, Nuovo Cimento 30A, 393 (1975).

39) V. Novikov, M. Shifman, A. Vainstein and V. Zakharov, ITEP preprint, 1979.

40) M. Shifman, A. Vainstein and V. Zakharov, Nucl. Phys. B147, 385,448 (1978).

41) See also M.-K. Gaillard, these proceedings.

42) G. Abrams et al., SLAC preprint SLAC-PUB-2331.

43) Studies of the connection of the OZI rule with gluonium states have been made by J. Bolzan, K. Geer, W. Palmer and S. Pinsky, Phys. Rev. Lett. 35, 419 (1975); also J. Bolzan, W. Palmer and S. Pinsky, Phys. Rev. D14, 3202 (1976).

44) G. Veneziano, Nucl. Phys. B117, 519 (1976).

45) E. Witten, Harvard preprint HUTP 79/A007.

46) M. Chanowitz, Phys. Rev. D12, 918 (1975); S. Brodsky, D. Coyne, T. deGrand and R. Horgan, Phys. Lett. 73B, 203 (1978); see M. Krammer and H. Krasemann, DESY preprint DESY 79/20, for a nice review.

47) See M. Davier, these proceedings.

48) A. Billoire, R. Lacaze, A. Morel and H. Navelet, Phys. Lett. 80B, 381 (1979).

49) M. Krammer, Phys. Lett. 74B, 361 (1978).

50) A. De Rujula, R. Giles and R. Jaffe, Phys. Rev. D17, 285 (1978).

51) Here we differ from Ref. 50), which allows color-triplet Higgs breakings.

52) A recent discussion is given by A. Casher, H. Neuberger and S. Nussinov, Tel-Aviv preprint TAUP-747/79; cf., also H. Neuberger, preprint TAUP-721/79.

53) J. Bjorken and L. McLerran, SLAC preprint SLAC-PUB-2308.

54) G. Steigman and R. Wagoner, Stanford preprint ITP-633, April 1979.

55) G. LaRue, W. Fairbank and A. Hebard, Phys. Rev. Lett. 38, 1011 (1977); G. LaRue, W. Fairbank and J. Phillip, Phys. Rev. Lett. 42, 142,1019 (1979).

56) This result is contained in work of J. Bahcall, S. Frautschi and G. Steigman, Ap. J. 175, 307 (1972). I thank G. Steigman for useful discussions and clarifications of all these points.

* * *

DISCUSSION

Chairman: W. Jentschke

Sci. Secretaries: A. Contin and R. Ross

S.J. Lindenbaum: I note with interest your first diagram that indicated, as you stated, that what happened inside jets was quite complicated. Therefore I think that a statement that one narrower jet accompanied by one wider jet was evidence for a single gluon emission from one of the quarks is not entirely founded. I believe in the possibility that the strong interactions which are non-perturbative are large -- they could also include final-state particle interactions in the language of the pre-QCD era. What is your view of this?

J.D. Bjorken: The experimentalists can probably answer this better than I can, but the evidence presented looks very favourable for the QCD picture; however, it certainly does require a careful set of control, Monte Carlo experiments. I think some of that has been done; namely one takes the best model of two-jet production, putting in resonance decays and all that kind of thing, and simulates the experiment with conventional assumptions to see whether one can get the observed behaviour or whether one really needs something like gluons. I think a fair amount of that kind of simulation has been done but perhaps an experimentalist would like to comment on that.

S.J. Lindenbaum: Sorry, as far as I know, they have not taken into account explicitly final-state interactions and I would worry about that because as you point out, these things are very strongly interacting even in the region of one fermi.

J.D. Bjorken: I'll pass to the experimentalists on that.

P. Söding (comment): Resonance effects have been taken into account in the Monte Carlo calculations of two-jet production with which the e^+e^- data at PETRA have been compared. The main arguments against resonance and other hadronic final-state interaction effects being the reason for the observed jet broadening are: i) the strong increase of this effect with Q^2, and ii) the fact that the jets tend to stay flat in one plane while they broaden *in* that plane. An interpretation of these facts purely in terms of resonances does not seem natural.

S.J. Lindenbaum: Another point: I also noted with interest your statement that the degree of quark-gluon mixing could affect the OZI rule. As you may know, we have written a paper which shows that the OZI rule does not work satisfactorily in production processes, such as $\pi^- p \to \phi\phi n$, and others. On the other hand, it seems to work well in decays of particles. Do you believe the quark-gluon mixing could be quite different in these two cases and explain this anomaly?

J.D. Bjorken: I would rather not comment on this question.

W. Nahm: As you talked about broken QCD and in particular broken strings shaking off baryons, can you comment about the Centauro events in cosmic rays?

J.D. Bjorken: McClarren and I have speculated on that. We have three models. The first is just a glob of very dense quark matter which is metastable and is destabilized on its passage through the atmosphere and then explodes. It needs no primordial quark, it does not have to be a fractional charge for that mechanism to work.

Then we speculated that, maybe, to hold this quark together at high enough density, it would be advantageous to have the heavy quark as a core.

Then the third speculation, which gives more or less the same phenomenology, was a different mechanism but involved the picture I showed; what happened was that one had a primary proton which then fragmented into these primordial quarks of small charges, but these immediately decay into the quarks of large baryon number, emitting a large number of baryons as secondary products. Then, what one saw in the Centauro were all these "fireball" secondary baryons. It is pretty wild and it is marginally compatible with other cosmic-ray data.

HEAVY LEPTONS

G. Flügge
Deutsches Elektronen-Synchrotron DESY, Germany

ABSTRACT

A summary of our present knowledge about the new heavy lepton τ is given.

I. INTRODUCTION

Only a few years have passed since the third lepton τ was first observed at SLAC in 1975[1]. Yet we are already in a position to argue about the details of its properties.

The existence of this new particle has been undoubtedly confirmed in nine different experiments[2-10]. Soon it became clear that the heavy sequential lepton hypothesis[11] (standard model) was the best candidate to give a proper description of the τ.

It will be the aim of this talk to review[12,13,14] the experimental properties of the new particle, compare them to the standard model and discuss, how far other hypotheses can be excluded.

II. PRODUCTION AND DECAY IN THE STANDARD MODEL

Lepton pair production in e^+e^- reactions can be predicted with certainty by quantum electrodynamics (QED). For the production of a pair of pointlike spin 1/2 particles $\tau^+\tau^-$ we get

$$\sigma_{\tau\tau} = \sigma_{\mu\mu}\,((3\beta - \beta^3)/2) \qquad (1)$$

where

$$\sigma_{\mu\mu} = (4\pi\alpha^2)/(3s) = 21.71\ \text{nb}/E_b^2 \qquad (E_b = s^{1/2}/2 = \text{beam energy})$$

is the cross section for $e^+e^- \to \mu^+\mu^-$ and β is the velocity of the τ. $\sigma_{\tau\tau}$ rises quickly from the threshold at $s^{1/2} = 2M_\tau$ and approaches $\sigma_{\mu\mu}$ asymptotically.

In the standard model a third sequential lepton τ is added to the old leptons μ and e. It is described by an additional term

$$\bar{\tau}\,\gamma_\alpha(1 + \gamma_5)\,\nu_\tau$$

in the weak leptonic current. This implies that a new lepton with its own massless left-handed neutrino takes part in the conventional weak interaction.

Possible decay modes of the τ into e, μ (leptonic) or hadrons (semihadronic) plus neutrinos are shown in fig. 1A,B. In first approximation, each decay mode $(e\,\bar{\nu}_e)$, $(\mu\,\bar{\nu}_\mu)$ and $d\bar{u}$ (three colours) contributes 20 % to the total branching ratio. Detailed calculations[11,14] yield a leptonic branching ratio of

$$B_e = BR(\tau \to e\nu\nu) = 16.8\ \%\ . \qquad (2)$$

The only uncertainty in this calculation comes from the assumptions for the hadronic part. An independent estimate of this contribution from QCD[15] yields

$$B_e = BR(\tau \to e\nu\nu) = 17.5\ \%. \qquad (3)$$

Consequently, the decay into leptons constitutes a large fraction of τ decays. Since also

the hadronic system tends to contain only one charged particle, the combination of one lepton and one charged particle is often used as a clean signature for τ pair production.

III. THRESHOLD BEHAVIOUR AND PROPERTIES OF THE τ

τ mass

The basic parameter of the τ mass can be deduced from the threshold behaviour (1). Until 1977 the mass of the τ was rather unprecisely determined[12]. Mainly for this reason a certain scepticism remained that the τ might be confused with a charm particle. A major break-through in this issue came with the discovery by the DASP group that τ production was already present at the ψ' resonance[16] (fig. 2a). From the inclusive electron production of fig. 2a a mass of $M_\tau = 1.807 \pm 0.02$ GeV could be determined by the DASP group. The DESY-Heidelberg group followed very quickly with an even better determination of the mass[8]: $M_\tau = 1.790\ ^{+0.007}_{-0.010}$ GeV. Both values were finally topped by the excellent measurement of the DELCO group[9] at SPEAR which is shown in fig. 2b. This measurement of the inclusive electron production in two-prong events sets a mass value of $1.782\ ^{+0.003}_{-0.004}$ GeV to be compared with the D meson mass of $M_D = 1.868 \pm 0.001$ GeV.

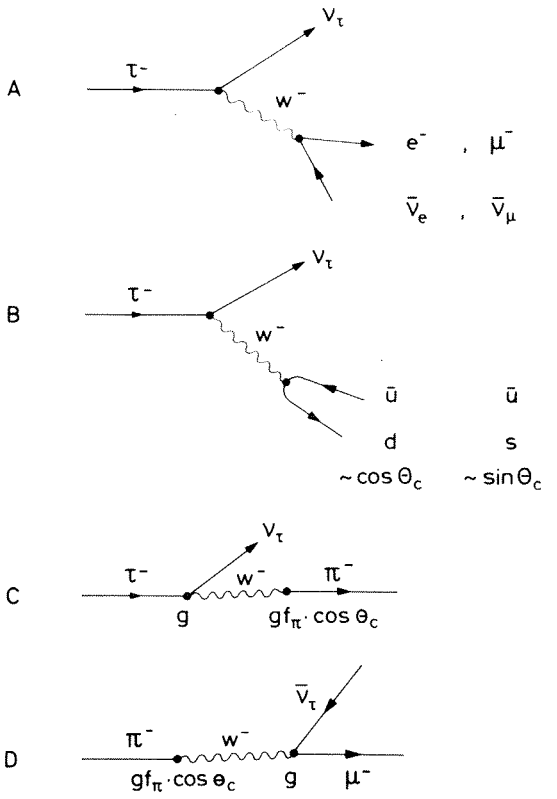

Fig. 1 Leptonic and semihadronic decays of the heavy lepton τ.

τ spin

Another parameter that can be determined from the threshold behaviour is the τ spin. The curves in fig. 2 demonstrate the expectation for different spins of the produced pair of pointlike particles. The data confirm previous observations first

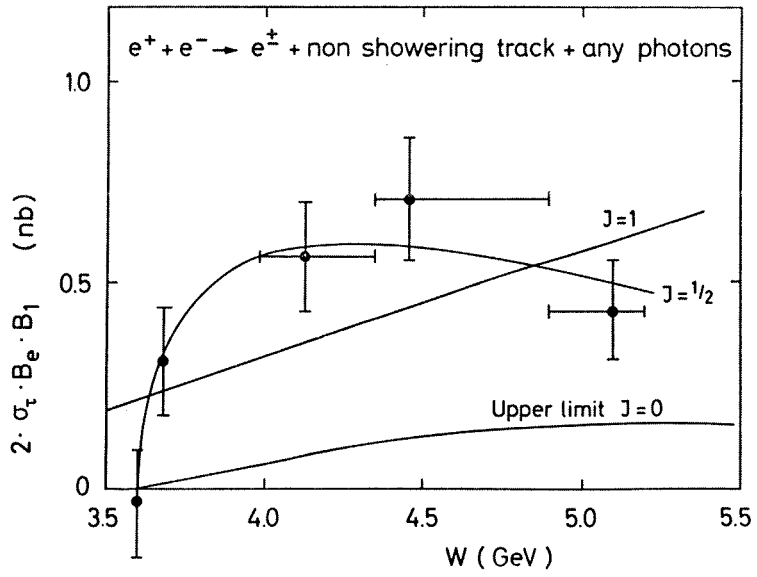

Fig. 2a DASP: cross section for inclusive electron production in the two-prong class with any number of photons. The solid curves are fits assuming pair production of pointlike particles with spin 0, 1/2 and 1.

stated by the PLUTO group[3]: spin 0, 1 and 3/2 can be excluded - spin 1 and 3/2 mainly since they deviate strongly at higher energies. Spin 0 is out anyway since it yields only 1/4 of $\sigma_{\mu\mu}$ asymptotically.

Pointlike τ structure

New data have become available very recently at energies of 9.4 GeV[17] (Table 1). The cross section is well compatible with the expectation (1) for a pointlike structure of the τ. To quantify this statement one may introduce a formfactor $F_\tau(s) = 1 \pm s/\Lambda_\pm^2$ of the τ multiplying (1) by $|F_\tau(s)|^2$.

The data of table 1 yield the following lower limits for the cut-off parameters $\Lambda_\pm$ (PLUTO[17]):
$\Lambda_+ > 22$ GeV $\quad \Lambda_- > 19$ GeV
There is no indication for a further heavy lepton τ' in the data. With the predicted branching ratios for a new sequential lepton[11] we get a limit of:
$M_{\tau'} > 4.3$ GeV (95 % C.L.) PLUTO[17]

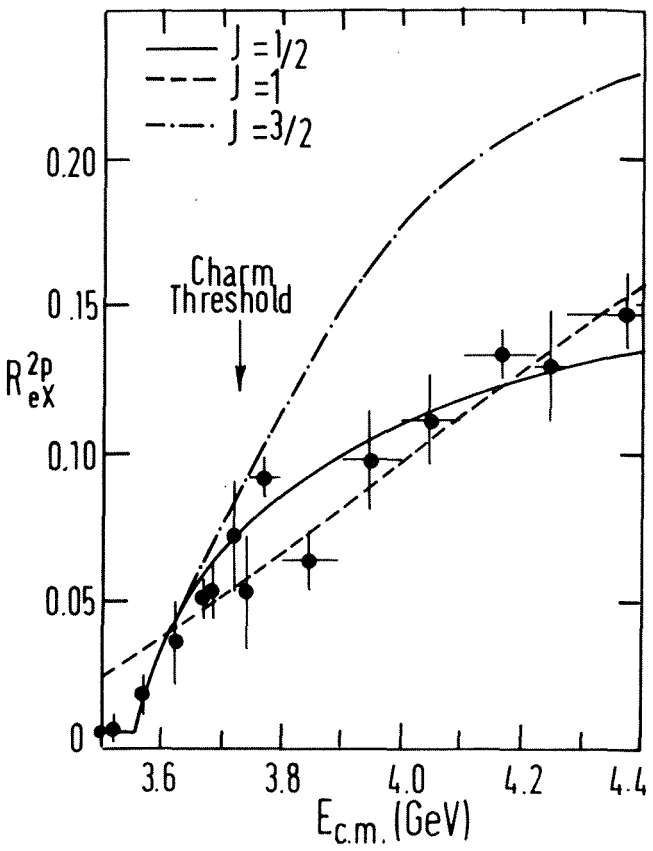

Fig. 2b DELCO: inclusive electron production in the two-prong class with any number of photons. The ratio of the electron to μ pair production is plotted versus CM energy. Data are compared with the prediction for spin 1/2, 1 and 3/2 pair production.

$e^+ e^- \rightarrow$	data	τ prediction
μ e	5	4.6
μ μ	3	3.0
μ hadron	5	3.5
μ ρ	7	9.2
μ + 1 track	7	7.0
μ + 3 tracks	7	4.3
background	2	
total ./. background	32 ±6	31.6

Table 1
PLUTO: τ production at $E_{CM} = 9.45$ GeV. Including radiative corrections (7 %) and systematic errors (20 %) one gets $\sigma_{\tau\tau}$ (9.4 GeV) $= (0.94 \pm 0.25)\sigma_{\tau\tau}$ (QED) (preliminary).

IV. LEPTONIC DECAYS

The leptonic decays can be calculated in the standard model without further assumptions. The branching ratios B_e and $B_\mu = BR(\tau \rightarrow \mu\nu\nu)$ differ only by a small phase space cor-

rection

$$B_\mu = 0.973\ B_e. \qquad (4)$$

The DASP[4], PLUTO[3,18] and SLAC-LBL[19] groups have checked the ratio B_μ/B_e from a comparison of τ events containing e or μ. The mean value[14] of 0.99 ±0.2 is in good agreement with the expectation. One may, therefore, combine various measurements of B_μ and B_e to evaluate a world average under the assumption (4). Table 2 summarizes the results published so far. The mean value of

$$B_\mu/0.973 = B_e = 17.1 \pm 1.0\ \%$$

is in excellent agreement with the theoretical expectations (2) and (3).

Table 2

Summary of leptonic branching ratios. For the average, $B_\mu = 0.973\ B_e$ is assumed and the statistical (first) and systematic (second) errors are added quadratically.

collaboration	$B_e = BR(\tau \to e\mu\mu)$ % $B_\mu = BR(\tau \to \mu\nu\nu)$ %	reference
SLAC-LBL	$\sqrt{B_e \cdot B_\mu} = 18.6 \pm 1.0 \pm 2.8$	2
	$B_\mu = 17.5 \pm 2.7 \pm 3.0$	2
PLUTO	$B_\mu = 15.0 \pm 3.0$	3,18
	$B_e = 16.5 \pm 5.6$	3,18
Lead-Glass-Wall	$\sqrt{B_e \cdot B_\mu} = 22.4 \pm 3.2 \pm 4.4$	5
Ironball	$B_\mu = 22\ ^{+\ 7}_{-\ 8}$	7
MPP	$B_\mu = 20 \pm 10$	6
DASP	$\sqrt{B_e \cdot B} = 18.2 \pm 2.8$	4
DELCO	$B_e = 16.0 \pm 1.3$	9
	$B_\mu = 21.0 \pm 5.0 \pm 3.0$	20
World average	$B_e = B_\mu/0.973 = 17.1 \pm 1.0$	

Experiments always measure the simultaneous decay of a τ pair. Therefore, the branching ratios of table 2 are necessarily determined from a product of two branching fractions. Consequently a purely experimental determination of B_e and B_μ can only be achieved, if at least three products of the branching ratios B_e, B_μ, $B_{1p} = BR(\tau \to \nu + 1$ charged particle) and $B_{3p} = BR(\tau \to \nu + \geq 3$ charged particles) are measured simultaneously. (E. g. the PLUTO values of table 2 were obtained from a simultaneous measurement of $B_e \cdot B_\mu$, $B_\mu \cdot B_{1p}$, $B_\mu \cdot B_{3p}$). G. Feldman has made a constrained fit to all available data to get a consistent set of the above four branching fractions[13]. The result of

$$B_\mu/B_e = 1.13 \pm 0.16$$

is again in good agreement with the expectation (4). Therefore applying the constraint (4) he gets

$$B_\mu/0.973 = B_e = 17.5 \pm 1.2\ \%$$

in good agreement with the above mean value.

V. SEMIHADRONIC DECAYS

Since the τ mass is high enough to allow for semihadronic decays (fig. 1 B), we have an excellent tool to check whether the new particle does in fact participate in the conventional weak interaction of the standard model. If this is the case, it should couple to two kinds of hadronic currents,

vector currents $J^P = 1^-$,

axial vector currents $J^P = 0^-, 1^+$,

where J^P is the spin parity of the hadronic final state. Due to the conservation of the vector current (CVC), no scalar final states occur in the vector part.

1. Vector current

The vector current with $J^P = 1^-$ leads to a prediction of the decay $\tau \to \nu\rho$. Assuming CVC, $B_e = 16.8$ %, $M_\rho = 0.77$ GeV and $M_\tau = 1.8$ GeV one gets[11,14]

$BR(\tau \to \nu\rho) = 25.3$ %.

Preliminary results on this decay mode are

$BR(\tau \to \nu\rho) = (24 \pm 9)$ % DASP[21],

$BR(\tau \to \nu\rho) = (21.1 \pm 3.7)$ % MARK II[10].

The mean value of (21.5 ± 3.4) % agrees with the expectation.

2. Axial vector current

Since the axial vector current is not conserved, its divergence can also contribute to the hadronic current. Therefore, $J^P = 0^-$ and 1^+ final states are allowed. Consequently, the τ will decay into π and A_1 (if the A_1 exists) or other 0^- and 1^+ states.

($\tau \to \nu\pi$) decay

This decay plays a central rôle in the discussion of the weak current involved in τ decay since it constitutes the "inversion" of the π decay. It can, therefore, unambiguously be predicted from the pion coupling constant f_π (fig. 1 C, D). With $B_e = 16.8$ %, $f_\pi = 0.129$ GeV and $M_\tau = 1.8$ GeV we get[11,14]

$BR(\tau \to \nu\pi) = 9.5$ %.

The PLUTO group studied inclusive pion production[22] from the reaction:

$e^+ e^- \to \pi^\pm$ + 1 charged particle + no photons. (5)

32 events of class (5) were seen in the 4 to 5 GeV energy range. On the other hand, only 8.9 ± 1.0 events were expected from hadron misidentification, $\tau \to \nu\rho$ decay and hadronic sources. They obtain a branching ratio of

$BR(\tau \to \nu\pi) = (9.0 \pm 2.9 \pm 2.5)$ % PLUTO[22],

where the second error indicates the systematic uncertainty. Going along very similar lines, the SLAC-LBL group found a branching ratio of

$BR(\tau \to \nu\pi) = (9.3 \pm 1.0 \pm 3.8)$ % SLAC-LBL[23,13].

DELCO studied[20] events of the type

$e^+ e^- \to e^\pm$ + 1 hadron + no photons. (6)

They observed 17.4 events after background subtraction. 19.3 events are expected, out of which only 6.9 events are due to other sources than $\tau \to \nu\pi$ decay (mainly $\tau \to \nu\rho$). The resulting branching ratio is

$BR(\tau \to \nu\pi) = (8.0 \pm 3.2 \pm 1.3)\ \%$ DELCO[20].

Preliminary results[10] from MARK II on signature (5) are

$BR(\tau \to \nu\pi) = (10.6 \pm 1.9)\ \%$ MARK II[10].

The present world average of (9.8 ±1.4) % is in good agreement with the theoretical expectation.

$(\tau \to \nu A_1)$ decay

This second candidate for an axial vector piece in the hadronic current can only be calculated if one introduces further assumptions about the relative size of the axial and vector current (Weinberg sum rules). With $B_e = 16.8\ \%$, $M_\tau = 1.8$ GeV and $M_{A_1} = 1.07$ GeV we get

$BR(\tau \to \nu A_1) = 8.1\ \%$.

The PLUTO collaboration has searched[24] for events from the reaction

$e^+ e^- \to e^\pm$ (or $\mu^\pm$) $+ \pi^\mp \pi^+ \pi^-$

in the energy range from 4 to 5 GeV. They found 40 events of this type including 13 background events (mainly from hadron misidentification).

The $\pi^+\pi^-$ mass distribution shows a strong ρ peak, indicating that the whole signal is due to the decay $\tau \to \nu\rho^0\pi$. Quantitatively the limit for uncorrelated 3π decay is

$$\frac{\Gamma(\tau \to \nu\, 3\pi,\ \text{no}\ \rho)}{\Gamma(\tau \to \nu\, 3\pi)} \leq 0.32 \quad (95\ \%\ \text{C.L.}).$$

Assuming I = 1 for the $\rho\pi$ system one can determine a branching ratio of

$BR(\tau \to \nu\rho\pi) = (10.8 \pm 2.6 \pm 2.2)\ \%$ PLUTO[24].

The existence of a $\rho\pi$ final state with negative G-parity in itself proves that an axial piece is present in the hadronic weak current in τ decays, provided only first class currents are present (by definition of first class currents[25]). To get a statement independent of the latter assumption, the spin parity of the $\rho\pi$ system was studied. The density distribution in a 3-dimensional Dalitz plot of the masses of the two $\pi^+\pi^-$ combinations and the $\rho\pi$ system was investigated. Only the $J^P = 1^+$ s-wave and the $J^P = 2^-$ p-wave gave an acceptable description of the data. Fig. 3a shows the mass distribution of the 3π system together with the expectation from a Monte Carlo calculation for different partial waves. The p and d waves give a very bad account of the data. Only the

$J^P = 1^+$ s-wave

is acceptable. This proves again the existence of an axial part in the hadronic current. In particular, there are no indications for a 1^- s-wave from second class axial currents.

The 3π mass distribution is much better described assuming a resonance of $0.7 \leq M \leq 1.2$ GeV and $0.4 \leq \Gamma \leq 0.5$ GeV in the 1^+ s-wave (fig. 3b). This indicates that the observed decay may indeed be due to

$\tau \to \nu A_1 \to \nu \rho \pi$.

The evidence is not compelling, however.

The SLAC-LBL group has studied[26] the reaction

$e^+ e^- \to \mu^\pm + \pi^\mp \pi^+ \pi^- + \geq 0$ photons.

They found a branching ratio of $BR(\tau \to \nu + 3\pi + n\,\pi^0) = (16 \pm 6)\ \%$. From a comparison of 0 γ and 1, 2 γ data the purely charged decay mode can be estimated

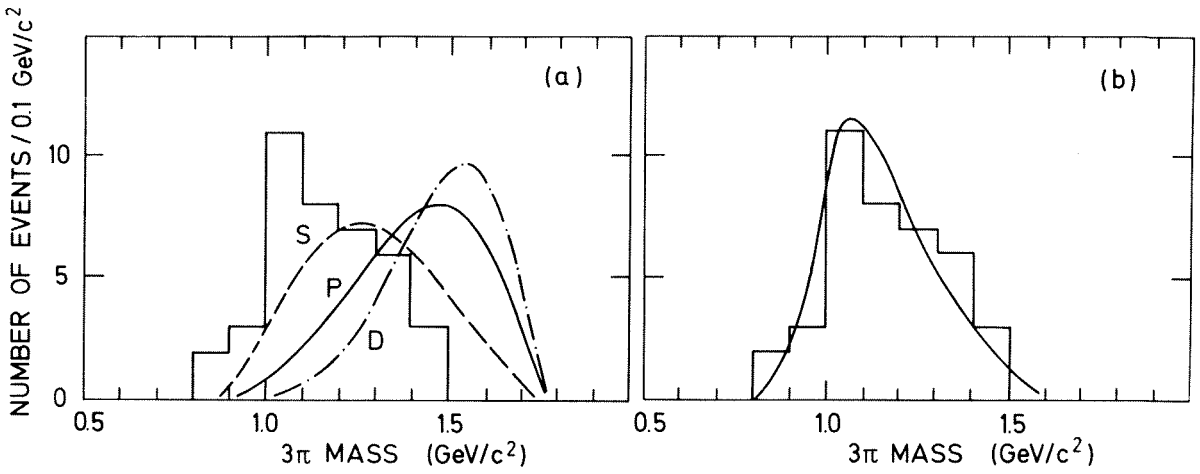

Fig. 3 PLUTO: ρπ decay of the τ. Data corrected for background and acceptance.

a) Mass distribution of the 3π system in the ρ band ($0.68 < M_{\pi^+\pi^-} < 0.86$ GeV). The curves represent phase space calculations for different partial waves of the ρπ system.

b) The same mass distribution with a fit of a resonant s-wave with $M_{A_1} = 1.0$ GeV and $\Gamma_{A_1} = 475$ MeV.

$BR(\tau \to \nu + 3\pi) = (7 \pm 5)\%$ SLAC-LBL[26]

in good agreement with the PLUTO result. An acceptable description of the 3π mass distribution is again obtained from a fit assuming $(\tau \to \nu\, A_1)$ decay with $M_{A_1} = 1.1$ GeV and a width $\Gamma_{A_1} = 200$ MeV.

3. Strangeness

Since the τ mass is below the charm threshold, decays involving strange particles should be suppressed by $tg^2\theta_c \simeq 5\%$. The DASP group measured[4] the ratio of kaon to pion production in two-prong events with one electron, which are dominated by τ production. Their result

$\sigma(e^+e^- \to e + K)/\sigma(e^+e^- \to e + \pi) = (7 \pm 6)\%$ DASP[4]

is in accordance with theory.

4. Hadron continuum

The remaining part of the semihadronic decay modes,

$\tau \to \nu +$ hadron continuum,

can be calculated from the quark model. Using CVC, the quark model with colour amd assuming that the vector part is equal to the axial part one obtains[11,14] $BR(\tau \to \nu +$ continuum$) = 21.8\%$. Only a small fraction of the hadronic final states is expected to contain a single charged particle[27]. Therefore, a rough test of this number can be obtained from a comparison with experimental results on multiprong final states:

$BR(\tau \to \nu + \geq 3$ prongs$) = (30 \pm 10)\%$ PLUTO[3]

$= (35 \pm 11)\%$ DASP[4]

$= (32 \pm 4)\%$ DELCO[9,28]

The constrained fit described in section IV yields

$BR(\tau \to \nu + \geq 3 \text{ prongs}) = (30.6 \pm 3.0)\ \%$ without (2) [13].

The experimental results agree quite well with the theoretical prediction since half the A_1 branching ratio ($A_1 \to \rho^0 \pi^+$) has to be added to the continuum value.

VI. 'FORBIDDEN' DECAY MODES

Several decays, which are not allowed by the standard model, have been searched for. None of them has been detected. At present the best limits are (all decays without neutrinos):

$BR(\tau \to 3$ charged particles)	$<$ 1.0 %	(95 % C.L.)	PLUTO[14]
$BR(\tau \to 3$ charged leptons)	$<$ 0.6 %	(90 % C.L.)	SLAC-LBL[12]
$BR(\tau \to e\ \gamma)$	$<$ 2.6 %	(90 % C.L.)	SLAC-LBL[12]
$BR(\tau \to \mu\gamma)$	$<$ 0.35 %	(90 % C.L.)	MARK II[10]
$BR(\tau \to \gamma)$	$<$ 0.8 %	(90 % C.L.)	MARK II[10]

VII. τ NEUTRINO

Decay spectrum and properties of 'ν_τ'

The form of the leptonic decay spectrum can be calculated in the standard model. Any deviations from the assumption of a massless lefthanded neutrino will lead to a softening of the spectrum[29].

The shape of the muon spectrum in the early SLAC-LBL and PLUTO results favoured V-A coupling of the τ and set a limit of less than about half a GeV on the neutrino mass. However, conclusive data became available only recently from the DELCO group[30]. Fig. 4 shows their inclusive electron spectrum in the energy range $3.57 \leq E_{cm} \leq 7.4$ GeV excluding the ψ"(3770). The expectations for V±A are indicated in the figure. The shape of the spectrum can be characterized by the Michel parameter ρ which is $\rho = 0.75$ for V-A, $\rho = 0$ for V+A and $\rho = 0.375$ for V or A. The experiment yields

$\rho = 0.72 \pm 0.15$ DELCO[30]

(including a systematic error of 0.11). This value is in good agreement with V-A, excludes V+A and disfavours V or A by 2.3 standard deviations.

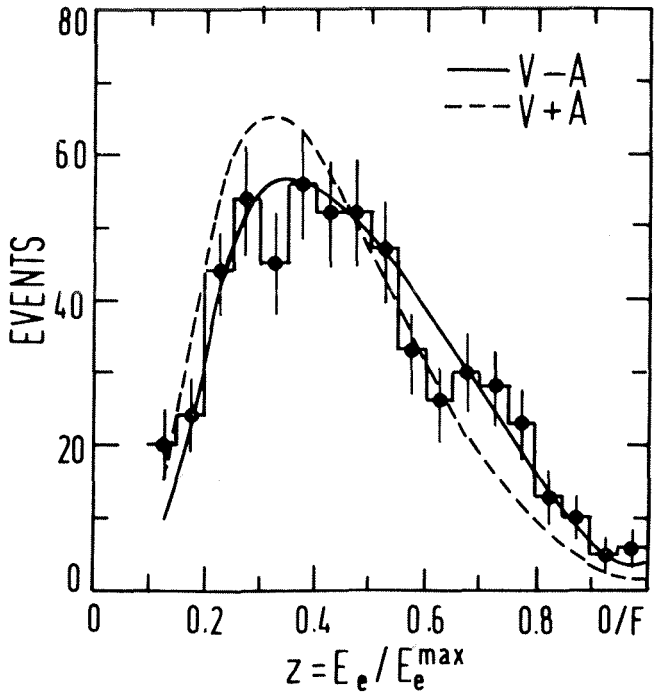

Fig. 4 DELCO: electron momentum distribution for two-prong events. Data are compared with the prediction for V-A (solid curve) and V+A (dashed curve) coupling of the τ.

If one assumes V-A interaction, the shape of the spectrum allows to set a limit on the neutrino mass. A finite mass corresponds to an effective decrease of ρ. The DELCO data yield an upper limit of 250 MeV (95 % C.L.).

Lifetime and nature of 'ν_τ'

So far all experimental findings are consistent with the τ being coupled to a massless lefthanded neutrino 'ν_τ'. Let us finally investigate, whether this could be one of the old neutrinos.

The relevant experimental information still needed is the coupling strength of the τ-'ν_τ' vertex. In the standard model a full strength would yield a lifetime

$$\tau_\tau = B_e \left(\frac{M_\mu}{M_\tau}\right)^5 \tau_\mu = 2.8 \times 10^{-13} \text{sec.}$$

Upper limits of the τ lifetime are available from the experiments PLUTO[31], SLAC-LBL[12] and DELCO[30]. From the best value given by the DELCO group[30]

$$\tau_\tau < 2.3 \times 10^{-12} \text{ sec (95 \% C.L.)} \qquad \text{DELCO}^{30)}$$

one can deduce that the coupling is at least 12 % of the full strength.

On the other hand we know from the absence of τ production in neutrino beams that the coupling to the τ is limited to less than 2.5 %[32]. Therefore, the 'ν_τ' cannot be identical with ν_μ or $\bar{\nu}_\mu$.

The possibilities of 'ν_τ' being either $\bar{\nu}_e$ (or $\bar{\nu}_\mu$) can also be excluded experimentally for massless neutrinos with V±A coupling. There would be a statistical factor of 2 in either B_e or B_μ, due to two identical neutrinos in the final state[33]. This is excluded by the data discussed in section IV.

Thus we are left with the one possibility that 'ν_τ' might be identical with ν_e. This case cannot be excluded on purely experimental grounds, since neutrino measurements are not yet available.

We can show, however, that simple mechanisms for such couplings proposed in SU(2)xU(1) gauge theories can be excluded. The simplest case would be that the τ appears in a singlet in addition to the (e ν_e) and (μ ν_μ) doublets[34]. Due to lepton number mixing this model leads to appreciable neutral current contributions:

$$\text{BR}(\tau \to \begin{matrix} e \\ \mu \end{matrix} + \text{hadrons}) \simeq 0.30$$

$$\text{BR}(\tau \to 3 \text{ charged leptons}) \simeq 0.05$$

This is excluded from the SLAC-LBL and PLUTO data (section VI).

Another possibility would be that the ν_τ is heavier than the τ[35]. The τ would then decay through lepton number mixing. The sum of coupling strengths to ν_e and ν_μ would have to be larger than 12 % of the full strength from the lifetime limit. With the μe universality[36] limit from π decay

$$\Gamma(\pi \to e\ \nu)/\Gamma(\pi \to \mu\ \nu) = \text{theory} \times (1.03 \pm 0.02)$$

and the upper limit on the ν_μ coupling of 2.5 % this is excluded.

VIII. SUMMARY

Table 3 gives a summary of the experimental knowledge about τ, which is now clearly established as a new heavy lepton with the mass $M_\tau = 1.782\ ^{+.003}_{-.004}$ GeV. All properties of this new particle are as expected for a sequential left-handed lepton with conventional weak coupling to its own massless neutrino. It should be noted, however, that the orthoelectron hypothesis (the neutrino being of the ν_e type) as well as pure V or pure A coupling cannot firmly be excluded.

Table 3

Summary of τ parameters. World averages or best values are given.

Parameter	Units	Prediction	Exp. Value	Experiments
Mass	GeV	-	$1.782\ ^{+.003}_{-.004}$	PLUTO, SLAC-LBL, DASP DESY-Heidelberg, DELCO
Neutrino mass	MeV	0	<250 (95 % C.L.)	SLAC-LBL, PLUTO, DELCO
Spin		1/2	1/2	PLUTO, DASP, DELCO, DESY-HEIDELBERG
Lifetime	10^{-13} s	2.8	<23 (95 % C.L.)	PLUTO, SLAC-LBL, DELCO
Michel parameter		0.75^{++}	0.72 ±.15	DELCO
Leptonic branching ratios				
$B_\mu/.973 = B_e$	%	16.8	17.1 ±1.0 17.5 ±1.2+	SLAC-LBL, PLUTO, Lead-Glass-Wall Ironball, MPP, DASP, DELCO
B_μ/B_e		.973	.99 ± .20 1.13 ± .16+	SLAC-LBL, PLUTO, DASP
Semihadronic BR				
$\tau^- \to \nu_\tau\ \pi^-$	%	9.5	9.8 ±1.4	PLUTO, SLAC-LBL, DELCO, MARK II
$\tau^- \to \nu_\tau\ \rho^-$	%	25.3	21.5 ±3.4	DASP, MARK II
$\tau^- \to \nu_\tau\ A_1^-$	%	8.1	10.8 ±3.4	PLUTO, SLAC-LBL
$\tau^- \to \nu_\tau$+≥3 prongs	%	~ 26	32 ±4 30.6 ±3.0+	PLUTO, DASP, DELCO
$\tau^- \to K^- .../\tau^- \to \pi^- ...$		.05	.07 ± .06	DASP

\+ From ref. 13.
++ V-A prediction. $\rho(V+A) = 0$ is excluded, $\rho(V \text{ or } A) = 0.375$ disfavoured by the data.

Till now the new lepton τ has remained a domain of e^+e^- physics. Within three years, most of its properties have been established. It was the particle that destroyed the four lepton - four quark symmetry (which had just been established) and gave a new impetus to the old puzzle of μ-e universality. Today it is the corner stone of a third generation of quarks and leptons.

REFERENCES

1) M.L. Perl et al., Phys. Rev. Lett. 35, 1489 (1975); 38, 117 (1976).

2) G.J. Feldman et al., Phys. Lett. 63B, 466 (1976); M.L. Perl et al., Phys. Lett. 70B, 487 (1977).

3) PLUTO Coll., J. Burmester et al., Phys. Lett. 68B, 297 (1977); 68B, 301 (1977).

4) DASP Coll., R. Brandelik et al., Phys. Lett. 70B, 125 (1977).

5) A. Barbaro-Galtieri et al., Phys. Rev. Lett. 39, 1058 (1977).

6) H.F.W. Sadrozinski, Proc. of the 1977 Int. Symp. on Lepton and Photon Interactions at High Energies, Hamburg (August 1977).

7) J.G. Smith et al., Phys. Rev. D18, 1 (1978).

8) W. Bartel et al., Phys. Lett. 77B, 331 (1978).

9) W. Bacino et al., Phys. Rev. Lett. 41, 13 (1978).

10) K.G. Hayes, talk given at the APS meeting, Washington (April 1978); G. Gidal, invited talk at this conference.

11) Y.S. Tsai, Phys. Rev. D4, 2821 (1971); SLAC-PUB 2105 (1978); H.B. Thacker, J.J. Sakurai, Phys. Lett. 36B, 103 (1971); J.D. Bjorken, C.H. Llewellyn-Smith, Phys. Rev. D7, 887 (1973).

12) M.L. Perl, Proc. of the 1977 Int. Symp. on Lepton and Photon Interactions at High Energies, Hamburg (August 1977).

13) G.J. Feldman, Proc. of the 19th Intern. Conf. on High Energy Physics, Tokyo (August 1978).

14) G. Flügge, Z. Physik C1, 121 (1979); G. Flügge, Proc. of the Vth Int. Conf. on Experimental Meson Spectroscopy, Boston (April 1977).

15) C.S. Lam, T.M. Yan, Phys. Rev. D16, 703 (1977).

16) DASP Coll., R. Brandelik et al., Phys. Lett. 73B, 109 (1978).

17) O. Meyer, private communication.

18) M. Rößler, Thesis, Hamburg (1978), Internal Report F14-78/01 (unpubl.).

19) F.B. Heile et al., Nucl. Phys. B138, 189 (1978).

20) W. Bacino et al., Phys. Rev. Lett. 42, 6 (1979).

21) B.H. Wiik, G. Wolf, DESY 78/23 (1978) (unpubl.).

22) PLUTO Coll., G. Alexander et al., Phys. Lett. 78B, 162 (1978).

23) G.J. Feldman, Int. Conf. on Neutrino Physics, Purdue 1978.

24) PLUTO Coll., G. Alexander et al., Phys. Lett. 73B, 99 (1978); W. Wagner, Thesis, Aachen (1978); PLUTO Coll., G. Alexander et al., to be published.

25) S. Weinberg, Phys. Rev. 112, 1375 (1958).

26) J.A. Jaros et al., Phys. Rev. Lett. 40, 1120 (1978).

27) F.J. Gilman, D.H. Miller, Phys. Rev. D17, 1846 (1978).

28) J. Kirkby, SLAC Summer Inst. on Particle Physics, 1978, SLAC-PUB-2231.

29) K. Fujikawa, N. Kawamoto, Phys. Rev. D14, 59 (1976) with further references.

30) W. Bacino et al., Phys. Rev. Lett. 42, 749 (1979).

31) PLUTO Coll., G. Alexander et al., Phys. Lett. 81B, 84 (1979).

32) A.M. Cnops et al., Phys. Rev. Lett. 40, 144 (1978).

33) C.H. Llewellyn-Smith, Proc. Royal Soc. A355, 585 (1977); J.D. Bjorken, C.H. Llewellyn-Smith, Phys. Rev. D7, 887 (1973); F.E. Low, Phys. Rev. Lett. 14, 238 (1965).

34) G. Altarelli, N. Cabibbo, L. Maiani, R. Petronzio, Phys. Lett. 67B, 463 (1977); D. Horn, D.D. Ross, Phys. Lett. 67B, 460 (1977).

35) H. Fritzsch, Phys. Lett. 67B, 451 (1977).

36) D.A. Bryman, C. Picciotto, Phys. Rev. D11, 1337 (1975); E. DiCapus et al., Phys. Rev. 133B, 1333 (1964).

JET ANALYSIS

P. Söding
Deutsches Elektronen-Synchrotron DESY, Hamburg, Germany.

Abstract

Methods and results of jet analysis in e^+e^- → hadrons are discussed, with emphasis on effects that indicate deviations from the simple $q\bar{q}$ collinear jet picture.

1. Introduction

The existence of collinear back-to-back jets in the process e^+e^- → hadrons was demonstrated in the remarkable work of the LBL-SLAC collaboration at SPEAR at an energy of $W = 2E_{BEAM} = 7.4$ GeV[1]. It was also shown in this experiment that the angular distribution of the jet axis agreed precisely with the expectation for spin $\frac{1}{2}$ particle-antiparticle pairs, confirming the quark parton model. This underlines a point that will be basic to my discussion: The jet direction can be quite well determined already at low energy and with neutrals undetected. Important further progress was made last year by the PLUTO collaboration at DORIS[2]. They showed that the process e^+e^- → $\Upsilon(9.46)$ → hadrons leads to final states of much larger sphericity than the collinear 2-jet processes in the nonresonant continuum at neighboring energies do. This was intriguing as a first hint towards a possible 3 gluon decay mechanism of the Υ, as expected in QCD.

The central issue today remains whether there is clear evidence for phenomena beyond those predicted by the naive quark parton picture. I would like to emphasise that QCD predicts deviations from the simple quark jet picture of e^+e^- annihilation into hadrons which are already very drastic in the continuum at the higher PETRA/PEP energies. Some of these deviations go like $\alpha_s(W^2)\, W^2$. They must appear as outstanding features of the data even in a qualitative analysis, if QCD is correct.

Concerning quantitative predictions, these are possible in perturbative QCD for observables that do not discriminate between

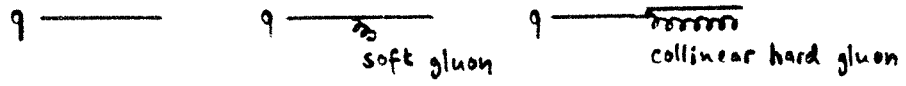

QCD deals, however, with elementary quarks and gluons. The hadronization processes of the quarks and gluons are not calculable. We experimenters measure the final state hadrons. We therefore have to test QCD exploiting features of the final hadron configuration that can be shown to be very unlikely to have resulted from collinear $q\bar{q}$ pairs fragmenting into hadrons. As will be seen, such tests are possible.

We recall the most popular variables used in the analysis of jets[3]:

Sphericity $S = \frac{3}{2}\,\mathrm{Min}\,\frac{\sum p_\perp^2}{\sum p^2} = \begin{cases} 0 & \text{(line)} \\ 1 & \text{(sphere)} \end{cases}$

Thrust $T = \text{Max} \dfrac{\Sigma|p_{\parallel}|}{\Sigma|p|} = \begin{cases} 1 & \text{(line)} \\ 2/3 & \text{(disk)} \\ 1/2 & \text{(sphere)} \end{cases}$

Sphericity and thrust tend to give quite similar results for the jet axes. This is demonstrated in Figs. 1 and 2. Note that thrust is conserved in decays and therefore is a 'good' variable in perturbative QCD. Both of these variables, however, are insensitive to a 3-jet substructure in a planar event.

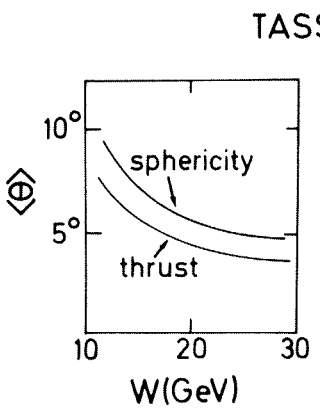

Fig. 1: Mean angular deviation of the sphericity and thrust axes from the true jet direction, for Field-Feynman Monte Carlo jets[4]) propagated through the TASSO detector (neutrals undetected).

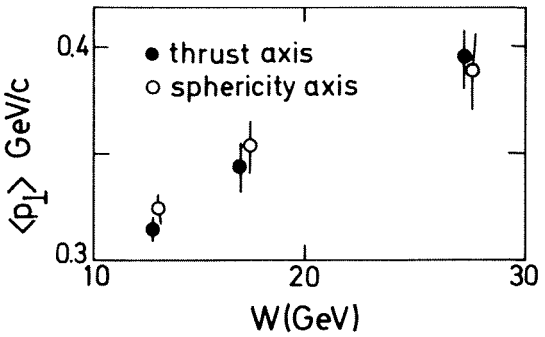

Fig. 2: Mean transverse momentum of the charged hadrons measured in the TASSO detector at PETRA at different total energies $W = 2 E_{BEAM}$, relative to the thrust/sphericity axis.

2. Υ (9.46) → 3 gluons → 3 jets ?

A major battleground in the attempt to check QCD predictions is presently the decay of the $\Upsilon(9.46)$. This has been investigated in the PLUTO detector at DORIS[2]). An excellent presentation of the state of the analysis of these data has been given at this Conference by S. Brandt[5]). Very detailed results on the distribution of many different quantities were presented, for example thrust, triplicity (a generalization of thrust to 3 axes), smallest and largest jet energies, and smallest and largest angle between the 3 axes defined by maximizing triplicity (Fig. 3). The off-resonances continuum data are in good agreement with the Field-Feynman $q\bar{q}$ jet model[4]). In sharp contrast to this, the non-electromagnetic resonant decays are totally different. Collinear back-to-back jets are ruled out as the dominant final states. The data are in very good agreement with a 3 gluon decay model in which the fragmentation of the gluon is assumed to be similar to that of a quark. The 3 gluon process,

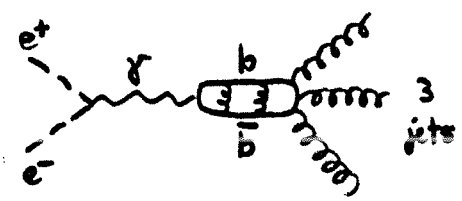

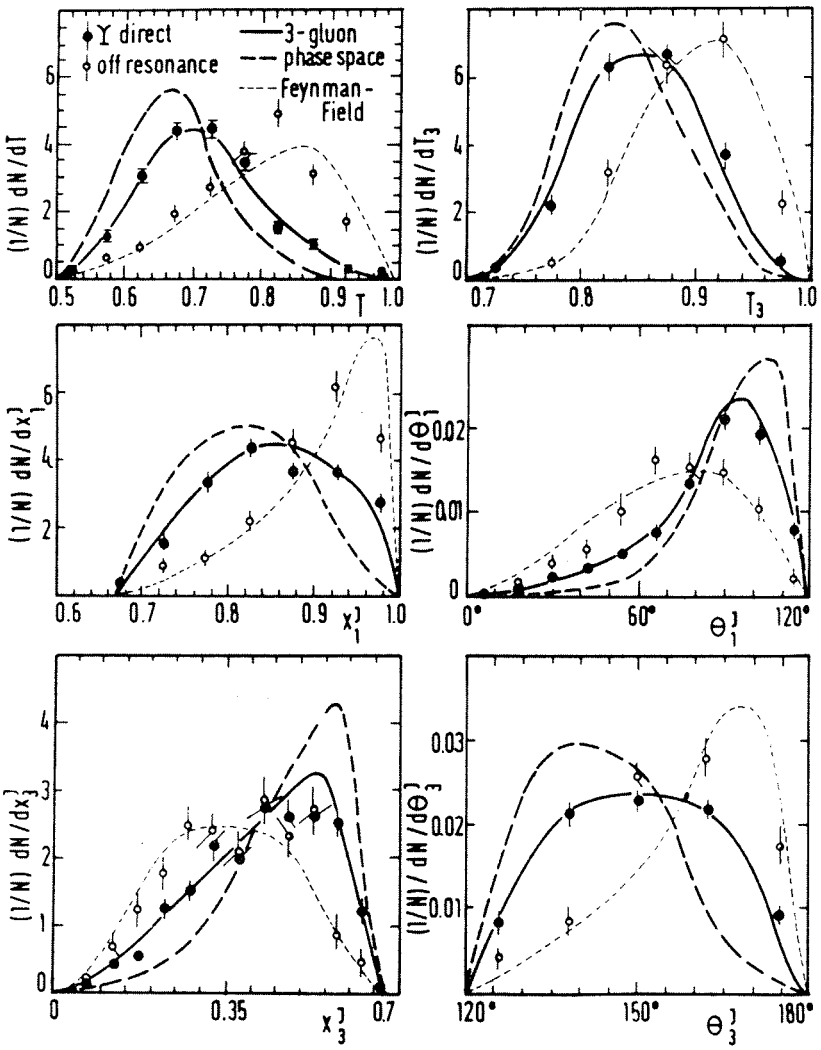

Fig. 3: Experimental distributions from PLUTO at the Υ resonance. Shown are thrust T, triplicity T_3, reconstructed gluon energies x_1^J, x_3^J and reconstructed angles θ_1^J, θ_3^J between gluons, compared with Monte-Carlo calculations based on various models.

analogous to triplet positronium decay, represents the lowest order QCD contribution to $\Upsilon \to$ hadrons. In spite of the low energy there is a clear distinction, both in the data and the model, from simple phase-space like behaviour.

3. Gluon bremsstrahlung at the highest PETRA energies?

In the $e^+e^- \to$ hadrons continuum, first order perturbative QCD involves the graphs

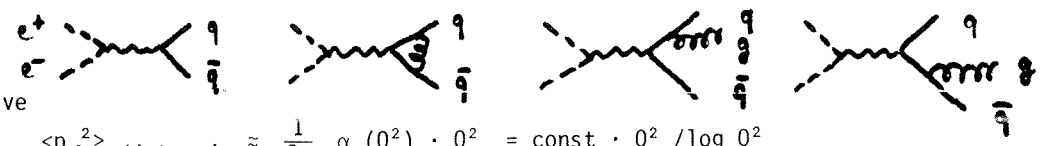

They give

$$\langle p_\perp^2 \rangle_{g/\text{jet axis}} \approx \frac{1}{3\pi}\,\alpha_s(Q^2)\cdot Q^2 = \text{const}\cdot Q^2/\log Q^2$$

and therefore large effects are predicted[6,7] at the highest energy at which data have so far been taken at PETRA, namely W = 27.4 GeV, $Q^2 = W^2 = 750\ GeV^2$.

Not yet committing ourselves to specific calculations, we can easily set up a list of qualitative effects on the $p_\perp$ distributions of the observed hadrons that are expected if gluon bremsstrahlung exists:

i) $\langle p_\perp^2 \rangle$ will increase with W.

ii) The increase, if observed, should come from a small fraction of the events that have relatively large $p_\perp$. This is due to the smallness of $\alpha_s(Q^2)$. Thus rather than a general broadening of the $p_\perp$ distribution (something which could conveivably also arise in the quark hadronization process), one expects a long tail of the $p_\perp$ distribution to develop.

iii) As the sketch at right explains, fast hadrons have a chance to carry a large fraction of the transverse momentum of their parent quark or gluon. This will lead to a strong rise of the observed $\langle p_\perp^2 \rangle$ with $z = p_h/p_{BEAM}$, a phenomenon often called 'seagull effect'.

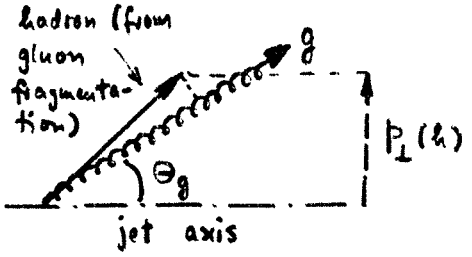

iv) Since hard non-collinear gluons occur with probability $\sim \frac{\alpha_s(Q^2)}{\pi} \sim 10\ \%$ one would in nearly all cases expect at most one of the two jets to appear broadened in transverse momentum space[7].

These effects have been looked for in the data taken with the TASSO detector. Let me emphasize that all these data are still preliminary, as more statistics is presently being accumulated and the checks on the data are being further refined. It is also very important for these tests that one is not passing a threshold for production of a new flavor. There is good evidence that in the energy range W = 13 GeV to 27.4 GeV which we have studied, no new flavor has appeared. This is discussed in the talks by Roger Cashmore[8] and Günter Wolf[9] at this conference.

In Figs. 4 and 5 the evidence for an increase of the overall $\langle p_\perp^2 \rangle$ with W and for the 'seagull' effect is presented. Both figures show significant deviations from the Field-Feynmann $q\bar{q}$ jet behavior[4] that describes lower energy data quite well*). Comparison with the prediction from a QCD calculation extended to include q and g hadronization in a least model-dependent way, presented recently by Hoyer et al.[5], demonstrates that the effects are of the size expected from perturbative QCD. The data show

*) Resonance formation and decays, which are included in the Field-Feynman model, are the cause for a seagull effect to occur also in $q\bar{q}$ jets. This is, however, a quantitatively much smaller effect, and there is no reason to expect it to be strongly energy dependent.

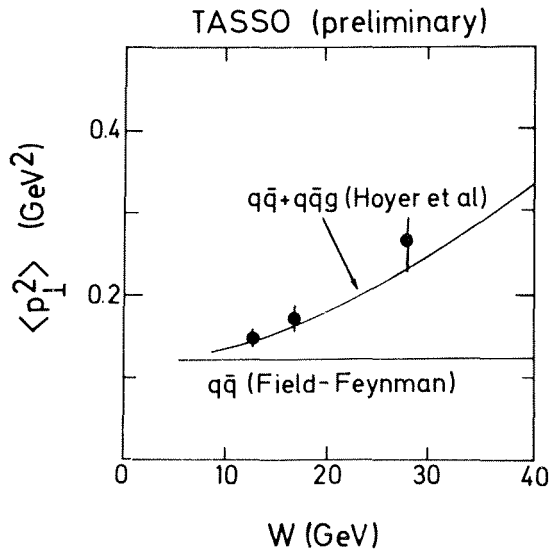

Fig. 4: Mean squared transverse momentum of the charged hadrons with respect to the jet (thrust) axis, as a function of the total e^+e^- cms energy W.

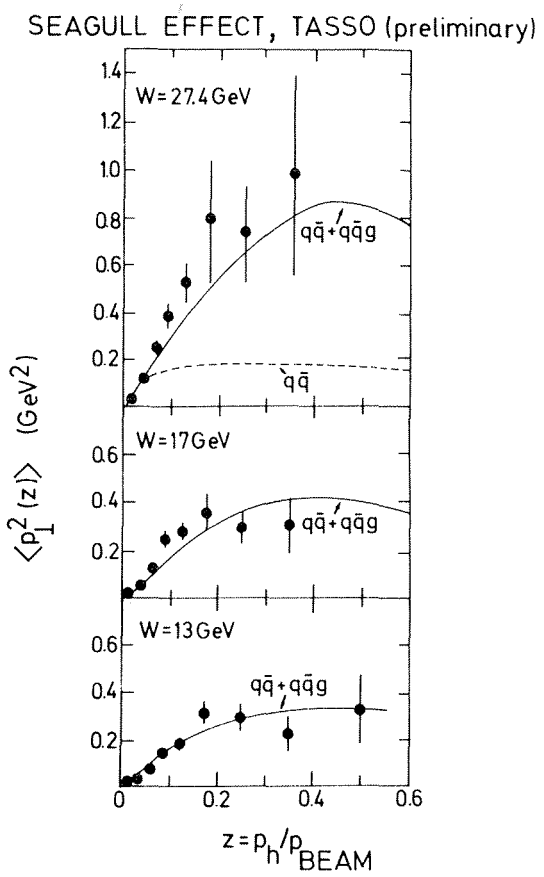

Fig. 5: Mean squared transverse momentum of the charged hadrons with respect to the jet axis as a function of fractional hadron momentum z, at different total e^+e^- cms energies W.

evidence also for a qualitative change in the shape of the $p_\perp$ distribution with increasing W, such that a tail is developed. This has been discussed by Roger Cashmore[8]. We have checked with Monte Carlo studies that resolution or acceptance effects of the detector or the analysis procedure have no significant effect on these results.

One-sided jet broadening is tested in Fig. 6. The jet axis was here determined from the thrust of only the particles in the 'narrow' jet. There is of course

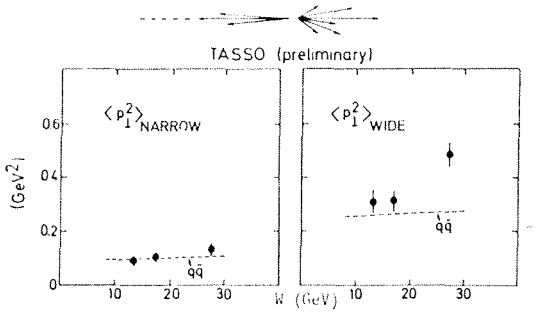

Fig. 6: One-sided jet broadening, expected in 1st order perturbative QCD, is appearing at the highest PETRA energy.

a trivial difference between the $\langle p_\perp^2 \rangle$ on the 'narrow' and 'wide' side, due to the built-in bias in the selection of the two sides. The effect of this bias can be seen from the curves labelled $q\bar{q}$, showing the effect of an identical selection on 2-jet Field-Feynman events. There remains a clear indication in the data of a true one-sided jet broadening at the highest W. It would appear difficult to find a plausible explanation for such an effect in terms of some pecularity of the hadronization process in a pure $q\bar{q}$ picture.

Next, let us discuss correlations between the hadrons produced. These may be expected to be still more sensitive to gluon bremsstrahlung effects than the single-particle $p_\perp$ data discussed so far. This is because hard non-collinear gluon bremsstrahlung will occur in only a small fraction of the events but these may often have several correlated hadrons of large $p_\perp$, occasionally grouped together such as to form a high-$p_\perp$ jet. We can exploit this fact by studying 'event shapes', in particular to distinguish topologies like

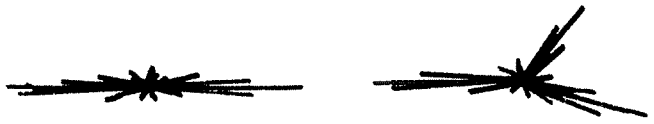

One method to do this uses the Fox-Wolfram moments[10]

$$H_\ell = \frac{4\pi}{2\ell+1} \sum_{m=-\ell}^{\ell} \left| \sum_h \frac{|\vec{p}|}{W} Y_\ell^m(\hat{p}) \right|^2$$

which provide a rotation-invariant characterization of the event shape. These moments can also be considered the coefficients of an expansion of the momentum-flow autocorrelation function of the events into a Legendre series. For a reflection invariant distribution $H_1 = H_3 = 0$, and for ideal $q\bar{q}$ jets (without nonperturbative broadening) $H_2 = H_4 = 1$. Calculations for realistic $q\bar{q}$ jets without gluon bremsstrahlung are shown in Fig. 7 along with the data. While at W = 17 GeV H_2 and H_4 are consistent with the $q\bar{q}$ model, at W = 27.4 GeV they are not. The deviation again provides evidence for a broadening of the event shape compared with pure $q\bar{q}$ jets, setting in at higher W.

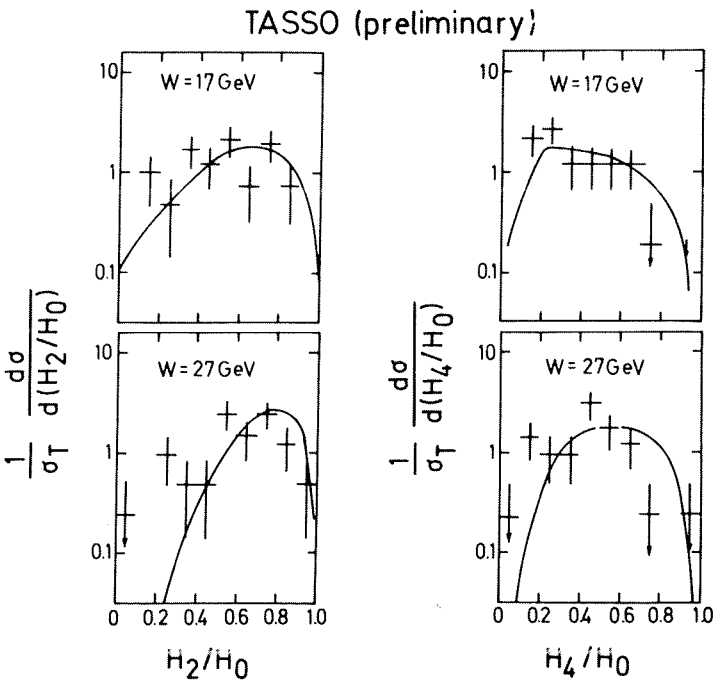

Fig. 7: Distribution of Fox-Wolfram moments at 17 and 27.4 GeV total e^+e^- energy. Curves are for pure $q\bar{q}$ jets.

A more direct method of studying event shapes is based on a paper by S.L. Wu and G. Zobernig[11]. For each event one considers the second rank tensor built from

the hadron momenta

$$\sum_h p_i\, p_k \qquad (i,k = x, y, z)$$

and rotates the coordinate system such that $\hat{x}$, $\hat{y}$, $\hat{z}$ are the eigenvectors associated with its largest, second largest, and smallest eigenvalue respectively. The principal jet axis is then in x direction, the 'event plane' is the xy plane, and z defines the direction in which the sum of the squared momentum components is smallest. The momentum vectors in this coordinate system are plotted for a rather typical event at W = 27.4 GeV in Fig. 8. A pronounced 2-jet

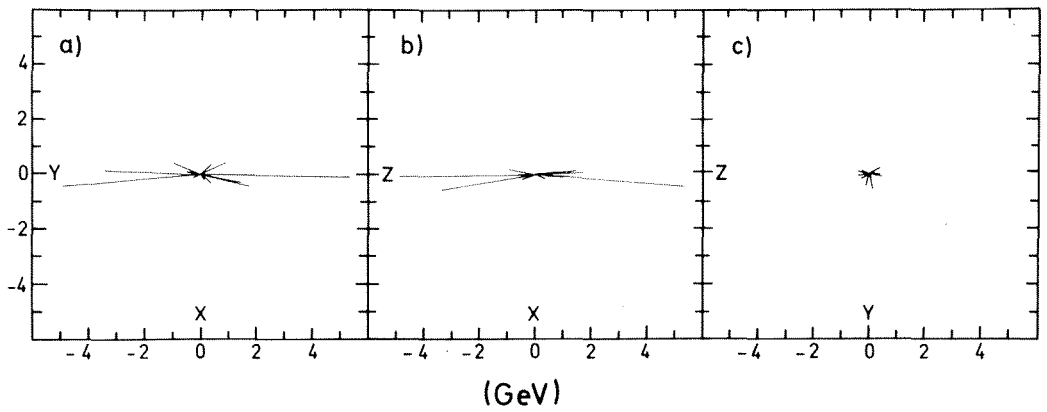

Fig. 8: A typical 2-jet event at W = 27.4 GeV, measured in TASSO. Plotted are the momentum vectors of the charged particles, a) projected on the 'event plane', b) looking at the event plane from the side, and c) viewed along the jet axis.

shape is apparent. Some of the events, however, were found to have a different appearance. Examples are shown in Fig. 9.

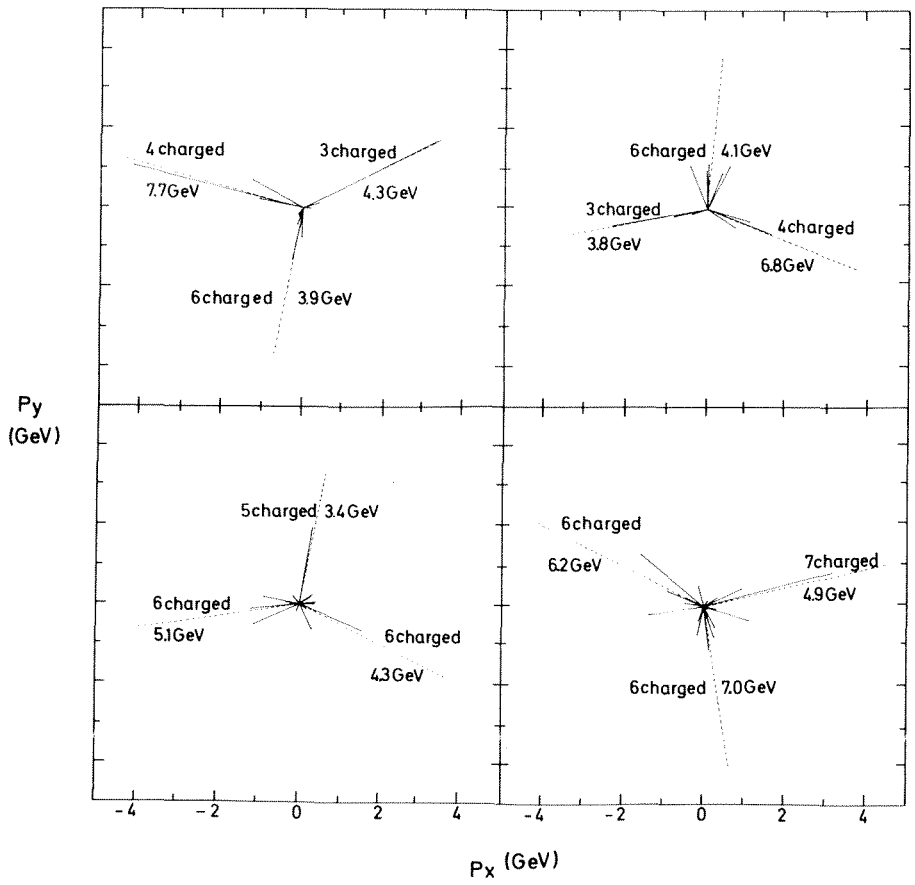

Fig. 9: Four events having topologies suggesting deviations from the simple $q\bar{q}$ quark jet picture, measured in TASSO at W = 27.4 GeV. Plotted are the momentum vectors of the charged particles, projected on the 'event plane' (see the text for the definition of this plane). The events are rotated such that if a single jet axis is fitted, it will point into the x direction. The dotted lines show the directions of the jet axes when 3 axes are fitted.

The momentum projections in the xy plane are then used to group the hadrons into 3 sets and to find the 3 corresponding jet directions [11]. For back-to-back 2-jet events two of these three jet axes will form an angle of 180^0 between them, while for true 3-jet events all angles between axes would significantly differ from 180^0. Also indicated in Fig. 9 are the charged hadron energy and multiplicity for each of the jets so defined.

We now proceed to a more quantitative discussion of these event shapes. In Fig. 10 the average $\langle p_\perp^2 \rangle_{OUT}$ and $\langle p_\perp^2 \rangle_{IN}$ per event is plotted, where 'OUT' refers to the component perpendicular to the event plane (z component), and 'IN' to the component in the event plane and perpendicular to the principal jet axis (y component). Comparing these two distributions we note that they must be trivially different, due to the bias introduced by choosing the event plane on the basis of the momentum tensor. To asess this bias, Monte Carlo back-to-back $q\bar{q}$ jets [4,12,13] were subjected to an identical analysis as the real events. The resulting $\langle p_\perp^2 \rangle_{OUT}$ and $\langle p_\perp^2 \rangle_{IN}$ distributions for these are shown as curves in Fig. 10. The observed distribution of $\langle p_\perp^2 \rangle_{OUT}$ is now seen to be very similar to that calculated for $q\bar{q}$ jets. For the latter, this distribution is determined by the fragmentation of the quarks into hadrons, including resonances and weak decay processes. Since the first order bremsstrahlung process $e^+e^- \to q\bar{q}g$ results in a planar $q\bar{q}g$ configuration, one expects $\langle p_\perp^2 \rangle_{OUT}$ to remain essentially unchanged by gluon bremsstrahlung to that order. This agrees with the observation of Fig. 10 and again confirms that the average hadronic $\langle p_\perp^2 \rangle$ in the q fragmentation model is more or less correct. The distribution measured for $\langle p_\perp^2 \rangle_{IN}$, on the other hand, shows a few events with far-out values of $\langle p_\perp^2 \rangle_{IN}$,

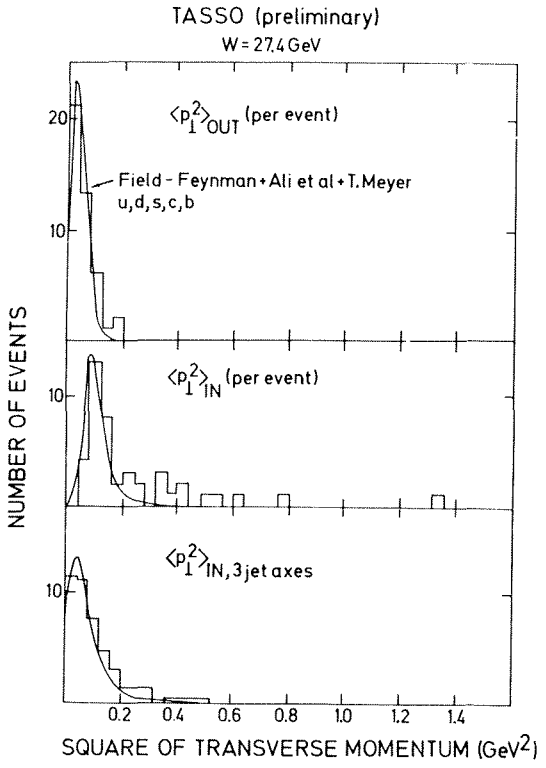

Fig. 10: Distribution of the average squared transverse momentum component out of the event plane (top), and in the event plane (center), for events at W = 27.4 GeV (averaging over charged hadrons only). The curves are for $q\bar{q}$ jets without gluon bremsstrahlung. Comparison of these distributions gives evidence that broadening (compared to $q\bar{q}$ jets) occurs in one plane. The bottom figure shows $\langle p_\perp^2 \rangle$ per jet when 3 jet axes are fitted, again compared with the q jet model.

in a region where the Monte Carlo calculation predicts negligible probability for a $q\bar{q}$ jet. Thus, we observe 11 events with $\langle p_\perp^2 \rangle_{IN} > 0.3$ GeV^2 while < 1 is expected from the $q\bar{q}$ model. To summarize: The events observed at W = 27.4 GeV are consistent with being planar to a degree determined by the smearing effect of the hadronization process; within the plane, however, a small percentage of the events shows enlarged transverse momenta with respect to the jet axis.

Instead of considering the transverse momentum relative to one common jet axis for the event, we can also fit 3 axes as described before and define the transverse momentum of each hadron relative to the axis of the jet to which it is associated. This results in a relatively narrow $\langle p_\perp^2 \rangle$ distribution (per jet) which agrees well with the calculated distribution for $q\bar{q}$ jets. This is shown in the bottom part of Fig. 10. Thus, interpreting the events as 3-jet events results in transverse momentum properties of the jets consistent with those of the q jet parametrization.

So far we have discussed evidence for deviations from the simple $q\bar{q}$ 2-jet picture, and I argued that effects are apparent in the data which result in final hadron configurations quite unlike those that would be expected to occur with nonnegligible probability from fragmentation processes of $q\bar{q}$ pairs. These effects appeared to be qualitatively consistent with the expected properties of gluon bremsstrahlung. Since perturbative QCD makes quantitative predictions, we can ask whether our measured rate of production of gluon bremsstrahlung event candidates is consistent with that prediction. To investigate this we rely on our determination of the angles between the 3 jet axes, which I believe to be the quantity least likely to be in gross error. A symmetric angular plot with events at W = 27.4 GeV is sketched below. Ordering the angles $\Theta_1 \leq \Theta_2 \leq \Theta_3$ puts all the events into 1/6 of the triangle. The 1st order QCD cross section $\frac{1}{\sigma_0} \frac{d\sigma}{d\Theta_1 \, d\Theta_2} (e^+e^- \to q\bar{q}g)$ varies relatively slowly over most of the angular region except when one of the angles approaches 180°. Let us define 'hard noncollinear bremsstrahlung candidates' by $\Theta_1 > 40^\circ$, $\Theta_3 < 160^\circ$; this ensures that

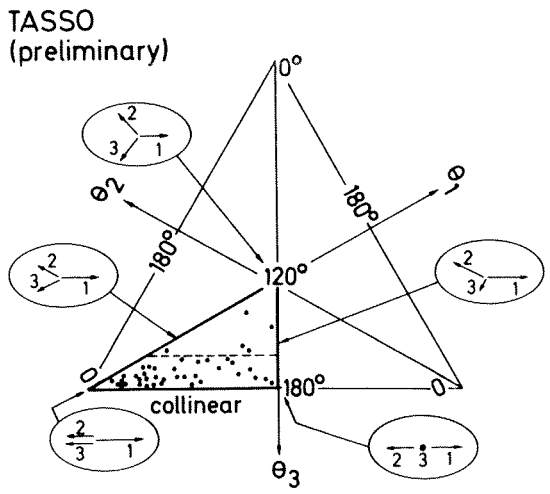

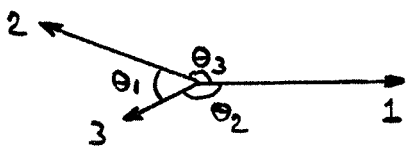

the smallest energy E_3 of any of the three jets is > 4 GeV. We find 5 candidates, while the prediction is 9 (assuming 5 flavors and Λ = 0.5 GeV in the calculation of $\alpha_s(W^2)$). I consider this as good an agreement as can be expected in view of the small statistics, the uncertainty from excaping neutrals, and the high degree of preliminarity of this analysis. In any case, from these numbers it is also obvious that a rather high rate for events of characteristic non-collinear topology is predicted by QCD perturbation theory at these high PETRA/PEP energies, of the order of a few percent of the total hadron production cross section. Thus, if this theory is correct we must soon confirm these results with a statistically much improved evidence.

* * *

Acknowledgement

I wish to thank all my colleagues in the TASSO collaboration and at DESY who made the measurements possible that provided the meat of this talk and who let me use the results of their work on these data.
For help, ideas, and clarification in connection with this talk I am particularly indebted to R. Barlow, W. Braunschweig, Y. Eisenberg, W. Koch, H. Kowalski, D. Lüke, Tom Meyer, G. Mikenberg, M. Schliwa, T. Walsh, B. Wiik, G. Wolf, Sau Lan Wu, P. Zerwas, and G. Zobernig.

References

1) G. Hanson et al., Phys. Rev. Letters 35,1609 (1975)

2) Ch. Berger et al., Phys. Letters B78,176 (1978)

3) For a discussion and references, see S. Brandt and H.D. Dahmen, Particles and Fields (Z. Physik C) 1,61 (1979)

4) R.D. Field and R.P. Feynman, Nucl. Phys. B136,1 (1978)

5) S. Brandt, Experimental search for Υ decay into 3 gluons, these proceedings

6) A. De Rujula, J. Ellis, E.G. Floratos and M.K. Gaillard, Nucl. Phys.B138,387 (1978); G. Kramer and G. Schierholz, Phys. Letters 82B,108 (1979)

7) P. Hoyer, P. Osland, H.G. Sander, T.F. Walsh and P.M. Zerwas, DESY 79/21 (1979), to be published

8) R. Cashmore, Results of the TASSO Collaboration, these Proceedings

9) G. Wolf, High Energy Trends in e^+e^- Physics, Rapporteur Talk, these Proceedings

10) G.C. Fox and S. Wolfram, Nucl. Phys. B149,413 (1979)

11) Sau Lan Wu and G. Zobernig, Particles and Fields (Z. Physik C) 2(1979), to be published

12) A. Ali, J.G. Körner, J. Willrodt and G. Kramer, Particles and Fields (Z. Physik C)1, 2o3 (1979); ibid. 1,269 (1979); and paper to be published

13) Tom Meyer (Wisconsin), private communication

DISCUSSION

Chairman: L.S. Cheng

Sci. Secretaries: G.V. Goggi and C. Peroni

G. Preparata: What is the fragmentation function of the gluon chosen in the $\Upsilon \to 3g$ analysis?

P. Söding: In the Pluto analysis the fragmentation function used was the quark fragmentation function.

G. Preparata (statement by questioner): If the gluon fragmentation function has been chosen to be the same as for quarks, this contradicts the QCD expectation that gluons radiate softer particles than quarks. In the light of this, one should be more careful before claiming experimental agreement with QCD.

P. Söding: The data agree with this model and they do not seem to show a spectacular rise of the multiplicity in the Y region.

S. Brandt: I would like to comment on the question raised, how the simple assumption that gluons fragment like quarks which was used in our Monte Carlo model influences the event multiplicities. The mean jet multiplicity is assumed to rise logarithmically and not linearly with jet energy. Therefore, although the mean gluon energy of $\Upsilon \to 3g$ is only $^2/_3$ of the quark energy of $e^+e^- \to q\bar{q}$, the total multiplicity of 3g Monte Carlo events is larger than that of $q\bar{q}$ events at the same E_{cm}. In fact the surplus in multiplicity corresponds to that we observe experimentally on the Y resonance as compared to the continuum.

V.A. Khoze: Can the seagull effect be at least partly connected with resonance decays?

P. Söding: In the Field-Feynman model the seagull effect is present and caused by resonances, but this model does not account for the large seagull effect observed. To explain it by resonances one would have to make a model in which resonance production drastically changes with energy.

S. Brodsky: Is there any evidence for hard photons plus two-jet events at the Υ or for $\gamma\gamma \to$ jet-jet events?

P. Söding: Not to my knowledge. The event rates are still too small.

e^+e^- PHYSICS BELOW J/ψ RESONANCE

J.E. Augustin
Laboratoire de l'Accélérateur Linéaire, Centre d'Orsay, 91405 Orsay, France.

ABSTRACT

Some recent results of e^+e^- physics in the 1 to 2 GeV region are reviewed. They begin with studies of electromagnetic final states in wide angle bremsstrahlung and in photon-photon collisions. Next, the measurements of the hadronic production ratio R are presented, together with the new determination of the inclusive K° ratio. Then the exclusive multipion channels and the status of claimed vector meson recurrences is reviewed, as well as new results on electromagnetic form factors in the time-like region.

INTRODUCTION

e^+e^- collisions below 3 GeV c.m. energy have been intensively studied in the recent years, especially between 1 and 2 GeV. These studies are aimed both at a precise measurement of the total cross section and inclusive particle production, and at a search for vector meson recurrences by looking at exclusive channels. The e^+e^- storage rings covering this domain are Vepp 2M at Novosibirsk, Adone at Frascati and DCI at Orsay. Vepp 2M energy range goes up to 1.4 GeV, which is about the lower energy limit of DCI and Adone. Data taking has stopped at Adone since June 1978 and we are in the situation where only one machine covers a given range in energy. The experiments concerned are : OLYA at Novosibirsk, $B\bar{B}$, MEA and $\gamma\gamma 2$ at Frascati, M3N and DM1 at Orsay. Only MEA and DM1 have a magnetic analysis for momentum measurement. OLYA, $\gamma\gamma 2$ and M3N allowed charged particles and photon detection.

Because of the small amount of time alloted to my talk, I cannot do justice to all the work done in this field, and I have only selected some aspects of the results. Section 1 covers new QED studies and section 2 some results on total and inclusive cross sections. In section 3 the most prominent inclusive channels are discussed and in section 4 results on proton and kaon form factors are covered.

1. ELECTROMAGNETIC FINAL STATES

a) $e^+e^- \to e^+e^-\gamma$ has been studied at Frascati[1] by the $\gamma\gamma 2$ group in the two kinematical cases where the three final particles are emitted at large angle (wide angle Bremsstrahlung) or only one electron and the γ ray are at large angle, and the other electron is detected as small angle (virtual compton scattering). The results are in agreement with predictions in both cases. The e-γ invariant mass spectra were searched for a heavy electron e^*, and new upper limits for the coupling constant of this hypothetical $e^* \to e\gamma$ are obtained for a mass in the range 0.3 to 2.5 GeV.

b) $e^+e^+ \to e^+e^+\ell^+\ell^-$ where $\ell^+\ell^-$ stands for e^+e^- or $\mu^+\mu^-$ is the simplest photon-photon collisions channel. At Orsay, the two rings system of DCI has been used by an Orsay-Clermont collaboration[2] to investigate this process at 2×1.2 GeV.

The only particles detected were the lepton pair whose momenta and angles were measured in the DM1 detector. The use of two e^+ beams eliminated the elastic scattering and annihilation background to the photon-photon events. For 8.8 nb^{-1} of integrated luminosity corresponding to 1300 Moeller scattering events, 88 $\gamma\gamma$ events have been detected with a background contamination of 6 ± 2. They correspond to $\gamma\gamma$ collisions in a range of small x ($x = \frac{E_\gamma}{E_{beam}} \simeq 0.1$) and small invariant mass (W ≃ 200 MeV). This clean sample of events has been used to test the theory on the distributions of the polar and azimuthal angles, of the velocity of the pair center of mass, of the transverse momentum and of the pair invariant mass. As an example, this last distribution is shown on figure 1. The agreement with theory is excellent, and shows that photon-photon collisions are well understood. The next step will be the study of $\pi\pi$ and $K\bar{K}$ C = + final states.

2. R AND INCLUSIVE CROSS SECTIONS

A) The ratio of the total hadronic cross section to the point like $\mu^+\mu^-$ cross section in the energy range 1 to 2 GeV has been measured by the experiments $\gamma\gamma 2$[1], M3N[3-4] and MEA[5]. The measurement results from a multipion statistical analysis of the observed topologies of charged particles and photons. The assumptions made are almost indentical for these experiments :

a) all particles in the final state are pions

b) Lorentz invariant phase space angular and momentum distributions

c) maximum multiplicity 7 pions (M3N) or 6 below 2 GeV and 8 above ($\gamma\gamma 2$)

d) two body ($\pi^+\pi^-$, K^+K^- , $p\bar{p}$) final states are not included.

Moreover, in the $\gamma\gamma 2$ analysis, the 5 pions channel is constrained such that

$$\sigma(4\ \pi^{\pm}\ \pi^{\circ}) = 2\ \sigma(2\ \pi^{\pm}\ 3\ \pi^{\circ}).$$

Assumption b can be checked by looking at the variation of efficiencies with the model for some specific channels. Assumption a is probably more delicate. As we will see, already at these energies, about 1 out of 4 of the multihadronic events includes a K pair. These kaons and their decay products tend to mix up topologies, but the total cross section measurement is probably safe at the 10 % level because it is only the differences between the true and assumed efficiencies which enters in.

The overall accuracy of the measurements depends then most on the total solid angle of the detector (70 % of 4π for M3N and 90 % of 4π for the improved $\gamma\gamma 2$ apparatus).

The results are shown on figure 2 as $R = \sigma_{TOT}/\sigma_{\mu\mu}$ with $\sigma_{\mu\mu}$ = 87 nb/s. The $\gamma\gamma 2$ and M3N points are shown together with a point from the MEA group, previous measurements from the $\gamma\gamma$ group[6] and the Mark I SLAC-LBL collaboration at SPEAR[7]. It is worth noticing that radiative corrections have been applied to the $\gamma\gamma 2$ data, but not to the M3N one. In any case, the systematic uncertainty is of order 10 to 20 % due to the hypothesis made. Between 1.5 and 2.2 GeV the mean value for the Orsay data is R = 2.18 ± .07 (± .2). The Frascati data seems to show a slight minimum around 2 GeV. The fact that already at 1.5 GeV, R has

reached a reasonable vicinity to the quark parton model value of 2 is comparable to the precocious scaling observed in deep inelastic lepton scattering. Taking the QCD time like result at face value

$$R = \sum_{u,d,s} Q_i^2 \left(1 + \frac{\alpha_s(s)}{\pi}\right)$$

and α_s given by Yndurain[8] one gets[4] R = 2.16 to 2.26 at 1.5 GeV with a normalization point between .45 and . 15 GeV. A more precise determination of R is clearly necessary to reach definite conclusions on QCD applicability.

B) As far as inclusive cross sections are concerned, many interesting results have been obtained[1] by the MEA group. I think that the most interesting new result is a DM1 measurement[9] of the inclusive K°_s cross section between 1.6 and 2.2 GeV. An evaluation of R_K given by $2\,\sigma_{K^\circ_s} / \sigma_{\mu\mu}$ is plotted on figure 2(b). It seems to stay constant around .5 already at these energies. R_{K° values have been measured at 3.6 GeV by Pluto[10] and SLAC-LBL[11] and $R_{K^\pm}$ by Dasp[12]. The DM1 measurement is consistent with a constancy of R_K in the whole range of the old physics - but measurements have to be done between 2.2 and 3.6 GeV.

In terms of the quark parton model, a value of $R_K = 1/3$ is expected from direct production of strange quarks. The remaining part of R_K could then, following Field and Feynman[13], be translated into a 10 % probability that $u\bar{u}$ and $d\bar{d}$ quarks get dressed using an $s\bar{s}$ pair, if such a statement is meaningful at these energies.

3. EXCLUSIVE CHANNELS

a) 4 pions : $\pi^+\pi^-\pi^+\pi^-$ and $\pi^+\pi^-\pi^\circ\pi^\circ$

The 4 charged pions channel is the only one in which photoproduction experiments and previous Adone data have clearly established[14] a vector meson recurrence, the $\rho'(1600)$. New data on $e^+e^- \to \pi^+\pi^-\pi^+\pi^-$ come from the DM1 experiment[9] at Orsay. The M3N[3] , $\gamma\gamma 2$[1] and MEA[5] experiments have also measured it together with the $\pi^+\pi^-\pi^\circ\pi^\circ$ final state. These results are shown on figure 3. A very clear ρ' signal is visible in the 4 charged pions channel, but a word of caution is in order : the left side of the resonance comes from Novosibirsk data[15], except from one point from Orsay at 1.35 GeV - so that relative normalization problems may occur. The accuracy of the high energy side is greatly improved by the DM1 data. For the $\pi^+\pi^-\pi^\circ\pi^\circ$ channel, besides this relative normalization uncertainty, the structure seems quite different.

If quasi two body final states dominate, isospin symmetry relates these two channels[16]: for example, $A_1\pi$ or $A_2\pi$ would contribute equally, whereas $\rho\varepsilon$ and ρf contribute two times more to $4\pi^\pm$, and $\omega\pi$ and $\rho^+\rho^-$ only to $\pi^+\pi^-2\pi^\circ$.

The $\gamma\gamma 2$ group has chosen to fit independently their $4\pi^\pm$ data together with Novosibirsk one. Using a p^3 threshold dependence, where p is the c.m. momentum of the quasi-two body, they get an excellent fit of a resonance with the following parameters

$$M = 1649 \pm 23 \text{ MeV} \quad \Gamma_{FWHA} = 500 \pm 50 \text{ MeV} \quad \Gamma_{ee} = 3.1 \pm .2 \text{ KeV}$$

and a threshold at $\sim$ 900 MeV. One question about this fit is that a p^3 factor is quite arbitrary since a $\rho' \to \rho\varepsilon$ or $A_1\pi$ has a p factor only, and $A_2\pi$ would need a p^5 term. Also, the question of the $\pi^+\pi^-\pi^\circ\pi^\circ$ channel is left open.

On the contrary, the M3N group at Orsay has first measured the $\omega^\circ\pi^\circ$ content of the $\pi^+\pi^-\pi^\circ\pi^\circ$ channel. The resulting cross section is quite flat, and so the remaining part was fitted jointly with the 4 $\pi^\pm$ channel. A one resonance fit cannot be found, and the M3N group suggest that two structures could exist ; the second being almost decoupled from the 4 charged pions channel. As an example they get

$$m_1 = 1533 \pm 21 \text{ MeV} \qquad \Gamma_1 = 202 \pm 70 \text{ MeV}$$

$$m_2 = 1690 \pm 14 \text{ MeV} \qquad \Gamma_2 = 180 \pm 87 \text{ MeV}$$

Magnetic detectors result for the $4\pi^\pm$ go further in analysing the final state : MEA[1] and DM1[9] confirm the photoproduction[14] result of a $\rho^\circ\pi^+\pi^-$ dominance. The question of $A_1\pi$ or even $A_2\pi$ is much more difficult because of the symmetrization of identical particles which is important. DM1 finds that in the 2 GeV region, the $A_1\pi$ channel does not seem to dominate. On the contrary in the low energy side the rise of the cross section is predicted to necessitate[17] $A_1\pi$ dominance. Detailed dynamical studies are necessary in both channels, and in the whole energy range. In particular the existence of a $\rho'(1250)$ is still an open question.

b) The other multipion channels have been extracted by the unfolding procedure, but the $\gamma\gamma 2$ and M3N groups give somewhat different results, especially in the $4\pi^\pm$ 2 π° channel where Adone data is consistently higher than the Orsay points. In these channels, hints for relatively narrow ($\Gamma \lesssim$ 50 MeV) resonances have been found : at 1820 MeV at Adone[18], and at Orsay[3] in 5 π at 1770 MeV and in 5 π and 3 π at 1660 MeV. Preliminary 5π data from the DM1 group is shown in figure 4 together with the previous M3N measurements. The DM1 data does not show evidence for the 1770 structure, but is not incompatible with the 1660 one. The 4 $\pi^\pm\pi^\circ$ final state is found by DM1 to be more than 50 % $\omega^\circ\pi\pi$.

c) New exclusive channels, containing kaons, have been measured by the DM1 experiment[9] at Orsay. For example the $K^+K^-\pi^+\pi^-$ channel gives a cross section quite flat between 1.8 and 2.2 GeV with a mean value of order 4 nb. Dynamically, the DM1 group finds this channel dominated by $K^*K\pi$. A resonance in the $K^{*\circ}$ inclusive final state has been claimed by the MEA group[19] at a mass of 2130 MeV. A preliminary analysis of the DM1 data in this region does not seem to show this effect, but an analysis identical to the MEA group one has not yet been done.

4. π, K and p FORM FACTORS

A very precise measurement of the pion form factor near threshold done at Novosibirsk[20] confirms the value predicted by an analytic fit of all existing data[21] both in the time-like and space-like regions.

The $e^+e^- \to p\bar{p}$ cross section near the threshold has been measured by the DM1 group[22]. Analysed in terms of hypothetical e^+e^- couplings of the narrow Baryonium states[23], they result in upper limits of

$$B_{p\bar{p}} \times \Gamma_{ee} < 10 \text{ eV} \quad \text{for the 1935 MeV state}$$

and

$$Bp\bar{p} \times \Gamma_{ee} < 25 \text{ eV} \quad \text{for the 2020 MeV state.}$$

The resulting squared proton form factor, assuming $|G_E|^2 = |G_M|^2$ is in agreement with the Adone[24] measurement and with $p\bar{p} \to e^+e^-$ results[25], and confirms a value about an order of magnitude higher than simple extrapolations of the space-like dipole fit.

The DM1 has also measured the charged and neutral kaon form factors in the energy range 1.6 to 2.2 GeV. In figure 5 their result is compared to previous Adone[26] data and to a ρ-ω-ϕ extrapolation by F. Renard[27]. The K° form factor remains quite small, but the K^+ one seems to show a structure in the 1.6 to 1.7 GeV region. If a definite isospin state dominated the $K\bar{K}$ channel, the K° and $K^\pm$ form factors would be equal. This is not the case and would indicate an interference effect.

One has here an example of the complicated behaviour of exclusive channels. Definite conclusions on the existence of vector meson recurrences besides the $\rho'(1600)$ effect will need detailed dynamical studies and coupled channels analysis. Other DM1 results also show that kaonic channels give a fruitful way to study this energy region where resonance and asymptotic properties mix together. Such a transition region ought to be of importance for the understanding of hadronic physics, and asks for an important experimental effort. It seems that an interesting region is almost between the Vepp 2M and DCI energies. The situation would be very improved by the construction of the Frascati 1 to 2.4 GeV ALA project[28]. In any case, new and better detectors are expected to operate soon at Novosibirsk and Orsay.

* * *

REFERENCES

1) M. Spinetti, Results from Adone, Report LNF 79/25(P), Frascati (1979).
R. Baldini, these proceedings.

2) A. Courau et al., Phys. Lett. B, 145 (1979).

3) G. Cosme et al., Nucl. Phys., B 152, 215 (1979).

4) C. Paulot, thèse L.A.L. Orsay (1979).

5) B. Esposito et al., Lett. Nuov. Cim., 25, 5 (1979) and 19, 21 (1977).

6) R. Baldini et al., Lett. Nuov. Cim., 24, 324 (1979).

7) J.E. Augustin et al., Phys. Rev. Lett., 34, 764 (1975).

8) F.J. Yndurain, Nucl. Phys. B 136, 533 (1978).

9) J.C. Bizot et al. Communication to this Conference.

10) J. Burmester et al., Phys. Lett., 67B, 367 (1977).

11) V. Lüth et al., Phys. Lett., 70B, 120 (1977).

12) R. Brandelik et al., Phys. Lett., 67B, 363 (1977).

13) R.P. Feynman and R.D. Field, Nucl. Phys., B136, 1 (1978).

14) Review of Particle Properties, Phys. Lett., 75B, 122 (1978) and references therein.

15) V. Sidorov, in Proceedings of the 18th Intern. Conf. on High Energy Physics, Tbilisi (USSR), July 1976. Edited by N.N. Bogolyubov et al., pB 13.

16) J. Layssac and F.M. Renard, Lett. Nuov. Cim., 1, 197 (1971) and Nuov. Cim,6A,134 (1971)

17) T.N. Pham, C. Roiesnel, T.N. Truong, Phys. Lett., 80B, 119 (1978).

18) C. Bemporad, in Proceedings of the 1977 Int. Symp. on Lepton and Photon Interactions at High Energies, Hamburg, Aug. 25-31, edited by F. Gutbrod(Desy, Hamburg, 1977), p. 165.

19) B. Esposito et al., Lett. Nuov. Cim., 22, 305 (1978).

20) V.I. Vasserman et al., Yad. Fiz., 28, 968 (1978).

21) A. Quenzer et al., Phys. Lett., 76B, 512 (1978).

22) B. Delcourt et al., Preprint Orsay, LAL 79-12 (1979).

23) see G. Flügge, in Proceedings of the 1978 Tokyo Conference, edited by S. Homma et al..

24) M. Castellano et al., Nuov. Cim., 14 A, 1 (1973).

25) G. Bassompierre et al., Phys. Lett., 68 B, 477 (1977).

26) M. Bernardini et al., Phys. Lett., 46 B (1973).

27) F.M. Renard, Nucl. Phys., B 82 (1974).

28) G. Belletini and R. Bertrani, Frascati, Report LNF-79/17(R) (1979).
ALA Design Report, Frascati LNF-78/15 (1978).

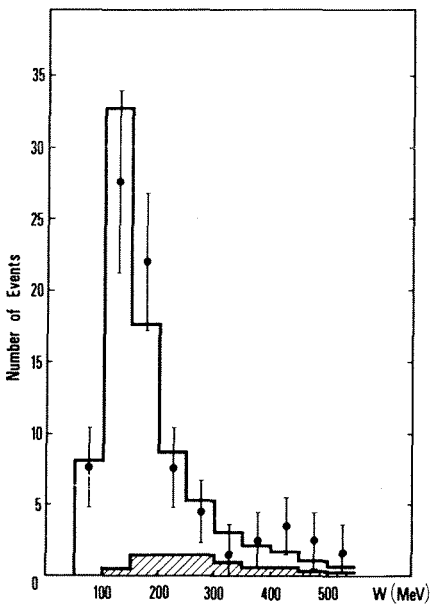

Fig. 1 : Invariant mass distribution of the lepton pairs from photon-photon collisions
Solid line : Monte-Carlo prediction ; Shaded area : muon contribution.

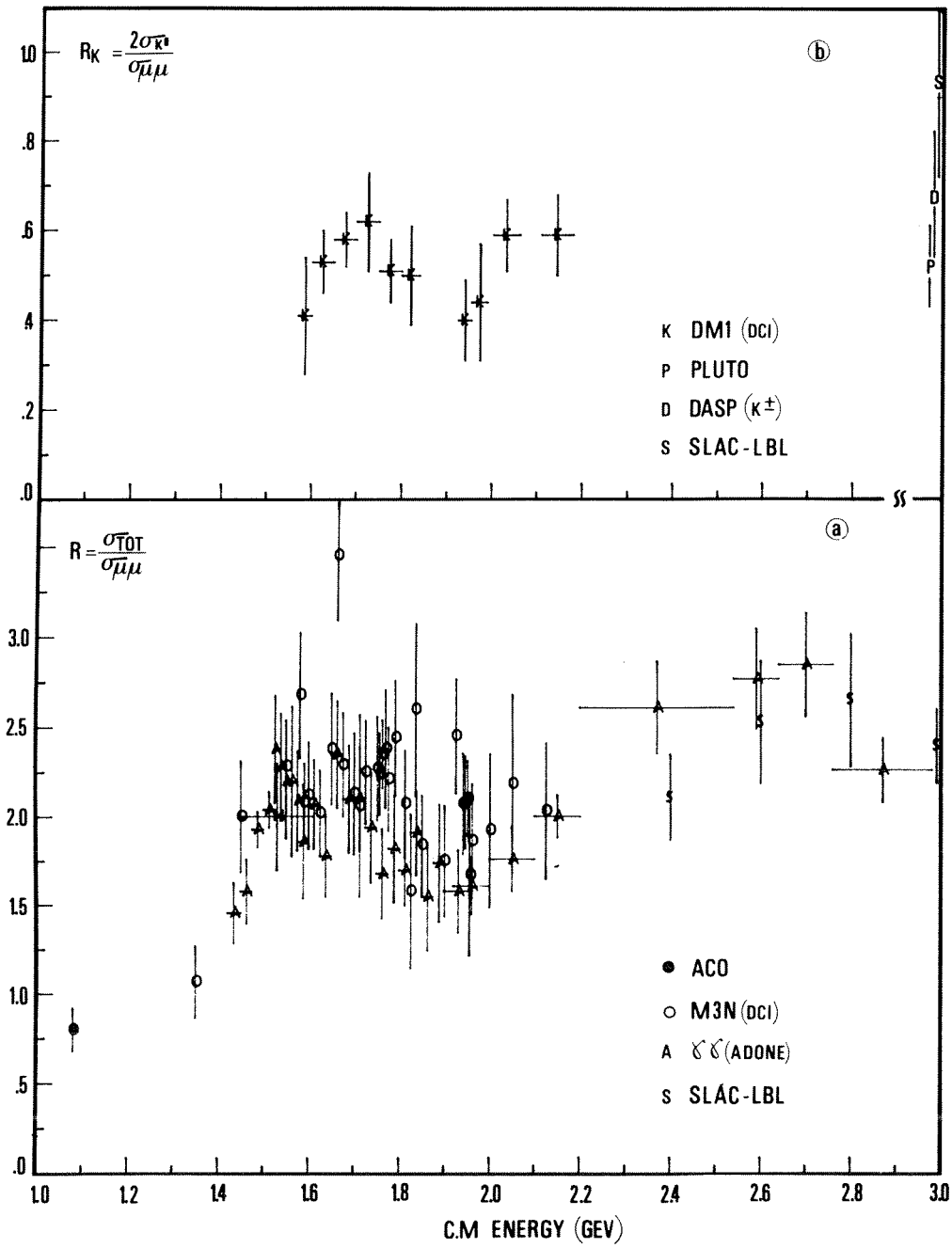

Fig. 2 a : R values between 1.1 and 3 GeV, and

2 b : $R_K = \frac{2\sigma_{K^0_S}}{\sigma_{\mu\mu}}$ with 3.6 GeV points : K^0 from Pluto and Spear, and $K^{\pm}$ from Dasp.

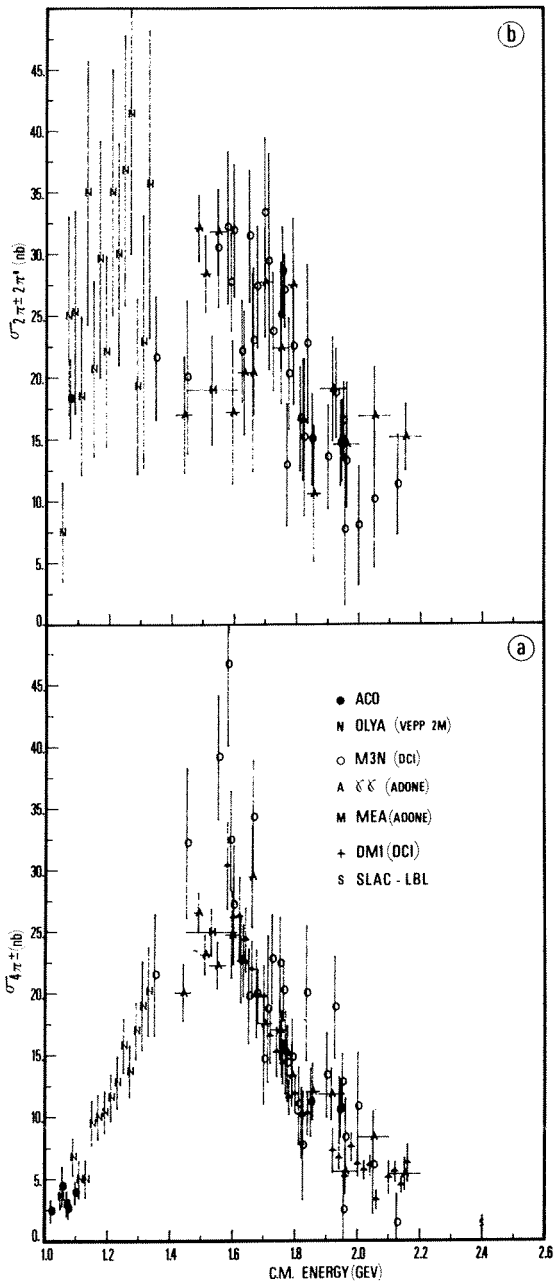

Fig. 3 : Cross section for the production of (a) 4 $\pi^{\pm}$ and (b) 2 $\pi^{\pm}$ 2 π° final states.

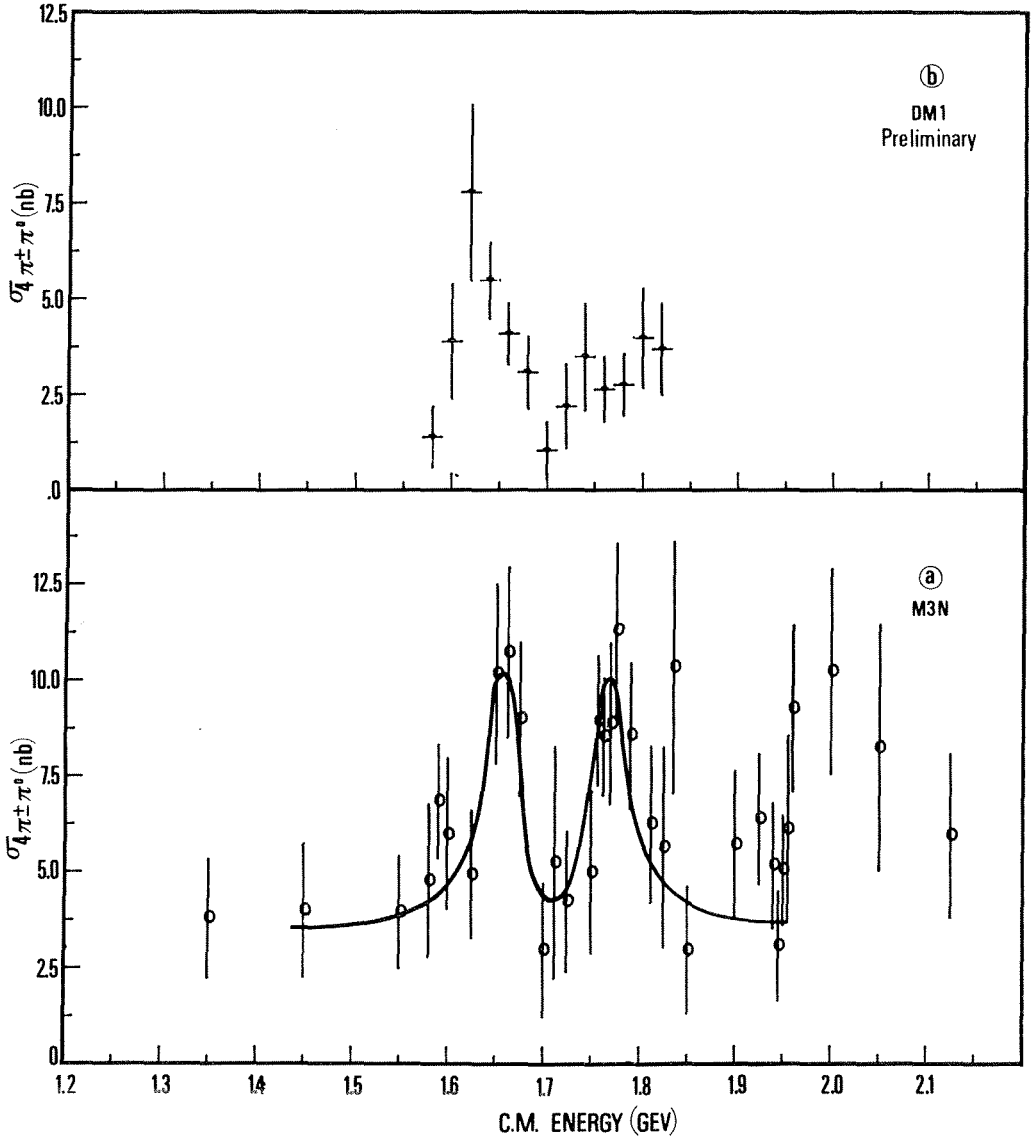

Fig. 4 : 5 pion cross section (4 $\pi^{\pm}\pi^{\circ}$) as measured by (a) M3N and (b) DM1 experiments at DCI.

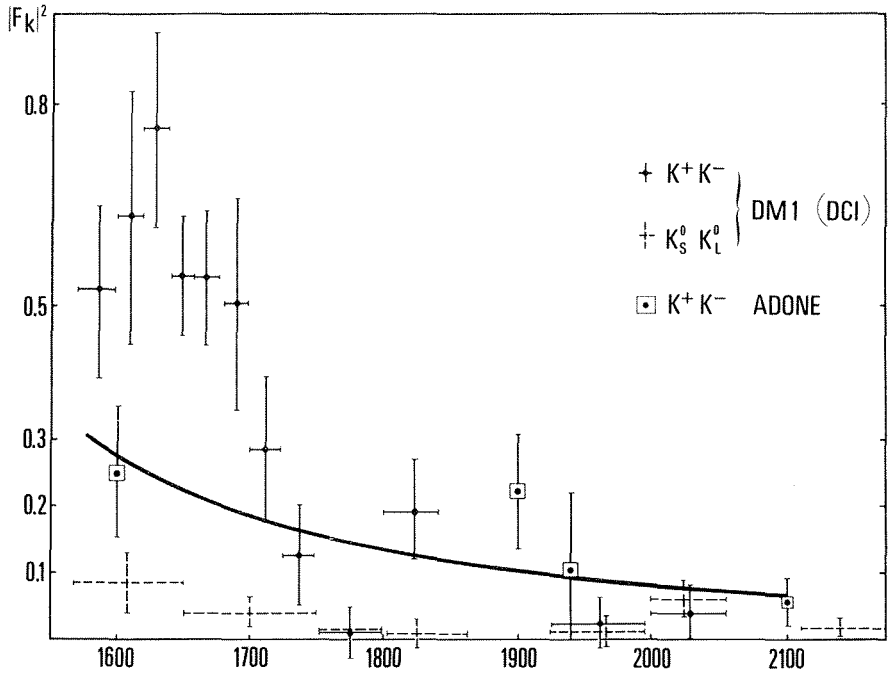

Fig. 5 : Kaon form factors. Full line : $\rho\omega\phi$ tail for K^+K^- from Renard.

DISCUSSION

Chairman: L.S. Cheng

Sci. Secretaries: G.V. Goggi and C. Peroni

G. Wolf: You showed data on the proton form factor, can they be described by the dipole form factor?

J. Augustin: The data are at least a factor of 10 above the simple extrapolation of the dipole form factor. They are consistent with computations using vector meson dominance for the time-like form factor.

A. Zichichi: I would like to make a comment on the so-called "dipole form factor". About 10 years ago we have shown (on data having been taken at the Adone storage ring) that the dipole fit was ruled out for the description of the π and K electromagnetic form factor.

T. Ferbel: Is there any information on two-pion decay rates of the ρ' mesons, and, if low, is there any theoretical understanding of that?

J. Augustin: There is no measurement of 2π decay of ρ' in storage rings. Only kinematical separation from e^+e^- final states allows one to measure the $\pi^+\pi^-$ decays and this is not possible at these energies with the present detectors.

A.J.G. Hey: Could you comment on the status of the proposed $\rho'(1250)$?

J. Augustin: Although it is not killed yet, it might be there with a smaller partial width than the one expected from recurrence models.

G. Preparata: Are you then in disagreement with Baldini's conclusions in his talk of yesterday?

J. Augustin: No; if one thinks that it has, say, 3 to 4 keV partial width into e^+e^-, then it is not there. It might be there with a smaller partial width, as inferred from the DESY-Frascati experiment, for example, in the interference experiment.

RESULTS ON CHARMONIUM FROM THE CRYSTAL BALL*

Presented by C. M. Kiesling (Representing the Crystal Ball Collaboration†)

Stanford Linear Accelerator Center
Stanford University, Stanford, California 94305

† CalTech: R. Partridge, C. Peck, F. Porter.
Harvard University: W. Kollmann, M. Richardson, K. Strauch, K. Wacker.
Princeton University: D. Aschman, T. Burnett, M. Cavalli-Sforza, D. Coyne, H. Sadrozinski.
Stanford University (HEPL): R. Hofstadter, I. Kirkbride, H. Kolanoski, A. Liberman, J. O'Reilly, J. Tompkins.
SLAC: E. D. Bloom, F. Bulos, R. Chestnut, J. Gaiser, G. Godfrey, C. Kiesling, M. Oreglia.

ABSTRACT

Results from the Crystal Ball experiment at SPEAR are presented. A preliminary analysis of the 3 photon final state from the $J/\psi(3095)$ and of the cascade decays of the $\psi'(3684)$ yield new upper limits on the controversial states X(2820), $\chi(3455)$ and the even C-parity state at 3.59 GeV. From inclusive γ-ray spectra of the J/ψ and ψ' preliminary branching ratios for $\psi' \to \chi$ states and upper limits for $J/\psi, \psi' \to \eta_c, \eta_c'$ are given.

1. INTRODUCTION

In the past years it has become evident that certain crucial questions as to the validity of the charmonium interpretation of the narrow resonances J/ψ, ψ' and the states discovered subsequently in e^+e^- can only be answered with a good photon detector. The essential features of such a detector are full coverage of solid angle, high detection efficiency for photons at all energies, good energy resolution and good angular resolution. These features are well approximated by the Crystal Ball Detector System as shown schematically in Fig. 1. Its main components are: (i) a highly segmented shell of NaI(Tℓ) 16 rad. lengths thick covering 94% of 4π (referred to as "the Ball" proper); (ii) a set of cylindrical proportional and magnetostrictive wire chambers inside this shell. The solid angle is extended to 98% of 4π by endcaps of 20 r.l. NaI(Tℓ) behind magnetostrictive wire chambers. The photon detector is supplemented by two muon detectors at 90^o to the beam axis (not shown in Fig. 1).

This report presents new (and preliminary) results on exclusive and inclusive reactions and is structured as follows: In Section 2 the detector system is described in detail and its performance during the first half-year of running is reported. Section 3 contains the analysis and the results on the reaction $\psi' \to \gamma\gamma\, J/\psi$, $J/\psi \to \ell^+\ell^-$ and the reaction $J/\psi \to \gamma\gamma\gamma$. In Section 4 initial studies and preliminary results are reported on absolute branching ratios of $\psi' \to \chi\gamma$ and upper limits for the reactions $\psi' \to \gamma\eta_c'$, $\gamma\eta_c$ and $J/\psi \to \gamma\eta_c$ are obtained with $\sim$25% of our final statistics. Finally, some conclusions are drawn on the now changing picture of the existing charmonium states vis-à-vis the results reported.

* Work supported by the Department of Energy under contract number DE-AC03-76SF00515.

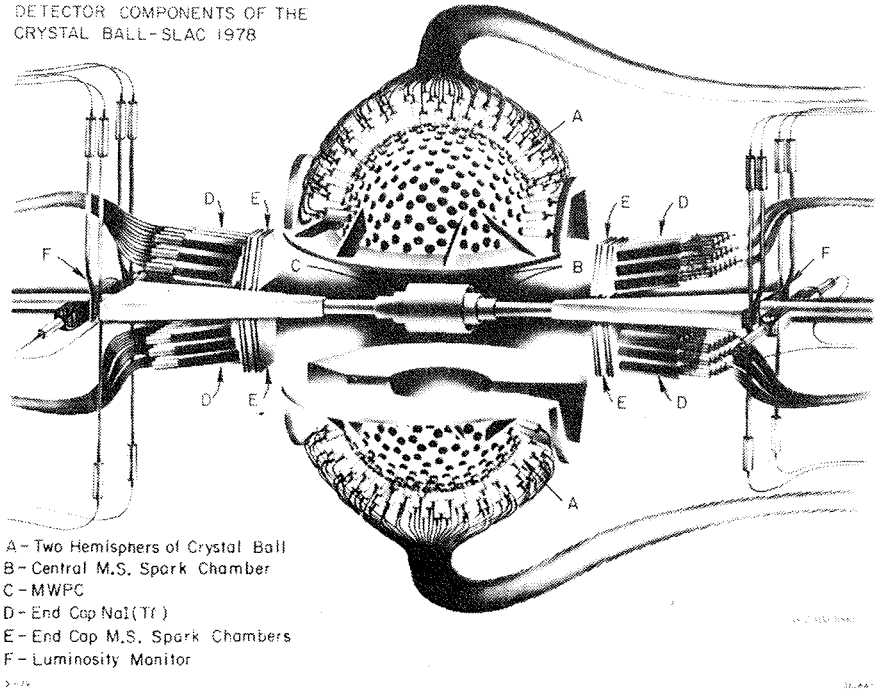

Fig. 1. Schematic representation of the components of the Crystal Ball Detector System.

2. THE CRYSTAL BALL DETECTOR SYSTEM

2.1. Components

The Ball has an outer radius of 66.0 cm and is divided into two hemispheres, each of which is segmented to contain 336 crystals; each crystal is a truncated triangular pyramid. The crystals are optically separated from each other and viewed by individual phototubes. The crystal surfaces are treated in order to give uniform light output (to within ±4%) for a given energy deposition at various points along the crystal.

The beampipe (1.5 mm of aluminum) is surrounded by a set of cylindrical proportional and magnetostrictive wire chambers: the proportional chamber has two gaps with both anode wire and cathode strip read-out and is sandwiched between two double gap magnetostrictive wire chambers. The solid angles subtended are 94% of 4π for the innermost spark chamber, 80% for the proportional chamber and 71% of 4π for the outer spark chamber. The endcaps consist of 4 units of 15 hexagonal crystals (20 rad. lengths of NaI(Tℓ)) each behind 4 gaps of magnetostrictive wire chambers. The solid angle thus covered by NaI and tracking chambers is 98% of 4π. The system is complemented by a luminosity monitor and two muon arms at 90^{o} with respect to the beam axis, each of which consists of 4 arrays of porportional tubes sandwiching iron slabs; the 2 arms subtend a total solid angle of 15% of 4π. These arms will be used for μ-identification and to check the π/e separation capabilities by the ball proper.

Each crystal of the Ball is viewed axially by an SRC L50B01 phototube. Signal readout in the CAMAC-standard electronics involves amplification, integration, holding and an analog multiplexer; all channels are read out sequentially by a fast ADC. The main com-

ponent of the detector trigger is the analog sum of the signals from the Ball, representing the energy deposited in NaI by each event. Energies from subsets of crystals and charged multiplicities (provided by the MWPC) are used in the OR of triggers. More details of the apparatus and triggers are contained in Refs. 1 and 2.

2.2. Performance

The outstanding feature of the Crystal Ball is its energy resolution due to the use of NaI(Tℓ). In a prototype experiment (assembly of 54 crystals) using electrons spanning 50 MeV to 4 GeV in energy, a resolution of

$$\frac{\Delta E}{E}\ (\mathrm{FWHM}) \;=\; \frac{2.8\%}{\sqrt[4]{E(\mathrm{GeV})}}$$

has been achieved[3]. In the actual experiment we presently obtain a resolution worse by roughly a factor of 2. We believe that this discrepancy is mainly caused by changes in time of the calibration between crystals, which we hope to reduce using a light pulser system which we recently developed. The presently used calibration procedure is described in Ref. 4. The angular resolution for photons is $\sim 1.5^{\circ}$.

In order to check the performance of the entire detector system various QED processes have been measured at different center-of-mass energies. As an example, the process

$$e^+e^- \rightarrow \gamma\gamma$$

is quoted at the J/ψ and the ψ''. At both energies the measured differential cross section (after radiative corrections) agrees with the expected values within the errors of ~5% in an angular acceptance interval of $|\cos\theta| < 0.8$.

3. EXCLUSIVE REACTIONS

A great wealth of results has been accumulated by several experiments on the decays of the J/ψ and ψ'. Nonetheless the candidates proposed for the pseudoscalar states of charmonium are difficult to explain within the framework of the charmonium model[5]. Since most charmonium transitions are accompanied by monochromatic photons, it is not surprising that the Crystal Ball may significantly contribute to the traits and understanding of the charmonium picture.

Results on exclusive decay channels from ψ' reported here are based on the analysis of cascade decays for ~1/4 of the presently available statistics. Results from the reaction J/ψ → 3γ are based on the full J/ψ statistics of 339 nb^{-1}.

3.1. $\psi' \rightarrow \gamma\gamma\ J/\psi,\ J/\psi \rightarrow \ell^+\ell^-$

For the analysis of the cascade decays the following event selection criteria have been applied: 4 tracks in the main ball were required with energy depositions per track greater than 20 MeV, 2 of them had to be neutral shower tracks as checked by the central wire chambers and a simple shower recognition algorithm. To ensure that no additional tracks were present in the events an energy deposition of less than 10 MeV in the endcaps was required. In order to minimize the problems arising from overlapping showers, a minimal opening angle between any two tracks of $\cos\theta < 0.9$ was required. The J/ψ in the final state is easily selected in the e^+e^- decay mode where an invariant mass of

3.1 ± .3 GeV was required for the lepton pair. The $\mu^+\mu^-$ decay channel for the J/ψ was selected by requiring an energy deposition pattern for the two charged tracks characteristic for minimum ionizing particles, i.e., ~200 MeV deposited in 1-3 adjacent crystals. Furthermore, since the μ's stem from the J/ψ, the angle between the minimum ionizing tracks had to be > 140°. Finally two cuts on the photon were applied: the energy sum of the two photons had to roughly match the ψ' - J/ψ mass difference ($E_1 + E_2$ > 480 MeV), and the invariant mass of the two photons should not lie in the η mass region defined by $M_{\gamma\gamma}$ = 549 ± 40 MeV. The overall acceptances for the various cascade processes have been determined by Monte Carlo calculations to range between ~34% and ~48%.

Customarily the cascade reactions are presented in a plot of higher vs. lower (γ - J/ψ) invariant mass, where each of the two γ's is combined with the J/ψ four vector. This two-dimensional plot including ~1/4 of the final statistics is shown in Fig. 2a. It should be noted that the events have not been subjected to kinematic fits. Clearly visible are 2 clusters corresponding to the χ-states of mass 3.55 GeV and 3.51 GeV. The clusters are elongated in the low mass variable indicating the effects of Doppler broadening and NaI(Tℓ) resolution. The high mass combination is observed with the resolution expected from NaI(Tℓ) alone. Thus the excellent energy resolution of the device enables us to easily determine the sequence of the γ-ray emission (i.e., low γ was emitted first). Note furthermore that no pronounced clustering is found in the region of 3.410, 3.455 and 3.6 GeV. The smallness of possible signals at these masses becomes even clearer looking at the high-mass projection in Fig. 2b. No accumulation of events besides the two dominant χ-states is observed. In Table 1 branching ratios for the states χ(3510) and χ(3550) through the cascade process are given and compared with other experiments. The branching ratios for the 3 other states listed in the table should be taken as conservative overestimates as no signal could be established. The well-established χ(3410) state thus seems to have a smaller cascade branching ratio that previously reported by some experiments[6]. Two possible candidates for the η_c' (both the χ(3455) and χ(3591) are only observed in the cascade decays) are not observed in our data. While we wish to refrain from giving upper limits at this stage, we notice that our "signals" at these two masses are significantly lower than the ones claimed by the original experiments[7,8]. New measurements by the Mark II collaboration reported at this conference[10] fail to reproduce the χ(3455) signal which is in agreement with the results presented in this report (see also Table 1). This leaves the χ(3591) for further discussion. We certainly need more statistics to decide about this state. The observed number of events in Fig. 2, however, is at least a factor of 3 below the claimed signal[7].

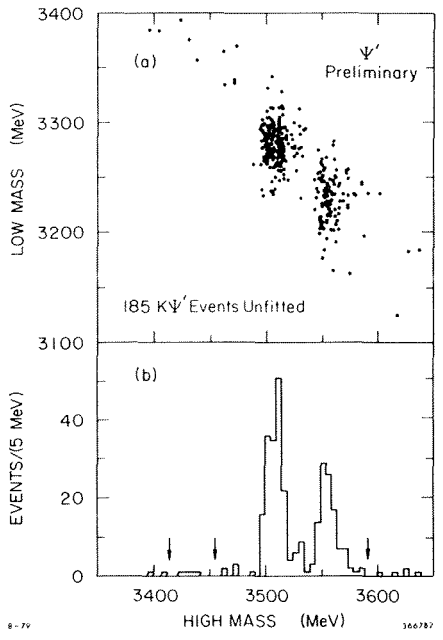

Fig. 2. (a) High mass vs. low mass for the γ - J/ψ mass combination in the ψ' → γγ J/ψ final state. (b) Projection onto the high mass solution.

Table 1

Preliminary Branching Ratios for $\psi \to \gamma\chi$, $\chi \to \gamma\, J/\psi$

χ mass [GeV]	Observed Events	Branching Ratio [%] Other Experiments	This experiment
3.553	104	$1.3 \pm .3$ [a]	$1.3 \pm .3$
3.507	180	$2.3 \pm .4$ [a]	$2.5 \pm .6$
3.409	6 ?	$.14 \pm .09$ [b]	$.1 \pm .06$ [d]
3.455	5 ?	$< .12$ [c]	$.07 \pm .06$ [d]
3.590	6 ?	$.18 \pm .06$ [b]	$.09 \pm .07$ [d]

a) Ref. 8; b) Ref. 7; c) Ref. 10.
d) Caution: no background has been subtracted; for more recent upper limits see Ref. 15.

3.2. $J/\psi \to \gamma\gamma\gamma$

Events of the type $J/\psi \to \gamma\gamma\gamma$ were selected according to the following criteria: Three neutral tracks were required in an angular interval with respect to the beam of $|\cos\theta| \leq 0.8$. The energy deposited for each track had to be ≥ 20 MeV and a minimum opening angle between any two tracks of $\cos\theta_{\gamma\gamma} < 0.9$ was required (as for the cascade events, see above). Since the final state considered consists of 3 showering particles depositing all their energy in the ball, a total energy cut of $2.7 \leq E_{TOT} \leq 3.4$ GeV and a momentum balance cut $\left|\sum_{i=1}^{3} \vec{P}_i\right| < 0.5$ GeV was imposed. A specific background related to the particular angular dimensions of the NaI crystals is due to the reaction $J/\psi \to \gamma\pi^o\pi^o$. This reaction which has similar strength as the 3γ final state may produce two high energetic π^o's $\left(|\vec{P}_{\pi^o}| \gtrsim 1.4 \text{ GeV/c}\right)$. These π^o's in turn decay into two photons with the most likely opening angle of $\sim 15^o$. In general the decay photons will hit two adjacent crystals and form two strongly overlapping showers which will be recognized by the initial event selection as one shower. A closer inspection of the shower patterns, i.e., the energy depositions in crystals close to the shower center, show a characteristic lateral broadening of the shower which in nearly all cases is correlated with another broad shower in the event thus corroborating the hypothesis of the reaction $J/\psi \to \gamma\pi^o\pi^o$ faking a 3γ event. All "broad shower" events were consequently removed from the 3γ sample. Finally, the events were subjected to a 4c kinematic fit with errors for the photon energies and angles as quoted above.

The resulting Dalitz plot for the 411 events satisfying the above selection criteria is shown in Fig. 3. The kinematical boundaries of the Dalitz plot as defined by the cuts as well as the positions of the η and η' bands corresponding to the 2-body reactions $J/\psi \to \gamma\eta,\eta'$ are indicated. Substantial clustering of events around the η and η' bands is observed. The projection of the Dalitz plot onto the low $\gamma\gamma$ mass axis (not the mass squared as in the Dalitz plot proper!) shows clear signals from the $J/\psi \to \gamma\eta,\gamma\eta'$ channels (see Fig. 4a). The high mass projection is shown in Fig. 4b. Most remarkable is the absence of a signal at 2.82 GeV which has been found by the DASP collaboration at DORIS[11]. Assuming our mass resolution of ~25 MeV at 2.8 GeV, one would have expected 53 events in 2

bins above background centered at 2.82 GeV, using the branching ratio quoted in Ref. 11 and taking into account the losses due to the acceptance cuts described above.

In order to determine upper limits for the branching ratio $J/\psi \to \gamma X(X \to \gamma\gamma)$ a likelihood fit to the two-dimensional Dalitz plot incorporating contributions from the reactions $J/\psi \to \gamma\eta$ ($\eta \to \gamma\gamma$), $J/\psi \to \gamma\eta'$ ($\eta' \to \gamma\gamma$), $J/\psi \to \gamma\gamma\gamma$ (direct decay), $e^+e^- \to \gamma\gamma\gamma$ (QED) was performed (the QED contribution has been calculated from first principles and is thus an absolute prediction). Furthermore, the reaction $J/\psi \to \gamma X(X \to \gamma\gamma)$ has been included in the fits assuming masses for the X between 2.7 GeV and 3.04 GeV. No signal could be established in the given mass range. Around 2.82 GeV one arrives at an upper limit for the branching ratio of the reaction $J/\psi \to \gamma X$, $X \to \gamma\gamma$ of $Br(J/\psi \to \gamma X(2820), X \to \gamma\gamma) < 3 \times 10^{-5}$ (90% C.L.) which corresponds to < 6 events above background. The upper limit for an X anywhere in the mass range of 2.7 - 3.04 GeV is $< 5 \times 10^{-5}$.

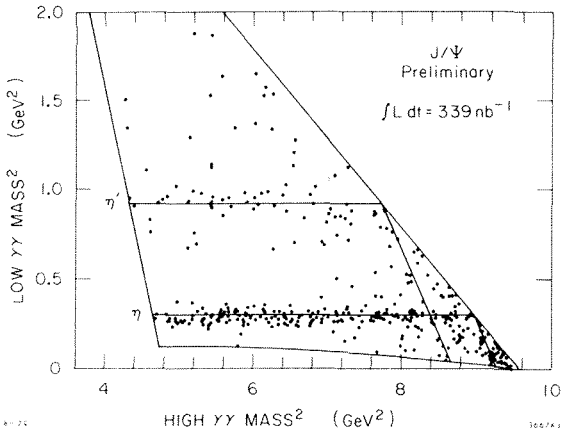

Fig. 3. Dalitz plot for the reaction $J/\psi \to \gamma\gamma\gamma$.

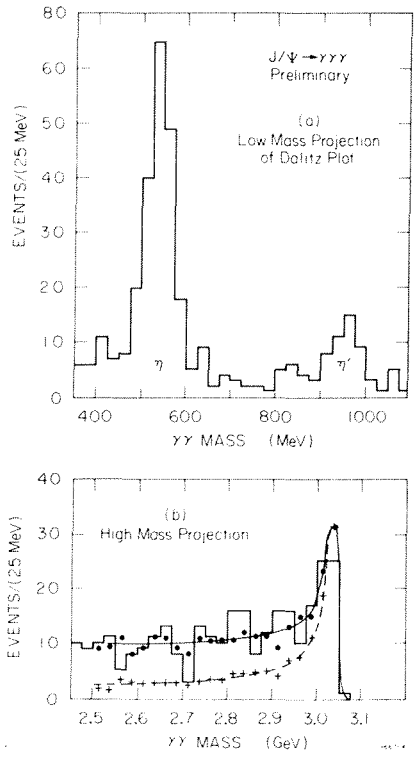

Fig. 4. (a) Projection of the Dalitz plot onto the low mass variable. (b) Projection of the Dalitz plot onto the high mass variable. The solid curve is the result of the likelihood fit to the two-dimensional Dalitz plot as described in the text. The broken line is the predicted contribution from $e^+e^- \to \gamma\gamma\gamma$ (QED).

The curves shown in Fig. 4 are taken from the fit which did not include an X contribution. As a byproduct one obtains the branching ratios for $J/\psi \to \gamma\eta, \gamma\eta'$ which are summarized in Table 2. In contrast to Refs. 11 and 12 on observes a higher yield of η' and a consequently increased ratio of η'/η.

Our experimental upper limits on $\psi \to \gamma\eta_c \to \gamma\gamma\gamma$ can be compared with theoretical predictions: Using the standard result[5] on the η_c branching ratios, the theoretical curve for the overall branching fraction $\psi \to \gamma\eta_c \to \gamma\gamma\gamma$ intersects the experimental upper limit at an η_c mass of 2.975 GeV corresponding to a monochromatic γ-ray of 120 MeV. In other words we can exclude η_c production consistent with the standard assumptions for the charmonium model for η_c masses lower than 2.975 GeV but cease to test them for higher masses (corresponding to lower monochromatic γ-rays).

Table 2

Preliminary Results for the Branching Ratios for $J/\psi \to \gamma\gamma\gamma$ Final States

Decay	Ref. 11	Ref. 12	This Experiment
$J/\psi \to \gamma\eta$	(.82 ± .2)	(1.3 ± 4)	$(1.15 \pm .17) \times 10^{-3}$
$\to \gamma\eta'$	(2.2 ± 1.7)	(2.3 ± .7)	$(6.3 \pm 1.6) \times 10^{-3}$
$\frac{Br(\eta')}{Br(\eta)}$	2.7 ± 2.2	1.8 ± .8	5.5 ± 1.3
$J/\psi \to \gamma X(7820)$	(1.4 ± .4)	< 3.2	$< .3 \times 10^{-4}$
$J/\psi \to \gamma\eta_c$			$< .5 \times 10^{-4}$
$m(\eta_c) \varepsilon [2.7, 3.04$ GeV]			

4. INCLUSIVE REACTIONS

Probably the most sensitive tool in the search for the charmonium pseudo-scalars consists in the inclusive γ spectra to which each radiative decay of the J/ψ or ψ' would contribute a monochromatic γ-ray irrespective of the decay channel of the coupled system. The disadvantage, however, of the inclusive spectra arises from the expected background under these potential lines since most of the detected photons originate from π^o and η decays. The understanding of this background is crucial in an attempt to maximize the signal/noise ratio, e.g., by means of π^o/η reconstruction and removal of the paired photons.

The preliminary analysis presented here is not yet sophisticated enough to exploit the full power of the Crystal Ball, i.e., to identify those γ's in a general n photon final state originating from π^o/η and derive an energy dependent correction function to account for the subtraction efficiency. Therefore all results quoted subsequently will be derived from the totally inclusive, i.e., unsubtracted photon spectrum. Only angular acceptance cuts for the photons have been imposed ($\cos\theta_\gamma < .71$) in order to make sure that the photon direction was covered by all three central wire chambers.

4.1. Determination of branching ratios for the χ-states

First branching ratios for the three established χ-states and their cascades from the ψ' are determined in order to show the capability of the experiment to measure monochromatic lines using inclusive spectra. A qualitative inclusive spectrum at the ψ' with π^o's removed is shown in Fig. 5. Clearly visible are the three monochromatic lines from ψ' to the χ-states and the Doppler broadened lines from at least 2 χ-states to the J/ψ (see labelling in Fig. 5). The statistics correspond to ~200K ψ' or 1/4 of the full data sample. The line strengths have been obtained by fitting Gaussians to the various peaks superposed on a general polynomial background to the unsubtracted spectrum (not shown).

The results of these fits, corrected for angular acceptance, photon conversion in the beampipe and various other losses are summarized in Table 3. It should be pointed out that the errors are entirely dominated by systematics and therefore have a chance to decrease as the understanding of the apparatus proceeds.

Table 3 displays overall consistency between Ref. 9 (radiative ψ' decays to χ-states), Ref. 8 (cascade decays of the ψ') and this experiment. Note in particular the internal consistency of the cascade branching ratios determined within this experiment from the inclusive spectrum and the cascade process (Section 3.1) itself.

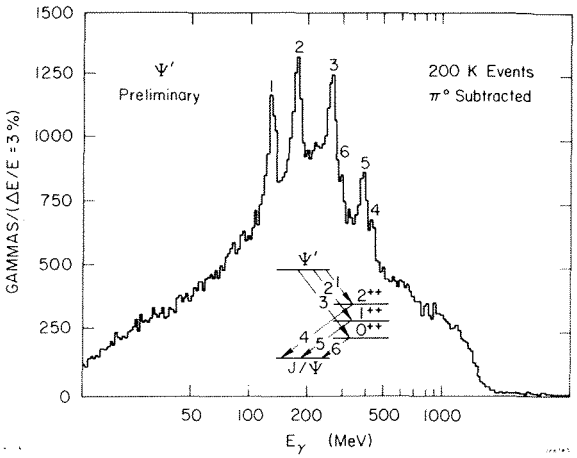

Fig. 5. Inclusive γ spectrum at the ψ'; γ's originating from π^0's have been removed.

Table 3

Preliminary Results on χ Branching Ratios from Inclusive Spectra at the ψ'

Reaction	Branching Ratio [%]	
	Other Experiments	This Experiment
$\psi' \to \gamma\chi(3553)$	7.0 ± 2.0 [a]	7.5 ± 1.7
$\to \gamma\chi(3507)$	7.1 ± 1.9 [a]	7.5 ± 1.7
$\to \gamma\chi(3409)$	7.2 ± 2.3 [a]	7.6 ± 1.7
$\psi' \to \gamma\chi(3507) \to \gamma J/\psi$	$2.3 \pm .4$ [b]	$2.3 \pm .5$
$\psi' \to \gamma\chi(3507) \to \gamma J/\psi$	$1.3 \pm .3$ [b]	$1.5 \pm .4$

a) Ref. 9; b) Ref. 8.

4.2. Search for additional structure

4.2.1. $\psi' \to \gamma\chi$

Besides the prominent lines (with results given in Table 3) no obvious additional structure within our resolution is visible in the ψ' spectrum. A systematic analysis of the γ spectrum has been carried out on the same ψ' data sample as above to determine upper limits for the branching ratios of $\psi' \to \gamma\eta_c'$, $\gamma\eta_c$ for photon energies of $\gtrsim$ 70 MeV* corresponding to η_c' masses of $\lesssim$ 3615 MeV. The procedure to find the upper limits on monochromatic photons as a function of photon energy (using 5 MeV energy steps) follows closely

* We have not yet verified our photon resolution below 70 MeV and thus limit ourselves to higher energies for the time being.

the one outlined above for χ-states. The upper limits for a monochromatic photon at the ψ' fall from ~1.5% at E_γ = 70 MeV to ~0.5% at E_γ = 640 MeV* (excluding, of course, the regions around the χ-states where the 90% C.L. upper limits jump to values around 10%). In particular, at an η_c' mass of 3.59 GeV (see Ref. 7) an upper limit for the branching ratio $\psi' \to \gamma\chi(3.59)$ of 1.4% is measured. The standard prediction[5] of the branching ratio for magnetic dipole transitions at the ψ' intersects the data at an energy for the monochromatic γ-ray of ~120 MeV, i.e., the sensitivity of the presented data is not yet good enough to test the model for level splittings ($\psi' - \eta_c'$) below 120 MeV. The hindered M1 transition $\psi' \to \gamma\eta_c$ with a γ-ray of ~640 MeV predicts a branching ratio of ~0.3% (see Ref. 14), to be compared with the measured upper limit of 0.5%.

4.2.2. $J/\psi \to \gamma\chi$

The unsubtracted J/ψ inclusive spectrum as of now shows no structure which could be associated with a monochromatic γ-ray of measurable size.

Thus upper limits have been determined at the J/ψ in the analogous way as described for the ψ'.

The results are shown in Fig. 6 which displays the upper limit (90% C.L.) for the branching ratio $J/\psi \to \gamma\chi$ based on ~300K J/ψ reactions (~30% of the final statistics) as a function of the photon energy. Also depicted is the prediction using the standard charmonium dipole transitions[5]. Here the crossover point is at ~75 MeV. It is interesting to note that recent calculations incorporating spin-dependent quark forces (Ref. 14) prefer a $J/\psi - \eta_c$ level split around 75 MeV. At the X(2820) the upper limit is down to .4%, a factor of 4 better than a previous determination[9].

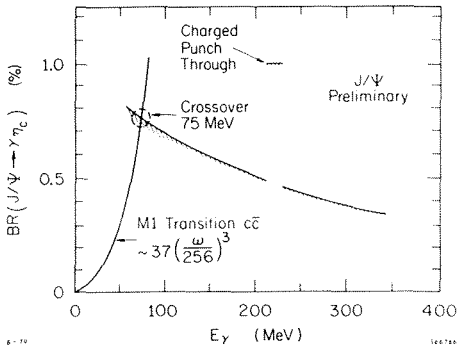

Fig. 6. Upper limit for the branching ratio $J/\psi \to \gamma\eta_c$ as a function of the γ-ray energy. Also shown is the expected yield using the standard model[5].

5. CONCLUSION

The results presented here, although preliminary, strongly suggest a revision of the assignment of charmonium states. While the three χ-states remain established beyond doubt, serious problems seem to arise for the η_c candidate X(2820) and two (alternative!) η_c' candidates at 3.455 GeV and 3.591 GeV. Given the almost optimal capabilities of the Crystal Ball to detect the $J/\psi \to \gamma\eta_c \to \gamma\gamma\gamma$ final state, we consider our upper limits as the death sentence for the X(2820) state. The non-observation of the χ(3455) by both our experiment and the SLAC-LBL collaboration[10] in the cascade mode makes its existence very unlikely. The same can be said for the state observed[7] in the cascade mode at 3591 MeV; due to the low (~90 MeV) energy of the primary photon, the Crystal Ball is the only experiment that can confirm or deny this result. Lack of observation of a 3591 MeV state in both inclusive spectra and cascade decays makes its existence at the level previously published[7] unlikely.

* Due to some low level contamination of the γ spectrum from minimum ionizing particles, the upper limit around 210 ± 20 MeV is ~2%.

The disappearance of the X(2820) and the $\chi(3455)$ is certainly welcome by the proponents of the simpler charmonium model, given the well-known difficulties of the model to fit the large splittings and the transition rates required by the above assignments. The burden of finding the theoretically necessary pseudoscalar partners of the J/ψ and ψ' is still on the experimenters. If the model predictions of the radiative decays of J/ψ and ψ' into η_c and η_c' are roughly correct and the level splittings between $J/\psi - \eta_c$ and $\psi' - \eta_c'$ are no smaller than ~30 MeV (the branching ratios being proportional to E_γ^3), there is a fair chance that these states will be found in the Crystal Ball experiment.[+]

[+] Note added in proof:

A preliminary analysis performed after this conference on the π^o subtracted inclusive spectra of the J/ψ and ψ' suggests monochromatic γ-rays from both resonances to a state with a mass around 2977 MeV at a level compatible with the upper limits presented at this conference (see also Ref. 15). This state could be a possible candidate for the η_c.

* * *

REFERENCES

1) E. D. Bloom for the Crystal Ball Collaboration. Invited talk at the XIVth Rencontre de Moriond, 1979. To be published in the Proceedings of the Moriond Conference.

2) J. E. Gaiser et al., Compact Multiwire Proportional Chambers and Electronics for the Crystal Ball Detector. IEEE Trans. on Nucl. Sci., Vol. NS-26, No. 1, 173 (1979).

3) Y. Chan et al., Design and Performance of a Modularized Na(Tℓ) Detector. IEEE Trans. on Nucl. Sci., Vol. NS-25, No. 1, 333 (1978).

4) I. Kirkbride et al., Use of a Low Energy Photon Accelerator for Calibrating a Large Na(Tℓ) Array in a High Energy Physics Experiment. IEEE Trans. on Nucl. Sci., Vol. NS-26, No. 1, 1535 (1979).

5) T. Appelquist, R. M. Barnett and K. Lane, Annu. Rev. Nucl. Part. Sci., Vol. 28, 387 (1978).

6) B. H. Wiik and G. Wolf, DESY Report 23 (1978).

7) W. Bartel et al., Phys. Lett. 79B, 492 (1978).

8) W. M. Tanenbaum et al., Phys. Rev. D17, 1731 (1978).

9) C. J. Biddick et al., Phys. Rev. Lett. 3B, 1324 (1977).

10) J. Weiss, These Proceedings.

11) W. Braunschweig et al., Phys. Lett. 67B, 243,249 (1977).

12) DESY-Heidelberg Collaboration, Proceedings of the 1977 Hamburg Conference, p. 117.

13) W. D. Apel et al., Phys. Lett. 72B, 500 (1978).

14) E. Eichten, F. Feinberg, Preprint HUTP-79/A022 (1979).

15) E. D. Bloom, Report presented at the 1979 International Symposium on Lepton and Photon Interactions at High Energies, Fermi Lab (1979).

DISCUSSION

Chairman: S.C.C. Ting

Sci. Secretaries: C. Best and H. Gennow

J. Rosner: Can you state in a little more detail the basis for your belief that one can place a useful limit on the branching ratio $J/\psi \to \gamma\eta_c$ for $E_\gamma > 35$ MeV?

C.M. Kiesling: Yes, if you remember the two plots which I gave you for the ψ'. We have a reduction of the photon background of a factor of ten if you subtract π^0's, and this gives you immediately the required sensitivity. So if we understand the correction then we are right there, that is the main problem.

G. Barbiellini: Do you have any evidence for direct photon emission in the J/ψ decay?

C.M. Kiesling: This question bears essentially on our ability to subtract the π^0's; this is the essential problem in this game. We have not been able to yet, and this is the reason why I did not give you any numbers to faithfully subtract π^0's; and it is only after you have subtracted the π^0's that you can really say what remains -- I mean something like di-photons. In addition, we have the particular problem with the overlapping showers, where suddenly one photon comes to two photons. So we really have to study what our actual spectrum from the π^0's in our detector looks like in order to make any statement like that.

RESULTS FROM THE MARK II DETECTOR AT SPEAR

G. S. Abrams, M. S. Alam, C. A. Blocker, A. M. Boyarski, M. Breidenbach, C. H. Broll, D. L. Burke, W. C. Carithers, W. Chinowsky, M. W. Coles, S. C. Cooper, W. E. Dieterle, J. W. Dillon, J. Dorenbosch, J. M. Dorfan, M. W. Eaton, G. J. Feldman, H. G. Fischer, M. E. B. Franklin, G. Gidal, G. Goldhaber, G. Hanson, K. G. Hayes, T. Himel, D. G. Hitlin, R. J. Hollebeek, W. R. Innes, J. A. Jaros, P. Jenni, A. D. Johnson, J. A. Kadyk, A. J. Lankford, R. R. Larsen, D. Lüke, V. Lüth, J. F. Martin, R. E. Millikan, M. Nelson, C. Y. Pang, J. F. Patrick, M. L. Perl, B. Richter, J. J. Russell, D. L. Scharre, R. H. Schindler, R. F. Schwitters, S. R. Shannon, J. L. Siegrist, J. Strait, H. Taureg, M. Tonutti, G. H. Trilling, E. N. Vella, R. A. Vidal, M. I. Videau, J. M. Weiss, and H. Zaccone

(presented by G. Gidal[†])

Stanford Linear Accelerator Center, Stanford, CA 94305
and
[†]Lawrence Berkeley Laboratory, Berkeley, CA 94720

ABSTRACT

We present some recent results from the Mark II detector at SPEAR*: (1) observation of some new D meson decay modes, including the Cabibbo suppressed K^-K^+ and $\pi^-\pi^+$ modes, (2) measurements of the $\rho\nu$ and $\pi\nu$ decays of the τ, and (3) some new data on ψ decays.

The Mark II detector has been in operation at SPEAR since the end of 1977 and has accumulated data over a wide range of energies between the $\psi(3100)$ and 7.4 GeV. Figure 1 shows the integrated luminosity as a function of E_{cm}. The logarithmic scale is used to indicate large runs at several energies in addition to systematic scans.

A schematic drawing of the detector is shown in Figure 2. Moving outward from the interaction region, the detector consists of two layers of cylindrical scintillation counters, 16 layers of cylindrical drift chambers,[1] 48 scintillation counters for time of flight (TOF), an aluminum solenoidal coil which produces a 4.1 kg axial magnetic field, 8 lead-liquid argon barrel shower counters,[2] iron hadron absorbers and two planes of proportional tubes, covering 55% of the solid angle, for muon detection. There are also shower detectors in the endcap regions: one of lead and liquid argon, and the other of two layers of lead and proportional chambers. The most common trigger[3] requires at least one charged track to be within the central 75% of the solid angle and a second charged track within approximately 85% of the solid angle.

The performance of the major components of the detector can be summarized as follows. The drift chambers measure the azimuthal coordinates of charged tracks to a rms accuracy of 200 μ at each layer. When tracks are constrained to pass through the known beam position, the rms momentum resolution can be parametrized as $\delta p/p = [(0.005\,p)^2 + (0.0145)^2]^{\frac{1}{2}}$, where p is measured in GeV/c. The tracking efficiency is greater than 95% for tracks with

* Mark II measurements of the radiative decays of the $\psi'(3684)$ and of inclusive baryon production are discussed by J. Weiss elsewhere in these proceedings.

$p > 100$ MeV/c over 75% of 4π sr. Figure 3 shows the difference between the expected time and the measured time for 2.08 GeV Bhabhas and is fit by a Gaussian with $\sigma = .270$ ns. For hadrons, the rms resolution is closer to .300 ns and leads to a 1σ separation between π's and K's at 1.35 GeV/c and between K's and p's at 2.0 GeV/c. Figure 4a shows the energy dependence of the γ detection efficiency of the Liquid Argon barrel shower counters. This is measured with the reactions $\psi \to \pi^+\pi^-\pi^o$ and $\psi \to 2\pi^+2\pi^-\pi^o$ in which one observed γ is used to predict the position of the other γ. This γ efficiency, together with the geometric acceptance, then translates into the π^o and η^o detection efficiencies shown in Figure 4b. The energy resolution of the Liquid Argon barrel modules is given by $\delta E/E = \frac{0.115}{\sqrt{E}}$ as measured by Bhabhas. Electron identification efficiencies vary between 0.64 below 5 GeV/c, for 0.85 and 1.0 GeV/c, up to 0.97 at higher momenta.

I. New D meson decay modes

We report the first observation of Cabibbo suppressed decays of charmed particles. In the standard model, with SU(3) in variance, one predicts

$$\frac{\Gamma(D^o \to K^-K^+)}{\Gamma(D^o \to K^-\pi^+)} = \frac{\Gamma(D^o \to \pi^-\pi^+)}{\Gamma(D^o \to K^-\pi^+)} = \tan^2\theta_c \approx .05 \quad .$$

To study the D decays we primarily depend on the 2840 nb^{-1} accumulated at 3.771 GeV (ψ''). Since D's are produced in pairs at this energy, oppositely charged track pairs with net momentum in the range 288 ± 30 MeV/c were selected as candidates for two body decays.

The TOF system provides about a 2.5 σ separation between π's and K's at the 850 MeV/c particle momentum typical of such decays. The probability that each track is a π or a K is assigned from the TOF,and, the product of the individual probabilities for a given final state hypothesis was required to be greater than 0.3. The corresponding two body invariant mass spectra are shown in Figure 5. Correctly identified D^o's appear near 1863 MeV/c^2, while D^o's in which one particle has been misidentified will appear shifted by ~120 MeV/c^2. In addition to the dominant $K^{\pm}\pi^{\mp}$ decay mode, a clear K^-K^+ signal is seen and there is an excess of $\pi^-\pi^+$ events in the D^o region. Figure 6 shows the same events as a scatter plot of the measured invariant mass against the beam constrained mass[4]. A likelihood fit to the signals and estimated backgrounds give 234.5 ± 15.8 $K^{\pm}\pi^{\mp}$ decays, 22.1 ± 5.2 K^+K^- decays, and 9.3 ± 3.9 $\pi^+\pi^-$ decays. Introducing the relative efficiencies gives

$$\frac{\Gamma(D^o \to K^-K^+)}{\Gamma(D^o \to K^-\pi^+)} = .113 \pm .030 \quad \text{and} \quad \frac{\Gamma(D^o \to \pi^-\pi^+)}{\Gamma(D^o \to K^-\pi^+)} = .033 \pm .015$$

We have also looked at the two body decays from the data taken in the region of $\sqrt{s}$ between 3.8 and 4.5 GeV. Here we also required a recoil mass > 1.8 GeV and p_K < 1.3 GeV/c. For events satisfying each mass hypothesis, the two body invariant mass and the recoil mass spectrum for events lying in the three central D^o mass bins are shown in Figure 7. In the $K^{\pm}\pi^{\mp}$ channel, the familiar DD, DD^*, and D^*D^* peaks are evident in the recoil spectrum. The K^+K^- channel recoil spectrum shows the same structure. The shaded regions correspond to the 45 K^+K^- events above background predicted from our measurement of $\Gamma(D^o \to K^+K^-)$ above. This higher energy data thus qualitatively confirms the observation of the K^+K^- Cabbibo suppressed decay. The $\pi^+\pi^-$ recoil distribution does not obviously show the characteristic structure and so it would be difficult to attribute all 39 shaded $\pi^+\pi^-$ events above the estimated background to $D^o \to \pi^+\pi^-$. The background uncertainties prohibit the use of this data to obtain precise branching fractions.

To study other decay modes of the D meson we again rely on the relatively background-free invariant mass spectra obtained with the ψ'' data. Figure 8 shows the beam constrained mass plots for the D decay channels $K^{\pm}\pi^{\mp}\pi^o$, $K^o\pi^-\pi^+$, $K^o\pi^o$, $K^o\pi^{\pm}$, and $K^o\pi^{\pm}\pi^{\pm}\pi^{\mp}$. The K^o's are detected from their $\pi^+\pi^-$ decay with an efficiency of $\approx$ 35% and are constrained to the K^o mass. The π^o's are reconstructed from 2 observed γ's whose energies are adjusted to give the π^o mass.An additional cut on the difference between the observed mass and the recoil mass is made before beam constraint. All these modes are seen, with resolutions well described by the Monte Carlo program.

The sensitivity of this experiment to the decay mode $D^o \to \bar{K}^o\pi^o$ is ~1/25 that for $D^o \to K^-\pi^+$, giving a (preliminary) value for the ratio

$$\frac{\Gamma(D^o \to K^-\pi^+)}{\Gamma(D^o \to \bar{K}^o\pi^o)} = 1.6 \pm 0.9 \ .$$

Most theoretical estimates[5] of charmed meson hadronic decay rates include the assumption of color selection, highly suppressing D^o decays into $\bar{K}^o$ or $\bar{K}^{*o}$ with respect to D^o decays into K^- or K^{*-}. On the other hand, Fritzsch[15] has recently argued that such color selection rules can easily be invalidated by the emission or absorption of soft gluons , predicting ~2 for the above ratio.

II. The $\rho\nu$ and $\pi\nu$ decays of the τ

Oppositely charged two prongs with coplanarity angle >20° were selected from the data in the $\sqrt{s}$ region between 4.5 and 6.0 GeV. For the $\rho\nu$ decay we also require two photons detected in the barrel modules. Figure 9 shows the $\gamma\gamma$ invariant mass for accepted photons and indicates a large π^o signal. We require $M(\gamma\gamma) < 200$ MeV/c^2 and adjust the γ energies to the π^o mass constraint ($\chi^2 < 6.0/1df$). The TOF, Liquid Argon, and muon systems were used when possible to identify the charged particles as kaon, proton, muon, or electron. All other tracks were called $\pi^{\pm}$. Figure 10a then shows the $\pi^{\pm}\pi^o$ invariant mass. Figure 10b shows the same distribution for events in which one of the charged tracks is a lepton. A clear ρ signal is observed. Because the lepton requirement insures only one entry per event and adds credence to the supposition that the ρ's come from τ decays, we concentrate on the ρ-lepton events to obtain a branching fraction. Events are normalized to $e\mu$ events in the same data sample. The solid curve in Figure 10b is the result of a fit to the data in the flat background + a Breit Wigner. The Monte Carlo used to obtain the efficiency assumes that the ρ's have two origins: $\tau \to \rho\nu$ and $\tau \to (A_1\nu + 4\pi$ continuum). The efficiency for detecting ρe events is 6.4%, for detecting $\rho\mu$ events is 2.7%, and for detecting $e\mu$ events is 12.9%. Taking all events in Figure 10b as ρ-lepton, there are 64 ρe events and 21 $\rho\mu$ events. After background subtraction (~10%) this gives

$$BR_{\tau\to\rho\nu} \cdot BR_{\tau\to e\bar{\nu}\nu} = .0435 \pm .0085$$

$$BR_{\tau\to\rho\nu} \cdot BR_{\tau\to\mu\bar{\nu}\nu} = .0329 \pm .0100$$

$$\sqrt{BR_{\tau\to e\bar{\nu}\nu} \cdot BR_{\tau\to\mu\bar{\nu}\nu}} = 18.5 \pm 1.2\% \quad ;$$

with μ-e universality this gives

$$BR_{\tau\to\rho\nu} = (21.1 \pm 3.7)\%$$

and

$$\frac{BR_{\tau\to\rho\nu}}{BR_{\tau\to e\bar{\nu}\nu}} = 1.14 \pm 0.22$$

in excellent agreement with the theoretical prediction of Gilman and Miller[16] of 1.20, providing a check of the vector part of the weak coupling. The momentum spectrum of the 85 ρ lepton events is compared with the Monte Carlo prediction in Figure 11 and shows excellent agreement.

To study the $\pi\nu$ decay we also require the "pion" track to be positively identified by the muon system, and that there be no detected γ's with E > 100 MeV. This leaves 443 such πx events. The principal source of background is feed-down from the reactions $\tau^{\pm} \to \rho^{\pm}\nu$, $A_1^{\pm}\nu$, continuum. The Monte Carlo program is used to subtract this ~40% background in each pion momentum bin. The pion energy spectrum for the remaining events is shown in Figure 12. A Monte Carlo simulation of $\tau \to \pi\nu$ gives the distribution shown as the solid line, and a branching ratio

$$BR_{\tau\to\pi\nu} = (10.6 \pm 1.9)\% \quad ,$$

The comparison with previously reported results is shown in Table I.

III. Some decays of the ψ

We have accumulated ~430 nb^{-1} at the ψ -- half with the LA shower counters, half without. For the data with shower counter information, events with two charged prongs and at least 2 observed γ's were fit with SQUAW to the hypothesis $\psi \to \pi^+\pi^-\gamma\gamma$. TOF information was used to eliminate tracks other than pions. The $\gamma\gamma$ invariant mass is shown in Figure 13a and exhibits a clean π^o peak with a σ of 10 MeV. The $\pi^+\pi^-$ invariant mass distribution is shown in Figure 13b. The recoiling γ's are required to form a π^o ($.12 < M_{\gamma\gamma} < .15$ GeV), and events with charged ρ's ($0.60 < M_{\pi^+\pi^o} < 0.90$ GeV) are eliminated. A ρ^o peak is clearly seen. In Figure 13c we show the $\pi^+\pi^-\gamma$ invariant mass with π^o's eliminated. A clean η' signal is observed. The resulting branching ratios are given in Table II and compared to other measurements.

This work is supported by the U.S. Department of Energy under contract number W-7405-ENG-48 .

Table I

Summary of τ Decay Measurements

	This Experiment	Previous Measurements	
$BR_{\tau\to\rho\nu}$	(21.1 ± 3.7)%	(24 ± 9)%	(ref. 9)
$BR_{\tau\to\pi\nu}$	(10.6 ± 1.9)%	(9 ± 3.8)%	(ref. 6)
		(8 ± 3.5)%	(ref. 7)
		(9.3 ± 3.9)%	(ref. 8)

Table II

Measured Branching Fractions for $\psi \to \rho\pi$ and $\psi \to \eta'\gamma$

Decay Mode	This Measurement	Previous Measurements	
$BR(\psi \to \eta'\gamma)$	$3.4 \pm 0.7 \times 10^{-3}$	$3.8 \pm 1.3 \times 10^{-3}$	(ref. 10)
		$2.2 \pm 1.7 \times 10^{-3}$	(ref. 11)
		$2.4 \pm 0.7 \times 10^{-3}$	(ref. 12)
$BR(\psi \to \rho\pi)$	0.0132 ± 0.0021	0.010 ± 0.002	(ref. 12)
		0.012 ± 0.003	(ref. 13)
		0.013 ± 0.003	(ref. 14)
$\Gamma(\rho^o\pi^o)/\Gamma(\rho^\pm\pi^\mp)$	0.56 ± 0.06	0.63 ± 0.22	(ref. 12)
		0.59 ± 0.17	(ref. 14)

References

1. W. Davies-White et al., Nucl. Instrum. and Methods 160, 227 (1979).

2. G. S. Abrams et al., IEEE Trans. on Nucl. Sci. NS-25, 309 (1978).

3. M. Breidenbach, et al., IEEE Trans. NS-25, 706 (1978).

   H. Brafman, et al., IEEE Trans. NS-25, 692 (1978).

4. By "beam constrained mass" we mean $(E_B^2 - p^2)^{\frac{1}{2}}$, where p is the measured total momentum of the decay particles and E_B is the known beam energy.

5. N. Cabibbo and L. Maiani, Phys. Lett. 73B, 418 (1978).

   D. Fakirov and B. Stech, Nucl. Phys. B133, 315 (1978).

6. G. Alexander et al., Phys. Lett. 78B, 162 (1978).

7. W. Bacino et al., Phys. Rev. Lett. 42, 6 (1979).

8. G. Feldman et al., Int. Conf. on Neutrino Physics -- Neutrinos 78, p. 647, E. C. Fowler, ed. (Purdue University).

9. S. Yamada, Proc. of 1977 Int. Symp. on Lepton and Photon Interactions, Hamburg, 1977, p. 69.

10. D. L. Scharre, SLAC preprint SLAC-PUB-2321 (1979).

11. W. Braunschweig et al., Phys. Lett. 67B, 243 (1977).

12. W. Bartel et al., Phys. Lett. 64B, 483 (1976).

13. W. Braunschweig et al., Phys. Lett. 63B, 487 (1976).

14. B. Jean-Marie et al., Phys. Rev. Lett. 36, 291 (1976).

15. H. Fritzsh, CERN Ref. Th. 2648, 28 March 1979 (unpublished)

16. F.J.Gilman and D.H.Miller, Phys.Rev. D17, 1846(1978) and private communication.

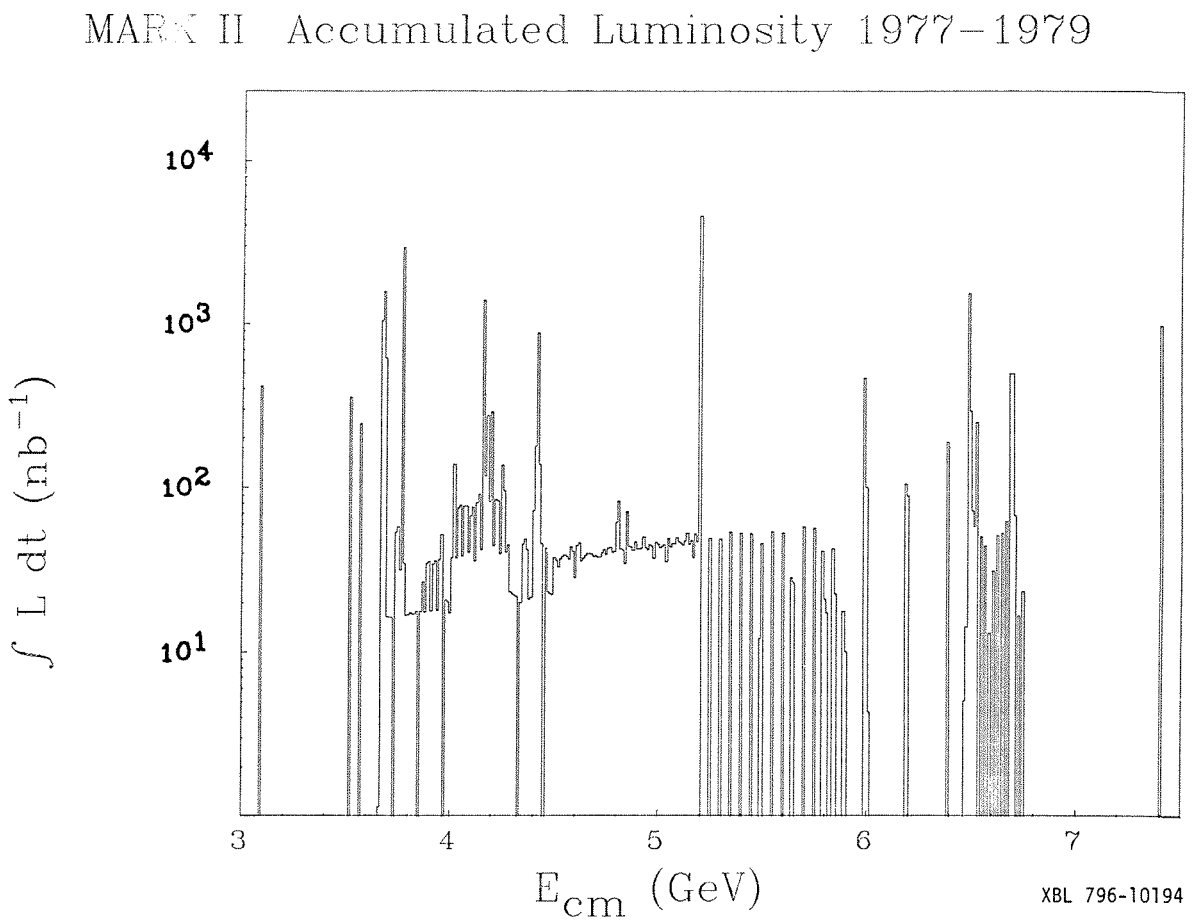

Fig. 1 Integrated luminosity for Mark II detector at SPEAR, 1977-1979

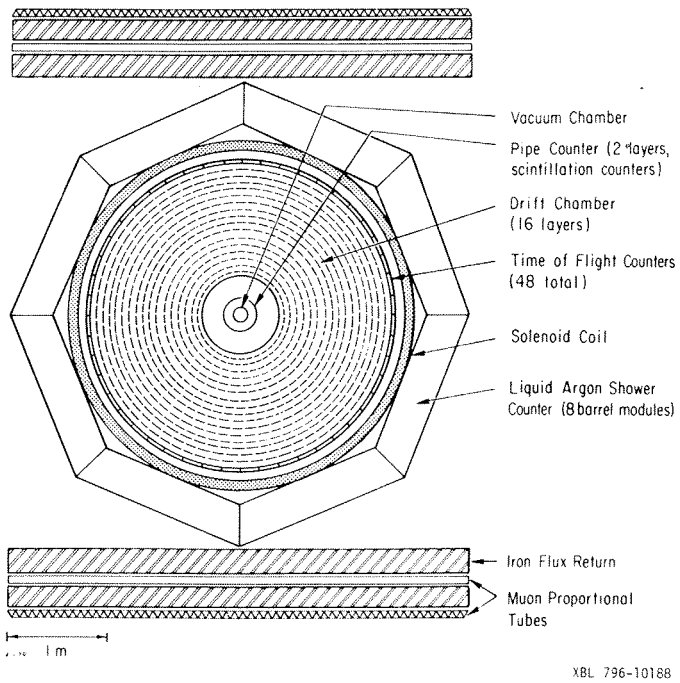

Fig. 2 Schematic drawing of the Mark II detector looking along the incident beams. The side muon detectors and the endcap shower counters are not shown.

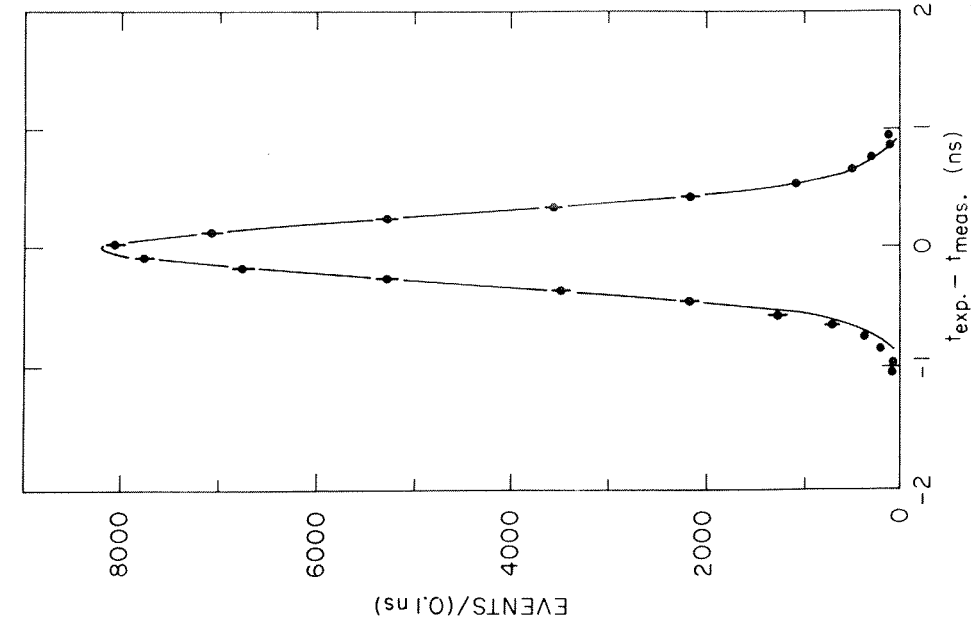

Fig. 3 Difference between expected and measured time at TOF system for Bhabha events at E_{cm} = 4.16 GeV. The curve represents the expected distribution for 0.270 ns resolution.

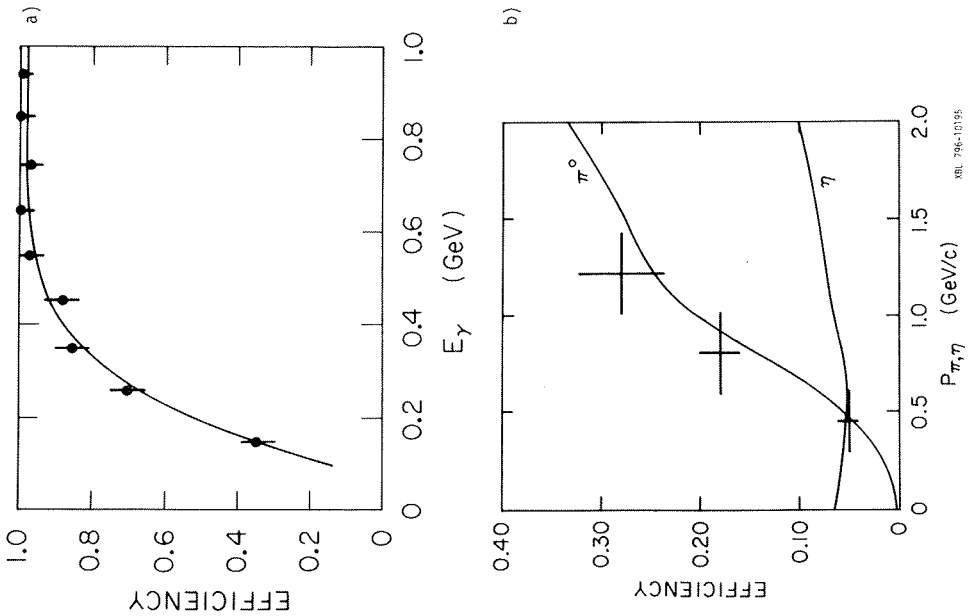

Fig. 4 a) Measured energy dependence of γ detection efficiency. Curve is a Monte Carlo calculation.
b) The π^0 and η^0 detection efficiencies. Geometry (seven LA barrel modules in this case) and branching fractions are included. Data points are measured π^0 values; curves are Monte Carlo calculations.

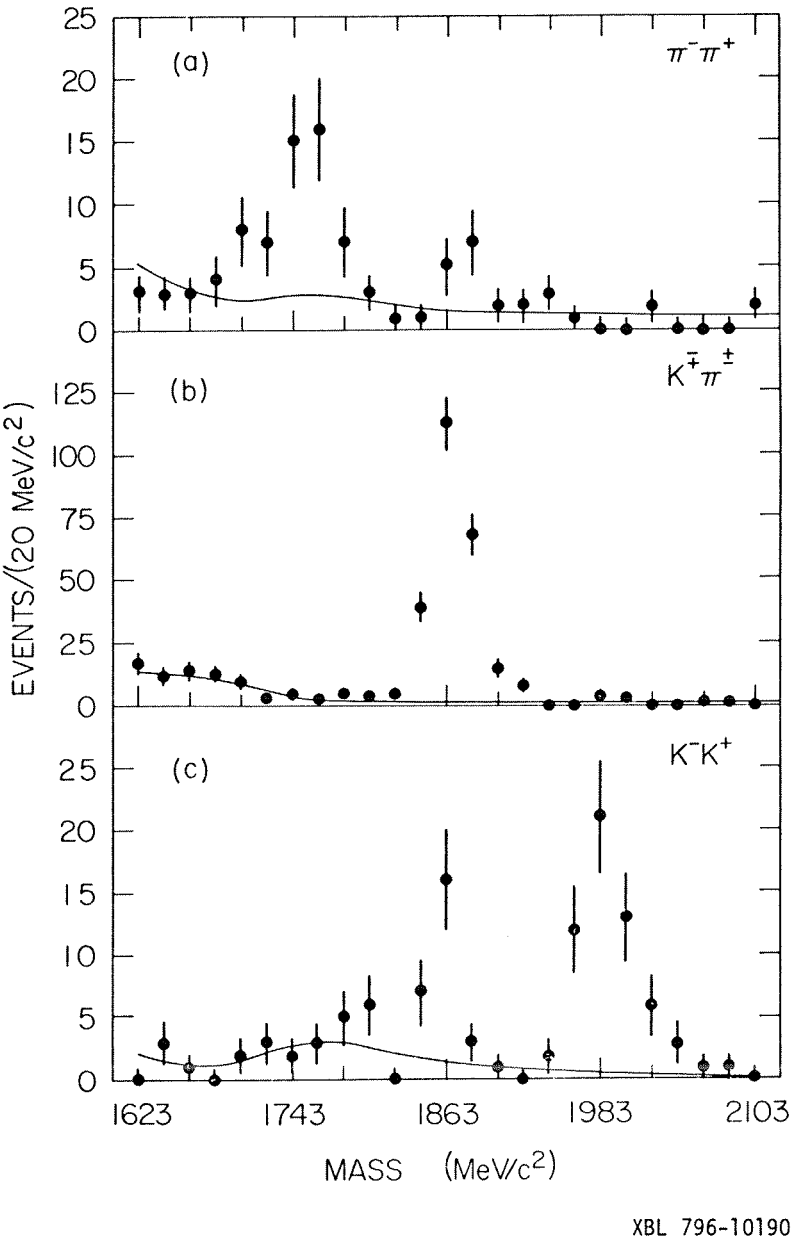

Fig. 5 Invariant mass of two particle combinations which have a momentum within 30 MeV/c of the expected D^0 momentum and TOF information consistent with the indicated particle masses.

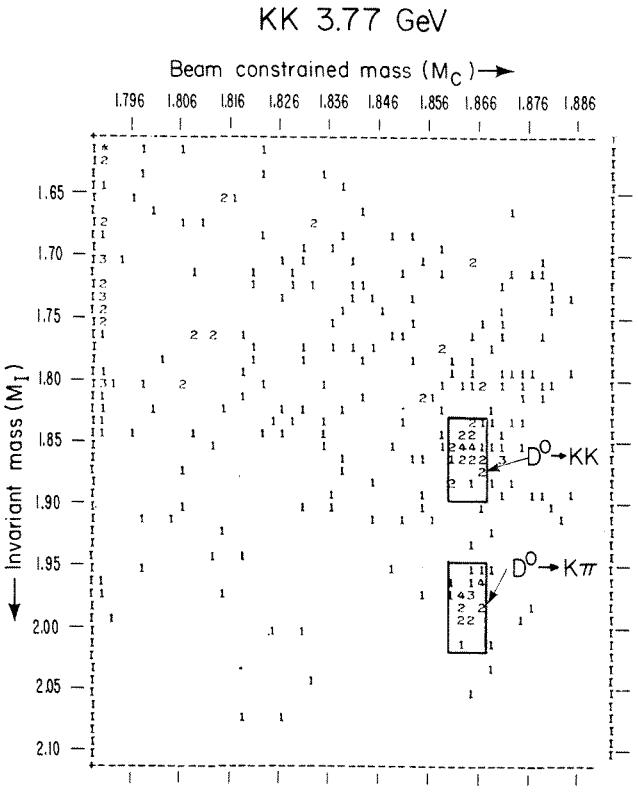

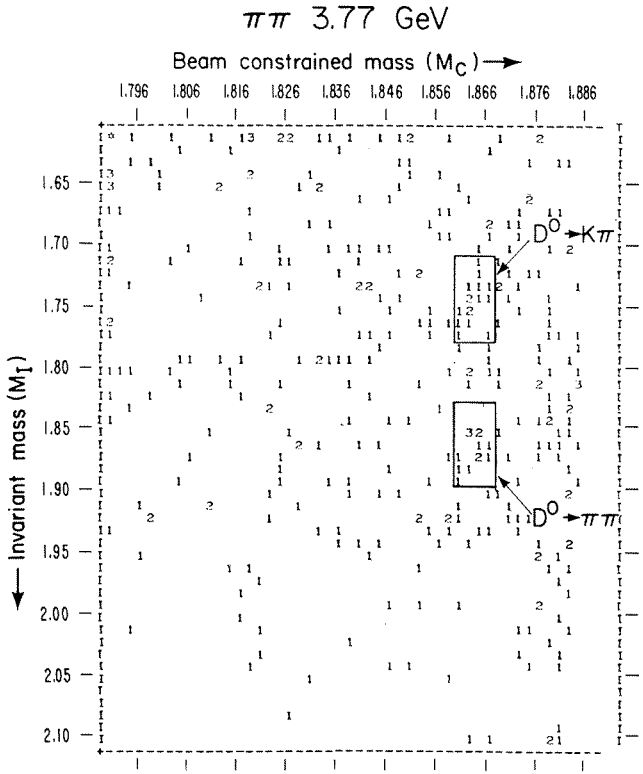

Fig. 6 Invariant mass (M_I) vs. beam constrained mass (M_C) for the K^+K^- and $\pi^+\pi^-$ mass assignments. The rectangular area was chosen from equivalent $K^{\pm}\pi^{\mp}$ mass plot.

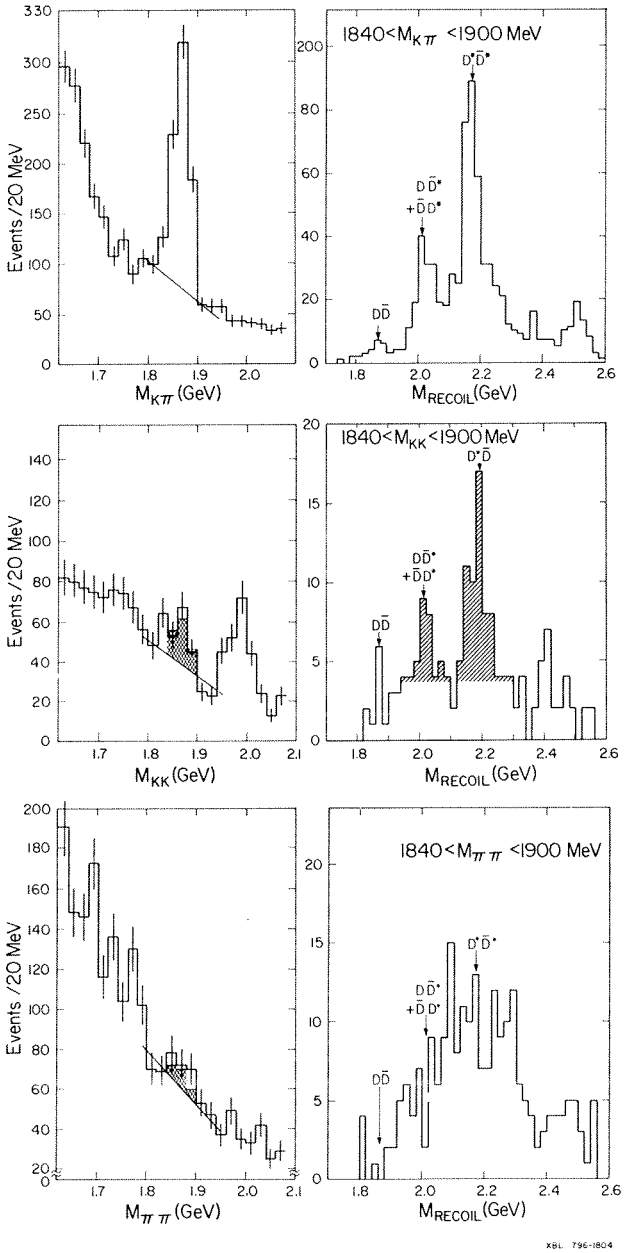

Fig. 7 Two body invariant mass and recoil mass spectrum against D (1.84 < M < 1.90), for each two body mass hypothesis. Data has $\sqrt{s}$ between 3.8 and 4.5 GeV.

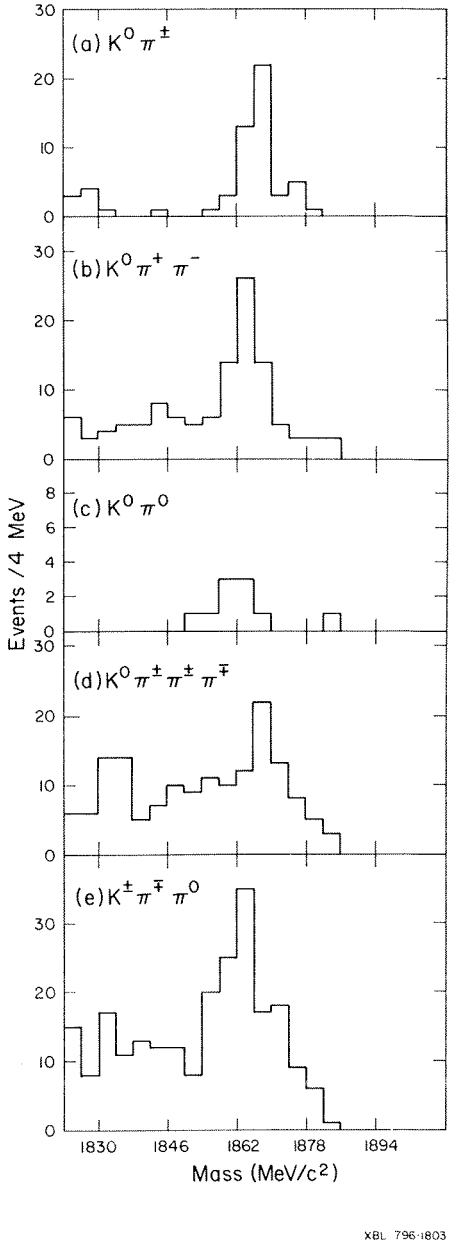

Fig. 8 Beam constrained mass spectra for some D meson decay channels: (a) $K^0\pi^\pm$, (b) $K^0\pi^+\pi^-$, (c) $K^0\pi^0$, (d) $K^0\pi^\pm\pi^\pm\pi^\mp$, and (e) $K^\pm\pi^\mp\pi^0$.

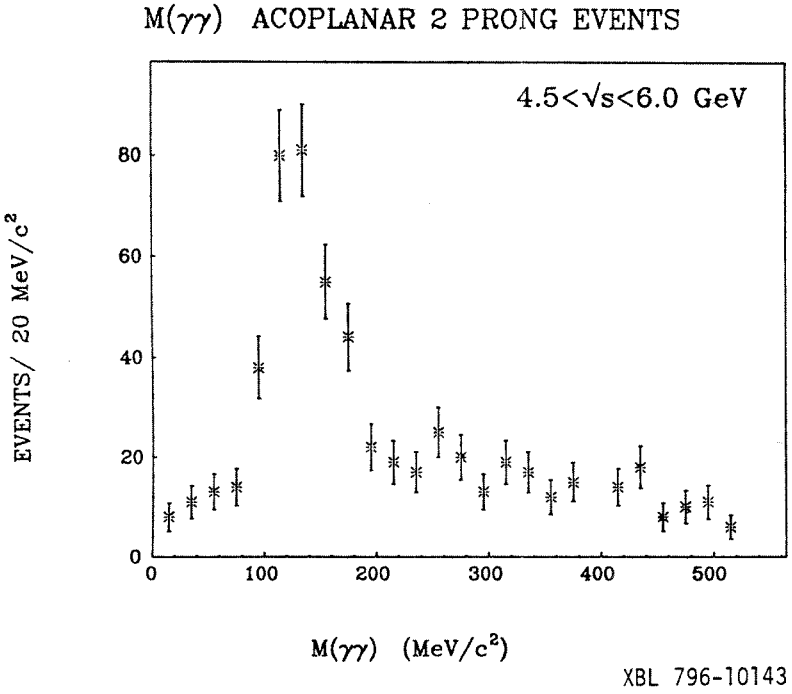

Fig. 9 γ-γ mass for acoplanar 2 prongs

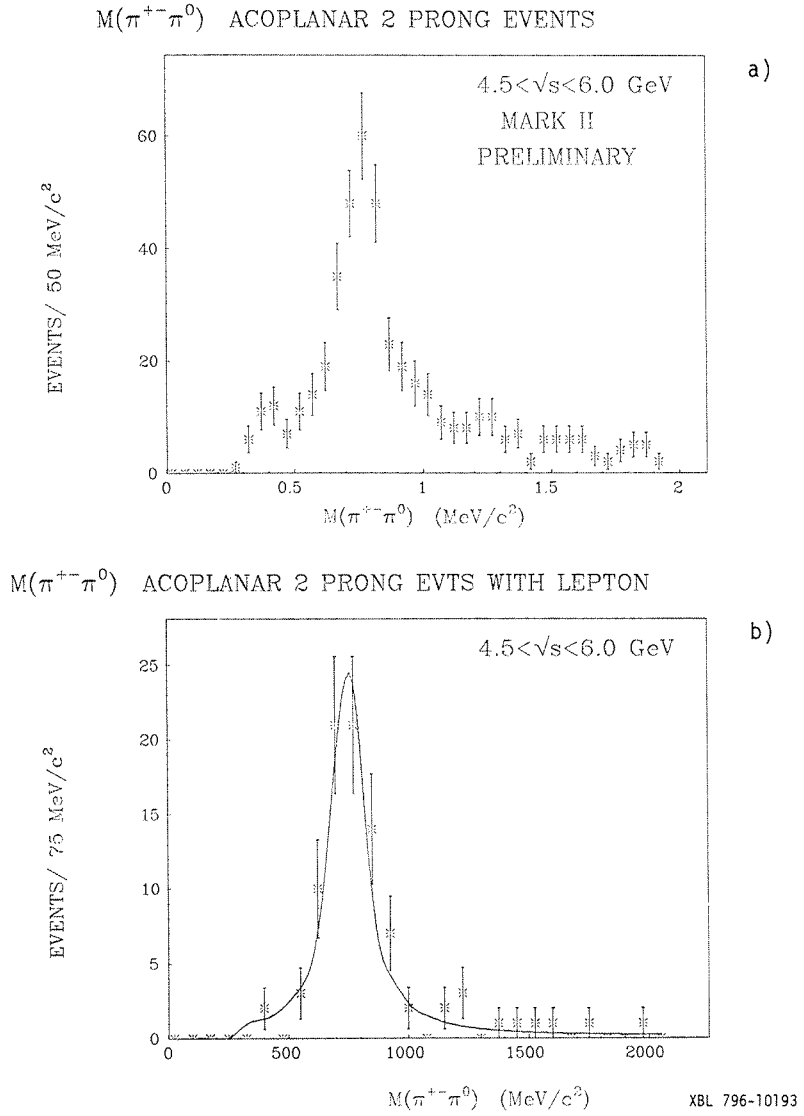

Fig. 10 $M(\pi^{\pm}\pi^0)$ for (a) all acoplanar two prong events with π^0 and (b) those events in which the other charged track is identified as a lepton

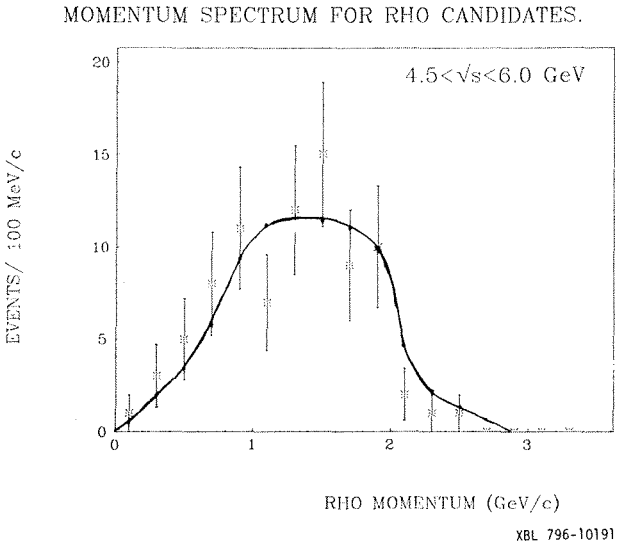

Fig. 11 Momentum spectrum for rho candidates

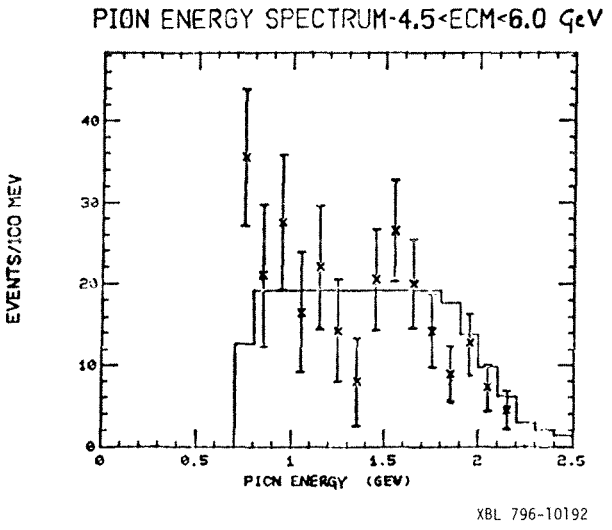

Fig. 12 Pion energy spectrum for acoplanar πx events

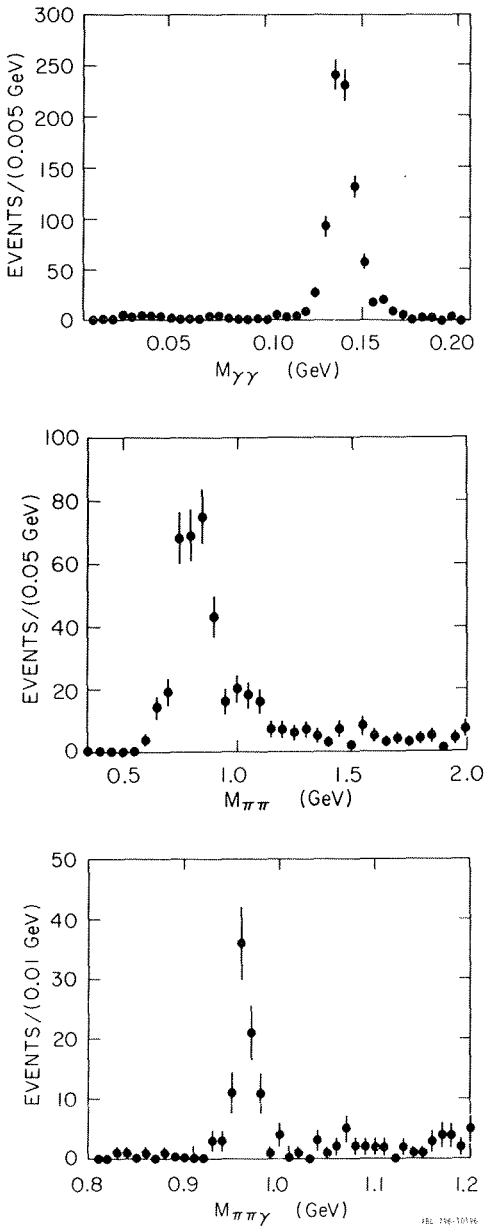

Fig. 13 Invariant mass distributions for events which fit $\psi \to \pi^+\pi^-\gamma\gamma$. (a) $\gamma\gamma$ mass, (b) $\pi^+\pi^-$ mass recoiling against π^0 with $\rho^\pm$ candidates removed, (c) $\pi^+\pi^-\gamma$ mass with events containing a π^0 removed.

DISCUSSION

Chairman: S.C.C. Ting

Sci. Secretaries: C. Best and H. Gennow

G. Barbiellini: What is your limit on the τ-neutrino mass?

G. Gidal: I am not prepared to say anything about that now.

A. Bodek: Do you have any number for the branching ratio of the $K^*\pi$ decay mode of the D (this is in view of the fact that the ISR Split Field Magnet group claims to see the D in this decay mode but not in any other)?

G. Gidal: No, we do not have a number. Qualitatively we see in the D^+ Dalitz plot fairly small amounts of K^*, of the order of less than 20%. In the $K^0\pi^+\pi^-$ Dalitz plot there is a large contribution from K^*'s. A lot of these things depend on detailed understanding of the efficiencies over the Dalitz plot and they will be forthcoming.

TESTS OF QUANTUM ELECTRODYNAMICS AT PETRA

James G. Branson

Deutsches Elektronen-Synchrotron, Hamburg, W. Germany.

ABSTRACT

Results from three PETRA experiments on $e^+e^- \longrightarrow e^+e^-$ and $e^+e^- \longrightarrow \mu^+\mu^-$ are presented. These are used to test for deviations of the photon propagator from $1/q^2$ or for nonpoint-like behavior of one of the particles γ, e or μ. Quantum Electrodynamics is found to be valid down to distances of 4×10^{-16} cm.

Over the years quantum electrodynamics has been tested[1] over and over again in many reactions and has so far been found to be an exact theory of the eletromagnetic interaction. With the advent of high energy operation of the e^+e^- storage ring PETRA, QED can be tested more stringently than previously in ways where one might expect the first breakdowns to occur. By colliding high energy e^+ and e^- beams, we can check QED's validity at larger values of momentum transfer than ever before. This implies we look at the very short distance behavior of the interactions.

There are two areas which I think are very interesting to check. The most popular theories of the weak, strong and electromagnetic interactions are theories of pointlike particles coupling to each other. Among these pointlike particles are the leptons, quarks, photon, gluons and the weak bosons. It is possible that these particles themselves are made up of some very tightly bound constituents. This can be probed by measuring very high q^2 interactions. The results of experiments using leptons and photons are the easiest to interpret.

Another possibility which would cause a deviation from QED at large q^2 would be the existence of a high mass particle like the photon. We have seen among the leptons and quarks that there is a mass spectrum of particles that have the same characteristics. We now know of 5 quark flavors which interact in a fashion very similar to each other. The three kinds of leptons and their neutrinos are even more similar to each other, the only difference being the mass. The same sort of mass spectrum is possible for photon like particles.

In order to make the test for a heavy photon most transparent, I prefer to parameterize any deviation from QED in terms of a value with the dimensions of mass. If there is a heavy photon of mass Λ, then the only change in QED is that the photon propagator is modified:

$$\frac{1}{q^2} \longrightarrow \frac{1}{q^2} + \frac{1}{q^2 - \Lambda^2}$$

The same modification to Bhabha scattering and μ pair production would be made if there were a form factor for each lepton or γ of the form

$$F(q^2, \Lambda_+^2) = 1 + \frac{q^2}{q^2 - \Lambda_+^2} \quad .$$

Values of Λ have been computed by the three experiments MARK J, PLUTO and TASSO for the above form as well as for

$$F(q^2, \Lambda_-^2) = 1 - \frac{q^2}{q^2 - \Lambda_-^2} \quad .$$

With a form factor, the cross section for Bhabha scattering becomes:

$$\frac{d\sigma}{d\Omega} = \frac{\alpha^2}{2s}\left[\frac{q'^4 + s^2}{q^4} \mid F(q^2,\Lambda_S^2) \mid^2 + \frac{2q^4}{q'^2 s}\,\mathrm{Re}(F(q'^2,\Lambda_S^2)\,F^*(s,\Lambda_T^2)) + \frac{q'^4 + q^4}{s^2}|F(s,\Lambda_T^2)|^2\right]$$

where $q'^2 = -s\sin^2(\Theta/2)$, $q^2 = -s\cos^2(\Theta/2)$ and I have allowed for a different value of Λ and spacelike regions.

The cross section for μ pair production becomes

$$\frac{d\sigma}{d\Omega} = \frac{\alpha^2}{2s}\,\frac{q'^4 + q^4}{s^2}\,|F(s,\Lambda_T^2)|^2$$

The three experiments MARK J, PLUTO and TASSO have made tests of QED. Their detection methods and acceptances are different from each other so I will very briefly describe the measurements.

MARK J measures the angular distribution for Bhabha scattering in three layers of lead-scintilator sandwich shower counters. The angular range covered is for $|\cos\Theta| < .97$. However, since the charge of the electron is not determined, only the sum of foreward and backward scattering can be compared to QED. Muon pair production is also measured by the detector with a drift chamber iron magnet system.

PLUTO and TASSO use cylindrical proportional and drift chambers in a solenoidal field to measure Bhabha scattering in the range $|\cos\Theta| < .8$. In addition, these experiments use a small angle luminosity monitor, which also measures Bhabha scattering, to normalize the angular distribution.

All of the experiments apply radiative corrections[2] to the data. The calculation of these corrections includes the effects of τ loops and of hadronic vacuum polarization.

The angular distribution for Bhabha scattering measured in the MARK J detector is shown in figure 1. The cross section $d\sigma/d(\cos\Theta)$ is multiplied by s so that data at three machine energies, 13, 17 and 27.4 GeV can be compared against one curve. All of the data points agree well with the expectation from QED and no unexpected s dependence is seen. These data are computed from over 4000 Bhabha scattering events at each energy. The Bhabha scattering data of PLUTO and TASSO are shown in figures 2 and 3. Again agreement with QED is quite good. In addition to the Bhabha scattering data, MARK J has measured 7 $\mu^+\mu^-$ events from one photon interactions with 8 events expected.

Using these data, the three groups have calculated 95% confidence level lower limits on $\Lambda_\pm$. These are displayed in Table 1.

Table 1

95% Confidence Level Limits

MARK J

FORM FACTOR	$1 - \frac{q^2}{q^2 - \Lambda_-^2}$	$1 + \frac{q^2}{q^2 - \Lambda_+^2}$
$\Lambda_S >$	43	33
$\Lambda_T >$	49	35
$\Lambda_S = \Lambda_T >$	53	45

TASSO

FORM FACTOR	$1 - \frac{q^2}{q^2 - \Lambda_-^2}$	$1 + \frac{q^2}{q^2 - \Lambda_+^2}$
$\Lambda_S = \Lambda_T >$	43	49

PLUTO

FORM FACTOR	$(1 - q^2/\Lambda^2)^{-1}$	$(1 + q^2/\Lambda^2)^{-1}$
$\Lambda_S = \Lambda_T >$	38	60

MARK J has computed values for the assumption that the Λ's for spacelike and timelike graphs are different and for the assumption that they are equal. The values of Λ for MARK J and TASSO are roughly the same for approximately equal integrated luminosity.

As seen in the table, PLUTO uses a slightly different parameterization than the other two groups. These are equal in the case of a minus sign,

$$(1 - q^2/\Lambda_-^2)^{-1} = 1 - \frac{q^2}{q^2 - \Lambda_-^2}$$

but are not equal in the case of the plus sign,

$$(1 + q^2/\Lambda_+^2)^{-1} = 1 + \frac{q^2}{-q^2 - \Lambda_+^2} \neq 1 + \frac{q^2}{q^2 - \Lambda_+^2} .$$

The PLUTO form makes a somewhat larger modification to the cross section for large q^2. PLUTO's value for Λ_+ for this choice is 60 GeV, which would change to roughly 50 GeV if the other form were used. All three experiments then have nearly the same limits on the breakdown of QED. The relative size of the two limits with opposite signs in the form factor only depends on whether the high q^2 data came out slightly lower or slightly higher than the QED expectation. If the data agreed exactly with QED, the two limits would be equal.

In terms of structure in the leptons or photons, both the values of Λ for the plus and minus sign in the form factor are of interest since for instance if the electron were made up of tightly bound constituents with charge greater than 1, Λ_- would have a finite value whereas if the constituent charges were less than 1, then Λ_+ would have a finite value. For these values of $\Lambda_\pm \simeq 50$ GeV, the electron, muon and photon are probed for any structure down to distances of 4×10^{-16} cm.

In case of a heavy photon, probably the value of Λ_+ is more relevant than Λ_- if one assumes that the heavy photon and normal photon couple in phase. If they were 180^0 out of phase, then the heavy particle would "cut off" the electromagnetic interaction at very large q^2. The lower limit on the mass of a heavy photon is just equal to the value of $\Lambda_\pm$. Of course the weak neutral boson Z_o would also have an effect on the cross sections tested here. However, in the Wienberg-Salam model, the mass of the Z_o is quite large and the vector coupling is quite small for measured values of $\sin^2\Theta_w$. If, however, there were some low mass Z_o, it could have a larger vector coupling. The ratio of the coupling of a Z_o to that of the mass is about 15% lower than the limit on heavy photon.

In summary, QED has been tested at shorter distances and at larger momentum transfer than before. So far, we have found no deviation from the expected cross sections. However, as more statistics are accumulated at PETRA, our limit will become more stringent or we may find the first evidence for a breakdown of QED.

REFERENCES

1) J.G. Asbury et al., Phys. Rev. Letters 18, 65 (1967)./ H. Alvensleben et al., Phys. Rev. Letters 21, 1501 (1968)./ V. Alles-Borelli et al., Nuovo Cimento 7A, 345 (1972)./ H. Newman et al., Phys. Rev. Letters 32, 483 (1974)./ J.E. Augustin et al., Phys. Rev. Letters 34, 233 (1975)./ L.H. O'Neill et al., Phys. Rev. Letters 37, 395 (1976)./ D.P. Barber et al., Phys. Rev. Letters 42, 1110 (1979).

2) S.A. Berends et al., Phys. Lett. 63B, 432 (1976) and private communication.

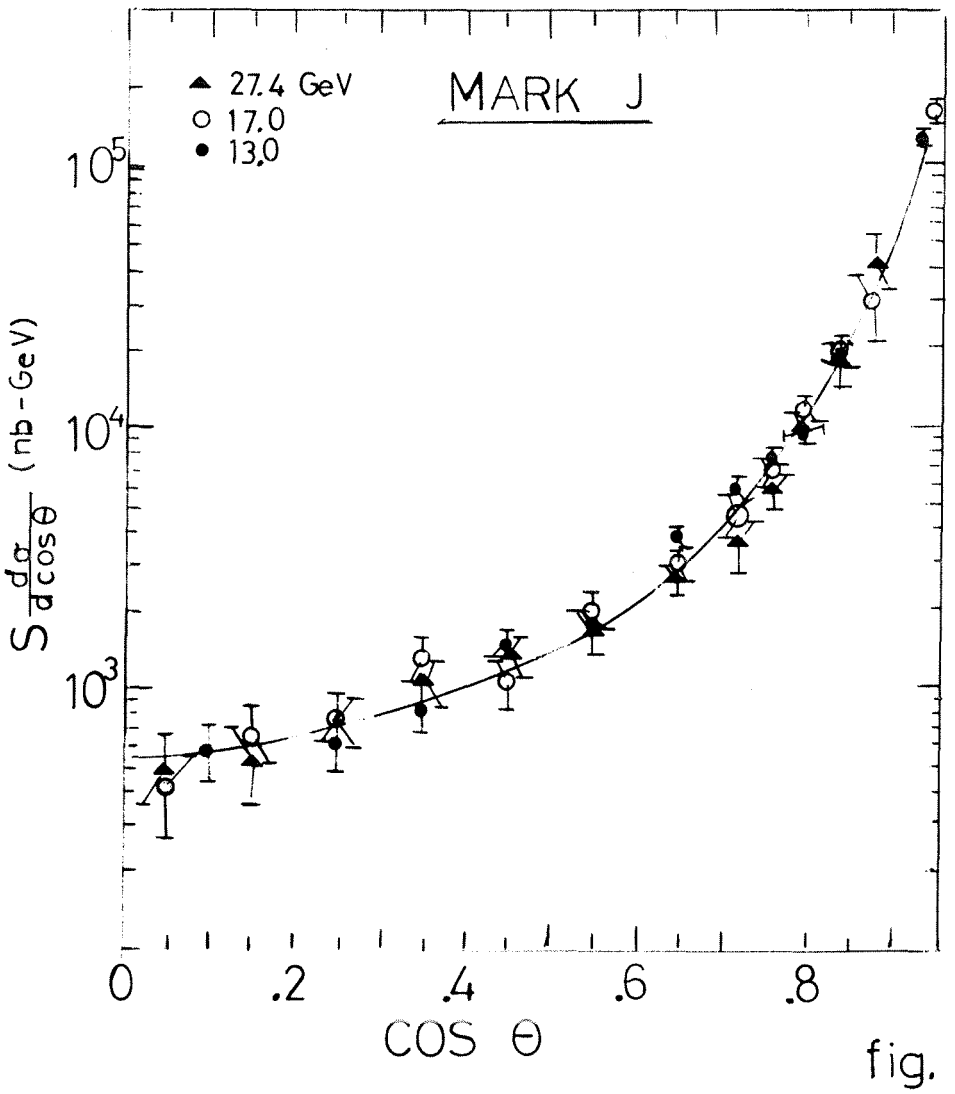

fig. 1

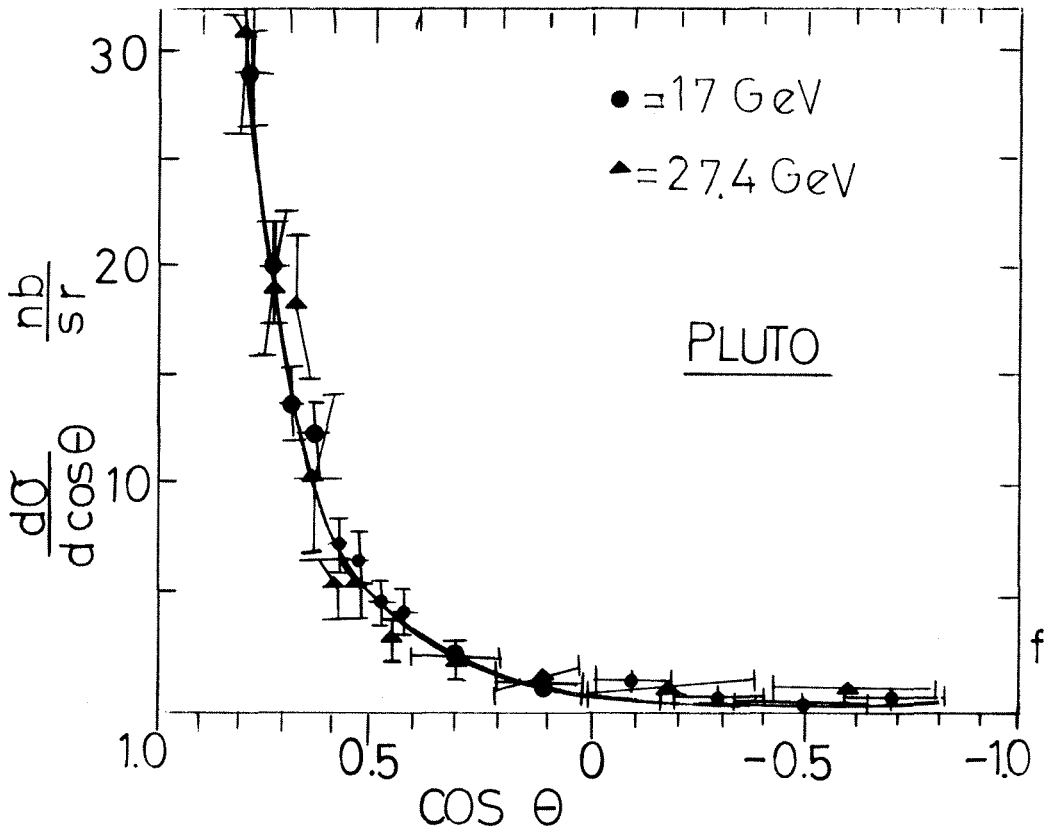
30
20
10
1.0
0.5
0
-0.5
-1.0
COS Θ
dσ/dcosΘ nb/sr
● = 17 GeV
▲ = 27.4 GeV
PLUTO

fig. 2

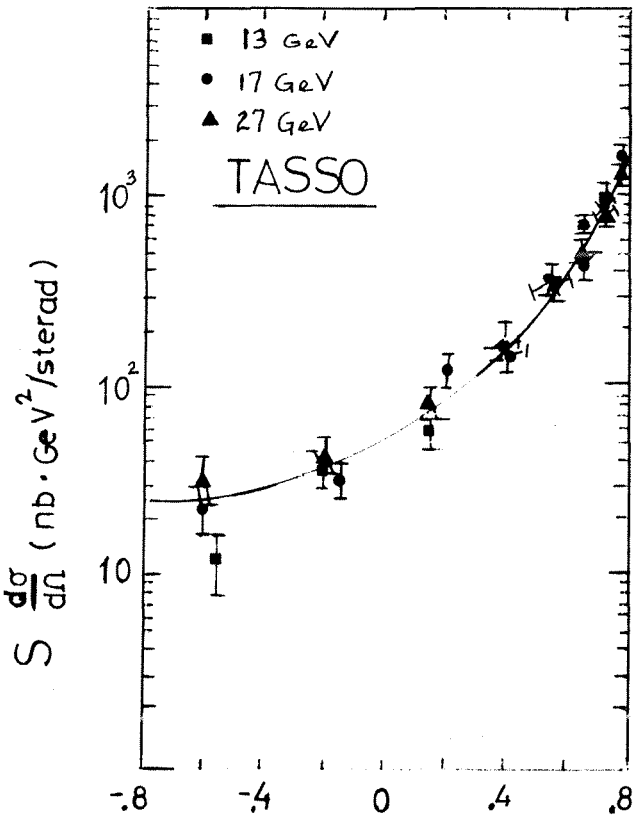
■ 13 GeV
● 17 GeV
▲ 27 GeV
TASSO
10³
10²
10
S dσ/dΩ (nb · GeV²/sterad)
-.8
-.4
0
.4
.8

fig. 3

A MEASUREMENT OF $e^+e^- \longrightarrow$ hadrons at $\sqrt{s}$ = 27.4 GeV

D. Barber, U. Becker, H. Benda, A. Böhm, J. Branson, J. Bron, D. Buikman, J. Burger, C.C. Chang, M. Chen, D.P. Cheng, Y.S. Chu, P. Duinker, H. Fesefeldt, D. Fong, M. Fukushima, M.C. Ho, H.K. Hsu, R. Kadel, D. Luckey, C.M. Ma, G. Massaro, T. Matsuda, H. Newman, J.P. Revol, M. Rohda, H. Rykaczewski, T.T. Shui, H.W. Tang, S.C.C. Ting, K.L. Tung, F. Vannucci, M. White, T.W. Wu, P.C. Yang.

Aachen-Annecy-DESY-M.I.T.-NIKHEF-Peking Collaboration

Presented by James G. Branson, DESY, Hamburg, W. Germany.

ABSTRACT

During the initial running of PETRA at 27.4 GeV, we have measured the reaction $e^+e^- \longrightarrow$ hadrons using the MARK J detector. We find a value of R of 4.1 ± .5 (statistical) ± .7 (systematic). Events are analyzed in terms of thrust and sperocity. Overall, we find no evidence for a new threshold in hadron production up to the present energy.

During April and May, PETRA has been running with a beam energy of 13.7 GeV. Up to the present time, we have detected 101 hadronic events mainly from the process $e^+e^- \longrightarrow$ hadrons using the MARK J detector. Since PETRA has opened up a large new energy region, between 10 GeV and 27 GeV, it is most interesting to determine if a threshold for production of new hadronic particles has been crossed. The most mundane new particles would be those with the quantum number "top". They would contain a t quark which is thought to belong in a doublet with the b quark, a component of an upsilon. The t quark should have charge 2/3. Of course it is also quite possible that a charge 1/3 quark could have a lower mass than the t quark or that there is a new color degree of freedom at high energy. There may be a threshold for some particles that we know nothing about.

The data on $e^+e^- \longrightarrow$ hadrons taken so far is consistent with a simple model in which the electron and positron annihilate, producing a timelike photon. The photon then decays to a quark antiquark pair. The quark and antiquark each produce a hadron jet by pulling more $q\bar{q}$ pairs out of the sea. These final state interactions between the quarks do not alter the cross section very much. The cross section is also only slightly modified by radiative corrections. This allows a simple comparison to the process for $e^+e^- \longrightarrow \mu^+\mu^-$ which proceeds by the same process. The ratio is simply

$$R = \frac{\sigma(e^+e^- \longrightarrow \text{hadrons})}{\sigma(e^+e^- \longrightarrow \mu^+\mu^-)} = \sum_{\substack{\text{flavors} \\ \text{colors}}} (q_i)^2$$

When we have crossed a threshold for production of a new kind of quark, the sum is then extended and the ratio R increases.

Another signal for production of a new particle is a change in the jet behavior of the events. In the simple model, the $q\bar{q}$ pair decay to hadrons with limited momentum transverse to the direction of the initial quark or antiquark. This transverse momentum is independent of energy except for relatively small possible effects of gluon emission. Then, as the center of mass energy increases, the initial quark has more momentum and the events become more and more jetlike.

However, if a very massive quark is produced near threshold, its momentum is rather

small. The massive particle containing this quark should then decay with the daughter particles randomly distributed in direction. This type of event would be very spherical and such behavior would persist quite far above threshold if the mass of the particle is large. Thus production of spherical events is simply a kinematical property of the production of a massive quark near enough to threshold. The result is that we would expect to see a class of very spherical events, from the new particles, mixed with the jetlike events. This is a statistically more powerful way of looking for new flavor production.

To study the hadronic events, we used the MARK J detector which has been previously described[1]. It consists of an electromagnetic shower counter followed by a hadron calorimeter. These both cover a solid angle of nearly 4π steradians. In addition, muons are identified and momentum analyzed in a drift chamber iron magnet system. To identify hadronic events, we require that at least 65% of the center of mass energy be deposited in the detector. Our overall energy resolution is less than 20% σ because a very large fraction of the energy is deposited in the shower counter.

To calculate the acceptance of the detector and to compare data to the expectations from the quark parton model we use a detailed Monte Carlo program. This generates events by producing $q\bar{q}$ pairs, the relative flavor productions being determined by the square of the quark charges. In general, we use u, d, s, c and b quarks; however, to test for the existence of a new flavor, we generate events with t quarks of charge 2/3 and mass 12 GeV. The initial quarks then fragment, producing hadrons according to the Feynman-Field Monte Carlo method. For the results I will show, we have used fragmentation functions

$$D(z) \propto (1 - z)^2$$

for all flavors. We have tried a constant D(z) for charmed, bottom and top quarks and found that this does not significantly effect our conclusions. The average $p_\perp$ of the primary mesons is 323 MeV.

The unstable mesons are then allowed to decay, with branching ratios taken whenever possible from the data. For the bottom and top particles, we have used the expectations of Ali et al.[2] which include 30% semileptonic decays. The final particles are traced through the detector depositing energy in the counters and causing hits in the drift chambers. From this information, counter ADCs and TDCs are generated as well as drift wire TDCs. All of this information is then passed on to the same analysis program used for normal data. The same cuts are applied and the acceptance is found to be .785.

Other processes are also generated by the Monte Carlo to measure our sensitivity to them. We find that $e^+e^- \longrightarrow \tau^+\tau^-$ contributes 0.3 to R. Also, $e^+e^- \longrightarrow e^+e^-$ + hadrons contributes 0.1.

Up to the time I left Hamburg, we had analyzed 101 hadronic events at 27.4 GeV. Of these, 12 have tracks that penetrate more than one meter of iron. This fraction is up substantially from the 13 and 17 GeV data and is insensitive to punchthrough. From these 101 events, we compute the value of R shown in Table 1 along with our previously reported values at 13 and 17 GeV.

Table 1

$\sqrt{s}$ (GeV)	13	17	27.4
R	4.5 ± .5 ± .7	4.9 ± .6 ± .7	4.1 ± .5 ± .7

The contamination from τ pair production and two photon processes has been subtracted. If the effects of initial state radiation are corrected for, the value of 4.1 changes to 3.7. The data at the three energies are in agreement with a constant value of R but of course this must be checked more thoroughly by taking data at intermediate energies. At any rate there is no evidence for an increase in R which would signal the production of new particles.

We have analyzed the jet behavior of the data in terms of the quantities, thrust and spherocity, defined below.

$$T = \max \left[\frac{\Sigma\, p_{/\!/}}{\Sigma\, p} \right] \qquad \text{and} \qquad S' = (4/\pi) \min \left[\frac{\Sigma\, p_{\perp}}{\Sigma\, p} \right]^2$$

These are parameters of each event that are maximized or minimized by choosing a single jet axis with respect to which $p_{/\!/}$ and $p_{\perp}$ are calculated.

Since we have a calorimetric detector, we do not measure the momenta of individual particles in a jet. We do however measure the energy flow for an event. Thrust and spherocity are defined in terms of particle momenta but, in fact, for these, only the energy flow is needed. We are therefore able to test the jet behavior by a method we call pseudotracks. A track is defined for each hit counter. The direction of the track is determined from the position of the hit and the magnitude from the energy depositied. Using this method, we reproduce the jet axis with either thrust or spherocity with an RMS error of less than 10 degrees.

Thrust distributions for energies of 13, 17 and 27.4 GeV are shown in figures 1a), 1b) and 1c). The solid lines are Monte Carlo calculations with u, d, s, c and b quarks and the dashed line in figure 1c) is with the addition of a t quark. At 13 and 17 GeV, the data and Monte Carlo agree quite well. At 27.4 GeV, the data are in reasonable agreement with the Monte Carlo although they may tend to be less strongly peaked. The data do not agree with the curve including top. In the region from .5 to .7, we would expect 12 events if top were being produced and we see zero. This is statistically quite powerful but perhaps model dependent. For instance, if the top quark were stable, we would not see a signal in the low thrust region from it.

Finally, we have calculated average values of thrust and spherocity, corrected for detector smearing, which are shown in Table 2. These are in good agreement with the Monte Carlo expectations.

Table 2

Corrected Average Thrust and Spherosity

$\sqrt{s}$	13	17	27.5
<T>	.82 ± .01	.85 ± .01	.87 ± .01
<S'>	.32 ± .03	.24 ± .03	.17 ± .03

In conclusion, we have studied hadron production for 27.4 GeV electron positron collisions and found no evidence for a new threshold in either the value of R or in the thrust distribution. In particular, a new charge 2/3 quark seems to be ruled out. We do not yet have enough information to comment of new leptons although we do recognize a probable τ signal in the data in the μ hadron mode.

* * *

REFERENCES

1) D.P. Barber et al., Phys. Rev. Letters 42, 1113 (1979).

2) A. Ali, J.G. Körner, G. Kramer, and J. Wilrodt, DESY Report 78/51 and 78/67 (1978) unpublished.
A. Ali, Z. Physik B, Particles and Fields 1, 25 (1979).
A. Ali and E. Pietarinen, DESY Report 79/12 (1979), unpublished.

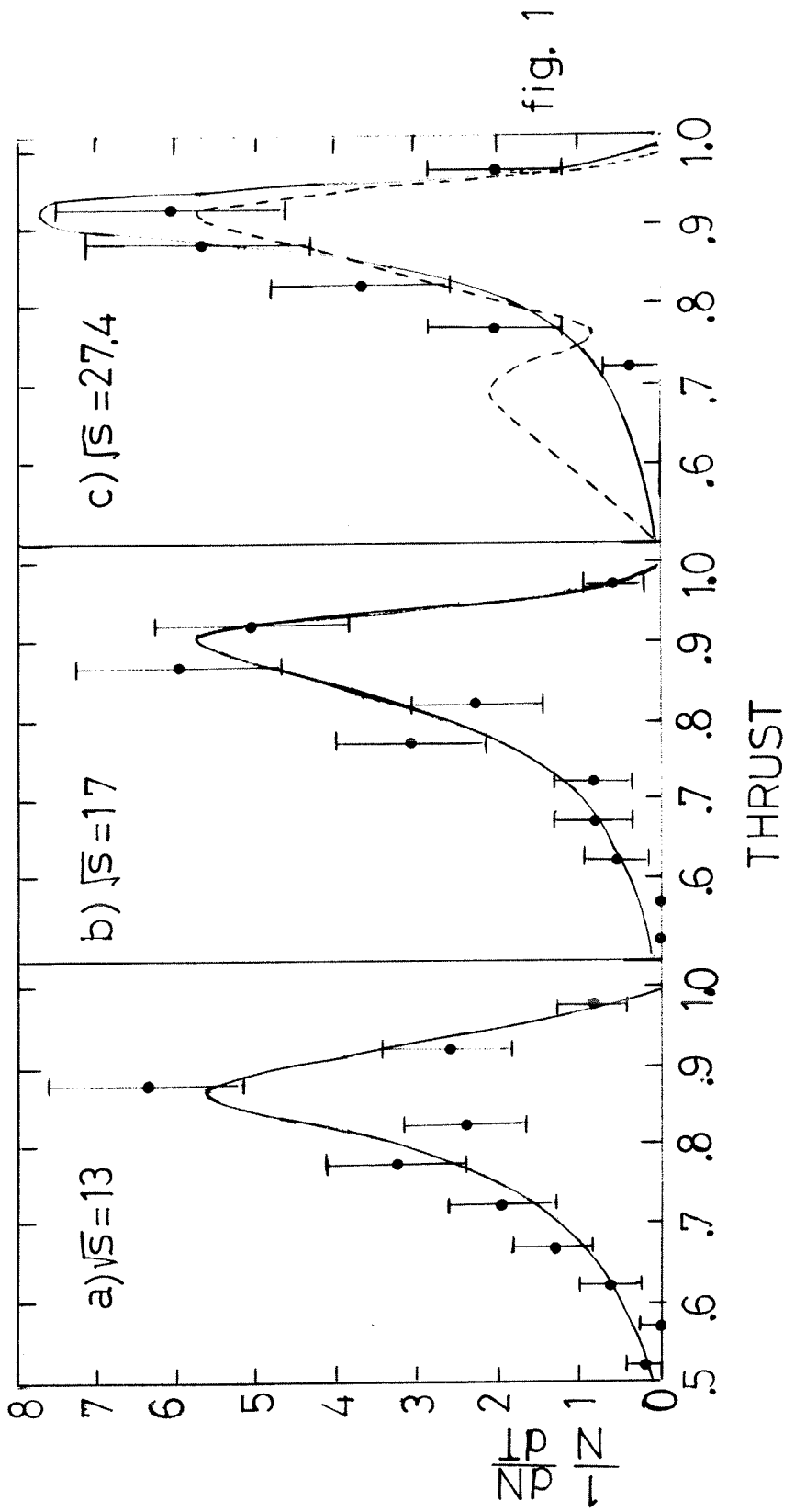
fig. 1
a) √s=13
b) √s=17
c) √s=27.4
1/N dN/dT
THRUST
0
1
2
3
4
5
6
7
8
.5
.6
.7
.8
.9
1.0

THE HADRONIC FINAL STATE IN e^+e^- ANNIHILATION AT C.M. ENERGIES OF 13, 17 AND 27.4 GeV

TASSO Collaboration
(Aachen,Bonn,DESY,Hamburg,Imperial College,Oxford,Rutherford,Weizman,Wisconsin)

(Presented by R.J. Cashmore, Department of Nuclear Physics, Oxford)

ABSTRACT

Results on the hadronic final state in e^+e^- annihilation at 13, 17 and 27.4 GeV are presented. There is no compelling evidence for the existence of the t quark in these data, which are in general agreement with a simple quark parton model. Some tentative indications of QCD effects are observed in the p_T^2 distributions.

1. THE TASSO DETECTOR AND EXPERIMENT

The TASSO detector is sited at one of the intersection points at the PETRA e^+e^- storage ring at DESY and has been described in detail previously[1]. The data described here have been obtained with only a part of the final detector. This consists of a large magnetic solenoid, 440 cms in length and with a radius of 135 cms producing a field of 0.5 Tesla parallel to the beam axis. The solenoid is filled with tracking chambers to allow measurement of the charged particles produced in the interactions. A luminosity monitor, which measures small angle Bhabha scattering, consists of eight counter telescopes mounted symmetrically with respect to the beam line and interaction point.

A particle emerging from the interaction point traverses the beam pipe and one of 4 scintillation counters which form a cylinder around the beam pipe, before entering a low mass cylindrical proportional chamber, a drift chamber and a set of time of flight counters. The proportional chamber has four gaps each containing anode wires parallel to the beam axis. The efficiency of the anode wires was 97%. The drift chamber contains 15 layers, 9 with sense wires parallel to the axis (zero-degree layers) and 6 with the sense wires oriented at approximately $\pm 4^\circ$ to the axis (stereo layers). The efficiency of each layer was found to be 96% together with a resolution of approximately 0.3 mm. Finally there are 48 time of flight counters (TOF) mounted between the drift chamber and the coil.

The 27.4 GeV data were obtained with the following trigger (which differs slightly from that used at 13 GeV and 17 GeV[1]): A coincidence between beam pick up signal, any beam pipe counter and any TOF counter gated information from 6 of the 9 zero degree layers of the drift chamber into a hardwired logic unit. This unit searched for tracks and determined their transverse momentum. Simultaneously the hits in the proportional chamber were gated into a separate processor which searched for track segments. A track was finally defined as the coincidence between a track from the drift chamber processor, a track segment from the proportional chamber processor and a TOF counter which was set. The trigger demanded either two tracks coplanar with the beam axis or at least four tracks. The transverse momentum of these tracks with respect to the beam axis was required to exceed 320 MeV/c. The resulting trigger rate was in the range of 1.0-2.0 Hz.

The luminosity was determined from measurements of the Bhabha cross-section at small angles. Large angle Bhabha scattering observed in the central detector was found to be consistent with these values within the statistical and systematic errors.

The resulting data samples and integrated luminosity are summarized in Table 1.

Table 1

Data samples and integrated luminosities

Energy	13	17	27.4
$\int Ldt$ (nb^{-1})	31.0	39.2	99.2
Triggers (K)	~ 350	~ 300	~ 300

2. THE SELECTION OF MULTIHADRON EVENTS AND THE MEASUREMENT OF R

In this section the criteria applied to select multihadron events from the 27.4 GeV data are described (these again differ slightly from those employed at 13 and 17 GeV[1]). Two steps were used to select the multihadron events:

At least 3 tracks were required in the projected r-ϕ plane (perpendicular to the beam axis) with at least 2 fully reconstructed in three dimensions. The three tracks have $d < 2.5$ cms and $|z| < 10$ cms, where d is the distance of closest approach in the r-ϕ plane and z is the z coordinate of the point of closest approach to the z axis (the beam axis). Furthermore at least one charged track must be in each of the two hemispheres oriented along the beam direction and the sum of the absolute values of the momenta should exceed 1 GeV. Approximately 120 events remained after applying these criteria.

An excess of events at low W (invariant mass) was apparent which we ascribed to beam gas and $\gamma\gamma$ interactions[2]. By considering events with $10 < |z| < 30$ cms we have been able to study beam gas effects. Requiring the sum of the absolute value of the momenta to exceed 9 GeV in an event ($\sum_i p_i \geq 9$ GeV) effectively removes all such events. The $\gamma\gamma$ interactions mainly populate low W also and thus this cut removes essentially all the $\gamma\gamma$ background too. That the $\gamma\gamma$ process was present can be deduced from our observation of

(i) events with one tagged electron

(ii) $\gamma\gamma \to \mu^+\mu^-$ and e^+e^- in the central detector

and we have checked that these events are consistent with the expected energy dependence of the $\gamma\gamma$ process.

In the second step to obtain multihadron events we applied the following criteria

(i) $\sum_i p_i \geq 9$ GeV (45 events remain)

(ii) events with one charged track in one hemisphere recoiling against the remaining tracks in the opposite hemisphere were removed. This is designed to remove heavy lepton contamination[3] (2 events are removed).

The remaining events, 43 in total, constituted the multihadron sample at 27.4 GeV and contains essentially no background.

In order to measure the total cross-section (and R) we have calculated the detection efficiency for events to trigger the apparatus and satisfy our selection criteria, using a 2 jet Monte Carlo program[4]. The detection efficiency was found to be 0.75 at 27.4 GeV

and fairly stable to changes in the input to the 2-jet Monte Carlo. The resulting value for R was 5.0 ± 0.8 which after radiative corrections led to a value of

$$R = 4.6 \pm 0.8 \pm 0.9$$

where the two contributions to the error are our estimates of the statistical and systematic errors respectively.

The values of R that we have measured are summarized in Table 2.

Table 2

The value of $R = \sigma_{hadrons}/\sigma_{\mu\mu}$

Energy (GeV)	13	17	27.4
R	$5.6 \pm 0.7 \pm 1.1$	$4.0 \pm 0.7 \pm 0.8$	$4.6 \pm 0.8 \pm 0.9$

Our expectations for R within the quark model are

u d s c b $\quad R = 11/3$

u d s c b + t $\quad R = 5$

From our results on R it is clear that we have no evidence for or against the existence of a new charge 2/3 or 1/3 quark or a charge 1 lepton.

3. INCLUSIVE PROPERTIES OF THE HADRONIC FINAL STATE

(i) Single particle inclusive spectra

Within the simple quark parton model the inclusive cross-section $\left(\frac{S}{\beta}\right)\frac{d\sigma}{dx_E}$ should scale with C.M. energy[5]. β is the particle velocity, $x_E = \frac{2E_h}{W}$ and $S = W^2$. At present we do not determine the particle type and hence we have used the quantity $S\frac{d\sigma}{dx}$ with $x = P/P_{beam}$. The resulting inclusive distributions are shown in Fig. 1. It is clear that scaling exists for $x \geq 0.2$. Only with greater statistics will we be able to look for the expected scaling violations in these distributions. It is also worth noting that the inclusive distribution at low x in the 13 GeV data exceeds that at the other energies which when taken with the larger value of R might indicate large production of $b\bar{b}$ states at this energy.

(ii) Multiplicities and rapidity distributions

The mean charged multiplicities we observe are in excess of simple extrapolations of the form[6]

$$\langle n \rangle = 2.1 + 0.7 \ln s$$

from lower energies. Thus the increase in $\langle n \rangle$ is not due solely to a lengthening of the rapidity plateau, it must rise as well.

4. JET PROPERTIES OF THE HADRONIC FINAL STATE

In the simplest quark parton model we expect the final hadronic system to be obtained from an initial $q\bar{q}$ system, resulting in jets of particles surrounding the original quark

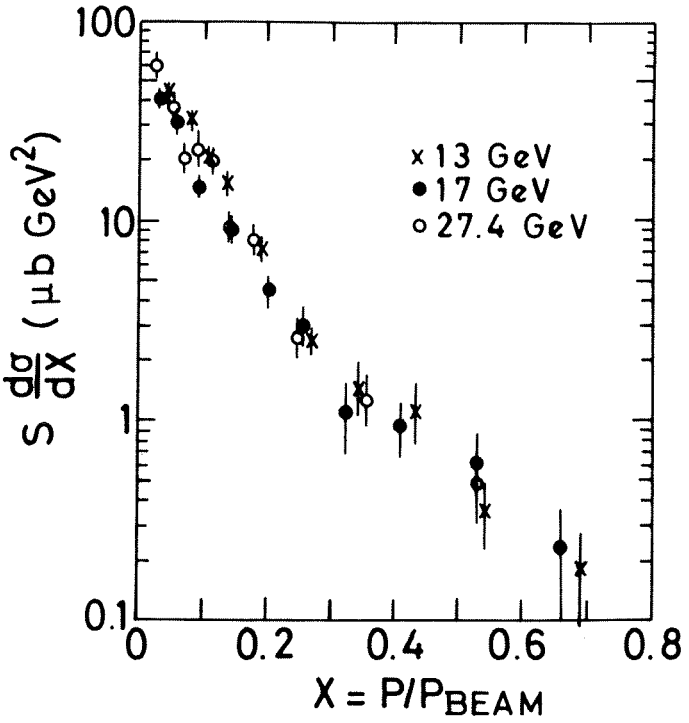

Fig. 1 The Inclusive Hadron Spectrum

direction having 'smallish' transverse momentum with respect to this direction. Within QCD modifications of this picture are expected where the quarks radiate gluons[7,8].

In order to study these jets we have defined the jet axis by minimizing the sphericity[9]

$$S = \frac{3}{2} \min \frac{\sum_i (p_T^i)^2}{\sum_i (p^i)^2}$$

where p^i is the momentum of a particle and p_T^i is its transverse component with respect to the axis. Studies using theoretically more desirable quantities e.g. thrust[8] lead to similar conclusions[10]. With the jet defined in this way we have studied

(a) sphericity distributions

(b) p_T^2 distributions

(c) jet axis angular distribution .

Our current low statistics (∿150 events at all energies) make the determination of the jet axis distribution (c) difficult. However the sum of all 3 energy samples is consistent with the expected form

$$\frac{d\sigma}{d\Omega} \propto 1 + \cos^2\theta$$

To study (a) and (b) we need to compare the data to a model. We have used the quark jet model described by Field and Feynman[4] with extensions to include c and b quark production[11]. The main assumptions are listed below

(i) quarks are produced according to the square of their charges

$$u\bar{u} : d\bar{d} : s\bar{s} : c\bar{c} : b\bar{b} = 4 : 1 : 1 : 4 : 1$$

(ii) quarks pairs are created in the fragmentation in the ratios

$$u\bar{u} : d\bar{d} : s\bar{s} = 2 : 2 : 1$$

(iii) the fragmentation function $f(\eta)$ is given by

$$f(\eta) = 1 - a + 3a\eta^2$$

with $a = 0.77$ $\eta = 1-z$ $z = E/Eq$

(iv) pseudoscalar mesons are produced as frequently as vector mesons

(v) the input mean p_T in the quark fragmentation is

$$\langle p_T^q \rangle = 0.250 \text{ GeV}$$

(vi) a statistical model is used for the decays of mesons containing c and b quarks

(vii) the masses of mesons containing b quarks are in the range $5.5 \rightarrow 6$ GeV

It is against this background that we have searched for the existence of the t-quark or QCD gluon effects.

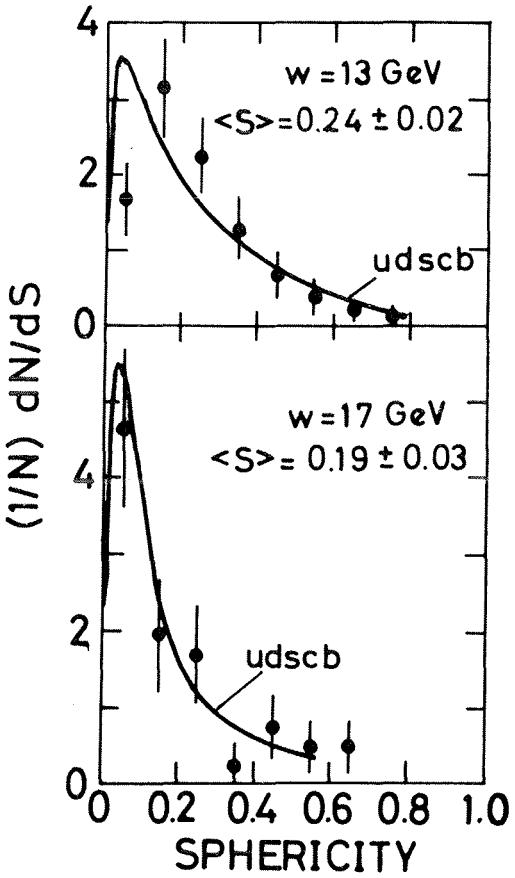

Fig. 2a Sphericity distributions at 13 and 17 GeV. The curves are from the two jet Monte Carlo with u,d,s,c,b quarks.

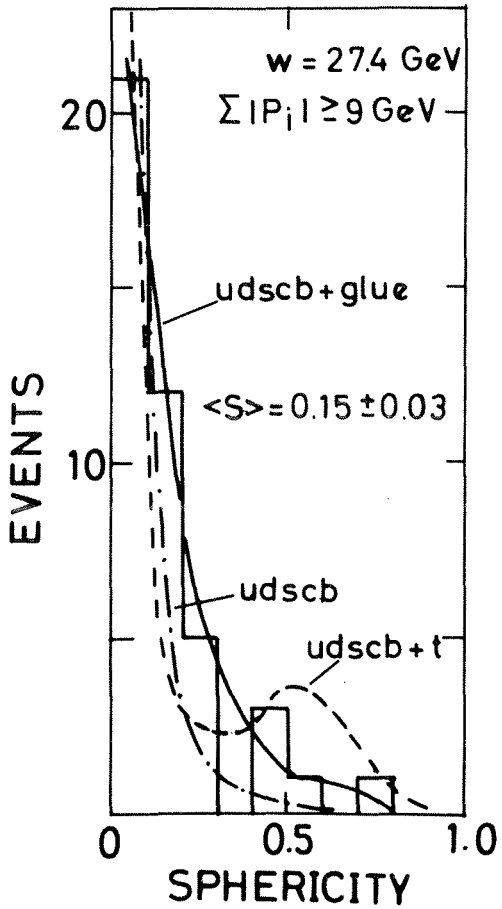

Fig. 2 b Sphericity distribution at 27.4 GeV together with different model predictions.

(a) Sphericity distributions

In Fig. 2a the sphericity distributions at 13 and 17 GeV are shown. The model, containing u,d,s,c and b quarks, clearly fits the data well. However at 27.4 GeV (Fig. 2b) the predicted distribution is clearly too narrow and the data contain some high sphericity events. To understand this distribution we have considered three modifications:

(i) inclusion of a t quark: the model distribution is still too narrow at low sphericity and predicts more events (7.5) at sphericities greater than 0.5 than are observed (2.0). Thus it is unlikely that production of a new quark is responsible.

(ii) a wider p_T distribution in the model: if we use $\langle p_T^q \rangle = 0.500$ GeV good agreement with the data is obtained (not shown). However there is little physical motivation for following this course.

(iii) include QCD effects: if QCD effects are included in the udscb quark jet model[12] good agreement with the data is obtained as indicated in Fig. 2b.

Thus we conclude that it is unlikely that new charge 2/3 quarks are produced at these energies. The explanation probably lies in (ii) or (iii). To investigate this we have studied the p_T distributions with respect to the jet axis.

(b) P_T distributions

We have observed that the $\langle p_T \rangle$ and $\langle p_T^2 \rangle$ are increasing with energy as indicated in Table 3.

Table 3

$\langle p_T \rangle$ and $\langle p_T^2 \rangle$ as a function of energy

Energy GeV	13	17	27.4
$\langle p_T \rangle$ GeV	0.313 ± 0.009	0.344 ± 0.012	0.393 ± 0.016
$\langle p_T^2 \rangle$ GeV^2	0.145 ± 0.010	0.175 ± 0.014	0.276 ± 0.029

The broadening p_T distribution with C.M. energy is clearly demonstrated in Fig. 3.

Changing $\langle p_T^q \rangle$ in the jet model to a value of 0.500 GeV reproduces $\langle p_T \rangle$ and $\langle p_T^2 \rangle$ but the resulting fit to the distribution is poor indicating that the correct explanation probably does not lie in a steady broadening of both jets.

Within QCD we expect one jet to broaden (by gluon emission) more frequently than both and we have searched for such indications within the data. In each event we have classified the two jets as a 'low $\langle p_T \rangle$' jet and a 'high $\langle p_T \rangle$' jet according to their values of $\langle p_T \rangle$. We have then evaluated $\langle p_T \rangle$ and $\langle p_T^2 \rangle$ for each of these categories, the results for the latter quantity being summarized in Table 4.

A bias is clearly introduced in the selection of the jets. However the difference is not constant with energy but increases in a manner qualitatively consistent with the predictions of QCD.

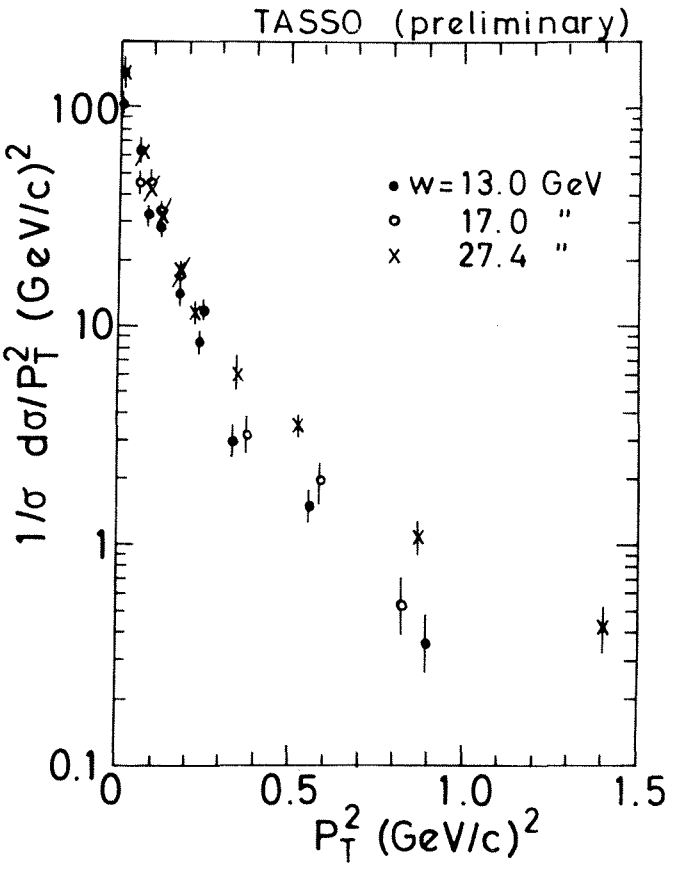

Fig. 5 The p_T^2 distribution measured relative to the spehericity axis.

Table 4

$\langle p_T^2 \rangle$ of 'low' and 'high' $\langle p_T \rangle$ jets

Energy GeV	13	17	27.4
$\langle p_T^2 \rangle_{low}$ GeV^2	0.105 ± 0.01	0.11 ± 0.01	0.18 ± 0.02
$\langle p_T^2 \rangle_{high}$ GeV^2	0.21 ± 0.02	0.24 ± 0.03	0.43 ± 0.05

Thus we conclude that the data are not represented by a two jet model but are qualitatively closer to a QCD interpretation. However the current statistical accuracy of the data precludes any quantitative proof of the QCD model. Finally we have some evidence for 3 jet events within our data[10].

5. CONCLUSIONS

The data (R, $S\frac{d\sigma}{dx}$) demonstrate general consistency with the simple quark model ideas without any compelling evidence for the existence of a new quark. The naive models of quark fragmentation leading to jets do not reproduce the data at 27.4 GeV, the predicted sphericity

and p_T^2 distributions being too narrow. However merely increasing $\langle p_T^q \rangle$ in the model is not the solution, the data being more in qualitative agreement with QCD. Before any quantitative conclusions on QCD can be drawn a much larger data sample is required together with a more detailed analysis of the events.

* * *

REFERENCES

1) R. Brandelik et al., PL 83B (1979) 261.

2) J. Parisi et al., PR D4 (1971) 2927;
S.J. Brodsky et al., PR D4 (1971) 1532;
S.J. Brodsky et al., PRL 41 (1978) 672.

3) G. Feldman, Invited paper at the XIX International Conference on High Energy Physics 1978, Tokyo, Japan.

4) B. Anderson et al., NP B135 (1978) 273;
R.D. Field and R.P. Feynman, NP B136 (1978) 1.

5) S.D. Drell et al., PR 187 (1969) 2159.

6) B.H. Wiik and G. Wolf, DESY 78/23.

7) J. Ellis et al., NP B111 (1976) 253.

8) A. de Rujula et al., NP B138 (1978) 387.

9) J.D. Bjorken and S.J. Brodsky, PR D1 (1970) 1416.

10) P. Soding, Invited paper at the EPS International Conference on High Energy Physics 1979, Geneva, Switzerland.

11) T. Meyer, Private communication.

12) H.G. Sander, Private communication.

EXPERIMENTAL SEARCH FOR T DECAY INTO 3 GLUONS

PLUTO Collaboration

Ch. Berger, H. Genzel, R. Grigull, W. Lackas, F. Raupach, W. Wagner,
I. Physikalisches Institut der RWTH Aachen.[6]

A. Kolvning, E. Lillestöl, E. Lillethun, J.A. Skard,
University of Bergen, Norway.[1]

H. Ackermann, G. Alexander[2], F. Barreiro, J. Bürger, L. Criegee,
H.C. Dehne, R. Devenish, G. Flügge, G. Franke, W. Gabriel, Ch. Gerke,
G. Horlitz, G. Knies, E. Lehmann, H.D. Mertiens, K.H. Pape, H.D. Reich,
B. Stella[3], U. Timm, P. Waloschek, G.G. Winter, S. Wolff, W. Zimmermann,
Deutsches Elektronen-Synchrotron DESY, Hamburg.

O. Achterberg, V. Blobel, L. Boesten, H. Kapitza, B. Koppitz, W. Lührsen,
R. Maschuw, R. van Staa, H. Spitzer,
II. Institut für Experimentalphysik der Universität Hamburg.[6]

C.Y. Chang, R.G. Glasser, R.G. Kellog, K.H. Lau, B. Sechi-Zorn, A. Skuja,
G. Welch, G.T. Zorn[4],
University of Maryland, U.S.A.[5]

A. Bäcker, S. Brandt, K. Derikum, C. Grupen, H.J. Meyer, B. Neumann,
M. Rost, G. Zech,
Gesamthochschule Siegen.[6]

T. Azemoon[7], H.J. Daum, H. Meyer, O. Meyer, M. Rössler, D. Schmidt,
K. Wacker,
Gesamthochschule Wuppertal.[6]

(Presented by S. Brandt)

ABSTRACT

The triplicity method was used to search for triple jets in the decay of T(9.46) into charged and neutral hadrons as an indication of the 3-gluon decay of the T. A comparison of the results with phase space, $q\bar{q}$ and 3-gluon predictions shows that the data is best described by a 3-gluon decay model.

1) Partially supported by the Norwegian Research Council for Science and Humanities.
2) On leave from University Tel Aviv, Israel.
3) On leave from University of Rome, Italy, partially supported by INFN.
4) U. of Md. General Research Board Grantee for 1978.
5) Partially supported by Department of Energy, U.S.A.
6) Supported by the BMFT, Germany.
7) Now at University College London, England.

Quantum chromodynamics predicts the 3-gluon decay of heavy quarkonium such as the $\Upsilon(9.46)$ meson and the $(t\bar{t})$ expected at higher mass. It should give rise to a 3-jet structure of the hadrons emitted in such decays. The observation of such a structure would be considered an important confirmation of QCD. In a previous paper[1] we have compared event topologies of charged hadrons from Υ decay with expectations from the 3-gluon process and other models. In the present study we also use information on neutral hadrons registered in the shower counters[2] (covering a solid angle of 94 % of 4π) which were added to the original PLUTO detector. Moreover, we tried to identify the 3 jets directly. Details of the experiment, the event selection criteria and the bin by bin subtraction of background from the non-resonating continuum and the Υ decay via the vacuum polarisation were already described[1,2].

To find the 3 jets the triplicity method[3] was used: The final state hadrons with the momenta $\vec{p}_1, \vec{p}_2, \ldots \vec{p}_N$ are grouped into 3 non-empty classes C_1, C_2, C_3 with the total momenta

$$\vec{P}(C_\ell) = \sum_{i \in C_\ell} \vec{p}_i; \qquad \ell = 1, 2, 3.$$

Triplicity is defined+) by

$$T_3 = (1/\sum_{i=1}^{N} |\vec{p}_i|) \max_{C_1,C_2,C_3} \{|\vec{P}(C_1)| + |\vec{P}(C_2)| + |\vec{P}(C_3)|\}.$$

It ranges between $T_3 = 1$ for a perfect 3-jet and $T_3 = 3\sqrt{3}/8 = 0.65$ for a completely spherical event. Those classes C_ℓ^* of particles yielding the maximum T_3 are identified with the hadrons originating from the fragmentation of the gluon ℓ. Thus the jet momenta are the $\vec{P}(C_\ell^*)$, cf. fig. 1. We rename them $\vec{P}_1, \vec{P}_2, \vec{P}_3$ with the convention $P_1 \geq P_2 \geq P_3$. The jet directions are given by the unit vectors $\hat{n}_\ell = \vec{P}_\ell / P_\ell$ and the angles between the 3 jets by

$$\cos\theta_1^J = \hat{n}_2 \cdot \hat{n}_3, \qquad \cos\theta_2^J = \hat{n}_3 \cdot \hat{n}_1, \qquad \cos\theta_3^J = \hat{n}_1 \cdot \hat{n}_2.$$

Then by identifying gluon and jet directions the gluon energies are (E_{cm} is the cm energy of the e^+e^- system)

$$E_\ell^J = E_{cm} \sin\theta_\ell^J / (\sin\theta_1^J + \sin\theta_2^J + \sin\theta_3^J)$$

or, in dimensionless variables, $x_\ell^J = 2 E_\ell^J / E_{cm}$.

+) It should be noted that thrust[4] is defined analogously by partition of momenta into 2 classes

$$T = (1/\sum_{i=1}^{N} |\vec{p}_i|) \max_{C_1,C_2} \{|\vec{P}(C_1)| + |\vec{P}(C_2)|\}.$$

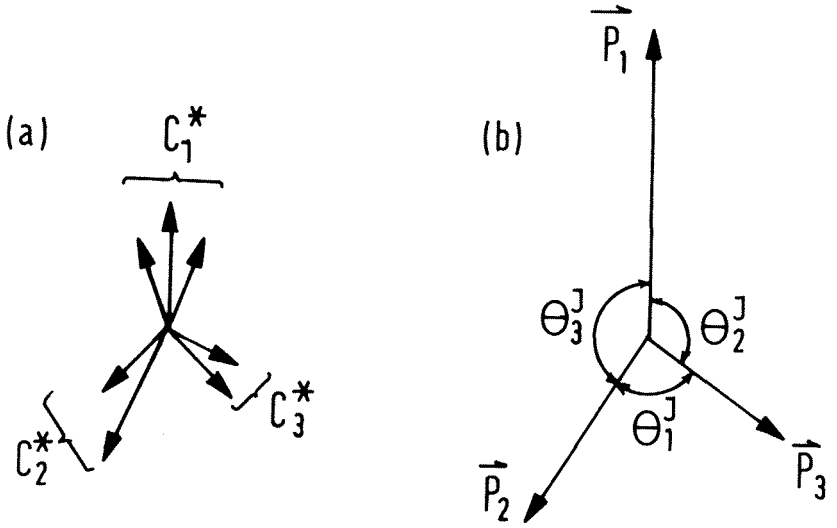

Fig. 1 Momentum configuration of hadrons (a) and jets (b) obtained by grouping hadrons into 3 classes.

The quantities E^J, x^J, θ^J as computed from the jets are expected to be identical to the gluon quantities E, x, θ only if the jets do not overlap in space. Since this is not always the case (expecially at the relatively low mass of the Υ) the measured quantities cannot be directly compared to theoretical predictions. We have therefore generated Monte-Carlo events using the 3-gluon decay matrix element[5] and giving the gluon jets the same features (transverse momentum and multiplicity distributions) as those we observed for hadron jets of similar energy in the continuum. For comparison we also generated $q\bar{q}$ two-jet events according to the Field-Feynman model[6] (using u, d and s quarks only) and events following a pure phase space with a mean multiplicity as observed on the Υ resonance. For the 3 sets of Monte-Carlo events the influence of the PLUTO detector and all experimental cuts were also simulated.

Our results are summarized in fig. 2 which shows the distributions of thrust T, triplicity T_3, the reconstructed gluon energies x_1^J, x_3^J and the angles between the gluon directions θ_1^J, θ_3^J. (It turns out that x_2^J and θ_2^J are not very discriminative. Therefore their distributions are not shown but the mean values are included in table 1 below.) In all distributions there is a clear difference between the data from the direct decay of the Υ (full data points) and the off-resonance events at E_{cm} = 9.4 GeV (open circles) which are subjected to the same analysis. The latter are rather well described by the Field-Feynman model. The Υ data are in very good agreement with the 3-gluon model. However, we observe a significant difference between the Υ data and phase space predictions. The observed mean values for the measured quantities and the corresponding predictions from the 3-gluon and phase space models are listed in table 1. The errors quoted are statistical only.

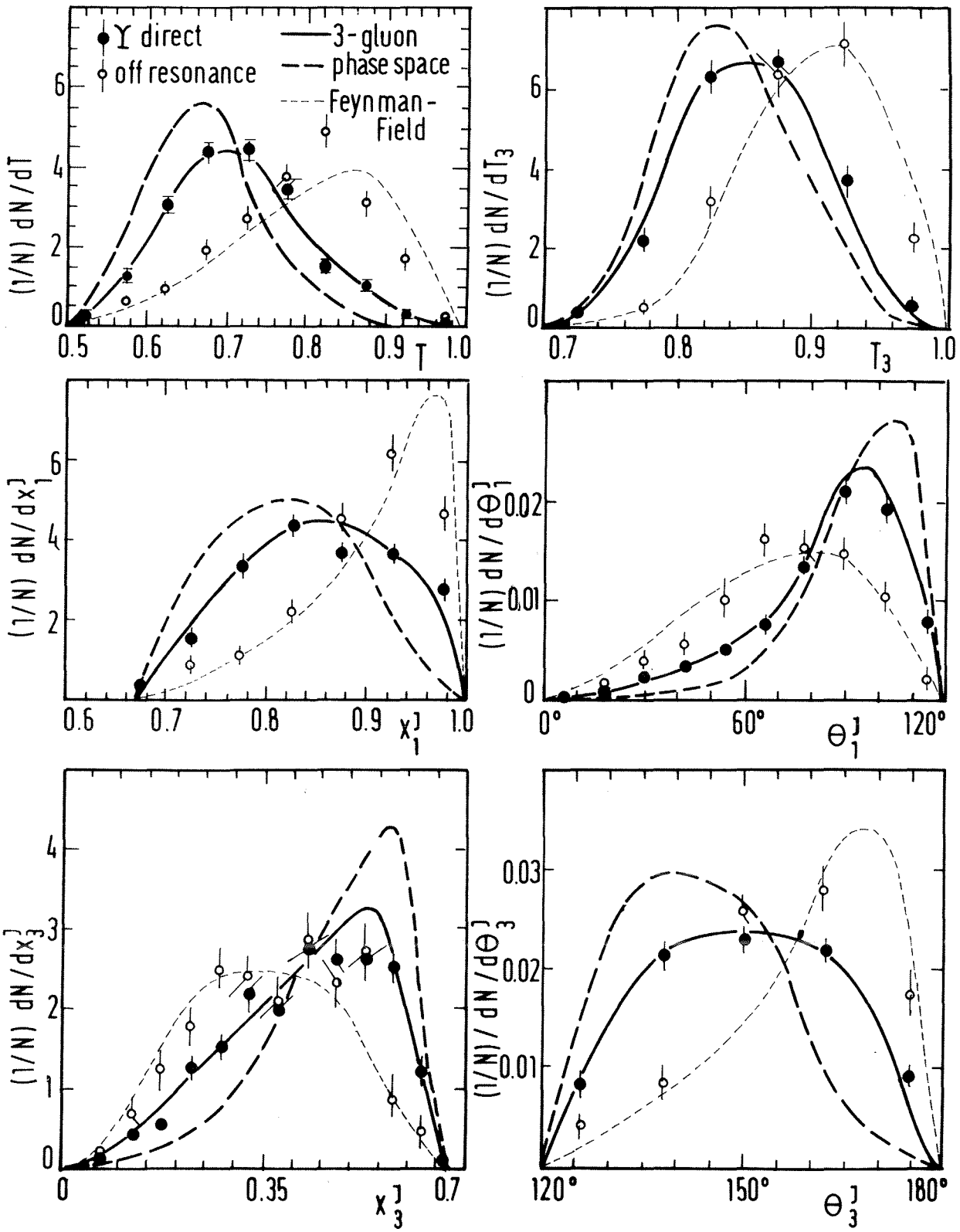

Fig. 2 Experimental distributions of thrust T, triplicity T_3 reconstructed gluon energies x_1^J, x_3^J and reconstructed angles θ_1^J, θ_3^J between gluons compared to Monte-Carlo calculations based on various models.

Table 1

Observed mean values and corresponding predictions of 3-gluon and phase space models.

	T direct data	3-gluon MC	phase space MC
$\langle T \rangle$	0.715 ±0.004	0.712 ±0.003	0.671 ±0.003
$\langle T_3 \rangle$	0.858 ±0.002	0.850 ±0.002	0.838 ±0.002
$\langle x_1^J \rangle$	0.855 ±0.004	0.853 ±0.003	0.819 ±0.002
$\langle x_2^J \rangle$	0.722 ±0.004	0.724 ±0.003	0.700 ±0.002
$\langle x_3^J \rangle$	0.423 ±0.006	0.422 ±0.005	0.481 ±0.004
$\langle \theta_1^J \rangle$	84.1^o $\pm 1.0^o$	85.5^o $\pm 0.8^o$	93.2^o $\pm 0.6^o$
$\langle \theta_2^J \rangle$	125.6^o $\pm 0.7^o$	124.3^o $\pm 0.5^o$	122.9^o $\pm 0.4^o$
$\langle \theta_3^J \rangle$	150.3^o $\pm 0.6^o$	150.2^o $\pm 0.5^o$	144.0^o $\pm 0.4^o$

In summary, we conclude that the decay structure of the T is clearly inconsistent with a simple $q\bar{q}$ or a pure phase space model. We cannot rule out more elaborate phase space models including resonances since these have many adjustable parameters. We should like to emphasize the fact that all experimental distributions are very well described if one assumes the 3-gluon decay of the T meson.

* * *

REFERENCES

1) PLUTO Collab., Ch. Berger et al., Phys. Lett. 82B (1979) 449.

2) PLUTO Collab., Ch. Berger et al., Phys. Lett. 76B (1978) 243 and Phys. Lett. 78B (1978) 176.

3) S. Brandt and H.D. Dahmen, Z. Physik C, Particles and Fields 1 (1979) 61.

4) S. Brandt, Ch. Peyrou, R. Sosnowski and A. Wroblewski, Phys. Lett. 12 (1964) 57; E. Farhi, Phys. Rev. Lett. 39 (1977) 1587.

5) K. Koller and T.F. Walsh, Phys. Lett. 72B (1977) 227; 73B (1978) 504; Nucl. Phys. B140 (1978) 449; K. Koller, H. Krasemann and T.F. Walsh, Z. Physik C, Particles and Fields 1 (1979) 71.

6) R.D. Field and R.P. Feynman, Nucl. Phys. B136 (1978) 1.

RESULTS FROM PLUTO AT PETRA

PLUTO Collaboration *

ABSTRACT

Results obtained at the e^+e^- storage ring PETRA by the PLUTO collaboration at c.m. energies of 13, 17 and 27.4 GeV are presented. New limits on QED cut-off parameters are determined from Bhabha scattering; at 27.4 GeV the limits are $\Lambda_+ > 38$ GeV and $\Lambda_- > 60$ GeV. The measured values of the total hadronic cross section, and the study of the jet character of the hadronic events are well consistent with the expected production of b mesons (with $q_b = 1/3$), but do not require additional new quarks with charge 2/3. Hadronic events from two-photon exchange processes are observed with comparable rates as events from one-photon exchange. First results on the hadronic cross section in $\gamma\gamma$ collisions are given.

1. INTRODUCTION

In this report results are presented obtained with the detector PLUTO at the e^+e^- storage ring PETRA. Since the start of physics runs in December '78 data were taken at c.m. energies E_{cm} = 13, 17 and 27.4 GeV. They allow a first look at hadronic final states from one-photon exchange[1] and two-photon exchange processes at previously unreached energies and allow sensitive tests on the validity of QED at large momentum transfers.

The detector PLUTO at PETRA has the following components: The inner detector consists of 13 cylindrical proportional chambers, operating in a magnetic field of 1.65 T. They provide a momentum resolution of $\sigma_p/p = 3\ \% \cdot p$ (p in GeV/c) at $p \gtrsim 3$ GeV/c. Photon and electron energies are measured in a set of shower counters. The central detector is surrounded by two lead scintillator shower counters:

1) $90^o > \Theta > 52^o$ cylindrical shower counters of 8.6 r.l.
2) $55^o > \Theta > 15^o$ end cap shower counter, 10.6 r.l..

In order to measure photons and electrons produced at small angles, the detector is equipped with two forward spectrometers, consisting of two shower counters:

3) $15^o > \Theta > 4^o$ lead scintillator shower counter (LAT), 14 r.l. with 4 planes of proportional tubes
4) $4^o > \Theta > 1.3^o$ lead glass shower counter (SAT), 12.5 r.l. with 4 planar proportional wire chambers.

For muon identification the flux return yoke is surrounded by an iron house, covered by planar drift chambers, to increase the total thickness of the hadron absorber to about 1 m iron equivalent.

The trigger, gated by the bunch crossing signal, is designed to be sensitive to QED events and to hadronic events from both one-photon exchange and two-photon exchange processes. The detector was triggered by one of the following conditions:

1) Two coplanar or $\gtrsim$ 3 arbitrary tracks detected by the wire logic of the central detector;
2) more than 3 GeV energy deposited in the central shower counter;
3) more than 3 GeV in both forward spectrometers;
4) 2 x 0.5 GeV or 1 x 3 GeV energy in the forward spectrometers together with either

* Contribution presented by V. Blobel

1 GeV shower energy or $\geq$ 1 track in the central detector.

2. BHABHA SCATTERING

The luminosity is determined by measuring the high rate of small angle Bhabha scattering $e^+e^- \to e^+e^-$, governed by small q^2, where QED is known to hold. The lead glass counters (SAT) of the forward spectrometer in the angular region $23 < \Theta < 70$ mrad are used for this purpose. This luminosity measurement has been checked with the Bhabha event rate in the LAT ($70 < \Theta < 260$ mrad), and in the central detector shower counters. The rates agree generally within 5 % (LAT) and 6 % (central detector). The total integrated luminosities are 43 nb^{-1}, 88 nb^{-1} and 103 nb^{-1} at 13, 17 and 27.4 GeV, respectively.

Bhabha scatters in the central detector are identified by the end cap and barrel shower counters, the charge signs by inner track chambers. The large angular region of $0.8 \gtrsim \cos\Theta \gtrsim -0.8$ allows a sensitive test on the validity of QED because of the very large q^2. Usually a possible break down of QED is described by a photon-propagator modification[2] in the lowest order Feynman diagrams. Introducing form factors F_T and F_S, depending on cut-off parameters Λ,

$$F_T = \left(1 \mp \frac{S}{\Lambda^2_{T\pm}} \right)^{-1} \qquad F_S = \left(1 \mp \frac{q^2}{\Lambda^2_{S\pm}}\right)^{-1}$$

the Bhabha cross section is modified to

$$\frac{d\sigma}{d\Omega} = \frac{\alpha^2}{2S} \left\{ \frac{q'^4 + S^2}{q^4} |F_S|^2 + \frac{2q'^4}{q^2 S} \mathrm{Re}\,(F_T F_S^*) + \frac{q'^4 + q^4}{S^2} |F_T|^2 \right\} (1 + c\,(\Theta))$$

$$S = 4\,E_{beam}^2 \qquad q^2 = -\,s \sin\Theta/2 \qquad q'^2 = -\,s \cos^2\Theta/2$$

The parameters Λ_T and Λ_S refer to timelike and spacelike photons, respectively, the plus and minus signs to different ways to formulate a modified QED. $c\,(\Theta)$ is a radiative correction term[3].

The data at all energies agree well with the QED expectation ($1/\Lambda^2 = 0$). A QED violation would show up in a deviation at large scattering angles ($\cos\Theta < 0$). A fit assuming $\Lambda_S = \Lambda_T$ results at all energies in values of $1/\Lambda^2$ consistent with zero. Converting the fitted values into lower limits at the 95 % C.L. of the cut-off parameter Λ we obtain the following values:

E_{cm} = 17 GeV	$\Lambda_+ > 37$ GeV	$\Lambda_- >$	49 GeV
E_{cm} = 27.4 GeV	$\Lambda_+ > 38$ GeV	$\Lambda_- >$	60 GeV

3. THE TOTAL HADRONIC CROSS SECTION

To select hadronic events, all background events from beam halo particles, beam-gas reactions, QED reactions, cosmic rays and also two-photon exchange reactions have to be separated. The event selection is done by requiring $\geq$ 2 non collinear ($\Delta\phi < 150^0$) charged tracks, and applying a cut in the energy observed in the central detector (including neutral energy). The latter cut is particularly effective to discriminate beam gas events. Radiative scatters are removed by excluding any 2 or 3 prong events in which a track had

an associated shower energy > 0.3 × E_{beam}. Contributions from τ-pair production are removed using the prong number and distribution of neutral energy of these events.

The acceptance factor ε of hadronic events is obtained from a Monte-Carlo study, using the Feynman and Field model[4] (with u, d and s quarks) in a realistic simulation of the detector. The result is ε = 0.72 (average). For the determination of the total cross section additional corrections are necessary for radiation effects (- 10 %), and for the estimated contribution by two-photon exchange events derived from a Monte-Carlo study. The resulting values of $R = \sigma_{had}/\sigma_{\gamma\gamma}$ are given below:

E_{cm} = 13 GeV	R = 5.0 ± 0.5	(statistical	
E_{cm} = 17 GeV	R = 4.3 ± 0.5	(statistical	±20% (system.))
E_{cm} = 27.4 GeV	R = 3.7 ± 0.8	(statistical	

The systematic errors of 20% are mainly due to uncertainties in the luminosity determination and in the acceptance calculation.

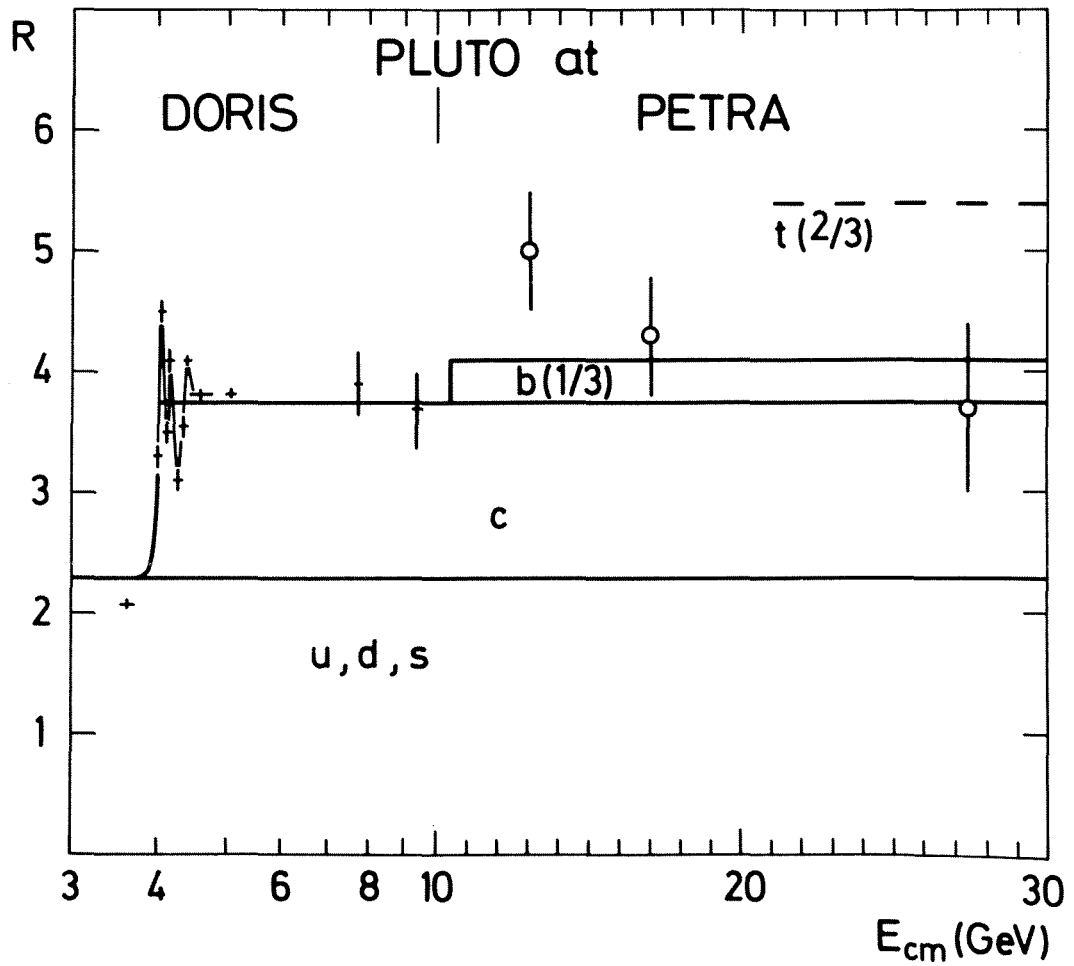

Fig. 1: Ratio R versus center of mass energy

The R values are shown in Fig. 1 together with values measured by PLUTO below 10 GeV[5]. The QCD expectation $R = 3 \Sigma Q_i^2 (1 + \alpha_s/\pi)$ is also shown. In the asymptotic regions the total cross sections are saturated by the contributions from the u, d, s and c quarks below 10 GeV, the higher energy data allow for a small increase due to a charge 1/3 quark (b). The 27.4 GeV data do not show evidence for an increase of R due to a potential new charge 2/3 quark (t).

4. JET ANALYSIS

For the investigation of the hadronic event topologies a minimum of 4 tracks was required in addition to the criteria given in Chapter 3. The jet character of the hadronic events[6] is measured by the quantity thrust, defined by

$$T = \max \frac{\sum_i |P_{Li}|}{\sum_i |p_i|}$$

where the p_{Li} are the longitudinal momenta w.r.t. an axis, which is chosen to maximize T. The range of T is between 1/2 for perfectly isotropic events and 1 for ideally jetlike events. If the transverse momenta of jet particles are assumed to be nearly constant with energy, the mean thrust should grow with increasing energy. Using the thrust axis as determined from all charged particles the ratio of $\langle p_L \rangle$ to $\langle p_T \rangle$ at $E_{cm} = 27.4$ GeV becomes as large as 3.1 ± 0.3.

Fig. 2a shows the observed mean values of $\langle 1 - T \rangle$ between 7.7 and 27.4 GeV, showing a clear decrease with increasing energy. The distributions of the observed thrust are shown in Fig. 2b-f for the different energies. Also shown are curves from a Monte-Carlo study based on the Feynman and Field model of quark parton jets, with full simulation of the detector and radiative corrections. The distributions generally follow the expected behaviour, using u, d and s quarks only. Also shown in Fig. 2a is the dependence of $\langle 1 - T \rangle$, if $b\bar{b}$ pair production and decay is included[7]. In the thrust distributions at higher energies the additional contributions for the c and b quarks are included. At 27.4 GeV in addition the expectation is shown, if a new heavy quark (2/3 charge) is added, assuming a threshold a few GeV below 27.4 GeV. No evidence is found for this additional contribution, which results in values of T around 0.7.

The observed mean transverse momenta w.r.t the thrust axis show a slight increase with energy between 13 and 27.4 GeV from 0.37 ± 0.01 to 0.43 ± 0.02 GeV. Part of this increase can be attributed to effects from the limited resolution and uncertainties in the determination of the jets axis. The effect of gluon emission in the quark pair production leads to a natural broadening of the energy flow in the final state, giving an increase of the mean transverse momentum. However, with present statistics no detailed analysis of these effects is possible.

5. TWO PHOTON EXCHANGE PROCESSES

Hadronic events from two-photon exchange processes[8] receive growing interest in the PETRA energy region. The basic diagram for this reaction is shown on top of the next page.

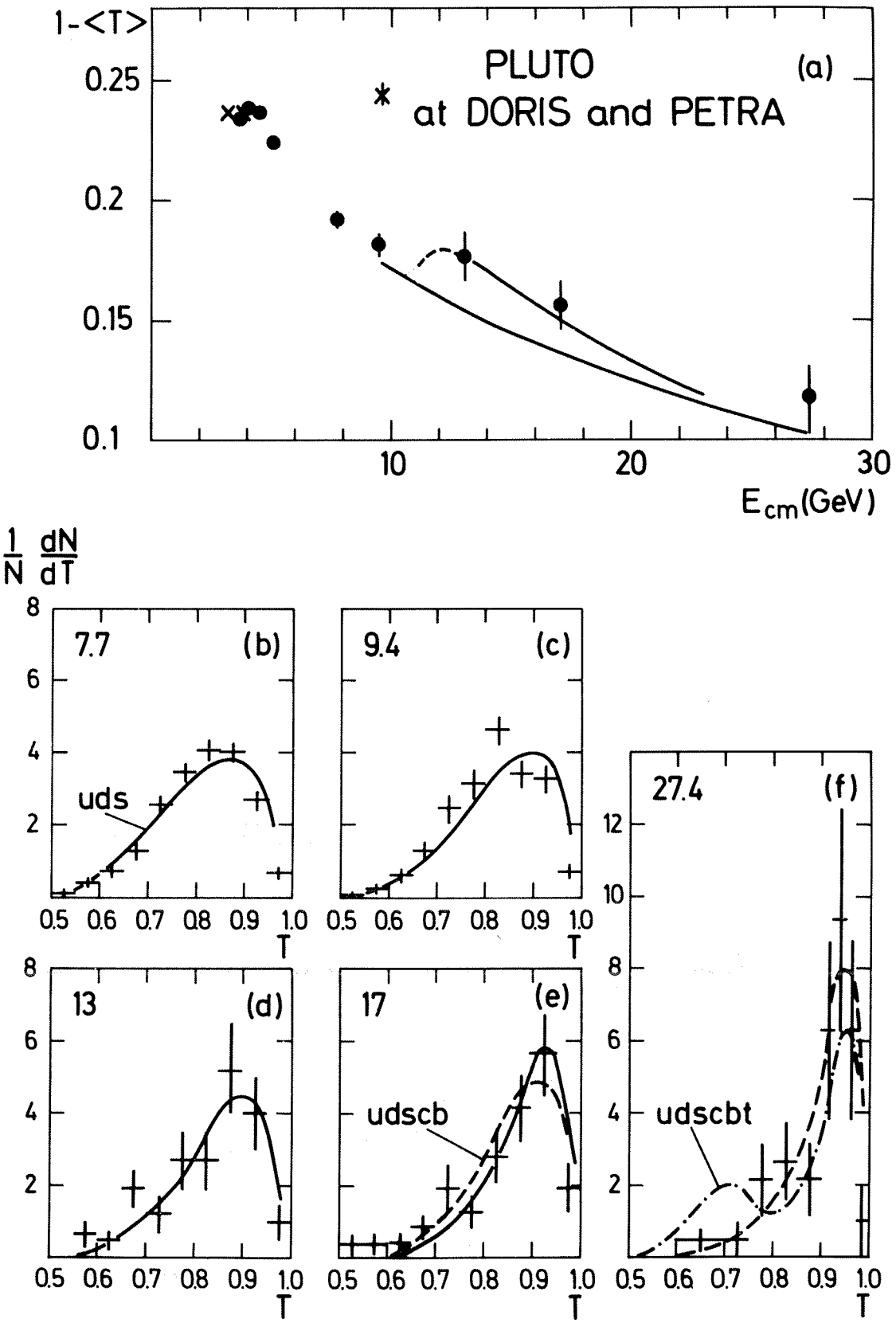

Fig. 2: (a) Mean observed values of <1-T> as a function of energy and (b) - (f) distributions of thrust for the different energies. The curves are explained in the text.

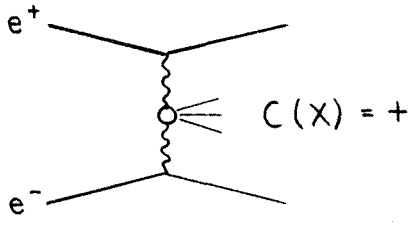

The genuine two-photon cross section $\sigma(\gamma\gamma \rightarrow$ hadrons) can be extracted from the measured cross section $\sigma(e^+e^- \rightarrow e^+e^- + X)$ using calculated flux factors of the incoming photons, usually in the 'equivalent photon approximation'. For a first analysis of our data taken at PETRA we have used events tagged in at least one of the forward spectrometers. The distribution of the vertices along the beam line, of the energy in the tagging counters and of the total energy and transverse momenta of the hadronic particles shows, that a 'single tag' is already a clean signature of 2γ events.

To reduce second order QED processes, we demand at least 3 particles in the central detector (3 tracks or 2 tracks + additional independent shower). Using tags in the SAT at 13 and 17 GeV (average $q^2 \approx 0.07$ and $0.11\ \mathrm{GeV}^2$), the sample consists of 51 events with a background of 11 events. The data are compared to the Monte Carlo expectation assuming a constant $\gamma\gamma$ cross section with a limited p_T of 300 MeV/c, with flux factors calculated in the equivalent photon approximation, which should be applicable at least in the region of high W of our sample. From a comparison to the data we get the total cross section $\sigma(\gamma\gamma \rightarrow$ hadrons) as a function of the visible invariant mass W_{vis}, shown in Fig. 3, together

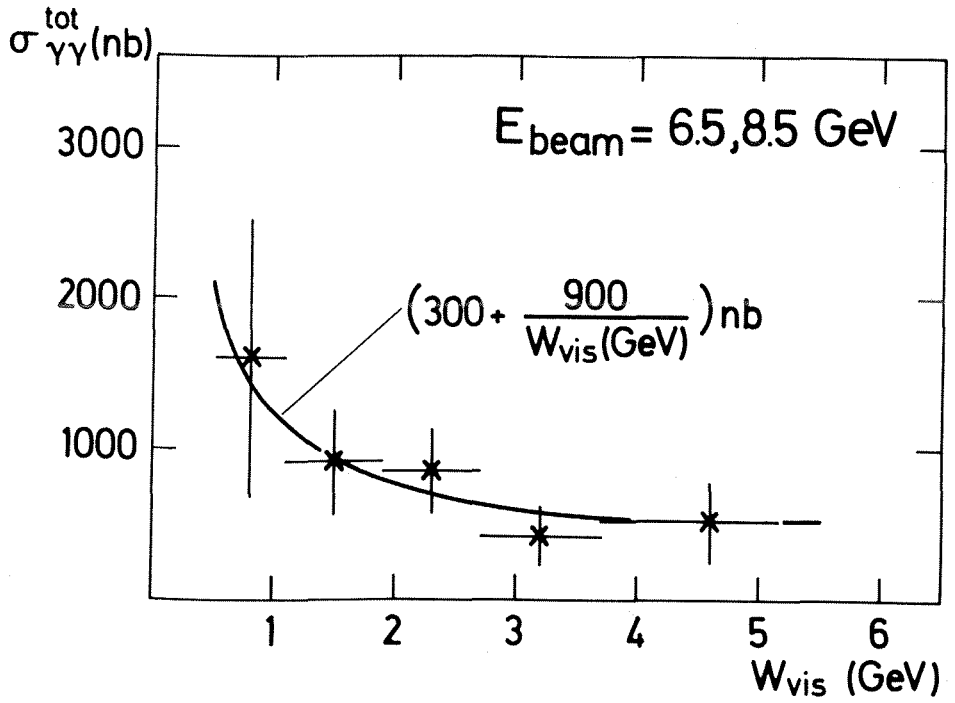

Fig. 3: First results on the total cross section $\sigma(\gamma\gamma \rightarrow$ hadrons) as a function of the visible invariant mass W_{vis}.

with a parametrization

$$\sigma(\gamma\gamma \rightarrow \text{hadrons}) = (300 + \frac{900}{W_{vis}(\text{GeV})}) \text{ nb.}$$

The constant term agrees in magnitude with the values expected for the diffractive part. The data taken at 27.4 GeV have an average q^2 as large as 0.4 GeV^2 even in the SAT; a preliminary analysis of these data indicates a q^2 dependence of hadronic production, which is being studied.

* * *

REFERENCES

1) PLUTO collaboration, Ch. Berger et al., Phys. Lett. 81B,410 (1979).

2) S.D. Drell, Ann. Phys. (New York) 4,75 (1958).

3) F.A. Berends, K.J.F. Gaemers, R. Gastmans, Nucl. Phys. B57,381 (1973); F.A. Berends, G.J. Komen, Nucl. Phys. B115,114 (1976) and Phys. Lett. 63B,433 (1976).

4) R.D. Field and R.P. Feynman, Nucl. Phys.B136,1 (1978).

5) PLUTO collaboration, J. Burmester et al., Phys. Lett. 66B,395 (1977); A. Bäcker, Thesis, Siegen (1977), Internal Report DESY F33-77/03 (unpublished); PLUTO collaboration, Ch. Berger et al., Z. Physik C1,343 (1979).

6) PLUTO collaboration, Ch. Berger et al., Phys. Lett. 78B,176 (1978).

7) A. Ali et al., DESY Report 79/16 (1979), to be published.

8) H. Terazawa, Rev. Mod. Phys. 45,615 (1973).

RESULTS FROM ADONE

R. Baldini Celio

Laboratori Nazionali di Frascati dell'I.N.F.N., Frascati, Italy.

ABSTRACT : A short review on recent experimental results obtained at Adone, on multihadronic $e^+ e^-$ annihilation is given.
Results and comments concern:
I) R values, compared with QCD and EVMD predictions,
2) Charged and neutral multiplicities, Threshold for "energy crisis", G parities and SU_3 checks,
3) $\sigma(2\pi^+ 2\pi^-)$: evidence for a large $\rho''(1600)$,
4) $\sigma(\pi^+ \pi^- 2\pi^0)$: non evidence for a $\rho'(1250)$,
5) $\sigma(2\pi^+ 2\pi^- 2\pi^0)$: evidence and interpretation of 1820.

-.-.-.-.-.-.-.-.-.-.-.-

The results I'll report about are partially the latest results coming from the Frascati $e^+ e^-$ storage ring Adone. Recently interesting results have been obtained on QED tests, search for an heavy electron, $\gamma\gamma$ interactions [I], but I dont have enough space to quote them. I'll concentrate on results on multihadronic $e^+ e^-$ annihilation, mainly coming from the $\gamma\gamma 2$ experiment. Soon results on total cross sections and two body reactions will come also from MEA and $B\bar{B}$ experiments.

Let me recall that Adone, which is the discoverer of the constancy of R, is an $e^+ e^-$ storagering covering the energy interval $1.4 \lesssim W \lesssim 3.1$ Gev with a typical luminosity $L \sim 2 \times 10^{29}$ cm^{-2} sec^{-1} at W=2Gev, which drops at W < 1.6 Gev.

Detectors features, several times reported, are sketched in Table I. In february 78 the $\gamma\gamma 2$ apparatus was modified to study more carefully the I.5 region. A resistive tubes core was added, increasing the total solid angle ($\sim$ 90%) and lowering the minimum energy ($T_{\pi^\pm} \gtrsim 20$ Mev) for tracking charged particles.

All data have been collected in sweeping mode. A first result, which comes adding all the Adone experiments, is that no ψ-like particle exists in the full energy range ($1.42 \lesssim W \lesssim 3.1$ Gev) at a level of $\sim 0.05\, \Gamma_{ee}(J/\psi)$ with 90% C.L..

Let me review the standard hypothesis done for calculating detection efficiencies to achieve cross sections:

I) produced particles are mainly π. From the bulk of data on $\sigma(k^\pm X)$, $\sigma(k^0_S X)$ by MEA, $\gamma\gamma$ ($\sigma(k^* k) \lesssim 8$nb, 95% C.L. at W= I.5 Gev) and mainly DCI-DMI we Know $\sigma(k\bar{k}X)/\sigma_{tot} \gtrsim 20$–30% at $W \gtrsim 1.6$Gev [2]: that means a correction on R evaluation, due to this hypothesis, which is $\sim$ 15% at I.6Gev and $\sim$ 0 at 3. Gev.

2) Particles momenta are distributed according an I.P.S. distribution. This hypothesis can be checked looking at the momenta inclusive distribution, which is well represented by a thermodynamical spectrum already at low energies, compared

with what is expected according I.P.S. weighting each process with its mean partial cross section (fig.I).

3) Isospin relations have been used, not necessary to get σ_{TOT}, but useful to reduce uncertainties on the smallest cross sections

I = 0 rigorous $\sigma(\pi^+\pi^- 3\pi^0) = 0.5\ \sigma(2\pi^+ 2\pi^- 1\pi^0)$

I = I stat. ground $\sigma(\pi^+\pi^- 4\pi^0) \simeq \sigma(3\pi^+ 3\pi^-) \simeq 0$

$R = \sigma_{TOT}(e^+e^- \to \text{hadrons}) / \sigma_{\mu\mu}$ behaviour

To have a complete panorama data at energies lower and greater than Adone covered energies are reported. Total cross sections have been evaluated by VEPP2M-OLYA data[3] assuming $\sigma(\pi^+\pi^-\pi^0)$, not measured, to be negligible. Data from SPEAR-MARKI have been reanalysed by these people and are not the published ones. Data from DCI-M3N[4] have not been reported and are in general good agreement with Adone-$\gamma\gamma 2$ data. Two body reactions ($e^+e^- \to \pi^+\pi^-, K\bar{K}$) have not been considered.

As a comment on R behaviour two steps appear: a first step toward a plateau value ~ 2 at $W \lesssim 2$ Gev and a second step toward a plateau value ~ 2.5 at $2 < W \lesssim 3$ Gev.

In general theoretical expectations do not fit the first step in R, essentially because theories expect the asymptotic value $R_o = 3\sum_{q=1}^{3} Q_q^2 = 2$ should be reached from above also at the lowest energies (fig.2).

I) QCD prediction example[5] :

$$R_1 = 3\sum_{q=1}^{3} Q_q^2\, \beta_q\, \frac{3-\beta_q^2}{2}\left\{1 + \frac{4}{3}\alpha_s(W^2) f(\beta_q)\right\}$$

$m_u = m_d \simeq 0.34$ Gev $\quad m_\lambda \simeq 0.50$ Gev

$\alpha_s \simeq 12\pi / 33 \ln \frac{W^2}{\Lambda^2}$. $\Lambda \simeq 0.5$ Gev $(\Gamma_{ee}(J/\psi))$

$f(\beta) \simeq \frac{\pi}{2\beta} - \frac{3+\beta}{4}\left(\frac{\pi}{2} - \frac{3}{4\pi}\right)$

2) EVMD + local duality prediction[6] :

simple choices reported here work very well on $J/\psi, \Upsilon$ families and predict $R_o = 2.5$

ρ FAMILY $\quad \Delta M_i^2 = 1\ \text{Gev}^2$ OR $2M_\rho^2$ (VENEZIANO)

$\Gamma_i^{ee} \propto M_{e_i}^{-1} \quad \Gamma_i^{\tau\sigma} \propto M_{e_i}$

ω, ϕ FAMILIES : ACCORDING SU_3 SCALING

Multiplicities, G - parities

Mean charged and neutral multiplicities are reported in fig.3. New logW fits are reported also. Comparing neutral multiplicities with 0.5 times charged multiplicities clearly the so called "energy crisis"(usually interpreted as due to η 's production) appears at higher energies, in good agreement with SPEAR-MARKI data.

A threshold for such a phenomenon is at W~2 Gev.

Before considering the various channels cross sections let us divide them according their G - parities. $G^+ = \sum_n \sigma(\ n_{EVEN}\ \pi\ )$ dominance is expected. SU_3 gives a more precise prediction, if the quarks structure is ρ and ω - like :

$$\frac{|A(\gamma \to \zeta^-)|^2}{|A(\gamma \to \zeta^+)|^2} = \frac{\int_{m_\phi}^{W} \sigma(W, \zeta^-)\,dW}{\int_{m_\phi}^{W} \sigma(W, \zeta^+)\,dW} = \frac{|Q_u - Q_d|^2}{|Q_u + Q_d|^2} = \frac{1}{9}$$

Data have been collected at Adone in sweeping mode, so real means in energy can be done. Adone-$\gamma\gamma 2$ data are in fair agreement with SU_3 prediction, if no dramatic contribution to G^- is present for $M_\phi < W < 1.42$ Gev. DCI-M3N data disagree strongly with SU_3 predictions[3].

Channels cross sections

$\sigma(e^+e^- \to 2\pi^+ 2\pi^-)$

To fully interpret this cross section a full overlap should be useful among VEPP2M-OLYA and Adone-$\gamma\gamma 2$ data. Playing the exercise to fit this cross section with only one Breit-Wigner a large ρ"(I600) is obtained with $M_{\rho''} \simeq$ I600 Mev, $\Gamma_{\rho''} \simeq$ 500 Mev, $\Gamma^{ee}_{\rho''} \simeq$ 3 Kev. Dalitz plot analysis by MEA experiment strongly favoured $\rho'' \to \rho\pi\pi$ with $\pi\pi$ in S-wave respect to I.P.S..

$\sigma(e^+e^- \to \pi^+\pi^- 2\pi^0)$

Two contributions are expected to this cross section : 0.5 $\sigma(e^+e^- \to 2\pi^+ 2\pi^-)$ if the aforementioned ρ"(I600) is assumed (with $\pi\pi$ in S wave) and $\rho_{tail} \to \omega\pi^0$, which can be predicted by ω decay coupling constants[7]. This contributions, added incoherently, almost saturate the cross section at low energies. On the other hand ρ'(I250) is expected large by local duality[6] and common sense (in analogy with ψ, ψ' and Υ, Υ') :

$$M_{\rho'}\Gamma^2_{\rho'}/(M^2_{\rho''} - M^2_{\rho'}) = M_\rho \Gamma^2_e/(M^2_{\rho'} - M^2_\rho) \quad \Gamma_{\rho'} \cong \Gamma_\rho\, M_{\rho'}/M_\rho \quad \Rightarrow \quad \Gamma^2_{\rho'} \simeq 4 \text{ kev} : \sigma^{\rho'}_{PEAK} = 150 \div 250 \text{ nb}$$

$$\left(\Gamma^{\rho'}_{TOT} = 250 \div 150 \text{ Mev}\right)$$

No room exists for such a cross section. All other evidencies on ρ'(I250) coupling to γ appear questionable. The simplest conclusion is the ρ'(I250) does not exist or it is not coupled to γ .

$\sigma(e^+e^- \to 2\pi^+ 2\pi^- 1\pi^0) + \sigma(e^+e^- \to 2\pi^+ 2\pi^- 2\pi^0)$

Complications are present to achieve I,2 π^0 identification in detail. On large energy intervals certainly $\sigma(2\pi^+ 2\pi^- 2\pi^0)$ dominates. The agreement with DCI-M3N data is good only if $\sigma_4 = \sigma(2\pi^+ 2\pi^-) + \sigma(2\pi^+ 2\pi^- 1\pi^0) + \sigma(2\pi^+ 2\pi^- 2\pi^0)$ is compared.
The higher point at W = I.82 Gev represents, integrated in energy, the bump ($\Gamma \sim$ 30 Mev) already published by all the 3 experiments at Adone[8]. From these cross section

data $2\pi^+2\pi^-2\pi^0$ appears to be the resonant channel, with $\Gamma_{ee} < 100$ ev. A ϕ recurrence interpretation for this bump is unlike : Γ_{ee} is too small, there is no evidence for a kaonic signal in MEA experiment, simplest kaonic channels do not predict a signal mainly on a $\Lambda c^{\pm} n\pi^0$ channel. An interpretation as a barionium state is possible. In fact general rules predict (if $J^P = I^-$ barionium states exist) a Ba (I = 1) state near $N\bar{N}$ threshold and Ba (I = 0) state at lowest energies. π^0- transitions between these states are allowed, being the Ba (I = 1) main decay and 5π is the plausible Ba (I = 0) decay; therefore

$$Ba\,(I=1) \to \pi^0\, Ba\,(I=0) \to 2\pi^+2\pi^-2\pi^0$$

-.-.-.-.-.-.-.-.-.-.-.

References:

(I) C.Bacci et al., to be published on Physics Letters

(2) M.Spinetti,Rencontre de Moriond (I979)
A.Cordier, " " " "

(3) V.A.Sidorov,Comm. to High Energy Physics Conf.,Tblisi (I976)

(4) F.Laplanche,Comm. to Lepton-Photon Interaction Symp.,Hamburg (I977)

(5) T.Appelquist,H.D.Politzer,Phys.Rev. I2 (I975)43

(6)M. Greco,Nuclear Phys. 63B (I973) 398
M. Greco,Phys. Lett. 77B (I978) 84

(7) F.M.Renard,Nuovo Cimento 64A (I969) 979

(8) B. Esposito et al., Phys. Lett. 68B (I978) 389; C.Bacci et al. Phys.Lett. 68B (I978) 393; G.Barbiellini et al.,Phys. Lett. 68B (I978) 397.

TABLE I

EXPERIMENT	$\gamma\gamma 2$	MEA	BB
TECHNIQUES	SCINT.+SPARK CH.+PB CONV. PROP.RES.TUBES CORE	MWPC+WG. SPARK CH.+ FE CONV. B=2-2.5 KG K/ 400 P 600 Mev/c	MAGNST.CH.+CAL.SCINT.+ FLASH TUBES
SOLID ANGLES $\frac{\Delta\Omega}{4\pi}$	TRIGGER=.4I+.I5 $C^{\pm}$ DET.=.90 γ DET.=.66	MAGN.AN.=.35	$C^{\pm}$ DET.=.75
$T_{\pi^{\pm}}$ TRIGGER CUTS	I20 Mev	I30 Mev	60 Mev
L MONITOR	ee WIDE ANGLES	ee WIDE ANGLES	ee WIDE ANGLES

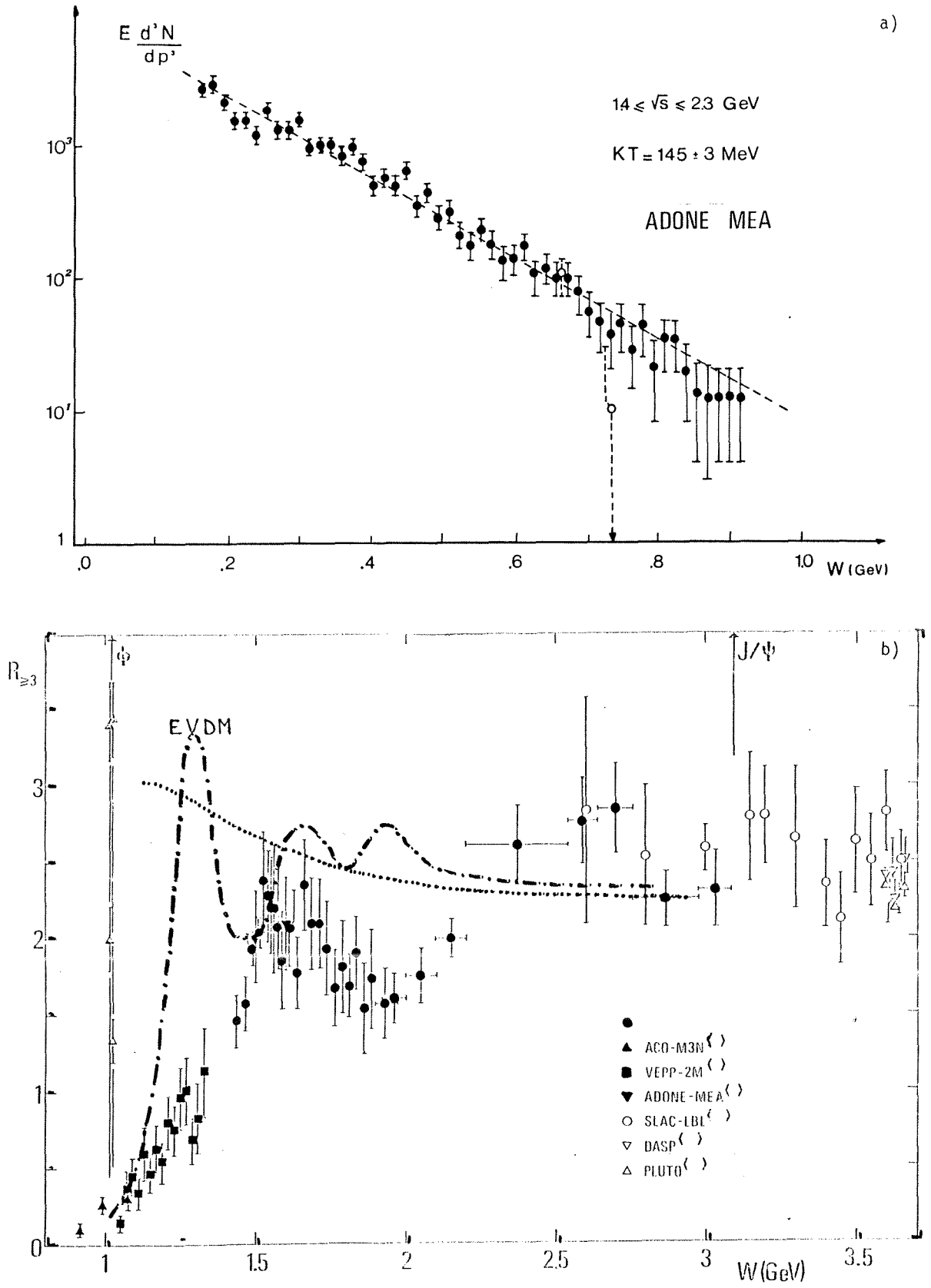
a)
E d³N/dp³
1.4 ≤ √s ≤ 2.3 GeV
KT = 145 ± 3 MeV
ADONE MEA
10³
10²
10¹
1
.0
.2
.4
.6
.8
1.0
W (GeV)
b)
R≥3
Φ
J/Ψ
EVDM
3
2
1
0
1
1.5
2
2.5
3
3.5
W(GeV)
ACO-M3N
VEPP-2M
ADONE-MEA
SLAC-LBL
DASP
PLUTO

Fig. 1

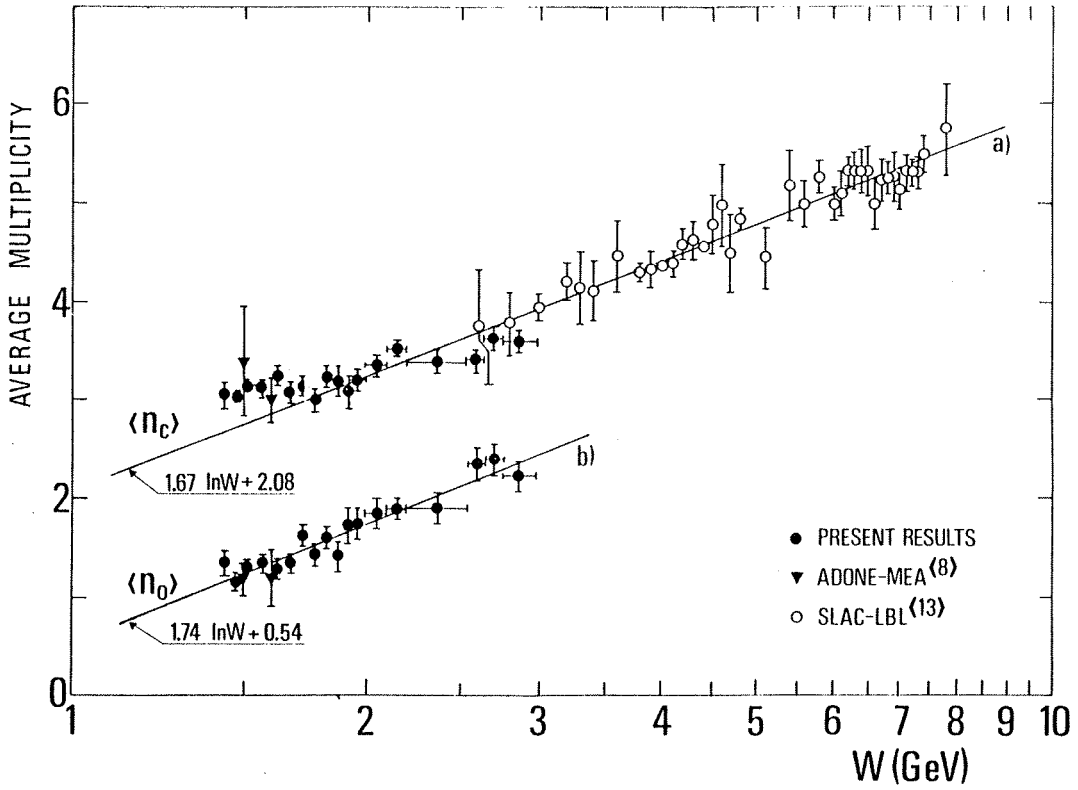
AVERAGE MULTIPLICITY
W (GeV)
⟨nc⟩
1.67 lnW + 2.08
⟨n0⟩
1.74 lnW + 0.54
a)
b)
PRESENT RESULTS
ADONE-MEA (8)
SLAC-LBL (13)

Fig. 2

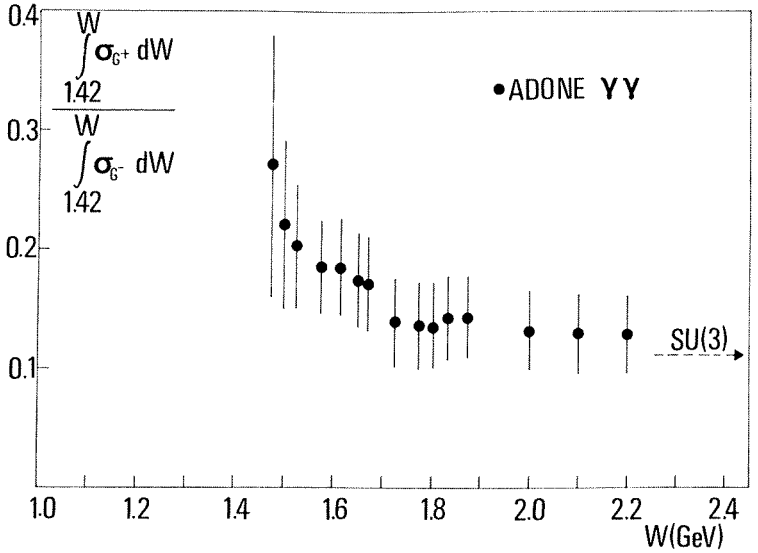
ADONE ΥΥ
SU(3)
W(GeV)

Fig. 3

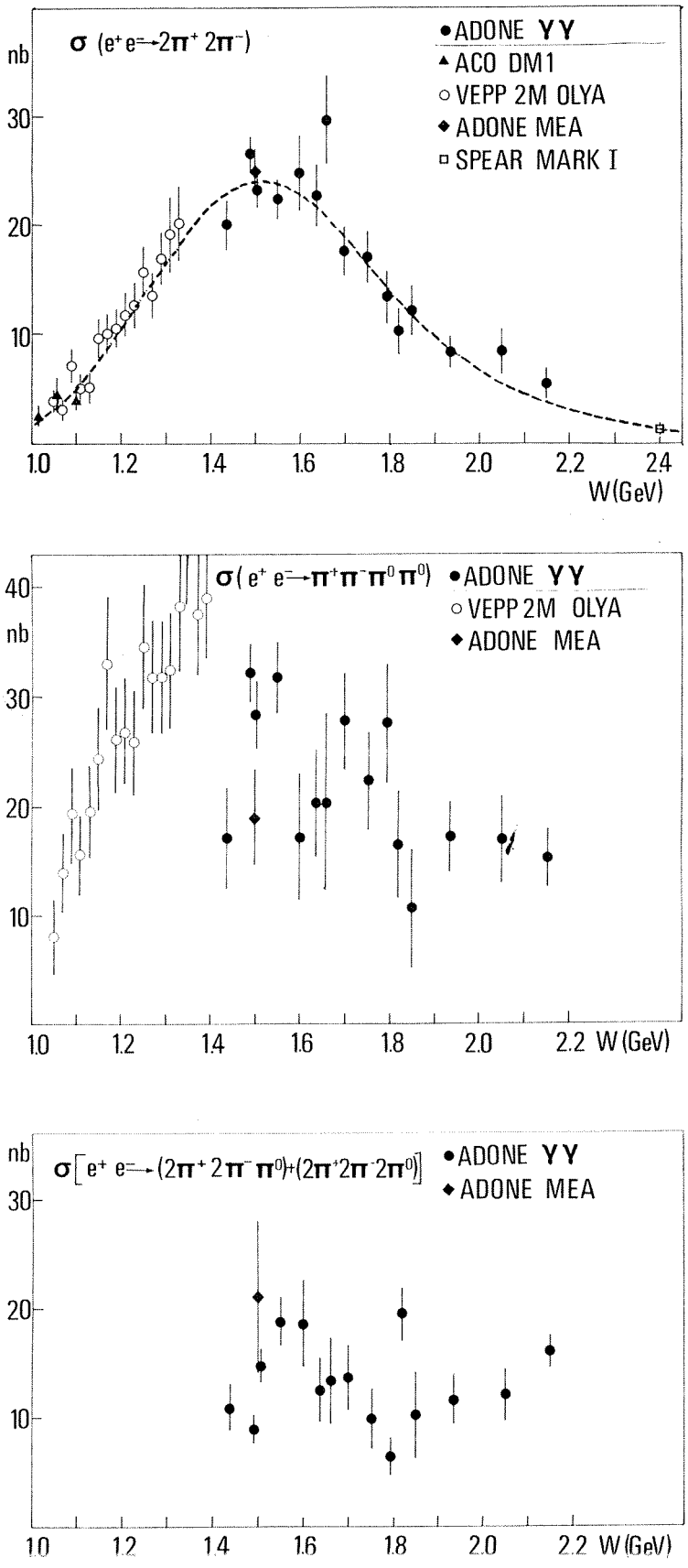
σ (e⁺e⁻→2π⁺2π⁻)
●ADONE γγ
▲ACO DM1
○VEPP 2M OLYA
◆ADONE MEA
□SPEAR MARK I
nb
30
20
10
1.0
1.2
1.4
1.6
1.8
2.0
2.2
2.4
W(GeV)
σ(e⁺e⁻→π⁺π⁻π⁰π⁰)
●ADONE γγ
○VEPP 2M OLYA
◆ADONE MEA
40
nb
30
20
10
1.0
1.2
1.4
1.6
1.8
2.0
2.2 W(GeV)
σ[e⁺e⁻→(2π⁺2π⁻π⁰)+(2π⁺2π⁻2π⁰)]
●ADONE γγ
◆ADONE MEA
nb
30
20
10
1.0
1.2
1.4
1.6
1.8
2.0
2.2 W(GeV)

Fig. 4

SOME FIRST RESULTS FROM THE MARK II AT SPEAR

G.S. Abrams, M.S. Alam, C.A. Blocker, A.M. Boyarski, M. Breidenbach, C.H. Broll, D.L. Burke, W.C. Carithers, W. Chinowsky, M.W. Coles, S. Cooper, B. Couchman, W.E. Dieterle, J.B. Dillon, J. Dorenbosch, J.M. Dorfan, M.W. Eaton, G.J. Feldman, H.G. Fischer, M.E.B. Franklin, G. Gidal, G. Goldhaber, G. Hanson, K.G. Hayes, T. Himel, D.G. Hitlin, R.J. Hollebeek, W.R. Innes, J.A. Jaros, P. Jenni, A.D. Johnson, J.A. Kadyk, A.J. Lankford, R.R. Larsen, M.J. Longo, D. Lüke, V. Lüth, J.F. Martin, R.E. Millikan, M.E. Nelson, C.Y. Pang, J.F. Patrick, M.L. Perl, B. Richter, J.J. Russell, D.L. Scharre, R.H. Schindler, R.F. Schwitters, S.R. Shannon, J.L. Siegrist, J. Strait, H. Taureg, V.I. Telnov, M. Tonutti, G.H. Trilling, E.N. Vella, R.A. Vidal, I. Videau, J.M. Weiss, H. Zaccone.

Presented by J.M. Weiss†

†Stanford Linear Accelerator Center
Stanford University, Stanford, California 94305

and

Lawrence Berkeley Laboratory and Department of Physics
University of California, Berkeley, California 94720

ABSTRACT

Preliminary results are given from the Mark II experiment at SPEAR on radiative decays of the $\psi'(3684)$ and on inclusive baryon production from 3.67 to 7.4 GeV center-of-mass energy. A 90% confidence level upper limit of 0.12% is given for $BR[\psi' \to \gamma\eta_c'(3455)] \times BR[\eta_c'(3455 \to \gamma\psi)]$.

1. INTRODUCTION

This paper presents some first results from the Mark II experiment at the Stanford Linear Accelerator Center e^+e^- storage ring facility SPEAR. These include results on:

i) radiative decays of the $\psi'(3684)$;

ii) inclusive baryon production in e^+e^- annihilation.

A number of other topics are discussed by G. Gidal elsewhere in these proceedings[1].

2. THE MARK II DETECTOR

A schematic diagram of the Mark II detector is shown in Fig. 1. Particles originating in the intersection region pass through a thin stainless steel vacuum pipe, a cylindrical scintillation pipe counter, 16 layers of cylindrical drift chambers[2], and a layer of 48 time-of-flight (TOF) scintillation counters.

They then may penetrate the 1.3 radiation length solenoidal coil and enter one of 8 lead-liquid argon (LA) shower counters[3] (14 r.ℓ.) which surround the inner detector. In addition, a muon detection system uses proportional tubes interspersed among the split magnet flux returns shown in Fig. 1 and additional iron absorbers on the top and sides which are not shown in the figure. Finally, both endcap regions of the detector are covered by additional shower detectors.

Performance features may be summarized here by:

i) 200μ average spatial resolution for the drift chambers which provide highly efficient tracking for $p > 100$ MeV/c over 75% of 4π ster. and some coverage out to 85% of 4π ster.

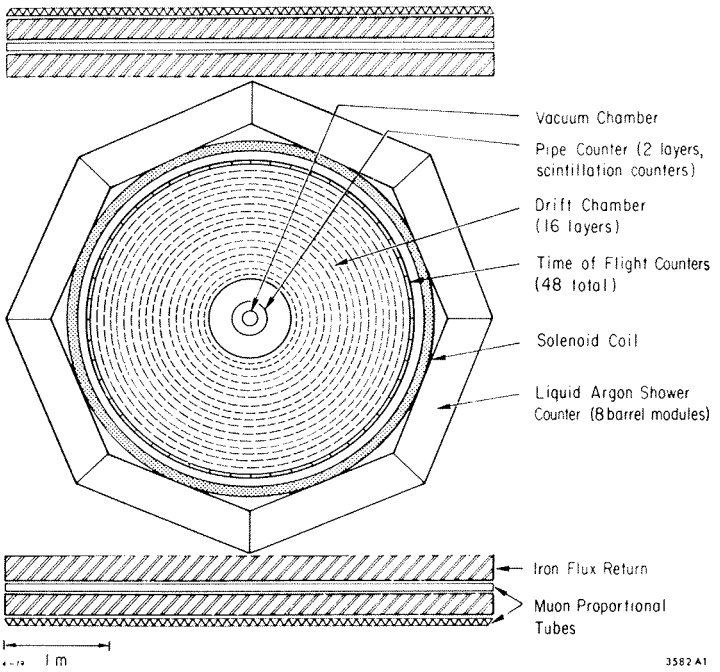

Fig. 1. Schematic view of the Mark II detector.

ii) 300 psec. time-of-flight resolution for hadrons (270 psec. for Bhabha events) over 75% of 4π ster. giving 1σ π/K separation at 1.3 GeV/c and 1σ K/p separation at 2.0 GeV/c.

iii) $\delta E/E = .12/\sqrt{E}$ (E in GeV) energy resolution for photons and electrons from the liquid argon shower counters which cover 73% of 4π ster. The efficiency of these devices has been measured using the photons in fully-constrained $\psi \to \pi^+\pi^-\pi^o$ and $\pi^+\pi^-\pi^+\pi^-\pi^o$ events and agrees well with detailed Monte Carlo calculations. This efficiency rises from about 30% at $E_\gamma = .15$ GeV to approximately 85% at $E_\gamma = .30$ GeV and 95% above .55 GeV.

3. RADIATIVE DECAYS OF THE $\psi'(3684)$

Events of the form

$$\psi' \longrightarrow \gamma\gamma\psi \qquad \psi \to \begin{cases} e^+e^- \\ \mu^+\mu^- \end{cases} \qquad (1)$$

are selected by the following criteria:

i) exactly 2 tracks of opposite charge from the primary vertex with an invariant mass between 2.8 and 3.4 GeV ($p_e < 1.75$ GeV/c).

ii) At least 2 photons found in the liquid argon, each separated from the nearest charged track by at least 0.2 m. ($E_\gamma > .1$ GeV). More than 2 photons are allowed due to the possibility of spurious "photons" generated from random preamplifier noise.

These events are then fit to the hypothesis (1) using the program SQUAW with 5 constraints. Figure 2(a) shows the $\gamma\gamma$ mass spectrum for events satisfying (1) with a $\chi^2 < 15$. The events in the prominent η peak at .548 GeV coming from $\psi' \to \eta\psi$ are then eliminated by requiring $m_{\gamma\gamma} < .530$ GeV, leaving events which are candidates for the desired cascade decay

$$\psi' \longrightarrow \gamma\chi \qquad \chi \longrightarrow \gamma\psi \qquad \psi \longrightarrow \ell^+\ell^- \tag{2}$$

The high mass $\gamma\psi$ combinations are plotted in Fig. 2(b) and show two clear peaks corresponding to the $\chi(3505)$ and $\chi(3550)$. In addition, there is a smooth background consistant in both size and shape with that expected from $\psi' \to \pi^o\pi^o\psi$. While there is no clear peak corresponding to the $\chi(3410)$, the events near that mass are consistant with the small branching ratio previously observed for that state[4,5,6,7]. On the other hand, there is no evidence in these data for a peak at 3455 MeV which has been previously reported[4] as $\chi(3455)$ and which has been suggested as a candidate for the pseudoscalar η_c'. Table 1 presents preliminary branching ratios obtained using our knowledge of the detector acceptance.

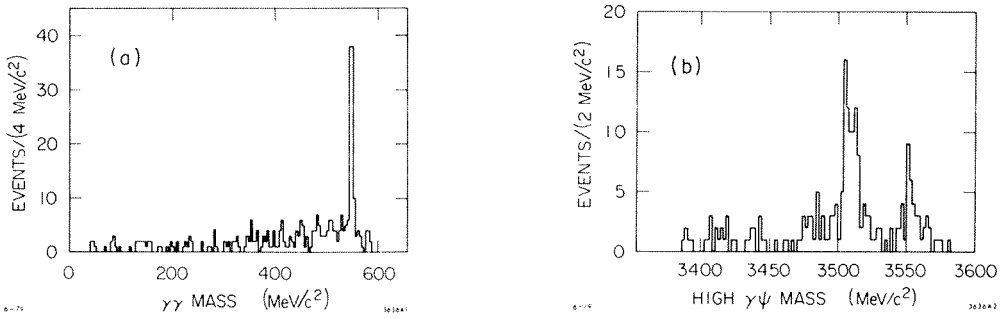

Fig. 2(a). $\gamma\gamma$ mass spectrum for events satisfying $\psi' \to \gamma\gamma\psi(\psi \to \ell^+\ell^-)$.

2(b). High mass $\gamma\psi$ combinations.

Table 1

Summary of Branching Ratios* $\psi' \to \gamma\gamma\psi$

	Mark II %	Mark I[4] %	DESY-Heidelberg[7] %
η	3.8 ± .5	4.3 ± .8	3.6 ± .5
$\chi(3550)$	1.2 ± .3	1.0 ± .6	1.0 ± .2
$\chi(3505)$	2.5 ± .3	2.4 ± .8	2.5 ± .4
$\chi(3455)$	<.12**	.8 ± .4	<.25
$\chi(3410)$	.08 ± .08	.2 ± .2	.14 ± .09

* $BR[\psi' \to \gamma\chi] \times BR[\chi \to \gamma\psi]$

** 90% confidence level

4. INCLUSIVE BARYON PRODUCTION IN e^+e^- ANNIHILATIONS

The inclusive production of $\bar{p}$, Λ and $\bar{\Lambda}$ has been studied with data concentrated in the center-of-mass energy range 4.5-6.0 GeV covering the region of a previously reported rise in $R(p+\bar{p})$[8]. Multi-hadron events with at least 3 detected tracks are selected. The time-of-flight system is used to identify p and $\bar{p}$ to 2.0 GeV/c using a weight method which is helpful above 1.3 GeV/c. However, only the $\bar{p}$ results are used here due to beam-gas backgrounds. The Λ and $\bar{\Lambda}$ are observed by their $p\pi^-$ and $\bar{p}\pi^+$ decay modes with an rms mass resolution of about 4 MeV.

Preliminary results, corrected for acceptance, are presented in Fig. 3 as a ratio of the inclusive cross-section to the μ-pair production cross-section. For the proton case, $R(\bar{p}+p) = 2\sigma_{\bar{p}}/\sigma_{\mu\mu}$. All errors shown are statistical only and do not include an estimated systematic uncertainty of ±30%, believed largely energy independent[9].

The measurements are consistant with previous experiments[8,10]. They show in detail, however, that the rise in the inclusive baryon production in e^+e^- annihilation is smooth and occurs principally between 4.6 and 5.2 GeV center-of-mass energy.

This work is supported by the U.S. Department of Energy under contract number DE-AC03-76SF00515.

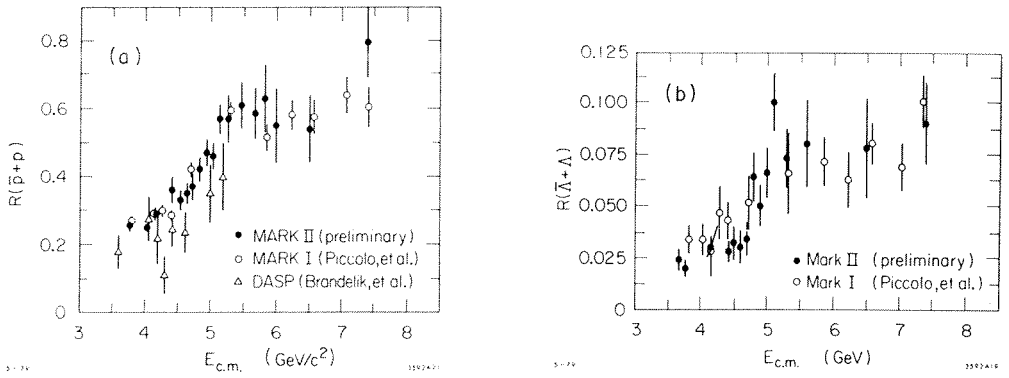

Fig. 3(a). Inclusive $\bar{p}$ production vs. c.m. energy.

3(b). Inclusive Λ and $\bar{\Lambda}$ production vs. c.m. energy.

REFERENCES

1) G. Gidal, Proc. of EPS Int. Conf. on High Energy Physics, Geneva, Switzerland, 27 June - 4 July, 1979.

2) W. Davies-White et al., Nucl. Instrum. and Methods 160, 227 (1979).

3) G.S. Abrams et al., IEEE Trans. on Nucl. Sci. NS-25, 309 (1978).

4) J.S. Whitaker et al., Phys. Rev. Lett. 37, 1596 (1976).

5) W. Braunschweig et al., Phys. Lett. 57B, 407 (1975).

6) V. Blobel, Proc. of the XIIth Rencontre de Moriond, Flaine, France, March 1977.

7) W. Bartel et al., DESY Report DESY 78/49 (1978).

8) M. Piccolo et al., Phys. Rev. Lett. 39, 1503 (1977).

9) This uncertainty is dominated by model dependence of the acceptance calculation which is still at a preliminary stage.

10) R. Brandelik et al., Nucl. Phys. B148, 189 (1979).

A STUDY OF e^+e^- ANNIHILATION INTO HADRONS IN THE 1600-2200 MeV ENERGY RANGE WITH THE MAGNETIC DETECTOR DM1 AT DCI

J.C. Bizot, J. Buon, A. Cordier, B. Delcourt, I. Derado*, P. Eschstruth, L. Fayard, J. Jeanjean, M. Jeanjean, F. Mané, J.C. Parvan, M. Ribes, F. Rumpf, J.L. Bertrand, D. Bisello**.

Laboratoire de l'Accélérateur Linéaire Université de Paris-Sud - 91405 Orsay.

ABSTRACT

We present here the results obtained with the Magnetic Detector DM1 on the Orsay e^+e^- colliding beams (DCI) for $1570 < \sqrt{S} < 2180$ MeV. The total integrated luminosity is 936 nb^{-1} over the whole energy range. Kinematics of annihilation events is determined by momentum measurements on the charged particles with an accuracy $\Delta p/p \simeq 2.5$ % at 500 MeV/c over a solid angle $\Omega = .6 \times 4\pi$ sr. Cross sections are given for e^+e^- annihilation into $p\bar{p}$, into four and five pions : $\pi^+\pi^-\pi^+\pi^-$ including $\rho^+\pi^+\pi^-$, $\pi^+\pi^-\pi^+\pi^-\pi^\circ$ including $\omega\pi^+\pi^-$, and into strange mesons K^+K^-, $K^\circ_S K^\circ_L$, KK^*, $K\bar{K}\pi\pi$ including $K^*K\pi$, inclusive K°_S. Limits on rare channels like baryonium states, $\phi^\circ\pi^\circ$, $\phi^\circ\eta^\circ$ are also obtained.

Data taking with the Magnetic Detector DM1 on the DCI colliding beam rings began in April 1978.

The detector [1] consists of four concentric cylindrical multiwire proportional chambers in a uniform magnetic field of .82T and covers a solid angle of $.6 \times 4\pi$ sr. In each chamber are measured both the azimuthal angle (in a plane normal to the beam line) and the longitudinal coordinate (along the beam line) of charged particle impacts with accuracy $r\Delta\phi = .7$ mm and $\Delta z = 2$ mm respectively. The thickness of each chamber is $.7 \times 10^{-3}$ Radiation Length, the vacuum chamber thickness being 12×10^{-3} R.L. The trigger requires that at least two charged particles reach the third chamber (75 MeV/c for the minimum transverse momentum). The system detects charged particles and measures their momentum with an accuracy $\frac{\Delta p}{p} = \frac{p}{500\ \text{MeV/c}} \times 2.5$ %. Twenty five scintillators surrounding the magnet are used to eliminate cosmic ray background by time of flight.

For every event we measure the time difference between the beam collision and the chamber signal. This allows us to make a very accurate estimate of the contamination of two body channels (e^+e^-, $p\bar{p}$, K^+K^-) by unidentified cosmic rays : the jitter of the chambers is 30 ns and the time between collisions is 300 ns.

We have used only the lower of the two DCI rings. The luminosity has been improved during the past year and now reaches 4.8×10^{29} cm^{-2} s^{-1} at 1.8 GeV total energy. Data were taken in energy steps of the same order as the beam dispersion (1 to 2 MeV total energy). The results are combined in wider intervals to get enough statistics. The energy intervals chosen are indicated by horizontal bars in the figures. The total analysed luminosity is 936 nb^{-1} over the energy regions 1570-1840, 1925-2060 and 2110-2180 MeV.

---

*) Present address : Max Planck Institut für Physik. D8 München 40, Germany.

**) On leave from Istituto di Fisica, ISN Sectione di Padova, Italy.

Selection of channels

Charged two body events (e^+e^-, K^+K^-, $p\bar{p}$) are selected by cuts on the angle ζ between the two tracks, the difference Δp between the two momenta, and the average value p_A of the two momenta. Typical cuts are $|\zeta - 180°| < 5°$ to $10°$, $\Delta P/p_A < 7$ to 15 % and p_A equal to the predicted value within 7 to 10 %.

Charged four body events ($\pi^+\pi^-\pi^+\pi^-$, $K^\circ_S(\to\pi^+\pi^-)$ $K^\pm\pi^\mp$, $K^+K^-\pi^+\pi^-$) are selected in three or four visible tracks. In the case of four visible tracks, cuts are applied on total momentum and reconstructed energy assuming the nature of the particles. For three visible tracks (not yet used for $K^+K^-\pi^+\pi^-$) cuts are applied on reconstructed energy with the momentum of the unseen particle set equal to the missing momentum.

For $\pi^+\pi^-\pi^+\pi^-\pi^\circ$, special care must be taken to avoid contamination by radiative four charged pion events. So we require a minimum missing momentum (12 % of the energy of one beam) and a minimum angle between the missing momentum and the beam line (10°).

K°_S are identified by their decay into $\pi^+\pi^-$. In order to suppress background from pion events, a minimum distance of 6 mm from the decay vertex to the beam line is required, cuts are also applied to the angle between the two pions, and to the direction of their total momentum. The background below the K°_S mass is estimated from side bins and subtracted.

Luminosity measurement

The on-line measurement is done with small angle Bhabha scattering[2]. The final determination is achieved using large angle Bhabha scattering. The e^+e^- are contaminated by unidentified cosmic rays (3 % very accurately known), $\mu^+\mu^-$ (8 % estimated by QED) and $\pi^+\pi^-$ (giving a 1 % systematic error). The two determinations agree with each other within 10 %. To the statistical error on the luminosity measurement (100 Bhabha events/nb^{-1}) we add a 10 % systematic error for possible uncontrolled variations of detection efficiency.

Efficiency determination

For each channel the efficiency has been determined by a Monte Carlo method taking into account the efficiency of detection of the MWPC and the production dynamics. As the detector does not cover a 4π solid angle, the efficiency may depend on the dynamics. We give the results for what we think the likeliest dynamics and include as systematic errors the differences with other possible dynamics. Radiative corrections of the bremsstrahlung type have been included in the Monte Carlo calculation. This has been done in the peaking approximation, using the formulas of Bonneau and Martin[3].

RESULTS

$p\bar{p}$ cross section

Events selection for this channel could not be done for the whole solid angle as the cosmic-ray veto-system is not sufficiently efficient : cosmic ray muons having the same momentum inside the apparatus as $p\bar{p}$ are stopped by the magnet coil or iron. We have used only the azimuthal range $-70° < \phi_p < 160°$ where cosmic-rays are scarce or enter the system through the scintillator in the direction of what we think to be the proton : a real proton

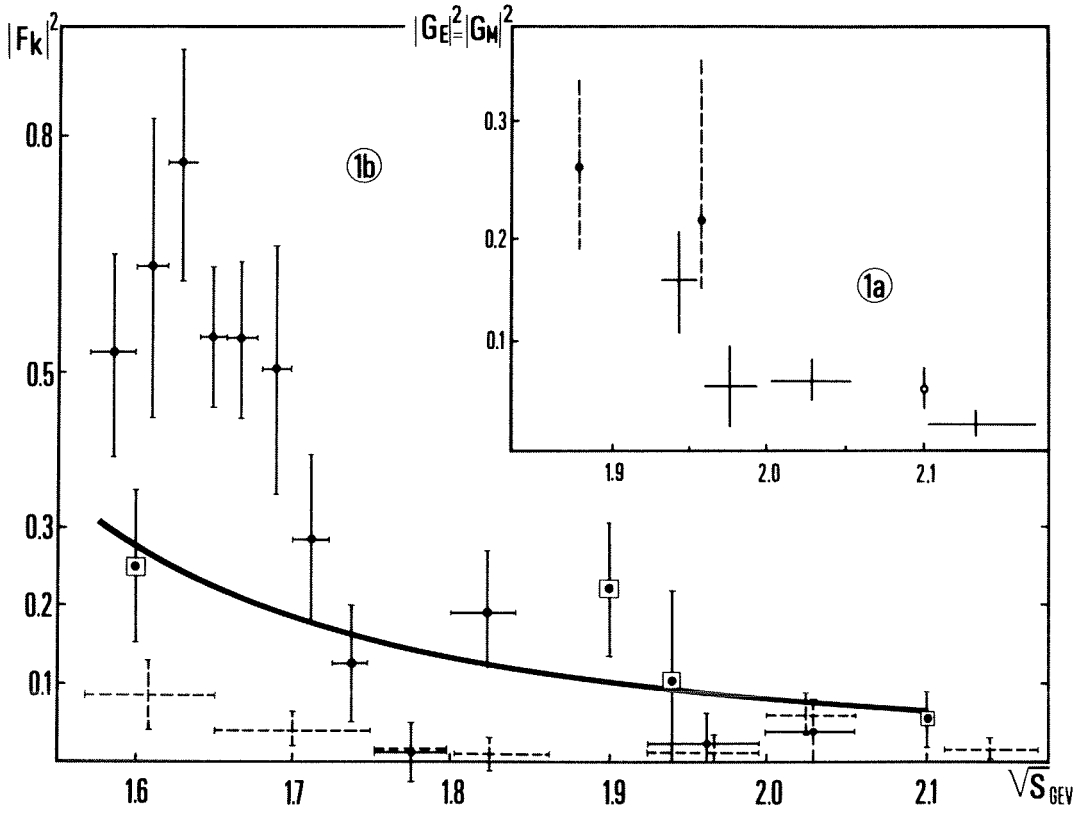

Figure 1 : Two body form factors
a - $p\bar{p}$ assuming $|G_E|^2 = |G_M|^2$
◊ ref.5) ♦ ref.4) + this experiment
b - K^+K^- and $K^\circ_S K^\circ_L$
K^+K^- = ⊡ ref.8) + this experiment - Full line theory ref.7)
$K^\circ_S K^\circ_L$ = -+- this experiment

cannot reach this scintillator at these energies. The signal obtained in the p_A distribution with the above cuts is quite clean. Assuming identical electric and magnetic form factors, the overall detection efficiency is ≃ 17 %. With the same assumption, fig. 1.a shows the squared form factor versus energy. Results of Castellano and al[4] and Bassompierre and al[5] are also shown.

The question arises whether one of the previously reported[6] baryonium states at 1935 and 2020 MeV could be a 1^{--} resonant state decaying into e^+e^-. Our results give the following limits on $\Gamma_{e^+e^-} B_{p\bar{p}}$ for these two states within 95 % confidence level.

$$m = 1935 \text{ MeV} \quad \Gamma = 9 \text{ MeV} \quad \Gamma_{e^+e^-} B_{p\bar{p}} < 1 \times 10^{-5} \text{ MeV}$$

$$m = 2020 \text{ MeV} \quad \Gamma = 24 \text{ MeV} \quad \Gamma_{e^+e^-} B_{p\bar{p}} < 2.5 \times 10^{-5} \text{ MeV}$$

K^+K^- and $K^\circ_S K^\circ_L$ cross section

The K^+K^- signal is clearly seen for $\sqrt{S} < 1700$. The efficiency is well known as there is only one form factor. It is equal to 27 %. For the K°_S channel we require a clearly recognized K°_S and a missing mass consistent with a K°_L. The signal is clear but weak. The efficiency amounts to 14 %. The form factors of K^+K^- and $K^\circ_S K^\circ_L$ are given in fig. 1.b. We see that the $K^\circ_S K^\circ_L$ form factor is 10 times less than the K^+K^- for $\sqrt{S} < 1700$ MeV indicating that $K\bar{K}$ is mainly produced by a pure SU3 photon. Fig. 1.b also gives the prediction obtained by Renard[7] using only ρ, ω and ϕ contribution, and the results of Bernardini and al[8].

$\pi^+\pi^-\pi^+\pi^-$ production

This channel has a rather large cross section in this energy range. Its dynamics are dominated by $\rho^\circ\pi^+\pi^-$ production but no clear structure is found either in the $\rho^\circ\pi^\pm$ invariant

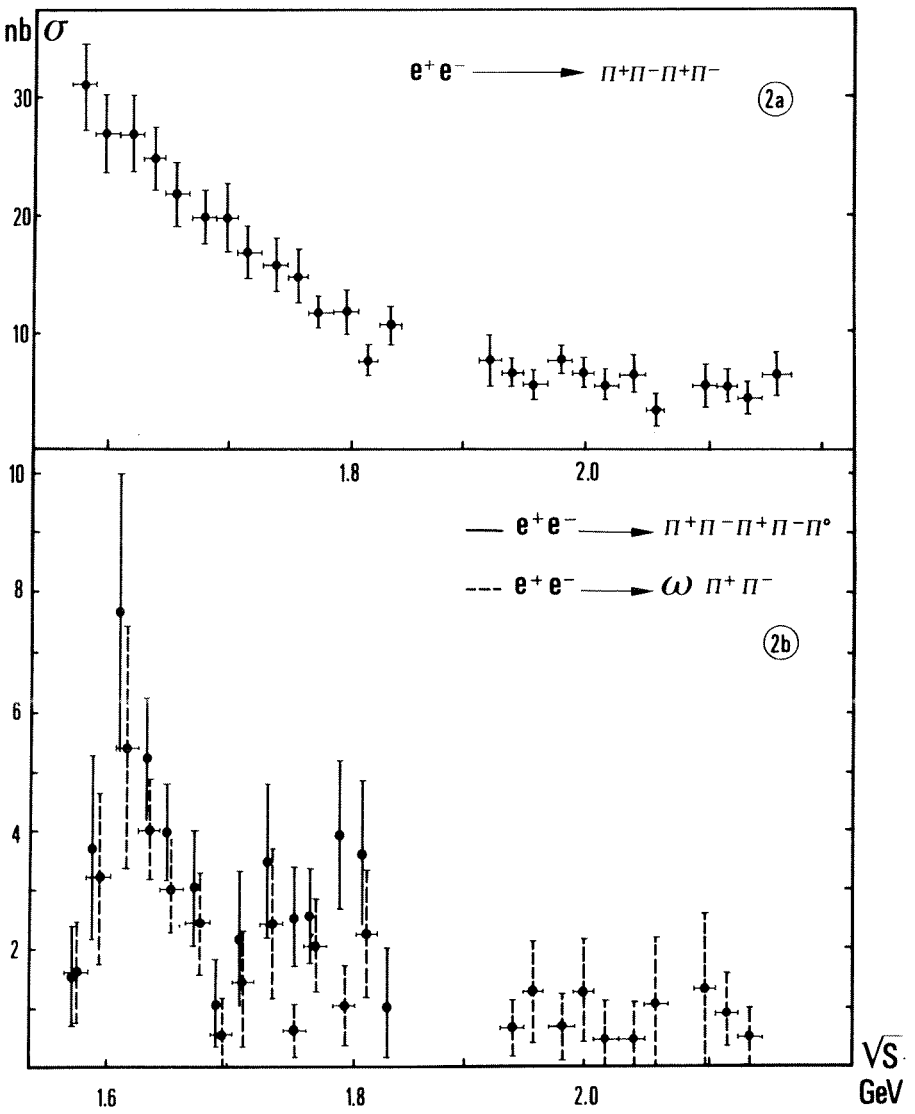

Figure 2 : Multipion cross sections
a - $\pi^+\pi^-\pi^+\pi^-$ b - $\pi^+\pi^-\pi^+\pi^-\pi^\circ$

mass distribution or in the $\pi^+\pi^-$ mass recoiling in front of the ρ. The efficiency depends on the production dynamics but is roughly the same for any simple dynamics as long as there is a ρ production : at 1800 MeV we get 42.2 % for pure phase space production and, for the following ρ production dynamics : 48.5 % for πA_1 (m = 1100, Γ = 300), 49.6 % for ρ plus a $\pi^+\pi^-$ pair in s wave, 51.0 % for $\rho\varepsilon$ (m = 1200, Γ = 600). So we have used at each energy the $\rho\pi\pi$ efficiency for computing the cross section (fig. 2.a). In the quoted error are combined quadratically statistical errors and an error of 10 % for possible variations of detection efficiency. To these errors we must add a 12 % systematic error for the dynamics and the luminosity determination.

The cross section agrees with the high energy part of previously reported ρ'[9].

$\pi^+\pi^-\pi^+\pi^-\pi^\circ$ production

In order to avoid contamination by $\pi^+\pi^-\pi^+\pi^-$, the events are selected from a region of the missing momentum-missing mass scatter-plot where this contamination is sufficiently weak. We have not yet completely analysed the remaining contamination and the cross section we give may be overestimated. However in the 1570-1700 MeV energy range, about 70 % of the selected events are seen to come from $\omega^\circ\pi^+\pi^-$ production. We are then able to determine correctly $\omega^\circ\pi^+\pi^-$ cross section. The efficiency depends only slightly on the production dynamics : 10.7 % for $\omega\pi^+\pi^-$ in phase space and 9.9 % for $\pi^+\pi^-\pi^+\pi^-\pi^\circ$ in phase space at 1650 MeV total energy. The results given fig. 2.b are not corrected for radiative effects and must be considered as preliminary.

$K^+K^-\pi^+\pi^-$ production

The $K^+K^-\pi^+\pi^-$ events are well separated on the scatter-plot : they have a zero total momentum and an apparent energy close to $\lambda\sqrt{S}$, assigning four pions masses ; λ varies with energy : .65 for $\sqrt{S} \simeq$ 1600 MeV to .8 for $\simeq$ 2150 MeV. Although the particles are not individually identified, we are able to study the production dynamics : we choose from the 4 possibilities the mass assignement giving the best value for the reconstructed energy. The production is dominated by $K^{*\circ}$ Kπ. No evident ρ structure appears in the high energy part (> 1925 MeV) of the data.

There is no evident structure either in three body mass spectra including the $K^{*\circ}$ or the $K^\pm\pi^\mp$ recoiling in front of $K^{*\circ}$. In particular $K^{*\circ}\bar{K}^{*\circ}$ production if any is weak. Again the efficiency depends on dynamics (8.9 % for pure phase space and 12.5 % for $K^{*\circ}$ with opposite Kπ in s wave at 2130 MeV) but is roughly the same for all simple dynamics producing $K^{*\circ}$. So we take this value for computing the cross section given in fig. 3.a.

Inclusive K°_S production

The efficiency for detecting a K°_S decaying into $\pi^+\pi^-$ is slightly momentum dependent and is evaluated by a Monte-Carlo technique. The production angular distribution is assumed to be isotropic. In the low energy part ($\sqrt{S}$ < 1800 MeV), where the KK^* production is dominant, this assumption introduces at most 10 % systematic error. The detection efficiency is essentially zero below 120 MeV/c. This loss at low momentum is estimated from an extrapolation of the momentum spectrum to zero momentum. The correction amounts to 5 %. The data are

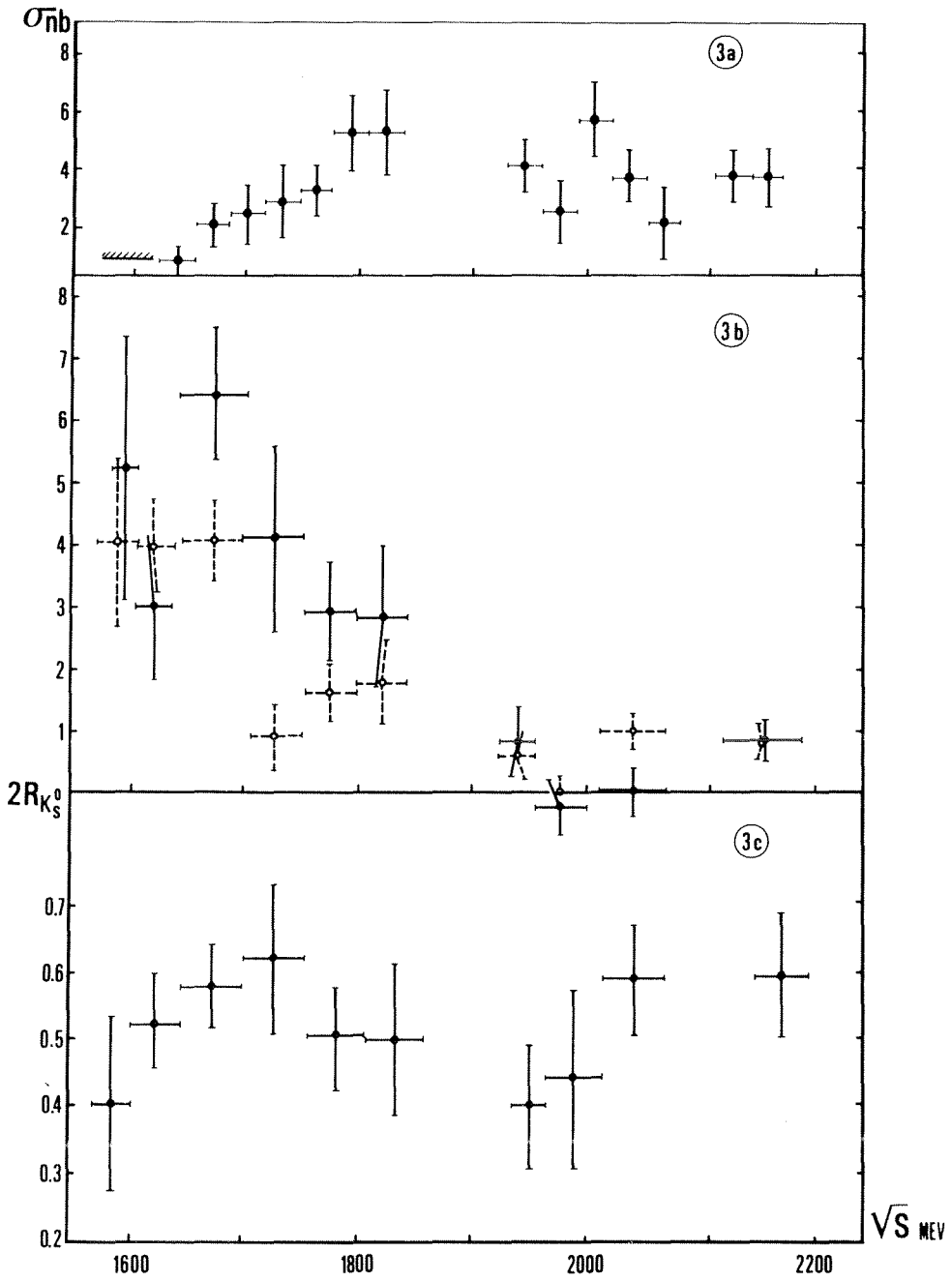

Figure 3 : Strange meson cross sections
a - $K^+K^-\pi^+\pi^-$ b - $K^0_S K^\pm\pi^\mp$: -⊕- and $K^0_S K^{*0}$ ⊕ c - $R_{K^0} = 2\,\sigma_{K^0_S}/\sigma_{\mu\mu}$

corrected for the unobserved decay mode $K^0_S \to \pi^0\pi^0$.

In fig. 3.c the neutral kaon production is compared to muon pair production. Assuming an equal number of K_S and K_L, the ratio $R_{K^0} = 2\sigma_{K^0_S}/\sigma_{\mu\mu}$ is given between 1570 and 2180 MeV. In this energy region R_{K^0} stays almost constant. Its value, about .5, is somewhat higher

than .33 as expected from the direct production of a $s\bar{s}$ pair by a photon.

$K^\circ_S K^\pm \pi^\mp$ production

This channel is selected from events with 3 or 4 visible tracks, two of them compatible with a decay $K^\circ_S \to \pi^+\pi^-$. No cut on the flight distance of the K°_S is necessary for the four prong events, as the contamination by other channels is small. We also require one of the two possibilities, assigning a K and a π to the two remaining tracks (one missing at most), to be equal to centre of mass energy within 2.5 %.

The kinematics of the observed events is consistent with a dominant K^*K production.

We select also the $K^\circ_S K^{*\circ}$ channel by requiring only a clearly recognized K°_S and a missing mass consistent with a $K^{*\circ}$.

Fig. 3.b shows the measured cross sections of $K^\circ_S K^\pm \pi^\mp$ and $K^\circ_S K^{*\circ}$. They are only important in the low energy region ($\sqrt{S}$ < 1800 MeV).

From these preliminary data, the $K^\circ K^{*\circ}$ production seems to be more important than the $K^\pm K^{*\mp}$ as is expected if KK^* is produced by a pure SU3 photon.

Upper limits on ϕ production

We have examined the K^+K^- pair at the ϕ invariant mass in $K^+K^-\pi^+\pi^-$ events and get the upper limit for $\sqrt{S}$ > 1775 MeV :

$$\sigma(\phi\pi^+\pi^-) < .5 \text{ nb} \qquad (90\ \%\ \text{C.L.})$$

We have also looked for $\phi\pi^\circ$ and $\phi\eta^\circ$ in all two prong events with two not aligned tracks : we assume that the two particles are K^+ and K^- and take the phase space for which the two kaons form a ϕ and the missing mass is consistent with a π° or a η° . We find for $\sqrt{S}$ > 1700 MeV :

$$\sigma(\phi\pi^\circ) < 2 \text{ nb} \qquad (90\ \%\ \text{C.L.})$$

$$\sigma(\phi\eta^\circ) < 2 \text{ nb} \qquad (90\ \%\ \text{C.L.})$$

* * *

REFERENCES

1) J. Jeanjean and al., Nucl. Instr. and Meth. 117, 349 (1974).
A. Cordier and al., Nucl. Instr. and Meth. 133, 237 (1976).

2) J.E. Augustin, Internal Report DCI 12-74.

3) G. Bonneau and F. Martin, Nucl. Phys. B27, 381 (1971).

4) M. Castellano and al., Nuovo Cimento 14A, 1 (1973).

5) G. Bassompierre and al., Phys. Lett. 68B, 477 (1977).

6) A.S. Caroll and al.,Phys. Rev. Lett. 32, 247 (1974), V. Chaloupka and al., Phys. Lett. 61B, 487 (1976), W. Bruckner and al.,Phys. Lett. 67B, 222(1977), P. Benkheiri and al., Phys. Lett. 68B, 483 (1977).

7) F.M. Renard, Nucl. Phys. B82, 1 (1974).

8) M. Bernardini et al., Phys. Lett. 46B, 261 (1973).

9) See for example G.J. Feldman in Proceedings of Tokyo Conference (1978) p. 777.

SESSION III

THEORY

Chairmen: S. Ferrara
H. Fritzsch
P. Matthews
B. Zumino

Sci. Secretaries: P. Aurenche
I. Bigi
A. Din
F. Martin
R. Petronzio
W. Zakrzewski

Rapporteurs talks:

J. Iliopoulos	Gauge symmetries
M.K. Gaillard	QCD phenomenology
A. De Rújula	Quantum chromo dynamite
G. Preparata	QCD: problems and alternatives

Invited papers:

J. Wess	Supergravity in superspace formulation
D.B. Fairlie	Instantons

GAUGE SYMMETRIES

J. Iliopoulos
Laboratoire de Physique Théorique de l'Ecole Normale Supérieure, Paris, France

"In the limited number of the mathematically existent simple field types and the simple equations possible between them, lies the theorist's hope of grasping the real in all its depth"

A. Einstein

ABSTRACT

This is a report on the recent applications of gauge theories to weak and electromagnetic interactions as well as grand unified theories. Due to the imposed length limitation it can be, at best, a compilation of subjects and references. For this reason I shall not cover topics which have been discussed extensively in other recent reports[1].

1. PRESENT ENERGIES

1.1 SU(2) x U(1)

Since the Tokyo conference last year nothing happened to shake our confidence in the simple $SU(2)_L \times U(1)$ [2,3] model of weak and electromagnetic interactions. Let me summarize briefly its present status :

The basic unit is a "family" consisting of fifteen two-component complex spinor fields organized in four left-handed doublets and seven right-handed singlets. The prototype is the electron family :

$$\begin{pmatrix} \nu \\ e^- \end{pmatrix}_L ; \quad \begin{pmatrix} p \\ n \end{pmatrix}_L^{\text{blue}} , \quad \begin{pmatrix} p \\ n \end{pmatrix}_L^{\text{white}} , \quad \begin{pmatrix} p \\ n \end{pmatrix}_L^{\text{red}}$$

$$e_R^- ; \; p_R, \; n_R \quad \text{(blue, white, red)}$$

The sum of the charges vanishes, as required by the cancellation of the triangle anomalies[4]. At present, we know of two complete families (electron-muon) and an almost complete third one (tau). No hint exists in the framework of $SU(2)_L \times U(1)$ concerning the total number of families. The gauge symmetry is broken spontaneously from $SU(2)_L \times U(1)$ to $U(1)_{e.m.}$ through a complex isodoublet of Higgs scalars[3]. In the simplest version, one neutral scalar particle survives.

Our confidence in this model is based on the following qualitative as well as quantitative predictions among which, all those who can be tested with existing machines, have been verified experimentally.

i) The neutral currents. In general, we would expect, for every flavor, a

parameter to determine the strength of the neutral current relatively to the charged one and another to fix the ratio of the vector and axial parts. In the simplest model[3], in which the breaking comes through isodoublet scalars, they are all expressible in terms of a single one, the angle θ_W. This is brilliantly confirmed by the fact that the values of θ_W from neutrino reactions and those from polarized electron scattering coincide.

ii) The charmed particles[5] were predicted to decay preferentiably to strange particles in agreement with observation. Their Cabibbo suppressed decays were also recently reported[6]. Mark II finds $\Gamma(D^0 \to \pi^+\pi^-)/\Gamma(D^0 \to K^-\pi^+) = 0.033 \pm 0.015$ and $\Gamma(D^0 \to K^+K^-)/\Gamma(D^0 \to K^-\pi^+) = 0.113 \pm 0.03$. A rough estimation yields $\sim \sin^2 \theta_c \sim 5\%$ with large uncertainties both from the presence of the other angles in the six family model[7] and the possible corrections to the simple-minded quark diagrams (penguin contributions etc.). I want also to mention that a similar order of magnitude agreement is obtained from the charmed particle production data in neutrino reactions where the Cabibbo suppressed process $\nu + d \to c + \mu^-$ competes with the allowed one $\nu + s \to c + \mu^-$ [8].

iii) The renormalisability of the theory requires the cancellation of triangle anomalies[4]. In the standard model this happens between leptons and quarks in the family. Therefore the discovery of a new lepton (τ) was interpreted as the opening of a third family. It seems that the b quark is healthy[9] and the discovery of t will confirm or invalidate this picture.

iv) The intermediate vector bosons are out of our reach for the moment. Their masses are fixed, as functions of θ_W. When $\sin^2 \theta_W$ varies from 0.2 to 0.23 we find $m_W \simeq 84 - 79$ GeV and $m_Z \simeq 94 - 90$ GeV. They will be discovered in the $p\bar{p}$ colliding beam facility, under construction at CERN[10]. The Z-γ interference may be seen earlier at PETRA or PEP, if the luminosity is sufficient. Note also that a richer group structure can produce lighter Z's with larger interference terms at low energies[11].

v) Finally, there is the prediction for the Higgs scalar (or scalars) but we shall come back to this problem presently.

Before finishing this brief review let me give an estimated time-table for the evolution of the subject in the near future. I will be glad to discuss privately with anyone wishing to bet on any of the detailed predictions. As I said at the beginning, the situation with the SU(2) x U(1) model looks perfect but alternative models do exist and, for a real experimental confirmation one has to go through the following steps :

i) For the moment what we know for sure is only that we have a Fermi theory of weak interactions with a very particular neutral current. In this theory the mass of the W plays the role of the cut-off. Assuming C.V.C., the magnitude of the radiative corrections to β- and μ-decays[12] gives us an upper limit for this cut-off of the order of 150 GeV.

ii) The next step will be the discovery of the W's and Z. Estimated time 3-4 years. By that time we shall know that Yukawa was right.

iii) A detailed study of their properties will reveal the existence of the Yang-Mills self-couplings[13]. Since it is a difficult experiment, even for L.E.P., I guess 12 to 15 years. Only then shall we know whether Glashow was right.

iv) This is still not good enough. We want to prove that we have a renormalizable field theory, i.e. we want to prove that Weinberg and Salam were right. I can offer no guess on how long it is going to take. If the Higgs is light it may be found earlier than the previous step, otherwise one has to be able to measure a higher order effect very precisely. Since this is a very important point I will discuss it in more detail.

1.2 The Higgs sector

The elementary scalar fields in gauge theories are needed in order to trigger the spontaneous symmetry breaking. Physical scalars are necessary for the taming of the high energy behaviour of scattering amplitudes. Notice that these points are precisely the least understood in the traditional framework of perturbation theory. In fact, in all known examples, this role is played by collective excitations, not by elementary fields. In superconductivity we just have a two-fermion correlation function, not even a bound state[14]. Furthermore, the mass generation through a Higgs scalar in the standard model is unsatisfactory because it requires the introduction of very small Yukawa coupling constants. For all these reasons I prefer to consider this system as a very convenient parametrization of our ignorance concerning the mechanism of spontaneous symmetry breaking as well as the high energy behaviour of the theory. Fortunately, the only measurable effect which depends on the existence of elementary Higgs fields is the physical scalar particle. In the case of a dynamical symmetry breaking[15] one expects a whole spectroscopy of bound states. In the Weinberg-Salam model one can derive rough order of magnitude limits for the mass of the remaining physical neutral particle : $0(10\ \text{GeV}) \lesssim m_H \lesssim 0(1\ \text{TeV})$[16,17]. The upper limit comes from the requirement that the quartic Higgs coupling constant stays smaller than one*), while the lower results from demanding that the radiative corrections to the effective potential do not upset the pattern of spontaneous symmetry breaking. In fact, if all the breaking comes from radiative corrections[19] one obtains $m_H \sim 10.5$ GeV [20] in which case its detection may be possible in the near future.

My own prejudice is that no Higgs scalar will be discovered even at LEP energies[21]. Notice that this will have no dramatic effect at any measurable process. For example, the predicted $e^+e^- \to W^+W^-$ cross section varies only by

(*) In the framework of grand unified theories (see below) this upper limit can be improved[18] by requiring that the φ^4 coupling constant does not increase too much up to the grand unification mass. A limit of 200 GeV is obtained.

about 5% when the Higgs mass moves from 10 GeV to 1 TeV [22], and this is still among the most sensitive ones. However, the upper limit shows that the absence of a Higgs scalar means that a sector of the theory will become strongly interacting, in other words one expects typical strong interaction behaviour (bound states, resonances, etc.) at energies of the order of 1000 GeV.

A particular realization of this idea is provided by the "technicolor" scheme[23] which assumes that the role of the Higgs particles is played by pseudoscalar bound states of a new type of quarks. These "techniquarks" develop strong interactions at a scale of 1 TeV where one expects a whole new spectroscopy of "technihadrons" (techni- ρ , techni- ω , etc.). The moral of the story is that physics may become rich and complicated, just a little above our reach.

1.3 The parameters of the SU(2) x U(1) model

In our present understanding of field theory, masses and coupling constants are, in general, free parameters to be determined by experiment. Symmetry principles (Poincaré, global internal symmetries, gauge symmetries or supersymmetries) impose relations among them but, until now, there has been no satisfactory way to compute, from first principles, the value of a mass or a coupling constant.

The simplest SU(2) x U(1) model with just one family contains 7 parameters which can be taken to be the three fermion masses, (the neutrino is assumed massless, so the model contains, in fact, a discreet γ_5 symmetry) the two coupling constants e and θ_W and, finally, the W-mass and the physical Higgs mass. Adding the n^{th} family brings 2n new parameters to a total of $n(n + 1) + 5$.

This growing number poses tantalizing questions, the first of which concerns the number of families[24]. It is clear that this question cannot be answered in the framework of the standard model but we can look for some experimental or theoretical hints. The observed helium abundance in the universe gives an upper bound for the number of massless (or nearly massless) neutrino types[25] and hence the number of families, assuming the neutrino will remain massless (maybe a dubious assumption). The surprising thing is that this number turns out to be small, 3-4. It may be that new neutrinos are not massless, after all, and a better determination of the ν_τ mass will be much welcome. Let me also mention that this astrophysical bound has been shown to be invalid if one assumes that the present universe contains a large net number of neutrinos of any type[26] (ν_e e.g.), comparable to the number of photons. I do not know of any reasonable mechanism to produce such number but, on the other hand, I feel uneasy with the thought that today, in 1979, we have discovered essentially all existing families.

Looking for theoretical hints, we first notice the upper limit of

sixteen quark flavors (i.e. eight families) before we loose the asymptotic freedom of Q.C.D.[27]. Furthermore we can put bounds on the masses of heavy fermions but I know of no way to translate them into bounds on the number of families. The fermion-Higgs Yukawa coupling constant becomes of the order of one when $m_f \sim m_W/g$. This means that strong interactions appear for fermion masses of a few hundred GeV. Similar conclusions can be reached by studying the contribution of fermion loops to the Higgs potential[28]. Notice, however, that both results depend on the simplest Higgs system of the Weinberg-Salam model.

An independent argument makes use precisely of the great success of the model, namely the relation $\rho = m_{W^\pm}^2/(m_Z^2 \cos^2\theta_W) = 1$ which, experimentally is equal to 1.004 ± 0.018. Fermion loops renormalize the masses of the intermediate vector bosons and we find[29]

$$\rho = 1 + \sum_f \frac{G}{8\sqrt{2}\pi^2}\left[m_1^2 + m_2^2 + \frac{2 m_1^2 m_2^2}{m_1^2 - m_2^2} \ln \frac{m_2^2}{m_1^2}\right]_f \qquad (1)$$

where the sum extends over all fermion isodoublets with masses m_1 and m_2. Notice that for $m_1 = m_2$ the correction in (1) vanishes, i.e. we get no information on the possible existence of fermion isodoublets with small mass splittings. If $m_2 = 0$ we obtain $\left[\sum_f m_1^2\right]^{1/2} \lesssim 500$ GeV. With increasing accuracy in the measurement of ρ this limit can be improved.

The conclusion is that a LEP with an energy $\gtrsim 100$ GeV/beam may discover all existing families.

Let me now consider the special case of the Kobayashi-Maskawa model with six families and seventeen parameters. We can try (i) to extract, as much as possible, their values from the available data or (ii) to enlarge the model with additional symmetries in order to obtain relations among them. The first direction has been reviewed recently[1], so let me only add some remarks concerning the second one[30].

We have the option of adding discreet or continuous symmetries. As a general rule, global continuous symmetries should be avoided since their breaking will produce unwanted Goldstone bosons. This leaves us with a group of the form $SU(2)_L \times U(1) \times K$ where K is either a discreet or a gauge symmetry(*). This central theme comes with a large number of variations. Discreet symmetries involve reflections and/or permutations of the fields and, among the gauge symmetries that have been used I would like to mention, in particular, the well-known $SU(2)_L \times SU(2)_R \times U(1)$ ref.[32] scheme and the $SU(2)_L \times U(1) \times SU(2)_H$ [33] model where $SU(2)_H$ mixes the different families "horizontally", i.e. the fermions which are singlets and doublets under $SU(2)_L$ transform as triplets of $SU(2)_H$.

All these models yield several interesting relations among masses and mixing angles, the most famous of which is

(*) Another possibility is to enlarge the group SU(2) itself. For a recent application of this idea see ref. 31).

$$tg\,\theta_c \approx \sqrt{\frac{m_d}{m_s}} \qquad (2)$$

If we take $m_d/m_s \sim 0.05$, eq. (2) gives $\theta_c \simeq 0.22$ rad. in excellent agreement with experiment.

Another commonly obtained mass formula is

$$m_t^2 \approx \frac{m_b^2\, m_\mu\, m_c}{m_d\, m_s} \qquad (3)$$

which predicts m_t roughly between 10 and 15 GeV, with large uncertainties.

All these relations are obtained in each model by a judicious choice of the Higgs system which often is quite complex. However I do not think that this complexity is, necessarily, a disadvantage of the theory. As I said earlier, I consider the Higgs mechanism as reflecting a deeper and, probably, rich structure and one should try to keep successful relations, like eq.(2), regardless of how many Higgs scalars it takes. The attractiveness of the model should not be judged by its Higgs sector.

If I gave the impression that our freedom in the choice and implementation of the additional symmetry K is such that any desired result could be obtained, let me correct it by quoting some general theorems of the no-go type, which tell us what is the price we must pay in each case. It turns out that the most important limitation comes from the requirement of avoiding flavor changing neutral currents. Strictly speaking we know nothing about their absence in transitions involving the b or t quarks, but it may sound reasonable and aesthetically attractive to raise this point to a general principle[34]. The price is the following : (i) quarks with the same helicity and charge have the same weak isospin[34]. This guarantees that no gauge bosons participate in flavor changing neutral processes to order G and αG. However, such processes may still occur through Higgs exchange. If one insists in their natural absence one obtains the second result[35].(ii) The Cabibbo-like mixing angles of the fermion mass matrix are either zero or undetermined.

1.4 CP violation

The predictions of the "standard" model are reviewed in ref.[1]. I have nothing new to add except to join in urging the experimentalists for an order of magnitude increase in the measurement of the CP violating parameter $|\varepsilon'|/|\varepsilon|$. This could allow for a distinction between the six-quark model and a superweak theory.

Let me instead say a few words on the problem of contaminating the strong interactions with P and T violation. We learnt that taking into account, in QCD, classical Euclidean field configurations with non-zero winding number (instantons) results into adding an effective term in the Lagrangian of the form[36]

$$\mathcal{L}_{eff} = \theta\, T_c\, \varepsilon_{\mu\nu\rho\sigma}\, F^{\mu\nu} F^{\rho\sigma}$$

$F^{\mu\nu}$ being the covariant curl of the gluon field. $\mathcal{L}_{eff}$ violates both P and T but, as long as QCD is considered alone, one could choose $\theta = 0$. However, this choice is not always possible in the presence of CP-violating weak interactions since one expects the value of θ to be renormalized by higher order corrections[37]. If one insists, as one should, on a natural (i.e. no parameter fitting) absence of T violation from strong interactions, one is faced with the following options : (i) The simplest solution is to have a massless quark for every axial U(1) current[38,39]. In the standard model this implies $m_u = 0$. Then $\mathcal{L}_{eff}$ can be rotated away. Unfortunately, one has to forsake some nice results on broken chiral dynamics[40]. (ii) The U(1) chiral symmetry could be spontaneously broken. No massless quark is required, but a pseudo-Goldstone particle should appear. One needs a non-minimal Higgs system and one of the surviving physical particles, the axion, will have a very small mass[39] (of the order of 1 MeV or smaller). Such a light particle seems to be excluded experimentally[39,41] and efforts to make it heavy in the framework of the standard model have not been very successful[42].
(ii) One could decide that weak interactions violate CP softly or spontaneously[43], in which case no infinite renormalization of θ is introduced. By a clever choice of the Higgs system the finite effects could be made small[44,45]. In particular, if the theory is left-right symmetric, non-vanishing contributions arise only at the two-loop level[45]. This gives $\theta_{eff} \sim 10^{-13}$ while the present limits on the neutron dipole moment require only $\theta_{eff} < 10^{-11}$. Some people have a prejudice against a spontaneous CP violation because it is generally believed that such violations disappear at high temperature and this would jeopardize the mechanism for producing a net baryon number in the early universe (see below). However, it has been recently pointed out[46], that such restoration of symmetry does not happen always. Maybe, one should check some realistic models from this point of view. (iv) Finally, one could stick to the simple solution of (i) or (ii) but remedy the shortcomings by introducing new kinds of quarks. For example, the technicolor scheme mentioned earlier can solve this problem[47] if one unifies at high energies (1 TeV) the color and technicolor groups into a simple gauge group. The absence or presence of fundamental scalars is not essential. In the second case, the corresponding axion will take its mass from the interactions that break the large gauge group and it will be one thousand times heavier.

1.5 Supersymmetry

Before leaving the domain of accessible physics I would like to mention some work based on supersymmetry[48]. Supersymmetry transformations change integer spin fields into half integer ones and vice versa ; thus a given irreducible representation contains both fermions and bosons. Their masses are degenerate, which implies that supersymmetry must be broken. The corresponding current is spinorial ; it follows that a spontaneous breaking will produce a massless Goldstone fermion[49]. It is tempting to identify it to one of the known neutrinos, (I just remind you that the only exact degeneracy in physics

involves the photon, the neutrinos and perhaps, the graviton) but this is incorrect. A Goldstone particle, boson or fermion, must satisfy Adler's low energy theorem[50], which says that the amplitude for emission or absorption of a soft Goldstone particle vanishes. The electron neutrino does not satisfy this condition[51]. The question now is : where is the Goldstone fermion ? We can give three answers : (i) Try to identify it with the right-handed neutrino, which, indeed, is not coupled[52]. (ii) Use the analog of the Higgs mechanism. This can only be done in supergravity. (iii) Introduce a new quantum number and contrive so that the Goldstone fermion, together with several other particles, carry it[53]. One can build realistic models based on this idea in which all particles have partners with the opposite statistics : the photon has a spin 1/2 "photino", the quarks have scalar associates, the gluons have spinor "gluinos" etc. The experimental consequences of such models have been examined in ref.[54]. For other applications of supersymmetry to unified theories see ref. [55].

2. GRAND UNIFIED THEORIES

2.1 SU(5)

As there is a "standard" gauge theory for low energy phenomena, in the same way, there is also a "standard" grand unified theory. The former is based on SU(3) x SU(2) x U(1), the latter on SU(5) [56]. In fact, it is the only group which contains a 15-dimensional ($\bar{5}$ + 10) anomaly free representation with the correct SU(3) x SU(2) x U(1) fermion assignment. I consider this fact as quite remarkable because, in order to obtain a successful grand unified theory, two things must conspire : the first is the group structure we just mentioned. The second comes from the dynamics. At present energies we have three distinct coupling constants. Each one evolves according to its own renormalization group equation. The three curves, with the appropriate normalization, must meet[57]. This is usually expressed as a prediction for $\sin\theta_W$. In SU(5) we obtain[57-60] $\sin^2\theta_W \sim 0.2 \pm 0.01$ while different weighted averages of experimental measurements give[59] $\sin^2\theta_W \sim 0.23$ with an error of about 0.015. This is still not the end of the story. The unification mass, i.e. the point where the three curves meet, is the mass of the gauge bosons which do not correspond to generators of SU(3) x SU(2) x U(1). They transmit highly forbidden processes such as proton decays (see below). Too low a rate will rule out the model if not its inventor. In SU(5) one obtains[60] $M \sim 10^{14}$ GeV - 10^{15} GeV corresponding to a proton life-time $\tau_p \sim 10^{30}$ y - 10^{31} y. One can turn the argument the other way round[61] : The present limit on τ_p is 2×10^{29} y. This implies $M \gtrsim 10^{14}$ GeV. On the other hand, we know the evolution equation for the electromagnetic fine structure constant which gives a rising curve. We obtain a limit by requiring that $\alpha(M)$ should not exhibit a Landau ghost for $M < 10^{14}$. This gives $\alpha(0) \lesssim 1/25$.

Other predictions of SU(5), involving fermion masses depend on the

detailed Higgs structure. The simplest assignment through the 5-dimensional representation, yields results in poor agreement with experiment[62]. One obtains that at $\sim 10^{15}$ GeV $m_e = m_d$; $m_\mu = m_s$; $m_\tau = m_b$ which gives $m_d / m_s \sim 1/200$, an order of magnitude smaller than estimates from chiral dynamics. A more interesting relation is[63] $m_\tau = m_b$; $m_\mu = 3 m_s$; $3 m_e = m_d$. It can be approximately derived if one uses a Higgs system with three 5- and one 45-dimensional representations. For more detail on SU(5) phenomenology see ref.[62].

2.2 Other grand unification theories

SU(5) has no room for right-handed neutrinos. Parity violation, which is observed at present energies, becomes a fundamental law of Nature. Present experimental evidence notwithstanding, it is attractive to speculate that this violation is a low-energy accident and that the underlying theory is ambidextrous. This leads us to extend $SU(2)_L \times U(1)$ to $SU(2)_L \times SU(2)_R \times U(1)$ ref.[32]. For phenomenological purposes it is enough that the gauge bosons of $SU(2)_R$ should be a few times heavier than $W^{\pm}$. Several of the mass relations which we mentioned earlier arise now naturally. The simplest grand-parent of this model is a grand unified theory based on SO(10) [64] with each fermion family (including ν_R), belonging to a 16-dimensional representation. In the long journey from SO(10) down to $SU(3) \times SU(2)_L \times U(1)$ Nature may choose various paths. She can take the direct road (just one big break) or she may decide to go through one (or more) of the intermediate subgroups. Particularly interesting among the latter are[65] $SU(4) \times SU(2)_L \times SU(2)_R$ or $SU(4) \times SU(2)_L \times U(1)$. They both incorporate the attractive idea of lepton number as a fourth color[66] and, since now we have an extra parameter, namely the mass scale of the intermediate breaking, we can accommodate a value of $\sin^2 \theta_W \simeq 0.23$. Mass relations can again be obtained but they depend on the choice of the Higgs system and the breaking pattern. For example, through one 10 and one 126 [65] we can obtain again $m_\tau = m_b$; $m_\mu = 3 m_s$; $3 m_e = m_d$

Among the other grand unified schemes I want to mention two which have quite particular features :

The first is based on the exceptional group E_6 [67]. It has 78 gauge bosons which gives eight neutral currents, including the electromagnetic one. The fermions are placed in two 27-dimensional representations. It contains as a maximal subgroup a product of three SU(3)'s which can be taken to be $SU(3)_C \times SU(3)_L \times SU(3)_R$. The gauge bosons belong to

$$78 = (8,1,1) + (1,8,1) + (1,1,8) + (3,\bar{3},\bar{3}) + (\bar{3},3,3)$$

while the fermions give

$$27 = (3,3,1) + (\bar{3},1,\bar{3}) + (1,\bar{3},3)$$

The first are left-handed quarks, the second left-handed anti-quarks while the third ones must be leptons. We still have six quark flavors but only two

(u and c) have charge 2/3. The other four have charge -1/3. Instead of t we predict a b'. If R in PETRA still refuses to take the big jump....

All the previous models share the questionable privilege of predicting a unification energy which will remain inaccessible to direct experimental observation for any forseeable future. The last model I want to mention dares to go against most accepted taboos[66,68]. When everybody talks about QCD and confinement it postulates integer charge, freely escaping unstable quarks. The unification group is $[SU(4)]^4 \times P$ where P is a discreet symmetry which interchanges the different factors. The breaking pattern which interests us here is $[SU(4)]^4 \rightarrow SU(3)_R \times SU(3)_L \times G$ where $SU(3)_R \times SU(3)_L$ is a chiral color group of strong interactions and G is some group which contains $SU(2)_L \times U(1)$. The two SU(3) factors are very crucial because they induce a factor of two in the β-function and make the strong interaction coupling constant decrease much faster with energy. This means that this scheme will predict a unification mass of almost human proportions, $M \sim 10^5$ GeV. Unfortunately the other two coupling constants g_2 and g_1 of $SU(2)_L$ and U(1) obey still the same renormalization group equations and have a tendency to meet much further, near 10^{14} GeV. This difficulty can be translated in a prediction for θ_W which here is $\sin^2 \theta_W = 0.3$ in serious disagreement with the data. However, enlarging the group to $[SU(2n)]^4$ with $n \geq 3$ (in fact n = 3 may be more appropriate now that we have three families) yields good values[69], for instance $\sin^2 \theta_W = 5/24$ for n = 3. Some physicists may see some day the grand unification.

2.3 Baryon decays

The most dramatic prediction of grand unified theories is the one about the ultimate decay of baryons. We all want to know how long we are allowed to live.

The subject has been reviewed extensively[70], so I shall only give the latest results. All models predict life times as low as $\sim 10^{31}$ y. Based on SU(6) wave functions one obtains for SU(5) [71]

$$\tau_p \sim 10^{31} \text{ y}$$

Dominant decay modes :

$p \rightarrow e^+ \pi^0$	($\sim$ 35%)	$n \rightarrow e^+ \pi^-$	(50%)
$p \rightarrow e^+ \rho^0$	($\sim$ 17%)	$n \rightarrow e^+ \rho^-$	(25%)
$p \rightarrow e^+ \omega^0$	($\sim$ 21%)	$n \rightarrow \bar{\nu} \pi^0$	(8%)
$p \rightarrow e^+ \eta^0$	($\sim$ 12%)	.	
$p \rightarrow \bar{\nu} \pi^+$	($\sim$ 9%)	.	
$p \rightarrow \bar{\nu} \rho^+$	($\sim$ 4%)	.	

For SO(10) the numbers may vary by as much as 30-40% and depend on the particular breaking pattern[71], but the orders of magnitude remain the same. Easily detectable, two-body decay modes seem to dominate.

The low unification mass theories allow for decays of the form[70] $p \to 3\nu + \pi^+$ which can dominate with branching ratio as high as 80%. However the mode $e^+ \pi^0$ can also be appreciable.

The most exciting is that planned experiments promise, after a year of operation, a sensitivity of the order of $\tau_p \sim 10^{33}$ y. Do you want to bet ?

Let me finish with the obvious remark : Proton decay is too important to be left to theorists.

2.4 The baryon number of the Universe

In traditional cosmological models baryons and anti-baryons were created in pairs since the Hamiltonian was assumed to respect the baryon number. Any net baryon number should be put in by hand as an initial condition. In the so-called "symmetric" cosmologies it was argued that, within some range of temperatures ($\sim$ 1 GeV), a phase transition occurs[72] which results in a spontaneous symmetry breaking and thermal radiation becomes unstable against separation of nucleons from antinucleons. The situation was compared to what happens in a ferromagnet where a domain structure appears. According to this view our presence is due to a local fluctuation.

The trouble with this theory is that there is no evidence for the presence of large amounts of antimatter anywhere in the Universe[73]. No trace of antinucleons has been detected in cosmic rays and no large-scale annihilations have been observed. This difficulty, although not absolutely conclusive, makes the whole subject worth a fresh start.

In fact, since our present theories of elementary particle interactions predict a violation of both baryon number and charge conjugation, they offer a unique opportunity to settle this old question[74].

The most probable scenario seems to be the following[75] : at a very early stage, at temperatures comparable to the Planck mass $kT \sim 10^{19}$ GeV, gravitational interactions establish thermal equilibrium for all particles. The relevant parameters are H, the expansion rate of the Universe, which is proportional to $(kT)^2$ and Γ_i, the rate for a particular process i. At $kT \sim 10^{19}$ GeV, if we assume all masses to be much smaller than this value, all Γ_i's are much less than H. Two kinds of processes may give rise to baryon number creation : the decays of superheavy gauge or Higgs bosons, which we shall call collectively X-bosons, and the baryon number violating scattering processes among fermions. The latter will turn out to be unsufficient to explain the observed baryon asymmetry. So we shall concentrate on the former. As the Universe cools down H becomes of the same order as Γ_X and a significant number of X's decay. If, at this time, $kT \lesssim M_X$ the X-bosons have dropped out of thermal equilibrium and the decay products have no chance to

reproduce, through collisions, new X's. A net baryon number will remain. Therefore the important thing is to compare kT and M_X for T such that $\Gamma_X \approx H$. If X is one of the gauge bosons $M_X \sim 10^{15}$ GeV while $\Gamma_X \approx H$ for $kT \gtrsim 10^{17}$ GeV. Thus gauge boson decays do not produce any net baryon number. On the contrary the Higgs particles have a much smaller coupling constant, therefore a lower Γ_X, which in turn gives a $kT \sim 10^{14}$ GeV. It follows that the dominant mechanism for generation of baryons is the decay of super-Higgs's. Detailed calculations support this view. Finally let me point out that any baryon asymmetry in the initial conditions will most probably be washed out during the first stage of thermal equilibrium. In other words, God did not make the world all at once. He let it be created.

2.5 The problem of gauge hierarchies[76]

A remarkable feature of grand unified theories is the enormous difference in the mass scales they contain. Traditionally these scales are introduced through the vacuum expectation values of Higgs scalars. One has to manage so that $\langle \Phi \rangle = V \sim 10^{15}$ GeV and $\langle \varphi \rangle = v \sim 10^2$ GeV, in other words one must make sure that, after the superheavy spontaneous breaking, some scalars remain with masses of order v and not of order V [77]. In fact one can show that this condition is both necessary and sufficient for such a hierarchy of symmetry breakings to occur[77]. The matrix of the second derivatives of the potential evaluated at $\Phi = V$ must have some zero (or very small in the scale of V) eigenvalues. It is easy to verify that, in general, one can enforce this condition since one disposes of free counterterms for the masses of the Higgs scalars. This enforcement can be achieved at any order of perturbation theory by fine tuning of the parameters. It is precisely what, in technical language, is called an "unnatural relation".

Let me make a digression at this point and emphasize that the problem is essentially the same with that of the cosmological constant in any theory with spontaneously broken symmetries[78]. Again, the constant can be put to zero, but only after order by order adjustment of the parameters. We know that supersymmetric invariant field theories guarantee that scalars which are members of a massless supermultiplet will remain massless. I have no realistic example of a grand unified theory based on supersymmetry and it may be that the only sensible way to solve the problem is in the framework of supergravity theories. However, let me describe here a general method, that of dimensional reduction[79], which may, or may not, be used in combination with supergravity, and which naturally produces superheavy masses.

It is the generalization of the old idea of Kaluza and Klein[80]. Starting from pure gravity in a five dimensional space, with metric tensor $g_{\hat{\mu}\hat{\nu}}$, $\hat{\mu}, \hat{\nu} = 0,\ldots,4$, one looks for solutions in which the components of g do not depend on the last coordinate. The result is that $g_{\hat{\mu}\hat{\nu}}$ describes a direct product of the ordinary 4-dimensional space times a circle of dimension of the inverse of the Planck mass (the only scale of the problem). Since the

manifold is periodic in the last coordinate, we obtain a quantized quantity which can be identified with the electric charge. The electromagnetic field A_μ $\mu = 0,\ldots,3$ is identical with $g_{\mu 4}$. g_{44} is a scalar. We thus obtain a U(1) gauge theory. It possesses the interesting property of containing naturally a superweak CP violation[81].

A completely straightforward generalization of this idea, just increasing the number of extra dimensions, is not very enlightening because it yields a gauge theory based on a direct product of U(1) factors. The correct generalization to an arbitrary gauge group requires a fibre bundle structure of space-time[82]. However, here I would like to follow a different line[79] : Let us start with the Einstein theory in 4 + D dimensions, coupled to a Yang-Mills theory of a compact group G. Let (x^μ , θ^i) be the coordinates and $A^a_{\hat{\mu}}$ the Yang-Mills potential. We look for solutions of the form

$$g_{\hat{\mu}\hat{\nu}} = \begin{pmatrix} g_{\mu\nu}(x) & 0 \\ 0 & g_{ij}(x) \end{pmatrix} \; ; \; A^a_\mu = 0 \; ; \; A^a_i = A^a_i(\theta^j) \qquad (4)$$

and $R_{\mu\nu} = 0$. g_{ij} is supposed to describe a D-dimensional, compact, space-like space S. It turns out that such solutions exist only if S can be viewed as a homogeneous space on G which means that S is isomorphic to the coset space G/H with respect to the subgroup H. Once such a solution is found, we can take it as describing the vacuum state and examine quantum fluctuations around it. In practice, one tries to expand all fields around the classical solution and integrate the action over the coordinates of the space S. The resulting 4-dimensional field theory contains an infinite set of spin 0,1 and 2 fields with masses quantized as $N.M_{Planck}$ with N being given in terms of the Casimir operators of G (In the simple U(1) theory N were integers). Thus the spectrum consists of massless and superheavy particles. The subgroup H remains as an unbroken gauge symmetry.

I do not know how to apply these ideas in a realistic model and, even on the conceptual level, my understanding is extremely limited . For example, nothing is known about the uniqueness and stability properties of the classical solution and the spectrum of states has been worked out for particular fluctuations. Furthermore, at least in a particular case, it seems that the theory contains a tachyon[83]. Nevertheless, I consider the whole idea extremely interesting and deserving further investigation.

2.6 The family problem

Why are there useless elementary particles ? How many are they ? Do the three families belong to some large representation of a big group and all their partners managed to get superheavy masses ?[84] Why all quarks are color triplets ? Are they ? What if the upsilon is a quix-antiquix[85] (color sextet quark) bound state ? Does the τ belong to an $SU(2)_L$ triplet[85] ? Why is everybody asking the same old questions and nobody is answering them ?[86] Is supergravity going to help ? I don't know and I don't take bets.

3. ONE, TWO, THREE,..., INFINITY OR ZERO ?

The gauge group of present day phenomenology is U(1) x SU(2) x SU(3). Guess what is going to happen next. Trying to answer this question, theorists have invented grand unified models, supersymmetries, extended symmetries and so on. However, the real question is : what is so special about SU(5), SO(10) or any other group and why any of them should be the basis for a fundamental theory ? Perhaps as we go up in energy, we shall discover higher and higher groups : one, two, three,..., infinity ?

The unconventional way to answer this question is to say that, since no group is more special than the others, none will be chosen. At very high energy there is no symmetry[87]. This brings us to the most daring speculation, the one that claims not only to discover the laws of nature, but also to prove that they are the only possible ones. The idea is that our present equations of QCD and SU(2) x U(1), with the specific values of their parameters, are infrared fixed points of some generalized renormalization group transformations, which act, not only on the values of the parameters appearing in the equations, but also on the form of the equations themselves[88]. At very high energies (10^{19} GeV ?) there is no symmetry and no equations of definite form. Complete chaos. But it does not matter. You can start anywhere, you will end up always at the same point, namely U(1) x SU(2) x SU(3).

Needless to say, we are very far from implementing such an ambitious program. We can nevertheless test the idea in some specific examples[89]. I will describe one of them.

Let us consider a Yang-Mills theory based on a group G which is not invariant under Lorentz transformations. The gauge potential $A_\mu^a(x)$ has two indices, a and μ, but no vector transformation properties are attached to the index μ. The gauge transformation with an element u(x) of the gauge group is :

$$A_\mu^a(x) \longrightarrow u^{aa'}(x)\, A_\mu^{a'}(x) + \left[\frac{\partial u(x)}{\partial x^\mu}\, u^{-1}(x)\right]^a \qquad (5)$$

We can now define the Yang-Mills field $F_{\mu\nu}^a(x)$ as usual and we write a gauge invariant Lagrangian

$$\mathcal{L}(x) = -\frac{1}{4}\, \eta^{\mu\nu\rho\sigma}\, F_{\mu\nu}^a(x)\, F_{\rho\sigma}^a(x) \qquad (6)$$

If we assume, for simplicity, translational invariance, $\mathcal{L}$ given by (6) is unique. The only difference from the Lorentz invariant case is that now we have a set of independent coupling constants $\eta^{\mu\nu\rho\sigma}$. Taking into account the antisymmetry of $F_{\mu\nu}$ and eliminating a divergence term proportional to $\varepsilon^{\mu\nu\rho\sigma}$, we are left with 20 independent coupling constants. We make contact with the covariant theory in the special case where space-time has a metric $g^{\mu\nu}$ and

$$\eta^{\mu\nu\rho\sigma}_{\text{covariant}} = \frac{1}{\varepsilon g^2}\left(g^{\mu\rho}g^{\nu\sigma} - g^{\mu\sigma}g^{\nu\rho}\right) \qquad (7)$$

g is the coupling constant of the covariant theory.

Now that we have set the framework, we proceed in the usual way. We define the β-functions as

$$\beta^{\mu\nu\rho\sigma} = \frac{\partial \eta^{\mu\nu\rho\sigma}(\mu)}{\partial \ln \mu} \qquad (8)$$

and we compute them at the one-loop level. The explicit formula is given in ref.[89]. The important result is that the symmetric solution (unique coupling constant) is an infrared attractive fixed point. If we start somewhere in its vicinity we shall fall on it. Lorentz invariance does not have to be imposed on the fundamental theory. At low energies the theory is necessarily Lorentz invariant.

Of course this analysis does not show that the covariant solution is the only attractive fixed point. And, more important, it allows only for variations of the values of the parameters, not the form of the equations. It would be very interesting if we were to derive gauge invariance by the same principle, but I have no concrete results to report yet. Nevertheless, I consider that the idea is very profound and this example sufficiently successful to deserve the greatest attention.

⊕ ⊕
⊕

REFERENCES

1) J. Ellis, "Neutrino 79", Bergen, 1979, CERN TH 2701.

2) S.L. Glashow, Nucl. Phys. 22, 579 (1961).

3) S. Weinberg, Phys. Rev. Lett. 19, 1264 (1967) ; A. Salam, Proc. 8th Nobel Symp., ed. N. Svartholm, Stockholm, 1968.

4) C. Bouchiat, J. Iliopoulos and Ph. Meyer, Phys. Lett. 38B, 519 (1972) ; D.J. Gross and R. Jackiw, Phys. Rev. D6, 477 (1972).

5) S.L. Glashow, J. Iliopoulos and L. Maiani, Phys. Rev. D2, 1285 (1970).

6) G.S. Abrams et al., Phys. Rev. Lett. 43, 481 (1979).

7) M. Kobayashi and T. Maskawa, Prog. Theor. Phys. 49, 652 (1973) ; L. Maiani, Phys. Lett. 63B, 183 (1976) ; J. Ellis, M.K. Gaillard and D.V. Nanopoulos, Nucl. Phys. B109, 213 (1976) ; S. Pakvasa and H. Sugawara, Phys. Rev. D14, 305 (1976).

8) J.Steinberger, private communication.

9) A preliminary evidence for the discovery of b-hadrons at SPS was reported at this Conference.

10) C. Rubbia, these proceedings.

11) For some recent examples see : G.V. Dass and P.R. Babu, Nucl. Phys. B149, 343 and 356 (1979) ; E.H. de Groot, G.J. Gounaris and D. Schildknecht, Bielefeld preprint BI-TP 79/15.

12) A. Sirlin, Nucl. Phys. B71, 29 (1974) ; S.S. Shei, A. Sirlin and H.S. Tsao, Phys. Rev. D19, 981 (1979).

13) K.J.F. Gaemers and G.J. Gounaris, Zeitschr. f. Phys. C1, 259 (1979).

14) T.D. Lee, private communication.

15) R. Jackiw and K. Johnson, Phys. Rev. D8, 2386 (1973) ; J. Cornwall and R. Norton, Phys. Rev. D8, 2446 (1973) ; S. Weinberg, Phys. Rev. D19, 1277 (1979) ; H. Pagels, Rockefeller U. preprint COO-2232B-180.

16) S. Weinberg, Phys. Rev. Lett. 36, 294 (1976) ; A.D. Linde, Zh. Eksp. Teor. Fiz. Pis'ma Red. 23, 73 (1976) ; Phys. Lett. 70B, 306 (1977) ; J.S. Kang, Phys. Lett. 84B, 109 (1979).

17) M. Veltman, Acta Phys. Pol. B8, 475 (1977) ; Phys. Lett. 70B, 253 (1977) ; D.A. Dicus and V.S. Mathur, Phys. Rev. D7, 3111 (1973) ; B.W. Lee, C. Quigg and H.B. Thacker, Phys. Rev. Lett. 38, 383 (1977) ; C.E. Vayonakis, Lett. Nuov. Cim. 17, 383 (1976) ; M. Green, Phys. Rev. D19, 3161 (1979) ; Nucl. Phys. B153, 187 (1979).

18) N. Cabibbo, L. Maiani and G. Parisi, CERN TH 2683.

19) S. Coleman and E. Weinberg, Phys. Rev. D7, 1888 (1973).

20) E. Gildener and S. Weinberg, Phys. Rev. D13, 3333 (1976) ; J. Ellis, M.K. Gaillard, D.V. Nanopoulos and C.T. Sachrajda, Phys. Lett. 83B, 339 (1979).

21) L.N. Chang and J.E. Kim, Phys. Lett. 81B, 233 (1979) ; J.P. Leveillé, Phys. Lett. 83B, 123 (1979) ; G.J. Gounaris, D. Schildknecht and F.M. Renard, Phys. Lett. 83B, 191 (1979) ; E. Ma, Hawaii preprint UH-511-334-79 ; D.R.T. Jones and S.T. Petkov, CERN TH.2661 ; J. Finjord, CERN TH 2663 ; G. Barbiellini et al. DESY 79/27.

22) M. Lemoine and M. Veltman, Utrecht preprint.

23) S. Dimopoulos and L. Susskind, Nucl. Phys. B155, 237 (1979) ; S. Dimopoulos, these proceedings ; E. Eichten and K. Lane, to be published.

24) S.L. Glashow, Harvard preprint HUTP-78/015 ; HUTP-79/A029 ; HUTP-79/A040.

25) J. Yang, D.N. Schramm, G. Steigman and R. Rood, Chicago preprint EFI-78.26 ; P. Hut, Phys. Lett. 69B, 85 (1977) ; M.A.B. Bég, W.J. Marciano and M. Ruderman, Phys. Rev. D17, 1395 (1978). For a possible experimental determination of the number of neutrino species see K.J.F. Gaemers, R. Gastmans and F.M. Renard, Phys. Rev. D19, 1605 (1979).

26) A.D. Linde, Phys. Lett. 83B, 311 (1979) ; S. Dimopoulos and G. Feinberg, Columbia preprint CU-TP-158.

27) See however L. Maiani, G. Parisi and R. Petronzio, Nucl. Phys. B136, 115 (1978).

28) P.Q. Hung, Phys. Rev. Lett. 42, 873 (1979) ; H.D. Politzer and S. Wolfram, Phys. Lett. 82B, 242 (1979), Err. 83B, 421 (1979).

29) M. Veltman, Nucl. Phys. B123, 89 (1977) ; M.S. Chanowitz, M. Furman and I. Hinchliffe, Phys. Lett. 78B, 285 (1978) ; Nucl. Phys. B153, 402 (1979).

30) It is impossible to give a complete list of references. The following are some of the most recent published papers. Some review articles are also included.
S. Weinberg, Festschr. in honor of I.I. Rabi, New York Academy of Sciences 1977 ; H. Fritzsch, CERN TH 2699 ; H. Georgi and D.V. Nanopoulos, Phys.

Lett. 82B, 392 (1979) ; Nucl. Phys. B155, 52 (1979) ; H. Fritzsch, Nucl. Phys. B155, 189 (1979) ; J.M. Frère, Phys. Lett. 80B, 369 (1979) ; S. Pakvasa and H. Sugawara, Phys. Lett. 82B, 105 (1979) ; C.E. Vayonakis, Phys. Lett. 82B, 224 (1979) ; K. Higashijima, T.K. Kuo and P.G. Lauwers, Phys. Lett. 83B, 213 (1979) ; G. Segré, H.A. Weldon and J. Weyers, Phys. Lett. 83B, 351 (1979) ; D. Grosser, Phys. Lett. 83B, 355 (1979) ; E. Derman, Phys. Rev. D19, 317 (1979) ; D. Wyler, Phys. Rev. D19, 330 (1979) ; C.D. Froggatt and H.B. Nielsen, Nucl. Phys. B147, 277 (1979) ; H. Sato, Nucl. Phys. B147, 433 (1979) ; M. Horibe, J. Ishida and A. Sato, Nucl. Phys. B152, 36 (1979) ; T. Hagiwara, Phys. Lett. 84B, 465 (1979); T. Yanagida TU/79/196 ; H. Grosse and A. Martin, CERN TH 2513 ; D. G. Sutherland and G. Zoupanos, Glasgow preprint ; R. Barbieri, G. Morchio and F. Strocchi, S.N.S. 10/79 ; G.G. Volkov and A.G. Liparteliani, this Conference.

31) H. Georgi and A. Pais, Phys. Rev. D19, 2746 (1979).

32) S. Weinberg, Phys. Rev. Lett. 29, 388 (1972) ; J. Pati and A. Salam, Phys. Rev. D10, 275 (1974) ; H. Fritzsch and P. Minkowski, Nucl. Phys. B103, 61 (1976) ; R.N. Mohapatra and J. Pati, Phys. Rev. D11, 566, 2558 (1975) ; G. Senjanovic and R.N. Mohapatra, Phys. Rev. D12, 1502 (1975) ; A. De Rujula, H. Georgi and S.L. Glashow, Ann. of Phys. 109, 258 (1977).

33) S. Barr and A. Zee, Phys. Rev. D17, 1854 (1978) ; F. Wilczek and A. Zee, Phys. Lett. 70B, 418 (1977) ; Phys. Rev. Lett. 42, 421 (1979) ; C.L. Ong, Phys. Rev. D19, 2738 (1979).

34) S.L.Glashow and S. Weinberg, Phys. Rev. D15, 1958 (1977) ; E. A. Paschos, Phys. Rev. D15, 1966 (1977) ; F.E. Paige, E.A. Paschos and T.L. Trueman, Phys. Rev. D15, 3416 (1977) ; H. Georgi and D.V. Nanopoulos, Phys. Lett. 82B, 95 (1979).

35) R. Barbieri, R. Gatto and F. Strocchi, Phys. Lett. 74B, 344 (1978) ; R. Gatto, G. Morchio and F. Strocchi, Phys. Lett. 80B, 265 (1979) ; R. Gatto, UGVA-DPT 1979/04-199 and references therein ; M.S. Chanowitz, J. Ellis and M. K. Gaillard, Nucl. Phys. B128, 506 (1977).

36) G. 't Hooft, Phys. Rev. Lett. 37, 8 (1976) ; Phys. Rev. D14, 3432 (1976) ; R. Jackiw and C. Rebbi, Phys. Rev. Lett. 37, 172 (1976) ; C.G. Callan, R.F. Dashen and D.J. Gross, Phys. Lett. 63B, 334 (1976).

37) J. Ellis and M.K. Gaillard, Nucl. Phys. B150, 141 (1979).

38) R.D. Peccei and H.R. Quinn, Phys. Rev. Lett. 38, 1440 (1977) ; Phys. Rev. D16, 1791 (1977).

39) S. Weinberg, Phys. Rev. Lett. 40, 223 (1978) ; F. Wilczek, Phys. Rev. Lett. 40, 279 (1978).

40) S.L. Glashow and S. Weinberg, Phys. Rev. Lett. 20, 224 (1968) ; M. Gell-Mann, R.J. Oakes and B. Renner, Phys. Rev. 175, 2195 (1968).

41) J. Ellis and M.K. Gaillard, Phys. Lett. 74B, 374 (1978).

42) J. Kandaswamy, P. Salomonson and J. Schechter, Phys. Rev. D19, 2757 (1979) ; See however P. Ramond and G.G. Ross, Phys. Lett. 81B, 61 (1979) ; V. Baluni, Phys. Rev. Lett. 40, 1358 (1978).

43) T.D. Lee, Phys. Rev. D8, 1226 (1973).

44) G. Segré and H.A. Weldon, Phys. Rev. Lett. 42, 1191 (1979) ; S. Barr and P. Langacker, Phys. Rev. Lett. 42, 1654 (1979) ; A.B. Lahanas and C.E. Vayonakis, Phys. Rev. D19, 2158 (1979) ; A.B. Lahanas and N.J. Papadopoulos, Lett. Nuov. Cim. 18, 123 (1977) ; H. Georgi, HUTP-78/A010.

45) M.A.B. Bég and H.S. Tsao, Phys. Rev. Lett. 41, 278 (1978) ; M.A.B. Bég, D.J. Maloof and H.S. Tsao, Phys. Rev. D19, 2221 (1979).

46) R.N. Mohapatra and G. Senjanovic, Phys. Rev. Lett. 42, 1651 (1979) and to be published.

47) S. Dimopoulos and L. Susskind, CU-TP-148 ; S. Dimopoulos, Phys. Lett. 84B, 435 (1979).

48) J. Wess and B. Zumino, Nucl. Phys. B70, 39 (1974).

49) P. Fayet and J. Iliopoulos, Phys. Lett. 51B, 461 (1974) ; P. Fayet, Phys. Lett. 58B, 67 (1975).

50) S.L. Adler, Phys. Rev. 137, B1022 (1965) ; 139, B1638 (1965).

51) W.A. Bardeen, unpublished ; B. de Wit and D.Z. Freedman, Phys. Rev. Lett. 35, 827 (1975).

52) J. Iliopoulos, Proc. Intern. Storage Ring Metting, Flaine, France, (Feb. 1976), p. 35.

53) P. Fayet, Phys. Lett. 69B, 489 (1977) ; 70B, 461 (1977).

54) G.R. Farrar and P. Fayet, Phys. Lett. 76B, 575 (1978) ; 79B, 442 (1978).

55) Y. Ne'eman, Phys. Lett. 81B, 190 (1979) ; D. Fairlie, ibid 82B, 97 (1979) ; E. Squires, ibid 82B, 395 (1979) ; J.G. Taylor, ibid 83B, 331 (1979) and 84B, 79 (1979) ; P.H. Dondi and P.D. Jarvis, ibid 84B, 75 (1979).

56) H. Georgi and S.L. Glashow, Phys. Rev. Lett. 32, 438 (1974).

57) H. Georgi, H.R. Quinn and S. Weinberg, Phys. Rev. Lett. 33, 451 (1974).

58) M.S. Chanowitz, J. Ellis and M.K. Gaillard, Nucl. Phys. B128, 506 (1977) ; A.J. Buras, J. Ellis, M.K. Gaillard and D.V. Nanopoulos, Nucl. Phys. B135, 66 (1978) ; D.V. Nanopoulos and D.A. Ross, CERN TH 2536.

59) E.A. Paschos, to be published.

60) T.J. Goldman and D.A. Ross, Phys. Lett. 84B, 208 (1979) ; W.J. Marciano, COO-2232B-173.

61) S.L. Glashow and D.V. Nanopoulos, HUTP-79/A035.

62) J. Ellis, these proceedings ; D.V. Nanopoulos, CERN TH 2534.

63) H. Georgi and C. Jarlskog, HUTP-79/A026.

64) H. Georgi, Particles and Fields, 1974 ; H. Fritzsch and P. Minkowski, Ann. of Phys. 93, 193 (1975) ; For an extension to O(10) see F.T. Hadji-oannou, to be published.

65) H. Georgi and D.V. Nanopoulos, HUTP-79/A039.

66) J.C. Pati and A. Salam, Phys. Rev. D8, 1240 (1973).

67) F. Gürsey, P. Ramond and P. Sikivie, Phys. Lett. 60B, 177 (1976) ; F. Gürsey and M. Serdanoglou, Lett. Nuov. Cim. 21, 28 (1978) ; Y. Achiman and B. Stech, Phys. Lett. 77B, 389 (1978) ; Q. Shafi, ibid 79B, 301 (1978) ; H. Ruegg and T. Schucker, UGVA-DPT 1979/05.198.

68) J.C. Pati and A. Salam, Phys. Rev. Lett. 31, 661 (1973) ; Phys. Rev. D10, 275 (1974) ; V. Elias, J.C. Pati and A. Salam, Phys. Rev. Lett. 40, 920 (1978) ; J.C. Pati, UMD 79-066.

69) V. Elias and S. Rajpoot, IC/78/159.

70) D.V. Nanopoulos, HUTP-78/A062 ; J.C. Pati, UMD 79-078.

71) M. Machacek, HUTP-79/A018 and 79/A021.

72) R. Omnès, Phys. Rep. 3C, No 1 (1972).

73) G. Steigman, 1971 Cargèse Lectures.

74) A.Y. Ignatiev, N.V. Krosnikov, V.A. Kurmin and A.N. Tevkhelidze, Phys. Lett. 76B, 436 (1978) ; M. Yoshimura, Phys. Rev. Lett. 41, 381 (1978) ; S. Dimopoulos and L. Susskind, Phys. Rev. D18, 4500 (1978) ; Phys. Lett. 81B, 416 (1979) ; A.D. Sakharov, Zh. Eksp. Teor. Fiz. 76, 1172 (1979); D. Toussaint, S.B. Treiman, F. Wilczek and A. Zee, Phys. Rev. D19, 1036 (1979) ; J. Ellis, M.K. Gaillard and D.V. Nanopoulos, Phys. Lett. 80B, 360 (1979) ; A. Yildiz and P.H. Cox, HUTP-79/A019 (1979) ; S. Barr, G. Segré and H.A. Weldon, UPR-0127 T ; N.J. Papastamatiou and L. Parker, Phys. Rev. D19, 2283 (1979) ; D. Toussaint and F. Wilczek, Phys. Lett. 81B, 238 (1979).

75) S. Weinberg, Phys. Rev. Lett. 42, 850 (1979) ; D.V. Nanopoulos and S. Weinberg, to be published.

76) E. Gildener, Phys. Rev. 14, 1667 (1976) ; K.T. Mahanthappa and D.G. Unger, Phys. Lett. 78B, 604 (1978) ; A.J. Buras, J. Ellis, M.K. Gaillard and D.V. Nanopoulos, Nucl. Phys. B135, 66 (1978) ; K.T. Mahanthappa, M.A. Sher and D.G. Unger, Phys. Lett. 84B, 113 (1979) ; O.K. Kalashnikov and V.V. Klimov, Phys. Lett. 80B, 75 (1979) ; F.T. Hadjioannou, A.B. Lahanas and C.E. Vayonakis, ibid 84B, 427 (1979) ; Q. Shafi, CERN TH 2667 ; M. Magg and Q. Shafi, ibid TH 2714 ; H. Georgi, HUTP-79/A036.

77) S. Weinberg, Phys. Lett. 82B, 387 (1979).

78) A.D. Linde, JETP Lett. 19, 320 (1974) ; M. Veltman, unpublished ; see however, D.A. Ross and M. Veltman, Nucl. Phys. B95, 135 (1975).

79) E. Cremmer and J. Scherk, Nucl. Phys. B103, 399 (1976) ; B108, 409 (1976) ; B118, 61 (1977) ; Z. Horvath, L. Palla, E. Cremmer and J. Scherk, ibid B127, 57 (1977) ; J.F. Luciani, ibid B135, 111 (1978) ; J. Scherk and J.H. Schwarz, ibid B153, 61 (1979) ; C. Omero and R. Percacci, to be published.

80) Th. Kaluza, Sitzungber. Preuss. Akad. Wiss. Berlin, Math. Phys. K1, 966 (1921) ; O. Klein, Z. Phys. 37, 895 (1926).

81) W. Thirring, Acta Phys. Aust. Suppl. IX, 256 (1972).

82) R. Kerner, Ann. Inst. H. Poincaré 9, 143 (1968).

83) E. Cremmer, private communication.

84) H. Georgi, HUTP-79/A013.

85) H. Georgi and S.L. Glashow, HUTP-79/A027.

86) All my colleagues, private communication.

87) H.B. Nielsen in Scottish Univ. Summer School 1977.

88) S. Ciulli, private communication.

89) H.B. Nielsen and M. Ninomiya, Nucl. Phys. B141, 153 (1979) ; see also S. Chadha and H.B. Nielsen, to be published and papers submitted to this Conference.

QCD PHENOMENOLOGY

Mary K. Gaillard
LAPP, Annecy-le-Vieux, France, and CERN, Geneva, Switzerland

ABSTRACT

Selected topics in QCD phenomenology are reviewed: the development of an effective jet perturbation series with applications to factorization, energy flow analysis and photon physics; implications of non-perturbative phenomena for hard scattering processes and the pseudoscalar mass spectrum; resonance properties as extracted from the combined technologies of perturbative and non-perturbative QCD.

The long-standing, solid prediction of what is now known as "perturbative QCD" is the asymptotic Q^2 dependence of the moments of deep inelastic scattering structure functions. Its formal derivation[1] using the light-cone operator product expansion (OPE)[2] and renormalization group equations (RGE)[3] has now been reformulated[4] in the language of perturbation theory. In addition to making the underlying physics more transparent, this formulation has the advantage that it can be applied to processes for which a light-cone analysis was not appropriate: Drell-Yan dilepton production, semi-inclusive lepton-nucleon and e^+e^- interactions, high p_T phenomena in hadron interactions, jet analyses, and photon interactions. The result is that there is now a basis for treating these processes in terms of a perturbative expansion in the "running" coupling constant $\alpha_s(Q^2)$, where Q^2 is a momentum transfer characteristic of the process studied, a procedure which had, in fact, already been adopted by optimistic phenomenologists[5].

I shall outline the arguments involved in the perturbation theory derivation of the moment equation, indicate how it is extended to other processes, and comment on various phenomenological applications. QCD perturbation theory is known to be inadequate on phenomenological grounds because it cannot account for confinement, and in fact non-perturbative phenomena have been discovered[6] through the study of classical QCD Lagrangians. I shall briefly discuss possible effects of these phenomena on the results of perturbative QCD. However, calculations of non-perturbative phenomena are in their infancy, and results obtained so far can only be considered as indicative. I shall air once again the U(1) problem, which is the issue as to whether the observed pseudoscalar mass spectrum is compatible with QCD, and finally, I shall describe the most ambitious attempt made so far to calculate resonance properties using the full apparatus of perturbative and non-perturbative QCD phenomenology. There are other applications of QCD to hadrons, notably heavy quark decays[7] and the properties of heavy onia[8], which I will not be able to cover. Recent progress in the calculation of electromagnetic form factors[9] will be reported by De Rújula.

1. MOMENTS IN PERTURBATION THEORY

The standard prediction for deep inelastic structure functions takes the form:

$$M_n(Q^2) = \int_0^1 x^n F(x,Q^2)\,dx = M_n(Q_0^2)\left(\frac{\alpha_s(Q^2)}{\alpha_s(Q_0^2)}\right)^{\gamma_n}\left[1+O\left(\frac{1}{\ln Q^2}\right)+O\left(\frac{1}{Q^2}\right)+\cdots\right], \quad (1.1)$$

where x is the usual Bjorken scaling variable;

$$\alpha_s(Q^2) \equiv \frac{12\pi}{33-N_f}\frac{1}{\ln Q^2/\Lambda^2} = g_s^2/4\pi$$

is the strong coupling constant; Q_0 is an arbitrary normalization point conventionally chosen so that $\alpha_s(Q^2) < \alpha_s(Q_0^2) << 1$, and γ_n is a computable number ("anomalous dimension"). The higher-order terms in $(\ln Q^2)^{-1}$ are calculable[10], but the $(Q^2)^{-n}$ terms are partly due to controllable mass effects[11] and partly due to "higher twist" effects which cannot be calculated with present technology. There are two obvious difficulties in confronting (1.1) with the data: experiments are carried out at finite Q^2, and one does not know *a priori* when the Q^{-n} terms will become negligible, and arbitrarily small values of $x = Q^2/2m_p E_{had}$ cannot be attained in finite energy experiments except for small Q^2. Whether or not present data confirm the predictions (1.1) is a controversial issue which will be discussed by de Rújula. We shall assume their validity and sketch their derivation in perturbation theory, so as to display the intuitively plausible features of quark and gluon interactions which may then be generalized to the analysis of other exclusive and semi-inclusive processes.

First recall the OPE-RGE approach, which is based on the observation that the deep inelastic scattering cross-section is related via the optical theorem to the imaginary part of the amplitude for forward Compton scattering of a highly virtual photon (or W, Z) by a proton. The latter amplitude is given by the matrix element between proton states of a time-ordered product of two current operators:

$$\sigma(lN \to l+X) \propto \mathrm{Im}\langle p|T(J_\mu(q), J_\nu(-q)|p\rangle . \tag{1.2}$$

The operator product expansion[2] says that the non-local (q^2-dependent) time-ordered current product can be expressed as a sum of local operators with the q^2 dependence appearing in multiplicative coefficients:

$$T(J_\mu(q), J_\nu(-q)) = \sum O_i(0)\frac{C_i(\ln Q^2)}{Q^{d_i-2}}, \quad Q^2 = -q^2 > 0, \tag{1.3}$$

where d_i is the dimension of O_i in units of mass. The power of Q on the right-hand side is determined by dimensional analysis: the current $J_\mu = \bar{q}\gamma_\mu q$ has dimension three and there is an implicit factor d^4x (d = -4), so the total dimension of the left-hand side is two. For $Q^2 \to \infty$ the dominant term is the one of lowest dimension. (In the Bjorken limit, one takes instead $\nu = p\cdot q \to \infty$, ν/Q^2 fixed; the leading terms in this case have lowest "twist" = dimension minus spin.) The matrix elements $\langle p|O_i|p\rangle$ are unknown, but the Q^2 dependence is contained entirely in the C_i which are determined from the RGE giving the result (1.1) for the leading term.

While this procedure is very formal, the result has nevertheless a simple physical interpretation[12,13]. Once the moments are inverted the deep inelastic cross-section can be expressed as a sum over point-like lepton-parton scattering cross-sections, with, however, Q^2-dependent parton distribution functions:

$$\sigma(\text{"}\gamma\text{"} + N \to X) = \sum_i \int \frac{f_i(x, \ln Q^2)}{x}\sigma(\text{"}\gamma\text{"} + p_i \to X) . \tag{1.4}$$

The influence of quark-gluon interactions is made explicit by the integral equation for the derivative of the distribution functions[13]:

$$\frac{df_i(x,\ln Q^2)}{d\ln Q^2} = \frac{\alpha_s(Q^2)}{2\pi}\int_x^1 \sum_j f_j(y,\ln Q^2)\,T_{ji}\,\frac{dy}{y} \quad . \tag{1.5}$$

The change in the probability of finding parton i at x depends on the probability T_{ji} that it was emitted by parton j at $y > x$ via, for example, gluon bremsstrahlung by a quark (Fig. 1a) or quark pair creation by a gluon. This picture provides an intuitive understanding[12] of the qualitative features of scaling violations. As Q^2 increases, the lepton probe resolves each parton into many partons and "sees" increasingly softer quarks and an increasing anti-quark component. It has also the practical advantage that use of Eq. (1.5) rather than Eq. (1.1) allows a test[14] of the theory without data at small x. However, at this stage, if we forget the formal derivation (1.1)-(1.3), we are still speaking a parton language: the Q^2 dependence of α_s is put in by hand and transverse momentum is neglected.

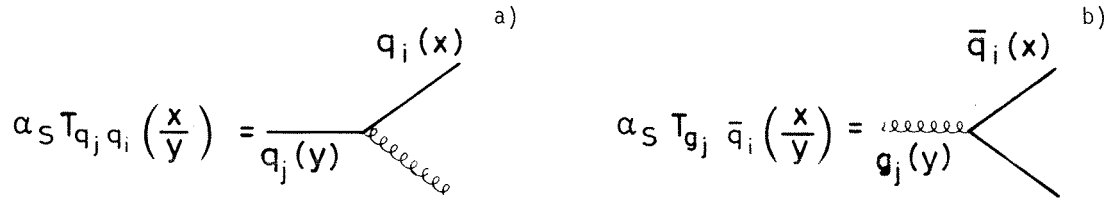

Fig. 1 Primary mechanisms for the Q^2 evolution of structure functions: a) momentum softening via gluon bremsstrahlung and b) sea enhancement via quark pair creation.

Next we turn to perturbation theory[15]. QCD, a theory of quarks interacting with massless vector gluons, has many similarities with QED, the theory of leptons interacting with massless vector photons. Notably we encounter certain infinities in evaluating amplitudes: a) "infrared" singularities; the divergence associated with soft-gluon emission (Fig. 2a) is cancelled by divergences arising from virtual gluon corrections (Fig. 2b); b) "mass" singularities occur when a quark emits a collinear gluon because the quark can remain on mass shell. If k_T is the transverse momentum of the gluon, the bremsstrahlung amplitude is

$$dk_T^2\,\frac{\alpha_s(k_T^2)}{k_T^2} \propto \frac{dk_T^2}{k_T^2 \ln k_T^2} = d(\ln\ln k_T^2)\,, \tag{1.6}$$

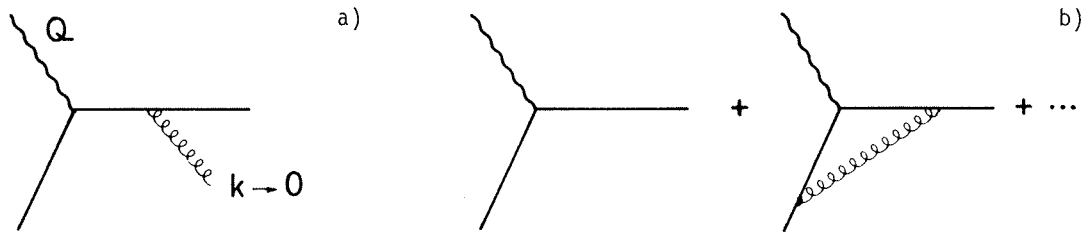

Fig. 2 Diagrams which combine to cancel infrared divergences: a) soft gluon bremsstrahlung and b) virtual gluon corrections.

where the use of the running coupling constant in Eq. (1.6) takes into account virtual gluon radiative corrections. Mass singularities vanish in the sum over collinear configurations of fixed total energy which are physically indistinguishable. Now consider a contribution to deep inelastic scattering illustrated in Fig. 3. Because the gluon bremsstrahlung spectrum diverges for small transverse momentum [Eq. (1.6)], the favoured configuration has all k_T^2 and q_T^2 small and ordered:

$$k_{1T}^2 > k_{2T}^2 > \cdots > k_{nT}^2 \; ; \; q_{1T}^2 > q_{2T}^2 > \cdots > q_{3T}^2 \; . \tag{1.7}$$

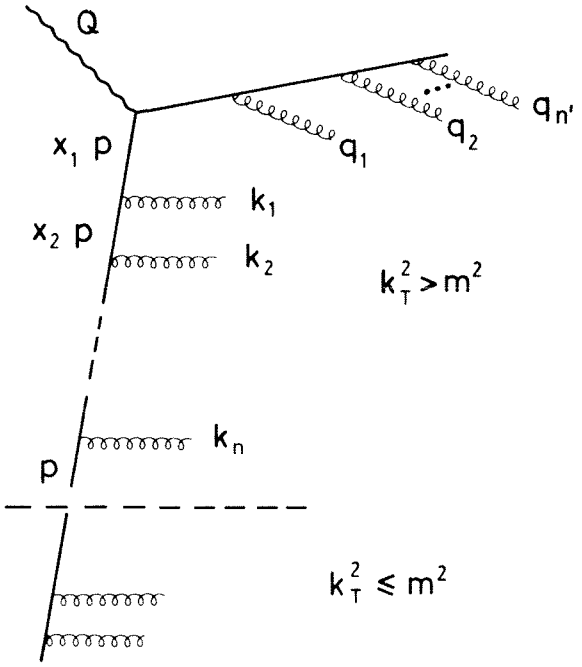

Fig. 3 Multigluon bremsstrahlung contribution to deep inelastic scattering

For inclusive final states, the sum over final-state configurations eliminates mass singularities arising from small q_{iT}. For the incoming quark line, we have to integrate over all the k_{iT}^2. Because of the form (1.6) for the bremsstrahlung spectrum, this integration takes a particularly simple form:

$$\int_0^{\ln\ln Q^2} dz_1 \int_0^{z_1} dz_2 \cdots \int_0^{z_{n-1}} dz_n = \frac{1}{n!}(\ln\ln Q^2)^n + \cdots \; . \tag{1.8}$$

Next we perform the x integration; since the dominant contribution comes from small k_T^2 we can neglect the transverse momenta of the quark lines. Since the scattering is from a quark of fractional momentum x_1, it plays the role of the Bjorken scaling variable and we get

$$\int_0^1 dx_1 \, \delta(1 - x/x_1) \int_{x_1}^1 dx_2 \, T(x_1/x_2) \cdots \int_{x_{n-1}}^1 dx_n \, T\left(\frac{x_{n-1}}{x_n}\right) T(x_n) \; , \tag{1.9}$$

where $\alpha_s T(x/y)$ is the amplitude of Fig. 1a. The folded integrals of formula (1.9) can be unfolded by taking moments; integrating (1.9) over x weighted with x^m gives

$$\int_0^1 dx \, x^m \, [(1.9)] = (T_m)^n \; ; \quad T_m = \int_0^1 dx \, x^{m+1} \, T(x) \; . \tag{1.10}$$

The moments of the structure functions are obtained by summing over n; the result is an exponential

$$M_m \propto \sum_n \frac{1}{n!} \left(T_m \ln\ln Q^2\right)^n = e^{T_m \ln\ln Q^2} = (\ln Q^2)^{T_m} \; , \tag{1.11}$$

which is the same as Eq. (1.1) with $T_m = -\gamma_m$. Actually, the procedure used, which incorporates virtual gluon radiative corrections by the replacement $\alpha_s \to \alpha_s(k_T^2)$ at each vertex, is a valid procedure as long as k_T^2 is large enough so that each quark line is sufficiently off-shell to be insensitive to bound-state effects. For this reason the chain in Fig. 3 has been divided into a subchain with $k_T^2 > m^2 = O(\text{GeV})$, to which the integration and summation procedure described above is applied, and a subchain with $k_T^2 < m^2$, which is left unspecified but which does not govern the Q^2 dependence.

Note that

a) Taking the derivative of Eq. (1.11) we get

$$\frac{dM_m}{d\ln Q^2} \propto \frac{1}{\ln Q^2} T_m M_m \propto \alpha_s(Q^2) T_m M_m \,, \tag{1.12}$$

which is obtained from the Altarelli-Parisi equation (1.5) by taking the m^{th} moment.

b) The result (1.11) corresponds to the "leading log approximation". For example, we neglected the lower end of the integrations ($z_i > \ln \ln m^2$) in Eq. (1.8) and the transverse quark momentum.

c) The perturbation theory result can easily be reinterpreted in terms of the operator product expansion. The squared amplitude corresponding to Fig. 3 is the imaginary part of the "ladder" contribution to Compton scattering (Fig. 4), which by definition has only large momenta $|k^2| > m^2$ running across its rungs. Once the momentum integrations are performed, one gets an effectively local biquark operator with a Q^2-dependent coefficient. Adding on the "soft" rungs at the bottom part of the chain of Fig. 3 corresponds to taking the matrix element between hadron states.

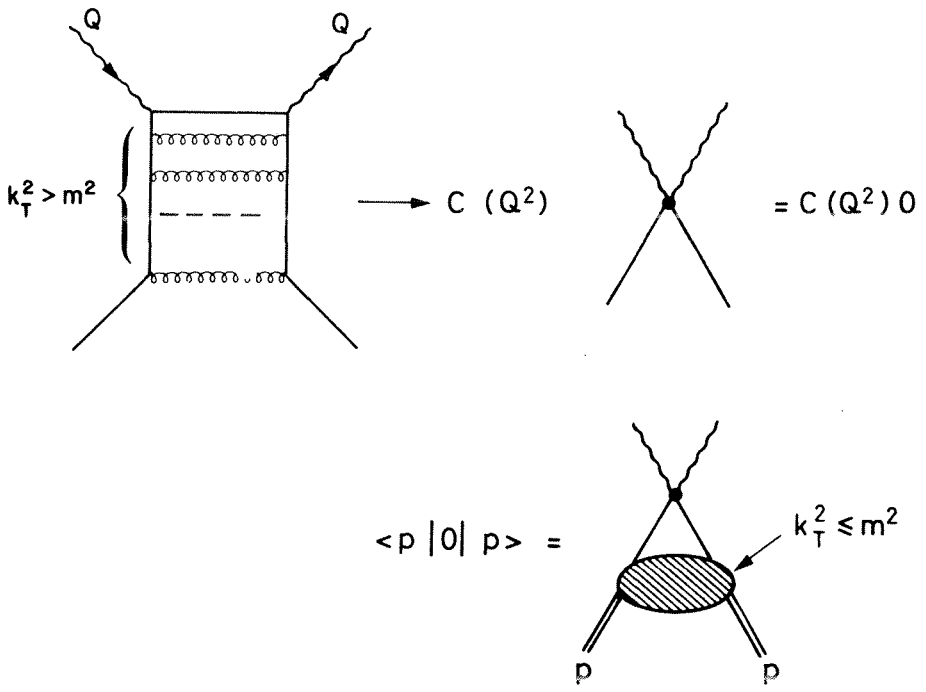

Fig. 4 Operator interpretation of the contribution of Fig. 3

2. FACTORIZATION AND JETS

We saw that the favoured configuration for a hard scattering process is one in which bremsstrahlung gluons are all nearly collinear with an incoming or outgoing quark line. This corresponds to a two-jet configuration. The first subdominant configuration is one in which one high p_T gluon is emitted. This forces a quark far off-mass-shell, and one power of $\ln Q^2$ is lost; the amplitude is then

$$\alpha_s^n (\ln Q^2)^{n-1} = O(\alpha_s(Q^2)) . \tag{2.1}$$

In this order we have to have either k_{1T} or q_{1T} large with $k_{i>1}$, $q_{i>1}$ again all nearly collinear. If large transverse momentum is emitted further down the chain, all the quarks above it are forced off-shell so that more powers of $\ln Q^2$ are lost. The hard gluon (as well as soft ones) is of course also dressed with collinear fragments, and one gets a three-jet configuration as illustrated in Fig. 5. What we see emerging is an effective perturbation series in $\alpha_s(Q^2)$.

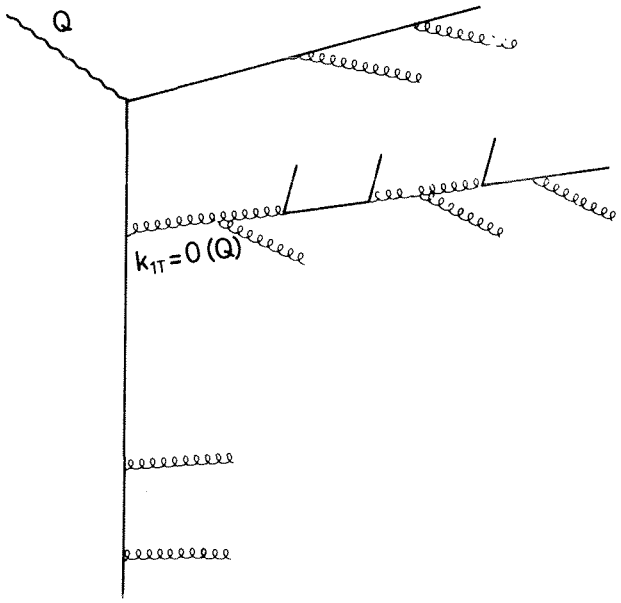

Fig. 5 A leading subdominant contribution to deep inelastic scattering or e^+e^- annihilation giving a three-jet final state

For example, to zeroth order in $\alpha_s(Q^2)$ e^+e^- → two jets via a quasi-collinear configuration analogous to Fig. 3; in order $\alpha_s(Q^2)$ we get the three-jet configuration of Fig. 5, and so forth. In addition, for a process involving a hadronic target or trigger particle, the soft piece ($k_T^2 \leq m^2$) at the bottom of the chain is independent of the number of hard transverse gluons emitted at the top of the chain. This means that the hadron structure/fragmentation function is a universal factor. For example, if the inclusive deep inelastic scattering cross-section is

$$\sigma(\text{"}\gamma\text{"} + N \to X) = \frac{1}{x} f_q(x, Q^2)\, \sigma(\text{"}\gamma\text{"} + q \to q) + \cdots , \tag{2.2}$$

the cross-section for the leading subdominant process with an extra-high p_T jet is given by

$$\sigma(\text{"}\gamma\text{"} + N \to 2 \text{ high } p_\perp \text{ jets}) = \frac{1}{x} f_q(x,Q^2)\,\sigma(\text{"}\gamma\text{"} + q \to q + g) + \cdots, \qquad (2.3)$$

where the cross-section on the right-hand side is to be calculated to lowest order in perturbation theory using the effective quark-gluon coupling constant $\alpha_s(p_T^2)$.

This result is known as "factorization" in the sense that the unknown function which incorporates the bound-state properties is independent of the number of high p_T jets observed in the final state. A more general definition of factorization arises in the description of a process involving more than one target, projectile, or trigger hadron. Factorization was first studied in the lowest non-trivial order in perturbation theory[16]. A quark structure function is determined in perturbation theory by writing the cross-section for deep inelastic lepton-quark scattering in the usual parton language:

$$\sigma(\text{"}\gamma\text{"} + q \to X) \equiv \sum_i \frac{1}{x} f_{i/q}(x,Q^2)\,\sigma(\text{"}\gamma\text{"} + i \to i), \qquad (2.4)$$

where $\sigma(\gamma + i \to i)$ is the point-like cross-section (e.g. Fig. 6a) for scattering from a parton i, and $f_{i/q}(x,Q^2)$ is by definition the distribution function for finding a parton i in a quark. The total cross-section can be calculated in perturbation theory via diagrams such as those in Fig. 6. Next, one calculates the cross-section for the production of Drell-Yan massive lepton pairs in quark-quark scattering via diagrams such as that of Fig. 7, and one finds that the result can be expressed in the form

$$\sigma(qq \to \mu^+\mu^- + X) = \sum_i \frac{1}{x_1 x_2} f_{i/q}(x_1)\, f_{\bar{i}/q}(x_2)\left[\sigma(i + \bar{i} \to \mu^+\mu^-) + O\left(\frac{1}{\ln Q^2}\right) + \cdots\right] + O\left(\frac{1}{Q^2}\right), \qquad (2.5)$$

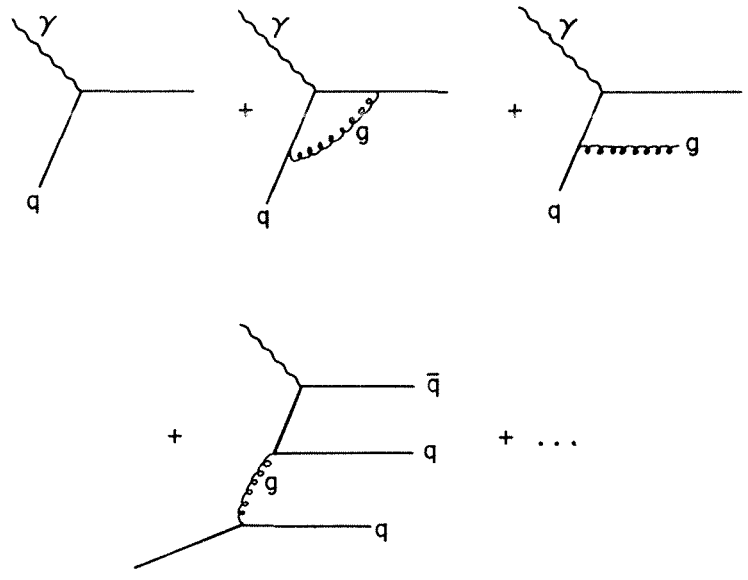

Fig. 6 Diagrams for deep inelastic lepton-quark scattering

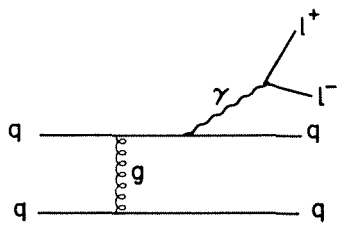

Fig. 7 Diagram contributing to the production of Drell-Yan lepton pairs by quarks

where $f_{i/q}$ and $f_{\bar{i}/q}$ are the quantities extracted from the calculation of (2.4), and $\sigma(i + \bar{i} \to \mu^+\mu^-)$ is the point-like parton-antiparton annihilation cross-section. The structure functions in fact contain mass singularities

$$f_{q/q} = \delta(x-1) + C\alpha_s(Q^2)\ln(Q^2/\mu^2) + \cdots , \tag{2.6}$$

but these are absorbed in a universal factor, which means that [to $O(1/Q^2)$] the Drell-Yan cross-section is calculable in terms of the deep inelastic scattering cross-section. Keeping just the first term in brackets in (2.5) gives just the usual Drell-Yan formula; the $O(1/\ln Q^2)$ terms can also be calculated, and a large amount of work has gone into their study and comparison with data[17].

Analogously, the fragmentation functions for partons into quarks can be defined by calculating perturbatively the cross-section for "one-quark inclusive" e^+e^- annihilation (Fig. 8), and relating it to the fragmentation functions via the formula

$$\sigma(e^+e^- \to q + X) = \sum_i \sigma(e^+e^- \to i + \bar{i})\, D_{q/i}(z) . \tag{2.7}$$

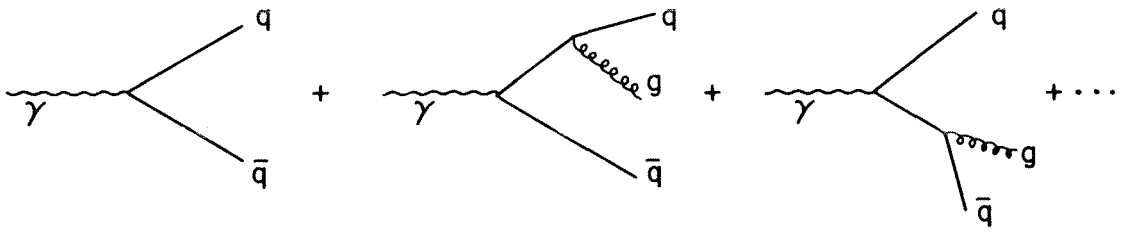

Fig. 8 Diagrams for $e^+e^- \to q + X$

Then a calculation of the two-quark inclusive cross-section shows that it can be expressed as

$$\sigma(e^+e^- \to q + q' + X) = \sum_i \sigma(e^+e^- \to i\bar{i})\left[D_{q/i}(z)D_{q'/\bar{i}}(z') + O(\ln^{-1}Q^2)\right] . \tag{2.8}$$

Similarly, the semi-inclusive deep inelastic cross-section contains as factors the quark structure and fragmentation functions:

$$\sigma(\text{"}\gamma\text{"} + q \to q' + X) = \frac{1}{x}\sum_{i,j} f_{i/q}(x)\, D_{q'/j}(z)\left[\sigma(\text{"}\gamma\text{"} + i \to j) + O(\ln^{-1}Q^2\right] , \tag{2.9}$$

where "γ" is a virtual photon, a $W^{\pm}$, or a Z^0, and high p_T hadron production in hadron collisions contains three "soft" factors:

$$\sigma(q + q' \to q''(p_\perp) + X) = \sum \frac{1}{xx'} f_{i/q}(x)\, f_{j/q'}(x')\, D_{q''/k}(z)\left[\sigma(i + j \to k(p_\perp/z) + X) + O(\ln^{-1}p_\perp^2)\right] , \tag{2.10}$$

where the cross-section on the right-hand side is calculated to lowest order in the running coupling constant $\alpha_s(p_T^2)$.

The results (2.5) to (2.10) have been shown[4,18] to be correct when leading logs are summed to all orders, with the infrared finite $O(\ln^{-1} Q^2)$ or equivalently $O[\alpha_s(Q^2)]$ corrections determined by the next-to-leading logs, analogous to Fig. 5, and so on. However, the results have been demonstrated only for quarks and gluons as target, projectile, and trigger particles, since perturbation theory cannot probe the bound-state properties of the theory. The hope is that the soft blobs at the end of the ladders remain Q^2-independent and factorizable in the presence of non-perturbative effects which are necessarily present. We shall comment later on this point.

3. ENERGY FLOW ANALYSIS

Since the properties of hadrons are not amenable to study in perturbative QCD alone, one would like to find tests of the theory which are independent of these properties. This is the principal motivation behind the various tests of energy flow patterns in e^+e^- annihilation which have recently been proposed. We saw that QCD perturbation theory justifies a perturbative expansion in the effective coupling constant. In e^+e^- annihilation the dominant configuration is two-jet-like, as in Fig. 3; the first subdominant configuration contains three jets, all with large relative $p_T = O(Q)$, and can be calculated from the simple quark-gluon bremsstrahlung amplitude using as coupling constant $\alpha_s(p_T^2) = \alpha_s(Q^2)[1 + O(\ln^{-1} Q^2)]$. On the other hand, for a 1^{--} $q\bar{q}$ resonance, the dominant contribution is a three-jet configuration $(\bar{q}q)_{1^-} \to 3$ gluons.

Just as the observation of a $(1 + \cos^2\theta)$ distribution for two-jet events, characteristic of the production of point-like spin-$\frac{1}{2}$ particles, gave strong support to the physical reality of quarks, we hope that various angular correlations which can be measured in three-jet events on and off resonance will show the patterns expected for spin-one gluons. When multijet events show up with clearly separated jets, their properties can be directly studied in terms of the energies and angles of separate jets. I think that few theorists expected to be seeing so soon such beautiful three-jet candidates as were shown during the talks of Söding and Wolf. At lower energies, for example at the Υ mass, three-jet structures are not visible to the eye, and a number of analyses have been proposed for extracting the hypothesized underlying jet structure and measuring the spin of the gluon. These tests are all based on the principle of avoiding infrared and mass singularities by summing over states which are physically indistinguishable in a theory of quarks and massless gluons. The same criteria also minimize sensitivity to our ignorance of the mechanism by which quarks and gluons are forced to "hadronize" to form the final state which is actually observed.

As a first example, consider the Sterman-Weinberg quantity which measures the fraction of energy flow through a cone of finite angle. For example, one can calculate perturbatively[19,20] the probability that a fraction ε of the total energy in e^+e^- annihilation lies outside a region defined by two back-to-back cones of half-angle δ. This quantity diverges if ε or δ is made arbitrarily small:

$$\frac{\sigma(\varepsilon,\delta)}{\sigma} \underset{\varepsilon,\delta\to 0}{\propto} \frac{\alpha_s}{\pi} \ln\varepsilon \ln\delta + O(\alpha_s^2). \tag{3.1}$$

This divergence reflects the fact that for small ε and δ, one is approaching a perfect two-jet configuration which is sensitive to quasi-collinear or soft multigluon emission, and the perturbation series no longer converges. So in order for such a test to be useful, one has to choose ε, δ sufficiently large:

$$|\ln\varepsilon \ln\delta| << \frac{\pi}{\alpha_s(Q^2)} \quad . \tag{3.2}$$

In addition, we know that jets have an intrinsic p_T spread, presumably governed by hadronization effects which cannot be calculated perturbatively, but which are hopefully Q^2-independent. In order for these effects to contribute negligibly to the measured energy fraction outside a biconical region, we also have to choose

$$\varepsilon, \delta >> \varepsilon_{had}, \delta_{had} \sim \frac{\langle p_\perp^2 \rangle_{had}}{Q^2} \tag{3.3}$$

where $\langle p_T \rangle_{had}$ can at present only be determined experimentally. That the criterion (3.3) is still difficult to satisfy at energies as high as 10 GeV can be seen from Fig. 9, where the average energy flow as a function of the angle δ, measured at 9.4 GeV, is compared with the QCD calculation[21]. Nevertheless, such tests should become feasible at higher energies since the hadronization effects should fall like Q^{-2}, while the perturbative contribution drops only logarithmically. Figure 10 shows[20] the probability, analogous to (3.1), for fractional energy flow outside the principal jet cones in deep inelastic scattering at two values of Q^2; the predictions are nearly indistinguishable. In addition, one can hope to improve comparison between theory and data by a re-summation of the perturbation expansion so as to account for the dominant contribution from multigluon soft/collinear bremsstrahlung, as will be discussed by De Rújula. Since many of the hadronization effects are kinematic in that finite values of

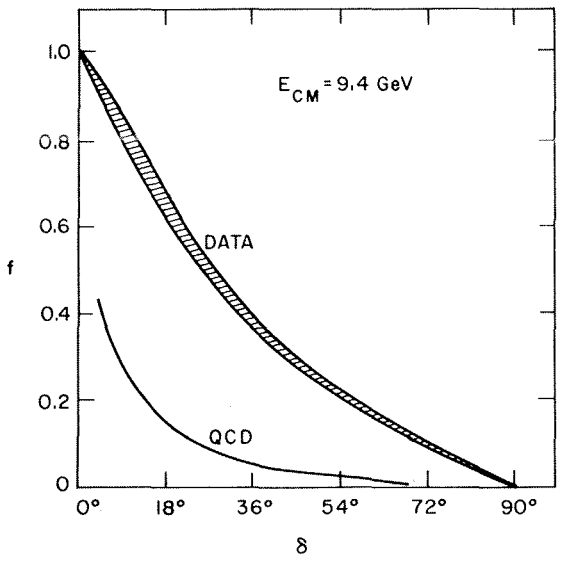

Fig. 9 Comparison[21] of data with QCD prediction for the average energy fraction outside a cone of half-angle δ

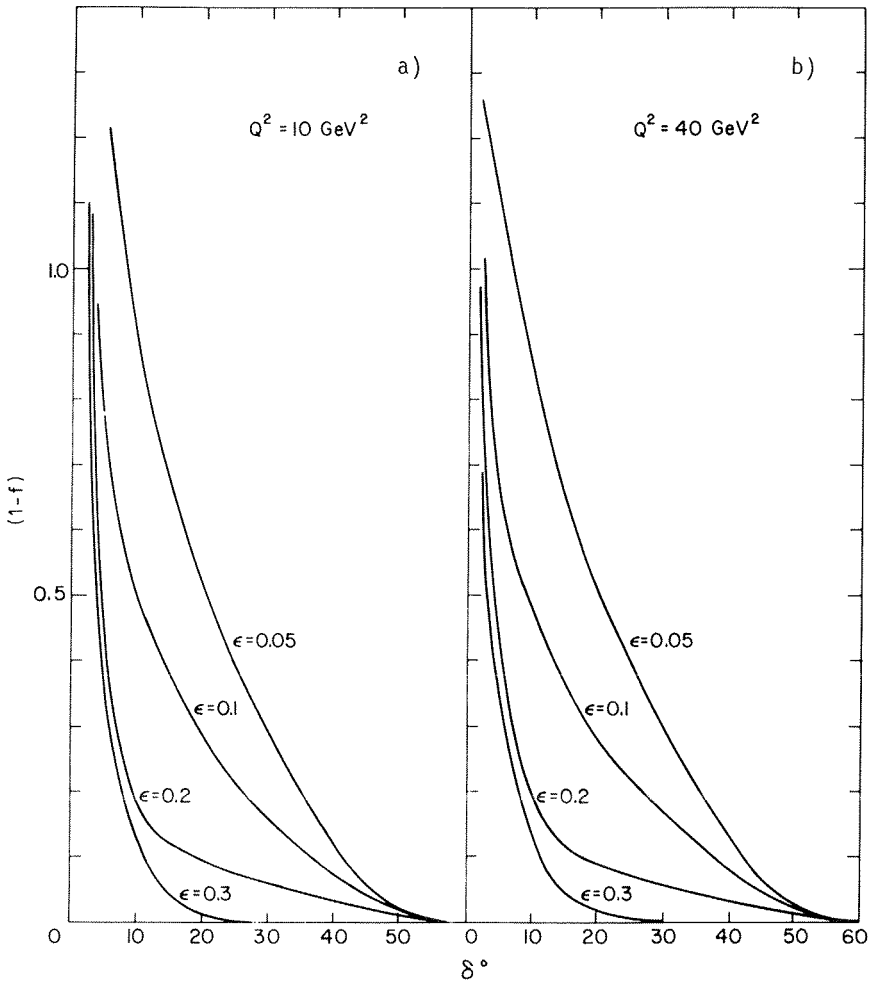

Fig. 10 The calculated probability[20] 1-f that a fraction ε of the energy in the hadronic final-state rest frame in deep inelastic scattering will lie outside back-to-back cones of half-angle δ

$\langle\varepsilon\rangle$, $\langle\delta\rangle$, etc., are directly related to the final-state multiplicity, a re-summation which incorporates multiquanta final state will more closely resemble the true multihadron final state. Of course no improvement of the perturbation series will be able to reproduce the final confining stage of hadronization.

The Sterman-Weinberg procedure tests only the perturbatively induced deviations from ideal two-jet events. There are many other observables which can be calculated perturbatively and which are more specific to the search for gluon jets. The most popular energy flow variables are thrust[22] (T), which measures the sum of parallel energies with respect to the axis which maximizes the parallel energy in one hemisphere of the event sphere; spherocity (S)[23], which measures the sum of transverse energies with respect to the axis which minimizes that quantity; and sphericity ($\hat{S}$)[24], which differs from spherocity in that it measures the sum of energies squared. Thrust and spherocity are "good" variables in that they are indistinguishable for physically indistinguishable collinear configurations, and therefore free of infrared singularities and insensitive to the details of hadronization in the limit of vanishing $\langle p_T \rangle_{had}$. Sphericity does not enjoy these properties, but is apparently[25,26] better

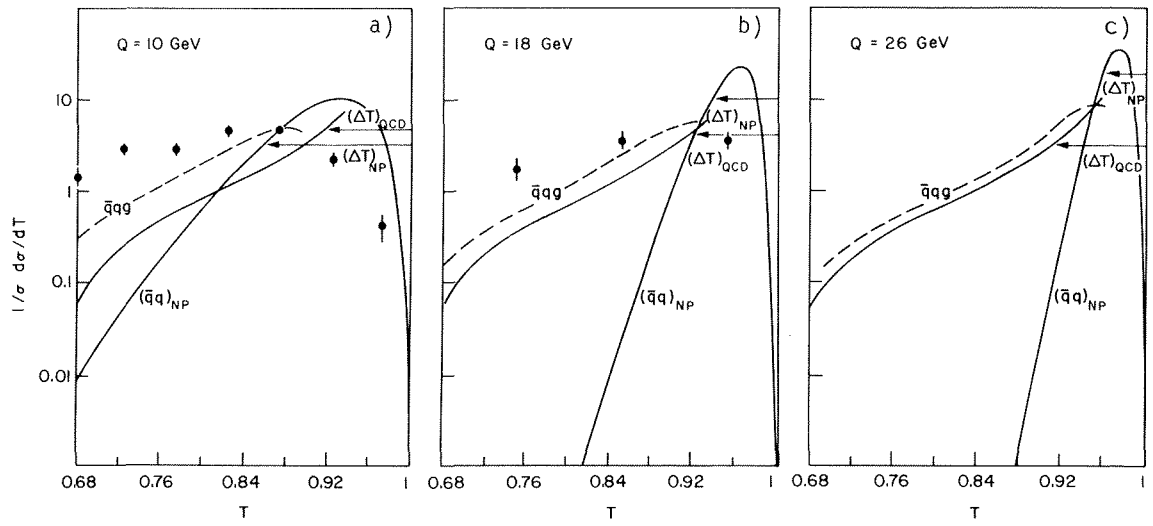

Fig. 11 Thrust distribution[27] for e^+e^- → hadrons at three centre-of-mass energies in order α_s in perturbative QCD. The solid (dashed) lines $q\bar{q}g$ show hard gluon bremsstrahlung without (with) hadronization, and are to be compared with a two-jet model $(q\bar{q})_{NP}$ and the data[28] at 9.4 and 17 GeV (resolution smearing not unfolded).

suited to data analysis than is spherocity. Thrust seems to enjoy the approval of both theorists and experimentalists. In Fig. 11 we show predicted thrust distributions[27] for e^+e^- → hadrons at three energies. The curves marked $(\bar{q}q)_{NP}$ represent a simple model for hadronized two-jet events; the solid $(\bar{q}qg)$ curves are the calculated gluon bremsstrahlung contributions, and the dashed curves are their hadronized versions. The data points[28] are at 9.4 and 17 GeV. Figure 12 shows[27] thrust distributions on resonance, where $(\bar{q}q)_{NP}$ is an estimate of the contributions from the non-resonant e^+e^- → $\bar{q}q$ background and the indirect decay $\Upsilon \to \gamma \to \bar{q}q$. The solid (ggg) curve is calculated from $\Upsilon \to 3$ gluons, and the dashed

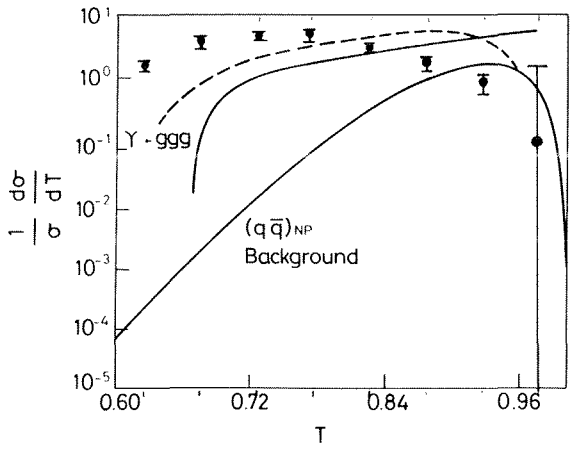

Fig. 12 Thrust distributions[27] on resonance for $\Upsilon \to 3g$ with (dashed) and without (solid) hadronization effects. The two-jet $(q\bar{q})_{NP}$ background is normalized to 1/6 of the three-gluon contribution. The data points[28] are with the two-jet contribution subtracted out (resolution smearing not unfolded).

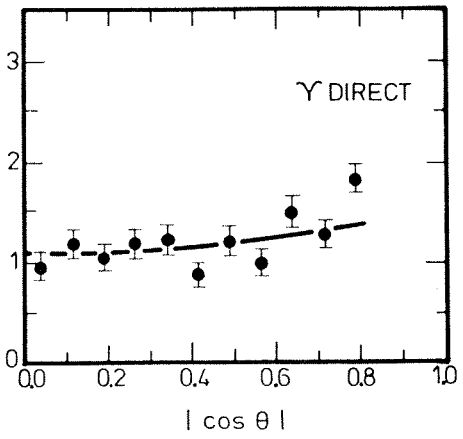

Fig. 13 Measured[29] angular distribution of the sphericity axis and theoretical[30] curve on resonance with the $e^+e^- \to q\bar{q}$ contribution subtracted out

line is hadronized. Figure 13 shows the angular distribution[29] of the thrust axis with respect to the beam direction compared with the prediction[30] for the QCD $\Upsilon \to 3g$ matrix element. The agreement is quite good and the assumption of scalar gluons, for example, cannot reproduce the data.

As discussed by Söding, analysis of the Υ data in terms of the above variables shows consistency with the $\Upsilon \to 3$ gluons hypothesis and a clear deviation from the two-jet-dominated continuum. However, one would like more specific evidence for a three-jet structure of the final state. Analyses of increasing complexity, but still based on "good" (singularity-free) variables, have been proposed. For example, "triplicity"[26] (T_3) is a generalization of thrust which measures the fractional energy parallel to the set of three axes which maximizes this quantity. Triplicity has the property that $T_3 = 1$ for a perfect three-jet event; so measuring both thrust and triplicity allows, in principle, the identification of an event as a three-jet configuration, as illustrated in Table 1. The analysis of the Υ final states in terms of triplicity has been discussed by Söding. Still more sophisticated analyses involve higher moments[31] in the (linearly combined) fractional momenta, up to a full reconstruction[27,32] of the energy flow as a function of the angle in the event plane. Other tests[30,33] exploit the fact that three quanta define three axes in the event plane, and various angular correlations (beam-jet, jet-jet, beam-event plane) can be exploited to test the spins of the final-state quanta.

As discussed by Söding, analyses such as these have been applied to the data in e^+e^- annihilation to look for the three-gluon decay of 1^{--} onia, hard gluon bremsstrahlung in $q\bar{q}$

Table 1
Range of T and T_3 for different event type

Event configuration	Thrust	Triplicity
Two jets	$T = 1$	$T_3 = 1$
Three jets	$\frac{2}{3} < T < 1$	$T_3 = 1$
Multi-jet	$\frac{1}{2} < T < 1$	$3\sqrt{3}/8 < T_3 < 1$
Sphere	$T = \frac{1}{2}$	$T_3 = 3\sqrt{3}/8$

final states in the continuum, and thresholds for new flavour production which are characterized by low thrust and high spherocity. Further applications include the study of cascade onium decays[27,34]. For example, the decays

$$1^{--} \to P + \gamma \quad (\hookrightarrow \text{hadrons}) \,, \tag{3.4}$$

where P is a 0^-, 0^+, or 2^+ state, are predicted to be dominated by a two-gluon hadronic final state. Jet angular correlations with respect to the photon and beam directions are sensitive to the spins of the gluons and of the hadronically decaying state.

Energy flow analysis can also be applied to the final state in hadron-induced reactions. The process[35,36]

$$\ell + N \to \ell' + 3 \text{ jets} \,, \tag{3.5}$$

where two jets have high p_T relative to one another and to the target fragmentation jet, can arise from mechanisms like that of Fig. 5. It is found[36] that contributions to thrust and spherocity distributions have a much higher "hadronization" to "perturbative QCD" ratio than do the corresponding distributions in e^+e^- annihilation, while tests involving angular correlations[36] between the lepton and hadron planes appear to offer more promising tests of the theory. Other applications include[37]

$$pp \to e^+e^- + \text{high } p_\perp \text{ jet} \,, \tag{3.6}$$

arising from the diagrams of Fig. 14, and[38]

$$pp \to \text{high } p_\perp \text{ jets} \,. \tag{3.7}$$

The process (3.7) is potentially very rich, as it involves in lowest order a variety of QCD perturbation theory diagrams (Fig. 15), including the otherwise elusive three-gluon vertex

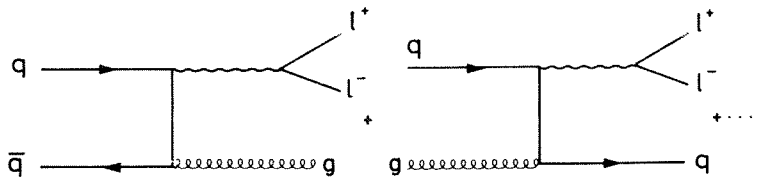

Fig. 14 Contributions to the production of Drell-Yan lepton pairs with large transverse momentum

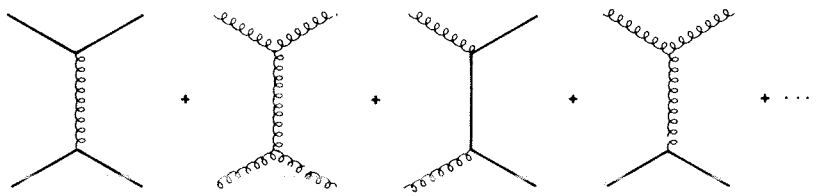

Fig. 15 Contributions to high p_T scattering in hadron collisions

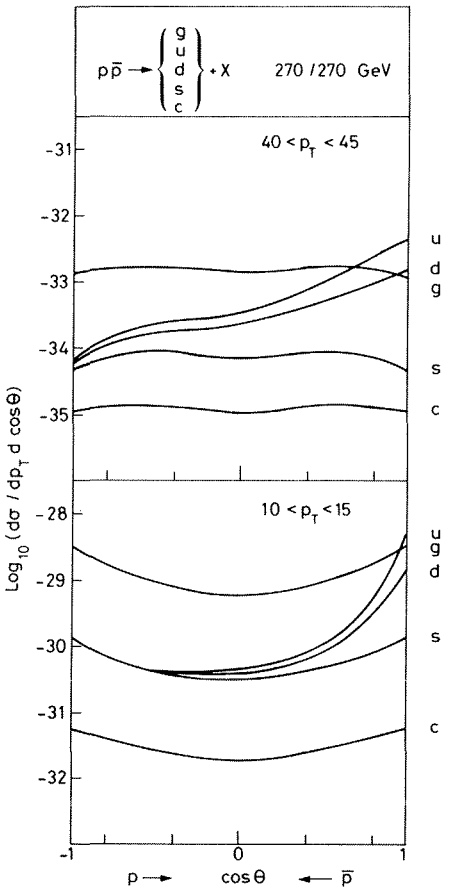

Fig. 16 Calculated[39] angular distributions for jets from different fragmenting quanta in pp̄ collisions at 540 GeV c.m. energy

which is fundamental to the theory. Figure 16 shows a calculation[39] of the angular distributions for jets induced by different types of quanta in pp̄ collisions at 540 GeV centre-of-mass energy. Different quanta arise from different elementary scattering mechanisms, and their relevant importance depends on the parallel momentum of the scattered system, since the initial-state quanta have fractional momentum distributions which depend on their nature. If jet quantum numbers could be identified, these processes would provide detailed tests of the theory. In any case they appear to provide a rich source of gluon jets.

4. PHOTON PHYSICS

As first discussed in terms of the operator product expansion[40], and more recently in the diagrammatic language[41] of perturbation theory, a real or quasi-real photon does not always act like a hadron. To see this[15], consider the deep inelastic scattering of a highly virtual photon from a quasi-real one (Fig. 17). Just as for scattering from a proton, the favoured configuration is for the k_{iT} small and ordered [Eq. (1.7)]. However, because the vertex at the bottom of the chain is point-like, the result of the k_T integration is quite different. Instead of Eq. (1.8) we get

$$\alpha \int^{Q^2} \frac{dk_{1T}^2}{k_{1T}^2 \ln k_{1T}^2} \int^{k_{1T}^2} \frac{dk_{2T}^2}{k_{2T}^2 \ln k_{2T}^2} \cdots \int^{k_{n-2T}^2} \frac{dk_{n-1T}^2}{k_{n-1T}^2 \ln k_{n-1T}^2} \int^{k_{n-1T}^2} \frac{dk_{n-1T}^2}{k_{n-1T}^2} \,. \qquad (4.1)$$

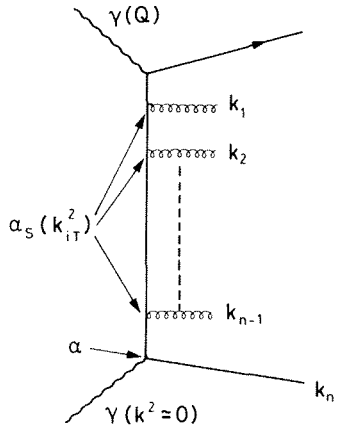

Fig. 17 Multigluon bremsstrahlung contribution to deep inelastic scattering from a photon

The k^2_{nT} integration gives simply $\ln(k^2_{n-1T})$, which cancels the log in the k^2_{n-1T} integration, and so on, giving simply $\alpha \ln Q^2$ for the expression (4.1). The x integration is the same as in Eq. (1.9), except that at the bottom of the chain the $q \to q$ transition function $T(x_n)$ is replaced by a $\gamma \to q$ transition function $T^\gamma(x_n)$. Then taking the m^{th} moment and summing over n gives

$$M^\gamma_m \propto \ln Q^2 \, T^\gamma_m \sum_n (T_m)^n = \frac{\ln Q^2 \, T^\gamma_m}{1 - T_m} \qquad (4.2)$$

instead of Eq. (1.11). The result (4.2) is valid as long as $k_{nT} > m^2$ such that $\alpha_s(m^2)/\pi \ll 1$. In the case where the gluon emission chain continues down to some $k^2_{jT} \lesssim m^2$ before the quark-photon interaction closes the chain, the perturbative treatment has to be stopped at $k^2_{nT} = k^2_{j+1T} > m^2$, giving the result (1.11) with the low k_T contributions absorbed once again into a non-calculable, Q^2-independent distribution function. However, since

$$T_n = -\gamma_n < 0 \quad , \quad \gamma_n > \gamma_{n-1} \qquad (4.3)$$

the higher moments, which govern the high-x region, are suppressed much more strongly with increasing Q^2 in (1.11) than in (4.2), so that for large Q^2 the contribution of (4.2) will be dominant except at very small x. In operator language, the result can be expressed as follows. In addition to the biquark operator of Fig. 4, with coefficient $O(\alpha)$, there is a biphoton operator (Fig. 18) with coefficient $O(\alpha^2)$. But while the matrix element of the biquark operator between photon states is $\alpha \times$ [soft wave function], the matrix element of the biphoton operator is unity. The result[41] for the photon structure function is shown in Fig. 19.

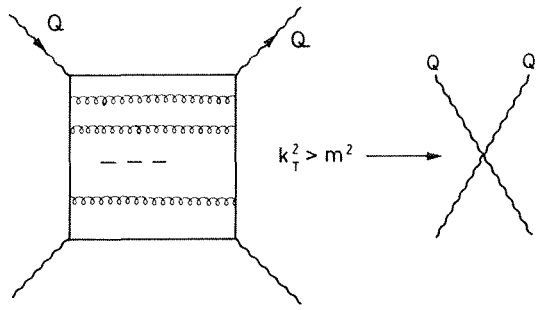

Fig. 18 Operator interpretation of Fig. 17

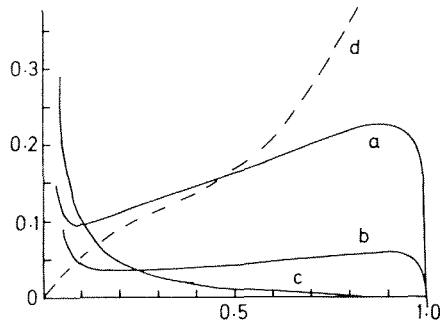

Fig. 19 The functions xq^γ_k and xg^γ in units of $(\alpha/\pi)\ell n Q^2$ [41]: a) xq for $Q_k = \frac{2}{3}$; b) xq for $Q_k = \frac{1}{3}$; c) xg; d) xq for $Q_k = \frac{2}{3}$ in Born approximation (no strong interactions).

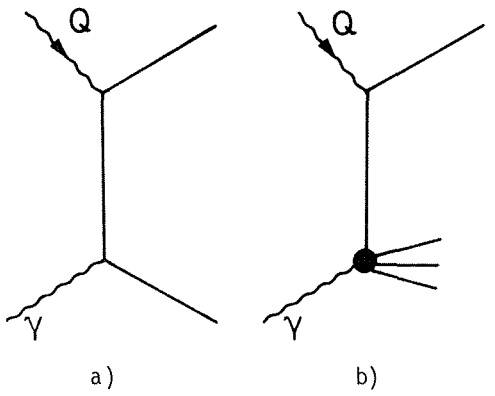

Fig. 20 Two calculable mechanisms for hard processes involving photons: a) point-like photon interaction and b) scattering from a parton

The photon has also a purely point-like contribution to hard scattering processes, so that processes involving real photons and large momentum transfers are dominated by two calculable mechanisms: a QED contribution (Fig. 20a), and a parton scattering contribution (Fig. 20b). These two contributions have different kinematic characteristics which allow them to be distinguished[42,43] experimentally and therefore tested separately. Applications include production of photons[44] with large transverse momentum relative to the jet axis in e^+e^- annihilation, two-photon processes[42,45] in e^+e^- scattering, and production of high p_T photons in photon-hadron scattering[43]. These processes measure the fourth power of the charge of the exchanged quark and so can be used to distinguish Gell-Mann - Zweig charge assignments from those of the Han-Nambu model, for example[46].

5. INSTANTON PHENOMENOLOGY

The study of non-perturbative phenomena in QCD has led to the observation[6,47] that the physical vacuum is a superposition of states $|n\rangle$ with non-trivial gluon field configurations which can be represented by:

$$|\theta\rangle = \sum_n e^{in\theta} |n\rangle \quad , \tag{5.1}$$

where the angular parameter θ which specifies the true vacuum is *a priori* arbitrary. Amplitudes for physical processes can be represented as vacuum-to-vacuum matrix elements of some (non-local) operator O:

$$\langle\theta|O|\theta\rangle = \sum e^{i(n-n')} \langle n|O|n'\rangle = \sum_\nu e^{i\nu\theta} \langle O\rangle_\nu \quad , \tag{5.2}$$

where the equality on the right incorporates the fact that amplitudes involving tunnelling between vacua depend only on the difference $\nu = n-n'$, and ν is the topological quantum number

$$\nu = \frac{\alpha_s}{8\pi} \int d^4x \, \tilde{F}^i_{\mu\nu}(x) F^i_{\mu\nu}(x) \quad , \tag{5.3}$$

where $F^i_{\mu\nu}$ is the gluon field strength tensor and $\tilde{F}^i_{\mu\nu}$ its dual:

$$\tilde{F}^i_{\mu\nu} = \varepsilon_{\mu\nu\rho\sigma} F^{i\rho\sigma} \quad . \tag{5.4}$$

The operator (5.3) is odd under P and CP, so that if $\theta \neq 0$, the amplitude (5.2) violates P and CP as discussed in the talk of Iliopoulos. Here we shall ignore this possibility. All known solutions of the classical gluon field equations are self-dual or anti-self-dual:

$$\tilde{F}^i_{\mu\nu} = \pm F^i_{\mu\nu} \quad . \tag{5.5}$$

The calculation of an amplitude $\langle O \rangle_\nu$ in (5.2) can be represented in a semi-classical approximation as the corresponding Feynman amplitude in the presence of an external field with the property (5.3) and weighted with an exponential damping factor e^{-S}, where S is the classical action:

$$S = \frac{1}{4}\int d^4x\, F^i_{\mu\nu}(x)\, F^i_{\mu\nu}(x) = \pm \frac{2\pi}{\alpha_s}\nu \quad > 0 \tag{5.6}$$

for (anti-)self-dual solutions (5.5). For small α_s, non-perturbative effects are strongly damped for large ν. The case $\nu = 0$ reduces to the usual (zero external field) perturbative treatment, and the largest non-trivial field contribution is the one-(anti-)instanton configuration[6] with $\nu = \pm 1$. This configuration corresponds to an effective external field localized at a space-time point z with space-time extension ρ. In this case α_s in Eq. (5.6) is effectively the running coupling constant defined in Eq. (1.1) with the substitution $Q \to 1/\rho$, so that the effects of small instantons are increasingly suppressed. If processes involving high-momentum transfer are sensitive only to vacuum fluctuations over a space-time extension characteristic of the interaction, $\rho \sim 1/Q$, then retention of only the tunnelling amplitudes of smallest action may represent a good approximation to non-perturbative effects.

The simplest such effect which can be studied is the non-perturbative contribution to $e^+e^- \to$ hadrons[48], which is determined by the imaginary part of the photon vacuum polarization. The one-instanton contribution is illustrated in Fig. 21a with quantum fluctuations (gluon exchange corrections to quark loops) neglected. The calculation differs from the free quark, or parton model, calculation in that the quark propagator has to be evaluated in the presence of an external instanton field[49]. The amplitude is then integrated over the instanton position z and size ρ, weighted by a density function $d(\rho\Lambda, m_q/\Lambda)$. The size integration diverges for large ρ, but the imaginary part is finite and gives a correction to the cross-section ratio

$$R = \frac{\sigma(e^+e^- \to \text{hadrons})}{\sigma(e^+e^- \to \mu^+\mu^-)}, \quad \frac{(\Delta R)_{\text{inst.}}}{R} \simeq \left(\frac{Q}{1\,\text{GeV}}\right)^{-12} (\ln Q^2)^{N_f}, \tag{5.7}$$

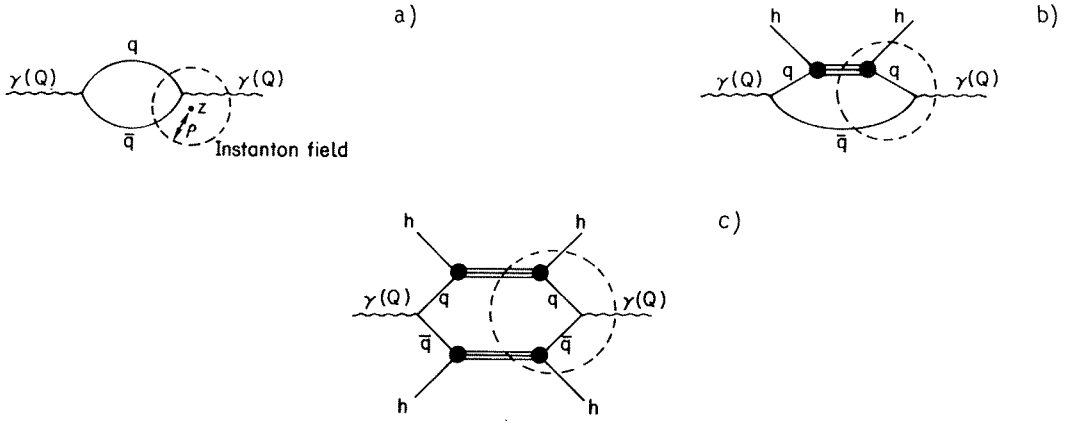

Fig. 21 Diagrams for evaluating instanton effects in a) $e^+e^- \to$ hadrons, b) $\ell + h \to \ell' + X$ or $e^+e^- \to h + X$, c) $h + h' \to \ell^+\ell^- + X$, $\ell + h \to \ell' + h' + X$ or $e^+e^- \to h + h' + X$.

where N_f is the number of quarks with $m_q \lesssim Q$, and conventional estimates of Λ and m_q have been used in determining the scale factor of 1 GeV. For $Q \lesssim 1$ GeV the correction (5.7) is O(1), implying a breakdown of the approximation used, but it becomes rapidly negligible for higher Q^2, suggesting a nice rationale for precocious scaling: the resonance region necessarily involves the non-perturbative aspects of QCD, but immediately above this region we recover the parton model results.

As the next step in complexity we can consider processes involving a hadron as the target or trigger particle, illustrated in Fig. 21b where h can be the target nucleon in deep inelastic scattering or the trigger hadron in one-particle semi-inclusive e^+e^- annihilation. The corrections[50] to the Q^2 dependence again turn out to be $O(Q^{-12})$, but there is a correction O(1) to the normalization. This is again intuitively plausible because the input quark distribution $F(Q_0^2)$ [or fragmentation function $D(Q_0^2)$] is in any case not calculable in perturbative QCD and is expected to reflect the non-perturbative aspects of the theory which determine the properties of hadrons as bound states.

Finally, we can consider the two-hadron semi-inclusive processes illustrated in Fig. 21c, which can represent Drell-Yan lepton pair production, one-particle semi-inclusive deep inelastic scattering, or two-particle semi-inclusive e^+e^- annihilation. In the one-(anti-) instanton approximation these processes fail to exhibit factorization[51]. For example, if Fig. 21b represents inclusive deep inelastic scattering, the resulting cross-section can be parametrized in terms of a structure function $F(x, Q^2)$, but the Drell-Yan cross-section extracted from Fig. 21c does not factorize in terms of the product of structure functions $F(Q^2, x_1)\, F(Q^2, x_2)$. On the other hand, the Q^2 dependence does factorize. If the moments of the structure functions are

$$\int_0^1 dx\, x^n F(x, Q^2) = A_n (\ln Q^2)^{\gamma_n} + O(Q^{-12}) \tag{5.8}$$

the appropriate double moments of the Drell-Yan cross-section take the form

$$\int_0^1 dx_1\, dx_2\, x_1^n x_2^m\, \sigma_{DY}(x_1, x_2, Q^2) \propto A_{nm} (\ln Q^2)^{\gamma_n+\gamma_m} + O(Q^{-12}), \tag{5.9}$$

$$A_{nm} \neq A_n A_m .$$

It is therefore of interest to test independently the factorization of normalization and of the Q^2 dependence in double moments.

As I emphasized before, the calculations done up to now are very rudimentary and should only be taken as indicative. Instanton phenomenology has also been applied to heavy-quark bound state systems[52], but the results depend on a cut-off which has to be imposed on the size integration[53].

6. THE U(1) PROBLEM

The U(1) problem[54] arises from the manifest chiral symmetry of the QCD Lagrangian:

$$\mathcal{L}_{QCD} = \bar{q} M q + \bar{q} \gamma_\mu D_\mu q + F^i_{\mu\nu} F^{i\mu\nu}, \tag{6.1}$$

where M is the quark-mass matrix. One can define vector and axial vector currents

$$V_\mu^\alpha = \bar{q}_\alpha \gamma_\mu q_\alpha \quad , \quad A_\mu^\alpha = \bar{q}_\alpha \gamma_\mu \gamma_5 q_\alpha \quad , \tag{6.2}$$

where α is a flavour index, which are conserved in the limit of vanishing quark mass, $M \to 0$, because in this limit the Lagrangian (6.1) conserves quark helicity. In the real world with finite quark masses, the symmetries associated with vector current conservation are observed to be approximate symmetries of the particle spectrum, while the "chiral" symmetries associated with axial current conservation are not. Chiral symmetry would imply approximately degenerate parity doublets; their absence is attributed to a spontaneous symmetry breaking such that the helicity-violating operators $\bar{q}_\alpha q_\alpha$ acquire (flavour independent) non-vanishing vacuum expectation values $\langle \bar{q}q \rangle \neq 0$. The original symmetry of the Lagrangian manifests itself through the appearance of massless (in the limit $M \to 0$) pseudoscalar particles called Goldstone bosons; the action of an axial charge on a state $|X\rangle$ relates it to the same state plus the appropriate pseudoscalar. For the I = 1 axial current

$$A_\mu^1 = \bar{u} \gamma_\mu \gamma_5 u - \bar{d} \gamma_\mu \gamma_5 d \quad , \tag{6.3}$$

which is conserved for $m_{u,d} = 0$, the Goldstone boson is the nearly massless pion $A|X\rangle \to |\pi X\rangle$. The U(1) problem is the absence of an equally light I = 0 pseudoscalar, since the isoscalar axial current

$$A_\mu^0 = \bar{u} \gamma_\mu \gamma_5 u + \bar{d} \gamma_\mu \gamma_5 d \tag{6.4}$$

is also conserved in the limit $m_{u,d} = 0$.

In fact the last statement is not true in QCD. The "anomalous" triangle diagram of Fig. 22 contributes a non-vanishing term to the divergence of the isoscalar current, while the analogous term for the isovector current cancels between the u- and d-exchange contributions. More generally, for an SU(n) flavour-symmetric current

$$A_\mu^n = \sum_{\alpha=1}^{n} \bar{q}_\alpha \gamma_\mu \gamma_5 q_\alpha \quad , \tag{6.5}$$

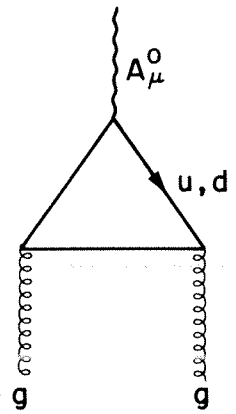

Fig. 22 Anomalous contribution to the isoscalar axial current divergence

the divergence is given by

$$\partial^\mu A^n_\mu = \sum_{\alpha=1}^{n} m_\alpha \bar{q}_\alpha \gamma_5 q_\alpha + \frac{n\alpha_s}{4\pi} \tilde{F}^i_{\mu\nu} F^{i\mu\nu} . \tag{6.6}$$

The last term on the right of Eq. (6.6) can also be written as the divergence of a current

$$K^n_\mu = \frac{n\alpha_s}{4\pi} \varepsilon_{\mu\rho\sigma\tau} A^{i\rho} F^{i\sigma\tau} \tag{6.7}$$

Then we can define a new "partially conserved" current

$$\tilde{A}^n_\mu = A^n_\mu - K^n_\mu ,$$

$$\partial^\mu \tilde{A}^n_\mu = \sum_\alpha m_\alpha \bar{q}_\alpha \gamma_5 q_\alpha , \tag{6.8}$$

and we are apparently back to the same problem. However, the current $\tilde{A}_\mu$ is not invariant under colour gauge transformations, so it has been argued[55] that its matrix elements, like those of quark and gluon fields, are unobservable, and the associated Goldstone boson is effectively confined. More recently, it has been pointed out[56] that non-perturbative effects violate chiral symmetry; the flavour singlet operator $\tilde{F}\cdot F$ which appears in vacuum tunnelling amplitudes [Eq. (5.2)] via the factor $e^{i\theta\nu}$ is a helicity-flip operator since it couples to $\bar{q}\gamma_5 q$ through the gluon-quark coupling.

However, it has been counter-argued[57] that an examination of the Ward identities involving only matrix elements of observable currents shows that the preceding remarks are insufficient to solve the U(1) problem. For example, if $\tilde{A}^n_\mu$ is conserved, one gets the identity

$$\lim_{p\to 0} p_\mu \langle T(\tilde{A}^n_\mu(p), \bar{q}_\alpha \gamma_5 q_\alpha)\rangle = \begin{cases} \langle \bar{q}_\alpha q_\alpha \rangle , & \alpha \le n \\ 0 , & \alpha > n . \end{cases} \tag{6.9}$$

The right-hand side of (6.9) has to be non-zero because of the non-observation of a chiral-symmetric particle spectrum, but the left-hand side can only be non-zero if there is a zero-mass pole giving the contribution illustrated in Fig. 23. This is one formulation of the U(1) problem. If we argue that the matrix element of Fig. 23 is unobservable, we have to consider instead the non-conserved current A_μ.

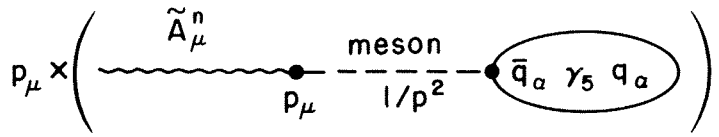

Fig. 23 Pole contribution to the amplitude of Eq. (6.9)

For M = 0 we get the Ward identity

$$\lim_{p\to 0} p_\mu \langle T(A^n_\mu(p), \bar{q}_\alpha \gamma_5 q_\alpha)\rangle = 2n \langle T(\nu, \bar{q}_\alpha \gamma_5 q_\alpha)\rangle + \langle \bar{q}_\alpha q_\alpha \rangle$$

$$= 2ni \frac{\partial}{\partial\theta} \langle \bar{q}_\alpha \gamma_5 q_\alpha \rangle + \langle \bar{q}_\alpha q_\alpha \rangle , \qquad (6.10)$$

where we have used the definition (5.3) and evaluated the amplitude between physical θ-vacuum states, Eq. (5.2). The left-hand side has to vanish since there is no (approximately) zero-mass pseudoscalar which can give a contribution like that of Fig. 23. Then the right-hand side determines the θ-dependence of vacuum expectation values of quark density operators; it can be solved by rewriting it in terms of the combination $\langle \frac{1}{2}\bar{q}_\alpha(1 \pm \gamma_5)q_\alpha\rangle$, giving

$$\langle \bar{q}_\alpha q_\alpha \rangle_\theta = \begin{cases} \cos(\theta/n) \langle \bar{q}_\alpha q_\alpha \rangle_0 & , \alpha \le n \\ \langle \bar{q}_\alpha q_\alpha \rangle_0 & , \alpha > n \end{cases} . \qquad (6.11)$$

This means that in the chiral SU(n) limit, the vacuum expectation values of $\langle\bar{q}q\rangle$ for the n massless quarks are θ-dependent, and furthermore if $\theta \neq 0$ they depend on the number of massless quarks. This is contrary to our customary thinking, according to which $\langle\bar{q}q\rangle$ is approximately flavour-independent and there is a smooth transition between the chiral SU(3) limit, where u, d, and s masses can be neglected, and the still better approximation of chiral SU(2) symmetry, $m_s \neq 0$, $m_{u,d} = 0$.

Is this limit-dependence a problem? Nature has chosen a fixed set of quark masses, and we cannot test experimentally the way amplitudes depend on how the chiral limit is approached. We have to rely on the experts to decide: at the time of writing, Crewther and Coleman are still arguing the issue. Crewther has offered a resolution[57,58] by speculating that the quasi-massless isoscalar Goldstone boson is absent only for isolated values of θ, one of them being the CP and P conserving value θ = 0 which nature has apparently chosen.

An alternative view[59] is that an isoscalar "pseudo-Goldstone boson" does occur, but that very large SU(3) symmetry-breaking effects in $(\bar{q}q)$-(gg) mixing give it a large mass so that it can be identified with the η′.

7. RESONANCE PROPERTIES IN QCD

As the final topic, I shall briefly describe the most ambitious attempt[60] to date to combine results of both perturbative and non-perturbative QCD in a calculation of resonance properties. Just as the deep inelastic scattering cross-section is expressible as the imaginary part of the matrix element of a non-local current-current product between nucleon states [Eq. (1.2)], the cross-section for e^+e^- annihilation into hadrons can be expressed as the matrix element of the same operator between vacuum states (vacuum polarization). However, in order to avoid the *a priori* uncalculable effects of thresholds and resonance structure for time-like Q^2, it is more convenient to relate the cross-section to the vacuum polarization through a dispersion relation; defining

$$\langle T(J_\mu(q), J_\nu(-q))\rangle = (q_\mu q_\nu - q^2 g_{\mu\nu})\Pi(Q^2),$$

$$Q^2 = -q^2 > 0, \qquad (7.1)$$

we can write a subtracted dispersion relation:

$$\Pi' = Q^2 \frac{\partial}{\partial Q^2} \Pi(Q^2) = \frac{Q^2}{\pi} \int_{s_{th}}^{\infty} \frac{\sigma(e^+e^- \to \text{hadrons}, s)\, ds}{(Q^2+s)^2} \quad . \tag{7.2}$$

Using the operator product expansion [Eq. (1.3)] for the current-current product, the left-hand side of (7.2) is expanded according to

$$\Pi' = \sum_i \frac{C_i(\ln Q^2)}{Q^{d_i}} \langle O_i \rangle = C_0(\ln Q^2) + \frac{C_2(\ln Q^2)\, m_q \langle \bar{q} q \rangle}{Q^4}$$

$$+ \frac{C_2'(\ln Q^2) \langle F^i_{\mu\nu} F^{i\mu\nu} \rangle}{Q^4} + O(Q^{-6}) \quad . \tag{7.3}$$

Contributions to the three leading operators in the expansion are shown in Fig. 24. In perturbation theory the vacuum expectation values of quark and gluon density operators vanish, but we know that $\langle \bar{q}q \rangle \neq 0$ because of the chiral asymmetry of the vacuum and $\langle F \cdot F \rangle \neq 0$ because of vacuum tunnelling. In addition, there are the $O(Q^{-12})$ non-perturbative effects discussed in Section 5. These are interpreted as a breakdown of the operator product expansion, which is therefore useful only for Q^2 large enough so that they are negligible. To the extent that the right-hand side of (7.3) can be calculated from theory, and the right-hand side of (7.2) can be evaluated using data, one gets a test of the theory. In particular, the leading term in (7.3) gives the asymptotic-freedom-corrected parton model result which relates R to the sum of squared quark charges.

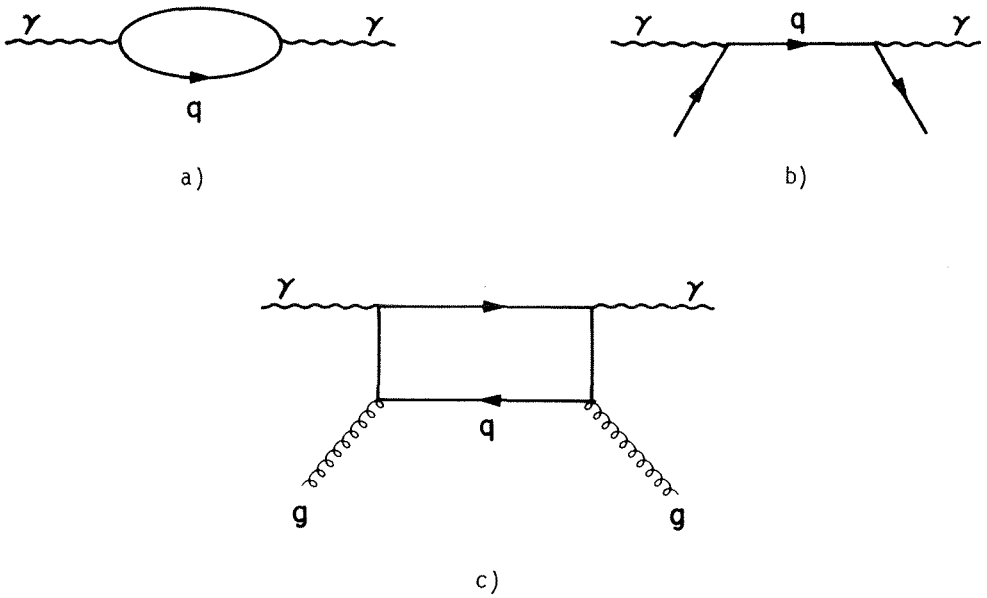

Fig. 24 Diagrams contributing to the leading operators in the current-current product expansion: a) unit operator, b) quark scalar density, c) gluon scalar density.

What one would like to do here is to probe resonance structure by chosing a value $Q^2 \sim 1$ GeV which emphasizes the resonance region of the dispersion integral, but this presents two major problems. For such low values of Q^2, higher-order terms in the expansion remain important, and the integrand in Eq. (7.2) does not converge rapidly enough to damp high Q^2 contributions to the integral. Shifman et al. have improved the situation by considering instead of (7.2) the quantity

$$\lim_{\substack{Q^2,n\to\infty \\ Q^2/n = M^2}} \frac{1}{(n-1)!} Q^{2n}\left(-\frac{d}{dQ^2}\right)^n \Pi \tag{7.4}$$

Then, instead of equating the left-hand sides of (7.2) and (7.3), one gets the relation

$$\frac{1}{\pi M^2}\int e^{-s/M^2}\sigma(s)\,ds = \hat{C}_1\langle 1\rangle + \hat{C}_2\frac{m\langle\bar{q}q\rangle}{2!M^4} + \frac{\hat{C}_2'}{2!M^4}\langle F\cdot F\rangle + \cdots \frac{h_n}{n!M^{2n}} + \cdots . \tag{7.5}$$

This trick provides a double miracle: the right-hand side converges much faster for moderate M^2, and the integral on the left-hand side is rapidly damped for $s > M^2$. Therefore if we choose, for example, $M^2 = m_\rho^2$, we can safely saturate the integral for the I = 1 part of the vector current with the ρ-meson contribution. The coefficient functions $\hat{C}_i$ in (7.5) are related to the C_i in (7.3) by

$$\hat{C}_i(\ln M^2) = C_i(\ln M^2)\left[1 + O\left(\frac{1}{\ln M^2}\right)\right] \tag{7.6}$$

and are calculated in the QCD leading log approximation. Some assumptions have to be made in evaluating the vacuum expectation values appearing in (7.5). The quantity $m\langle\bar{q}q\rangle$ is determined by standard soft-pion techniques

$$(m_u + m_d)\langle\bar{u}u + \bar{d}d\rangle \simeq -f_\pi^2 m_\pi^2 \tag{7.7}$$

$\langle F\cdot F\rangle$ can be evaluated for the presumably dominant one-instanton configuration, but the size integration diverges. The authors prefer to determine $\langle F\cdot F\rangle$ from their analogous sum rules for the charmonium states; the result corresponds to an instanton size cut-off $\rho < (200\ \text{MeV})^{-1}$, which seems plausible. They also find a non-negligible contribution from the four-quark operator, which they approximate by

$$\langle(\bar{q}q)(\bar{q}q)\rangle \simeq |\langle\bar{q}q\rangle|^2 = m_\pi^4 f_\pi^4/m_q^2\ , \tag{7.8}$$

and which can become large if the quark masses are very small. Using values of α_s and m_q which they justify on the basis of other calculations, they find [neglecting corrections O(1%)]

$$m_\rho^2 \simeq 0.6\ \text{GeV}\ ,\quad g_\rho^2/4\pi \simeq 2.42\ ,$$

in excellent agreement with the experimental values

$$m_\rho^2 = 0.602\ ,\quad g_\rho^2/4\pi = 2.36 \pm 0.18\ .$$

Equally remarkable results are obtained by considering currents with different quantum numbers, pseudoscalar densities, etc.

However, the results appear to depend strongly on the choice of the parameters α_s and m_q, which are taken smaller than the values accepted by most theorists. For example, their value of α_s is the one extracted from lowest-order QCD charmonium analysis, which has been found to suffer large higher-order corrections[61], rather than the higher values extracted from deep inelastic scattering data. In addition, the validity of their results depends on the $O(Q^{-12})$ non-perturbative corrections being negligible at the ρ mass. The effective scale parameter which was given as 1 GeV in Eq. (5.7) depends explicitly on m_q and α_s, and with the authors' undoubtedly controversial choice it is indeed $< m_\rho$. In spite of these caveats, it would seem difficult to ignore the success their analysis has met with.

Acknowledgements

I have enjoyed many instructive discussions with Rod Crewther, Sidney Coleman, John Ellis, Ronald Horgan, Vojtek Zakrzewski and especially Chris Sachrajda. The writing of this talk was completed at Fermilab, and it is a pleasure to thank Chris Quigg and the theory group for their hospitality. I am indebted to the scientific secretaries Ikaros Bigi and François Martin for invaluable help in preparing the manuscript.

REFERENCES

1) See: H.D. Politzer, Phys. Reports C14, 129 (1974).
A. Peterman (to be published in Phys. Reports).

2) K.G. Wilson, Phys. Rev. 179, 1499 (1969).
B.L. Ioffe, Phys. Lett. 30B, 123 (1969).
R.A. Brandt and G. Preparata, Nucl. Phys. B27, 541 (1971).
Y. Frishman, Ann. Phys. (NY) 66, 373 (1971).

3) E.C.G. Stueckelberg and A. Peterman, Helv. Phys. Acta 26, 499 (1953).
M. Gell-Mann and F. Low, Phys. Rev. 95, 1300 (1954).

4) C.H. Llewellyn Smith, Proc. 17th Int. Universitätswochen für Kernphysik, Schladming, 1978 [Acta Phys. Austriaca, Suppl. XIX, 331 (1978)].
K.H. Craig and C.H. Llewellyn Smith, Phys. Lett. 72B, 349 (1978).
Yu.L. Dokshitzer, D.I. D'yakanov and S.I. Troyan, Material for the 13th Leningrad Winter School, 1978 [SLAC TRANS-183 (1978)].
D. Amati, R. Petronzio and G. Veneziano, Nucl. Phys. B140, 54 (1978) and B146, 29 (1978).
For earlier related developments see, for example:
S.J. Chang and P.M. Fishbane, Phys. Rev. D 2, 1084 (1970).
V.N. Gribov and L.N. Lipatov, Sov. J. Phys. 15, 438 (1972).
I. Halliday, Nucl. Phys. B103, 343 (1976).
J. Frenkel, M.J. Shailer and J.C. Taylor, Nucl. Phys. B148, 228 (1979).
I. Hinchliffe and C.H. Llewellyn Smith, Phys. Lett. 65B, 281 (1971).
J.L. Cardy and G.B. Winbow, Phys. Lett. 52B, 95 (1974).

5) A partial list of references is:
R.F. Cahalan, K.A. Geer, J. Kogut and L. Susskind, Phys. Rev. D 11, 1199 (1975)
J. Ellis, M.K. Gaillard and G.G. Ross, Nucl. Phys. B111, 253 (1976).
T.A. De Grand, Y.J. Ng and S.-H. Tye, Phys. Rev. D 16, 325 (1977).
E.G. Floratos, Nuovo Cimento 43A, 241 (1977).
H.D. Politzer, Phys. Lett. 70B, 430 (1977).
R. Cutler and D. Sivers, Phys. Rev. D 16, 679 (1977).
B. Combridge, J. Kripfganz and J. Ranft, Phys. Lett. 70B, 234 (1977).
A.P. Contogouris, R. Gaskell and S. Papadopoulos, Phys. Rev. D 17, 2314 (1978).

6) A.A. Belavin, A.M. Polyakov, A.S. Schwarz and Yu.S. Tyupkin, Phys. Lett. 54B, 856 (1975).

7) N. Cabibbo and L. Maiani, Phys. Lett. 79B, 109 (1978).
M. Suzuki, LBL preprint 7948 (1978).
N. Cabibbo, G. Corbo and L. Maiani, Rome Univ. preprint ROM 79-145 (1979).
A. Ali and A. Pietarinen, DESY preprint 79/12 (1979).
See also M.K. Gaillard, Proc. SLAC Summer Inst. on Particle Physics, Stanford, 1978 (SLAC Report No. 215, 1978), p. 397.

8) A. Billoire, R. Lacaze, A. Morel and H. Navelet, Phys. Lett. 78B, 140 (1978); and Saclay preprint DPh-T/78/111 (1978).
W. Bernreuther, N. Marinescu and M.G. Schmidt, Heidelberg preprint HD-THEP-79-5 (1979).

9) G.P. Lepage and S.J. Brodsky, SLAC preprints SLAC-PUB-2348 and 2343 (1979).
For earlier work, see R. Coquereaux and E. de Rafael, Phys. Lett. 74B, 105 (1978).

10) E.G. Floratos, D.A. Ross and C.T. Sachrajda, Nucl. Phys. B129, 66 (1977) and B139, 545 (1978).
W.A. Bardeen, A.J. Buras, D.W. Duke, and T. Muta, Phys. Rev. D 18, 3998 (1978).

11) O. Nachtmann, Nucl. Phys. B63, 239 (1973) and B78, 455 (1974).

12) J. Kogut and L. Susskind, Phys. Rev. D 9, 697 (1974) and D 9, 3391 (1974).

13) G. Altarelli and G. Parisi, Nucl. Phys. B126, 298 (1977).

14) L. Baulieu and F.C. Kounnas, Paris preprint LPTENS 78/27 (1978).

15) I follow closely the descriptions given by C.H. Llewellyn Smith, Ref. 4, and C.T. Sachrajda, Proc. 10th GIFT Seminar on Theoretical Physics (1979), in preparation.

16) H.D. Politzer, Nucl. Phys. B129, 301 (1977).
C.T. Sachrajda, Phys. Letters 73B, 185 (1978).
C.T. Sachrajda, Phys. Letters 76B, 100 (1978).

17) B. Humpert and W.L. Van Neerven, COO-881-54/ Rev. (1978), Phys. Lett. B, to be published.
G. Altarelli, K. Ellis and G. Martinelli, MIT preprint, MIT-77619 (1979).
K. Harada, T. Kanako and N. Sakai, CERN preprint TH-2619 (1979).

18) R.K. Ellis, H. Georgi, M. Machacek, H.D. Politzer and G.G. Ross, Nucl. Phys. B152, 285 (1979).
S. Libby and G. Sterman, Phys. Rev. D 17, 2773 and 2789 (1978).

19) G. Sterman and S. Weinberg, Phys. Rev. Lett. 39, 1436 (1977).
See also:
B.G. Weeks, Phys. Lett. 81B, 377 (1979).
K. Shizuya and S.-H. Tye, Phys. Rev. Lett. 41, 787 and 1195(E) (1978).
M.B. Einhorn and B. Weeks, SLAC-PUB-2164 (1978).

20) P. Binétruy and G. Girardi, Phys. Lett. 83B, 339 (1979).

21) Data: Ch. Berger et al., PLUTO Collaboration, Phys. Lett. 82B, 449 (1979).
Calculation: I.I.Y. Bigi and T.F. Walsh, Phys. Lett. 82B, 267 (1979).

22) S. Brandt, Ch. Peyrou, R. Sosnowski and A. Wroblewski, Phys. Lett. 12, 57 (1964).
E. Farhi, Phys. Rev. Lett. 35, 1609 (1975).

23) H. Georgi and M. Macharek, Phys. Rev. Letters 39, 1237 (1977).

24) J.D. Bjorken and S.J. Brodsky, Phys. Rev. Lett. D 1, 1416 (1977).

25) Private communications from experimentalists.

26) S. Brandt and H.D. Dahmen, Z. Phys. C1, 61 (1979).

27) A. De Rújula, J. Ellis, E.G. Floratos and M.K. Gaillard, Nucl. Phys. B138, 387 (1978).

28) PLUTO Collaboration, see H. Meyer, *in* Highly Specialized Seminars, Erice, 1979.

29) Ch. Berger et al., PLUTO Collaboration, Phys. Lett. 78B, 176 (1978).

30) K. Koller, H. Krasemann and T.F. Walsh, Z. Phys. C1, 71 (1979).

31) G. Fox and S. Wolfram, Phys. Lett. 82B, 134 (1979); Phys. Rev. Lett. 41, 1581 (1979); and Nucl. Phys. B149, 413 (1979).
J.F. Donoghue, F.E. Low and S.Y. Pi, MIT preprint, MIT-CTP 771 (1979).

32) K. Koller and T.F. Walsh, Phys. Lett. 72B, 227 (1977) and E 73B, 504 (1978).
G. Parisi, Phys. Lett. 74B, 65 (1978).
C.L. Basham, L.S. Brown, S.D. Ellis and S.T. Love, Phys. Rev. Lett. 41, 1585 (1978), Phys. Rev. D 17, 2298 (1978), and Univ. of Washington preprint RLO-1388-759 (1978).
G. Parisi and R. Petronzio, Phys. Lett. 82B, 26 (1979).
E.G. Floratos, Saclay preprint DPh T/79/89 (1979).

33) H. Fritzsch and K.H. Streng, Phys. Lett. 74B, 90 (1978).
S.-Y. Pi, R.L. Jaffe and F.E. Low, Phys. Rev. Lett. 41, 142 (1978).
S.-Y. Pi and R.L. Jaffe, MIT preprint CPT 735 (1978), to appear in Phys. Rev. D Comments and Addenda.
J. Ellis and I. Karliner, Nucl. Phys. B148, 141 (1979).

34) M. Krammer and H. Krasemann, Phys. Lett. 73B, 58 (1978).
H. Krasemann, Z. Phys. C1, 189 (1979).

35) H. Georgi and H.D. Politzer, Phys. Rev. Lett. 40, 3 (1978).
G. Ranft and J. Ranft, Leipzig Univ. preprint 78-15 (1978).
A. Méndez, Nucl. Phys. B145, 199 (1978).
A. Méndez, A. Raychaudhuri and V.J. Stenger, Nucl. Phys. B148, 499 (1979).
J. Cleymans, Phys. Rev. D 18, 954 (1978).
G. Köpp, R. Maciejko and P.M. Zerwas, Nucl. Phys. B144, 123 (1978).
G. Altarelli and G. Martinelli, Phys. Lett. 76B, 89 (1978).
P. Mazzanti, R. Odorico and V. Roberto, Bologna preprint IFUB/78-11 (1978).
F. Hayot and A. Morel, Saclay preprint DPh-T/79/3 (1979).
K.H. Streng, T.F. Walsh and P.M. Zerwas, DESY preprint 79/10 (1979).

36) P. Binétruy and G. Girardi, CERN preprint TH-2611 (1979) to be published in Nucl. Phys. and *in* Highly Specialized Seminars, Erice, 1979.

37) J.B. Kogut, Phys. Lett. 65B, 377 (1976).
D. Lopez, Phys. Rev. Lett. 38, 461 (1977).
A.V. Radyshkin, Phys. Lett. 69B, 245 (1977).
J. Kogut and J. Shigimitsu, Nucl. Phys. B129, 461 (1977).
H. Fritzsch and P. Minkowski, Phys. Lett. 73B, 80 (1978).
G. Altarelli, G. Parisi and R. Petronzio, Phys. Lett. 76B, 351 and 356 (1978).
K. Kajantie and R. Raitio, Helsinki preprint HU-TFT 77-21 (1977).
F. Halzen and D. Scott, Phys. Lett. 79B, 123 (1978).
K. Kajantie and J. Lindfors, Helsinki preprint ISBN 951-45-1487-4 (1978).

38) H. Fritzsch and P. Minkowski, Phys. Lett. 69B, 316 (1977).
Z. Kunszt and E. Pietarinen, DESY preprint 79/18 (1979).
Z. Kunszt, E. Pietarinen and E. Reya, DESY preprint DESY 79/28 (1979).

39) R. Horgan, private communication.

40) E. Witten, Nucl. Phys. B120, 189 (1977).

41) C.H. Llewellyn Smith, Phys. Lett. 79B, 83 (1978).
W.R. Frazer and J.F. Gunion, Phys. Rev. D 19, 2447 (1979).

42) S.J. Brodsky, T.A. Debrand, J.F. Gunion and J.H. Weis, Phys. Rev. D 19, 1418 (1979).

43) Tu Tung-Sheng and Wu Chi-Min, CERN preprint TH-2646 (1979).
Chang Chao-Hsi, Tu Tung-Sheng and Wu Chi-Min, CERN preprint TH-2675 (1979).

44) G.R. Farrar and B.L. Ioffe, Phys. Letters 71B, 118 (1977).
K. Koller, T.F. Walsh and P.M. Zerwas, DESY preprint 78/77 (1978).

45) M. Abud, R. Gatto and C.A. Savoy, Univ. of Geneva preprint UGVA-DPT 1979/03-192 (1979).

46) C.H. Llewellyn Smith, *in* LEP Summer Study, Les Houches, 1978 (CERN 79-01, 1979), p. 35.

47) G. 't Hooft, Phys. Rev. Lett. 37, 8 (1976); Phys. Rev. D 14, 3432 (1976) and Erratum in D18, 2199 (1978).
C.G. Callan, R. Dashen and A.J. Gross, Phys. Lett. 63B, 334 (1976) and 66B, 375 (1977).

48) N. Andrei and D.J. Gross, Phys. Rev. D 18, 468 (1978).
L. Baulieu, J. Ellis, M.K. Gaillard and W.J. Zakrzewski, Phys. Lett. 77B, 290 (1978).
T. Appelquist and R. Shankar, Phys. Lett. 78B, 468 (1978).

49) L.S. Brown, R.D. Carlitz, D.B. Creamer and C. Lee, Phys. Lett. 70B, 180 (1977).

50) L. Baulieu, J. Ellis, M.K. Gaillard and W.J. Zakrzewski, Phys. Lett. 81B, 41 (1979).
C.A. Flory, LBL preprint 8499 (1979).

51) J. Ellis, M.K. Gallard and W.J. Zakrzewski, Phys. Lett. 81B, 224 (1979).

52) C.G. Callan, R. Dashen and D.J. Gross, Phys. Rev. D17, 2717 (1978).
F. Wilczek and A. Zee, Phys. Rev. Lett. 40, 83 (1978).
C.G. Callan, R. Dashen, D.J. Gross, F. Wilczek and A. Zee, Phys. Rev. 18, 4684 (1978).
W. Bernreuther et al., Ref. 8.

53) See, however, Appelquist and Shankar, Ref. 48.

54) S.L. Glashow, *in* Hadrons and their interactions (Academic Press Inc., New York, 1968), p. 83.
S. Weinberg, Phys. Rev. D 11, 3583 (1975).

55) J. Kogut and L. Susskind, Phys. Rev. D 11, 3594 (1975).

56) G. 't Hooft, Ref. 47.

57) R.J. Crewther, Phys. Lett. 70B, 349 (1977).

58) R.J. Crewther, Riv. Nuovo Cimento 2, No. 8 (1979) p. 63.

59) H. Goldberg, Northwestern University preprint NUB No. 2397 (1979).

60) M.A. Shifman, A.I. Vainshtein and V.I. Zakharov, Nucl. Phys. B147, 385, 448 and 519 (1979).

61) R. Barbieri, E. d'Emilio, G. Curci and E. Remiddi, CERN preprint TH-2622 (1979).

QUANTUM CHROMO DYNAMITE

Alvaro De Rújula*)
CERN, Geneva, Switzerland.

ABSTRACT

The explosion of interest in QCD makes a review both timely and impossible. In this talk I discuss aspects of QCD that were not covered by other speakers at the same Conference (EPS 79). These include topics in "non-perturbative" QCD (i.e. the 1/N expansion), in perturbative QCD (is it really being tested?, are form factors calculable?), and in the land of in-between (higher twists, duality, preconfinement...).

1. APOLOGETIC INTRODUCTION

QCD is neither in its infancy nor is it dead, but it is youthfully undecided and moving in many directions simultaneously. Reviewing its present status, as I was supposed to do in this talk, is a rather herculean task. Fortunately many aspects of QCD's theory and experiment have been covered by other speakers at this conference. Thus I only have to fill in some holes. This is a partial justification for the sporadic nature of this review. I will concentrate on four topics: non-perturbative effects and confinement (with emphasis on the 1/N approach); deep inelastic scattering (with emphasis on the theoretical uncertainties); the recent progress in understanding elastic form factors (with justifiable emphasis); and the attempts to bridge the QCD gap between perturbation theory and the hypothetical confining phase.

I will not attempt to give a fair reference list to the QCD classics.

2. SOLVING QCD

2.1 Why is it so hard?

Perhaps it is not. But one can point out limitations in our present technology that make some non-perturbative problems particularly untractable. Refer, for the sake of definiteness, to a light quark bound state: the pion or the ρ meson. Here, it can be argued that heavy quark effects are irrelevant. Moreover, the light quark "Lagrangian" masses are also thought to be irrelevant on the scale of the bound-state solution, the inverse pion radius. Thus, it is as if the theory had no relevant dimensionful parameters, the only parameter being the strength g of the coloured couplings. What then sets the scale of distances or energies? Renormalizable field theories provide a tricky answer: dimensional transvestism. The numerical value of the (running, renormalization point independent) dimensionless coupling constant, itself gives a meaning to the momentum scale. In an asymptotically free field theory at sufficiently large momentum

$$\alpha_s = g^2/4\pi = (b \ln Q^2/\Lambda^2)^{-1} , \qquad (1)$$

the value of the coupling is governed by a physical parameter Λ with dimensions of mass. And now we are in trouble: in a light quark bound-state problem where the momentum, mass, and size scales are to come out as the answer, QCD possesses no small parameter to justify

*) Sloan Foundation Fellow, on leave from Harvard University.

our modest tools: perturbation theory and/or a non-relativistic treatment. The α_s of Eq. (1) may take any value, including those large enough to invalidate Eq. (1), obtained from (renormalization group improved) perturbation theory. Life would be very different for quarks of mass $m_q >> \Lambda$, the low-level bound-state problem would be tractable although confinement and the forces between distant quarks would presumably be equally challenging.

Though confinement has been found to be difficult to prove, the struggle is not in vain: many an important insight has been gained from the different approaches, some of which I will proceed to comment upon; others, reviewed by other speakers, I will just mention.

2.2 The big guns approach

Heel goed[1], say some, the problem of confinement is essentially non-perturbative, so we will attack it with techniques that do not mention perturbation theory, such as direct minimization of the action. This approach has led to important discoveries: the resolution of the U(1) problem[1,2] (to which I will come back), the discovery of instantons and the non-trivial nature of the QCD vacuum[1,2], the suspicion that axions may exist[3], etc. The progress in these fields has been reviewed by Gaillard[4] and Fairlie[5], and I will not dwell on the subject. In spite of the elegance of the approach and the beauty of some results, it is not clear whether or not the explicit solutions to the QCD equations of motion found so far (instantons) are relevant to confinement.

2.3 The guess-the-answer approach

At the other extreme of the spectrum (of sophistication, ambition, or physical sense, depending on your taste) lie those who guess at a model of confined colour, distastefully call it a "bag", and proceed to do constructive phenomenology. Hey[6] has reviewed this field, with emphasis on recent work by Jaffe and Low[7] on the (so far neglected) effects of open decay channels on the spectrum of quark bound states.

A limitation (virtue?) of the bag approach is that it makes field theorists cry. Attempts to justify the bag in a field theoretic language have recently been revived by Lee[8] in a model where hadrons are bubbles in a perfect chromodielectric vacuum. A virtue of the model is that in certain limits it reproduces all of the different "bags" (MIT, SLAC) that have been satisfactorily used to describe the hadron spectrum.

I cannot refrain from mentioning the intriguing work of Nielsen and Ninomiya[9] presented in the parallel sessions. These authors emphasize that no longer does anybody in his right mind believe the vacuum to be empty. On the contrary, the QCD vacuum presumably has a complicated colourful structure. It is possible to guess vacuum structures whose energy density (calculated perturbatively: a weak point) is lower than zero, the energy density of the "vacuum" inside a hadron bag. The bag constant B must be bigger than the energy density gap between the ansatz outside vacuum and the vacant inside vacuum; equal to it if the ansatz was right. The limits on α_s as a function of B thus obtained are suspiciously close to our present rough experimental values of α_s.

2.4 Two "hidden parameter" approaches: lattices and 1/d expansions

As stated in Section 2.1, QCD does not really have a parameter in which to do perturbation theory. Several roundabout approaches to the non-perturbative aspects of QCD are based on the following incantation: Choose a "parameter" having some fixed value in Nature, say

d = 4, with d the number of space-time dimensions. Develop the theory in powers of this parameter (or of its inverse) around a value where the theory may be simpler (d = 2, d^{-1} = 0?) Hope that the extrapolation to the real world (d↑4, d↓4) converges fast enough for this "perturbation theory" to be sensible. Hope that one can prove that aspects of the simplified theory (confinement?) survive the limiting procedure.

The oldest and most developed of these roundabouts is the lattice[10]. Here, space is substituted by a set of points with spacing L, at which colour sources may sit. The colour fields link the colour sources. The approach has the advantage of taming *ab initio* the violent infrared behaviour of chromodynamics. The theory at fixed L may be expanded in powers of 1/g, with g the colour charge. For reasonable confinement criteria and sufficiently large g, the model confines quarks. The unsurpassed difficulty, it goes without saying, is in the limit L → 0. At least two recent steps in the lattice approach are worth mentioning.

The first is a theorem[11] of which I shall quote an abridged version, followed by an attempt to explain its enunciation.

Theorem: If static quarks are confined in a lattice Z_3 gauge theory (with coupling g), they are also confined in a lattice SU(3) gauge theory (with coupling κg, κ < ∞).

Z_3 is the centre of SU(3): the discrete set of group elements that commute with all elements of the group, $Z_3 = [1, \exp(2\pi i/3), \exp(4\pi i/3)]$. An optimist may react as follows: If the lattice is the way to understand confinement, the theorem is an enormous step forward; it reduces the group theory aspects from the complicated group SU(3) to its almost trivial centre. A pessimist may react as follows: It is hard to picture Z_3, a group of discrete transformations, in the continuous (L → 0) limit. Z_3 is not a gauge group in the sense of being associated with gauge gluons. How can one hope that the dynamics of confinement will have such an incidental connection (a non-trivial group centre) with the gauge particles that carry the forces? We shall have to wait and see.

A second and very intriguing advance in the lattice battleground is due to Kogut, Pearson and Shigemitsu[12]. They compute a suitably defined β-function (governing the momentum scale evolution of the coupling constant) in the strong coupling confining phase of the lattice theory, in a considerable number of inverse powers of g. They find that as they move towards the intermediate coupling regime (g↓1) the lattice β-function "tries to match" onto the conventional perturbative β-function of asymptotically free renown. I am not competent to judge the reliability of a truncated strong coupling expansion (or, for that matter, any other perturbation theory). But the result could be the first example where we see two ends of QCD (perturbative and confining) meet.

2.5 The 1/N expansion; another "hidden parameter" approach

Let N be the number of quark colours. In our neighbourhood, we have very good reasons to believe that N = 3. This is a rather large number, for after all, even the most abstract physicists count 1, 2, 3, many; and most phenomenologists count 1, 2, ∞. The hope (not yet a reality in four-dimensional QCD) is to solve the theory in powers of 1/N, and set N = 3 at the end[13]. This may be somewhat better than it sounds, since for many observables the actual expansion parameter is $1/N^2$, much as it is e^2 in QED. An optimist may even expect the effective perturbation parameter to be $1/4\pi N^2$, analogous to $\alpha = e^2/4\pi$. Notice that $\alpha = 1/137.035982(30)$ while for N = 3, $1/4\pi N^2 = 1/113.0973356(1)$, and dig it.

There are more serious reasons for listening to the songs of the 1/N mermaids. One of them is that one can argue that QCD, in the large N limit -- the zeroth approximation in the 1/N expansion -- leads to a qualitative picture of the hadron world not unlike reality. Moreover, some qualitative results of the 1/N approach (i.e. Zweig's rule for light particles) have not been obtained otherwise. Witten[14] turns this argument around to conclude that the 1/N expansion may be a fast converging one: N = 3 is large enough not to obliterate the N = ∞ picture.

In what follows I discuss the 1/N approach in more detail than any other assault on QCD, with the exception of good old perturbation theory. Two reasons are: i) the 1/N technology is simple enough that its rudiments can be explained in no time to a kiloperson audience[14]; ii) the approach has made more contact with phenomenology than have the other formal approaches (just recall the Z_3 theorem). But, I must pause for a warning: confinement has not been proved, even in the $N \to \infty$ limit. Some believe that as $N \to \infty$ the theory should *not* confine. Some believe that it should, but that the proof is not simpler as $N \to \infty$. More constructive groups[15] have found that the $N \to \infty$ limit of some (toy) theories is much simpler than what one would expect.

A technology for guessing results in the 1/N, "large" N expansion is essentially based on quark and gluon colour counting in Stükelberg-Feynman diagrams. Let a quark q^i be denoted by an arrow with a colour index i = 1, ..., N as in Fig. 1a. Let a gluon $A_{\mu j}^{\ i}$ be denoted by two oppositely directed coloured arrows; i,j = 1, ..., N as in Fig. 1b. The fact that A_j^i

Fig. 1

should be made traceless (there are $N^2 - 1$ and not N^2 coloured gluons in the adjoint representation on an SU(N) coloured gauge theory) is irrelevant in the large N limit. Believe it or not, we are now in a position to "derive" the suppression of the "sea constituency of hadrons" or the apparent absence of "four-quark exotics" in the Particle Data Tables. Consider the diagram of Fig. 2a, where some gluon exchanges are happening in a quark-antiquark bound state. Figure 2b is a redrawing of Fig. 2a, with the labelling convention just adopted. Notice that the coloured lines are continuous and that the colour index of the central ring may run from 1 to N; it is not constrained, as the other lines are, to have the colour of the incoming and outgoing quarks. Consider Fig. 2c with the gluon loop substituted by a quark loop. Should one catch the meson in this disguise, it would have a sea constituency or be exotic. But when one draws the coloured lines as in Fig. 2d, the N possibilities that we found for the internal line in the gluon counterpart (Fig. 2b) are no longer there. Thus the four-quark state is suppressed by a relative factor N in amplitude, *quod constituibat demonstraturum*[13,14].

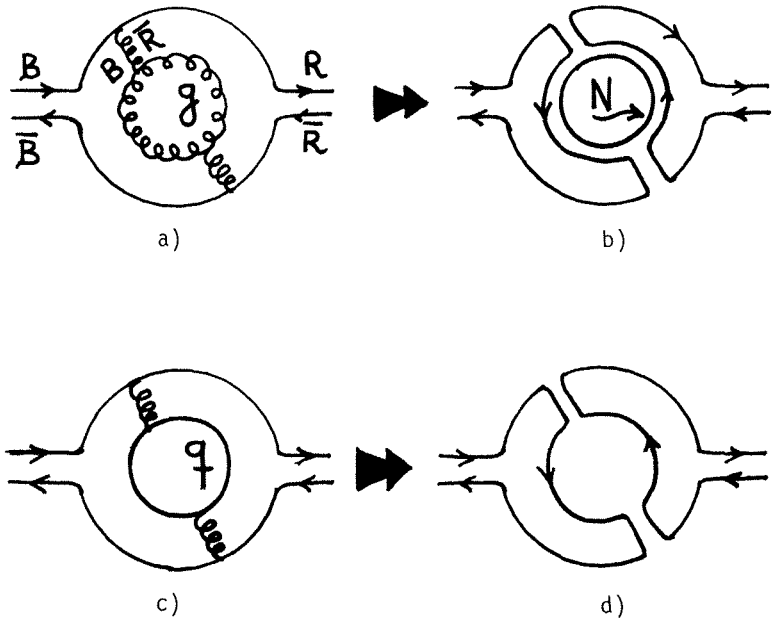

Fig. 2

A similar argument (with the additional information that a non-trivial large-N theory is obtained with a coupling $g/\sqrt{N}$, at fixed g) may be used to "prove" that the Zweig-Iizuka forbidden decay of Fig. 3a is suppressed in amplitude by a factor N, relative to the Zweig allowed counterpart of Fig. 3b or any of its purely gluonic (planar) dressings. Perturbation theory arguments can be advanced for the suppression of the total widths of heavy "onium" states (i.e. $J/\psi \to$ all $\approx J/\psi \to 3$ gluons) but the same arguments have no reason to hold for exclusive decays ($\psi' \to \psi\pi\pi$) or the "forbidden" decays of relatively light mesons ($\phi(s\bar{s}) \to$ $\to K\bar{K} > 5\phi \to \rho\pi$). Thus one may say that the 1/N expansion offers the only complete explanation of Zweig's rule. Unfortunately, we are not yet in a position to understand the actual numerology.

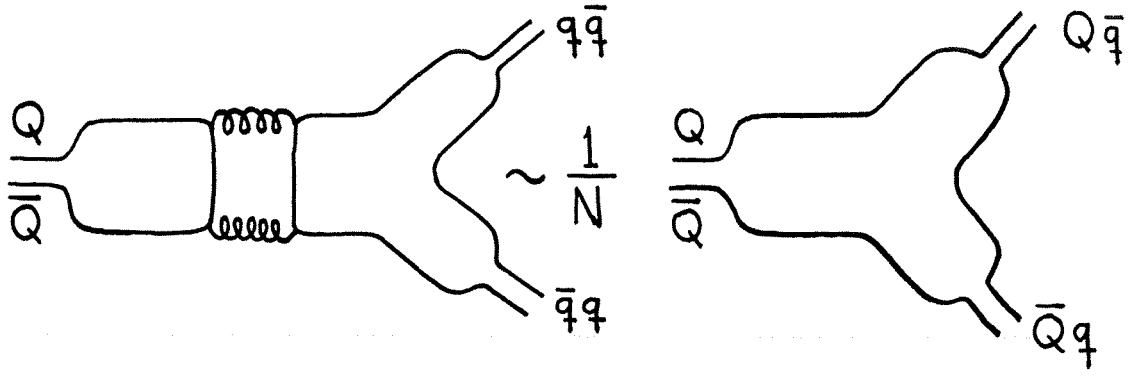

Fig. 3

In Table 1, I have collected a list of "classic" large-N results[13]. Notice they all refer to mesons.

Table 1

Classic 1/N statements

Claim ($N \to \infty$)	Particle Data (Michelin *)
$\forall J^{PC}$, $\exists \infty$ many mesons M	* * * * ...
M's are not exotic	* * (*?)
M's have finite masses: $m(M) \to$ const.	* * *
M's are narrower than their masses: $\Gamma(M \to MM) \to N^{-1}$	*
M's are quasi-free: $\sigma(MM \to MM) \to N^{-2}$	?
Glue balls must exist, but their production is strongly damped[16]: $\sigma(MM \to \text{Glue balls}) \to N^{-2}$	* * *
Zweig-Iizuka rule Small sea constituency	* * *
Meson interactions can be described with a phenomenological Lagrangian with multimeson exchanges	* (Regge?)

Some would accuse the above table of being "poetry" (much as the parton model was prose before QCD justified it). The rationale for the accusation is that QCD has not been exactly solved even as $N \to \infty$. The solution would involve an infinite sum of diagrams, but only planar ones, presumably a considerable simplification.

2.6 Recent progress in the 1/N expansion

At least four items are worth mentioning, of which I will discuss the last two:

i) Towards the summation of planar diagrams in toy theories [already quoted[15]].

ii) Further instanton confusion: does the gas evaporate as $N \to \infty$? [see Fairlie's talk[5]].

iii) The consistent inclusion of baryons in the large-N qualitative picture[14].

iv) Further understanding of the resolution of the U(1) problem[17].

No matter the number of quark colours, the natural generalization of a meson to $N \neq 3$ is a two-particle quark-antiquark colourless combination: $q^i \bar{q}_j$. The natural generalization of a baryon would be a completely antisymmetric N-quark compound: $\varepsilon_{ij\ldots\ell}\, q^i q^j \ldots q^\ell$.

The colour-counting diagramatic techniques get out of hand for a baryon whose number of constituents increases with N, but the problem is amenable to a path integral formulation. I will quote some results[14] of Witten's, established for heavy quarks and reasonably argued (quite explicitly in two-dimensional QCD) for light quark systems:

i) The mass of a baryon increases linearly with N. This sounds trivial, since N is the number of baryon constituent quarks. It sounds less trivial when one recalls that the perturbation parameter is 1/N: baryons are the monopoles of QCD (the mass of a conventional monopole is also proportional to the inverse of the coupling constant).

ii) The radius R of a baryon tends to a finite limit at large N. To be expected: a new colour is invented every time a new quark is added, $N \to N + 1$, and no exclusion principle makes the baryon bulge. Moreover, Witten argues, any quark moves in the self-consiste[illegible] Hartree-Fock potential of the others. Thus, in the large-N limit, Bjorken scaling would be strikingly precocious: it should set in for Q bigger than the parameters describing the motion of a single quark (R^{-1}, m_q) and not for Q bigger than the nucleon mass ($m_N \sim Nm_q$, NR^{-1}). It would be nice to believe these arguments[18] for N = 3.

iii) Cross-sections for meson-baryon and baryon-baryon scattering are O(1) at large N, a breakdown of "additivity".

The so-called U(1) problem has remained a field of controversy for many years. A naive, imprecise, and easy to improve way of stating the problem is the following[19]. Return to the old three-quark days, q = (u, d, s). Consider the eightfold-way octet of axial currents $A_\mu^\alpha = \bar{q}\gamma_\mu\gamma_5\lambda^\alpha q$. Their divergencies are $O(m_q)$. This makes theorists correctly "suspect" that eight light pseudoscalars (π, K, η) should exist. The problem is that there is an extra U(1) current $A_\mu^0 = \bar{q}\gamma_\mu\gamma_5 q$, with an $O(m_q)$ divergence, but the corresponding singlet pseudoscalar (η'?) is not light enough to satisfy theorists. The U(1) problem can best be dramatized in terms of mass inequalities that the observed particles do not satisfy[20].

Here are some ups and downs of the U(1) battle, in a QCD framework:

1) Simple people skirt the problem[21] by pointing out that a $q\bar{q}$ *singlet* may annihilate into two or more gluons, implying a contribution to its mass ($q\bar{q} \to gg \to q\bar{q}$) that octets do not share.

2) As Gaillard reviewed[4], more sophisticated people state that in the presence of instantons, the U(1) current has an anomaly, it is not conserved (even in the $m_q \to 0$ limit) and the U(1) problem was not there to start with[1,2].

3) Supersophisticated people[19] have reasons to criticize both of the above paragraphs.

4) Diplomatic people[17] use the 1/N expansion to argue that the simple and sophisticated are both right. For N = 3 the anomaly is a non-perturbative effect, which cannot be smoothly turned off and investigated in perturbation theory. Not so in the 1/N expansion, say they. The current anomaly and the gluon annihilation diagrams are seen to be one and the same thing. In an attempt to tame the critics, Veneziano has proved[22] the Ward identities implied by this point of view, and Di Vecchia[23] has proved the statements to be right in explicitly solvable models that share many of the QCD's properties (two-dimensional CP_n). Their attempt [to tame the critics[24]] failed[24].

2.7 Inconclusions at half way

The proof that QCD does or does not confine quarks in one sense or another remains unconquered. I have only described aspects of a few approaches to QCD that have developed around attempts to understand confinement. A few other approaches are summarized in Fig. 4.

Fig. 4

Perhaps I convinced some sceptics that, although we do not understand confinement, the theoretical progress around this subject has been considerable. A cynic would conclude that the proof of confinement is among the things that one should make last.

Fairbank and collaborators[25] may be the only group that have made real progress in the subject of quark confinement. It is instructive to compare the community's lack of reaction to this situation (an anti-dogma claim) with the reaction to Weber's announcement of a gravitational wave signal (a pro-dogma claim). In the latter case, several groups rapidly improved upon the experiment with, alas, well-known negative results. In our business, such is the power of prejudice.

3. QCD IN PERTURBATION THEORY

Perturbative QCD is a theory of unconfined quarks and gluons, whose asymptotic freedom often allows us to do a consistent perturbation expansion at large momenta. Even the most solid results (asymptotic freedom itself, the formal derivation of the Q^2 evolution of moments of structure functions) can be agnostically criticized on grounds that we do not really know how non-perturbative and confining effects would affect the perturbative statements. In this situation we may follow one of three reasonable paths:

i) Attempt to build a theory superior to today's QCD [see the talk by Preparata[26]].

ii) Continue to apply perturbation theory to new observables or to higher orders in α_s. This is only reasonable if supplemented with point (iii).

iii) Be aware of the assumptions that provide the bridge between perturbation theory and the real world where quarks and gluons do not easily get out (i.e. softness of wave functions). Either attempt to bridge the gap theoretically, or let experiment interplay with perturbation theory to learn the amount of sense that the latter makes.

In the sections that follow I will describe progress and controversy in the second and third of the above entries.

Much of the history of quantitative QCD evolved around inclusive deep inelastic lepton scattering, and the understanding of scaling and deviations thereof. It is a curious history:

i) Scaling was predicted to be an asymptotic property ($Q^2 \gg m_p^2$) of hadron structure functions.

ii) Scaling was observed, but turned out to be precocious (correct to $\sim$ 20% at $Q^2 > 1$ GeV^2).

iii) QCD and its asymptotic freedom made scaling and the existence at long distances of strong-strong interactions, compatible. A specific pattern of scaling deviations was forecast.

iv) Scaling deviations consistent with the predicted behaviour were observed.

v) The liturgical appeal of the classic formal approach to the study of scaling deviations, based on the operator product expansion and renormalization group techniques, was lost as a more "physical" diagrammatic approach[27] developed (Altarelli-Parisi equations, sums of ladder graphs in physical gauges, etc.). Scores of theorists joined the game.

vi) Although the agreement between theory and experiment did nothing but improve, there developed doubt, scepticism and even serious criticism. The pleasant conclusion that

QCD is vindicated is now placed under serious scrutiny. This point I will discuss *ad nauseam*, concentrating on deep inelastic scattering.

3.1 Scaling deviations beyond the leading log

It is incredibly well known that the QCD prediction for the Q^2 evolution of x-moments of non-singlet*) structure functions F is particularly simple:

$$M_n \equiv \int_0^1 x^n F(x,Q^2)\, dx$$

$$M_n(Q^2) \simeq M_n(Q_0^2) \left(\frac{\ln Q^2/\Lambda^2}{\ln Q_0^2/\Lambda^2} \right)^{-d_n} \left[1 + O(\alpha_s) + O(1/Q^2)\right].$$

Target mass effects to all orders in m_p^2/Q^2 can be explicitly included into the above expression by use of Nachtmann moments[28]. The exponents d_n are explicitly known. The above formula, without the unspecified corrections, is generally called the "leading log" result. It corresponds, to the sum of all perturbation theory diagrams in the approximation $\alpha_s(Q^2) \ll 1$, $\alpha_s(Q^2) \ln Q^2/\Lambda^2 \sim O(1)$. (Recall that $\alpha_s \sim 1/\ln Q^2$.) I will explicitly discuss the "higher twist" $O(1/Q^2)$ corrections in the next section, and temporarily and *blindly* proceed as if they could be confidently neglected.

The neutrino data have been analysed by the experimentalists themselves in terms of moments of non-singlet structure functions. The well-publicized results are that the data are compatible with the leading log QCD prediction, that several ratios of the exponents d_n/d_m are determined to agree with a vector gluon theory, and that the value of Λ in the fits is a few hundred MeV [29]. To gauge the relevance of this leading log success, it is necessary and by no means sufficient to know how large the $O(\alpha_s)$ corrections are. Knowledge of these terms has recently been completed with the calculation of the singlet $O(\alpha_s)$ corrections[30]. Three statements are often quoted: the $O(\alpha_s)$ terms are so large that perturbation theory is doubtful; the $O(\alpha_s)$ corrections are small; it depends. I am faced with the hard task of explaining that none of these statements is entirely wrong.

Let me rewrite a bit more explicitly the prediction for a structure function moment, up to and including $O(\alpha_s)$ corrections:

$$M_n(Q^2) = \frac{K_n}{(\ln Q^2/\Lambda^2)^{d_n}} \left[1 + \frac{a_n + b_n \ln \ln Q^2/\Lambda^2}{\ln Q^2/\Lambda^2} + O(\alpha_s^2)\right],$$

where K_n is an unknown constant that reflects our ignorance of bound-state dynamics. The coefficients a_n and b_n are calculable (and calculated) in perturbation theory, the dimensionful parameter Λ is not. The source of confusion is that Λ and a_n (though not b_n) are "renormalization-scheme dependent". In a renormalizable field theory the meaning of the

*) A non-singlet structure function is one to which only matrix elements of quark operators (as opposed to quark and gluon operators) contribute. The combination F_2(ep-en) is an example, because gluons carry no isospin. The VA interference $xF_3(\nu$ or $\bar{\nu})$ is an example, because gluons have definite colour G-parity, and V and A currents have opposite charge conjugation.

parameters, say $\alpha_s(Q^2)$, must be ascertained with particular care. QED has a tractable low-energy limit, and there is a tacit agreement to define α through the Thompson limit of Compton scattering. But α could have been defined otherwise, $\alpha' \equiv 2\pi(g-2)_\mu$, to give an example. Calculations in terms of α or α' would look different, yet mean the same. QCD does not have a perturbatively tractable low-energy limit, and the definition of $\alpha_s(Q^2)$ used in a higher-order calculation must be made explicit. No definition or "renormalization scheme" is obviously the best, and experts have not reached a peace treaty on a standard procedure[31]. All this does not imply that two correct calculations of the same quantity in two different schemes may give different results: formally, the results are the same up to corrections of the first neglected order of perturbation theory. So much for generalities. Now, data analysis. The real question is whether the data are good enough to test QCD beyond the leading log predictions.

A popular and inelegant way of expressing the effect of $O(\alpha_s)$ corrections to the moment predictions is to reabsorb them into an n-dependent redefinition of $\Lambda \to \Lambda_n$ (strictly speaking this is not possible, but numerically speaking and given present experimental errors, it is all right). The data are then fitted to a "leading-log-like" expression with a free Λ parameter for each moment:

$$M_n(Q^2) \simeq \frac{K_n}{(\ln Q^2/\Lambda^2)^{d_n}}\left[1 + \frac{a_n + b_n \ln\ln Q^2/\Lambda^2}{\ln Q^2/\Lambda^2}\right] \simeq \frac{\overline{K}_n}{(\ln Q^2/\Lambda_n^2)^{d_n}} .$$

This does not eliminate the formal scheme-dependence of the predictions for Λ_n, but the ratios Λ_n/Λ_m are scheme-independent, as emphasized by Para and Sachrajda[32]. However convoluted, these ratios are a good place where theoretical $O(\alpha_s)$ corrections can be compared with experiment. In Fig. 5a two sets of neutrino data are compared with theory[32]. The horizontal axis is the order of the structure function moment n, the vertical logarithmic axis is Λ_n. Only Λ_n/Λ_m is scheme-independent so that the theoretical curve $\ln \Lambda(n)$ can be displaced in parallel up and down. Thus we reach an unprecedented situation: the theory agrees with two sets of data that appear to disagree with each other (see Fig. 5a). Apparently this "disagreement" is mainly due to human intervention[33] [choice of the number of flavours assumed in the expression for $\alpha_s(Q^2)$, etc.]. A look at the error bars implies the following conclusion: the neutrino data are not yet good enough to check QCD beyond leading log. In the present example this would imply measuring the upward trend of the theoretical curve in Fig. 5a. Para and Sachrajda[32] estimate that really conclusive tests of next-to-leading QCD corrections would require the measurement of structure function moments to 2% accuracy in the range $Q^2 = 3$ to 70 GeV^2. To this unprecedented accuracy radiative corrections become quite relevant.

The corresponding Λ_n analysis[32,34] for F_2[ep-en] is shown in Fig. 5b. In this case the error bars are small enough to be tempted to conclude that the $O(\alpha_s)$ QCD corrections are measured to agree with theory. This conclusion may be premature in view of the theoretical uncertainties to be discussed in the next chapter.

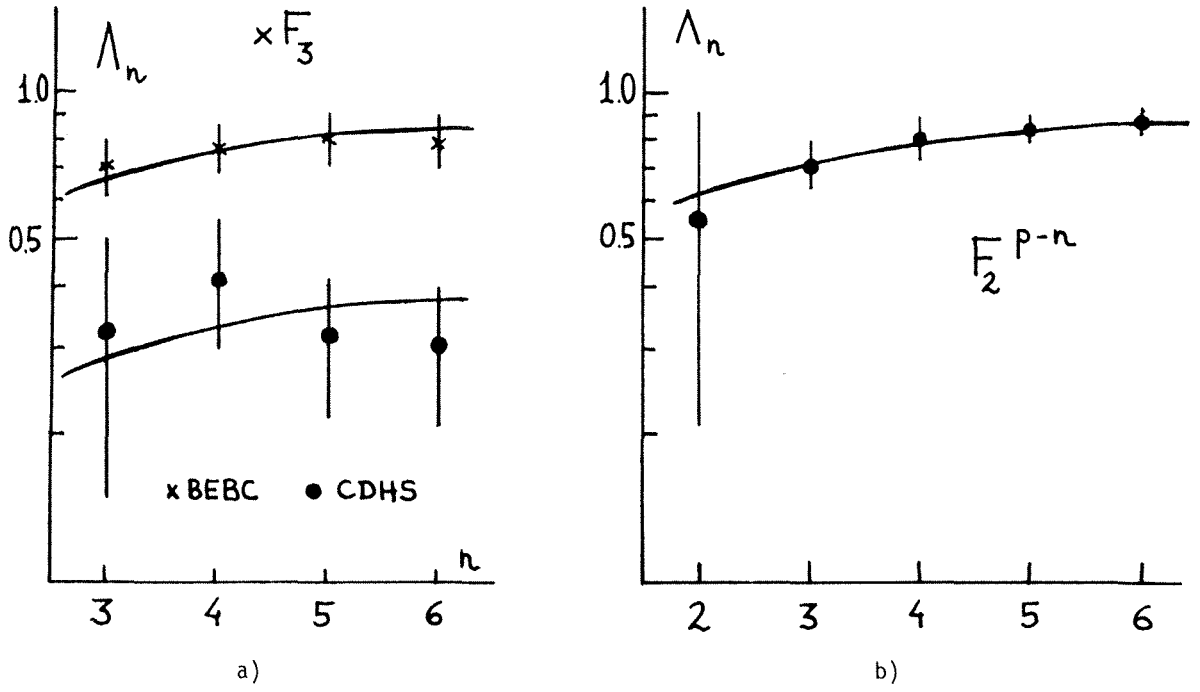

Fig. 5

3.2 Remembrance of higher twists[18)]

We have seen that the QCD prediction for the Q^2 evolution of structure function moments appears to agree with experiment, perhaps even to the level of $O(\alpha_s)$ corrections. A definite conclusion, however, can only be reached if the possible "higher-twist" effects are taken into account in the analysis of data. A higher twist is a contribution to the moments that dies away as a negative power of Q^2. Twist is also the mass dimension minus the spin of an operator constructed with quarks and gluon fields that contributes through its matrix elements to the structure function. The expressions for moments discussed in the previous section are leading-twist (T = 2) expressions. The complete perturbative QCD prediction for moments, when higher twists are taken into account, is of the form[18,35)]:

$$M_n(Q^2) = K_n \left[\ln^{-1} Q^2/\Lambda^2\right]^{d_n} \left[1 + O(\alpha_s) + \ldots\right] \times$$

$$\times \{1 + nt_n \frac{M_0^2}{Q^2} + O(1/Q^4) + \ldots\} ,$$

where the T = 4 $[1/Q^2]$ contribution is made somewhat explicit and the T ≥ 6 terms $[1/Q^4$, etc.] are not. The moment in the above expression is to be understood as a Nachtmann moment; the kinematical effects behaving as powers of m_p^2/Q^2 have been taken into account.

Higher-twist contributions come from several sources, depicted in Fig. 6, for squared amplitudes describing lepton scattering. All these effects have to do with breakdowns of the approximations entering the parton model or the leading twist results. Figure 6a refers to a non-zero p_T of the incoming quarks, a deviation from the approximation of wave-function softness: $\langle p_T \rangle / Q \ll 1$. Figures 6b and 6c are breakdowns of the impulse approximation of individual quark scattering. Figure 6b also breaks the approximation of free final-state quarks and is a perturbative alarm signaling the possibility of outgoing bound states.

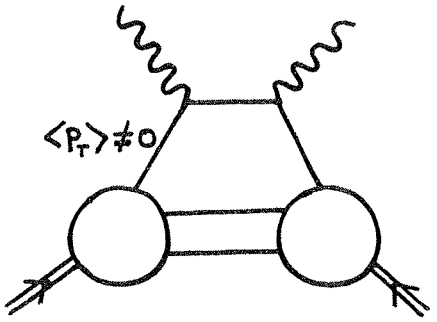

a)

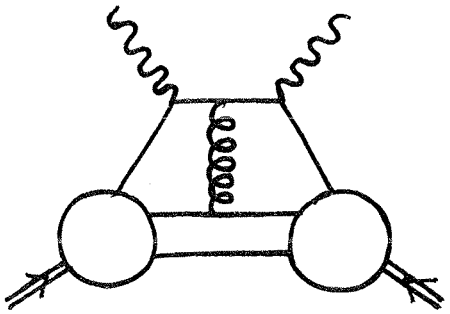

b)

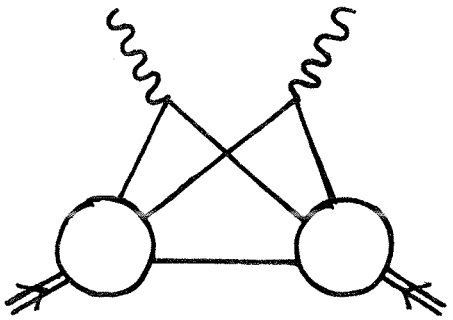

c)

Fig. 6

Notice the explicit factor n, the order of the moment, in the twist-four contribution of the lone formula of this section. Once this factor of n is made explicit, the unknown coefficient t_n (that one can normalize for a given n, say $|t_2| = 1$) is expected[18] to vary only logarithmically with n and Q^2. The combination $K_n t_n M_0^2$ corresponds to nucleon matrix elements of twist-four operators and is not calculable in perturbation theory, much as the corresponding twist-two object: the over-all normalization K_n. For not very large n, one expects $t_n \sim 1$ and the mass scale M_0 to be of the order of the relevant bound-state parameters with dimensions of mass: R_p^{-1}, $\langle p_T \rangle$, and perhaps Λ itself. The "large" mass in the problem m_p ($m_p^2 \sim 4 \langle p_T^2 \rangle$) has been taken care of via Nachtmann moments. Its large size is probably an accident connected with the fact that 3 is a large number (recall the discussion of precocious scaling in the 1/N approach); m_p plays no role in the description of scattering off individual quarks. For electroproduction data, which have high resolution and precision at relatively low Q^2, attempts have been made to extract the unknown twist-four quantity M_0 from the data. The result[18], $M^{ep} \sim 450$ MeV, agreed with theoretical expectation. The corresponding analysis has never been attempted in neutrino scattering, where questions of bad resolution in x may make the analysis difficult for theorists. In the next section I will quote an analysis of neutrino data with only higher twists (and no perturbative logs) and vice versa[36].

Unfortunately (for whoever may have jumped to early conclusions on neutrino scattering tests of QCD) the point is not that higher twists *may* be there, but that higher twists *must* be there for perturbation theory statements to be compatible with the existence of bound states. This is readily seen.

Consider a structure function $F(\xi,Q_0^2)$, where ξ is the correct scaling variable for analysing structure functions when $O(m_p/Q^2)$ effects are important; I will use the ξ variable for the sake of precision, without further comment[28]. Let Q_0^2 be large enough for form factors to have considerably damped off the elastic contribution and the nucleon resonances. A plot of $F(\xi,Q_0^2)$ versus ξ will not have resonance peaks visible to the naked eye (see Fig. 7). Suppose we use the first line of the lone equation of this section *(thus neglecting higher-twist effects)* to predict $F(\xi,Q_1^2)$ at a much smaller momentum transfer, $Q_1^2 \sim$ few GeV^2. The moments vary uniformly and logarithmically, and $F(\xi,Q_1^2)$ is predicted to be a *smooth* curve as indicated in Fig. 7.

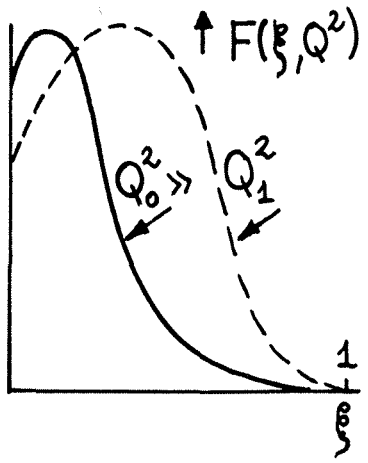

Fig. 7

Figure 8 shows an explicit example of predictions along these lines at Q^2 = 1, 2, 3 GeV^2 (the smooth dashed lines) and the actual data[37] (the bumpy lines; some idea of error bars is given here and there; the arrow is the position of the elastic peak). Terrible goof! Data and predictions disagree by factors of two on the resonances and by a lot more on the elastic delta function. All that has happened is that we have abused the twist-two moment prediction. But QCD is consistent enough to warn us that such T = 2 predictions are to be believed up to corrections of order [n (few hundred MeV)$^2/Q^2$]. For a fixed desired precision, fewer and fewer moments are predicted by the leading-twist analysis as Q^2 decreases. In terms of the structure function itself, rather than its moments, the presence of higher twists implies that the leading-twist predictions are to be believed, not in a local sense point by point in x, but on an average sense over intervals of width $\Delta x \sim M_0^2/Q^2$. This is what is needed for the T = 2 prediction to somehow interpolate the prominent low-Q^2 resonances [a phenomenon known to historians by the name of Bloom-Gilman duality[38].]

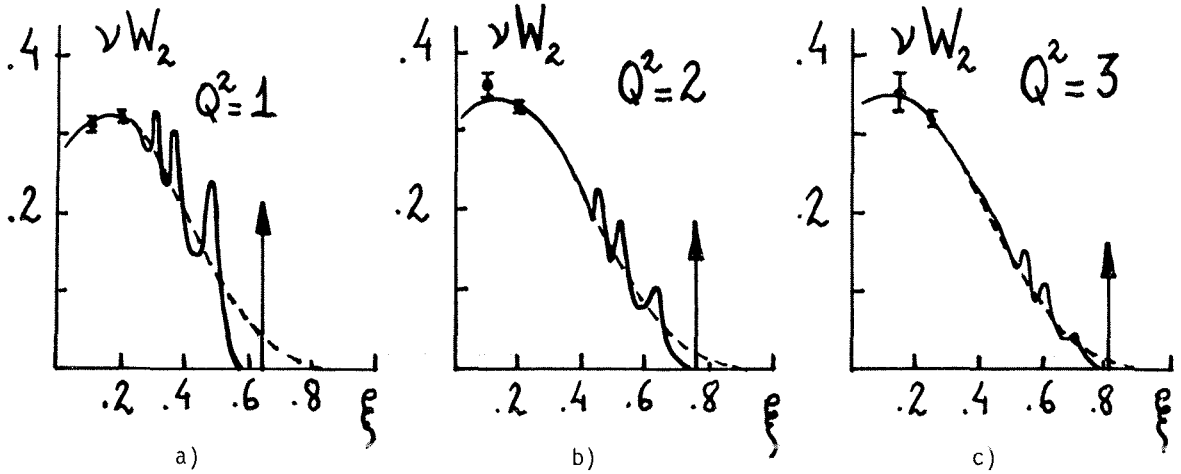

Fig. 8

3.3 A higher twist to recent analyses of neutrino data

There are several ways of ascertaining the possible impact of higher-twist uncertainties on neutrino data, which have so far only been fit to leading-twist expressions. Consider, for instance, the well-travelled plot versus $\ln Q^2$ of a non-singlet experimental moment $M_n(Q^2)$ raised to the inverse power of a theoretically calculated exponent d_n:

$$[M_n(Q^2)]^{1/d_n} = (K_n)^{1/d_n} \ln Q^2/\Lambda^2 \ .$$

This plot is expected to yield a straight line with intercept Λ^2 (or Λ_n^2) on the abscissa. Data for moments of xF_3, taken and analysed by the BEBC group, are shown in Fig. 9. Indeed, a straight (dashed) line can be drawn through the data points, and a relatively precise determination of Λ seems possible. But suppose we admit a twist-four uncertainty in $M_n(Q^2)$ of order $(1 \pm nM_0^2/Q^2)$ with $M_0^2(\nu) \sim \langle p_T^2 \rangle \sim (0.2\ \mathrm{GeV}^2)$ for the sake of definiteness. This would modify the previous straight line to a "trumpet" of uncertainty bound by the continuous lines in Fig. 9. The message is clear: the data on xF_3 are compatible with a leading-twist expression but, should one (as one should) include at least one extra parameter in the fit (M_0), the error bars on Λ would be much bigger.

Abbot and Barnett[36] have dramatized more quantitatively the uncertainties associated with higher-twist effects. They fit the BEBC-Gargamelle xF_3 moments and the CDHS xF_3 structure function either with the purely logarithmic QCD leading-twist predictions or with expressions containing higher-twist effects but no logarithmic Q^2-dependence. The power law fits are worse -- but not significantly worse -- than the logarithmic fits. Discouraged by this result, the quoted authors[36] do not fit to the theory, in which one expects *both* logarithmic and inverse power scaling deviations. But their analysis implies that the conclusion that we have seen the logs of perturbation theory is not tenable.

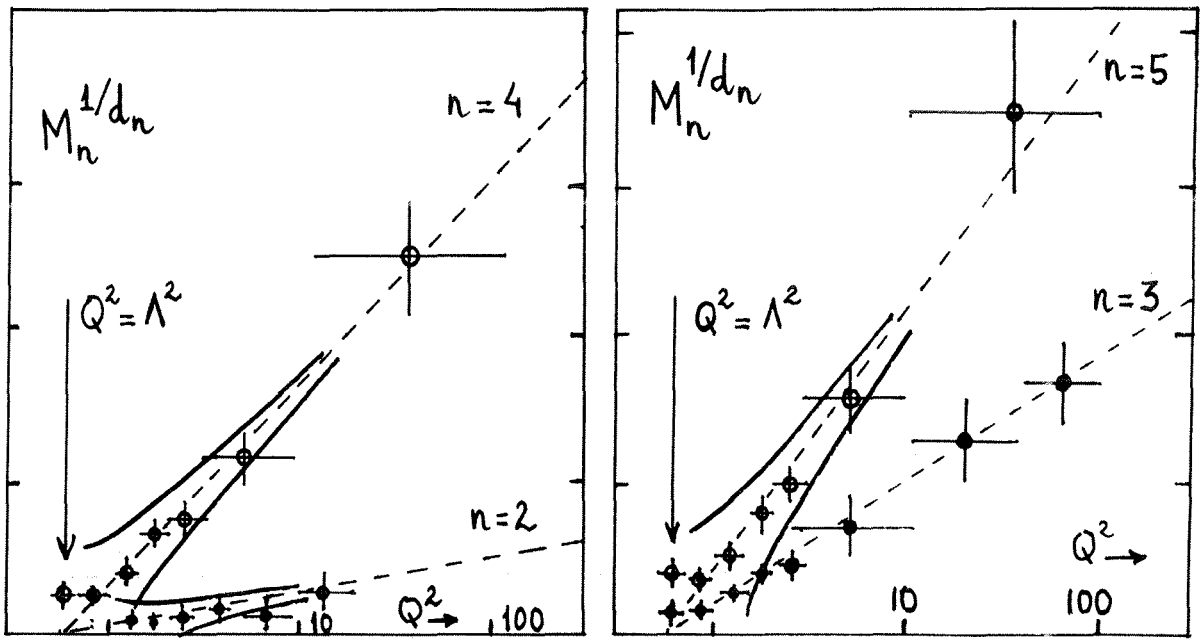

Fig. 9

Better experiments and stronger theoretical prejudices on higher-twist effects are urgently needed.

3.4 Tests of QCD in deep inelastic scattering: conclusions

The previous sections (3.2 and 3.3) were meant to moderate the temptation that arose in the one before: to conclude that perturbative QCD has definitely been tested in deep inelastic scattering experiments, in the leading log approximation or perhaps beyond it. The above is not a criticism of present experiments. On the contrary, the data are becoming precise enough, and experimentalists have learned so much theory that, with just another tiny little effort (plus $\sim$ 10 MSF), we may reach very definite conclusions.

A better control on higher twists (a measure or an upper bound on them) would constitute an important step towards the conclusion that perturbative QCD is being tested. This is because the perturbative prediction for moments of structure functions is a double series in powers of $(\ln Q^2)^{-1} \sim \alpha_s$ and powers of $1/Q^2$ (twists). The coefficients of the different twist contributions will only be calculable if and when the quark bound-state problem is solved. While it is not, the best we can do to ascertain whether QCD perturbation theory makes sense, requires a measurement of those coefficients. If indeed the form of the twist-four corrections to a given n^{th} moment is $\sim nM_0^2/Q^2$, their measurement should not be so difficult, since n and Q^2 are tunable. Once the twist-four contribution is estimated from the data, we know the values of (n,Q^2) for which higher-twist effects are likely to be smaller than the error bars. There and then, the tests of leading-twist perturbative predictions are serious. Incidentally, there is no reason why models of confinement, i.e. the bag model, could not be used to estimate higher-twist effects.

I have only discussed QCD tests within a *single* type of observable: moments of inclusive leptoproduction. Neither the emphasis on moments nor the choice of a single type of experiment are the optimal way to proceed. A sensible way of ascertaining the worth of QCD predictions for a single experiment is to compare them with predictions of other theories. This is not an entirely fair game, since there is no alternative theory scoring half as many Michelin stars as QCD in our general understanding of hadrons. But a scalar gluon "theory" can be and has been used to determine how specific the QCD predictions are for ratios of anomalous dimensions[39] (ratios of the d_n exponents of logs in the predicted behaviour of moments). Results[29] are given in Table 2.

Table 2

d_n/d_m ratios

n	m	QCD	ABCLOS	CDHS	QSD
6	4	1.29	1.29 ± 0.06	1.18 ± 0.09	1.06
5	3	1.456	1.50 ± 0.08	1.34 ± 0.12	1.12
7	3	1.760	1.84 ± 0.20	-	1.16
6	3	1.621	-	1.38 ± 0.15	1.14

The table seems to imply that experiments are almost precise enough to tell scalar from vector gluons. I do not think this conclusion would survive the growth of the error bars that would ensue from the (mandatory) allowance for at least an extra parameter in the fits (the M_0^2 of twist-four contributions). On the other hand, the numerical value of the coupling constant in the scalar theory (needed to fit the observed scaling deviations) is so large that there is no question that leading-twist perturbative QSD (S for scalar) is not a serious alternative.

Presumably the tightest tests of QCD are to be made by comparing *different* experiments, rather than milking one to the bitter end. An example is deep inelastic scattering versus hadron-hadron inclusive annihilation into lepton pairs [a subject covered by Altarelli[40] at this Conference]. In the leading log approximation, both experiments are described by the same Q^2-dependent structure functions[41]. But the $O(\alpha_s)$ deviations from this "sameness" are very large[42]. Thus the comparison should be a relatively easy and stringent test of perturbative QCD. Should deep inelastic scattering remain the most precise observable compatible with QCD, it could perhaps be considered, not only as a stringent consistency test, but also as a strong analogue of the Josephson junction; that is, the place where α (or α_s) is best measured. Once the parameters are consistently specified, one moves to other experiments for further tests. There is a long way to go QCD-testing.

3.5 QCD versus elastic form factors

An ancient superstition[43] about the elastic form factors of hadrons states that their power behaviour can be guessed by counting the minimal number of gluons that must be exchanged to "turn around" all valence quarks. The example of a baryon is given in Fig. 10. For an n-quark hadron, $F(Q^2) \sim 1/[Q^2]^{n-1}$, where the power behaviour is governed by the minimal number of hard propagators.

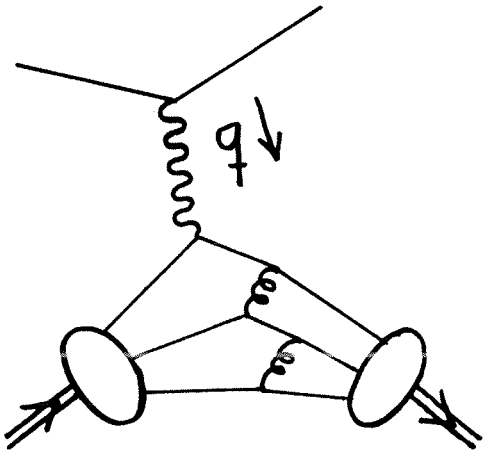

Fig. 10

A recent claim is that this superstition is to be believed (up to the ubiquitous $\ln Q^2$ corrections) as a QCD dictum. This was first seriously defended more than a year ago by Radyushkin and Efremov[44]. Subsequent work by the same authors, and by Lepage, Brodsky[45] and others[46] has considerably clarified the situation.

To repeat the litany: we do not yet understand hadron wave functions in QCD. A form factor, unlike a structure function, is a coherent object that knows about exquisitely delicate mechanisms such as the matching of phases between wave functions. Thus it is not easy to believe that today's underdeveloped QCD suffices to make precise statements about form factors. The present predictions on form factors, as we shall see, are not as strong as the corresponding structure function predictions, but they are also correct, I believe. Whether experiment agrees with them is another question.

The derivation of the form-factor results is lengthy and not always transparent. To me the clearest work is that of Lepage and Brodsky[45], who capitalize on recent progress in the understanding of high-momentum features of QED bound states[47]. Wave functions can be split by fiat into two pieces: a soft one and a hard one for which constituents are close to or far from being on-shell. The key statement is that a sufficiently hard hard wave function is perturbatively calculable in terms of the soft part. In QED the soft wave function is calculable and contains most of the hard facts of life. In QCD the soft wave function must be left unspecified, much as the matrix elements of operators contributing to structure functions are dumped into the normalization of moments at a reference momentum scale. So much for vague words. For a reasonably soft bound-state wave function, the pion form factor is predicted to behave at large Q^2 as[44,45]

$$F_\pi(Q^2) = \frac{16\pi}{3Q^2}\,\alpha_s(Q^2)\left|\sum_{n=0}^{\infty} a_n(\ln Q^2/\Lambda^2)^{-\gamma_n}\right|^2 + O\left(\frac{m^2}{Q^2}, \alpha_s\right)$$

The unspecified corrections are non-leading twist and non-leading log perturbative effects. The γ_n are the usual anomalous dimensions; the unknown coefficients a_n can be expressed in terms of the wave function at a reference momentum scale. Knowledge of $F(Q^2)$ at Q_0^2 is not enough to determine the different a_n and the subsequent ($Q^2 > Q_0^2$) fate of the form factor, in contrast with the situation for structure functions. The first coefficient a_0, however, can be related to the pion decay constant f_π. Since $\gamma_0 < \gamma_1 < \gamma_2 \ldots$ this implies an absolute prediction at super-asymptotic energies:

$$\lim_{\ln Q^2/\Lambda^2 \gg 1} F_\pi(Q^2) \to 16\pi\,\alpha_s(Q^2)\,\frac{1}{Q^2}\,f_\pi^2 .$$

To estimate when this prediction applies, let $a_0 \approx a_1$, $a_2 = a_3 = \ldots = 0$. The prediction would then be true at the 10% (60%) level at $Q^2 \simeq \Lambda^2\, e^{100}$ ($\Lambda^2 e^4$). To compare their results with data, Lepage and Brodsky invent input wave functions that they consider to be extreme cases. Their results for the magnetic form factor of the proton (for which the data extend to high Q^2) are shown in Fig. 11 as an allowed dashed region. The prediction is that $Q^4 G_M(Q^2) \sim \alpha_s^2(Q^2)$, while the data seem to level off to a constant (though apparently not to one fewer or extra power of Q^2). Conclusions would be premature in view of the fact that $O(\alpha_s)$ corrections have not been computed and higher-twist effects have not been estimated. Perhaps this "discrepancy" will teach us more than the flabbergasting successes

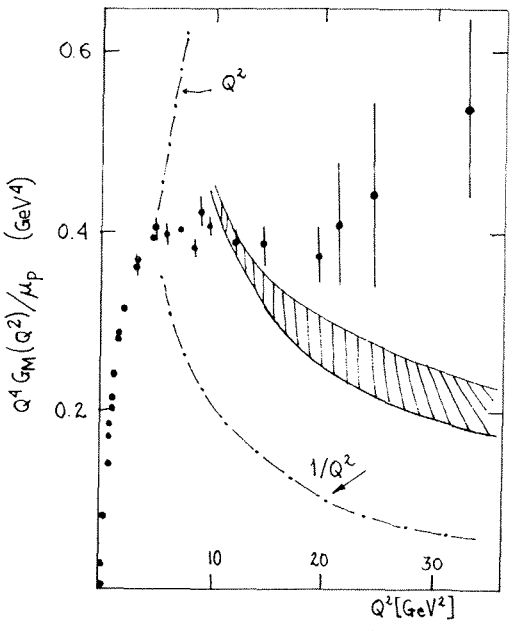

Fig. 11

of the leading log analyses of structure functions. Let me conclude by emphasizing that the extraction of the power behaviour of a form factor is an entirely non-trivial feat, relying heavily on delicacies of the quark spin structure in a colour singlet bound state and the approximate scale invariance of the underlying theory.

Should this progress in understanding form factors consolidate, then a Pandora's box of new exclusive and semiexclusive processes will be opened up to chromodynamic inspection.

3.6 Other advances in perturbation theory

Although several plenary speakers at this Conference dealt with QCD, I do not think we collectively managed to cover the subject, not even its perturbative aspects. Much of the recent work invading the press consists of rather straightforward applications. Now and then a novel feature or an unexpected application surfaces. The previous section was an example; others were discussed by other speakers. I know of four more particularly interesting pieces of work. Three of them I will proceed to discuss. The fourth is left unspecified, as a device for not offending anybody.

Parisi and Petronzio[48] elaborate on previous work[48], to emphasize that at very large Q^2 (accessible at Isabelle) the p_T distribution of lepton pairs in $pp \to \ell^+\ell^- + \ldots$ is completely calculable, even down to $p_T = 0$. This conflicts with the intuition that a memory of the "primordial p_T" of the original hadron constituents should be preserved. But the probability of gluon emission with p_T greater than a fixed number increases so quickly with Q^2 that, eventually, the only way for a lepton pair to come out with $p_T = 0$ is to originate from quarks that have emitted at least two gluons with large p_T's adding to zero. And this is calculable.

The multiplicity of heavy flavour production at very large Q^2 has been computed[49], with the result that it grows like $\exp(\sqrt{\ln Q^2})$, faster (slower) than any power of $\ln Q^2$ (Q^2). Reference to a hard reaction is crucial, one does not expect the result to apply to hadron-hadron collisions. Heavy flavours are invoked to justify the use of perturbation theory, but one is tempted to substitute them for heavy hadronic "clusters" and conclude that the results apply, up to a constant, to the total multiplicity. Unfortunately, more work is needed before it is decided at what energy a dramatic departure from the usual logarithmic multiplicity should be observable.

The "hadronic content" of the photon has always been an intriguing subject, and perturbative QCD has recently had its say[50]. The "structure function" of a photon in "$\gamma\gamma^*$" processes, as measured in $(e^+e^- \to e^+e^- + \text{hadrons})$ reactions, with the momentum transfer of one of the leptons remaining very small, is completely calculable. Non-perturbative effects, such as the ρ-meson contribution, die away as an inverse power of a logarithm, relative to the leading calculable result. Thus, the theoretical status of this process is half way between $\sigma_{tot}(e^+e^-)$ and the nucleon structure functions. The non-perturbative effects die away less rapidly than higher twists, but the leading result is completely calculable.

4. THE LAND OF IN-BETWEEN

In most of the previous sections I have discussed either "confinement" or "long distance" problems on the one hand and "perturbative" or "short distance" problems on the other, as if

they were separable subjects and as if the semantic distinctions really made sense. Exceptions to this unjustified dichotomic treatment were the discussion of coupling constant renormalization on a lattice and, to some extent, the diatribe on higher twists. Even at the present stage when confinement is not mastered, it is of course important to try to fathom the missing link with perturbation theory. I will comment on progress along two fronts, both of which carry misleading names: "duality" and "preconfinement".

4.1 QCD duality[51)]

QCD perturbation theorists deal with free quarks and gluons and most experimentalists with their bound states. Yet, *audaces fortuna juvat*, their results, for sufficiently "inclusive" and/or "smeared" observables, tend to agree. The example of low Q^2 structure functions we discussed in detail. Another example is $\sigma(e^+e^- \to \text{hadrons})$, plagued in reality with obvious "non-perturbative" effects: prominent resonances. Yet the experimental cross-section, when smeared with a sufficiently coarse energy resolution, agrees with the perturbative QCD calculation. Arguments as to why the process that confines quarks and gluons to real particles should not affect the perturbative calculation of some observables, have been given long ago[51,52)]. Ultimately, they rely on the uncertainty principle: the smearing of an observable such as $\sigma(e^+e^- \to \text{hadrons})$ with a bad energy resolution emphasizes the short time dynamics, with which QCD deals consistently. The long-range confining forces may only affect the "local" properties of $\sigma_{e^+e^-}(\sqrt{s})$, depleting the cross-section here to gather it in a resonance lump there, but not substantially changing its integral over some energy range. Whether these arguments are right, a pessimist would say, cannot be fully decided prior to an explicit understanding of quark bound states. But the arguments have recently been supported by explicit calculations within fully solvable non-relativistic confining potential models.

An example is the work of Bell and Bertlmann[53)] who, elaborating on the analysis of several authors[54)], investigate the degree to which the duality requirement

$$\int_{\Delta s} s\, \sigma_V\, d\sqrt{s} \simeq \int_{\Delta s} s\, \sigma_{q\bar{q}}\, d\sqrt{s} \ ,$$

is local. In the above expression $\sigma_{q\bar{q}}$ is the cross-section for the e^+e^- production of free heavy quarks and σ_V is the cross-section as a sum of the associated vector meson contributions. For three rather different types of potentials (logarithmic, Coulomb plus linear or cubic), duality is so local as to be true to better than 10%, resonance by resonance, except for the ground state[53)]. What this means is that the contribution of a resonance peak is roughly equal to the integral of $\sigma_{q\bar{q}}$ from half way to the previous resonance to half way to the next, irrespective of the details of the long-distance confining potential. It is not necessarily madness to forget about confinement.

Much more ambitious work along these lines has been published by Shifman, Vainstein and Zacharov[55)], and described by Gaillard[4)] at this Conference. These authors essentially argue that QCD and its local duality are good enough to compute perturbatively some properties of single bound states, such as the ρ-meson, which they indeed proceed to compute with astonishing numerical success. Their results have occasioned both awe and disbelief, and I hope we will be able to settle for the first.

4.2 "Preconfinement"

Several authors[56] have investigated the development of coloured showers in QCD perturbation theory. Consider e^+e^- annihilation at c.m.s. energy Q. This is a source of quarks of squared four-momentum up to $\sim Q^2$. As the primordial quarks emit gluons and quark pairs, their four-momentum degrades to, say, $Q_0^2 < Q^2$. The process can be investigated in perturbation theory, provided $\alpha(Q_0^2)$ is kept small enough ($Q_0^2 >> \Lambda^2$). Suppose one takes a "picture" of the developing shower when the four-momenta of individual quanta is of $O(Q_0^2)$. The claim is that one can organize this picture into colour singlet combinations of quanta, whose average invariant masses are also of $O(Q_0^2)$. The same is true of colour octet combinations. First notice that the result is non-trivial. Consider another asymptotically free theory with a much less violent infrared behaviour: $\lambda\phi_6^3$, scalars in six dimensions with cubic couplings. In this theory the mass of "colour singlet or octet" combinations (when individual quanta have degraded to the scale Q_0) is not of order Q_0, but remains of order Q. Should we assume that $\lambda\phi_6^3$ confines, it would be necessary to dream of a non-perturbative confinement mechanism that is operative down to short distances $\sim 1/Q$. In QCD, contrarywise, it is enough to assume that a long-distance mechanism is there to pick up, in the final hadronization process, low-mass colour singlets, rather than low-mass colour non-singlets. The role of confinement is relegated to small momenta and, whatever its detailed properties are, it should not greatly affect the over-all momentum flow in the process.

To summarize: as a consequence of the violent infrared behaviour of QCD, relatively soft and/or collinear gluons are so readily emitted that the outgoing mess can easily be "projected" into low-mass colour singlets. This, the task of confinement, is a soft one.

5. CONCLUSIONS

For the first time ever, we have a healthy and consistent field theory of hadrons.

QCD scores enormous qualitative successes. To name just some: it explains detailed features of the hadron spectrum[6], it offers deep justification for welcome colour-counting factors (in π^0 decay, e^+e^- annihilation, and lepton pair production) and, for the parton model, the tool that saved us from going the way nuclear physicists went. With the development of QCD, more and more features of hadron physics become understandable. There is no hint that QCD is wrong. QCD is beautiful.

But the details of the predicted scaling violations that are specific to QCD turned out to be a little harder to extract from a single experiment than some thought. Also, the understanding of confinement continues to defy some of the best and the brightest. These trivia, I sense at this Conference, have triggered a rather general mood of defeatism. I do not understand.

REFERENCES

1) G.'t Hooft, Phys. Rev. Lett. 37, 8 (1976); Phys. Rev. D 14, 3432 (1976).

2) A.M. Polyakov, Phys. Lett. 59B, 82 (1975); Nucl. Phys. B121, 429 (1977).
A.A. Belavin et al., Phys. Lett. 59B, 85 (1975).
C. Callan, R. Dashen and D.J. Gross, Phys. Lett. 63B, 334 (1976).
R. Jackiw and C. Rebbi, Phys. Rev. Lett. 37, 172 (1976).

3) S. Weinberg, Phys. Rev. Lett. 40, 223 (1978).
F. Wilczek, Phys. Rev. Lett. 40, 279 (1978).
For a recent review, see R.D. Peccei, Proc. Int. Conf. on High-Energy Physics, Tokyo, 1978 (Physical Society of Japan, Tokyo, 1979), p. 385.

4) M.K. Gaillard, these proceedings.

5) D. Fairlie, these proceedings.

6) A. Hey, these proceedings.

7) R.L. Jaffe and F.E. Low, Phys. Rev. D 19, 2105 (1979).

8) T.D. Lee, Phys. Rev. D 19, 1802 (1979).
R. Friedberg and T.D. Lee, Phys. Rev. D 18, 2623 (1978).

9) H.B. Nielsen and M. Ninomiya, One-loop numerical calculation of the MIT bag constant and Nielsen-Olesen unstable mode in SU(2) Yang-Mills, Niels Bohr Institute preprint (1979).

10) K.G. Wilson, Phys. Rev. D 10, 2445 (1974).
J.B. Kogut and L. Susskind, Phys. Rev. D 11, 395 (1975).

11) G. Mack, Confinement of static quarks in two-dimensional lattice gauge theories, to be published in Commun. Math. Phys.
G. Mack and V.B. Petkova, Confinement of lattice gauge theories with gauge groups Z_2 and SU(2), DESY preprint (1978).
D. Brydges, J. Fröhlich and E. Seiler, Diamagnetic and critical properties of Higgs lattice gauge theories, to appear in Nucl. Phys. B.
J. Fröhlich, Phys. Lett. 83B, 195 (1979).

12) J.B. Kogut, R.B. Pearson and J. Shigemitsu, Phys. Rev. Lett. 43, 484 (1979).

13) G.'t Hooft, Nucl. Phys. B72, 461 (1974).
For a list of references, see G. Veneziano, Proc. Int. Conf. on High-Energy Physics, Tokyo, 1978 (Physical Society of Japan, Tokyo, 1979), p. 725.

14) E. Witten, Baryons in the 1/N expansion, Harvard Univ. preprint (1979). The first half of this paper is a very readable introduction to the 1/N expansion, the source of whatever I say on this subject that happens to be clear.

15) E. Brezin et al., Commun. Math. Phys. 59, 35 (1978).
M. Casartelli, G. Marchesini and E. Onofri, Univ. of Parma preprint (1979).
J. Koplik, A. Neveu and S. Nussinov, Nucl. Phys. B123, 109 (1977).
C. Thorn, Phys. Rev. D 17, 1073 (1978).
R. Giles, L. McLerran and C. Thorn, Phys. Rev. D 17, 2058 (1978).
R. Brower, R. Giles and C. Thorn, Phys. Rev. D 18, 484 (1978).

16) G. Veneziano, Nucl. Phys. B117, 519 (1979).

17) E. Witten, Harvard Univ. preprint HUTP-79/A014 (1979).

18) A. De Rújula, H. Georgi and H.D. Politzer, Ann. Phys. 103, 315 (1977); Phys. Lett. 64B, 428 (1977).

19) For a review of the U(1) problem(s), see R. Crewther, preprint TH.2546-CERN (1977).

20) S. Weinberg, Phys. Rev. D 12, 3583 (1975).

21) A. De Rújula, H. Georgi and S.L. Glashow, Phys. Rev. D 12, 47 (1975).
N. Isgur, Phys. Rev. D 13, 122 (1976).

22) G. Veneziano, preprint TH. 2651-CERN (1979).

23) P. Di Vecchia, preprint TH.2680-CERN (1979).

24) R.J. Crewther, private communication.

25) G.S. LaRue, W.M. Fairbank and J.D. Phillips, Phys. Rev. Lett. 42, 142 (1979).

26) G. Preparata, these proceedings.

27) For a review and list of references, see C.H. Llewellyn Smith, Lectures at the 1978 Schladming School; and Oxford Univ. preprint 47/78 (1978).

28) O. Nachtmann, Nucl. Phys. B63, 237 (1973).
The QCD revival of the "target-mass-improved" scaling analysis was the cause of a good deal of misunderstanding. See A. De Rújula, H. Georgi and H.D. Politzer, Phys. Rev. D 15, 2495 (1977), and references therein.

29) P. Bosetti et al., Nucl. Phys. B142, 1 (1978).
J.G.H. de Groot et al., Particles and Fields, Z. Phys. 1, 143 (1979); Phys. Lett. 82B, 292 (1979). For a review, see D.H. Perkins, Oxford Univ. preprint 279 (1979).

30) E.G. Floratos, D.A. Toss and C.T. Sachrajda, preprint TH.2566-CERN (1979), and references therein.

31) W.A. Bardeen et al., Phys. Rev. D 18, 3998 (1978).
A. Gonzalez Arroyo, C. Lopez and F.J. Yndurain, Universidad Autónoma de Madrid preprint FTUAM 79-3 (1979) and preprint TH.2728-CERN (1979).
R. Barbieri et al., Phys. Lett. 81B, 207 (1979).
D.W. Duke and R.G. Roberts, Rutherford Lab. preprint RL-79-025 (1979).
D.W. Duke, Rutherford Lab. preprint RL-79-044 (1979).
For a recent review, see A. Peterman, Phys. Reports 53, 168 (1979).

32) A. Para and C.T. Sachrajda, preprint TH.2702-CERN (1979).

33) Presented by J. Wotschak at this conference (parallel session 2).

34) T.W. Quirk et al., Oxford Univ. preprint (1979).

35) S. Brodsky and G. Farrar, Phys. Lett. 31, 1153 (1973); Phys. Rev. D 11, 1309 (1975).
R. Blankenbecler and S. Brodsky, Phys. Rev. D 10, 2973 (1974).
A. De Rújula et al., Can one tell QCD from a hole in the ground? A drama to be published in the proceedings of the 1979 Erice School of Subnuclear Physics.

36) L.F. Abbot and R.M. Barnett, SLAC-PUB-2325 (1979).

37) E. Riordan et al., Phys. Rev. Lett. 33, 561 (1974); SLAC-PUB-1634 (1975), unpublished.

38) E. Bloom and F. Gilman, Phys. Rev. D 4, 2901 (1971).
M. Nauenberg, Acta Phys. Acad. Sci. Hung. 31, 51 (1972).

39) D. Bailin and A. Love, Nucl. Phys. B75, 159 (1974).
M. Glück and E. Reya, Phys. Rev. D 16, 3242 (1977); DESY preprint 79/13 (1979); Phys. Lett. 69B, 77 (1977).
V. Baluni and E. Eichten, Phys. Rev. Lett. 37, 1181 (1976); Phys. Rev. D 14, 3045 (1976).

40) G. Altarelli, these proceedings.

41) D. Amati, R. Petronzio and G. Veneziano, Nucl. Phys. B140, 54 (1978) and B146, 29 (1978).
H. Georgi et al., Phys. Lett. 78B, 281 (1978); Nucl. Phys. B152, 285 (1979).

42) J. Kubar-Andre and F.W. Paige, Phys. Rev. D 19, 221 (1979).
B. Humpert and W.L. van Neerven, Phys. Lett. 84B, 227 (1979) and 85B, 293 (1979); and Ambiguities in the calculation of infrared effects in Drell-Yan annihilation, to be published.
G. Altarelli, R.K. Ellis and G. Martinelli, Nucl. Phys. B143, 521 (1978).
K. Harada, T. Kaneko and N. Sakai, Nucl. Phys. B155, 169 (1979).
J. Abad and B. Humpert, Phys. Lett. 77B, 105 (1978) and 80B, 286 (1979).

43) V.A. Matveev, R.M. Muradyan and T.V. Tavkhelidze, Lett. Nuovo Cimento 7, 719 (1973).
S.J. Brodsky and G.R. Farrar, Phys. Rev. Lett. 31, 1153 (1973); Phys. Rev. D 11, 1309 (1975).
S.J. Brodsky and B.T. Chertok, Phys. Rev. D 14, 3003 (1976); Phys. Rev. Lett. 37, 269 (1976).
A.I. Vainshtein and V.I. Zakharov, Phys. Lett. 72B, 368 (1978).

44) A.V. Radyushkin, JINR preprint P2-10717 (1977).
A.V. Efremov and A.V. Radyushkin, JINR preprint E2-11983 (1978), Paper contributed to the Int. Conf. on High-Energy Physics, Tokyo, 1978.

45) G.P. Lepage and S.J. Brodsky, SLAC-PUB-2343 (1979) and 2348 (1979).
S.J. Brodsky et al., preprint TH.2731-CERN (1979).

46) G. Farrar and D.R. Jackson, CalTech preprint (1976).
G. Parisi, Ecole normale supérieure (Paris) preprint LPTENS 79-7 (1979).

47) W. Caswell and G.P. Lepage, Phys. Rev. A 18, 810 (1978), and references therein.

48) G. Parisi and R. Petronzio, preprint TH.2627-CERN (1979).
R.K. Ellis and R. Petronzio, preprint TH.2571-CERN (1978).
K. Konishi, A. Ukawa and G. Veneziano, preprints TH.2509-CERN and TH.2577-CERN (1979).
L. Pancheri and Y. Srivastava, Frascati preprint LNF 78/46 (1978).
G. Curci, M. Greco and Y. Srivastava, in preparation.

49) W. Furmanski, R. Petronzio and S. Pokorski, preprint TH.2625-CERN (1979).
A. Basetto, N. Ciafaloni and G. Marchesini, Pisa preprint SNS 4/1979.

50) E. Witten, Nucl. Phys. B120, 189 (1977).
W.R. Frazer and J.F. Gunion, Univ. California (San Diego) preprint UCS D10P10-199 (1979).
C.H. Llewellyn Smith, Univ. Oxford preprint (1979).

51) A. Bramon, M. Etim and M. Greco, Phys. Lett. 41B, 609 (1972).
M. Greco, Nucl. Phys. B63, 398 (1973).
J.J. Sakurai, Phys. Lett. 46B, 207 (1973).

52) S.L. Adler, Phys. Rev. D 10, 3714 (1974).
A. De Rújula and H. Georgi, Phys. Rev. D 13, 1296 (1976).
E. Poggio, H. Quinn and S. Weinberg, Phys. Rev. D 13, 1958 (1976).
R. Shankar, Phys. Rev. D 15, 755 (1977).
R.G. Moorhouse, M.R. Pennington and G.G. Ross, Nucl. Phys. B124, 285 (1977).

53) J.S. Bell and R.A. Bertlmann, preprint TH.2677-CERN (1979).

54) K. Ishikawa and J.J. Sakurai, Particles and Fields, Z. Phys. 1, 117 (1979).
J.S. Bell and J. Pasupathy, preprint TH.2636-CERN (1979).
J.S. Bell and J. Pasupathy, preprint TH.2649-CERN (1979).
M. Krammer and P. Leal-Ferreira, Rev. Bras. Fis. 6, 7 (1976).
C. Quigg and J.L. Rosner, Phys. Rev. D 17, 2364 (1978).

55) M.A. Shifman, A.I. Vainshtein and V.I. Zakharov, Nucl. Phys. B147, 385, 448, 519 (1979).

56) D. Amati and G. Veneziano, preprint TH.2620-CERN (1979).
A. Basetto et al., as cited in Ref. 49.

QCD: PROBLEMS AND ALTERNATIVES

Giuliano Preparata
CERN, Geneva, Switzerland, and Università di Bari, Italy

INTRODUCTION

Keeping to the title, my talk shall be divided in two parts, the first on the problems of QCD, the second on possible alternatives.

As will become clear, my critical attitude will not concern QCD itself but the now prevailing way (based on perturbation theory, and other doubtful approximations) of deriving consequences of it to be compared to the enormous amount of experimental data which is floating around in search of an explanation.

For it is a fact of life, which we have slowly learnt through the best part of the past 30 years, that the subnuclear world is built upon two very fundamental concepts: quarks and colour[1,2]. And if we try to embody these concepts in a quantum field theory (QFT) there is no doubt that we are inescapably led to QCD. Thus there is a non-negligible probability that the wonderful variety of hadronic phenomena is due to such a simple and beautiful QFT. But the task of a physicist at this stage is to check whether or not QCD gives a false description of the physical reality, as he knows it.

It belongs to the subnuclear physicist, therefore, to establish the necessary mathematical link between the fundamental world of QCD, populated by $3 \times F$ (F = number of flavours) quarks and 8 gluons, and the real world, which is crowded with a great number of interacting mesons and baryons (Fig. 1). We have strong reasons to believe (foremost among them the incredible elusiveness of quarks) that the link between the QCD world and the real world is established by the solution of the problem of confinement. The idea is that in a theory where SU(3) is an exact symmetry, the fundamental fields do not appear as physical states; but the Hilbert space of physical states comprises only colour-singlets, i.e. mesons and baryons. Nobody can deny this idea its enormous appeal, but so far we have witnessed the failure of all attempts to give it a well-defined mathematical substance. The problem looks, if not hopeless, at least tremendously difficult; and not even a germ of a solution appears to be in sight. It is perfectly obvious that the assaults on the problem of confinement

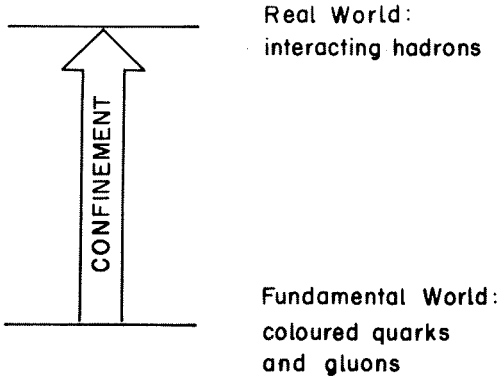

Fig. 1 The link between QCD and the real world

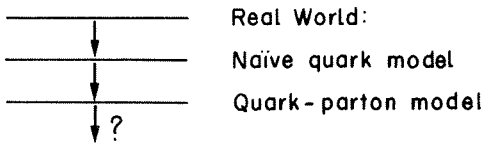

Fig. 2 The alternative strategy is to go from the real to the fundamental world

should be continued with all possible theoretical weapons, but, as I will argue later, it also appears that those weapons we have at our disposal, such as perturbation theory and instantons, are absolutely inadequate for coping with this formidable problem. But, are there alternative strategies? I believe that the answer is positive, provided we are willing to march in a direction opposite to the one which requires the solution, "tout court", of confinement. In other words, rather than attempt the great leap from the fundamental world to the real world, we should try out a long march, from the real world to its foundations. In the small or the big steps of this march we should be guided by the attentive observation and analysis of what happens in nature. Once we have conquered something firm, somewhere at midway, the problems we should solve, i.e. to establish the link with the fundamental world, will certainly be less difficult, and perhaps doable. Two important steps have already been taken in this direction: that of the spectrum of hadrons in the naive quark model, and that with regard to deep inelastic phenomena in the quark-parton model. Much of our intuition and understanding of subnuclear phenomena rests upon these two naive models. In the second part of this talk I shall describe possible further steps along this direction (see Fig. 2).

1. PROBLEMS WITH THE GENERALLY ACCEPTED (NAIVE) QCD

When one writes down the QCD Lagrangian,

$$L_{QCD} = -\frac{1}{4} F^a_{\mu\nu} F_a^{\mu\nu} + \sum_F \bar{q}_F(-i\not{\partial} + M)q_F \ , \tag{1}$$

$$F^a_{\mu\nu} = (\partial_\mu A^a_\nu - \partial_\mu A^a_\nu + g_0 \, if^{abc} A^b_\mu A^c_\nu)$$

$$D_\mu = \partial_\mu - ig_0 A^a_\mu \left(\frac{\lambda_a}{2}\right) \ , \tag{2}$$

one is immediately confronted with the problem of establishing its meaning. The Lagrangian L_{QCD} contains an extremely elegant formulation of a theory which has spin $\frac{1}{2}$ quarks of different flavours F, and is locally invariant under an SU(3) gauge group, the colour group, whose eight gauge fields A^a_μ (the gluons) mediate the interactions among quarks.

Looked at the Lagrangian level, QCD is nothing but the non-Abelian extension of quantum electrodynamics (QED), whose gauge group is U(1), the related gauge field is the photon, and the spin $\frac{1}{2}$ fermions are the leptons such as the electron and the muon.

But the analogy with QCD stops here. Whereas the real world of QED (made of interacting leptons and photons) can be clearly recognized in the QED Lagrangian, a very different situation presents itself in QCD. The real world, made out of (presumably) an infinite number of mesons and baryons, which interact strongly, does not seem to have anything to do with the beautifully simple QCD Lagrangian.

And yet the chances are that the two worlds are in fact related; but how? Nobody knows; confinement must be a non-perturbative phenomenon, and no systematic method is at hand to deal with a quantum field theory where the coupling among fields is strong. Several attempts have been made to demonstrate that QCD confines quarks and gluons, the most notable among them being through lattice gauge theories[3], and instantons[4]. No conclusive results have so far emerged; and it appears, as I will comment briefly later on, that the latter aproach is in very serious difficulties.

So, as far as confinement is concerned, the score -- put euphemistically -- is meagre. Where, then, are the successes of QCD? The usual claim is that one has been able to conquer a great deal of physics by making use of the perturbative methods, through what is now called "Perturbative QCD" and for which I would like to suggest the more appropriate name of "Naive QCD".

Owing to the necessarily non-perturbative link that connects QCD with the real world, it would seem hard to believe that perturbative QCD can be of any relevance to describing the subnuclear phenomena. Nevertheless, current literature is flooded with applications of QCD perturbation theory to all kinds of deep inelastic phenomena. How did all this happen? The use -- I should say the abuse -- of perturbative QCD rests on a number of theoretical ideas whose doubtful nature I shall endeavour to discuss and clarify.

1.1 Asymptotic freedom; is it a true property of non-perturbative QCD?

There can be no doubt that asymptotic freedom is a property of *perturbative* QCD[5]. In order to understand the meaning of this statement, let us consider a generic n-point function Γ_n (see Fig. 3), where the n-legs can represent any of the local fields that can be constructed in QCD. Γ_n is a function (neglecting discrete indices such as spin, colour, and flavour) of the renormalized QCD coupling constant g, which is defined to acquire the particular value g at the normalization momentum $q^2 = -\mu^2$ (see Fig. 4). Thus we can write:

$$\Gamma_n = \Gamma_n\left(g,\mu;\{(p_i p_j)\}\right) ,$$

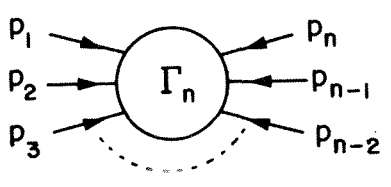

Fig. 3 The n-point Green's function Γ_n

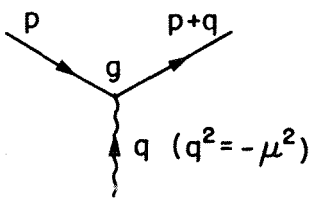

Fig. 4 The quark-gluon coupling

where $\{(p_i p_j)\}$ denotes the set of independent Lorentz scalars that can be formed with the external momenta p_i. The renormalization group equations for Γ_n [6] have a very simple form:

$$\mu \frac{\partial}{\partial \mu} \Gamma_n + \beta(g) \frac{\partial}{\partial g} \Gamma_n + \gamma_n(g) \Gamma_n = 0 ,$$

which tie together the effects of changing the normalization momentum and the value of the coupling constant g; $\beta(g)$ is the celebrated Callan-Symanzik function, and $\gamma_n(g)$ is the "anomalous dimension". As is well known[7], the solution of the previous equation is very simple, provided we define

$$t = -\frac{1}{2} \log \frac{\mu^2}{\mu_0^2}$$

$$k(g) = \int_{g_0}^{g} \frac{dg'}{\beta(g')}$$

The previous equation then becomes

$$\frac{\partial}{\partial t} \Gamma_n + \frac{\partial}{\partial k} \Gamma_n + \gamma_n(k) \Gamma_n = 0 ,$$

whose solution is

$$\Gamma_n\left(\mu, g_0; \{(p_i p_j)\}\right) = \Gamma_n\left(\mu_0, g(-t); \{(p_i p_j)\}\right) e^{\int_0^{-t} dt' \gamma_n(t')}$$

where the "running coupling constant" g(k) is the function obtained inverting the expression $k = k(g)$. Thus by asymptotic freedom (AF) we denote the property of those theories for which $\beta(g)$ has, for small values of g, negative values. If this happens, one can easily check from the solution of the renormalization group equations that when $t \to -\infty$, i.e. $\mu \to \infty$, the "running coupling constant" g(-t) tends to zero, provided g_0 is sufficiently small. AF has given rise to the hope that for large momenta (μ^2) one could master hadronic physics by the relatively simple tools of perturbation theory. Is this hope well founded? There are several ways in which, in a confined theory, this possibility would be ruled out. For instance:

i) The true, non-perturbative $\beta(g)$ is as shown in Fig. 5. Owing to confinement, for small momenta the coupling g_0 is necessarily very large, so that for large momenta one would reach the point g^*, rather than the point $g = 0$.

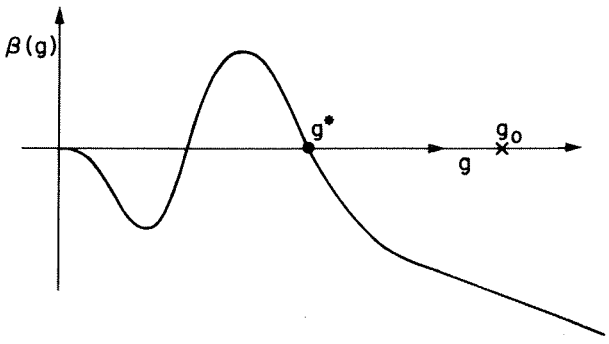

Fig. 5 A possible non-perturbative $\beta(g)$ for QCD

ii) Even if $\beta(g)$ has no other zero than the trivial one, there is no guarantee that in a theory with confined quarks and gluons the limit $g \to 0$ corresponds to the perturbative limit. In a world where confinement gives rise to an infinite string of hadrons of increasing mass, there will necessarily be very strong singularities in the coupling constant near $g = 0$, which might forbid any perturbative expansion in that neighbourhood.

1.2 Where, if anywhere, can perturbative QCD be applied?

Let us suppose that for miraculous reasons none of the possible barriers between the confined and the perturbative QCD at large momenta is operative; the question we must ask is, What kind of physical processes can we calculate?

It should be clear that the limit in which the renormalization group equations provide useful information is the deep Euclidean limit; which is defined by setting for the p_i's of the n-point Green's function Γ_n,

$$p_i = \lambda n_i$$
$$n_i n_j < 0 \ ,$$

and taking the limit $\lambda \to \infty$. The deep Euclidean limit is really a very peculiar limit. All four-momenta tend to infinite values, and all scalar products become infinitely large and *negative*. No known physical process, happening in Minkowski space, involves momenta of this type; and in order to relate the deep Euclidean limit to physical reality we need some extra assumptions. But before discussing the extra assumptions needed to apply AF to physically observable processes, let me stress that the requirement $n_i n_j < 0$ stems from the necessity to avoid, in the limit of large momenta, the dangerous regions where physical singularities are located; which might easily spoil the uniformity of the $g \to 0$ limit. In this respect we should remark that these singularities are precisely related to those hadronic states which should arise from the non-perturbative action of colour confinement.

The least doubtful application of AF is to e^+e^- annihilation into hadrons. The relevant Green's function is the vacuum-polarization tensor:

$\pi_{\mu\nu}(q^2) =$ 

.

Assuming the validity of once-subtracted dispersion relations, or equivalently the Wilson short-distance operator product expansion[8], we can make use of the deep Euclidean limit to infer that the famous ratio $R = \sigma(e^+e^- \to \text{hadrons})/\sigma(e^+e^- \to \mu^+\mu^-)$ is given by

$$R = 3 \sum_F Q_F^2 \ ,$$

a result which seems to agree with experiments. However, there are still experimental uncertainties of about one unit in R, which do not yet allow us to evaluate the precision of this prediction.

Much more difficult is the situation for all other deep inelastic processes, whose experimental study has tremendously enhanced our confidence in the primary role played by quarks in subnuclear phenomena. All such processes, in fact, are described by amplitudes which do involve, either in the initial or in the final states, low-lying hadronic states, whose p^2 is time-like and small!

But how has it happened, then, that the perturbative QCD scheme claims to describe, with great accuracy, scaling and its violations in deep inelastic lepton-hadron scattering? The reason rests on the fact that through the light-cone (LC) operator product expansion written down in 1970 by R. Brandt and the author[9], it is possible to show that the deep Euclidean region determines the asymptotic (large Q^2) behaviour of the moments of structure functions:

$$M_n(Q^2) = \int_0^1 dx\, x^{n-1} F(x,Q^2) \ .$$

But we should be aware of the fact that, whereas it is possible to prove the existence of a light-cone operator product expansion in perturbation theory, it is by no means clear that there exists such an expansion in a theory where quarks and gluons are confined. But even accepting the validity of an LC expansion, the range of processes to which AF may be applied stops here.

The fact that the renormalization group equations are very useful for summing "leading logs"[10] in perturbation theory, thus giving rise to a coherent and possibly consistent calculational scheme, should by no means be taken as a justification for their widespread uncritical use.

Thus we should remember that processes of very great interest such as

i) e^+e^- annihilation into hadrons (deep inelastic annihilation),

ii) lepton pair production in hadron-hadron collisions,

iii) jets in deep inelastic collisions,

iv) large p_T phenomena,

cannot be described by means of the perturbative QCD apparatus of AF. Thus much of the theoretical work that has recently been done to apply perturbative QCD to the previous processes, appears to have no theoretical foundation. The success that has nevertheless been claimed in this type of calculation is really a confirmation that the totality of deep inelastic phenomena seems to be fairly accurately represented by a quark-parton model, which perturbative QCD reproduces, along with its grave difficulties of interpretation, quite closely.

1.3 Is asymptotic freedom really observed?

If we accept the assumptions of AF in the deep Euclidean region and the LC operator product expansion, we see that we can make definite predictions for deep inelastic scattering in the Bjorken limit. Recently, a remarkable effort has gone into checking the predictions made by this theoretical scheme[11].

The experimental data in both electron(muon)-nucleon scattering and neutrino-nucleon scattering show a pattern of scaling violations which seems to go in the direction of the predictions of AF.

But let us look at this problem a bit more closely. One remarkable property of scaling, which has been known since the pioneering SLAC experiments, is its precocity, i.e. it shows up for values of Q^2 as low as 1 GeV^2. But we know from the renormalization group equations that, for such a low value of Q^2, QCD perturbation theory must break down. Thus AF has no

explanation to offer for "precocious scaling". However, let us go on, and consider the moments of several different structure functions and determine, from experiments, their Q^2 dependence. For non-singlet structure functions, the AF prediction to leading order reads

$$M_N(Q^2) \to A_N\left(\log \frac{Q^2}{\Lambda^2}\right)^{-d_N}$$

where d_N is calculable and Λ^2 is a parameter to be determined from experiment. In particular, Λ^2 can be determined by forming $M_N(Q^2)^{-1/d_N}$ and plotting it as a function of $\log Q^2/Q_0^2$, and finding out the intersection of the corresponding curve, which is predicted to be a straight line, with the axis of the abscissae. This intersection provides the value of $\log \Lambda^2/Q_0^2$. Actually it turns out that including higher-order corrections the parameter Λ^2 in the asymptotic expression of the moments is renormalized and acquires a calculable dependence on N. In Fig. 6 such a prediction for Λ_N [12] is reported along with the results of analyses of data from an FNAL experiment on μD scattering[13], and two CERN experiments[14] (BEBC and CDHS). We clearly see that something goes wrong. Those who would rush to cast doubts on some experiments should remember that the two neutrino experiments (BEBC and CDHS) have data in different ranges of Q^2 ($Q^2 \geq 1$ GeV^2, BEBC; $Q^2 \geq 6$ GeV^2, CDHS); on the other hand, the μD scattering experiments are affected by the deuteron smearing corrections, which become quite uncertain for high N-values. Just to illustrate the kind of troubles AF may be facing here,

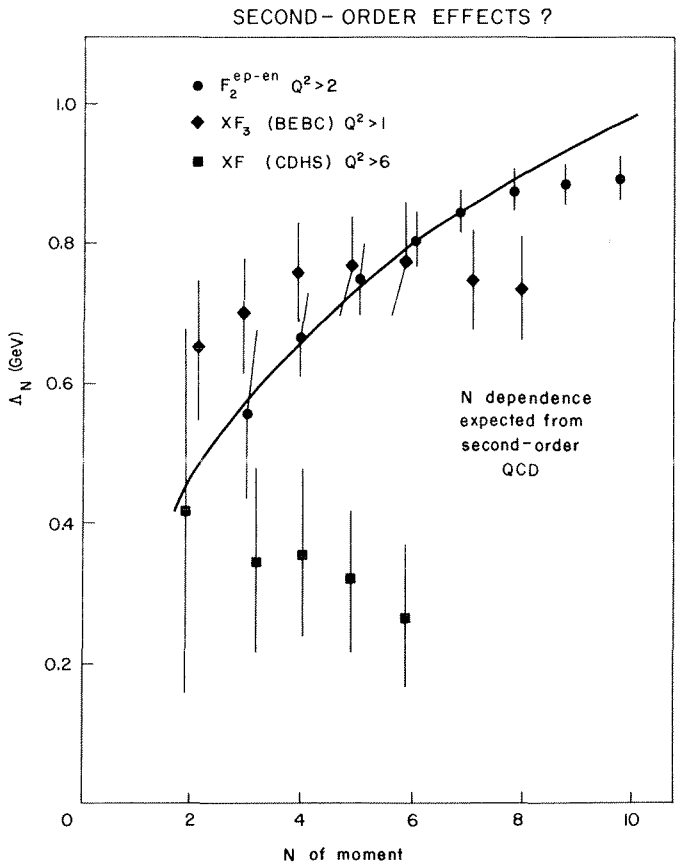

Fig. 6 A determination of Λ_N for non-singlet structure functions according to the authors of Ref. 12. The curve is the theoretical prediction including higher-order corrections.

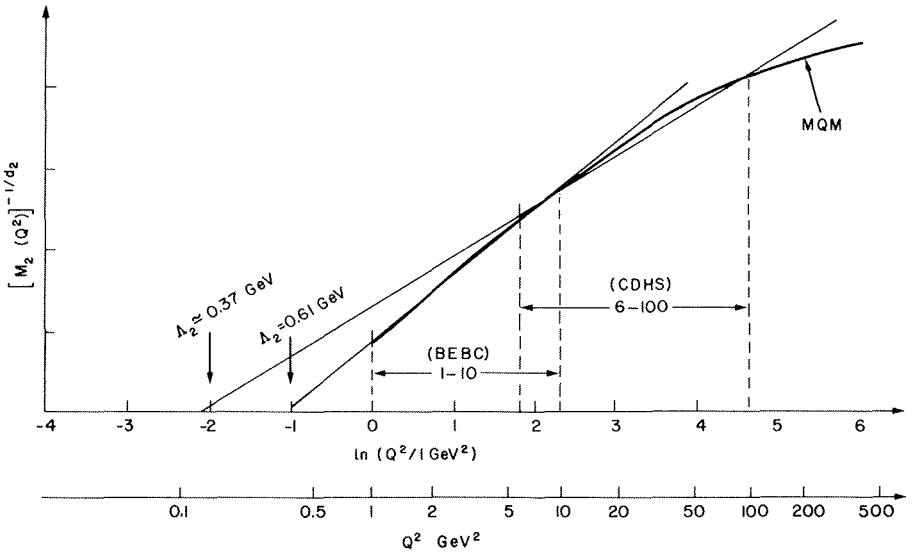

Fig. 7 The theoretical prediction of $\left[M_2(Q^2)\right]^{-1/d_2}$ according to Ref. 21

in Fig. 7 I have plotted the massive quark model (MQM) prediction for $M_2(Q^2)$ (see Section 2.2); we see that the dependence of $(M_2)^{-1/d_2}$ is not really linear, and that in different Q^2 regions we can fit with two different straight lines with different slopes, which accounts very nicely for what is experimentally observed. Certainly more data and more refined analyses are needed before one can reach a firm conclusion; however, the AF believer should find in these results some reasons for being worried. According to Duke and Roberts[12], AF seems to be in trouble also for the singlet structure functions (see Fig. 8), owing to the peculiar behaviour of the gluon momentum distribution functions. It is somewhat ironic that the only place in hadronic dynamics where important gluon effects are strongly suggested (who would, otherwise, carry the missing momentum?) is just where some serious trouble for the AF picture seems to develop. Another thing which should be of some concern to the AF theorist is the plot of the integral $I_2 = \int_0^1 F_2(x,Q^2)\,dx$ as a function of Q^2, where no sign of approaching the AF prediction of 5/42 is to be seen (see Fig. 9).

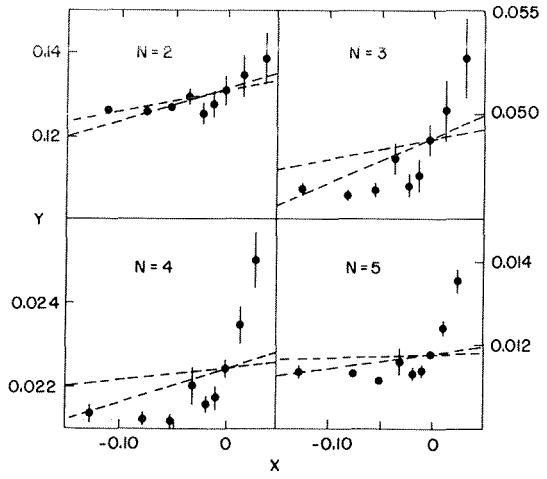

Fig. 8 The AF analysis of singlet structure functions of Ref. 12. The dashed lines are AF-predictions with two different choices for the gluon momentum distributions.

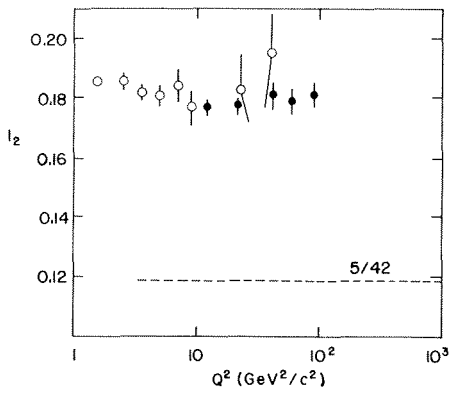

Fig. 9 A compilation[15] of the experimental results for I_2. The dashed line is the AF limit 5/42.

1.4 Can we trust instantons?

Much emphasis has recently been given to the possible role of instantons in many important non-perturbative problems of QCD, foremost among them being confinement. Recently Patrascioiu[16] has formulated some serious objections to the possibility of utilizing the Gaussian approximation to the integrals when massless fields are around, such as happens in QCD. He considers several simple examples that bear out his contention that infrared divergences must necessarily mar the results of instanton calculations in massless theories. If no way out is found to his objections, we must say farewell to the only non-perturbative approach that we have at our disposal for dealing with the difficulties of the confinement problem.

I shall conclude this part of my talk by stressing that our present understanding of QCD, based on perturbation theory and AF on the one hand, and on instantons and the Gaussian approximation to path integrals on the other, seems to be on very shaky ground. This does not mean that we should abandon QCD, but rather that we should try a different strategy. As indicated in the Introduction, instead of going from QCD to the real world, through the unsafe and obscure paths of AF and instantons, we should consider the possibility of learning from nature what the real meaning of QCD is. In the second part of this talk I shall endeavour to show that this road is not only practicable but that it also offers some extremely valuable insight into the world of subnuclear phenomena.

2. ALTERNATIVES TO "NAIVE QCD"

The naive quark model for low-energy phenomena and the quark-parton model for deep inelastic physics have been the first steps in the direction of unravelling the fundamental structure of the subnuclear world. It was the remarkable and unexpected success of such simple approaches that offered strong indications for the relevance of the notions of quarks and colour, whence QCD. After having discussed some of the difficulties which at present bar the road from which the QCD Lagrangian should lead us to the real world, we shall now examine what progress has been achieved along the direction of refining and unifying the naive quark model and the quark-parton approach to deep inelastic phenomena.

2.1 Beyond the naive quark model: the MIT bag

This is an original and imaginative approach to low-energy hadronic physics. Invented by a group of MIT theoreticians[17], the Bag approach circumvents the problem of establishing confinement directly from the QCD Lagrangian by adding to the QCD action a "cosmological term" proportional to the space-time volume of the bag; thus they write

$$W_{bag} = \int_{bag} d^4x \, L_{QCD} + B \int_{bag} d^4x \ .$$

From this action we can immediately find that the vacuum exists in two phases, one in which quarks and gluons can propagate freely (phase I), the other in which such propagation is impossible (phase II) (see Fig. 10).

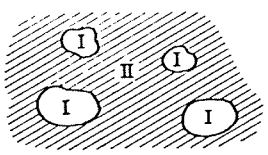

Fig. 10 The vacuum of the MIT bag is a two-phase system

In this way the vacuum becomes similar to a liquid (phase II) in which gas bubbles are formed (phase I), and from W_{bag} we can read off how much energy we have to spend in order to form the bubbles. This energy is just

$$E = BV ,$$

where V is the volume of the bubble. It is only inside the bubbles or bags that quarks and gluons can exist. In fact, in order to take quarks apart we must make bigger and bigger bubbles, which is going to require more and more energy; thus producing a free quark requires an infinite energy.

All this is very nice and extremely appealing; confinement has been introduced in a very simple and straightforward way. But how are we going to calculate in this theory? Let me say right away that from the point of view of calculation, the bag action does not represent any real improvement on the one of QCD; it has only the advantage of explicitly containing quark confinement. However, once we are sure that the theory confines, we can develop several approximation schemes to sort out the low-energy hadronic states.

This is not the place to review what has been achieved within this theoretical framework; there are several good reviews that can be consulted[18]. Here I shall rather point out the difficulties of the MIT bag approach which must be overcome before we can trust it as a good tool for describing hadrons.

i) The low-energy spectrum ($M \leq 1$ GeV) contains, besides the naive-quark-model states (pseudoscalar and vector mesons), also glueball states whose existence has never been established.

ii) There are bag surface modes which greatly complicate the hadronic spectrum from the expectations of the naive quark model. No experimental trace of such states has so far been revealed.

iii) Exotic states (i.e. different from $q\bar{q}$, and qqq configuration) should appear copiously in the spectrum, contrary to experimental evidence.

iv) The MIT bag, in the way it has been formulated so far, is not a second quantized theory; so all aspects of scattering, particle production, form factors, etc., cannot be analysed, thus limiting its theoretical scope enormously.

In spite of these difficulties, the MIT bag is certainly an important step beyond the naive-quark model. Its main achievement is, in my opinion, to have clarified that it is possible to accurately describe hadrons by imagining them as being made out of a small number of point-like quarks moving "almost" freely inside well-defined regions of space, the bags.

2.2 Beyond the parton model: the massive quark model

The MIT bag represents a step to free the naive quark model from some of its unappealing features, as for instance its non-relativistic character; the massive quark model (MQM)[19] was constructed in order to avoid the most troublesome aspect of the parton model, namely the non-observation of partons. Several field theoretical attempts have been tried out in order to deal with this grave problem of the parton model, by imagining that the bare nucleons had a point-like interaction with currents[20], but this line of approach had to be abandoned in the face of several difficulties of its own, paramount among them being the lack of the quark degree of freedom.

Thus, as far as I know, the MQM is the only attempt to treat *realistically* the way in which the quark degree of freedom intervenes in the physics of deep inelastic phenomena. Again, this is not the place to give a full description of this theory and of its results; in the following I will simply state what the main ideas are, and present some very recent results of an analysis of deep inelastic lepton-hadron scattering[21].

If we want to be *realistic* about deep inelastic physics, we must make sure that, whichever way we are going to deal with quarks, they will in no case appear in the final states. Some people will argue that in the quark parton model this realistic element is introduced by saying that after the elementary deep scattering has taken place, the confinement mechanism becomes operative by "dressing" the quarks so that they shall never appear "naked" in the final states. The reason why I find this argument unacceptable is that the effects of confinement do not appear, as they should, *explicitly* in the calculations. To say that these effects are "soft", without specifying "how soft", and omitting to give some approximate but quantitative description of them, does not help the parton model to surmount the barrier which separates it from the physical reality. The parton model diagrams may very well be a very useful and accurate "rule of thumb" for describing the physics of processes at large momenta, but they cannot constitute a scientific explanation of their physics. As I argued above, the same criticism does apply to the generalized use of asymptotic freedom which seems to be prevailing now.

How does the MQM cope, then, with the task of providing a realistic description of the physics at large momenta? The main assumptions are as follows:

i) The quark degrees of freedom exist only in *finite* space-time domains (bags).

ii) In the bag domains, quarks have the same behaviour as low (effective) mass hadrons; in particular, high-energy quark Green's functions exhibit Regge behaviour.

iii) Quarks, as in the quark parton model, have a point-like coupling to electromagnetic and weak currents.

Assumption (i) simply states that quarks are confined, and specifies the analyticity properties that a quark Green's function must possess in a field theory of confined quarks. In particular, any quark Green's function must be an *entire* function of the four-momentum squared of any of its quark legs. Assumption (ii) indicates what is the high-energy behaviour of a quark Green's function, and allows us to describe the globality of high-energy behaviour in terms of a few Regge trajectories. Finally (iii) gives an unambiguous physical meaning to the point-like nature of quarks.

Based on these three general assumptions we can work out all deep inelastic phenomena and derive, in a "realistic" fashion, most of the quark-parton-model results[20]. But the most interesting aspect of this approach is that it unifies the high-energy low p_T physics with deep inelastic physics. For instance, it turns out that Bjorken scaling for the current-hadron amplitude is nothing but Feynman scaling for the six-point $q\bar{q}$-hadron scattering (see Fig. 11). In this way we see that the scaling behaviour of deep inelastic scattering is nothing but the reflection of the same phenomenon in high-energy low p_T physics; its precocity is analogous to the precocity of Regge behaviour. This does not mean that the MQM *explains* scaling, but it certainly demonstrates that constancy (approximate) of high-energy cross-sections[22] and scaling in deep inelastic lepton-hadron interactions are but the two sides of the same coin.

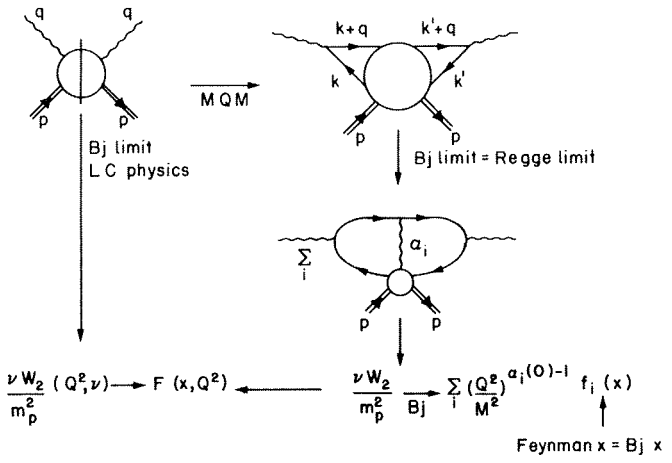

Fig. 11 The MQM unifies Feynman and Bjorken scaling

Another important aspect of this theory, which distinguishes it sharply from the parton model, is the prediction that the structure of final states is universal, i.e. it does not depend on the particular reaction, be it hadron-hadron, lepton-hadron, or e^+e^- collisions, chosen to produce hadronic matter. Experimental evidence is now accumulating in favour of this remarkable fact.

Before leaving the MQM, let me briefly report on some very recent application of MQM that P. Castorina, G. Nardulli and myself have made to deep inelastic structure functions[21]. Using all the constraints of Mueller-Regge analysis, we have been able to describe scaling *and* its violations for all observable structure functions in terms of only six parameters. Furthermore, scaling violations can be accounted for by only one parameter, and have the form of subasymptotic violations (coming from non-leading Regge trajectories) of the type:

$$\frac{F^{\text{non-scaling}}(x,Q^2)}{F^{\text{scaling}}(x)} \sim \frac{1}{(1-x)^{\frac{1}{2}}(Q^2)^{\frac{1}{2}}} .$$

A fit to the recent experimental data is presented in Figs. 12, 13 and 14.

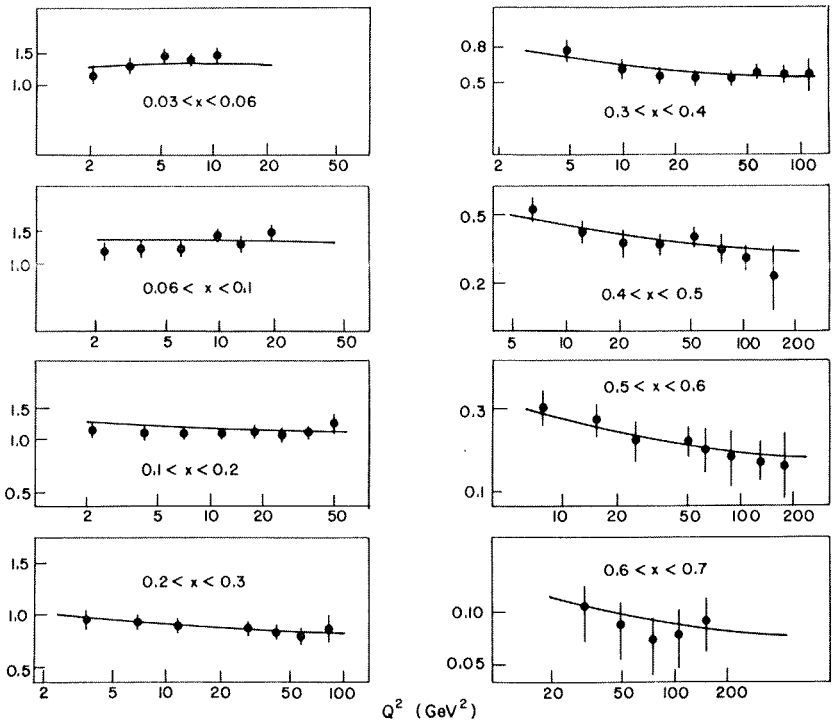

Fig. 12 CDHS[14] data versus the MQM predictions[21] for $F_2(x,Q^2)$

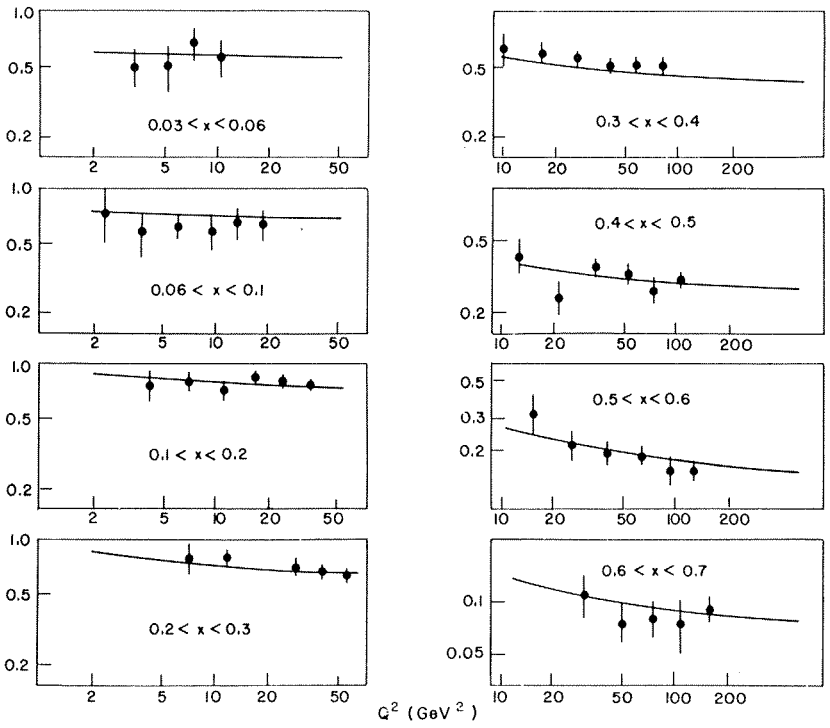

Fig. 13 CDHS data versus the MQM predictions[21] for $xF_3(x,Q^2)$

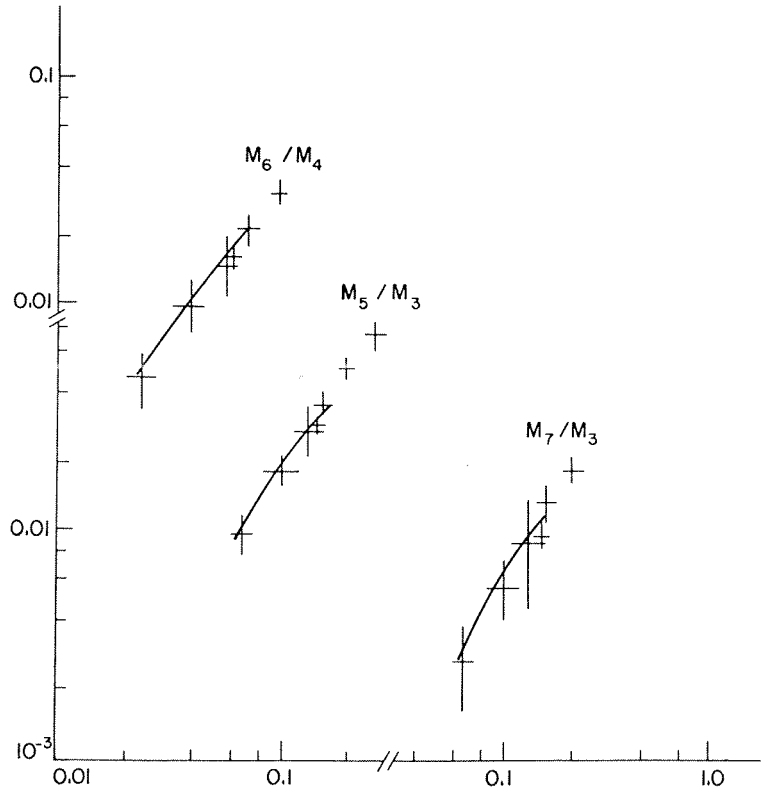

Fig. 14 A plot of different moments against each other. Experimental points are from BEBC[14] and the theoretical curves are the MQM predictions[21].

Thus we see that the MQM provides us with a predictive and precise description of a class of phenomena which have been thought to be the main testing ground of AF.

2.3 An intermediate step: the primitive world

After having experimented with theories which give a better understanding of the physics covered by the naive quark model and by the quark parton model, it appears appropriate to make a serious effort to unify the low-energy with the high-momentum aspects of the physics of quarks. It would be futile, however, to aim right away at a theory which gives a complete and accurate explanation of the most diverse phenomena of the subnuclear world. We would immediately be confronted with the problem of unitarity -- a problem which, in strong-coupling regimes, we are not able to handle.

So we must try a different strategy, and ask ourselves whether it is possible to construct a hadronic world where the main aspects of the naive quark model and of the quark parton model are contained in a very simple and *calculable* fashion, whereas the more subtle aspects of unitarity are reserved for a later attempt.

In order for this strategy to have any chance of being successful, it is clearly necessary that this world, which we shall call the "primitive world", be not too far away from the real world. Prima facie, such a requirement looks hopeless. Do we not know that strong interactions are strong? Not quite. For it is a fact, which we should have learnt by now, that the so-called strong interactions are characterized by fairly weak couplings, and this gives our strategy a really good fighting chance.

But before I shall describe one possible way of constructing the primitive world, let me briefly recall a few facts which give us confidence in our belief that strong interactions are by no means strong.

i) The success of the naive quark model. If strong interactions were really strong, because of unitarity corrections we would find no trace in nature of the simple dynamical systems that the naive quark model imagines.

ii) The remarkable validity of the Zweig rule. This happens not only for heavy mesons but also for the ϕ mesons, that is in a mass region where AF cannot be applied. As everybody knows, unitarity corrections of the type shown in Fig. 15 give a mixing between ϕ and ω, thus spoiling the validity of the Zweig rule. The only way for the rule to survive is for the unitarity corrections to be small[23]!

iii) At high energy, total cross-sections are much larger than the elastic cross-sections; even at the highest energies, hadrons are far from the black disks that a theory of *strong* strong interactions would lead us to expect.

On the basis of all that, we shall conceive a *"primitive world"* that is populated by non-interacting hadrons whose spectrum contains infinitely many states, and whose currents are described by point-like couplings to quarks. This world should be simple, calculable,

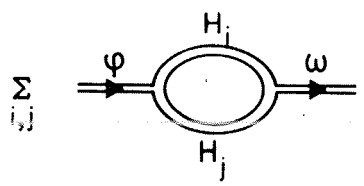

Fig. 15 The "radiative corrections" to the Zweig rule

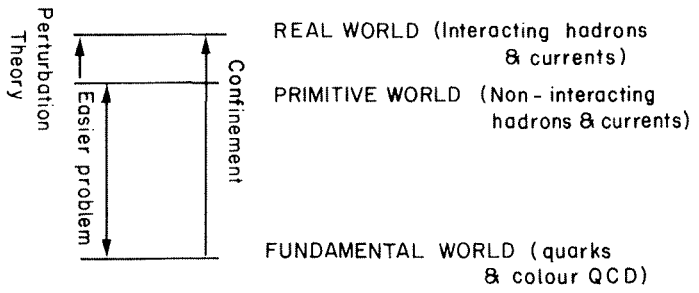

Fig. 16 The primitive world is an intermediate stage between the real and the fundamental worlds

and *perturbatively* related to the real world, so that interactions among hadrons can be calculated in a systematic fashion starting from the primitive world in a way analogous to that of perturbation theory in QED. There the primitive world is described by the free part of the Lagrangian, and its link with the real world of interacting leptons and photons is provided by treating the interaction Lagrangian as a perturbation. The strategy we envisage is thus pictured in Fig. 16.

2.4 How can we construct the primitive world?

The primitive world (PW), besides being simple and calculable, should contain the successful characteristics of the naive quark model and the quark parton model, and of their more refined and mature versions the MIT bag and the MQM, respectively. Thus it should:

i) contain an infinite number of mesons ($q\bar{q}$ states) and baryons (qqq states) lying on (approximately) linear and parallel Regge trajectories;

ii) have the quarks appearing only in *finite* space-time domains (bags), with a wave motion inside them that is as close as possible to a free motion;

iii) exhibit weak and electromagnetic currents coupled to quarks in a point-like fashion.

In the light of the previous discussion, I believe that any further motivation of these three points is superfluous. But, how do we go about implementing them? I believe that there are several possible ways of constructing a viable primitive world; the problem obviously is to work them out and to confront them with the real world. Those that come close to describing what happens in nature should be taken as possible candidates on which to construct the next step, i.e. the introduction of a perturbative interaction among hadrons.

So far, to my knowledge[24], only one proposal exists for the construction of the primitive world in the way I have described above: quark-geometrodynamics (QGD)[25]. Detailed reviews of this approach are available in the literature[26], so that I need focus only on its main ideas, and on a list of results.

QGD aims at giving a field theoretical description of the PW. However, it is abundantly clear that hadrons are non-local objects; the attribution to them of a local field can in fact make sense only as a means to account, in the sense of LSZ, for their asymptotic properties. In the light of the valiant if unsuccessful efforts of the last decades, the chances of obtaining something sensible along the direction of non-local field theories seem indeed very slim. Thus the only hopeful direction which seems open to our investigation is that of *multilocal* field theories, in which the fundamental fields do not depend on an infinite number of space-time points, but only on a *finite* number.

The idea, which was first contemplated by Yukawa in the early 1950's[27], is to describe families of hadrons by a multilocal field $\psi(x_1,x_2\ldots)$. Profiting from the lessons of the quark model, we introduce two types of multilocal fields (Greek indices stand for Dirac, colour, and flavour):

$$M_a^{\beta}(x_1,x_2) \qquad \text{for mesons}$$

$$B_{\alpha\beta\gamma}(x_1,x_2,x_3) \qquad \text{for baryons}$$

In this way it is guaranteed that the internal structure of mesons and baryons is correctly described by coloured quarks and by flavoured spin $\frac{1}{2}$ quarks.

Next we must specify the equations of motion for these fields as well as appropriate boundary conditions. Here we have a wide variety of choices; one of them, which seems to have very nice properties, will be described in a moment. As a solution of these equations we obtain an infinite spectrum of meson and baryon states, each of which is associated with a well-defined wave function whose only indeterminacy lies in a normalization factor. Such a factor will be fixed once we have specified the way in which currents operate on the hadronic w.f.'s. The choice of the current operators will obviously depend on the equations of motion that have been adopted for the bi- and tri-local fields.

At the end of this construction we obtain a PW which is equipped with a well-defined spectrum of zero-width hadrons that have current form factors, and deep inelastic structure functions that are completely non-trivial. Weak and electromagnetic processes will therefore provide us with a very stringent test of the adequacy of the PW that we have been able to construct. If the answers we obtain do not approximate to within, say, 10-20% what is experimentally measured, we had better have another try; for no perturbation theory will have a chance to take us from our PW to the real world.

2.5 The PW in quark geometrodynamics

Let me now briefly describe the steps through which the PW is constructed in QGD:

i) To each hadron we associate a w.f. which describes the quark degrees of freedom of mesons and baryons; for mesons we have (Greek indices are Dirac indices, while latin indices stand for colour and flavour)

$$\psi_{\alpha a}^{\beta b}(p;x_1,x_2) = e^{ip(x_1+x_2)/2}\,\psi(p;x_1-x_2)_{\alpha a}^{\beta b} ,$$

while for baryons we write

$$\psi_{\alpha a,\beta b,\gamma c}(p;x_1,x_2,x_3) = e^{ip(x_1+x_2+x_3)/3}\,\psi(p;x,y)_{\alpha a,\beta b,\gamma c} .$$

ii) Confinement is introduced *geometrically*, i.e. we ask that the w.f.'s vanish outside a compact region of the relative space-time coordinates; thus for mesons we impose

$$\psi(p;x) = 0 \qquad \text{for } x \notin R^4(p) ,$$

and for baryons

$$\psi(p;x,y) = 0 \qquad \text{for } x,y \notin R^8(p) \ ,$$

where $R^4(p)$ and $R^8(p)$ are compact regions which depend on the total hadron momentum p.

iii) Inside the regions R^4 and R^8 the w.f.'s obey differential equations of the Bethe-Salpeter type with vanishing kernels (i.e. with no potentials!); we therefore write:

$$\vec{D}_1 \psi \overleftarrow{D}_2 = 0 \qquad \text{for mesons,}$$

and

$$\vec{D}_1 \vec{D}_2 \vec{D}_3 \psi = 0 \qquad \text{for baryons,}$$

where $D_i = (-i\not{\partial}_i + m_i)$ is the Dirac operator for the quark inside the "bag" R; and m_i is the operational definition of the quark mass.

iv) On the boundaries of the regions R we impose the vanishing of appropriate scalar coefficients of our w.f.'s.

v) We keep only those solutions which reproduce free quark motion very closely.

It has been shown that at the end of this fairly straightforward procedure a hadronic spectrum is produced which handsomely meets the requirements we have set up in Section 2. In particular, the meson spectrum turns out to *coincide* with the naive non-relativistic quark model spectrum, even though this theory is fully relativistic. Where, however, we have a departure from the non-relativistic quark model is in the baryon spectrum[28]. For masses below 2 GeV the (idealized) spectra in the two approaches are as reported in Fig. 17. Failure to observe baryon resonances which belong to the representations $(70,0^+)$ and $(20,1^+)$ would be a strong support for our picture, which naturally leads to the dominance for baryons of the quark-diquark configurations.

Currents can also be introduced in a very simple fashion, and we obtain, besides the normalizations, very reasonable form factors having the asymptotic behaviour $1/Q^2$ for mesons and $(1/Q^2)^2$ for baryons. In the PW we have also calculated the current-particle matrix elements (see Fig. 18); here also, the results are very encouraging[26]. In particular, the asymptotic value of R in e^+e^- annihilation is given by

$$R_{as} = \frac{4}{\pi} \sum_{\substack{\text{(i=colour} \\ \text{and flavour)}}} Q_i^2 \ ;$$

a result which is extremely close to the experimental observations.

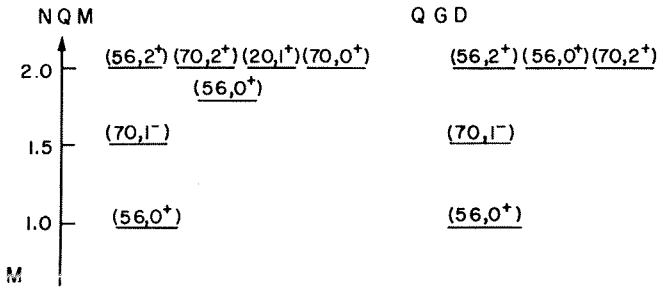

Fig. 17 The expected baryon spectrum in the naïve quark model (NQM) and in QGD

Fig. 18 The current-particle junction

Everything, so far, looks very good; however, I should add that we are only at the beginning of our exploration of this intriguing primitive world. A great number of calculations must be performed before we can talk about its features with a good degree of confidence.

2.6 Putting interactions in

There is a very simple way of introducing an interaction among the inhabitants of the primitive world. We define the three-meson and the baryon-baryon-meson couplings by the space-time overlap of the wave functions we have derived in setting up the PW. Thus we should consider diagrams such as Fig. 19, where the three-meson vertex is depicted.

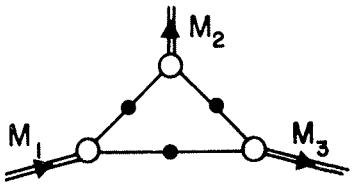

Fig. 19 The three-meson vertex. The dots denote the quark-tunnelling amplitudes.

But before we can start calculating in great detail, we must solve two problems: i) determine precisely the spin structure of the overlap integral; and ii) find out in which way our vertex behaves when particles are off-shell. The first problem should pose no real difficulty, but the second is a very fundamental issue, whose clarification would give new and deeper insight into several fascinating problems of hadronic dynamics, ranging from intermediate-energy nuclear physics to high-energy scattering.

For both problems the situation is at present quite fluid.

3. CONCLUSIONS

Besides having severe problems from the theoretical point of view, perturbative QCD appears to have met with its first serious crisis also on the experimental front (see Section 1). In the light of these troubles, the successes of perturbative QCD which are being incessantly claimed in the literature, reflect nothing but the fact that nature does seem to follow very closely the quark parton model, whose simple ideas were a very big puzzle and still remain so.

Perhaps a way out of this curious blend of confusion and simplicity is represented by the construction of a simple, well-defined primitive world. There, quarks will be both confined and almost free; a world which seems to be very near to the real one. I have indicated one of the ways of building up such a world, starting from a multilocal field theory of hadrons; but other possibilities may be envisaged. The results obtained so far strongly encourage us to continue on this path and to start building up the perturbative framework which should lead us from the primitive to the real world.

If this programme is successful we shall certainly have extremely valuable hints as to what the real QCD theory is. For the time being it would be a good thing if more and more people would stop celebrating the ephemeral triumphs of naive QCD and start thinking about the real nature of quantum chromodynamics.

REFERENCES

1) The naive quark model was first introduced by G. Morpurgo, Physics 2, 95 (1965), and later extended by R.H. Dalitz, 13th Int. Conf. on High-Energy Physics, Berkeley, 1966 (University of California Press, 1967), p. 344.

2) Colour was invented by O.W. Greenberg, Phys. Rev. Lett. 13, 598 (1964); and later developed into QCD by many people.

3) See the discussion of K.G. Wilson, *in* "Ettore Majorana" Int. School of Subnuclear Physics, Erice; New Phenomena in Subnuclear Physics (ed. A. Zichichi) (Plenum Press, New York, 1977), part A, p. 69.

4) See, for instance, C. Callan, R. Dashen and D. Gross, Phys. Rev. D 17, 2717 (1978).

5) This was shown by H.D. Politzer, Phys. Rev. Lett. 30, 1346 (1974); and by D. Gross and F. Wilczek, Phys. Rev. Lett. 30, 1343 (1974).

6) K. Symanzik, Commun. Math. Phys. 18, 227 (1970).
C.J. Callan, Phys. Rev. D 2, 1541 (1970).

7) S. Coleman, Renormalization and symmetry: A review for non-specialists, *in* Properties of the Fundamental Interactions, Proc. 1971 Erice Summer School (ed. A. Zichichi) (Ed. Compositori, Bologna, 1973), p. 605.

8) K.G. Wilson, Phys. Rev. 179, 1499 (1969).

9) R. Brandt and G. Preparata, Nucl. Phys. B27, 541 (1971).

10) See the talk by M.K. Gaillard at this conference.

11) See the reports by R. Turlay and E. Gabathuler at this conference.

12) D.W. Duke and R.G. Roberts, Analysis of nucleon structure function moments, Rutherford preprint RL-79-025 (1979).

13) B.A. Gordon et al., Phys. Rev. Lett. 41, 615 (1978).
H.L. Anderson et al., Phys. Rev. Lett. 40, 1061 (1978).

14) P. Bosetti et al. [BEBC], Nucl. Phys. B142, 1 (1978).
J.G.H. de Groot [CDHS], Z. Phys. 1, 143 (1979).

15) K.W. Chen, contribution to the Highly Specialized Seminar on Probing Hadrons with Leptons, Erice, 1979.

16) A. Patrascioiu, Phys. Rev. D 17, 2764 (1978).

17) A. Chodos, R.L. Jaffe, K. Johnson, C.B. Thorn and V.F. Weisskopf, Phys. Rev. D 9, 3471 (1974).

18) For an up-to-date review, see P. Hasenfratz and J. Kuti, Phys. Rep.

19) G. Preparata, Phys. Rev. D 7, 2973 (1973).

20) S.D. Drell and T.D. Lee, Phys. Rev. D 5, 1738 (1972).

21) P. Castorina, G. Nardulli and G. Preparata, A realistic description of deep inelastic structure functions; CERN preprint TH.2670 (1979).

22) In order to get Bjorken scaling it is sufficient that the increase of high-energy cross-sections and the shrinking of the diffraction peak are "geometrically" related, as observed experimentally.

23) This has been explicitly demonstrated by G. Fogli and G. Preparata, Nuovo Cimento 48A, 235 (1978). See also M. Roos and N. Törnqvist, paper presented at this conference.

24) Several attempts had been made in the last 10 years but they have focused on some limited aspects of the Primitive World: the following are a few examples:
G. Preparata, A relativistic quark model, *in* Subnuclear Phenomena, Proc. 1969 Erice Summer School (ed. A. Zichichi) (Academic Press, New York, 1970), p. 240.
M. Böhm, H. Joos and M. Krammer, Nucl. Phys. B51, 397 (1973).
H. Leutwyler and J. Stern, Nucl. Phys. B133, 115 (1978).

25) G. Preparata and N. Craigie, Nucl. Phys. B102, 478 (1976).
N. Craigie and G. Preparata, Nucl. Phys. B102, 497 (1976).

26) For a recent review, see G. Preparata, Quark geometrodynamics: a new approach to hadrons and their interactions, Proc. 1977 Erice Summer School (ed. A. Zichichi), to appear.

27) H. Yukawa, Phys. Rev. 91, 415 and 416 (1953).

28) G. Preparata and K. Szegö, Phys. Lett. 68B, 239 (1977); and Nuovo Cimento 47A, 303 (1978).

SUPERGRAVITY IN SUPERSPACE FORMULATION

J. Wess
Karlsruhe University, W. Germany

In the superspace formulation [1] of supergravity, the dynamics of the system has to be formulated in terms of the Vielbein-superfield $E_m{}^a(z)$ and the connection $\phi_{m\,a}{}^b(z)$. The connection is Lie-algebra valued and different structure groups impose different restrictions on $\phi_{m\,a}^{(z)\,b}$

The covariant tensor quantities which can be constructed in terms of the Vielbein and the connection and their derivatives are the torsion $T_{ab}{}^c$ and the curvature $R_{abc}{}^d$.

There are two types of equations which determine the dynamics of the system:

Constraint equations, they reduce the number of independent fields, but they do not impose any restrictions on the dependence of the fields on the four-dimensional space time variable x^m. The aim is to find all the constraints to minimalize the number of independent fields without eliminating them all.

Field equations are mass-shell conditions, they govern the x^m dependence of the fields and they should be such that the equations are local, causal and free of ghosts.

The equations are known for three cases:

a) N=1, Lorentz group as structure group [2].

$$\phi_{m\,\alpha\dot\alpha\,\beta\dot\beta} = -2\varepsilon_{\alpha\beta}\phi_{m\,\dot\alpha\dot\beta} + 2\varepsilon_{\dot\alpha\dot\beta}\phi_{m\,\alpha\beta}$$

Constraint equations:

$$T_{\underline{\gamma}\underline{\beta}}{}^{\underline{\alpha}} = 0\,, \quad T_{\gamma\beta}{}^{a} = T^{\dot\gamma\dot\beta\,a} = 0\,, \quad T_{\gamma}^{\dot\beta a} = 2i\sigma^a{}_{\gamma}{}^{\dot\beta}$$

$$T_{\gamma b}{}^{a} = T^{\dot\gamma}{}_{\beta}{}^{a} = 0\,, \quad T_{\alpha b}{}^{a} = 0\,.$$

Field equations:

$$T_{\alpha\dot{\alpha}}{}^{\beta} = 0$$

b) N=2 ,[3] Lorentz group as structure group: [4]

$$\phi_{e\ \alpha\dot{\alpha},\beta\dot{\beta}} = -2\varepsilon_{\alpha\beta}\phi_{e\dot{\alpha}\dot{\beta}} + 2\varepsilon_{\dot{\alpha}\dot{\beta}}\phi_{e\alpha\beta}$$

$$\phi_{e\alpha B}^{\ \ A\ \beta} = \Gamma_B^A \phi_{e\ \alpha}^{\ \ \beta}$$

$$\phi_{e\ A\dot{\beta}}^{\ \ \dot{\alpha}\ B} = \Gamma_A^B \phi_{e\ \ \dot{\beta}}^{\ \ \dot{\alpha}}$$

Constraint equations:

$$T_{D\,B\,A}^{\dot{\Gamma}\,\dot{\beta}\,\alpha} = T_{\Gamma\,\beta\,\dot{\alpha}}^{D\,B\,A} = 0$$

$$T_{\Gamma\beta}^{D\,B\,\alpha} = T_{D\,B}^{\dot{\Gamma}\,\dot{\beta}\,\alpha} = 0\,, \quad T_{\Gamma\,B}^{D\,\dot{\beta}\,A} = 2i\sigma^{\alpha}{}_{\Gamma}^{\dot{\beta}}\,\Gamma_B^D$$

$$T_{\Gamma\ \beta}^{D\ \ \alpha} = T_{D\ \beta}^{\dot{\Gamma}\ \ \alpha} = 0\,, \quad T_{\alpha\beta}^{\ \ \ A} = 0\,,$$

$$T_{\Gamma\,B\,\dot{\alpha}}^{D\,\dot{\beta}\,B} = T_{D\,\beta\,B}^{\dot{\Gamma}\,B\,\alpha} = 0$$

$$\oint_{ACD} g^{CB}\, T_{\Gamma\,B\,\dot{\alpha}}^{D\,\dot{\beta}\,A} = \oint_{ACD} g_{CB}\, T_{D\,\beta\,A}^{\dot{\Gamma}\,B\,\alpha} = 0$$

$$\gamma_D^{\Gamma}\, T_{\Gamma\,B\,\dot{\alpha}}^{D\,\dot{\beta}\,A} = \gamma_{\dot{\Gamma}}^{D}\, T_{D\,\beta\,A}^{\dot{\Gamma}\,B\,\alpha} = 0\,.$$

This set of equations reduces the number of independent fields to one irreducible multiplet under supersymmetry transformations, it has 40 fermionic and 40 bosonic components [5].

The field equations can be simply stated as

$$T_{\Gamma\,D\,\dot{\alpha}}^{D\,\dot{\beta}\,A} = T_{D\,\beta\,A}^{\dot{\Gamma}\,D\,\alpha} = 0\,.$$

They reduce the dynamical independent fields to the irreducible on mass-shell supersymmetry multiplet.

c) N=2 , direct product of the Lorentz group and SU(2) as structure group

$$\phi_{\mathcal{C}\,\alpha\dot{\alpha}\,\beta\dot{\beta}} = -2\varepsilon_{\alpha\beta}\phi_{\mathcal{C}\,\dot{\alpha}\dot{\beta}} + 2\varepsilon_{\dot{\alpha}\dot{\beta}}\phi_{\mathcal{C}\,\alpha\beta}$$

$$\phi_{\mathcal{C}\,\alpha B}^{\quad A\beta} = \delta_B^A \phi_{\mathcal{C}\,\alpha}^{\quad\beta} + \delta_\alpha^\beta \phi_{\mathcal{C}}^{\quad A}{}_{B}$$

$$\phi_{\mathcal{C}A\,\dot{\beta}}^{\quad\dot{\alpha}B} = \delta_A^B \phi_{\mathcal{C}}^{\quad\dot{\alpha}}{}_{\dot{\beta}} + \delta_{\dot{\beta}}^{\dot{\alpha}} \phi_{\mathcal{C}A}^{\quad B}$$

$$\phi_{\mathcal{C}}^{\quad A}{}_{B} = -\phi_{\mathcal{C}B}^{\quad\quad A}\,, \qquad \phi_{\mathcal{C}}^{\quad A}{}_{A} = 0\,.$$

The constraint equations are as before and in addition:

$$R_{\delta\gamma\,\alpha B}^{\mathcal{D}C\,A\alpha} = -R_{\delta\gamma\,A\dot{\alpha}}^{\mathcal{D}C\,\dot{\alpha}B} = 0$$

$$R_{\mathcal{D}C\,A\dot{\alpha}}^{\dot{\delta}\dot{\gamma}\,\dot{\alpha}B} = -R_{\mathcal{D}C\,\dot{\alpha}B}^{\dot{\delta}\dot{\gamma}\,A\dot{\alpha}} = 0$$

$$T_{\mathcal{G}\,\alpha A}^{\quad\mathcal{D}\alpha} = T_{\mathcal{G}\mathcal{D}\,\dot{\alpha}}^{\quad\dot{\alpha}A} = 0$$

The field equations are as before:

$$T_{\delta\mathcal{D}\,\dot{\alpha}}^{\mathcal{D}\dot{\beta}\,A} = T_{\mathcal{D}\beta A}^{\dot{\delta}\mathcal{D}\,\alpha} = 0$$

The number of independent fields is the same as before. The connection of the internal symmetry group SU(2) is expressed in terms of auxiliary fields which have to be eliminated via their field equations.

The field content and the absence of ghosts has been checked in the linearized approximation.

REFERENCES

1) J. Wess and B. Zumino, Phys. Lett. 66B (1977) 361.
2) J. Wess and B. Zumino, Phys. Lett. 74B (1978) 51.
3) S. Ferrara, J. Scherk, B. Zumino, Nucl. Phys. B 121 (1977) 393.
L. Brink, M. Gell-Mann, P. Ramont and J.H. Schwarz, Phys. Lett. 74B (1978) 336.
4) N. Dragon, R. Grimm, J. Wess, to be published.
5) B. de Wit and J.W. van Holten, Multiplets of Linearized SU(2) Supergravity, Stony Brook preprint, ITP-SB-79-21

DISCUSSION

Chairman: S. Ferrara

Sci. Secretaries: A. Din and W. Zakrzewski

J. Rosner: Will you be commenting or will Prof. Salam be commenting on the extension of SO(8) to SU(8) (in experimental terms)?

J. Wess: Prof. Salam will be discussing this question in his summary talk.

J.G. Taylor: What is the relation of your results for N = 2 with that of Gell-Mann et al.?

J. Wess: It is consistent with their work but they have not separated constraint and field equations.

J.G. Taylor: What is the impact of this new work on the Princeton work on confinement?

D. Fairlie: Unfortunately the work has not yet reached a stage at which this question can be answered.

INSTANTONS

D.B.Fairlie
Department of Mathematics, University of Durham, U.K.

ABSTRACT

Recent progress in multi-instanton calculations is reviewed.

Instantons are five years old this summer, and, with a persistence which belies their name, their study remains one of the growth areas of theoretical physics. They correspond to local minima of the Euclidean action, and in the physically interesting case of Yang Mills in 4 dimensions fall into classes associated with a topological number k given by

$$k = \frac{1}{16\pi^2} \int d^4x \, \mathrm{Tr}\,(F_{\mu\nu} F^*_{\mu\nu})$$

where $F^*_{\mu\nu} = \varepsilon_{\mu\nu\rho\sigma} F_{\rho\sigma}$ and the instantons are singularly free solutions of

$$F_{\mu\nu} = \pm F^*_{\mu\nu} ,$$

which means that they are solutions of the equations of motion in virtue of the Bianchi identities (1).

The major trend in the past few years has been the development of methods for the evaluation of multi-instanton effects, with a view to quantifying the effects of the dilute gas approximation, and to assess the practical importance of instanton contributions to strong interaction processes.

There are three areas where significant progress has been made.

The first of these is a consequence of the remarkable general k instanton solution found by Atiyah, Hitchin, Drinfield and Manin, using (2) powerful techniques in algebraic geometry. Many theorists including myself have been forced to revise our prejudice against the practical utility of modern pure mathematics on account of this work. The solution itself is simple, and may be verified by routine calculations, and I shall run through the construction of the 8k - 3 instantons with instanton number k in SU(2) to give the flavour of its structure, since it works for any compact Lie gauge group in a similar fashion. We take the coordinates x_μ ($\mu = 0,\ldots,3$) in Euclidean space and represent them in terms of the quaternion

$$x = x_0 - i\underline{x}\cdot\underline{\sigma} = \begin{pmatrix} x_0 - ix_3 & -x_2 - ix_1 \\ x_2 - ix_1 & x_0 + ix_3 \end{pmatrix} .$$

Consider now a $(k+1) \times k$ matrix Δ whose entries are quaternion valued, and are linear in x

$$\Delta_{ij}(x) = a_{ij} + b_{ij} x \qquad \begin{matrix} 1 \leq i \leq 1+k \\ 1 \leq j \leq k \end{matrix}$$

where a,b are quaternionic matrices.

Next construct a $(k+1) \times 1$ column vector $V(x)$, normalised so that

$$V^{+}V = 1$$

and in the orthogonal subspace to that spanned by Δ

$$V^{+}\Delta = 0.$$

Then provided $\Delta^{+}(x)\Delta(x)$ is real and invertible, which is tantamount to the requirement that $a^{+}a$, $b^{+}b$ and $a^{+}b$ are symmetric as $k \times k$ matrices of quaternions then

$$A_{\mu} = V^{+}\partial_{\mu}V$$

is the vector potential of a non singular self dual solution of SU(2) Yang Mills. All the non linearity of the problem has been pushed into the constraints on Δ, but so far the only explicit solutions known in any generality are the k instanton in SU(2k) (3) and the original t'Hooft solution,

$$A_{\mu} = \eta a_{\mu\nu}\partial_{\nu}\ell n\rho$$

$$\rho = 1 + \sum \frac{\lambda_i}{|x - a_i|^2}$$

which in the A D H M construction takes the form

$$V^{+}(x) = \phi^{-\frac{1}{2}}\left(1, \lambda_i \frac{x - a_i}{|x - a_i|^2} \right)$$

where the normalisation factor

$$\phi = 1 + \sum \frac{\lambda_i^2}{|x - a_i|^2} .$$

This mathematical work has provided the inspiration for a series of papers (4, 5, 6, 7) which have translated and extended the pioneering work of the Seattle group (8, 9) on the Green function in the presence of an arbitrary number of t'Hooft instantons and the functional determinant of fluctuations about the instanton solution in terms of the A D H M work.

The Green function for a scalar field transforming as the doublet representation of SU(2) in the presence of a general multi-instanton background is given by the simple and elegant formula (4,5)

$$G(x,y) = \frac{V^{+}(x)V(y)}{4\pi^2(x - y)^2} .$$

The latter papers in this series (6,7) constitute a mathematical tour de force, in expressing the Green function for the adjoint representation and the determinant up to a conformally invariant factor in the new language. Overlapping results on the determinant have been derived recently by the Russian group (10,11). Their result for the logarithm of the determinant

in the presence of an arbitrary t'Hooft solution is

$$\ell n\, DA \;=\; -\frac{1}{96\pi^2}\left(\int d^4x\, \ell n\, \tilde{\rho}\, \Box^2\, \ell n\, \tilde{\rho} \;+\; 16\pi^2 \sum_{i<j} \ell n\, |\, a_i - a_j|^2\right)$$

where

$$\tilde{\rho} \;=\; \rho\, |x - a_1|^2 \;\ldots\; |x - a_k|^2 \;.$$

The second topic I should like to mention is the development of the so-called CP(N - 1) models. These are generalisations of the so-called σ model, and are studied as two dimensional analogues of the Yang Mills system, possessing a topological invariant, multi-instanton self dual solutions,etc. They were first formulated by Eichenherr (12), as a two dimensional field theory described by a complex vector ξ_α which is normalised to unity and

$$|\xi_\alpha|^2 \;=\; 1$$

and each component is a function of two variables. There is a U(1) gauge invariance in the theory

$$\xi_\alpha' \;=\; e^{in(x)}\xi_\alpha$$

is a physically equivalent field to ξ_α .

A Lagrangian with this invariance is

$$\mathscr{L} \;=\; \partial_\mu\, \xi_\alpha^*\, \partial_\mu \xi_\alpha - (\xi_\alpha^*\, \partial_\mu \xi^\alpha)(\xi_\beta^*\, \partial_\mu \xi^\beta)$$

$$=\; D_\mu \xi_\alpha\, D_\mu \xi \qquad \text{where} \quad D_\mu = \partial_\mu - \xi_a\, \partial_\mu \xi_\alpha .$$

Now

$$|D_\mu \xi_\alpha \pm i\varepsilon_{\mu\nu} D_\nu \xi_\alpha|^2 \;\geqslant\; 0$$

gives

$$|D_\mu \xi_\alpha|^2 \;\geqslant\; \pm i\varepsilon_{\mu\nu}\partial_\mu (\xi_\alpha^*\, \partial_\nu \xi_\alpha) .$$

Now there is a topological charge in the theory

$$k \;=\; \frac{1}{2n}\int d^2x \partial_\mu (\xi_\alpha^*\, \partial_\nu \xi_\alpha)\varepsilon_{\mu\nu}$$

and we have

$$\int |D_\mu \xi_\alpha|^2 d^2x \;\geqslant\; 2\pi k \;.$$

Thus the condition of self duality $D_\mu \xi_\alpha = i\varepsilon_{\mu\nu} D_\nu \xi_\alpha$ gives a minimum of the action, and the condition is equivalent to the Cauchy Riemann conditions

$$\partial_{\bar{z}} \xi_\alpha \;=\; 0$$

The k instanton solution is described in terms of n(k + 1) - 1 complex parameters

$$\xi_\alpha \;=\; \frac{p_\alpha(z)}{|p_\alpha|}$$

where

$$p_\alpha(z) = c_\alpha \prod_{j=1}^{k} (s - a_\alpha^j)$$

The motive for studying these models is that they are mathematically simpler than the Yang Mills analogues, and it is hoped will give some insight into the behaviour of the latter. I wish to stress that here the instanton behaviour of CP(N - 1) models is present only in two dimensions. Recently Berg and Luscher (13), and Fateev et al (14) have succeeded in evaluating the instanton determinant in CP(1). Apart from renormalisation terms it is identical to the Coulomb gas potential of k positive and k negative charges at positions a_1^i, a_2^i respectively

$$\ell n \Delta = \sum_{i,j} \ell n |a_1^i - a_2^j|^2 - \sum_{i<j} \{ \ell n |a_1^i - a_1^j| + \ell n |a_2^i - a_2^j| \}$$

I conjecture on the basis of the results of (7 and 11) that the Yang Mills case will be representable in a similar form where a_1^i, a_2^i are quaternionic solutions of

$$V_1^+ V(x) = 0, \quad V_2^+ V(x) = 0$$

for some fixed vectors V_1 and V_2, following (11).

Before leaving the mathematical developments I should like to mention the multi-instanton solution of the Einstein equations due to Gibbons and Hawking (15).

The third area of development is the most controversial - and is centred on the question of the practical utility of instantons. There is a paper by Witten (16) which investigates the CP(N - 1) models in a 1/N expansion in which no instantons appear: and the claim is made that instanton effects die exponentially with N, and thus in a 1/N power expansion, the contribution of the Feynman diagrams will dominate. The other line of attack is the criticism of the quantisation of topological charge - this is equivalent to the assumption that asymptotically the gauge fields approach pure gauge fields at infinity. Though the 1/N expansion of the CP(N-1) model with instantons may be shown to have very interesting properties like dynamical mass generation and confinement by a topological Coulomb force (17), it has been confirmed that the N-dependence of one-instanton effects and the 1/N expansion do not match (18). This might however be the case when multi-instanton effects are taken properly into account.

My own view is that since multi-instantons are a feature of two, four and possibly eight real dimensional theories only, their effect cannot be negligible.

REFERENCES

1) A. Belavin, A. Polyakov, A. Schwarz and Yu Tyupkin, Phys. Lett. B 59, (1975) 85.

2) M.F.Atiyah, N. Hitchin, V. Drinfield and Yu I. Manin, Phys. Lett. 65,185 (1978) 185

3) V.C.Drinfield and Yu Manin Comm. Math. Phys. 63 (1978) 177.

4) E.F.Corrigan, D.B.Fairlie, P. Goddard and S.J.Templeton, Nuclear Physics B 140 (1978) 31

5) N.H.Christ, E.J.Weinberg and N.K.Stanton, Phys. Rev. D 18 (1978) 2013.

6) E.F.Corrigan, P. Goddard and S.J.Templeton, Nuclear Physics B 15 (1979) 93.

7) E.F.Corrigan, P. Goddard, H. Osborn and S.J.Templeton, Cal. Tech. Preprint.

8) L.S.Brown, R.D.Carlitz, D.B.Creamer and C. Lee, Phys. Lett. B 71 (1977) 103.

9) L.S.Brown and D.B.Creamer, Phys. Rev. D18 (1978) 3695.

10) A.S.Schwarz, Comm. Math. Phys. 64 (1979) 233.

11) A.A.Belavin, V.A.Fateev, A.S.Schwarz and Yu Tyupkin, Phys. Lett. B 83 (1979) 317.

12) H. Eichenherr, Nuclear Physics B 146 (1978) 215.

13) B. Berg and M. Lüscher, DESY Preprint (1979).

14) V.A.Fateev, I.V.Frolov and A.S.Schwarz, Nuclear Physics to appear.

15) G.W.Gibbons and S.W.Hawking, Phys. Lett. B 78 (1979) 430.

16) F. Witten, Nuclear Physics B 149 (1979) 285.

17) A.D.Adda, P. Di Vecchia and M. Lüscher, Nuclear Physics B 146 (1978) 63.

18) A.M. Din, P. Di Vecchia and W.J. Zakrzewski, CERN preprint 2645 (1979) (to be published in Nuclear Physics).